

A New Theory of Alzheimer's Disease

by

Felix S. Meier-Stephenson

Submitted in partial fulfilment of the requirements
for the degree of Doctor of Philosophy

at

Dalhousie University
Halifax, Nova Scotia
March 2014

© Copyright by Felix S. Meier-Stephenson, 2014

To V.

Table of Contents

List of Tables	xix
List of Figures	xxi
Abstract	xxvi
List of Abbreviations and Symbols Used.....	xxvii
Acknowledgements	xxxv
CHAPTER I. INTRODUCTION	1
1. Alzheimer’s Disease.....	1
1.1. Background.....	1
1.2. The Burden of AD	2
1.3. Pathology, Pathophysiology and Risk Factors of AD	3
1.3.1. Pathology	4
1.3.2. Pathophysiology	5
1.3.3. Risk Factors.....	6
1.3.4. Processes and Factors Implicated in AD Pathophysiology	7
1.3.5. β-Amyloid ($A\beta$)	10
1.3.5.1. APP Processing and β -Amyloid Generation	10
1.3.5.2. Posttranslational Modifications of β -Amyloid	12
1.3.5.3. Secondary/Tertiary Structure of β -Amyloid	13
1.3.5.4. Oligomerization and Fibrillogenesis.....	14
(a) Influence of $A\beta$ species and concentration	17
(b) Influence of pH.....	18
(c) Influence of Metal Ions	18

(d) Influence of Cell Membrane Components.....	19
1.3.5.5. Plaques.....	20
1.3.5.6. Intracellular β -Amyloid	21
1.3.5.7. Toxic Species of β -Amyloid	21
1.3.6. Neurofibrillary Tangles (NFTs)	22
1.3.7. Inflammation.....	23
1.4. Interaction of β-Amyloid with Endogenous Molecules and the Importance of the 'HHQK' Region	24
1.4.1. Interaction with Metal Cations.....	24
1.4.2. Interaction with Cell Membranes	26
1.4.2.1. Interaction with Membrane Proteins	26
1.4.2.2. Interaction with Membrane Lipids	26
1.4.3. Interaction with other Molecules	27
1.5. Current AD Hypotheses	27
1.5.1. Amyloid Cascade Hypothesis.....	29
1.5.2. Tau Hypothesis	31
1.5.1. Shortcomings of Current Hypotheses	33
2. Research Goals.....	34
3. References	36
CHAPTER II. ALZHEIMER'S DISEASE AS AN AUTOIMMUNE DISEASE OF THE INNATE IMMUNE SYSTEM.....	92
1. Introduction	92
2. The Physiologic Function of β-Amyloid: Aβ as an Antimicrobial Peptide	94

2.1. Introduction.....	94
2.2. Innate vs. Acquired Immunity.....	95
2.3. Effectors of the Innate Immune System	95
2.3.1. Bacteria	96
2.3.2. Viruses.....	100
2.3.3. Trauma	100
2.3.4. AMPs	100
2.4. Evolutionary Connections between AMPs and β-Amyloid	101
2.5. Structural Comparison of β-Amyloid to AMPs.....	102
2.5.1. Aβ Sequence, Constituent Amino Acid Residues & Charge State	104
2.5.2. Amphipathicity & Schiffer-Edmundson Helical Wheel.....	105
2.5.3. Boman Index.....	107
2.5.4. Heparin Affinity	107
2.5.5. AMP Activity Prediction	108
2.6. Mechanism of Action	108
2.6.1. Mechanisms of Action of Known AMPs	108
2.6.1.1. Non-Receptor Mediated AMPs.....	109
2.6.1.2. Receptor Mediated AMPs.....	110
2.6.1.3. AMP Mechanisms of Action.....	110
(a) Barrel-Stave Pore Formation Model.....	110
(b) Carpet-like Destruction Model	111
(c) Toroidal Pore Formation Model	111

(d) Aggregate Channel Model	112
2.6.1.4. Connection of Antibacterial and Immunomodulatory Effects.....	113
2.6.2. Effect of Metal Cations on the Activity of AMPs.....	113
2.6.3. Effect of Cholesterol on the Activity of AMPs	114
2.6.4. β-Amyloid's Mechanism of Action.....	114
2.7. β-Amyloid is Produced in Response to Infection	116
2.7.1. Introduction.....	116
2.7.2. Materials	117
2.7.2.1. Biological Materials.....	117
(a) Bacteria	117
(b) Mammalian Cells.....	118
2.7.2.2. Chemicals	118
2.7.2.3. Instrumentation.....	119
2.7.3. Methods.....	120
2.7.3.1. Preparation of β -Amyloid Stock Solutions.....	120
2.7.3.2. β -Amyloid Quantitation by BCA Assay.....	121
(a) Standard Assay (100 – 1000 $\mu\text{g}/\text{mL}$ total protein).....	122
(b) Microassay (0.5 – 10 $\mu\text{g}/\text{mL}$ total protein)	122
(c) Microwave Assay (0.5 – 10 $\mu\text{g}/\text{mL}$ total protein)	123
2.7.3.3. β -Amyloid Quantitation by ELISA.....	123
(a) Determination of $\text{A}\beta_{1-40}$ and $\text{A}\beta_{1-42}$ content.....	123
(b) Determination of oligomeric and total $\text{A}\beta$ content.....	124

2.7.3.4. Bacterial Cell Culture.....	126
2.7.3.5. Preparation of Bacterial Cell Cultures for Assays	127
2.7.3.6. Preparation of Bacterial Membrane Fragments.....	128
2.7.3.7. Mammalian Cell Culture	129
2.7.3.8. Preparation of Mammalian Cell Cultures for Assays	129
2.7.3.9. Preparation of primary rat neurons.....	130
2.7.3.10. A β production in mammalian cells induced by infection	130
2.7.4. Results & Discussion	132
2.7.5. Summary	135
2.8. Antibacterial Activity of β-Amyloid	136
2.8.1. Introduction.....	136
2.8.2. Materials	137
2.8.2.1. Biological Materials.....	137
2.8.2.2. Chemicals	138
2.8.3. Methods.....	138
2.8.3.1. Bacterial Cell Culture.....	138
2.8.3.2. Radial Diffusion Assay	138
2.8.3.3. Micro-Gel Well Diffusion Assay	140
2.8.3.4. Bacterial Growth Curve Assay (incl. CFU/time curves).....	140
2.8.3.5. Broth Microdilution Assay	141
2.8.4. Results & Discussion	142
2.8.4.1. Radial Diffusion Assay (RDA).....	142
2.8.4.2. Micro-gel Well Diffusion Assay	144

2.8.4.3. Bacterial Growth Curve Assay.....	147
(a) Development of the Growth Curve Assay (GCA)	147
(a) Incubation of <i>E. coli</i>	155
(b) Incubation of <i>S. marcescens</i>	156
(c) Incubation of <i>K. pneumoniae</i>	157
(d) Incubation of methicillin-resistant <i>S. aureus</i> (MRSA).....	158
(e) Incubation of methicillin-susceptible <i>S. aureus</i> (MSSA)	159
(f) Summary of parameters for all bacterial strains	160
2.8.4.4. Growth Curve Assays of A β dilution series.....	161
(a) A β ₁₋₄₀	162
(b) A β ₁₋₄₂	163
2.8.4.5. Growth Curve Assays of LL-37	165
2.8.4.6. Minimum Inhibitory Concentration (MIC).....	166
2.8.5. Summary	170
2.9. Antiviral activity.....	172
2.9.1. Introduction.....	172
2.9.2. Results & Discussion	173
2.9.3. Summary	178
2.10. Summary	179
3. Why Aβ Attacks Neurons	180
3.1. Introduction.....	180
3.2. Comparison of Mammalian and Bacterial Membranes.....	180

3.3. Comparison of Neuronal and Bacterial Membranes	182
3.4. Neurotoxicity of β-Amyloid	183
3.4.1. Introduction.....	183
3.4.2. Materials	183
3.4.2.1. Biological Materials.....	183
3.4.2.2. Chemicals	183
3.4.3. Methods.....	184
3.4.3.1. MTT Cell Viability Assay	184
3.4.4. Results & Discussion	185
3.4.5. Summary	187
3.5. Neurotoxicity of Known AMPs.....	188
3.5.1. Introduction.....	188
3.5.2. Materials	188
3.5.2.1. Biological Materials.....	188
3.5.2.2. Chemicals	189
3.5.3. Methods.....	189
3.5.4. Results & Discussion	189
3.5.5. Summary	191
3.6. Summary	192
4. Why AD is Progressive and Chronic.....	193
4.1. Mechanism for Progression and Chronicity of AD	193
4.1.1. Materials	194

4.1.1.1. Biological Materials.....	194
4.1.1.2. Chemicals	195
4.1.2. Methods.....	195
4.1.2.1. Preparation of Apoptotic and Necrotic Cell Supernatants and Lysates.....	196
4.1.2.2. Caspase-3/-7 Assay	197
4.1.2.3. Simulating the propagation of AD	198
4.1.3. Results & Discussion	198
4.1.3.1. Apoptosis	198
4.1.3.1. β -Amyloid production induced by apoptosis and necrosis	199
4.2. Summary	205
5. How it all fits together	206
5.1. AD is an autoimmune disease of the innate immune system.....	206
5.1.1. What is an autoimmune disease?.....	206
5.1.2. An autoimmune disease of the innate immune system?	207
5.2. The Vicious Cycle of Alzheimer’s Disease	208
5.2.1. A mechanism for the propagation of cell death in AD	208
5.3. Addressing gaps in current AD hypotheses	210
5.4. Summary	211
6. Conclusions	212
7. References	213
CHAPTER III. PENICILLIN AS A RISK FACTOR FOR ALZHEIMER’S DISEASE.....	240
1. Introduction	240

2.	Penicillin as a Risk Factor for AD	241
2.1.	Classes of Antibiotics and their Mechanism of Action	241
2.1.1.	β -Lactam Antibiotics	242
2.1.2.	Sulfonamides & Trimethoprim	242
2.1.3.	Quinolones	243
2.1.4.	Macrolides.....	243
2.1.5.	Tetracyclines & Glycylcyclines	243
2.1.6.	Aminoglycosides & Aminocyclitols	244
2.1.7.	Glycopeptides.....	244
2.2.	Materials	246
2.2.1.	Biological Materials	246
2.2.1.1.	Bacteria	246
2.2.1.2.	Mammalian Cells.....	246
2.2.2.	Chemicals	246
2.3.	Methods	247
2.3.1.	Killing bacteria	247
2.3.2.	Resazurin Cell Viability Assay	248
2.3.3.	Testing the Hypothesis.....	249
2.4.	Results & Discussion.....	249
2.4.1.	Preliminary Experiments.....	250
2.4.1.1.	Bacteria killing efficacy.....	250

2.4.1.2.	A β production induced by bacterial fragments and medium	253
2.4.1.3.	A β production induced by bacterial fragments obtained through γ -irradiation and autoclaving	254
2.4.1.4.	A β production induced by bacterial fragments obtained through treatment with antibiotics	255
3.	Conclusion & Future Work	261
4.	References	262
 CHAPTER IV. MICROWAVE-ASSISTED SOLID-PHASE PEPTIDE SYNTHESIS		264
1.	Introduction	264
2.	Solid-Phase Peptide Synthesis.....	266
2.1.	Principles of Solid-Phase Peptide Synthesis.....	266
2.2.	Principles of Microwave-Assisted Organic Synthesis	268
2.2.1.	Background.....	268
2.2.2.	Microwaves	268
2.2.3.	Microwave Dielectric Heating	269
2.2.4.	Dielectric Properties	271
2.2.5.	Conventional vs. Microwave Heating	273
2.2.6.	Microwave Effects	274
2.2.6.1.	Thermal Effects (Kinetics)	274
2.2.6.2.	Specific Microwave Effects	275
2.2.6.3.	Non-Thermal Microwave Effects	276
2.3.	Microwaves in SPPS	277
3.	Peptide Synthesis and Purification	279

3.1. Background	279
3.2. Materials	279
3.3. Methods	280
3.3.1. Peptide Synthesis Instrumentation	280
3.3.2. Peptide Synthesis Methods	280
3.3.3. Manual Peptide Cleavage	282
3.3.4. Peptide Purification Instrumentation and Materials	284
3.3.5. Peptide Purification Conditions	286
3.3.6. Mass Spectrometry	287
3.4. Results & Discussion	287
3.4.1. β-Amyloid-related peptides	287
3.4.1.1. $A\beta_{1-40}$	287
3.4.1.2. $A\beta_{1-42}$	290
3.4.1.3. $A\beta_{1-40}$ K28A Mutant	291
3.4.1.4. $A\beta_{12-17}$	292
3.4.1.5. VHHQKLAAAA.....	293
3.4.2. BBXB Series	294
3.4.2.1. BBXB $A\beta$	297
3.4.2.2. BBXB Tau	297
3.4.2.3. BBXB S100 β , BBXB C1qA, BBXB IL4_a & BBXB IL6_a	298
3.4.2.4. BBXB IL4_b, BBXB IL6_b & BBXB IL6_c.....	298
4. Conclusions	299
5. References	300

CHAPTER V. β-AMYLOID INTERACTION ASSAYS.....	305
1. Introduction	305
2. Peptide binding to sample vessels	306
2.1. Background.....	306
2.2. Materials	306
2.3. Methods	307
2.3.1. Coating glassware and plasticware.....	307
2.3.1.1. Silanisation.....	307
2.3.1.2. Blocking with BSA.....	307
2.3.2. Determination of protein binding.....	308
2.4. Results and Discussion	308
2.4.1. Time dependence of protein binding.....	308
2.4.2. Concentration dependence of protein binding.....	310
2.4.3. Dependence of protein binding on type of protein	312
2.5. Summary	315
3. GM1 Assay	316
3.1. Background.....	316
3.1.1. Current Aggregation Assays	316
3.1.2. Monosialoganglioside GM1 – Aβ Interactions.....	317
3.2. GM1 Assay Principle.....	318
3.3. Materials	320
3.4. Methods	320

3.4.1. Preparation of GM1 Assay 96-well plates	320
3.4.2. FAM-A β Preparation	321
3.4.1. GM1 Coating Variability	322
3.4.2. Limits of Detection and Quantitation of FAM-A β	323
3.4.3. Plate Washing and Sensitivity	324
3.4.4. Competitive Binding Assays	326
3.4.5. Thioflavin T Assay	326
3.4.6. PICUP Assay	326
3.4.7. Tricine-SDS-PAGE	327
3.5. Results and Discussion	328
3.5.1. Limits of Detection and Quantitation of FAM-A β	328
3.5.1. GM1 Coating Variability	330
3.5.2. Plate Washing.....	331
3.5.3. Sensitivity	335
3.5.4. Competitive Binding Assays	339
3.5.4.1. Influence of Metal Ions	339
3.5.4.2. Time Dependence of Zinc Effect	343
3.5.4.3. Influence of A β Antiaggregants	344
(a) A β Antiaggregants and Metals.....	344
(b) A β Aggregation Inhibitors	348
3.5.5. PICUP Assay	353
3.6. Summary	360

4.	Conclusions	362
5.	References	363
CHAPTER VI. CONCLUSIONS AND FUTURE DIRECTIONS		371
1.	Conclusions	371
2.	Future Directions.....	374
3.	References	377
APPENDIX A. PREDICTION OF A β AS AMP		378
APPENDIX B. RADIAL DIFFUSION ASSAY		380
APPENDIX C. THE GROWTH CURVE ASSAY		384
C.1.	Parameter Selection	384
C.2.	Results	390
C.2.1.	Incubation of <i>E. coli</i>	391
C.2.2.	Incubation of <i>S. marcescens</i>	395
C.2.3.	Incubation of <i>K. pneumoniae</i>	399
C.2.4.	Incubation of methicillin-resistant <i>S. aureus</i> (MRSA).....	403
C.2.5.	Incubation of methicillin-susceptible <i>S. aureus</i> (MSSA)	407
APPENDIX D. AMINO ACIDS		411
APPENDIX E. PEPTIDE SYNTHESIS CYCLES		416
APPENDIX F. ANALYSIS AND PURIFICATION OF SYNTHESISED PEPTIDES.....		418
F.1.	A β ₁₋₄₀	418
F.1.1.	Batch 1.....	418
F.1.2.	Batch 2.....	419

F.1.3. Batch 3.....	421
F.2. A β ₁₋₄₂	423
F.3. A β ₁₋₄₀ K28A	424
F.4. A β ₁₂₋₁₇	426
F.4.1. Batch 1.....	426
F.4.2. Batch 2.....	427
F.5. VHHQKLA AAA	432
F.6. BBXB Peptides.....	433
F.6.1. BBXB A β (YEVHHQKLVF)	433
F.6.2. BBXB Tau (SDDKKAKGAD).....	435
F.6.3. BBXB S100 β (GDKHKLKSEL).....	436
F.6.4. BBXB C1qA (KDPKKGHIYQ)	438
F.6.5. BBXB IL4_a (FYSHHEKDTR).....	440
F.6.6. BBXB IL4_b (Ac-QQFHRHKQLI)	442
F.6.7. BBXB IL6_a (FLQKKAKNLD)	443
F.6.8. BBXB IL6_b (NEGKKMRCEW)	444
F.6.9. BBXB IL6_c (ADCKAKRDTP)	445
APPENDIX G. PERMISSIONS	446
G.1. Permission for Figure I-1	446
G.2. Permission for Figures I-2 & I-3	451
G.3. Permission for Figure I-6	452
G.4. Permission for Figure I-7	453
G.5. Permission for Figure I-8	456
G.6. Permission for Figure I-9	459
G.7. Permission for Figures II-7, II-8 & II-9	464
G.8. Permission for Figure IV-4.....	467

G.9. Permission for Figure V-22A.....	471
G.10. Permission for Figure V-22B.....	475
REFERENCES	476

List of Tables

Table I-1	Processes and factors implied in AD pathophysiology.....	7
Table I-2	Intermediates in the pathway of A β fibrillization.	15
Table I-3	Current AD hypotheses.	28
Table II-1	Results of RDA with <i>E. coli</i> on TSB agar without cholesterol.	142
Table II-2	Results of RDA with <i>E. coli</i> on TSB agar with cholesterol.....	142
Table II-3	Result summary of the influence of A β ₁₋₄₀ , Cu ²⁺ , Zn ²⁺ , and cholesterol on the viability of <i>E. coli</i> , <i>S. marcescens</i> , <i>K. pneumoniae</i> , MRSA, and MSSA as determined by the Growth Curve Assay.	154
Table II-4	MIC Assay conditions for experiments using the GCA preparation protocol.	167
Table II-5	MIC assay conditions for experiments using MIC preparation protocol.....	168
Table II-6	Select MICs of A β determined by Soscia <i>et al.</i> (215).....	169
Table II-7	Antiviral activity of A β ₁₋₄₂ against HSV-1-GFP.	177
Table II-8	Similarities and differences between bacterial, mammalian neuronal and other mammalian cells.	182
Table II-9	Simulated neuron loss in AD.	202
Table III-1	Comparison of the efficacy of methods to kill bacteria.	251
Table IV-1	Comparison of frequency and quantum energy of a range of radiation types with the bond energy of select bond types (12-14).	269
Table IV-2	Dielectric constants, dielectric losses and loss tangent (<i>tan</i> δ) of various solvents (2.45 GHz, 20°C) (17, 18).	272
Table IV-3	Volume chart for the different steps of manual peptide cleavage.	283
Table IV-4	Equal solvent strength mixtures of MeOH/H ₂ O and MeCN/H ₂ O. Data from Ref. (44).	286
Table IV-5	Synthesis of A β ₁₋₄₀	289
Table IV-6	Synthesis of A β ₁₋₄₂	291

Table IV-7	Synthesis of A β ₁₋₄₀ K28A mutant.	292
Table IV-8	Synthesis of A β ₁₂₋₁₇	293
Table IV-10	Synthesis of VHHQKLAAAA.	294
Table IV-11	BBXB series peptides.	295
Table IV-12	Synthesized BBXB series peptides.	297
Table V-1	Recovery of BSA (20 μ g/mL) after incubation for 30 minutes and 24 hours.	309
Table V-2	Recovery of protein after incubation of different concentrations of BSA (2 μ g/mL and 20 μ g/mL) for 30 minutes.	312
Table V-3	Recovery of protein after incubation of A β ₁₋₄₂ (5 μ g/mL) samples for 30 minutes.	313
Table V-4	Comparison of physical parameters for A β ₁₋₄₂ and BSA.	314
Table V-5	Limit of Detection and Limit of Quantitation for FAM-A β	330
Table V-6	GM1 plate coating variability.	331
Table V-7	GM1 Assay IC ₅₀ values for FAM-A β ₁₋₄₀ and FAM-A β ₁₋₄₂ of NCE-217, NCE-370 and NCE-371 in presence of Cu ²⁺ and Zn ²⁺	348
Table V-8	ThT assay and GM1 Assay IC ₅₀ values for three series of A β aggregation inhibitors.	352

List of Figures

Figure I-1	The clinical continuum of Alzheimer's Disease	3
Figure I-2	Progression of AD	4
Figure I-3	Typical changes in the AD brain	6
Figure I-4	Primary sequence of A β and schematic representation of APP processing.	11
Figure I-5	Secondary structure of A β	13
Figure I-6	Intermediates and equilibria in A β fibrillization.....	16
Figure I-7	The Amyloid Cascade Hypothesis.....	29
Figure I-8	Updated version of the Amyloid Cascade by Beckerman.	30
Figure I-9	Hypothetical model integrating immunohistology and dynamic biomarkers of the AD pathological cascade.	32
Figure II-1	Schematic of Gram-positive and Gram-negative bacterial cell walls.....	97
Figure II-2	Chemical structures of lipid A portion of lipopolysaccharide (LPS) and lipoteichoic acid (LTA).	99
Figure II-3	Examples of AMPs with different secondary structures.	103
Figure II-4	Amino acid sequence of A β ₁₋₄₂	104
Figure II-5	Distribution of charged and hydrophobic residues in α -helical AMPs.....	105
Figure II-6	Helical wheel of the N-terminal helix (A β ₈₋₂₅).	106
Figure II-7	The barrel-stave model of AMP-induced killing.	111
Figure II-8	The carpet model of AMP-induced killing.	111
Figure II-9	The torroidal pore model of AMP-induced killing.....	112
Figure II-10	The aggregate channel model of AMP-induced killing.....	113
Figure II-11	A β secondary structures containing a flexible “hinge” region between two α -helices.	115
Figure II-12	Schematic of experimental procedure for A β production by neuronal cells.....	117

Figure II-13	ELISA workflow	124
Figure II-14	Oligomeric A β ELISA principle.	125
Figure II-15	A β production by neuroblastoma cells induced by bacterial infection.	132
Figure II-16	ELISA of rodent A β	133
Figure II-17	Time series of A β production by neuroblastoma cells induced by incubation with LPS and LTA.	135
Figure II-18	Influence of A β_{1-40} on viability of <i>E.coli</i> assessed by the Radial Diffusion Assay.....	143
Figure II-19	Spread frequency in the Micro-gel Well Diffusion Assay.	145
Figure II-20	Influence of A β_{1-42} on the viability of <i>E. coli</i> determined by Micro-gel Well Diffusion Assay.	146
Figure II-21	Influence of A β_{1-42} on the viability of MRSA determined by Micro-gel Well Diffusion Assay.	147
Figure II-22	Idealised bacterial growth curve and growth phases.	148
Figure II-23	Typical growth curve of a bacterial culture.....	149
Figure II-24	Influence of different additives on bacterial growth.	150
Figure II-25	The bacterial Growth Curve Assay.	151
Figure II-26	Bacterial Growth Curve Assay –Slope _{max} and t _{onset}	152
Figure II-27	Growth Curve Assay results for incubation of <i>E. coli</i>	155
Figure II-28	Growth Curve Assay results for incubation of <i>S. marcescens</i>	156
Figure II-29	Growth Curve Assay results for incubation of <i>K. pneumoniae</i>	157
Figure II-30	Growth Curve Assay results for incubation of MRSA.	158
Figure II-31	Growth Curve Assay results for incubation of MSSA.	159
Figure II-32	Dilution series of A β_{1-40} to determine its activity against different bacterial strains.	162
Figure II-33	Dose-response curves and IC ₅₀ values for incubation of <i>E. coli</i> with A β_{1-42}	164

Figure II-34 Antibacterial activity of LL-37 against <i>E. coli</i>	166
Figure II-35 Effect of A β ₁₋₄₂ pretreatment on VSV-GFP.....	175
Figure II-36 Antiviral activity of A β ₁₋₄₂ against HSV-1-GFP.....	176
Figure II-37 MTT assay.....	184
Figure II-38 Toxicity of A β ₁₋₄₀ and A β ₁₋₄₂ against SK-N-AS neuroblastomas and primary rat neurons.....	186
Figure II-39 Primary sequences of known AMPs LL-37 and cecropin A.....	189
Figure II-40 Toxicity of AMPs against SK-N-AS neuroblastomas and primary rat neurons.....	190
Figure II-41 Caspase-3/-7 assay principle.....	197
Figure II-42 Apoptosis in differently treated SK-N-AS neuroblastoma cells.....	199
Figure II-43 A β production by SK-N-AS neuroblastoma cells in response to apoptosis and necrosis.....	200
Figure II-44 Simulated neuronal loss in AD.....	202
Figure II-45 A β production by SK-N-AS neuroblastoma cells induced by incubation with GM ₁ and GM ₁ /A β	204
Figure II-46 The Vicious Cycle of Alzheimer’s Disease.....	209
Figure III-1 Chemical structures of used antibiotics.....	245
Figure III-2 Resazurin and related compounds.....	248
Figure III-3 Bacterial toxicity of antibiotics.....	252
Figure III-4 A β production in SK-N-AS neuroblastoma cells induced by incubation with bacterial medium and fragments.....	253
Figure III-5 A β production in SK-N-AS neuroblastoma cells induced by incubation with fragments of bacteria killed by γ -irradiation or autoclaving.....	254
Figure III-6 A β production in SK-N-AS neuroblastoma cells induced by incubation with fragments of bacteria killed by different antibiotics.....	256
Figure III-7 Effect of antibiotic-treated MSSA on total protein production by SK-N-AS neuroblastoma cells.....	257

Figure III-8	A β production in SK-N-AS induced by incubation with <i>E. coli</i> fragments.	259
Figure III-9	A β production in SK-N-AS induced by incubation with MSSA fragments.	260
Figure IV-1	General reaction scheme of SPPS.....	267
Figure IV-2	The electromagnetic spectrum.	268
Figure IV-3	Electric and magnetic field components in microwaves.	270
Figure IV-4	Modelling of inverted temperature gradients in microwave versus normal in oil-bath heating.	273
Figure IV-5	Manual peptide cleavage filter.....	283
Figure IV-6	Pseudoproline dipeptides for difficult A $\beta_{1-40/42}$ synthesis.	288
Figure V-1	Recovery of BSA after incubation for 30 minutes and 24 hours.	310
Figure V-2	Recovery of protein after incubation of different concentrations of BSA (2 and 20 $\mu\text{g}/\text{mL}$) for 30 minutes.....	311
Figure V-3	Recovery of protein after incubation of A β_{1-42} (5 $\mu\text{g}/\text{mL}$) for 30 minutes.	313
Figure V-4	Chemical structures of Thioflavin T and Congo Red.....	317
Figure V-5	Chemical structure of monosialoganglioside GM1.	318
Figure V-6	Schematic of the GM1 Assay principle.	319
Figure V-7	Limit of Detection and Limit of Quantitation for FAM-A β	329
Figure V-8	GM1 plate coating variability.	331
Figure V-9	GM1 Assay plate washing study – experiment 1.	332
Figure V-10	GM1 Assay plate washing study – experiment 2.	334
Figure V-11	Sensitivity of the GM1 Assay - experiment 1 – supernatant.....	335
Figure V-12	Sensitivity of the GM1 Assay - experiment 1 – assay plate.....	337
Figure V-13	Sensitivity of the GM1 Assay - experiment 2 – assay plate.....	338
Figure V-14	Influence of Cu ²⁺ and Zn ²⁺ on GM1 – A β_{1-40} binding and aggregation.	340
Figure V-15	Influence of Cu ²⁺ and Zn ²⁺ on GM1 – A β_{1-42} binding and aggregation.	341

Figure V-16 Influence of Zn^{2+} on GM1 – $A\beta_{1-42}$ binding and aggregation.....	342
Figure V-17 Time dependence of zinc effect.	344
Figure V-18 Influence of metal ions and $A\beta$ antiaggregants on GM1-binding by FAM- $A\beta_{1-40}$	346
Figure V-19 Influence of metal ions and $A\beta$ antiaggregants on GM1-binding by FAM- $A\beta_{1-42}$	347
Figure V-20 Chemical structures of $A\beta$ aggregation inhibitors.....	349
Figure V-21 Dose-response curves for $A\beta$ aggregation inhibitors determined by GM1 Assay.....	351
Figure V-22 Experimental configurations for the PICUP assay and $[Ru(Bpy)_3]^{2+}$ absorbance spectrum.....	355
Figure V-23 The new PICUP LED Irradiator.	356
Figure V-24 Tris-Tricine SDS-PAGE gel of PICUP assay.....	357
Figure V-25 The PICUP Multiplex LED Irradiator.....	358

Abstract

Alzheimer's Disease (AD) is a chronic progressive neurological condition, clinically characterized by memory deficits, cognitive and physical impairment, and personality changes.

Traditionally, AD was considered a type of protein folding disorder. Here, the concept of AD as an autoimmune disease of the innate immune system was developed. After exploring evolutionary connections between the AD peptide β -amyloid ($A\beta$) and known antimicrobial peptides (AMPs), and elucidating the structural similarities between $A\beta$ and AMPs, a mechanism of action for $A\beta$'s antimicrobial activity is proposed that is based on the compromise of bacterial membranes. Following these theoretical considerations, experimental evidence is presented for the production of $A\beta$ by cells in response to infection, and for $A\beta$'s antibacterial and antiviral activity. Rooted in similarities of the cell membranes of neuronal and bacterial cells in terms of lipid composition and transmembrane potential, it is hypothesised that $A\beta$'s neurotoxicity is caused by its misguided attack on neurons as an AMP. In reversing the concept of $A\beta$ as an AMP, the similarity of AMPs to $A\beta$ is demonstrated in experiments revealing the neurotoxicity of two AMPs, LL-37, and cecropin A. To determine a mechanism for the progressive nature of AD, it was shown that, although apoptosis may be involved in AD, it is actually necrosis that is responsible for the propagation of neuronal cell death so characteristic of AD. With the *Vicious Cycle of AD*, a scheme was devised, integrating the results obtained here with data and research from other groups, which explains the chronic and progressive nature of AD as a result of $A\beta$'s physiological role as an AMP and innate immune system effector.

Borne from $A\beta$'s activity as an AMP and its central role in the *Vicious Cycle of AD*, a question was investigated: do antibiotics, such as penicillin, that cause release of bacterial endotoxins due to their mechanism of action, trigger the *Vicious Cycle of AD* and thus lead to the development of AD? Preliminary evidence supporting this notion was presented.

List of Abbreviations and Symbols Used

Abbreviations

A β	β -amyloid peptide
A β ₅₆ *	A β oligomer, 56 kDa
AChE	acetyl cholinesterase
ACP	acyl carrier protein
AD	Alzheimer's Disease
ADDLs	A β -derived diffusible ligands
ADP	adenosine diphosphate
AGEs	advanced glycation endproducts
AIF	apoptosis-inducing factor
AMC	7-amino-4-methylcoumarin
AMP	antimicrobial peptide
AMSDb	Antimicrobial Sequences Database
APD	Antimicrobial Peptides Databank
APS	ammonium persulfate
ApoE	apolipoprotein E
ApoJ	apolipoprotein J
APP	β -amyloid precursor protein
APP _S - α	soluble α ectodomain of APP
APP _S - β	soluble β ectodomain of APP
AT	antithrombin
ATCC	American Type Culture Collection
ATP	adenosine triphosphate
a.u.	arbitrary units
BBB	blood-brain barrier
<i>B. burgdorferi</i>	<i>Borrelia burgdorferi</i>
BCA	bicinchoninic acid
BI	Boman index
BMP	bone morphogenetic proteins
Boc	<i>tert</i> -butoxycarbonyl (an amino acid N-terminal and side chain protecting group)
C83	83 amino acid residue C-terminal fragment of APP
C99	99 amino acid residue C-terminal fragment of APP
Caspases	cysteine-dependent <u>aspartate-directed proteases</u>
CD	circular dichroism

CD14/36/etc.	cluster of differentiation 14/36/etc.
CDCs	cholesterol-dependent cytolysins
CE	capillary electrophoresis
CFU	colony-forming unit
chol.	cholesterol
CMV	cytomegalovirus
CNS	central nervous system
<i>C. neoformans</i>	<i>Cryptococcus neoformans</i>
CoA	certificate of analysis
<i>C. pneumoniae</i>	<i>Chlamydomphila pneumoniae</i>
CR	Congo Red
CSF	cerebrospinal fluid
CtxB-HRP	Cholera toxin subunit B, HRP conjugate
DAMPs	damage-associated molecular patterns
DBU	1,8-diazabicyclo-[5.4.0]undec-7-ene
DIEA	diisopropylethylamine
DMAP	<i>p</i> -dimethylaminopyridine
DMEM	Dulbecco/Vogt modified Eagle's minimal essential medium
EC ₅₀	50% effective concentration
<i>E. coli</i>	<i>Escherichia coli</i>
EEO	electroendoosmosis
ELISA	Enzyme-Linked Immunosorbent Assay
ER	endoplasmatic reticulum
ESI	electrospray ionization
5-/6-FAM	5-/6-carboxyfluorescein
FBS	fetal bovine serum
FDG	fluorodeoxyglucose
FGF	fibroblast growth factor
Fmoc	9-fluorenylmethoxycarbonyl (an amino acid N-terminal protecting group)
GAG	glycosaminoglycan
GCA	growth curve assay
GFP	green-fluorescent protein
GM1	monosialoganglioside 1
HATU	<i>O</i> -(7-azabenzotriazole-1-yl)- <i>N,N,N',N'</i> -tetramethylammonium hexafluorophosphate
HBSS	Hank's Balanced Salt Solution
HBTU	2-(1- <i>H</i> -benzotriazole-1-yl)-1,1,3,3-tetramethylammonium hexafluorophosphate

HF	hydrogen fluoride
HFIP	1,1,1,3,3,3-hexafluoroisopropanol
HHV 6	human herpes virus type 6
HMGB1	high mobility group box 1
HMPB	4-(4-hydroxymethyl-3-methoxyphenoxy)butyric acid
4-HNE	4-hydroxynonenal
HOBt	<i>N</i> -hydroxybenzotriazole
HPLC	high-pressure liquid chromatography
HRP	horseradish peroxidase
HSV 1	Herpes simplex virus type 1
<i>H. pylori</i>	<i>Helicobacter pylori</i>
IC ₅₀	50% inhibitory concentration
IDE	insulin-degrading enzyme
IR	infrared
ISM	microwave frequencies assigned for the use in industrial, scientific, and medical fields
kdo	keto-deoxyoctulosonate (= 3-deoxy-D-mannoctulosonic acid)
<i>K. pneumoniae</i>	<i>Klebsiella pneumoniae</i>
LANCL1	lanthionine synthase-like protein-1
LB	Luria-Bertoni
LBP	LPS-binding protein
LDL	low-density lipoprotein
LED	light-emitting diode
LoD	limit of detection
LoQ	limit of quantitation
LPS	lipopolysaccharide
LRP	lipoprotein receptor-related protein
LTA	lipoteichoic acid
LTP	long-term potentiation
MALDI	matrix-assisted laser desorption/ionization
M _{avg.}	average molecular mass
M _{mono}	monoisotopic mass
MβCD	methyl-β-cyclodextrin
MBHA resin	4-methylbenzhydramine
MCI	mild cognitive impairment
MD-2	myeloid differentiation-2
MeCN	acetonitrile
MEM	minimum essential medium

MeOH	methanol
MHIICA broth	Mueller Hinton II Cation Adjusted broth
MIC	minimum inhibitory concentration
MRI	magnetic resonance imaging
MRSA	methicillin-resistant <i>Staphylococcus aureus</i>
mRNA	messenger RNA
MS	mass spectrometry
MS ⁿ	tandem mass spectrometry with n (=multiple, unspecified #) stages
MSSA	methicillin-susceptible <i>Staphylococcus aureus</i>
mtDNA	mitochondrial DNA
MTT	3-(4,5-dimethylthiazol-2-yl)-2,5-diphenyltetrazolium bromide
MW	molecular weight
MWDA	Micro-Gel Well Diffusion Assay
NAD ⁺	nicotinamide adenine dinucleotide
NADH	nicotinamide adenine dinucleotide hydride
NADP ⁺	nicotinamide adenine dinucleotide phosphate
NADPH	nicotinamide adenine dinucleotide phosphate hydride
NCE	new chemical entity
n/d	not determined
NFT	neurofibrillary tangle
NF κB	nuclear factor κB
NGF	neuronal growth factor
NLRs	NOD-like receptors
NMDA	<i>N</i> -methyl-D-aspartate
NMP	<i>N,N</i> -dimethylpyrrolidone
NMR	nuclear-magnetic resonance
NOD	Nucleotide-binding oligomerization domain containing protein
OPA	<i>o</i> -phthaldialdehyde
OtBu	<i>tert</i> -butyl ester (an amino acid side chain protecting group)
p3	an APP fragment
<i>P. aeruginosa</i>	<i>Pseudomonas aeruginosa</i>
PAMPs	pathogen-associated molecular patterns
pbf	2,2,4,6,7-pentamethyldihydrobenzofuran-5-sulfonyl (an amino acid side chain protecting group)
PBS	phosphate-buffered saline
PC	phosphatidylcholine
PCD	programmed cell death (= apoptosis)
PCR	polymerase chain reaction

PDB	Protein Data Bank
PDB ID	Protein Data Bank identification number
PEG	polyethyleneglycol
PEGA	polyethyleneglycol-polyacrylamide
Pen-Strep	penicillin-streptomycin
PET	positron emission tomography
PHFs	paired-helical filaments
pI	isoelectric point
PICUP	photo-induced cross-coupling of unmodified proteins
PP	polypropylene
PPAR γ	Peroxisome proliferator-activated receptor γ
PRRs	pattern/pathogen recognition receptors
PS	phosphatidylserine
<i>PSEN1/2</i>	<i>Presenilin-1/-2</i> genes
PTFE	poly(tetrafluoroethylene)
PVDF	polyvinylidene fluoride
(Q)SAR	(quantitative) structure activity relationship
RAGE	receptor for advanced glycation endproducts
RDA	radial diffusion assay
Ref.	reference
RFU	relative fluorescence units
RIG I	retinoic acid-inducible gene 1
RLRs	RIG I-like receptors
RNA	ribonucleic acid
ROS	reactive oxygen species
RP-HPLC	reversed-phase high-pressure liquid chromatography
rRNA	ribosomal RNA
[Ru(bpy) ₃] ²⁺	tris(2,2'-bipyridyl) ruthenium(II)
<i>S. marcescens</i>	<i>Serratia marcescens</i>
SDS-PAGE	sodium dodecylsulfate-polyacrylamide gel electrophoresis
S.E.M.	standard error of the mean
SM	sphingomyelin
SPPS	solid-phase peptide synthesis
SRs	scavenger receptors
TBST	Tris-buffered saline with Tween-20
tBu	<i>tert</i> -butyl (an amino acid side chain protecting group)
TFA	trifluoroacetic acid
TFE	trifluoroethanol

TGF	transforming growth factors
ThT	thioflavin T
TIS	triisopropylsilane
TLRs	Toll-like receptors
TMB	3,3',5,5'-tetramethylbenzidine
TMD	transmembrane domain
TMP	trimethoprim
Tris	tris(hydroxymethyl)aminomethane)
tRNA	transfer RNA
Trt	Trityl (an amino acid side chain protecting group)
TSB	tryptone soy broth
UV	ultraviolet
Vis	visible light
VSV	vesicular stomatitis virus
Wnt	combination of 'Wingless' and 'INT' genes
YADAMP	Yet Another Database of Antimicrobial Peptides

Symbols

A	pre-exponential factor (in Arrhenius equation)
Da	Dalton
D_p	penetration depth (m)
e	Euler's constant (e = 2.718...)
e'	dielectric constant
e''	dielectric loss
E_a	activation energy (kJ/mol) (in Arrhenius equation)
$\Delta G_{\text{chx} \rightarrow \text{water}}$	solvation free energy for an amino acid side chain of n residues to transfer from cyclohexane (chx) to water
g	g-force
Hz	Hertz
Gy	gray: SI derived unit of absorbed dose of ionising radiation
IU	international units
k	rate constant
k	Boltzmann constant (= 1.38×10^{-23} J/K)
K_a	association binding constant
k_a, k_{a+1}, k_{a+n}	association rate constants
kDa	kilo-Dalton
λ	wavelength (m, cm, or nm)
λ_{max}	wavelength of maximum absorption/emission (nm)
M	molar concentration (mol/L)
$M_{\text{avg.}}$	average molecular mass (g/mol)
$M_{\text{mono.}}$	monoisotopic molecular mass (g/mol)
n	number of amino acid residues
n	frequency (s^{-1})
OD_x	optical density at wavelength x nm (absorbance units)
$OD_{12\text{h}}$	optical density after 12h incubation time (absorbance units)
ΔOD_{final}	difference between OD_{max} and the last OD_{595} value (absorbance units)
$OD_{\text{Slope}_{\text{max}}}$	optical density at $\text{Slope}_{\text{max}}$ (absorbance units)
OD_{max}	max. optical density (absorbance units)
p	pressure (hPa)
rpm	revolutions per minute
T	temperature (K)
$\text{Slope}_{\text{max}}$	max. slope during exponential phase (OD/min)
t_{2x}	doubling time in the exponential phase (min)
$\tan \delta$	loss tangent
Δt_{max}	difference between $t_{OD_{\text{max}}}$ and t_{onset} (min)

$t_{OD_{max}}$	time of OD_{max} (min)
t_{onset}	time of onset of exponential phase in bacterial growth (min)
$t_{Slope_{max}}$	time of $Slope_{max}$ (min)
u	mass-to-charge ratio (m/z)
v/v	concentration (volume / volume)
w/v	concentration (weight / volume)

Acknowledgements

First and foremost, I would like to thank my supervisor, Dr. Donald Weaver, for the opportunity to pursue a research project of this scope. I benefitted tremendously from his insight and discussions about the many different areas of research involved in this project. But not only professionally was he of great help, also privately in understanding the challenges of starting a family. The German term '*Doktorvater*' ('doctorate father') is probably a more appropriate term than just 'supervisor' for his role in this part of my life.

Without the constant support and encouragement of my wife, Vanessa, I would not have been able to complete this work. Our two children, Liam and Emma, were a source of joy and delight during this time.

I would like to thank my parents, Karlheinz and Brigitte, for their generosity — financially, and so many other ways. I cannot forget to thank my aunt, Ilse, for her financial support that allowed my move to Canada in the first place; and my in-laws for their kindness.

I would like to thank Yanfei Wang, for her help in the biochemical and cell culture aspects of this work; Dr. Mark Reed, Dr. Fan Wu, Dr. Erhu Lu, Dr. Scott Banfield, Gordon Simms, Dr. Chris Barden, and Dr. Autumn Meek, for discussions and insight about organic, analytical, and computational chemistry. Also mentioned should be help by Todd Galloway, Rose (Qiangwei) Chen, Dr. Robert Boudreau, Dr. Luzhe Pan, and Pam Gallant with some biochemical and cell culture work. Furthermore, I would like to thank Dr. Ryan Noyce for performing experiments related to the antiviral activity of A β ; Xiao Feng for performing the mass spectrometric analysis of my peptide samples; Jürgen Müller and Todd Carter for their great work and pieces of glassware art; Dr. Raphael Garduno, Department for Microbiology and Immunology, for his introduction to working with bacteria; Dr. William Wong, Treventis, for deeper insight into bacterial work; Dr. Peter Wentzell, for answers about statistical analysis; Laural Fisher, for help with the peptide crystallisation attempt; Kurt Stover, Department of Psychology, for help in the penicillin project; and Colin Brien, for practical assistance in the peptide binding study and the GM1 Assay.

I gratefully acknowledge financial support by Dalhousie University in form of the Vitamin Scholarship, as well as assistance by Giselle Andrews and Cheryl Weaver in administrative matters.

Finally, I would like to thank all my friends in the Weaver group, the Department of Chemistry, and outside of work for their support and encouragement throughout my degree.

CHAPTER I.

INTRODUCTION

1. Alzheimer's Disease

1.1. Background

Alzheimer's Disease (AD) is a progressive neurological disease, clinically characterized by memory deficits, cognitive and physical impairment, and personality changes. Alois Alzheimer first described the disease in 1906 in a presentation given to the *Assembly of Southwestern German Doctors for the Insane* in Tübingen, Germany, which he published the following year (1, 2). In this article, he described the two hallmarks of the disease, "plaques" and "tangles" that he found during the autopsy of the brain of a patient, which he had followed since 1901 intrigued by the symptoms of her dementia. The term *Alzheimer's Disease* was introduced in 1910 in the 8th edition of Emil Kraepelin's *Textbook of Psychiatry* (3).

For the next 50 years, AD was considered a "normal part of aging". In the 1960s, however, a link between the cognitive decline of a patient and the numbers of plaques and tangles was discovered (4, 5), leading pathologists to recognize AD as a disease rather than a natural event in the process of aging. In 1984, Glenner and Wong isolated a peptide from fibrils found in AD patients' brains they termed *cerebrovascular amyloid protein* (it would now be designated ' $A\beta_{1-24}$ ') (6). In the early 1990s, a genetic link to early-onset familial AD was found (7-9). As well,

inheritance of the $\epsilon 4$ allele of the apolipoprotein E (ApoE) was identified as a risk factor for the development of late-onset sporadic AD (10). In 1997, Aricept™ (donepezil) became available; the first drug to lessen the symptoms of mild to moderate AD in some individuals by enhancing the levels of a neurotransmitter. Four other drugs have been brought to market since — galantamine, rivastigmine, and tacrine, acting in the same manner; and memantine, acting as NMDA¹ receptor antagonist — to treat symptoms of the disease. The progression and ultimate outcome of the disease remains unaltered despite over 100 years of its recognized existence.

1.2. The Burden of AD

In their World Alzheimer Report 2009, Alzheimer Disease International estimated that in 2010, AD would affect about 35.6 million people over the age of 65 worldwide, with an associated total cost of about US-\$604 billion (11). The projected incidence for 2030 and 2050 was 65.7 million and 115.4 million people, respectively.

With 1 in 20 Canadians over age 65, and 1 in 4 Canadians over age 85 having AD, it is the most common form of dementia (12). Besides its devastating effects on the affected patients and their families, it also constitutes a major burden for the health care system. The total annual cost of AD in Canada (2000-2001) was estimated to be about \$1.43 billion, second only to stroke amongst the most common neurological conditions (13). In 2004-2005, over 56,000 patients diagnosed with AD as primary or secondary condition were hospitalized in an acute care facility, staying for an average (median) of 11 days (13). The number of acute care hospitalizations across Canada for patients with AD increased by 38 % between 2000-2001 and

¹ NMDA receptor: N-methyl-D-aspartate receptor

2004-2005 (13). For 2008, the Alzheimer Society of Canada has estimated a total national societal cost of 14.9 billion Canadian Dollars, arising from 481,000 people with dementia, with a predicted tenfold increase, to 153 billion over the thirty years to 2038 (14). Since the number of Canadians aged 65 and older is growing, these numbers and the related cost are expected to increase proportionally in the future.

1.3. Pathology, Pathophysiology and Risk Factors of AD

After over 100 years of research, the root of AD has still not been conclusively established. However, it seems that AD is caused not by a single factor, but rather is the result of multiple risk factors that collectively overpower the body's natural self-repair and self-healing mechanisms in the brain. The cognitive decline in dementia is different from that of "regular aging" in that it shows an earlier onset, faster decline and ultimately leads to death.

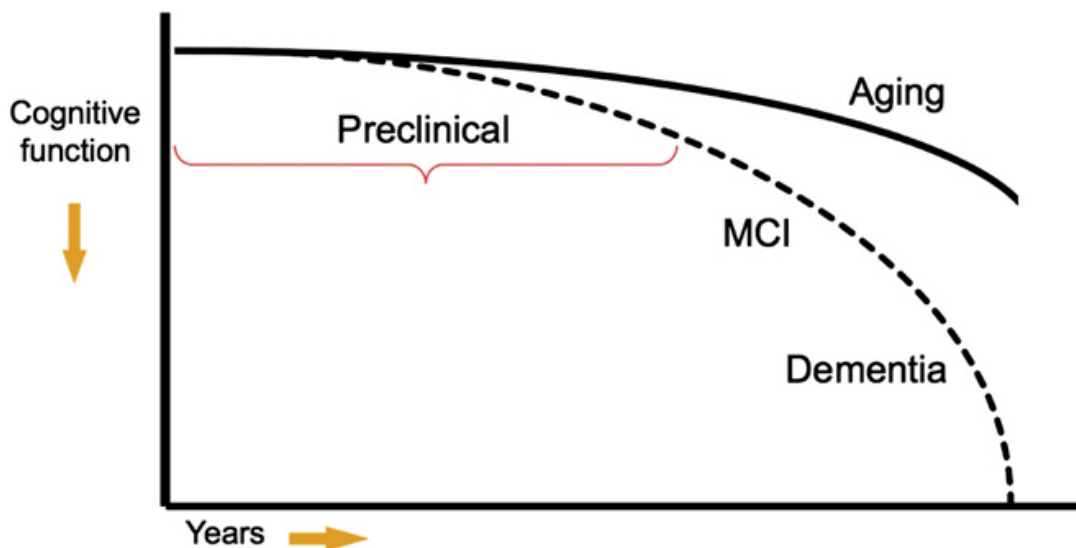


Figure I-1 The clinical continuum of Alzheimer's Disease

Hypothetical model for the pathological-clinical continuum of AD. AD begins in a asymptomatic, preclinical stage that precedes the development of mild cognitive impairment (MCI) and eventually dementia. The cognitive decline in AD is considerably steeper than in normal aging. Reprinted from Ref. (15) with permission from Elsevier.

It is also being recognized, that the clinical progression of AD can be described on a continuum, rather than occurring in distinct steps (Figure I-1) (15). AD begins in an asymptomatic, preclinical stage that can sometimes start over 20 years before the first occurrence of symptoms in the form of Mild Cognitive Impairment (MCI). MCI eventually develops into full dementia in a predictable pattern of functional loss (15). This predictable clinical pattern may become quite useful in identifying patients early enough in the disease to treat with available medications.

1.3.1. Pathology

AD shows a remarkably consistent pattern of affected brain regions as it progresses (16-25). Typically, it begins in the hippocampus where it impairs short-term memory formation. From there, it spreads to other limbic regions such as the amygdala and entorhinal cortex, and subsequently propagates to higher associative areas of the brain producing losses in memory, judgment and reasoning, and changes in behavior (Figure I-2).

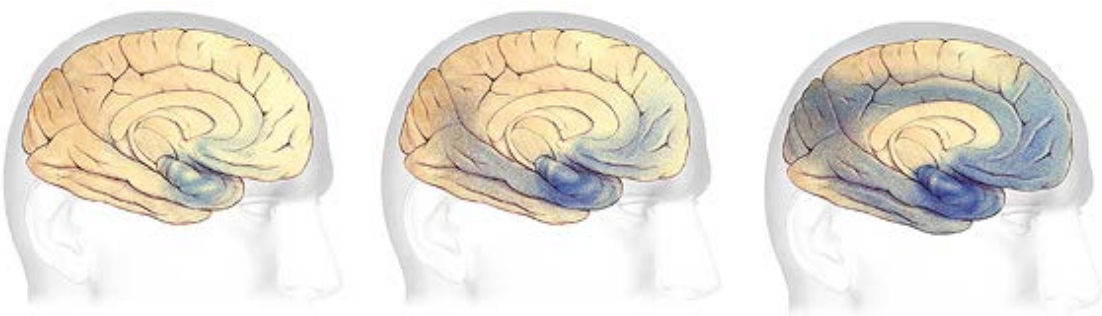


Figure I-2 Progression of AD

AD begins in the hippocampus where it impairs short-term memory formation. It spreads from the hippocampus to other limbic regions such as the amygdala and entorhinal cortex, and from these regions propagates to higher associative areas of the brain producing losses in memory, judgment and reasoning, and changes in behavior.

Reproduced and adapted with permission from: <http://www.alz.org/braintour/progression.asp> ; © 2013 Alzheimer's Association (www.alz.org). All rights reserved. Illustrations by Stacy Jannis.

Although great research efforts have gone into the development of tests and validation of biomarkers to detect AD in vivo, it can still not be diagnosed with absolute certainty solely based on the presentation of clinical symptoms. Therefore, the classical lesions have to be observable in *post mortem* analysis of microscopic sections of the hippocampus, amygdala, and the association cortices of the frontal, temporal, and parietal lobes to confirm a clinical diagnosis of AD (22, 26, 27).

1.3.2. Pathophysiology

The defining characteristic of AD is the accumulation of extracellular neuritic plaques in the brain, combined with the presence of intracellular neurofibrillary tangles (NFTs) in neuronal cells (22, 26). However, a range of other alterations occurring in AD brains and contributing to AD progression has been observed, as well. Those include synapse loss (28), decreased neurotransmitter levels (in particular acetylcholine) (29-31), neuron loss (32), formation of neuropil threads (33, 34), and dystrophic neurites (abnormal neuronal dendrites and axons) in association with A β plaques and NFTs (35-39). Other alterations of the cytoskeleton include a loss of microtubules in affected neurons (40-42), in addition to an alteration in normal microtubular architecture (43-45). As a result of these changes, in particular neuron and synapse loss, brain regions involved in learning and memory processes (including temporal and frontal lobes), are considerably reduced in size (Figure I-3). At gross examination, the Alzheimer's brain shows severe atrophy and a reduction in brain weight of usually more than 35 % (46).

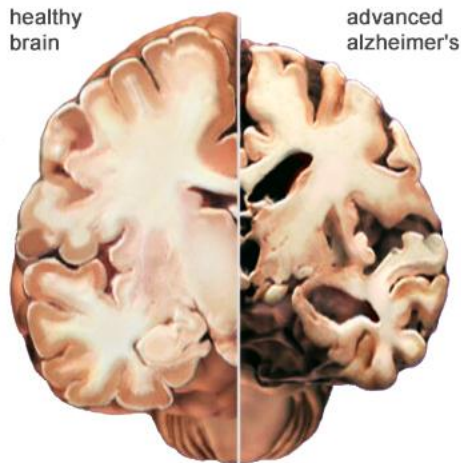


Figure I-3 Typical changes in the AD brain

At gross examination, the Alzheimer's Disease brain shows severe atrophy and a reduction in brain weight of usually more than 35 % (46).

Reproduced with permission from:

http://www.alz.org/braintour/healthy_vs_alzheimers.asp ; © 2013 Alzheimer's Association (www.alz.org). All rights reserved. Illustrations by Stacy Jannis.

1.3.3. Risk Factors

The major risk factors that have been identified so far are aging and genetic predisposition. The age of onset tends to be between 30-60 years of age; the genetic link appears to be present in 5-7 % of cases involving genes such as *APP*, *ApoE ε4*, *PSEN1*, and *PSEN2* (47). Other risk factors include diabetes, traumatic brain injury, stroke, hypercholesterolemia, hypertension, 'mild cognitive impairment' (MCI), Down's syndrome (Trisomy 21; *APP* is located on Chromosome 21), gender (women have 1.5x - 3x higher incidence linked to post-menopausal estrogen-deficiency), chronic inflammatory conditions, a history of episodes of clinical depression, stress, lack of physical exercise, inadequate exercising of the brain, unhealthy eating habits, obesity, low levels of formal education, and low socio-economic status (48, 49).

More recently, Rockwood and co-workers published findings that a suite of non-traditional risk factors such as a bone fracture or a not-fitting denture, combine to predict AD and dementia (50).

1.3.4. Processes and Factors Implicated in AD Pathophysiology

A large number of processes and factors have been implicated in AD (a non-exhaustive list is given in Table I-1), leading to the notion of AD as a multifactorial disorder rather than a single-cause disease. The ones most relevant for this thesis are described in greater detail in the next few paragraphs.

Table I-1 Processes and factors implied in AD pathophysiology

Process/Factor	Description ^a	References
Genetics	<p><i>APP</i> (some mutations cause increased production of Aβ₁₋₄₂); 33 mutations known</p> <p><i>PSEN1</i>, <i>PSEN2</i> (Presenilin-1 & -2 are the catalytic core of the γ-secretase complex; some mutations cause increased production of Aβ₁₋₄₂) (<i>PSEN1</i>: 185 & <i>PSEN2</i>: 13 mutations known)</p> <p><i>ApoE</i> ϵ4 (increases Aβ fibrillization; increases cholesterol in exofacial leaflet of synaptic plasma membrane; lipidation status influences Aβ metabolism)</p> <p>Down syndrome² (increased levels of Aβ due to third copy of chromosome 21)</p>	<p>(51-56)</p> <p>(51, 56-62)</p> <p>(63-74)</p> <p>(7, 75-78)</p>
Extracellular Aβ	<ul style="list-style-type: none"> - observed as oligomers and plaques - regulated via proteolysis by IDE - activates death receptors in cell lines - extracellular Aβ metabolism regulated by ApoE - may originate from excreted intracellular Aβ 	(51, 79-88)
Intracellular Aβ	<ul style="list-style-type: none"> - produced in ER and/or late Golgi compartments - causes synaptic dysfunction - causes mitochondrial toxicity - causes ER stress - causes neuroinflammation - increases tau phosphorylation - extracellular Aβ causes production of intracellular Aβ 	(61, 85, 89-110)

² Down syndrome is also known as trisomy 21, where three copies of chromosome 21 are present; the *APP* gene is located on this chromosome leading to its overexpression in Down syndrome patients.

Process/Factor	Description ^a	References
Reduced Aβ clearance	Receptor-mediated transport across BBB, e.g., RAGE, LRP, ApoE, ApoJ, PPAR γ Proteolysis by enzymes, e.g., neprilysin, IDE Microglia/astrocytes dysfunction Misfunction of aquaporin-4 water channel A β Autoantibodies	(111-116) (86, 117-121) (122, 123) (124) (125)
Hyper-phosphorylated Tau	<ul style="list-style-type: none"> - causes impaired axonal transport - leads to formation of PHFs & NFTs 	(126-134)
Metal Ions	<ul style="list-style-type: none"> - bind Aβ to produce ROS via Fenton(-like) chemistry and the Haber–Weiss reaction - Al³⁺ - Cu²⁺ - Fe³⁺ - Zn²⁺ 	(135-146) (147-153) (140, 154-164) (151, 165-170) (159, 169, 171-181)
Reactive Oxygen Species (ROS)	<ul style="list-style-type: none"> - cause oxidative stress - induce intracellular Aβ₁₋₄₂ production - cause oxidation of nucleic acids and proteins - cause peroxidation of lipids - activate microglia - modify tau phosphorylation 	(99, 136, 142, 153, 170, 182-190)
Cholesterol	<ul style="list-style-type: none"> - elevated levels increase Aβ production - controls interaction of Aβ with neuronal membranes (GM1) - Aβ disrupts cellular cholesterol homeostasis which induces tau phosphorylation - mitochondrial cholesterol exacerbates Aβ-induced inflammation and neurotoxicity 	(191-203)
Lipids	Membrane lipid composition determines A β aggregate assembly Lipid rafts involved in A β clearance by amyloid-degrading enzymes Lipid peroxidation: <ul style="list-style-type: none"> - inhibits NF-κB which induces expression of anti-apoptotic proteins - increases membrane rigidity - alters activity of membrane enzymes - alters membrane permeability 	(113, 204-228)
Calcium	<ul style="list-style-type: none"> - Aβ leads to disturbed calcium homeostasis by enhancing Ca²⁺ entry via channel activation or formation - increased intracellular Ca²⁺ enhances long-term depression leading to learning and memory deficits, and ultimately cell death by apoptosis 	(229-239)

Process/Factor	Description ^a	References
Mitochondria	<ul style="list-style-type: none"> - Aβ and tau impact mitochondrial respiration - Aβ inhibits key mitochondrial enzymes - Aβ may cause oxidative damage to mtDNA - Aβ causes impaired axonal transport of mitochondria in neurons 	(240-254)
Membranes	<ul style="list-style-type: none"> - interaction of Aβ with cell membranes stimulates its own production - Aβ interacts with a number of membrane components, e.g., cholesterol, fatty acids 	(255-259)
Glial cells (e.g., astrocytes, microglia)	<ul style="list-style-type: none"> - activated astrocytes and microglial found in AD brains in/around plaques - activated astrocytes degrade plaques and accumulate neuron-derived Aβ, but their lysis results in astrocytic amyloid plaques - microglia facilitate conversion of soluble and oligomeric Aβ into fibrils 	(46, 260-280)
Bacterial infection	- bacteria implicated in AD: <i>C. pneumoniae</i> , <i>B. burgdorferi</i> , <i>H. pylori</i> , <i>C. neoformans</i> ,	(281-287)
Viral infection	<ul style="list-style-type: none"> - viral DNA found in the core of senile plaques - viruses implicated in AD: HSV-1, HHV-6, CMV 	(285, 288-294)
Estrogen	Reduced estrogen levels increase risk for AD	(295-299)
Synapses	<ul style="list-style-type: none"> - Aβ impairs LTP (→ memory formation) - Aβ causes aberrations in synapse composition, shape, and density - hyperphosphorylated tau impairs axonal transport → starvation of synapses 	(28, 300, 301, 301-316)
Inflammation	<ul style="list-style-type: none"> - always found in AD brains - LPS-induced neuroinflammation causes increase in intracellular APP and Aβ - intracellular Aβ causes neuroinflammation 	(101, 317-321)
Apoptosis	<p>Apoptosis marker levels are elevated in AD brains</p> <p>Aβ levels elevated in apoptotic neurons</p> <p>Aβ causes neuronal apoptosis</p> <p>Cleavage of APP by caspases³ produces Aβ</p>	(99, 186, 322-333)
Necrosis	Aβ ₂₅₋₃₅ (20 μM) caused cell death in vitro with features consistent with necrosis, but not apoptosis	(334)

^a Acronyms: ApoE/J: Apolipoprotein E/J; APP: Amyloid-β precursor protein; BBB: Blood-brain barrier; mtDNA: mitochondrial DNA; *B. burgdorferi*: *Borrelia burgdorferi*; CMV: cytomegalovirus; *C. neoformans*: *Cryptococcus neoformans*; *C. pneumoniae*: *Chlamydomphila pneumoniae*; ER: endoplasmic reticulum; GM1: monosialoganglioside 1; HHV-6: human herpes virus type 6; HSV-1: Herpes simplex virus type 1; *H. pylori*: *Helicobacter pylori*; IDE: Insulin-degrading enzyme; LRP: Lipoprotein receptor-related protein; LTP: long-term potentiation; NF-κB: nuclear factor κB; NFTs: neurofibrillary tangles; PHFs: paired-helical filaments; PSEN1/2: Presenilin-1/-2; PPAR γ: Peroxisome proliferator-activated receptor γ; RAGE: receptor for advanced glycation end-products; ROS: reactive oxygen species.

³ Caspases (cysteine-dependent aspartate-directed proteases) are key enzymes in the apoptotic (cell death) cascade in cells

1.3.5. β -Amyloid ($A\beta$)

The majority of researchers in the field consider the $A\beta$ peptide to be the key component implicated in AD. Accordingly, extensive research has been conducted into its physiological generation, structure, aggregation, toxic species, and localization within the brain, which will be summarized in this section.

1.3.5.1. APP Processing and β -Amyloid Generation

$A\beta$ is derived from a much larger protein — β -amyloid precursor protein (APP). This protein is a transmembrane glycoprotein with a single transmembrane region, a large extracellular domain, and a short cytoplasmic tail (Figure I-4) suggesting a function as cell surface receptor (335). So far, eight differently spliced isoforms containing 695 to 770 amino acid residues have been identified (336, 337). APP is ubiquitously expressed in vertebrates (338), where expression levels depend on the developmental and physiological state of the cells; APP695 is the main transcript in neuronal cells (339, 340). Very high levels have been observed in the brain, where it constitutes 0.2% of the total mRNA in neurons (341). Its physiological functions are not fully understood yet; however, APP has been implicated in neuronal survival (342), neurite outgrowth and synaptogenesis (343), cell adhesion (344), inhibition of coagulation factors (345-347), inhibition of platelet activation (348), and modulation of copper homeostasis (349).

The $A\beta$ region of APP includes the 28 residues just outside the single transmembrane domain (TMD), plus the first 11–14 residues of that buried domain. Three enzymes can act upon APP to produce different fragments: α -, β - and γ -secretase (Figure I-4) (51, 350). Most commonly, APP is cleaved initially by the enzyme α -secretase to release the N-terminal (soluble)

APP_S-α from the 83 amino acid residue C-terminal fragment (C83). Subsequent cleavage within the transmembrane domain by γ-secretase yields the p3 fragment. Alternatively, APP can be first cleaved by β-secretase to produce the N-terminal (soluble) APP_S-β fragment, leaving a 99 amino acid residue C-terminal fragment (C99) behind, followed by γ-secretase cleavage which results in the formation of (mostly) Aβ₁₋₄₀ or Aβ₁₋₄₂. Aβ₁₋₄₀, being the most common isoform, is typically produced in the endoplasmic reticulum, while Aβ₁₋₄₂ is produced in the trans-Golgi network (90, 351). Cleavage of APP by the more common first pathway precludes the formation of Aβ.

A β-Amyloid(1-42) primary sequence:

Asp-Ala-Glu-Phe-Arg-His-Asp-Ser-Gly-Tyr - Glu-Val-His-His-Gln-Lys-Leu-Val-Phe-Phe-Ala-Glu-Asp-Val-Gly-Ser-Asn-Lys-Gly-Ala - Ile-Ile-Gly-Leu-Met-Val-Gly-Gly-Val-Val - Ile-Ala
 DAEFRHDSGY¹⁰ EVHHQKLVFF²⁰ AEDVGSNKG³⁰ IIGLMVGGVV⁴⁰ IA

B

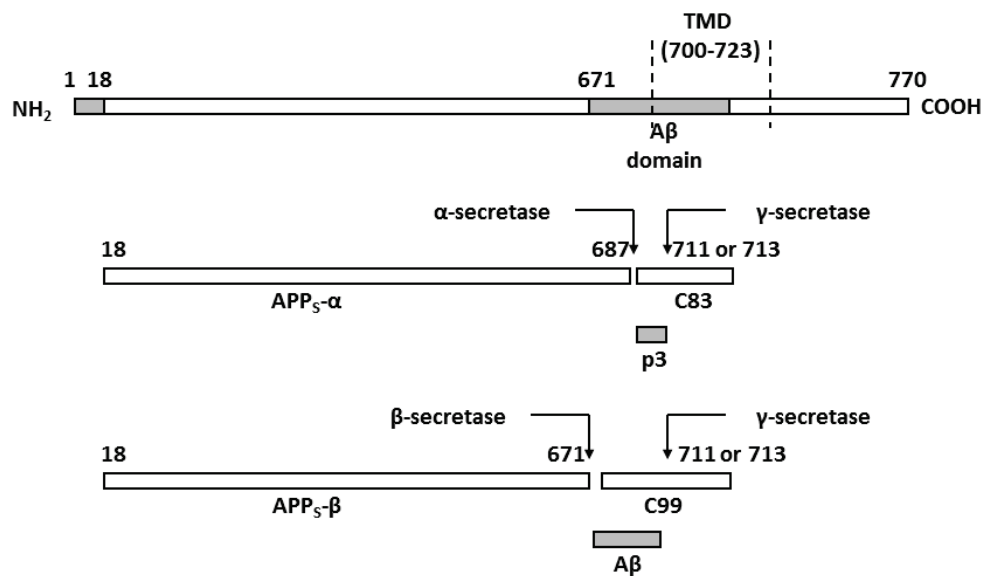


Figure I-4 Primary sequence of Aβ and schematic representation of APP processing.

A: Primary sequence of Aβ; three- and one-letter code. **B:** Top: Largest known splice variant of APP, containing a signal peptide (residues 1–17), and a single transmembrane domain (TMD) (residues 700–723). Middle: Constitutive α-secretase-mediated proteolytic cleavage of APP occurs after residue 687, yielding APPS-α (soluble ectodomain of APP) and the C83 fragment. Bottom: β-secretase mediated cleavage occurs after residue 671, yielding APPS-β (soluble ectodomain of APP) and C99. γ-secretase cleavage at position 711 or 713 releases the p3 peptide from C83 and Aβ₁₋₄₀/Aβ₁₋₄₂ from C99. Numbers represent amino acid positions; arrows indicate sites of secretase cleavages.

A β is found in healthy individuals in low nanomolar concentrations (CSF concentration 700-860 pg/mL) (352), and Bateman *et al.* demonstrated that A β has high synthesis and clearance rates (353). However, its physiological role is currently still not entirely clear. A few authors suggested a role as antioxidant (354, 355), others proposed its role as sealant of the vasculature in the cases of injury (356), and VC Meier-Stephenson has proposed its role as an antimicrobial peptide (AMP) of the innate immune system in the brain (357). Recently, Soscia *et al.* further provided experimental evidence of A β acting as an AMP (358).

1.3.5.2. Posttranslational Modifications of β -Amyloid

A β_{1-42} obtained from brain tissue of AD-inflicted individuals has been found to be surprisingly resistant to proteolysis (359). This stability has been related to the presence of posttranslational modifications, such as D-amino acids and isopeptide bonds (360-362), as well as nonenzymatic glycation modifications (363-365). Besides these modifications of single A β_{1-42} molecules, crosslinked A β species have also been found. Crosslinking may be induced by a number of molecules, e.g., Cu²⁺, aldehydes, or advanced glycation endproducts (AGEs). Cu²⁺ has been demonstrated to cause formation of dimers and trimers through crosslinking at Tyr-10 (366, 367). Aldehydes are well-known to crosslink proteins, a reaction utilised in the fixation of tissue samples with formaldehyde or glutaraldehyde. Endogenous aldehydes like formaldehyde, methylglyoxal, malondialdehyde, and 4-hydroxynonenal (4-HNE) have been found to enhance the rate of formation of β -sheets, oligomers and protofibrils in A β , and increase the size of its aggregates (368). Crosslinking of A β by advanced glycation endproducts (AGEs) proceeds through Maillard-type reactions of A β with reducing sugars (369).

Modifications of A β ₁₋₄₀, on the other hand, has been found to occur to a much lesser degree, thus allowing formation of a steady-state equilibrium between production and degradation (361, 362).

1.3.5.3. Secondary/Tertiary Structure of β -Amyloid

Upon cleavage from APP, A β initially exists in a random coil conformation before entering equilibrium with its α -helical and β -sheet conformations. The α -helical and random coil conformations are both soluble, non-toxic forms of the peptide. In fact, some results seem to suggest that in one or both of these conformations, A β may actually act as a neuroprotectant (370-372). However, when the equilibrium shifts to the β -sheet conformation, the A β monomers become insoluble (373), aggregate and subsequently precipitate as plaques (374).

A number of factors have been found to influence the secondary structure of A β (Figure I-5), e.g., pH, temperature and solvent variance, as well as the length of the A β fragment (375, 376).



Figure I-5 Secondary structure of A β .

The secondary structure of A β in a solvent mimicking conditions found in and around membranes (80 % HFIP, 20 % water) obtained by solution NMR. PDB ID: 1IYT (377)

In 1998, Giulian *et al.* suggested that the H₁₃H₁₄Q₁₅K₁₆ tetrapeptide domain within A β provided a structural basis for the immunopathology of AD, noting that A β ₁₃₋₁₆ was necessary for initial A β aggregation and subsequent microglial activation through a cell surface mechanism mediated by heparan sulfate proteoglycans (378). A study by Zagorski *et al.* involving A β ₁₋₂₈ at pH 4.0 showed that the α -helix of residues 13-20 (HHQKLVFF) would unfold at elevated temperature (379). The suggested mechanism proposed that deprotonation of residues Asp7, Glu11, Glu22, Asp23 in conjunction with protonation of residues His6, His13, and His14, destabilizes the α -helical structure (379). Furthermore, Tjernberg *et al.* identified in their deletion and substitution studies residues 14-23 (HQKLVFFAED) as the smallest region of A β capable to generate fibrils (380). Fraser *et al.* found in their studies comparing different A β fragments that fibrillogenesis depended on both electrostatic interactions involving His13 and Asp23 and hydrophobic interactions of residues 17-21 (381).

1.3.5.4. Oligomerization and Fibrillogenesis

The formation of plaques is a very complex process and the exact mechanism has eluded researchers so far. However, a growing number of studies give some insight into this process. As mentioned earlier, it is generally believed that a conformational change of A β monomers from a random coil or α -helical form to a β -sheet conformation initiates the process of amyloidogenesis. Numerous aggregates, on- and off-pathway to the fibrillization of A β have been identified so far, and it seems that sometimes different terms are used by different authors for very similar or maybe even the same species. The most commonly mentioned intermediates are summarized in Table I-2.

Table I-2 Intermediates in the pathway of A β fibrillization.

Data compiled from Refs. (382-384))

Aβ species	Characteristic	References
Monomers	soluble amphipathic molecule; generated from APP; potential α -helical, random coil or β -sheet conformation	(385-389)
Dimers	intracellular localization in vivo, in human brain extracts and in vitro; hydrophobic core; diameter of about 35 nm	(92, 390-394)
Trimers	observed in vivo in mouse models; potential key role as subunit of toxic oligomers	(395-397)
Small oligomers	observed in vivo in AD patients as well as in mouse models and in vitro; heteromorphous; comprising of 3 - 50 monomers; mostly transient and unstable, but toxic	(83-85, 395, 398-401)
Globular oligomers	observed in vitro; 5 nm diameter, dimers - pentamers	(402-406)
Annular oligomers	observed in cell culture and in vitro experiments; potential role as membrane-disrupting pores or ion channels	(407-409)
ADDLs	observed in murine and human brain extracts as well as in vitro; nonfibrillar; neurotoxic; 17-42 kDa; trimers to 24-mers	(402, 410-414)
Aβ₅₆*	observed in APP-transgenic mouse brain extracts; 56 kDa; causes impairment of spatial memory	(395)
Protofibrils	observed in vitro; short, flexible, rod-like structure; diameter 4 – 11 nm, length 20 - 200 nm; binding Congo red and thioflavin T; precursor of mature fibrils; toxic	(256, 405, 412, 415-423)
Fibrils	observed in AD patients as well as in mouse models and in vitro; bind Congo red and thioflavin T; stable; diameter 7 – 12 nm, three to six laterally associated filaments, characteristic cross- β -sheet structure that comprises an array of β -sheets propagating into a helical-twisted fibril with the β -strand perpendicular to the long axis of the fibril	(424-432)
Plaques	observed in vivo in AD patients as well as in mouse models; large extracellular A β deposits; predominantly composed of fibrils; not toxic; surrounded by dystrophic dendrites, axons, activated microglia and reactive astrocytes	(385, 433-435)
Diffuse plaques	observed in vivo in AD brains; contain mostly A β ₁₋₄₂	(43, 436-438)

Acronyms: A β ₅₆*: A β oligomer, 56 kDa; ADDLs: A β -derived diffusible ligands

The formation of these many intermediates are due to a corresponding number of equilibria, which are highly dependent on the experimental conditions, e.g., A β species, A β concentration, solvent, pH, and presence of metal ions, other proteins, lipids, interfaces and salts. A schematic of these intermediates and their equilibria is shown in Figure I-6.

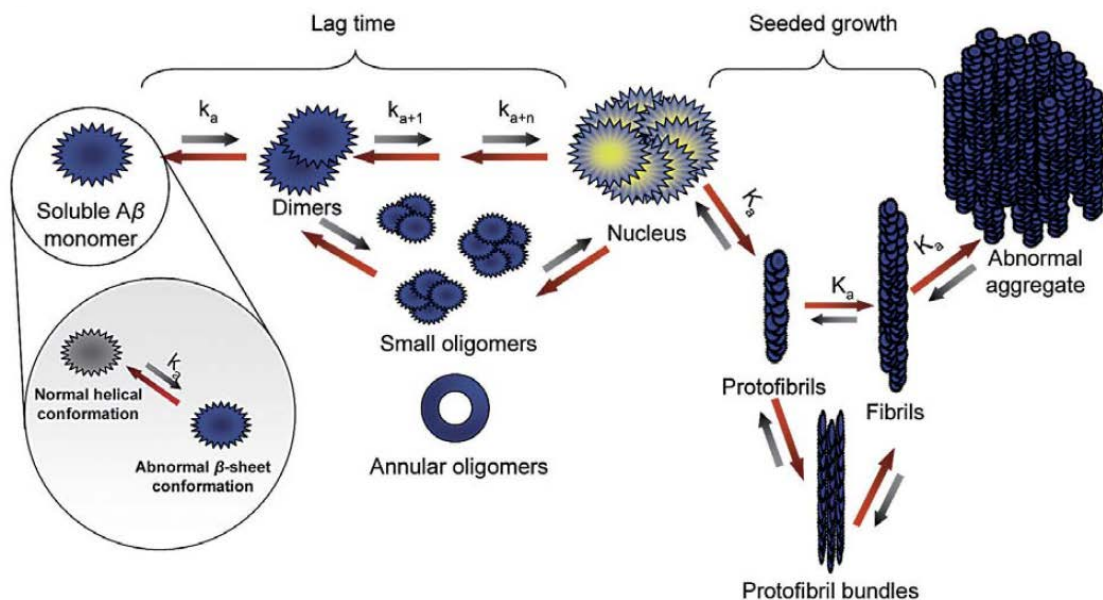


Figure I-6 Intermediates and equilibria in A β fibrillization.

This schematic shows some of the pathways suggested to be involved in the fibrillization of A β . A β normally exists in α -helical form; upon adoption of a β -sheet conformation and after a lag time, dimers, trimers and other small oligomers are formed, which eventually form the nuclei for the fibrillization of A β . Small globular and annular oligomers are proposed to be the actual toxic species of A β ; there is still debate about whether they are on-pathway intermediates for the formation of fibrils or if they form their own pathway (439, 440).

Reproduced with permission from Ref. (382); © by S. Karger AG, Basel.

A number of models have been developed to describe the fibrillization of A β ; the two most common are the *nucleation-dependent polymerization model* and the *template assembly model*.

The nucleation-dependent polymerization model (415, 441-444) postulates that amyloid fibril formation starts with the assembly of monomers into a “nucleus”, a process that is both thermodynamically and kinetically unfavorable (445, 446), and therefore the rate-limiting step. Once the nucleus is formed, it acts as a seed for exponential fibril growth by irreversibly adding more monomers. Naiki and Nakakuki found that the extension of A β_{1-40} fibrils in vitro can be described by a first-order kinetic model in which monomeric A β molecules attach consecutively

to the ends of pre-existing fibrils (447). Morinaga *et al.* found interfaces and agitation to play a critical role at low A β concentration for the nucleation of A β amyloid fibrils (448).

The template assembly model proposes that fibril elongation occurs via reversible addition of a soluble monomer to a pre-existing fibril; subsequently, the monomer conformation changes to an aggregation-competent state resulting in the irreversible association onto the end of the fibril (449, 450). Hasegawa *et al.* confirmed a first order mechanism for both the association of A β monomers onto and dissociation from the ends of existing fibrils (451).

The question of whether A β oligomers are on-pathway to the formation of fibrils is still debated, as they have been found to be not obligate for fibril formation (439, 440)

(a) Influence of A β species and concentration

The propensity for A β to aggregate is dependent on the species of A β involved, as well the concentration. Jarrett *et al.* established that A β_{1-42} has a considerably higher aggregation propensity than A β_{1-40} (452). This finding was reliably reproduced by other groups (83, 453). In a later study, Bitan *et al.* showed that A β_{1-40} and A β_{1-42} oligomerize through distinct pathways, with A β_{1-42} generally forming larger oligomers and involving several distinct transient structures that gradually rearranged into protofibrils (400).

With regards to concentration, using A β_{1-40} , Huang *et al.* showed that higher concentrations of the peptide would lead to a β -structured aggregate, whereas a lower concentration tended to form a more unstructured, unfolded aggregate. The critical concentration separating these two pathways was 10 μ M (454).

Since multiple different species of A β had been found in plaques, Hasegawa *et al.* studied in detail the peptide interactions when the two major forms of A β , A β_{1-40} and A β_{1-42} , are present in vitro. They looked at the fibrillization using pre-formed fibrils of both species to act as

“seeds”, and fresh, unaggregated A β (453). In their experiments, they found that the morphology of fibrillar A β formed is governed by the major component of fresh A β peptide in the reaction mixture, not by the morphology of pre-existing fibrils. Furthermore, they describe an inhibitory interaction between A β_{1-42} and A β_{1-40} that occurs during the nucleation phase, slowing fibril formation considerably. They attribute this to a minor difference in the conformation between A β_{1-42} and A β_{1-40} . Yan and Wang confirmed via NMR experiments that A β_{1-40} inhibited A β_{1-42} monomers from aggregating in an A β_{1-42} /A β_{1-40} ratio-dependent manner (455). They attributed this to the higher affinity for A β_{1-42} aggregates of A β_{1-40} monomers compared to A β_{1-42} monomers. Addition of A β_{1-40} to A β_{1-42} aggregates even resulted in the release of A β_{1-42} monomers.

(b) Influence of pH

Wood *et al.* showed that A β_{1-40} formed aggregates within minutes at a pH range of 5 – 6, whereas at pH 7.4, physiologic pH, hours or days were needed to complete fibrillization (456). They attributed the rapid aggregation of A β to relatively non-specific interactions between highly hydrophobic, neutral molecules that are present in the pH range of 5 – 6, close to the calculated isoelectric point of A β of 5.5. Klug *et al.* observed that A β aggregates formed by slow aging at physiologic pH were more cytotoxic than those formed at pH 5.0 (457).

(c) Influence of Metal Ions

Since a number of metal ions were found in AD plaques (169), metal binding of A β had been the focus of a number of research groups. Bush and co-workers found that Zn²⁺, Cu²⁺, and Fe³⁺ induce aggregation (174), in particular in slightly acidic conditions (163). Tougu *et al.*

showed that Zn^{2+} and Cu^{2+} prevent fibrillization while forming non-fibrillar $A\beta_{1-42}$ aggregates (171), although upon longer incubation (7 d) some conversion to fibrils was seen; a finding supported by others (157, 158, 458). Bolognin *et al.* found that aluminum and iron induce formation of annular protofibrils and fibrillar oligomers, whereas copper and zinc completely prevented the formation of soluble fibrillary aggregates (149). The interaction of $A\beta$ with metal ions will be discussed in more detail in Section 1.4.1. below.

(d) Influence of Cell Membrane Components

Lipids, as major constituents of cell membranes involved in a myriad of physiological processes, have naturally found attention as an interaction partner for $A\beta$. There is a large amount of literature for the involvement of gangliosides, in particular the monosialoganglioside GM1, and cholesterol in the aggregation of $A\beta$.

$A\beta$ has been shown to bind to GM1 in the brains of AD patients (459, 460) and that through this specific binding, the process of amyloid fibril formation is accelerated (460-463). Recently, Ikeda *et al.* (464) suggested a mechanism of $A\beta$ aggregation mediated by GM1 clusters on raft-like lipid bilayers composed of GM1, cholesterol, and sphingomyelin, where, depending on the $A\beta$ /GM1 ratio, $A\beta$ will assume different secondary structures. Subsequently, Fukunaga *et al.* showed that GM1 clusters mediate the formation of toxic $A\beta$ fibrils by providing a hydrophobic environment (465). Interestingly, GM1 was detected only on the surface of native and nerve growth factor (NGF)-treated PC12 cells (466), an important finding for the evaluation of experimental results obtained from differentiated cells. The interaction of $A\beta$ with GM1 will be discussed in more detail in Chapter V.

1.3.5.5. Plaques

Amyloid plaques are one of the hallmarks of Alzheimer's disease (1). These plaques comprise mainly of varying lengths of A β , with A β ₁₋₄₂ being the main alloform (78, 467-469). They form large insoluble aggregates, which are surrounded by dystrophic neurites, and activated glial cells (the neurons' supportive cells) (35, 37-39, 272, 470-472). Glial cells maintain brain plasticity and protect it from injury. Damage to or dysfunction of these cells may promote neurodegeneration, leading to impaired signalling in the brain (46).

The plaques are typically described as either "fibrillar" plaques (more defined), or diffuse plaques (amorphous or non-fibrillar) (43, 473, 474). Different conformations of A β were detected in these different types of plaques (475), and while some researchers argue the plaques develop by independent mechanisms (476), others argue that there is a morphologic continuum (477).

The plaques, once formed, are extraordinarily stable against resolubilization. Post-translational modifications, such as N-terminal degradation, isomerization, racemization, pyroglutamylation, oxidation, and covalently linked dimers are all thought to play a role in their increased stability (478)

While A β is the major component of the amyloid deposits, other molecules are also associated with or found in these deposits, for example, ferritin, components of the complement pathway, caspase-6, α 1-antichymotrypsin, α 2-macroglobulin, LDL-receptor related proteins, APP, cholesterol, acetylcholinesterase, laminin, glycosaminoglycans, and apolipoproteins E and J (70, 266, 326, 479-482).

1.3.5.6. Intracellular β -Amyloid

Initially, A β was considered solely an extracellular peptide (78, 483, 484). More recently, A β accumulation was also observed intracellularly in AD brains (103, 107, 109, 110, 437, 485-488), in AD mouse models (97, 98, 108, 110, 489) and in cultured neurons and neuronal cell lines (61, 90, 92, 102, 104, 339, 490-492), as well as in other brain cells, such as glial cells (493-495). Intracellular A β accumulation occurs early, before any signs of senile plaques or NFTs are detectable (97, 98, 108, 486, 496-499), and is now considered a key event in the development of synaptic and neuronal dysfunction (94, 98, 107, 500-502) and neuronal cell death (105, 110, 332, 333, 503). A β_{1-40} and A β_{1-42} are produced intracellularly in neurons at different sites (90) and γ -secretase specificity differs for intracellular vs. excreted A β leading to different A β_{1-42} /A β_{1-40} ratios for these two different A β pools (89). Depending on the cell line used in the experiments, A β was found to be cleaved off the APP in the endoplasmic reticulum (ER) (90, 504), the trans-Golgi network (351, 491, 505), or the endosomal-lysosomal system (506), however others found external A β being internalized (488, 507-509). Interestingly, Yang *et al.* as well as other groups found that application of extracellular A β_{1-42} induced the production of intracellular A β_{n-42} (104, 501, 510, 511).

Several molecular and cellular mechanisms, including tau hyperphosphorylation that leads to alterations in axonal structure and transport (94, 502, 512-515), ER stress and mitochondrial toxicity causing apoptosis, and inflammation are implied in the neurotoxicity of intracellular A β and its role in synaptic dysfunction (93, 94, 96, 98, 99, 105, 241, 242, 248, 516).

1.3.5.7. Toxic Species of β -Amyloid

Toxic actions of A β that have been observed include effects on membrane transport of ions, modification of ion channels, enhancement of calcium ion influx and glutamate toxicity,

generation of reactive oxygen species (ROS), activation of inflammatory responses and apoptotic pathways, and modification of signaling pathways, transcription, and interactions with cholesterol and lipoprotein transport (517).

Recent findings have cast doubt on the long-held belief that the neuritic plaques themselves are the toxic A β species (83, 96, 410, 518). Instead of a primary cause, the neuritic plaques may merely be the aftermath of neuronal destruction. Pre-fibrillar structures (including activated monomers) (519), small oligomers (400, 411, 418) and protofibrils (416, 418, 421) have been suggested to be the key neurotoxic effectors in AD, with small oligomers being the favoured candidate most recently (83, 410, 520). Oligomers significantly inhibit neuronal viability at 10 nM and are 10 times more potent than fibrils and about 40 times more potent than unaggregated peptide (520). However, another research group showed that A β fibrils form specifically on GM1 clusters and exhibit neurotoxic properties (521).

An issue with all these studies is that they rarely perform experiments with equivalent concentrations of A β oligomers and plaques to allow for a true comparison of their respective toxicities.

1.3.6. Neurofibrillary Tangles (NFTs)

Neurofibrillary tangles (NFTs), the other pathological feature of AD, are intraneuronal bundles of paired helical filaments composed of hyperphosphorylated tau protein (126, 127, 522). Tau (523, 524) is a widely expressed normal constituent of cellular microtubules chiefly maintaining their stability (525, 526). Besides providing stability to the cell, microtubules also function as the tracks for axonal transport of chemicals and small cell organelles (527, 528). Hyperphosphorylation as in AD causes tau to lose its ability to bind microtubules (128, 131, 529)

leading to cytoskeletal degeneration, neuronal dystrophy and ultimately cell death (129, 530-535).

NFTs are not specific to AD and are also found in a variety of other neurodegenerative conditions such as frontotemporal dementia, subacute sclerosing panencephalitis, Hallervorden-Spatz disease, Parkinson dementia complex, and dementia pugilistica (*boxer's dementia*) (536, 537).

1.3.7. Inflammation

It is now well recognized that AD also includes an inflammatory component. This notion is based on epidemiological findings showing a reduced prevalence of the disease upon long-term medication with anti-inflammatory drugs (538). As well, an increasing number of studies have provided evidence suggesting that A β deposition and NFT can activate an innate immune response triggered by an accumulation of activated glial cells, particularly microglia and astrocytes, in the same areas as the amyloid plaques (539, 540). Normally, glial cells maintain brain plasticity and protect the brain from injuries. Once activated, however, glial cells produce proinflammatory factors such as cytokines and chemokines, and activate the complement cascade presumably leading to a potentially pathological reaction in AD brains. This reaction may include neurodegeneration and the retraction of neuronal synapses, giving rise to cognitive deficits. The mechanism of inflammation by the body's innate immune response is based on the detection of different ligands that are not self-initiated and expresses highly conserved pattern recognition receptors (PRRs) to facilitate the clearance of debris. Among these highly conserved receptors, the most abundant factors that express on glial cells are the complement receptors (541, 542), Toll-like receptors (TLRs), and scavenger receptors (SR) (543-545). The innate immune system's response apparently also triggers the production of antibodies that recognize

human senile plaques in the central nervous system (CNS), which can be found in serum and CSF samples of AD patients (546, 547).

1.4. Interaction of β -Amyloid with Endogenous Molecules and the Importance of the 'HHQK' Region

Since A β at physiological pH contains multiple charged residues, it interacts not only with other A β peptides (to form oligomers), but also with a multitude of other endogenous molecules, amongst others, metal cations and cell membrane components. Comparing these interactions, it turns out that the HHQK region (residues 13-16, see Figure I-4) plays a major role in most of them.

1.4.1. Interaction with Metal Cations

Since early in the study of AD, reports showed that metal ion homeostasis is severely dysregulated in AD (167, 169, 216, 548-554). Trace metals, including Cu²⁺, Zn²⁺ and Fe³⁺ were also found in elevated concentrations in isolated amyloid plaques (169, 555).

A β itself was also found to bind both copper and zinc. Hou *et al.* determined the Cu²⁺ binding site to contain the residues Arg5, Val12, Leu17 (556). Atwood identified multiple affinity cooperative Cu²⁺ binding sites existing on A β , with A β ₁₋₄₂ exhibiting much stronger cooperative binding than A β ₁₋₄₀ (557). Syme *et al.* found residues His6, His13 and His14 to be responsible for zinc binding (558). Danielsson and co-workers confirmed these results, but added that the N-terminus was involved in the interaction, as well (559). Furthermore, they noted that this binding site is shared with Cu²⁺. An additional weaker binding site involving residues 23-28 was

also proposed (559). Yang *et al.* on the other hand, reported that only the His13 and His14 residues, but not His6 are involved in Zn²⁺ binding (560). In NMR-based experiments, Bin *et al.* found a pH-dependence of Cu-binding to A β in the pH range from 7.0 to 4.0 (561). Ghabelani *et al.* showed that Zn²⁺, as opposed to Cu²⁺, loses its binding specificity for the histidine residues at pH 5.5 (173).

Metal binding seems to affect A β in a number of ways. For example, Strozyk and co-workers found that zinc and copper modulate A β levels in human cerebrospinal fluid (562). They proposed that excessive interaction with copper and zinc may induce neocortical A β precipitation in AD, whereas soluble A β degradation is normally promoted by physiological copper and zinc concentrations (562). Danielsson *et al.* further explained that at high metal ion concentrations, the metal-induced aggregation should mainly originate from electrostatic interactions leading to decreased repulsion between A β molecules, whereas at low metal ion concentrations, metal binding induced a peptide secondary structure that counteracted aggregation (559). Moreover, zinc binding, in particular, was found to induce the formation of a helical peptide structure that results in aggregation of A β thus facilitating insertion into the cell membrane and pore formation (205, 563, 564).

Aluminum is another metal that has been implicated in AD through its presence in the amyloid plaques (147, 148, 565, 566). It's role as a precipitant, however, is controversial (567, 568). More recent evidence suggests a potential pathogenic role of A β — Al complexes (569)⁴. Furthermore, aluminum was found to enhance A β penetration of the BBB (570), alter Ca²⁺ homeostasis and mitochondrial function (150), and generate increased radicals and reactive oxygen species (ROS) which are also toxic to cells (139, 153, 163, 571, 572). Bush *et al.* further

⁴ The evidence is rather weak, though, since the Al — A β complexes were not more toxic than A β alone; Al was just not as "protective" as Cu or Zn (refer to their Fig. 6A & 7).

distinguished the A β species by showing that Al³⁺ in combination with A β ₁₋₄₂ generated significantly more radicals than A β ₁₋₄₀ (140, 141). This may provide a possible explanation for the higher toxicity of the former species, as will come up again later in this thesis.

1.4.2. Interaction with Cell Membranes

For A β to exert toxic effects on neuronal and glial cells, it first has to bind to cell membrane components. In particular, interactions with membrane proteins and membrane lipids play a critical role.

1.4.2.1. Interaction with Membrane Proteins

A number of membrane proteins have been identified, which can mediate the interaction between A β and the plasma membranes of cells implicated in AD. On neurons, these are APP, the NMDA receptor, and integrins, to name but a few; and on glial cells, e.g., the scavenger receptors A, BI and CD36, a complex involving CD36, and CD47 (573). These proteins have been shown to exhibit different binding capacities to A β monomers and A β fibrils (574).

1.4.2.2. Interaction with Membrane Lipids

Curtain *et al.* reported that the interactions of A β with model membrane lipids and insertion of A β into those membranes is regulated by the pH and cholesterol, and dependent on metal ion binding (205).

Based on in vitro studies of lipid bilayers, Devanathan and co-workers more recently presented data that support a mechanism in which peptide aggregation requires an environment rich in sphingomyelin and occurs largely on the bilayer surface in the absence of

cholesterol (206). In this study, the presence of cholesterol actually facilitated peptide insertion into the bilayer and promoted the aggregation process, leading to the formation of a less densely packed bilayer. The presence of Zn^{2+} enhanced insertion and aggregation, as well, and promoted large bilayer structural changes induced by peptide aggregates resulting in a more porous membrane (206). When considering the amount of cholesterol needed, Curtain *et al.* noted that at cholesterol contents above 0.2 mole fraction of the total lipid, insertion of $A\beta$ was completely inhibited (205).

1.4.3. Interaction with other Molecules

A multitude of other molecules have been shown to interact with and bind to $A\beta$ (575-579). Here, only one interesting example shall be mentioned. Shao and co-workers conducted binding studies on $A\beta_{1-40}$ and $A\beta_{1-42}$ with, amongst others, nicotine, which had been found previously to inhibit $A\beta$ amyloidogenesis (580). These NMR studies showed that nicotine binds to the His13 and His14 side-chains of the Tyr10-Val24 helical segment preventing the conversion of α -helix to β -sheet (575).

1.5. Current AD Hypotheses

There are several different hypotheses proposed for the underlying mechanism of the development of Alzheimer's disease (Table I-3). Each is able to piece together some of the facts derived through various experiments and observations, however, none to date has been truly comprehensive, leaving many unanswered questions. The following section will provide brief descriptions of the hypotheses most relevant to this thesis, followed by a discussion of their shortcomings.

Table I-3 Current AD hypotheses.

Hypotheses attempting to describe the underlying mechanism of AD development.

Hypothesis	Description	References
Cholinergic Hypothesis	Deficiencies in cholinergic signaling initiates the progression of the disease Refuted, since AChE inhibitors are only symptomatic, not curative drugs	(527, 581-584) (585, 586)
Amyloid Cascade Hypothesis	A β deposition causes AD pathology	(587-590)
Tau Hypothesis	Tau hyperphosphorylation leads to neurofibrillary degeneration (NFTs, neuropil threads, dystrophic neurites), one hallmark of AD pathology Destabilisation of the cytoskeleton impairs axonal transport	(130, 533, 591-593) (513, 594-596)
Calcium Hypothesis	Both, APP and A β increase intracellular Ca ²⁺ , leading to learning and memory deficits; altered Ca ²⁺ signalling contributes to neuronal degeneration	(230, 239, 597-599)
Metal Hypothesis	Zn ²⁺ and Cu ²⁺ accelerate A β aggregation Cu ²⁺ and Fe ³⁺ promote neurotoxic redox activity of A β and induce A β crosslinking	(600)
Aluminum-Amyloid Cascade Hypothesis	Al promotes A β fibrillization Al increases brain A β burden in animal models	(147, 148, 601-603)
Neurovascular Hypothesis	Decreased A β clearance caused by impairment of the LRP-1 at the BBB leads to increased A β levels in the brain	(604)
Biofloculant Hypothesis	A β is normally produced to bind neurotoxic solutes (e.g., metal ions); aggregation of A β into plaques helps to present these toxins to phagocytes	(605)
Mitochondrial Cascade Hypothesis	Oxidative mitochondrial damage amplifies ROS production and triggers three events: (1) cells generate A β , which further perturbs mitochondrial function, (2) compromised cells are removed via PCD mechanisms, (3) neuronal progenitor cells unsuccessfully attempt to re-enter the cell cycle, causing aneuploidy, tau phosphorylation, and NFT formation	(243, 244, 606)
Aβ Ion Channel Hypothesis	A β forms ion channels leading to disrupted ion homeostasis	(597, 607-610)
Microbe-Dementia / Pathogen Hypothesis	Infiltration of the brain by pathogens acts as a trigger or co-factor for AD	(291, 611, 612)
Alternate Aβ Hypothesis	Oxidative stress leads to production of A β which is protective against it as antioxidant	(613, 614)
Dual Pathway Hypothesis	A β and tau are linked by separate mechanisms driven by a common upstream molecular defect	(615)
Tau Axis Hypothesis	A β and tau act synergistically to cause AD Tau mediates A β toxicity at dendrites	(616)

Acronyms: A β :beta-amyloid; AChE: Acetylcholinesterase; AD: Alzheimer's Disease; BBB: blood-brain barrier; DNA: desoxyribonucleic acid; LRP-1: low density lipoprotein receptor related protein-1; NFT: neurofibrillary tangle; PCD: programmed cell death (apoptosis); RNA: ribonucleic acid; ROS: reactive oxygen species

1.5.1. Amyloid Cascade Hypothesis

Most researchers in the field consider A β a key molecule in the development of AD. Recognizing the importance of A β , in 1992 Hardy and Higgins developed the amyloid cascade hypothesis, which states that “deposition of [A β] is the causative agent of Alzheimer’s pathology and that the neurofibrillary tangles, cell loss, vascular damage and dementia follow as a direct result of this deposition” (587). It suggests that cleavage of the APP by secretase (now known as α -secretase) leads to non-amyloidogenic products, whereas processing of APP by the endosomal-lysosomal pathway leads to formation of the various species of A β (Figure I-7). An increased intraneuronal calcium concentration caused by A β leads to hyperphosphorylation of tau protein which forms paired helical filaments that can aggregate into neurofibrillary tangles. Furthermore, disruption of calcium homeostasis might directly lead to calcium-mediated neuronal death.

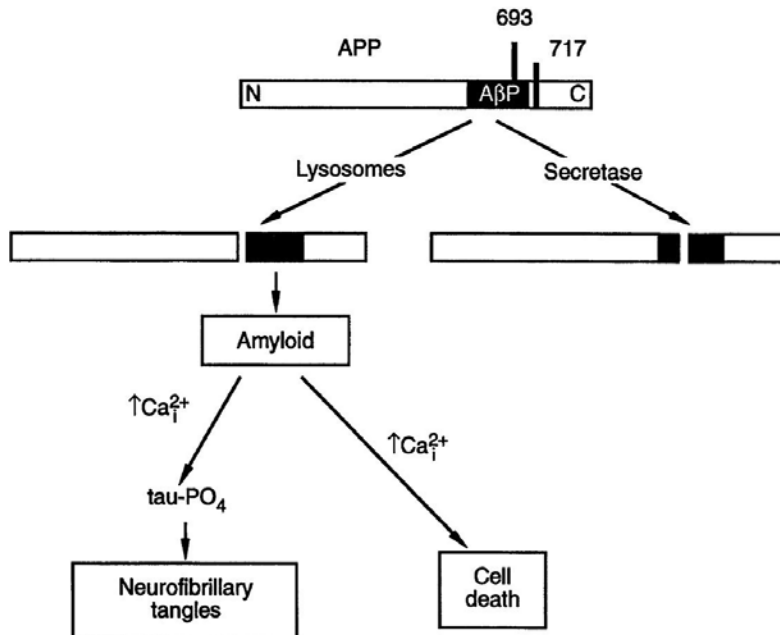


Figure I-7 The Amyloid Cascade Hypothesis
APP may be processed through two pathways, the secretase pathway leading to soluble products unable to form amyloids, and the lysosomal pathway generating A β that precipitates as amyloid and eventually causes neurofibrillary tangles and cell death, the hallmarks of AD. From Ref. (587). Reprinted with permission from AAAS.

Since its inception, the amyloid cascade hypothesis has been revised considerably to account for the many subsequent discoveries. Recently, the focus has shifted more to processes involving synapses, and to effects that render them dysfunctional early on in the course of the disease. The updated and expanded model presented by Beckerman (589) (Figure I-8) attempts to relate the normal function of A β to the pathologic development of the disease state. It now includes neuroinflammation and the toxic effects of soluble A β oligomers, and incorporates the neurofibrillary tangles into the overall scheme of the disease progression.

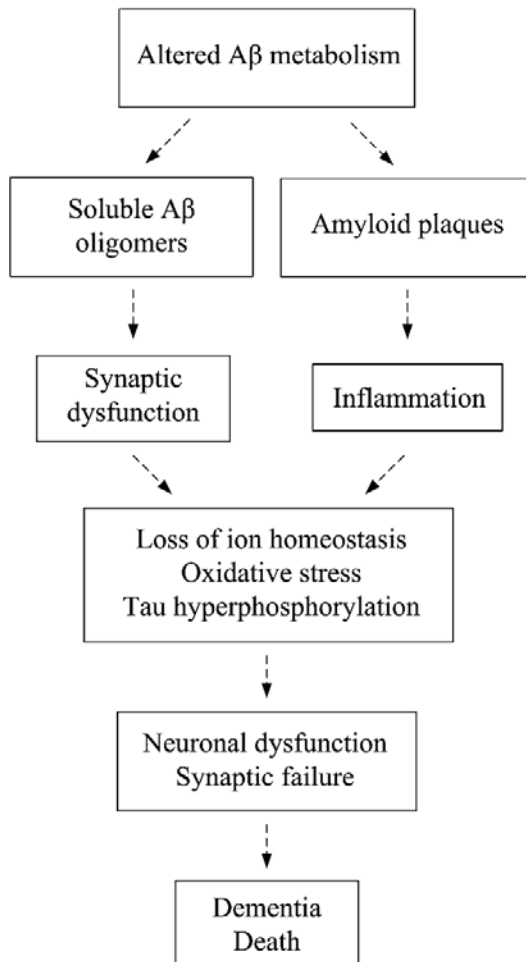


Figure I-8 Updated version of the Amyloid Cascade by Beckerman.

The updated version of the amyloid cascade now includes neuroinflammation and the toxic effects of soluble A β oligomers, and incorporates the neurofibrillary tangles into the overall scheme of the disease progression. From: Springer and M. Beckerman, *Cellular Signaling in Health and Disease*, Biological and Medical Physics, Biomedical Engineering, 2009, p. 370, Chapter 17 Alzheimer's Disease, M. Beckerman, Fig. 1, © Springer Science + Business Media, LLC 2009; with kind permission from Springer Science and Business Media.

1.5.2. Tau Hypothesis

The tau proteins belong to a group of proteins that are involved in stabilization of neuronal cytoskeleton (617-621). They are normally phosphorylated to varying degrees, but in AD, all the isoforms become hyperphosphorylated and can no longer perform their function, and possibly impair axonal transport processes (131, 530, 617, 622-628). This hyperphosphorylated tau can also form paired helical filaments (PHFs) (4, 629, 630) which aggregate into neurofibrillary tangles (NFTs) (485, 631-634), the other hallmark of AD besides amyloid plaques.

Arguments for tau being a central player in AD are that the tau proteins are hyperphosphorylated and begin to form tangles long before the *pathology* of the A β plaques (16, 635). Furthermore, the A β plaque load in AD brains often shows poor correlation with cognitive impairment (434). Arguments against tau's causative role are that signs of A β *aggregation* do actually precede the formation of tangles, that tangles are not necessarily found in all pathology samples of AD brains and that some inherited mutations of tau may lead to a frontotemporal dementia with Parkinsonism, but not AD (636, 637). In addition, hippocampal neuron loss in AD patients has been found to exceed extracellular NFT formation by a large margin (32). As well, findings based on human genetic analyses have now established that alterations in tau occur further downstream from A β accumulation (638-640), while corresponding results have been obtained in transgenic mouse models (641-643).

More recent research has provided evidence that tau expression seems to be necessary for neuronal dysfunction and behavioral deficits in AD subjects and animal models. Results from neuronal cell cultures (644, 645) and APP-transgenic mice (646, 647) seem to suggest that a decreased or absent tau expression alleviates the neurotoxic impact of A β .

Current research efforts are aimed at integrating findings for different pathophysiological processes into one coherent model. Jack *et al.* published a hypothetical model of dynamic

biomarkers (648) that incorporates A β and tau pathology as independent processes (see Figure I-9).

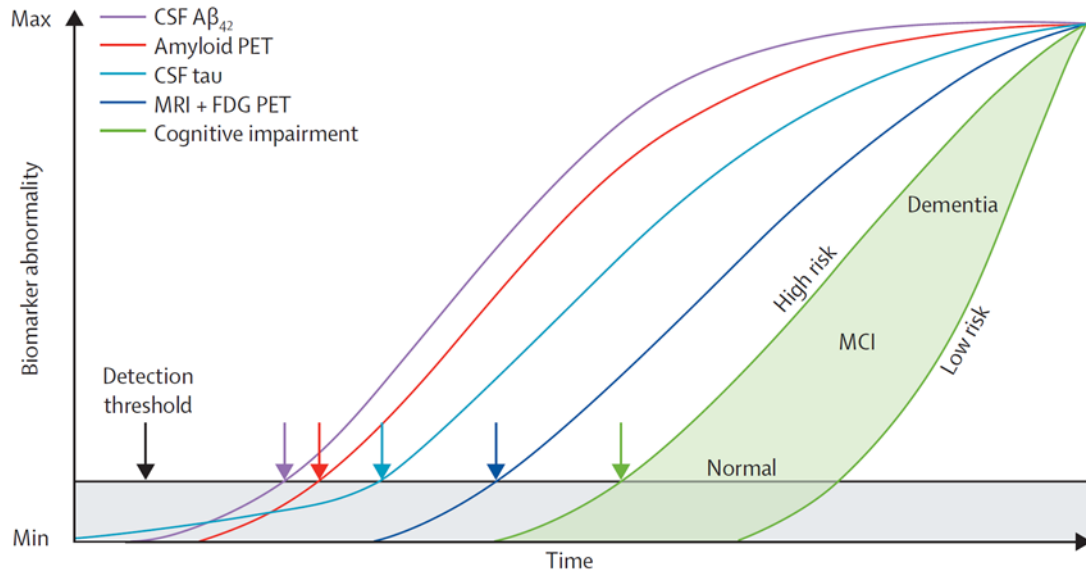


Figure I-9 Hypothetical model integrating immunohistology and dynamic biomarkers of the AD pathological cascade.

The degree of neurodegeneration is quantified by structural MRI and FDG PET (dark blue). By definition, the curves for all biomarkers converge at the point of maximum abnormality in the top right-hand corner of the plot. Cognitive impairment is depicted as a zone (light green-filled area) bordered by lines for low-risk and high-risk individuals. The biomarker detection threshold is represented by the black horizontal line; the grey area beneath denotes the zone in which abnormal pathophysiological changes occur below detectable levels. Early on, tau pathology precedes A β deposition in time, albeit at subthreshold levels. A β deposition then occurs independently and rises above the biomarker detection threshold (purple and red arrows) before CSF tau (light blue arrow). Eventually, hypometabolism on FDG PET and atrophy on structural MRI (dark blue arrow) rise above the detection threshold. Finally, cognitive impairment becomes evident (green arrow), where the age of onset and the cognitive responses depend on the individual's risk profile (light green-filled area).

Acronyms: A β = β -amyloid; CSF: central nervous system; FDG = fluorodeoxyglucose; MCI = mild cognitive impairment; MRI: magnetic resonance imaging; PET: positron emission tomography.

Reprinted from Ref. (648) with permission from Elsevier.

1.5.1. Shortcomings of Current Hypotheses

As the above discussion has illustrated, the current hypotheses do have some shortcomings that leave many unanswered questions about AD. For example, what would be the underlying physiologic role of A β ? Why would A β attack neurons? Why is AD chronic? Why does AD get worse over time? How is it all connected?

2. Research Goals

The goal of the research described in this thesis was the development of a new theory of Alzheimer's Disease based on currently available knowledge and experimental evidence gathered for this work. This theory should be molecular based rather than cellular (i.e., should permit a conceptualization of the aetiology and pathogenesis of Alzheimer's at a molecule/atom level of structural refinement) and thus, should afford the ability for medicinal chemistry to rationally design new chemical entities as putative therapeutics for the disease altering treatment of AD.

In developing the concept of AD as autoimmune disease of the innate immune system, Chapter II addresses the shortcomings of current AD hypotheses and provides solutions for unanswered questions about AD. The solutions to these unanswered questions include: [i] The physiologic role of A β is as antimicrobial peptide (AMP). [ii] The mechanism for A β 's attack on neurons is rooted in their similarity to bacteria. [iii] AD is chronic and worsens over time because necrotic cell death caused by A β spreads to adjacent neurons, while A β also prevents repair through neurogenesis. [iv] Since this process occurs only in a low percentage of attacked neurons, progression of the disease is slow but chronic. [v] These findings reveal that the processes involved in AD are not linear, as implied in the amyloid cascade, but are rather characterised by a positive feedback loop that was termed the '*Vicious Cycle of AD*'.

In Chapter III, a question borne from A β 's activity as AMP and its central role in the Vicious Cycle of AD is investigated: do antibiotics, such as penicillin, that cause release of bacterial endotoxins due to their mechanism of action, trigger the Vicious Cycle of AD and thus lead to the development of AD?

Chapter IV describes the synthesis and purification of a number of peptides related to AD and used in this work.

Finally, Chapter V deals with two projects involving interactions of A β with other molecules. The first one tackles the issue of peptide loss due to adsorption to sample and assay vessels. The second one describes the development of a new A β aggregation assay; it is based on the interaction of A β with the ganglioside GM1. Additionally, it includes the design of two new irradiators for use in photo-induced cross-coupling of unmodified proteins (PICUP), a technique that has been employed successfully in the analysis of A β aggregation.

3. References

1. Alzheimer, A. Über eine eigenartige Erkrankung der Hirnrinde. Vortrag in der Versammlung Südwestdeutscher Irrenärzte in Tübingen am 3. November 1906. *Allgemeine Zeitschrift für Psychiatrie und psychisch-gerichtliche Medizin* **1907**, *64*, 146-148.
2. Alzheimer, A.; Stelzmann, R. A.; Schnitzlein, H. N.; Murtagh, F. R. An English translation of Alzheimer's 1907 paper, "Über eine eigenartige Erkrankung der Hirnrinde". *Clin. Anat.* **1995**, *8*, 429-431.
3. Kraepelin, E. *Psychiatrie: ein Lehrbuch für Studierende und Ärzte. II. Band, Klinische Psychiatrie. I. Teil*; Johann Ambrosius Barth: Leipzig, 1910; , pp 1.
4. Kidd, M. Paired helical filaments in electron microscopy of Alzheimer's disease. *Nature* **1963**, *197*, 192-193.
5. Terry, R. D.; Gonatas, N. K.; Weiss, M. Ultrastructural Studies in Alzheimer's Presenile Dementia. *Am. J. Pathol.* **1964**, *44*, 269-297.
6. Glenner, G. G.; Wong, C. W. Alzheimer's disease: Initial report of the purification and characterization of a novel cerebrovascular amyloid protein. *Biochem. Biophys. Res. Commun.* **1984**, *120*, 885-890.
7. Heston, L. L.; Mastri, A. R. The genetics of Alzheimer's disease: associations with hematologic malignancy and Down's syndrome. *Arch. Gen. Psychiatry* **1977**, *34*, 976-981.
8. Schellenberg, G. D. Early Alzheimer's disease genetics. *J. Alzheimers Dis.* **2006**, *9*, 367-372.
9. Bertram, L.; Tanzi, R. E. The genetics of Alzheimer's disease. *Prog. Mol. Biol. Transl. Sci.* **2012**, *107*, 79-100.
10. Jack, C. R., Jr; Knopman, D. S.; Jagust, W. J.; Shaw, L. M.; Aisen, P. S.; Weiner, M. W.; Petersen, R. C.; Trojanowski, J. Q. Hypothetical model of dynamic biomarkers of the Alzheimer's pathological cascade. *Lancet Neurol.* **2010**, *9*, 119-128.
11. Ferri, C. P.; Sousa, R.; Albanese, E.; Ribeiro, W. S.; Honyashiki, M.; Acosta, D.; Blom, M.; Dudgeon, S.; Frantz, N.; Geiger, A.; Jansen, S.; Ketteringham, A.; Kinnaird, L.; Martensson, B.; Rees, G.; Schaper, F.; Splaine, M.; Tamitegama, T.; Westerlund, K.; Wortmann, M. World Alzheimer Report 2009. **2009**, *1*, 1-96.

12. Canadian study of health and aging: study methods and prevalence of dementia. *CMAJ* **1994**, *150*, 899-913.
13. Canadian Institute for Health Information. The Burden of Neurologic Diseases, Disorders and Injuries in Canada. **2007**.
14. Dudgeon, S. Rising Tide - The Impact of Dementia on Canadian Society. **2010**, 1-35.
15. Sperling, R. A.; Aisen, P. S.; Beckett, L. A.; Bennett, D. A.; Craft, S.; Fagan, A. M.; Iwatsubo, T.; Jack Jr., C. R.; Kaye, J.; Montine, T. J.; Park, D. C.; Reiman, E. M.; Rowe, C. C.; Siemers, E.; Stern, Y.; Yaffe, K.; Carrillo, M. C.; Thies, B.; Morrison-Bogorad, M.; Wagster, M. V.; Phelps, C. H. Toward defining the preclinical stages of Alzheimer's disease: Recommendations from the National Institute on Aging-Alzheimer's Association workgroups on diagnostic guidelines for Alzheimer's disease. *Alzheimer's and Dementia* **2011**, *7*, 280-292.
16. Braak, H.; Braak, E. Neuropathological staging of Alzheimer-related changes. *Acta Neuropathol.* **1991**, *82*, 239-259.
17. Braak, H.; Braak, E. Morphological criteria for the recognition of Alzheimer's disease and the distribution pattern of cortical changes related to this disorder. *Neurobiol. Aging* **1994**, *15*, 355-6; discussion 379-80.
18. Braak, H.; Braak, E.; Bohl, J. Staging of Alzheimer-related cortical destruction. *Eur. Neurol.* **1993**, *33*, 403-408.
19. Braak, H.; Braak, E. Staging of Alzheimer's disease-related neurofibrillary changes. *Neurobiol. Aging* **1995**, *16*, 271-8; discussion 278-84.
20. Braak, H.; Braak, E. Staging of Alzheimer-related cortical destruction. *Int. Psychogeriatr.* **1997**, *9 Suppl 1*, 257-61; discussion 269-72.
21. Braak, E.; Griffing, K.; Arai, K.; Bohl, J.; Bratzke, H.; Braak, H. Neuropathology of Alzheimer's disease: what is new since A. Alzheimer? *Eur. Arch. Psychiatry Clin. Neurosci.* **1999**, *249 Suppl 3*, 14-22.
22. Braak, H.; Braak, E. Evolution of neuronal changes in the course of Alzheimer's disease. *J. Neural Transm. Suppl.* **1998**, *53*, 127-140.
23. Braak, H.; Braak, E. Frequency of stages of Alzheimer-related lesions in different age categories. *Neurobiol. Aging* **1997**, *18*, 351-357.
24. Schoenheit, B.; Zarski, R.; Ohm, T. G. Spatial and temporal relationships between plaques and tangles in Alzheimer-pathology. *Neurobiol. Aging* **2004**, *25*, 697-711.

25. Duyckaerts, C.; Hauw, J. J. Diagnosis and staging of Alzheimer disease. *Neurobiol. Aging* **1997**, *18*, S33-42.
26. Dickson, D. W. Neuropathological diagnosis of Alzheimer's disease: a perspective from longitudinal clinicopathological studies. *Neurobiol. Aging* **1997**, *18*, S21-6.
27. Thal, D. R.; Braak, H. Post-mortem diagnosis of Alzheimer's disease. *Pathologie* **2005**, *26*, 201-213.
28. Mesulam, M. M. Neuroplasticity failure in Alzheimer's disease: bridging the gap between plaques and tangles. *Neuron* **1999**, *24*, 521-529.
29. Davies, P.; Maloney, A. J. Selective loss of central cholinergic neurons in Alzheimer's disease. *Lancet* **1976**, *2*, 1403.
30. Perry, E. K.; Gibson, P. H.; Blessed, G.; Perry, R. H.; Tomlinson, B. E. Neurotransmitter enzyme abnormalities in senile dementia. Choline acetyltransferase and glutamic acid decarboxylase activities in necropsy brain tissue. *J. Neurol. Sci.* **1977**, *34*, 247-265.
31. Bowen, D. M. Biochemistry of Dementias. *Proc. R. Soc. Med.* **1977**, *70*, 351-353.
32. Kril, J. J.; Patel, S.; Harding, A. J.; Halliday, G. M. Neuron loss from the hippocampus of Alzheimer's disease exceeds extracellular neurofibrillary tangle formation. *Acta Neuropathol.* **2002**, *103*, 370-376.
33. McKenzie, J. E.; Roberts, G. W.; Royston, M. C. Comparative investigation of neurofibrillary damage in the temporal lobe in Alzheimer's disease, Down's syndrome and dementia pugilistica. *Neurodegeneration* **1996**, *5*, 259-264.
34. Terry, R. D. Neuropathological changes in Alzheimer disease. *Prog. Brain Res.* **1994**, *101*, 383-390.
35. Dickson, T. C.; King, C. E.; McCormack, G. H.; Vickers, J. C. Neurochemical diversity of dystrophic neurites in the early and late stages of Alzheimer's disease. *Exp. Neurol.* **1999**, *156*, 100-110.
36. Hof, P.; Morrison, J. In *The cellular basis of cortical disconnection in Alzheimer disease and related dementing conditions*; Terry, R., Katzman, R. and Bick, K., Eds.; Alzheimer disease; Raven Press: New York, **1994**; pp. 197-229.
37. Masliah, E.; Mallory, M.; Deerinck, T.; DeTeresa, R.; Lamont, S.; Miller, A.; Terry, R. D.; Carragher, B.; Ellisman, M. Re-evaluation of the structural organization of neuritic plaques in Alzheimer's disease. *J. Neuropathol. Exp. Neurol.* **1993**, *52*, 619-632.

38. Praprotnik, D.; Smith, M. A.; Richey, P. L.; Vinters, H. V.; Perry, G. Filament heterogeneity within the dystrophic neurites of senile plaques suggests blockage of fast axonal transport in Alzheimer's disease. *Acta Neuropathol.* **1996**, *91*, 226-235.
39. Vickers, J. C.; Chin, D.; Edwards, A. M.; Sampson, V.; Harper, C.; Morrison, J. Dystrophic neurite formation associated with age-related β amyloid deposition in the neocortex: clues to the genesis of neurofibrillary pathology. *Exp. Neurol.* **1996**, *141*, 1-11.
40. Gray, E. G. Spongiform encephalopathy: a neurocytologist's viewpoint with a note on Alzheimer's disease. *Neuropathol. Appl. Neurobiol.* **1986**, *12*, 149-172.
41. Gray, E. G.; Paula-Barbosa, M.; Roher, A. Alzheimer's disease: paired helical filaments and cytomembranes. *Neuropathol. Appl. Neurobiol.* **1987**, *13*, 91-110.
42. Paula-Barbosa, M.; Tavares, M. A.; Cadete-Leite, A. A quantitative study of frontal cortex dendritic microtubules in patients with Alzheimer's disease. *Brain Res.* **1987**, *417*, 139-142.
43. Adlard, P. A.; Vickers, J. C. Morphologically distinct plaque types differentially affect dendritic structure and organisation in the early and late stages of Alzheimer's disease. *Acta Neuropathol.* **2002**, *103*, 377-383.
44. Knowles, R. B.; Gomez-Isla, T.; Hyman, B. T. A β associated neuropil changes: correlation with neuronal loss and dementia. *J. Neuropathol. Exp. Neurol.* **1998**, *57*, 1122-1130.
45. Knowles, R. B.; Wyart, C.; Buldyrev, S. V.; Cruz, L.; Urbanc, B.; Hasselmo, M. E.; Stanley, H. E.; Hyman, B. T. Plaque-induced neurite abnormalities: implications for disruption of neural networks in Alzheimer's disease. *Proc. Natl. Acad. Sci. U. S. A.* **1999**, *96*, 5274-5279.
46. Farfara, D.; Lifshitz, V.; Frenkel, D. Neuroprotective and Neurotoxic Properties of Glial Cells in the Pathogenesis of Alzheimer's Disease. *J. Cell. Mol. Med.* **2008**, *12*, 762-780.
47. Diamond, J. A Report on Alzheimer's Disease and Current Research. **2008**, *1*.
48. Ferri, C. P.; Prince, M.; Brayne, C.; Brodaty, H.; Fratiglioni, L.; Ganguli, M.; Hall, K.; Hasegawa, K.; Hendrie, H.; Huang, Y.; Jorm, A.; Mathers, C.; Menezes, P. R.; Rimmer, E.; Sczufca, M.; Alzheimer's Disease International. Global prevalence of dementia: a Delphi consensus study. *Lancet* **2005**, *366*, 2112-2117.
49. Mattson, M. P. Gene-diet interactions in brain aging and neurodegenerative disorders. *Ann. Intern. Med.* **2003**, *139*, 441-444.
50. Song, X.; Mitnitski, A.; Rockwood, K. Nontraditional risk factors combine to predict Alzheimer disease and dementia. *Neurology* **2011**, *77*, 227-234.

51. Scheuner, D.; Eckman, C.; Jensen, M.; Song, X.; Citron, M.; Suzuki, N.; Bird, T. D.; Hardy, J.; Hutton, M.; Kukull, W.; Larson, E.; Levy-Lahad, E.; Viitanen, M.; Peskind, E.; Poorkaj, P.; Schellenberg, G.; Tanzi, R.; Wasco, W.; Lannfelt, L.; Selkoe, D.; Younkin, S. Secreted amyloid β -protein similar to that in the senile plaques of Alzheimer's disease is increased in vivo by the presenilin 1 and 2 and APP mutations linked to familial Alzheimer's disease. *Nat. Med.* **1996**, *2*, 864-870.
52. De Jonghe, C.; Zehr, C.; Yager, D.; Prada, C. M.; Younkin, S.; Hendriks, L.; Van Broeckhoven, C.; Eckman, C. B. Flemish and Dutch mutations in amyloid β precursor protein have different effects on amyloid β secretion. *Neurobiol. Dis.* **1998**, *5*, 281-286.
53. Hendriks, L.; van Duijn, C. M.; Cras, P.; Cruts, M.; Van Hul, W.; van Harskamp, F.; Warren, A.; McInnis, M. G.; Antonarakis, S. E.; Martin, J. J. Presenile dementia and cerebral haemorrhage linked to a mutation at codon 692 of the β -amyloid precursor protein gene. *Nat. Genet.* **1992**, *1*, 218-221.
54. Nilsberth, C.; Westlind-Danielsson, A.; Eckman, C. B.; Condron, M. M.; Axelman, K.; Forsell, C.; Stenh, C.; Luthman, J.; Teplow, D. B.; Younkin, S. G.; Naslund, J.; Lannfelt, L. The 'Arctic' APP mutation (E693G) causes Alzheimer's disease by enhanced A β protofibril formation. *Nat. Neurosci.* **2001**, *4*, 887-893.
55. Suzuki, N.; Cheung, T. T.; Cai, X. D.; Odaka, A.; Otvos, L., Jr; Eckman, C.; Golde, T. E.; Younkin, S. G. An increased percentage of long amyloid β protein secreted by familial amyloid β protein precursor (β APP₇₁₇) mutants. *Science* **1994**, *264*, 1336-1340.
56. Cruts, M.; Theuns, J.; Van Broeckhoven, C. Locus-specific mutation databases for neurodegenerative brain diseases. *Hum. Mutat.* **2012**, *33*, 1340-1344.
57. Ankarcona, M. In *The Role of Presenilins in A β -Induced Cell Death in Alzheimer's Disease*; Barrow, C. J., Small, D. H., Eds.; A β peptide and Alzheimer's disease - Celebrating a century of research; Springer: London, **2007**; pp. 234-244.
58. Chan, Y.; Jan, Y. N. Presenilins, Processing of β -Amyloid Precursor Protein, and Notch Signaling. *Neuron* **1999**, *23*, 201-204.
59. Muller, U.; Winter, P.; Graeber, M. B. A presenilin 1 mutation in the first case of Alzheimer's disease. *Lancet Neurol.* **2013**, *12*, 129-130.
60. Verdile, G.; Gandy, S. E.; Martins, R. N. The role of presenilin and its interacting proteins in the biogenesis of Alzheimer's β amyloid. *Neurochem. Res.* **2007**, *32*, 609-623.
61. Sudoh, S.; Kawamura, Y.; Sato, S.; Wang, R.; Saido, T. C.; Oyama, F.; Sakaki, Y.; Komano, H.; Yanagisawa, K. Presenilin 1 mutations linked to familial Alzheimer's disease increase the

- intracellular levels of amyloid β -protein 1-42 and its N-terminally truncated variant(s) which are generated at distinct sites. *J. Neurochem.* **1998**, *71*, 1535-1543.
62. Li, Y. M.; Lai, M. T.; Xu, M.; Huang, Q.; DiMuzio-Mower, J.; Sardana, M. K.; Shi, X. P.; Yin, K. C.; Shafer, J. A.; Gardell, S. J. Presenilin 1 is linked with γ -secretase activity in the detergent solubilized state. *Proc. Natl. Acad. Sci. U. S. A.* **2000**, *97*, 6138-6143.
 63. Sadowski, M. J.; Pankiewicz, J.; Scholtzova, H.; Mehta, P. D.; Prelli, F.; Quartermain, D.; Wisniewski, T. Blocking the apolipoprotein E/amyloid- β interaction as a potential therapeutic approach for Alzheimer's disease. *Proc. Natl. Acad. Sci. U. S. A.* **2006**, *103*, 18787-18792.
 64. Ghebremedhin, E.; Schultz, C.; Braak, E.; Braak, H. High frequency of apolipoprotein E epsilon4 allele in young individuals with very mild Alzheimer's disease-related neurofibrillary changes. *Exp. Neurol.* **1998**, *153*, 152-155.
 65. Adalbert, R.; Gilley, J.; Coleman, M. P. A β , tau and ApoE4 in Alzheimer's disease: the axonal connection. *Trends Mol. Med.* **2007**, *13*, 135-142.
 66. Bell, R. D.; Sagare, A. P.; Friedman, A. E.; Bedi, G. S.; Holtzman, D. M.; Deane, R.; Zlokovic, B. V. Transport pathways for clearance of human Alzheimer's amyloid β -peptide and apolipoproteins E and J in the mouse central nervous system. *J. Cereb. Blood Flow Metab.* **2007**, *27*, 909-918.
 67. Koffie, R. M.; Hashimoto, T.; Tai, H. C.; Kay, K. R.; Serrano-Pozo, A.; Joyner, D.; Hou, S.; Kopeikina, K. J.; Frosch, M. P.; Lee, V. M.; Holtzman, D. M.; Hyman, B. T.; Spires-Jones, T. L. Apolipoprotein E4 effects in Alzheimer's disease are mediated by synaptotoxic oligomeric amyloid- β . *Brain* **2012**, *135*, 2155-2168.
 68. Corder, E. H.; Saunders, A. M.; Strittmatter, W. J.; Schmechel, D. E.; Gaskell, P. C.; Small, G. W.; Roses, A. D.; Haines, J. L.; Pericak-Vance, M. A. Gene dose of apolipoprotein E type 4 allele and the risk of Alzheimer's disease in late onset families. *Science* **1993**, *261*, 921-923.
 69. Sing, C. F.; Davignon, J. Role of the apolipoprotein E polymorphism in determining normal plasma lipid and lipoprotein variation. *Am. J. Hum. Genet.* **1985**, *37*, 268-285.
 70. Strittmatter, W. J.; Roses, A. D. Apolipoprotein E and Alzheimer disease. *Proc. Natl. Acad. Sci. U. S. A.* **1995**, *92*, 4725-4727.
 71. Wu, C. W.; Liao, P. C.; Lin, C.; Kuo, C. J.; Chen, S. T.; Chen, H. I.; Kuo, Y. M. Brain region-dependent increases in β -amyloid and apolipoprotein E levels in hypercholesterolemic rabbits. *J. Neural Transm.* **2003**, *110*, 641-649.

72. Hayashi, H.; Igbavboa, U.; Hamanaka, H.; Kobayashi, M.; Fujita, S. C.; Wood, W. G.; Yanagisawa, K. Cholesterol is increased in the exofacial leaflet of synaptic plasma membranes of human apolipoprotein E4 knock-in mice. *Neuroreport* **2002**, *13*, 383-386.
73. Seshadri, S.; Drachman, D. A.; Lippa, C. F. Apolipoprotein E epsilon 4 allele and the lifetime risk of Alzheimer's disease. What physicians know, and what they should know. *Arch. Neurol.* **1995**, *52*, 1074-1079.
74. Yu, G.; Chen, F.; Levesque, G.; Nishimura, M.; Zhang, D.; Levesque, L.; Rogaeva, E.; Xu, D.; Liang, Y.; Duthie, M.; George-Hyslop, P. H. S.; Fraser, P. E. The Presenilin 1 Protein Is a Component of a High Molecular Weight Intracellular Complex That Contains β -Catenin. *Journal of Biological Chemistry* **1998**, *273*, 16470-16475.
75. Heston, L. L. Alzheimer's dementia and Down's syndrome: genetic evidence suggesting an association. *Ann. N. Y. Acad. Sci.* **1982**, *396*, 29-37.
76. Armstrong, R. A. Correlations between the morphology of diffuse and primitive β -amyloid (A β) deposits and the frequency of associated cells in Down's syndrome. *Neuropathol. Appl. Neurobiol.* **1996**, *22*, 527-530.
77. Glenner, G. G.; Wong, C. W. Alzheimer's disease and Down's syndrome: sharing of a unique cerebrovascular amyloid fibril protein. *Biochem. Biophys. Res. Commun.* **1984**, *122*, 1131-1135.
78. Masters, C. L.; Simms, G.; Weinman, N. A.; Multhaup, G.; McDonald, B. L.; Beyreuther, K. Amyloid plaque core protein in Alzheimer disease and Down syndrome. *Proc. Natl. Acad. Sci. U. S. A.* **1985**, *82*, 4245-4249.
79. Armstrong, R. A.; Myers, D. β /A4 deposits and their relationship to senile plaques in Alzheimer's disease. *Neuroreport* **1992**, *3*, 262-264.
80. Arnold, S. E.; Hyman, B. T.; Flory, J.; Damasio, A. R.; Van Hoesen, G. W. The topographical and neuroanatomical distribution of neurofibrillary tangles and neuritic plaques in the cerebral cortex of patients with Alzheimer's disease. *Cereb. Cortex* **1991**, *1*, 103-116.
81. Fiala, J. C. Mechanisms of amyloid plaque pathogenesis. *Acta Neuropathol.* **2007**, *114*, 551-571.
82. Klein, W. L.; Krafft, G. A.; Finch, C. E. Targeting small A β oligomers: the solution to an Alzheimer's disease conundrum? *Trends Neurosci.* **2001**, *24*, 219-224.
83. Dahlgren, K. N.; Manelli, A. M.; Stine, W. B., Jr; Baker, L. K.; Krafft, G. A.; LaDu, M. J. Oligomeric and fibrillar species of amyloid- β peptides differentially affect neuronal viability. *J. Biol. Chem.* **2002**, *277*, 32046-32053.

84. Walsh, D. M.; Klyubin, I.; Fadeeva, J. V.; Rowan, M. J.; Selkoe, D. J. Amyloid- β oligomers: their production, toxicity and therapeutic inhibition. *Biochem. Soc. Trans.* **2002**, *30*, 552-557.
85. Walsh, D. M.; Klyubin, I.; Fadeeva, J. V.; Cullen, W. K.; Anwyl, R.; Wolfe, M. S.; Rowan, M. J.; Selkoe, D. J. Naturally secreted oligomers of amyloid β protein potently inhibit hippocampal long-term potentiation in vivo. *Nature* **2002**, *416*, 535-539.
86. Vekrellis, K.; Ye, Z.; Qiu, W. Q.; Walsh, D.; Hartley, D.; Chesneau, V.; Rosner, M. R.; Selkoe, D. J. Neurons regulate extracellular levels of amyloid β -protein via proteolysis by insulin-degrading enzyme. *J. Neurosci.* **2000**, *20*, 1657-1665.
87. Zhang, Y.; Hong, Y.; Bounhar, Y.; Blacker, M.; Roucou, X.; Tounekti, O.; Vereker, E.; Bowers, W. J.; Federoff, H. J.; Goodyer, C. G.; LeBlanc, A. P75 Neurotrophin Receptor Protects Primary Cultures of Human Neurons Against Extracellular Amyloid β Peptide Cytotoxicity. *J. Neurosci.* **2003**, *23*, 7385-7394.
88. DeMattos, R. B.; Cirrito, J. R.; Parsadanian, M.; May, P. C.; O'Dell, M. A.; Taylor, J. W.; Harmony, J. A.; Aronow, B. J.; Bales, K. R.; Paul, S. M.; Holtzman, D. M. ApoE and clusterin cooperatively suppress A β levels and deposition: evidence that ApoE regulates extracellular A β metabolism in vivo. *Neuron* **2004**, *41*, 193-202.
89. Grimm, H. S.; Beher, D.; Lichtenthaler, S. F.; Shearman, M. S.; Beyreuther, K.; Hartmann, T. γ -Secretase cleavage site specificity differs for intracellular and secretory amyloid β . *J. Biol. Chem.* **2003**, *278*, 13077-13085.
90. Hartmann, T.; Bieger, S. C.; Bruhl, B.; Tienari, P. J.; Ida, N.; Allsop, D.; Roberts, G. W.; Masters, C. L.; Dotti, C. G.; Unsicker, K.; Beyreuther, K. Distinct sites of intracellular production for Alzheimer's disease A $\beta_{40/42}$ amyloid peptides. *Nat. Med.* **1997**, *3*, 1016-1020.
91. Lee, H. K.; Kumar, P.; Fu, Q.; Rosen, K. M.; Querfurth, H. W. The insulin/Akt signaling pathway is targeted by intracellular β -amyloid. *Mol. Biol. Cell* **2009**, *20*, 1533-1544.
92. Walsh, D. M.; Tseng, B. P.; Rydel, R. E.; Podlisny, M. B.; Selkoe, D. J. The oligomerization of amyloid β -protein begins intracellularly in cells derived from human brain. *Biochemistry* **2000**, *39*, 10831-10839.
93. Friedrich, R. P.; Tepper, K.; Ronicke, R.; Soom, M.; Westermann, M.; Reymann, K.; Kaether, C.; Fandrich, M. Mechanism of amyloid plaque formation suggests an intracellular basis of A β pathogenicity. *Proc. Natl. Acad. Sci. U. S. A.* **2010**, *107*, 1942-1947.
94. Bayer, T. A.; Wirths, O. Intracellular accumulation of amyloid- β - a predictor for synaptic dysfunction and neuron loss in Alzheimer's disease. *Front. Aging Neurosci.* **2010**, *2*, 8.

95. LaFerla, F. M.; Green, K. N.; Oddo, S. Intracellular amyloid- β in Alzheimer's disease. *Nat. Rev. Neurosci.* **2007**, *8*, 499-509.
96. Li, M.; Chen, L.; Lee, D. H.; Yu, L. C.; Zhang, Y. The role of intracellular amyloid β in Alzheimer's disease. *Prog. Neurobiol.* **2007**, *83*, 131-139.
97. Wirths, O.; Multhaup, G.; Czech, C.; Blanchard, V.; Moussaoui, S.; Tremp, G.; Pradier, L.; Beyreuther, K.; Bayer, T. A. Intraneuronal A β accumulation precedes plaque formation in β -amyloid precursor protein and presenilin-1 double-transgenic mice. *Neurosci. Lett.* **2001**, *306*, 116-120.
98. Oddo, S.; Caccamo, A.; Shepherd, J. D.; Murphy, M. P.; Golde, T. E.; Kaye, R.; Metherate, R.; Mattson, M. P.; Akbari, Y.; LaFerla, F. M. Triple-transgenic model of Alzheimer's disease with plaques and tangles: intracellular A β and synaptic dysfunction. *Neuron* **2003**, *39*, 409-421.
99. Ohyaigi, Y.; Yamada, T.; Nishioka, K.; Clarke, N. J.; Tomlinson, A. J.; Naylor, S.; Nakabeppu, Y.; Kira, J.; Younkin, S. G. Selective increase in cellular A β_{42} is related to apoptosis but not necrosis. *Neuroreport* **2000**, *11*, 167-171.
100. Small, S. A.; Gandy, S. Sorting through the cell biology of Alzheimer's disease: intracellular pathways to pathogenesis. *Neuron* **2006**, *52*, 15-31.
101. Ferretti, M. T.; Bruno, M. A.; Ducatenzeiler, A.; Klein, W. L.; Cuellar, A. C. Intracellular A β -oligomers and early inflammation in a model of Alzheimer's disease. *Neurobiol. Aging* **2012**, *33*, 1329-1342.
102. Turner, R. S.; Suzuki, N.; Chyung, A. S.; Younkin, S. G.; Lee, V. M. Amyloids β_{40} and β_{42} are generated intracellularly in cultured human neurons and their secretion increases with maturation. *J. Biol. Chem.* **1996**, *271*, 8966-8970.
103. Tabira, T.; Chui, D. H.; Kuroda, S. Significance of intracellular A β_{42} accumulation in Alzheimer's disease. *Front. Biosci.* **2002**, *7*, a44-9.
104. Yang, A. J.; Chandswangbhuvana, D.; Shu, T.; Henschen, A.; Glabe, C. G. Intracellular accumulation of insoluble, newly synthesized A β_{n-42} in amyloid precursor protein-transfected cells that have been treated with A β_{1-42} . *J. Biol. Chem.* **1999**, *274*, 20650-20656.
105. Zhang, Y.; McLaughlin, R. W.; Goodyer, C.; LeBlanc, A. Selective cytotoxicity of intracellular amyloid β peptide1-42 through p53 and Bax in cultured primary human neurons. *J. Cell Biol.* **2002**, *156*, 519-529.

106. Yang, T. T.; Hsu, C. T.; Kuo, Y. M. Cell-derived soluble oligomers of human amyloid- β peptides disturb cellular homeostasis and induce apoptosis in primary hippocampal neurons. *J. Neural Transm.* **2009**, *116*, 1561-1569.
107. Gouras, G. K.; Almeida, C. G.; Takahashi, R. H. Intraneuronal A β accumulation and origin of plaques in Alzheimer's disease. *Neurobiol. Aging* **2005**, *26*, 1235-1244.
108. Billings, L. M.; Oddo, S.; Green, K. N.; McGaugh, J. L.; LaFerla, F. M. Intraneuronal A β causes the onset of early Alzheimer's disease-related cognitive deficits in transgenic mice. *Neuron* **2005**, *45*, 675-688.
109. Fernandez-Vizarra, P.; Fernandez, A. P.; Castro-Blanco, S.; Serrano, J.; Bentura, M. L.; Martinez-Murillo, R.; Martinez, A.; Rodrigo, J. Intra- and extracellular A β and PHF in clinically evaluated cases of Alzheimer's disease. *Histol. Histopathol.* **2004**, *19*, 823-844.
110. Chui, D. H.; Tanahashi, H.; Ozawa, K.; Ikeda, S.; Checler, F.; Ueda, O.; Suzuki, H.; Araki, W.; Inoue, H.; Shirotani, K.; Takahashi, K.; Gallyas, F.; Tabira, T. Transgenic mice with Alzheimer presenilin 1 mutations show accelerated neurodegeneration without amyloid plaque formation. *Nat. Med.* **1999**, *5*, 560-564.
111. Bates, K. A.; Verdile, G.; Li, Q. X.; Ames, D.; Hudson, P.; Masters, C. L.; Martins, R. N. Clearance mechanisms of Alzheimer's amyloid- β peptide: implications for therapeutic design and diagnostic tests. *Mol. Psychiatry* **2009**, *14*, 469-486.
112. Tahara, K.; Kim, H. D.; Jin, J. J.; Maxwell, J. A.; Li, L.; Fukuchi, K. Role of toll-like receptor signalling in A β uptake and clearance. *Brain* **2006**, *129*, 3006-3019.
113. Fan, J.; Donkin, J.; Wellington, C. Greasing the wheels of A β clearance in Alzheimer's disease: the role of lipids and apolipoprotein E. *Biofactors* **2009**, *35*, 239-248.
114. Wang, Y. J.; Zhou, H. D.; Zhou, X. F. Clearance of amyloid- β in Alzheimer's disease: progress, problems and perspectives. *Drug Discov. Today* **2006**, *11*, 931-938.
115. Deane, R.; Wu, Z.; Zlokovic, B. V. RAGE (yin) versus LRP (yang) balance regulates alzheimer amyloid β -peptide clearance through transport across the blood-brain barrier. *Stroke* **2004**, *35*, 2628-2631.
116. Camacho, I. E.; Serneels, L.; Spittaels, K.; Merchiers, P.; Dominguez, D.; De Strooper, B. Peroxisome-proliferator-activated receptor γ induces a clearance mechanism for the amyloid- β peptide. *J. Neurosci.* **2004**, *24*, 10908-10917.
117. Hellström-Lindahl, E.; Ravid, R.; Nordberg, A. Age-dependent decline of neprilysin in Alzheimer's disease and normal brain: Inverse correlation with A β levels. *Neurobiol. Aging* **2008**, *29*, 210-221.

118. Apelt, J.; Ach, K.; Schliebs, R. Aging-related down-regulation of neprilysin, a putative β -amyloid-degrading enzyme, in transgenic Tg2576 Alzheimer-like mouse brain is accompanied by an astroglial upregulation in the vicinity of β -amyloid plaques. *Neurosci. Lett.* **2003**, *339*, 183-186.
119. Wang, D. S.; Lipton, R. B.; Katz, M. J.; Davies, P.; Buschke, H.; Kuslansky, G.; Verghese, J.; Younkin, S. G.; Eckman, C.; Dickson, D. W. Decreased neprilysin immunoreactivity in Alzheimer disease, but not in pathological aging. *J. Neuropathol. Exp. Neurol.* **2005**, *64*, 378-385.
120. Gao, W.; Eisenhauer, P. B.; Conn, K.; Lynch, J. A.; Wells, J. M.; Ullman, M. D.; McKee, A.; Thatté, H. S.; Fine, R. E. Insulin degrading enzyme is expressed in the human cerebrovascular endothelium and in cultured human cerebrovascular endothelial cells. *Neurosci. Lett.* **2004**, *371*, 6-11.
121. Kurochkin, I. V.; Goto, S. Alzheimer's β -amyloid peptide specifically interacts with and is degraded by insulin degrading enzyme. *FEBS Lett.* **1994**, *345*, 33-37.
122. Thal, D. R. The role of astrocytes in amyloid β -protein toxicity and clearance. *Exp. Neurol.* **2012**, *236*, 1-5.
123. Hickman, S. E.; Allison, E. K.; El Khoury, J. Microglial dysfunction and defective β -amyloid clearance pathways in aging Alzheimer's disease mice. *J. Neurosci.* **2008**, *28*, 8354-8360.
124. Iliff, J. J.; Wang, M.; Liao, Y.; Plogg, B. A.; Peng, W.; Gundersen, G. A.; Benveniste, H.; Vates, G. E.; Deane, R.; Goldman, S. A.; Nagelhus, E. A.; Nedergaard, M. A paravascular pathway facilitates CSF flow through the brain parenchyma and the clearance of interstitial solutes, including amyloid β . *Sci. Transl. Med.* **2012**, *4*, 147ra111.
125. Boche, D.; Nicoll, J. A. The role of the immune system in clearance of A β from the brain. *Brain Pathol.* **2008**, *18*, 267-278.
126. Michaelis, M. L.; Dobrowsky, R. T.; Li, G. Tau neurofibrillary pathology and microtubule stability. *J. Mol. Neurosci.* **2002**, *19*, 289-293.
127. Jellinger, K. A.; Bancher, C. Neuropathology of Alzheimer's disease: a critical update. *J. Neural Transm. Suppl.* **1998**, *54*, 77-95.
128. Lu, M.; Kosik, K. S. Competition for microtubule-binding with dual expression of tau missense and splice isoforms. *Mol. Biol. Cell* **2001**, *12*, 171-184.
129. Lovestone, S.; Reynolds, C. H. The phosphorylation of tau: a critical stage in neurodevelopment and neurodegenerative processes. *Neuroscience* **1997**, *78*, 309-324.

130. Forman, M. S.; Trojanowski, J. Q.; Lee, V. M. Neurodegenerative diseases: a decade of discoveries paves the way for therapeutic breakthroughs. *Nat. Med.* **2004**, *10*, 1055-1063.
131. Goedert, M.; Spillantini, M. G.; Cairns, N. J.; Crowther, R. A. Tau proteins of Alzheimer paired helical filaments: abnormal phosphorylation of all six brain isoforms. *Neuron* **1992**, *8*, 159-168.
132. Lee, G.; Leugers, C. J. Tau and tauopathies. *Prog. Mol. Biol. Transl. Sci.* **2012**, *107*, 263-293.
133. Avila, J. The tau code. *Front. Aging Neurosci.* **2009**, *1*, 1.
134. Avila, J. Tau phosphorylation and aggregation in Alzheimer's disease pathology. *FEBS Lett.* **2006**, *580*, 2922-2927.
135. Greenough, M. A.; Camakaris, J.; Bush, A. I. Metal dyshomeostasis and oxidative stress in Alzheimer's disease. *Neurochem. Int.* **2013**, *62*, 540-555.
136. Hureau, C.; Faller, P. A β -mediated ROS production by Cu ions: structural insights, mechanisms and relevance to Alzheimer's disease. *Biochimie* **2009**, *91*, 1212-1217.
137. Dikalov, S. I.; Vitek, M. P.; Mason, R. P. Cupric-amyloid β peptide complex stimulates oxidation of ascorbate and generation of hydroxyl radical. *Free Radic. Biol. Med.* **2004**, *36*, 340-347.
138. Adlard, P. A.; Bush, A. I. In *Metal Ions and Alzheimer's Disease*; Malva, J. O., Rego, A. C., Cunha, R. A. and Oliveira, C. R., Eds.; Interaction between neurons and glia in aging and disease; Springer Science+Business Media, LLC: New York, NY, 2007; pp. 333-362.
139. Atwood, C. S.; Huang, X.; Moir, R. D.; Tanzi, R. E.; Bush, A. I. Role of free radicals and metal ions in the pathogenesis of Alzheimer's disease. *Met. Ions Biol. Syst.* **1999**, *36*, 309-364.
140. Huang, X.; Cuajungco, M. P.; Atwood, C. S.; Hartshorn, M. A.; Tyndall, J. D.; Hanson, G. R.; Stokes, K. C.; Leopold, M.; Multhaup, G.; Goldstein, L. E.; Scarpa, R. C.; Saunders, A. J.; Lim, J.; Moir, R. D.; Glabe, C.; Bowden, E. F.; Masters, C. L.; Fairlie, D. P.; Tanzi, R. E.; Bush, A. I. Cu(II) potentiation of alzheimer A β neurotoxicity. Correlation with cell-free hydrogen peroxide production and metal reduction. *J. Biol. Chem.* **1999**, *274*, 37111-37116.
141. Huang, X.; Atwood, C. S.; Hartshorn, M. A.; Multhaup, G.; Goldstein, L. E.; Scarpa, R. C.; Cuajungco, M. P.; Gray, D. N.; Lim, J.; Moir, R. D.; Tanzi, R. E.; Bush, A. I. The A β peptide of Alzheimer's disease directly produces hydrogen peroxide through metal ion reduction. *Biochemistry* **1999**, *38*, 7609-7616.

142. Tabner, B. J.; Mayes, J.; Allsop, D. Hypothesis: soluble A β oligomers in association with redox-active metal ions are the optimal generators of reactive oxygen species in Alzheimer's disease. *Int. J. Alzheimers Dis.* **2010**, *2011*, 546380.
143. Cherny, R. A.; Atwood, C. S.; Xilinas, M. E.; Gray, D. N.; Jones, W. D.; McLean, C. A.; Barnham, K. J.; Volitakis, I.; Fraser, F. W.; Kim, Y.; Huang, X.; Goldstein, L. E.; Moir, R. D.; Lim, J. T.; Beyreuther, K.; Zheng, H.; Tanzi, R. E.; Masters, C. L.; Bush, A. I. Treatment with a Copper-Zinc Chelator Markedly and Rapidly Inhibits β -Amyloid Accumulation in Alzheimer's Disease Transgenic Mice. *Neuron* **2001**, *30*, 665-676.
144. Opazo, C.; Huang, X.; Cherny, R. A.; Moir, R. D.; Roher, A. E.; White, A. R.; Cappai, R.; Masters, C. L.; Tanzi, R. E.; Inestrosa, N. C.; Bush, A. I. Metalloenzyme-like activity of Alzheimer's disease β -amyloid. Cu-dependent catalytic conversion of dopamine, cholesterol, and biological reducing agents to neurotoxic H₂O₂. *J. Biol. Chem.* **2002**, *277*, 40302-40308.
145. Jomova, K.; Valko, M. Advances in metal-induced oxidative stress and human disease. *Toxicology* **2011**, *283*, 65-87.
146. Stohs, S. J.; Bagchi, D. Oxidative mechanisms in the toxicity of metal ions. *Free Radic. Biol. Med.* **1995**, *18*, 321-336.
147. Exley, C. The aluminium-amyloid cascade hypothesis and Alzheimer's disease. *Subcell. Biochem.* **2005**, *38*, 225-234.
148. Exley, C. A molecular mechanism of aluminium-induced Alzheimer's disease? *J. Inorg. Biochem.* **1999**, *76*, 133-140.
149. Bolognin, S.; Messori, L.; Drago, D.; Gabbiani, C.; Cendron, L.; Zatta, P. Aluminum, copper, iron and zinc differentially alter amyloid-A β ₁₋₄₂ aggregation and toxicity. *Int. J. Biochem. Cell Biol.* **2011**, *43*, 877-885.
150. Drago, D.; Cavaliere, A.; Mascetra, N.; Ciavardelli, D.; di Ilio, C.; Zatta, P.; Sensi, S. L. Aluminum modulates effects of β amyloid(1-42) on neuronal calcium homeostasis and mitochondria functioning and is altered in a triple transgenic mouse model of Alzheimer's disease. *Rejuvenation Res.* **2008**, *11*, 861-871.
151. Exley, C. Aluminium and iron, but neither copper nor zinc, are key to the precipitation of β -sheets of A β ₄₂ in senile plaque cores in Alzheimer's disease. *J. Alzheimers Dis.* **2006**, *10*, 173-177.
152. Trapp, G. A.; Miner, G. D.; Zimmerman, R. L.; Mastri, A. R.; Heston, L. L. Aluminum levels in brain in Alzheimer's disease. *Biol. Psychiatry* **1978**, *13*, 709-718.

153. Bolognin, S.; Zatta, P.; Lorenzetto, E.; Valenti, M. T.; Buffelli, M. β -Amyloid-aluminum complex alters cytoskeletal stability and increases ROS production in cortical neurons. *Neurochem. Int.* **2013**, *62*, 566-574.
154. Bahadi, R.; Farrelly, P. V.; Kenna, B. L.; Curtain, C. C.; Masters, C. L.; Cappai, R.; Barnham, K. J.; Kourie, J. I. Cu^{2+} -induced modification of the kinetics of $\text{A}\beta(1-42)$ channels. *Am. J. Physiol. Cell. Physiol.* **2003**, *285*, C873-C880.
155. Dai, X. L.; Sun, Y. X.; Jiang, Z. F. Cu(II) potentiation of Alzheimer $\text{A}\beta_{1-40}$ cytotoxicity and transition on its secondary structure. *Acta Biochim. Biophys. Sin. (Shanghai)* **2006**, *38*, 765-772.
156. Lin, C. J.; Huang, H. C.; Jiang, Z. F. Cu(II) interaction with amyloid- β peptide: a review of neuroactive mechanisms in AD brains. *Brain Res. Bull.* **2010**, *82*, 235-242.
157. Pedersen, J. T.; Ostergaard, J.; Rozlosnik, N.; Gammelgaard, B.; Heegaard, N. H. Cu(II) mediates kinetically distinct, non-amyloidogenic aggregation of amyloid- β peptides. *J. Biol. Chem.* **2011**, *286*, 26952-26963.
158. Smith, D. P.; Ciccotosto, G. D.; Tew, D. J.; Fodero-Tavoletti, M. T.; Johanssen, T.; Masters, C. L.; Barnham, K. J.; Cappai, R. Concentration Dependent Cu^{2+} Induced Aggregation and Dityrosine Formation of the Alzheimer's Disease Amyloid- β Peptide. *Biochemistry* **2007**.
159. Bush, A. I. Copper, zinc, and the metallobiology of Alzheimer disease. *Alzheimer Dis. Assoc. Disord.* **2003**, *17*, 147-150.
160. Jun, S.; Saxena, S. The aggregated state of amyloid- β peptide in vitro depends on Cu^{2+} ion concentration. *Angew. Chem. Int. Ed Engl.* **2007**, *46*, 3959-3961.
161. Karr, J. W.; Kaupp, L. J.; Szalai, V. A. Amyloid- β binds Cu^{2+} in a mononuclear metal ion binding site. *J. Am. Chem. Soc.* **2004**, *126*, 13534-13538.
162. Hureau, C.; Balland, V.; Coppel, Y.; Solari, P. L.; Fonda, E.; Faller, P. Importance of dynamical processes in the coordination chemistry and redox conversion of copper amyloid- β complexes. *J. Biol. Inorg. Chem.* **2009**, *14*, 995-1000.
163. Atwood, C. S.; Moir, R. D.; Huang, X.; Scarpa, R. C.; Bacarra, N. M.; Romano, D. M.; Hartshorn, M. A.; Tanzi, R. E.; Bush, A. I. Dramatic aggregation of Alzheimer $\text{A}\beta$ by Cu(II) is induced by conditions representing physiological acidosis. *J. Biol. Chem.* **1998**, *273*, 12817-12826.
164. Hayashi, T.; Shishido, N.; Nakayama, K.; Nunomura, A.; Smith, M. A.; Perry, G.; Nakamura, M. Lipid peroxidation and 4-hydroxy-2-nonenal formation by copper ion bound to amyloid- β peptide. *Free Radic. Biol. Med.* **2007**, *43*, 1552-1559.

165. Amit, T.; Avramovich-Tirosh, Y.; Youdim, M. B.; Mandel, S. Targeting multiple Alzheimer's disease etiologies with multimodal neuroprotective and neurorestorative iron chelators. *FASEB J.* **2008**, *22*, 1296-1305.
166. Collingwood, J. F.; Mikhaylova, A.; Davidson, M.; Batich, C.; Streit, W. J.; Terry, J.; Dobson, J. In situ characterization and mapping of iron compounds in Alzheimer's disease tissue. *J. Alzheimers Dis.* **2005**, *7*, 267-272.
167. Deibel, M. A.; Ehmann, W. D.; Markesbery, W. R. Copper, iron, and zinc imbalances in severely degenerated brain regions in Alzheimer's disease: possible relation to oxidative stress. *J. Neurol. Sci.* **1996**, *143*, 137-142.
168. House, E.; Collingwood, J.; Khan, A.; Korchazkina, O.; Berthon, G.; Exley, C. Aluminium, iron, zinc and copper influence the in vitro formation of amyloid fibrils of A β ₄₂ in a manner which may have consequences for metal chelation therapy in Alzheimer's disease. *J. Alzheimers Dis.* **2004**, *6*, 291-301.
169. Lovell, M. A.; Robertson, J. D.; Teesdale, W. J.; Campbell, J. L.; Markesbery, W. R. Copper, iron and zinc in Alzheimer's disease senile plaques. *J. Neurol. Sci.* **1998**, *158*, 47-52.
170. Khan, A.; Dobson, J. P.; Exley, C. Redox cycling of iron by A β ₄₂. *Free Radic. Biol. Med.* **2006**, *40*, 557-569.
171. Tougu, V.; Karafin, A.; Zovo, K.; Chung, R. S.; Howells, C.; West, A. K.; Palumaa, P. Zn(II)- and Cu(II)-induced Nonfibrillar Aggregates of Amyloid- β (1-42) Peptide are Transformed to Amyloid Fibrils, both Spontaneously and under the Influence of Metal Chelators. *J. Neurochem.* **2009**.
172. Miller, L. M.; Wang, Q.; Telivala, T. P.; Smith, R. J.; Lanzirotti, A.; Miklossy, J. Synchrotron-based infrared and X-ray imaging shows focalized accumulation of Cu and Zn co-localized with β -amyloid deposits in Alzheimer's disease. *J. Struct. Biol.* **2006**, *155*, 30-37.
173. Ghalebani, L.; Wahlstrom, A.; Danielsson, J.; Warmlander, S. K.; Graslund, A. pH-dependence of the specific binding of Cu(II) and Zn(II) ions to the amyloid- β peptide. *Biochem. Biophys. Res. Commun.* **2012**, *421*, 554-560.
174. Bush, A. I.; Pettingell, W. H.; Multhaup, G.; d. Paradis, M.; Vonsattel, J. P.; Gusella, J. F.; Beyreuther, K.; Masters, C. L.; Tanzi, R. E. Rapid induction of Alzheimer A β amyloid formation by zinc. *Science* **1994**, *265*, 1464-1467.
175. Cuajungco, M. P.; Fagét, K. Y. Zinc takes the center stage: its paradoxical role in Alzheimer's disease. *Brain Res. Rev.* **2003**, *41*, 44-56.

176. Esler, W. P.; Stimson, E. R.; Jennings, J. M.; Ghilardi, J. R.; Mantyh, P. W.; Maggio, J. E. Zinc-induced aggregation of human and rat β -amyloid peptides in vitro. *J. Neurochem.* **1996**, *66*, 723-732.
177. Fitzgerald, D. J.; Maggio, J. E.; Esler, W. P.; Stimson, E. R.; Jennings, J. M.; Ghilardi, J. R.; Mantyh, P. W.; Bush, A. I.; Moir, R. D.; Rosenkranz, K. M.; Tanzi, R. E. Zinc and Alzheimer's disease. *Science* **1995**, *268*, 1920-1; author reply 1921-3.
178. Huang, X.; Atwood, C. S.; Moir, R. D.; Hartshorn, M. A.; Vonsattel, J. P.; Tanzi, R. E.; Bush, A. I. Zinc-induced Alzheimer's $A\beta_{1-40}$ aggregation is mediated by conformational factors. *J. Biol. Chem.* **1997**, *272*, 26464-26470.
179. Ichinohe, N.; Hayashi, M.; Wakabayashi, K.; Rockland, K. S. Distribution and progression of amyloid- β deposits in the amygdala of the aged macaque monkey, and parallels with zinc distribution. *Neuroscience* **2009**, *159*, 1374-1383.
180. Zhang, C. F.; Yang, P. Zinc-induced aggregation of $A\beta$ (10-21) potentiates its action on voltage-gated potassium channel. *Biochem. Biophys. Res. Commun.* **2006**, *345*, 43-49.
181. Faller, P. Copper and zinc binding to amyloid- β : coordination, dynamics, aggregation, reactivity and metal-ion transfer. *Chembiochem* **2009**, *10*, 2837-2845.
182. Yankner, B. A.; Duffy, L. K.; Kirschner, D. A. Neurotrophic and neurotoxic effects of amyloid β protein: reversal by tachykinin neuropeptides. *Science* **1990**, *250*, 279-282.
183. Jiang, D.; Li, X.; Liu, L.; Yagnik, G. B.; Zhou, F. Reaction rates and mechanism of the ascorbic acid oxidation by molecular oxygen facilitated by Cu(II)-containing amyloid- β complexes and aggregates. *J Phys Chem B* **2010**, *114*, 4896-4903.
184. Kang, J.; Park, E. J.; Jou, I.; Kim, J. H.; Joe, E. H. Reactive oxygen species mediate $A\beta$ (25-35)-induced activation of BV-2 microglia. *Neuroreport* **2001**, *12*, 1449-1452.
185. Multhaup, G.; Ruppert, T.; Schlicksupp, A.; Hesse, L.; Behr, D.; Masters, C. L.; Beyreuther, K. Reactive oxygen species and Alzheimer's disease. *Biochem. Pharmacol.* **1997**, *54*, 533-539.
186. Kadowaki, H.; Nishitoh, H.; Urano, F.; Sadamitsu, C.; Matsuzawa, A.; Takeda, K.; Masutani, H.; Yodoi, J.; Urano, Y.; Nagano, T.; Ichijo, H. Amyloid β induces neuronal cell death through ROS-mediated ASK1 activation. *Cell Death Differ.* **2005**, *12*, 19-24.
187. Sponne, I.; Fifre, A.; Drouet, B.; Klein, C.; Koziel, V.; Pincon-Raymond, M.; Olivier, J. L.; Chambaz, J.; Pillot, T. Apoptotic neuronal cell death induced by the non-fibrillar amyloid- β peptide proceeds through an early reactive oxygen species-dependent cytoskeleton perturbation. *J. Biol. Chem.* **2003**, *278*, 3437-3445.

188. Butterfield, D. A.; Reed, T.; Newman, S. F.; Sultana, R. Roles of amyloid β -peptide-associated oxidative stress and brain protein modifications in the pathogenesis of Alzheimer's disease and mild cognitive impairment. *Free Radic. Biol. Med.* **2007**, *43*, 658-677.
189. Sultana, R.; Perluigi, M.; Butterfield, D. A. Oxidatively modified proteins in Alzheimer's disease (AD), mild cognitive impairment and animal models of AD: role of A β in pathogenesis. *Acta Neuropathol.* **2009**, *118*, 131-150.
190. Egana, J. T.; Zambrano, C.; Nunez, M. T.; Gonzalez-Billault, C.; Maccioni, R. B. Iron-induced oxidative stress modify tau phosphorylation patterns in hippocampal cell cultures. *Biometals* **2003**, *16*, 215-223.
191. Sjogren, M.; Mielke, M.; Gustafson, D.; Zandi, P.; Skoog, I. Cholesterol and Alzheimer's disease--is there a relation? *Mech. Ageing Dev.* **2006**, *127*, 138-147.
192. Eckert, G. P.; Kirsch, C.; Leutz, S.; Wood, W. G.; Muller, W. E. Cholesterol modulates amyloid β -peptide's membrane interactions. *Pharmacopsychiatry* **2003**, *36 Suppl 2*, S136-43.
193. Gong, J. S.; Sawamura, N.; Zou, K.; Sakai, J.; Yanagisawa, K.; Michikawa, M. Amyloid β -protein affects cholesterol metabolism in cultured neurons: implications for pivotal role of cholesterol in the amyloid cascade. *J. Neurosci. Res.* **2002**, *70*, 438-446.
194. Runz, H.; Rietdorf, J.; Tomic, I.; de Bernard, M.; Beyreuther, K.; Pepperkok, R.; Hartmann, T. Inhibition of intracellular cholesterol transport alters presenilin localization and amyloid precursor protein processing in neuronal cells. *J. Neurosci.* **2002**, *22*, 1679-1689.
195. Colell, A.; Fernandez, A.; Fernandez-Checa, J. C. Mitochondria, cholesterol and amyloid β peptide: a dangerous trio in Alzheimer disease. *J. Bioenerg. Biomembr.* **2009**.
196. Arispe, N.; Doh, M. Plasma membrane cholesterol controls the cytotoxicity of Alzheimer's disease A β P (1-40) and (1-42) peptides. *FASEB J.* **2002**, *16*, 1526-1536.
197. Yip, C. M.; Elton, E. A.; Darabie, A. A.; Morrison, M. R.; McLaurin, J. Cholesterol, a modulator of membrane-associated A β -fibrillogenesis and neurotoxicity. *J. Mol. Biol.* **2001**, *311*, 723-734.
198. McLaurin, J.; Darabie, A. A.; Morrison, M. R. Cholesterol, a modulator of membrane-associated A β -fibrillogenesis. *Pharmacopsychiatry* **2003**, *36 Suppl 2*, S130-5.
199. Vestergaard, M.; Hamada, T.; Takagi, M. Using model membranes for the study of amyloid β :lipid interactions and neurotoxicity. *Biotechnol. Bioeng.* **2008**, *99*, 753-763.

200. Michikawa, M.; Gong, J. S.; Fan, Q. W.; Sawamura, N.; Yanagisawa, K. A novel action of alzheimer's amyloid β -protein (A β): oligomeric A β promotes lipid release. *J. Neurosci.* **2001**, *21*, 7226-7235.
201. Fan, Q. W.; Yu, W.; Senda, T.; Yanagisawa, K.; Michikawa, M. Cholesterol-dependent modulation of tau phosphorylation in cultured neurons. *J. Neurochem.* **2001**, *76*, 391-400.
202. Fernandez, A.; Llacuna, L.; Fernandez-Checa, J. C.; Colell, A. Mitochondrial cholesterol loading exacerbates amyloid β peptide-induced inflammation and neurotoxicity. *J. Neurosci.* **2009**, *29*, 6394-6405.
203. Yanagisawa, K. Cholesterol and A β aggregation. *Pharmacopsychiatry* **2003**, *36 Suppl 2*, S127-9.
204. Lau, T. L.; Ambroggio, E. E.; Tew, D. J.; Cappai, R.; Masters, C. L.; Fidelio, G. D.; Barnham, K. J.; Separovic, F. Amyloid- β peptide disruption of lipid membranes and the effect of metal ions. *J. Mol. Biol.* **2006**, *356*, 759-770.
205. Curtain, C. C.; Ali, F. E.; Smith, D. G.; Bush, A. I.; Masters, C. L.; Barnham, K. J. Metal ions, pH, and cholesterol regulate the interactions of Alzheimer's disease amyloid- β peptide with membrane lipid. *J. Biol. Chem.* **2003**, *278*, 2977-2982.
206. Devanathan, S.; Salamon, Z.; Lindblom, G.; Grobner, G.; Tollin, G. Effects of sphingomyelin, cholesterol and zinc ions on the binding, insertion and aggregation of the amyloid A β (1-40) peptide in solid-supported lipid bilayers. *FEBS J.* **2006**, *273*, 1389-1402.
207. Lemkul, J. A.; Bevan, D. R. Lipid composition influences the release of Alzheimer's amyloid β -peptide from membranes. *Protein Sci.* **2011**, *20*, 1530-1545.
208. Widenbrant, M. J. O.; Rajadas, J.; Sutardja, C.; Fuller, G. G. Lipid-Induced β -Amyloid Peptide Assemblage Fragmentation. *Biophys. J.* **2006**, *91*, 4071-4080.
209. Eehalt, R.; Keller, P.; Haass, C.; Thiele, C.; Simons, K. Amyloidogenic processing of the Alzheimer β -amyloid precursor protein depends on lipid rafts. *J. Cell Biol.* **2003**, *160*, 113-123.
210. Friedman, R.; Pellarin, R.; Caflich, A. Amyloid aggregation on lipid bilayers and its impact on membrane permeability. *J. Mol. Biol.* **2009**, *387*, 407-415.
211. Yip, C. M.; Darabie, A. A.; McLaurin, J. A β ₄₂-peptide assembly on lipid bilayers. *J. Mol. Biol.* **2002**, *318*, 97-107.

212. Grösgen, S.; Grimm, M. O. W.; Frieß, P.; Hartmann, T. Role of amyloid β in lipid homeostasis. *Biochimica et Biophysica Acta (BBA) - Molecular and Cell Biology of Lipids* **2010**, *1801*, 966-974.
213. Cordy, J. M.; Hooper, N. M.; Turner, A. J. The involvement of lipid rafts in Alzheimer's disease. *Mol. Membr. Biol.* **2006**, *23*, 111-122.
214. Mielke, M. M.; Lyketsos, C. G. Lipids and the pathogenesis of Alzheimer's disease: is there a link? *Int. Rev. Psychiatry.* **2006**, *18*, 173-186.
215. Arlt, S.; Beisiegel, U.; Kontush, A. Lipid peroxidation in neurodegeneration: new insights into Alzheimer's disease. *Curr. Opin. Lipidol.* **2002**, *13*, 289-294.
216. Gonzalez, C.; Martin, T.; Cacho, J.; Brenas, M. T.; Arroyo, T.; Garcia-Berrocal, B.; Navajo, J. A.; Gonzalez-Buitrago, J. M. Serum zinc, copper, insulin and lipids in Alzheimer's disease epsilon 4 apolipoprotein E allele carriers. *Eur. J. Clin. Invest.* **1999**, *29*, 637-642.
217. Florent-Bechard, S.; Desbene, C.; Garcia, P.; Allouche, A.; Youssef, I.; Escanye, M. C.; Koziel, V.; Hanse, M.; Malaplate-Armand, C.; Stenger, C. The essential role of lipids in Alzheimer's disease. *Biochimie* **2009**, *91*, 804-809.
218. Martins, I. C.; Kuperstein, I.; Wilkinson, H.; Maes, E.; Vanbrabant, M.; Jonckheere, W.; Van Gelder, P.; Hartmann, D.; D'Hooge, R.; De Strooper, B.; Schymkowitz, J.; Rousseau, F. Lipids revert inert A β amyloid fibrils to neurotoxic protofibrils that affect learning in mice. *EMBO J.* **2008**, *27*, 224-233.
219. Vestergaard, M.; Hamada, T.; Morita, M.; Takagi, M. Cholesterol, lipids, amyloid β , and Alzheimer's. *Curr. Alzheimer Res.* **2010**, *7*, 262-270.
220. Camandola, S.; Poli, G.; Mattson, M. P. The lipid peroxidation product 4-hydroxy-2,3-nonenal inhibits constitutive and inducible activity of nuclear factor κ B in neurons. *Brain Res. Mol. Brain Res.* **2000**, *85*, 53-60.
221. Chaudhary, P.; Sharma, R.; Sharma, A.; Vatsyayan, R.; Yadav, S.; Singhal, S. S.; Rauniyar, N.; Prokai, L.; Awasthi, S.; Awasthi, Y. C. Mechanisms of 4-hydroxy-2-nonenal induced pro- and anti-apoptotic signaling. *Biochemistry* **2010**, *49*, 6263-6275.
222. Perluigi, M.; Coccia, R.; Butterfield, D. A. 4-Hydroxy-2-Nonenal, a Reactive Product of Lipid Peroxidation, and Neurodegenerative Diseases: A Toxic Combination Illuminated by Redox Proteomics Studies. *Antioxid. Redox Signal.* **2012**.
223. Butterfield, D. A.; Bader Lange, M. L.; Sultana, R. Involvements of the lipid peroxidation product, HNE, in the pathogenesis and progression of Alzheimer's disease. *Biochim. Biophys. Acta* **2010**, *1801*, 924-929.

224. Tang, S. C.; Lathia, J. D.; Selvaraj, P. K.; Jo, D. G.; Mughal, M. R.; Cheng, A.; Siler, D. A.; Markesbery, W. R.; Arumugam, T. V.; Mattson, M. P. Toll-like receptor-4 mediates neuronal apoptosis induced by amyloid β -peptide and the membrane lipid peroxidation product 4-hydroxynonenal. *Exp. Neurol.* **2008**, *213*, 114-121.
225. Butterfield, D. A.; Lauderback, C. M. Lipid peroxidation and protein oxidation in Alzheimer's disease brain: potential causes and consequences involving amyloid β -peptide-associated free radical oxidative stress. *Free Radic. Biol. Med.* **2002**, *32*, 1050-1060.
226. Castegna, A.; Lauderback, C. M.; Mohammad-Abdul, H.; Butterfield, D. A. Modulation of phospholipid asymmetry in synaptosomal membranes by the lipid peroxidation products, 4-hydroxynonenal and acrolein: implications for Alzheimer's disease. *Brain Res.* **2004**, *1004*, 193-197.
227. Markesbery, W. R.; Lovell, M. A. Four-Hydroxynonenal, a Product of Lipid Peroxidation, is Increased in the Brain in Alzheimer's Disease. *Neurobiol. Aging* **1998**, *19*, 33-36.
228. Reed, T. T.; Pierce, W. M.; Markesbery, W. R.; Butterfield, D. A. Proteomic identification of HNE-bound proteins in early Alzheimer disease: Insights into the role of lipid peroxidation in the progression of AD. *Brain Res.* **2009**, *1274*, 66-76.
229. Pollard, H. B.; Rojas, E.; Arispe, N. A new hypothesis for the mechanism of amyloid toxicity, based on the calcium channel activity of amyloid β protein (A β P) in phospholipid bilayer membranes. *Ann. N. Y. Acad. Sci.* **1993**, *695*, 165-168.
230. Berridge, M. J. Calcium hypothesis of Alzheimer's disease. *Pflugers Arch.* **2010**, *459*, 441-449.
231. Berridge, M. J. Calcium signalling and Alzheimer's disease. *Neurochem. Res.* **2011**, *36*, 1149-1156.
232. Demuro, A.; Mina, E.; Kaye, R.; Milton, S. C.; Parker, I.; Glabe, C. G. Calcium dysregulation and membrane disruption as a ubiquitous neurotoxic mechanism of soluble amyloid oligomers. *J. Biol. Chem.* **2005**, *280*, 17294-17300.
233. Isaacs, A. M.; Senn, D. B.; Yuan, M.; Shine, J. P.; Yankner, B. A. Acceleration of amyloid β -peptide aggregation by physiological concentrations of calcium. *J. Biol. Chem.* **2006**, *281*, 27916-27923.
234. Kawahara, M.; Kuroda, Y. Molecular mechanism of neurodegeneration induced by Alzheimer's β -amyloid protein: channel formation and disruption of calcium homeostasis. *Brain Res. Bull.* **2000**, *53*, 389-397.

235. Suo, Z.; Fang, C.; Crawford, F.; Mullan, M. Superoxide free radical and intracellular calcium mediate A β ₁₋₄₂ induced endothelial toxicity. *Brain Res.* **1997**, *762*, 144-152.
236. Buxbaum, J. D.; Ruefli, A. A.; Parker, C. A.; Cypess, A. M.; Greengard, P. Calcium regulates processing of the Alzheimer amyloid protein precursor in a protein kinase C-independent manner. *Proc. Natl. Acad. Sci. U. S. A.* **1994**, *91*, 4489-4493.
237. Demuro, A.; Parker, I.; Stutzmann, G. E. Calcium signaling and amyloid toxicity in Alzheimer disease. *J. Biol. Chem.* **2010**, *285*, 12463-12468.
238. Ferreira, E.; Oliveira, C. R.; Pereira, C. M. The release of calcium from the endoplasmic reticulum induced by amyloid- β and prion peptides activates the mitochondrial apoptotic pathway. *Neurobiol. Dis.* **2008**, *30*, 331-342.
239. Supnet, C.; Bezprozvanny, I. The dysregulation of intracellular calcium in Alzheimer disease. *Cell Calcium* **2010**, *47*, 183-189.
240. Casley, C. S.; Canevari, L.; Land, J. M.; Clark, J. B.; Sharpe, M. A. β -amyloid inhibits integrated mitochondrial respiration and key enzyme activities. *J. Neurochem.* **2002**, *80*, 91-100.
241. Lustbader, J. W.; Cirilli, M.; Lin, C.; Xu, H. W.; Takuma, K.; Wang, N.; Caspersen, C.; Chen, X.; Pollak, S.; Chaney, M.; Trinchese, F.; Liu, S.; Gunn-Moore, F.; Lue, L. F.; Walker, D. G.; Kuppusamy, P.; Zewier, Z. L.; Arancio, O.; Stern, D.; Yan, S. S.; Wu, H. ABAD directly links A β to mitochondrial toxicity in Alzheimer's disease. *Science* **2004**, *304*, 448-452.
242. Manczak, M.; Anekonda, T. S.; Henson, E.; Park, B. S.; Quinn, J.; Reddy, P. H. Mitochondria are a direct site of A β accumulation in Alzheimer's disease neurons: implications for free radical generation and oxidative damage in disease progression. *Hum. Mol. Genet.* **2006**, *15*, 1437-1449.
243. Swerdlow, R. H.; Khan, S. M. A "mitochondrial cascade hypothesis" for sporadic Alzheimer's disease. *Med. Hypotheses* **2004**, *63*, 8-20.
244. Swerdlow, R. H.; Burns, J. M.; Khan, S. M. The Alzheimer's disease mitochondrial cascade hypothesis. *J. Alzheimers Dis.* **2010**, *20 Suppl 2*, S265-79.
245. Wang, X.; Perry, G.; Smith, M. A.; Zhu, X. Amyloid- β -derived diffusible ligands cause impaired axonal transport of mitochondria in neurons. *Neurodegener Dis.* **2010**, *7*, 56-59.
246. Eckert, A.; Schulz, K. L.; Rhein, V.; Gotz, J. Convergence of amyloid- β and tau pathologies on mitochondria in vivo. *Mol. Neurobiol.* **2010**, *41*, 107-114.

247. Eckert, A.; Schmitt, K.; Gotz, J. Mitochondrial dysfunction - the beginning of the end in Alzheimer's disease? Separate and synergistic modes of tau and amyloid- β toxicity. *Alzheimers Res. Ther.* **2011**, *3*, 15.
248. Keil, U.; Hauptmann, S.; Bonert, A.; Scherping, I.; Eckert, A.; Muller, W. E. Mitochondrial dysfunction induced by disease relevant A β PP and tau protein mutations. *J. Alzheimers Dis.* **2006**, *9*, 139-146.
249. Atamna, H.; Frey, W. H., 2nd Mechanisms of mitochondrial dysfunction and energy deficiency in Alzheimer's disease. *Mitochondrion* **2007**, *7*, 297-310.
250. Davis, J. N.; Hunnicutt Jr, E. J.; Chisholm, J. C. A mitochondrial bottleneck hypothesis of Alzheimer's disease. *Mol. Med. Today* **1995**, *1*, 240-247.
251. Gibson, G. E.; Starkov, A.; Blass, J. P.; Ratan, R. R.; Beal, M. F. Cause and consequence: Mitochondrial dysfunction initiates and propagates neuronal dysfunction, neuronal death and behavioral abnormalities in age-associated neurodegenerative diseases. *Biochimica et Biophysica Acta (BBA) - Molecular Basis of Disease* **2010**, *1802*, 122-134.
252. Dragicevic, N.; Mamcarz, M.; Zhu, Y.; Buzzeo, R.; Tan, J.; Arendash, G. W.; Bradshaw, P. C. Mitochondrial amyloid- β levels are associated with the extent of mitochondrial dysfunction in different brain regions and the degree of cognitive impairment in Alzheimer's transgenic mice. *J. Alzheimers Dis.* **2010**, *20 Suppl 2*, S535-50.
253. Hsu, M. J.; Sheu, J. R.; Lin, C. H.; Shen, M. Y.; Hsu, C. Y. Mitochondrial mechanisms in amyloid β peptide-induced cerebrovascular degeneration. *Biochim. Biophys. Acta* **2010**, *1800*, 290-296.
254. Riemer, J.; Kins, S. Axonal Transport and Mitochondrial Dysfunction in Alzheimer's Disease. *Neurodegener Dis.* **2012**.
255. Peters, I.; Igbavboa, U.; Schutt, T.; Haidari, S.; Hartig, U.; Rosello, X.; Bottner, S.; Copanaki, E.; Deller, T.; Kogel, D.; Wood, W. G.; Muller, W. E.; Eckert, G. P. The interaction of β -amyloid protein with cellular membranes stimulates its own production. *Biochim. Biophys. Acta* **2009**, *1788*, 964-972.
256. Lau, T.; Gehman, J. D.; Wade, J. D.; Perez, K.; Masters, C. L.; Barnham, K. J.; Separovic, F. Membrane interactions and the effect of metal ions of the amyloidogenic fragment A β (25–35) in comparison to A β (1–42). *Biochimica et Biophysica Acta (BBA) - Biomembranes* **2007**, *1768*, 2400-2408.
257. Askarova, S.; Yang, X.; Lee, J. C. Impacts of membrane biophysics in Alzheimer's disease: from amyloid precursor protein processing to A β Peptide-induced membrane changes. *Int. J. Alzheimers Dis.* **2011**, *2011*, 134971.

258. Price, K. A.; Crouch, P. J.; Donnelly, P. S.; Masters, C. L.; White, A. R.; Curtain, C. C. Membrane-targeted strategies for modulating APP and A β -mediated toxicity. *J. Cell. Mol. Med.* **2009**, *13*, 249-261.
259. Williams, T. L.; Serpell, L. C. Membrane and surface interactions of Alzheimer's A β peptide--insights into the mechanism of cytotoxicity. *FEBS J.* **2011**, *278*, 3905-3917.
260. Eikelenboom, P.; Veerhuis, R. The role of complement and activated microglia in the pathogenesis of Alzheimer's disease. *Neurobiol. Aging* **1996**, *17*, 673-680.
261. Siu, G.; Clifford, P.; Kosciuk, M.; Venkataraman, V.; Nagele, R. G. In *Glial Cells and A β Peptides in Alzheimer's Disease Pathogenesis*; Barrow, C. J., Small, D. H., Eds.; A β peptide and Alzheimer's disease - Celebrating a century of research; Springer: London, 2007; pp. 216-233.
262. Mrak, R. E.; Sheng, J. G.; Griffin, W. S. Glial cytokines in Alzheimer's disease: review and pathogenic implications. *Hum. Pathol.* **1995**, *26*, 816-823.
263. Walsh, D. T.; Bresciani, L.; Saunders, D.; Manca, M. F.; Jen, A.; Gentleman, S. M.; Jen, L. S. Amyloid β peptide causes chronic glial cell activation and neuro-degeneration after intravitreal injection. *Neuropathol. Appl. Neurobiol.* **2005**, *31*, 491-502.
264. Meda, L.; Baron, P.; Scarlato, G. Glial activation in Alzheimer's disease: the role of A β and its associated proteins. *Neurobiol. Aging* **2001**, *22*, 885-893.
265. Holcomb, L. A.; Gordon, M. N.; Benkovic, S. A.; Morgan, D. G. A β and perlecan in rat brain: glial activation, gradual clearance and limited neurotoxicity. *Mech. Ageing Dev.* **2000**, *112*, 135-152.
266. Haertig, W.; Bruckner, G.; Schmidt, C.; Brauer, K.; Bodewitz, G.; Turner, J. D.; Bigl, V. Co-localization of β -amyloid peptides, apolipoprotein E and glial markers in senile plaques in the prefrontal cortex of old rhesus monkeys. *Brain Res.* **1997**, *751*, 315-322.
267. Mohamed, A.; Posse de Chaves, E. A β internalization by neurons and glia. *Int. J. Alzheimers Dis.* **2011**, *2011*, 127984.
268. Nagele, R. G.; Wegiel, J.; Venkataraman, V.; Imaki, H.; Wang, K. C.; Wegiel, J. Contribution of glial cells to the development of amyloid plaques in Alzheimer's disease. *Neurobiol. Aging* **2004**, *25*, 663-674.
269. Serrano-Pozo, A.; Mielke, M. L.; Gomez-Isla, T.; Betensky, R. A.; Growdon, J. H.; Frosch, M. P.; Hyman, B. T. Reactive glia not only associates with plaques but also parallels tangles in Alzheimer's disease. *Am. J. Pathol.* **2011**, *179*, 1373-1384.

270. Wisniewski, H. M.; Wegiel, J. Spatial relationships between astrocytes and classical plaque components. *Neurobiol. Aging* **1991**, *12*, 593-600.
271. Thal, D. R.; Schultz, C.; Dehghani, F.; Yamaguchi, H.; Braak, H.; Braak, E. Amyloid β -protein (A β)-containing astrocytes are located preferentially near N-terminal-truncated A β deposits in the human entorhinal cortex. *Acta Neuropathol.* **2000**, *100*, 608-617.
272. Nagele, R. G.; D'Andrea, M. R.; Lee, H.; Venkataraman, V.; Wang, H. Y. Astrocytes accumulate A β ₄₂ and give rise to astrocytic amyloid plaques in Alzheimer disease brains. *Brain Res.* **2003**, *971*, 197-209.
273. Thal, D. R.; Hartig, W.; Schober, R. Diffuse plaques in the molecular layer show intracellular A β ₈₋₁₇-immunoreactive deposits in subpial astrocytes. *Clin. Neuropathol.* **1999**, *18*, 226-231.
274. Paresce, D. M.; Ghosh, R. N.; Maxfield, F. R. Microglial cells internalize aggregates of the Alzheimer's disease amyloid β -protein via a scavenger receptor. *Neuron* **1996**, *17*, 553-565.
275. Akiyama, H.; Mori, H.; Saido, T.; Kondo, H.; Ikeda, K.; McGeer, P. L. Occurrence of the diffuse amyloid β -protein (A β) deposits with numerous A β -containing glial cells in the cerebral cortex of patients with Alzheimer's disease. *Glia* **1999**, *25*, 324-331.
276. Ard, M. D.; Cole, G. M.; Wei, J.; Mehrle, A. P.; Fratkin, J. D. Scavenging of Alzheimer's amyloid β -protein by microglia in culture. *J. Neurosci. Res.* **1996**, *43*, 190-202.
277. Chung, H.; Brazil, M. I.; Soe, T. T.; Maxfield, F. R. Uptake, degradation, and release of fibrillar and soluble forms of Alzheimer's amyloid β -peptide by microglial cells. *J. Biol. Chem.* **1999**, *274*, 32301-32308.
278. DeWitt, D. A.; Perry, G.; Cohen, M.; Doller, C.; Silver, J. Astrocytes regulate microglial phagocytosis of senile plaque cores of Alzheimer's disease. *Exp. Neurol.* **1998**, *149*, 329-340.
279. Kurt, M. A.; Davies, D. C.; Kidd, M. β -Amyloid immunoreactivity in astrocytes in Alzheimer's disease brain biopsies: an electron microscope study. *Exp. Neurol.* **1999**, *158*, 221-228.
280. Wegiel, J.; Wang, K. C.; Tarnawski, M.; Lach, B. Microglia cells are the driving force in fibrillar plaque formation, whereas astrocytes are a leading factor in plaque degradation. *Acta Neuropathol.* **2000**, *100*, 356-364.
281. Balin, B. J.; Gerard, H. C.; Arking, E. J.; Appelt, D. M.; Branigan, P. J.; Abrams, J. T.; Whittum-Hudson, J. A.; Hudson, A. P. Identification and localization of *Chlamydia pneumoniae* in the Alzheimer's brain. *Med. Microbiol. Immunol.* **1998**, *187*, 23-42.
282. Kamer, A. R.; Craig, R. G.; Pirraglia, E.; Dasanayake, A. P.; Norman, R. G.; Boylan, R. J.; Nehorayoff, A.; Glodzik, L.; Brys, M.; de Leon, M. J. TNF- α and antibodies to periodontal

- bacteria discriminate between Alzheimer's disease patients and normal subjects. *J. Neuroimmunol.* **2009**, *216*, 92-97.
283. Urosevic, N.; Martins, R. N. Infection and Alzheimer's disease: the APOE epsilon4 connection and lipid metabolism. *J. Alzheimers Dis.* **2008**, *13*, 421-435.
284. Honjo, K.; van Reekum, R.; Verhoeff, N. P. Alzheimer's disease and infection: do infectious agents contribute to progression of Alzheimer's disease? *Alzheimers Dement.* **2009**, *5*, 348-360.
285. Nicolson, G. L. Chronic Bacterial and Viral Infections in Neurodegenerative and Neurobehavioral Diseases. *Lab Medicine* **2008**, *39*, 291-299.
286. Carter, C. Alzheimer's Disease: APP, γ Secretase, APOE, CLU, CR1, PICALM, ABCA7, BIN1, CD2AP, CD33, EPHA1, and MS4A2, and Their Relationships with Herpes Simplex, C. *Pneumoniae*, Other Suspect Pathogens, and the Immune System. *Int. J. Alzheimers Dis.* **2011**, *2011*, 501862.
287. Yucesan, C.; Sriram, S. *Chlamydia pneumoniae* infection of the central nervous system. *Curr. Opin. Neurol.* **2001**, *14*, 355-359.
288. Letenneur, L.; Peres, K.; Fleury, H.; Garrigue, I.; Barberger-Gateau, P.; Helmer, C.; Orgogozo, J. M.; Gauthier, S.; Dartigues, J. F. Seropositivity to herpes simplex virus antibodies and risk of Alzheimer's disease: a population-based cohort study. *PLoS One* **2008**, *3*, e3637.
289. Wozniak, M. A.; Mee, A. P.; Itzhaki, R. F. Herpes simplex virus type 1 DNA is located within Alzheimer's disease amyloid plaques. *J. Pathol.* **2009**, *217*, 131-138.
290. Kammerman, E. M.; Neumann, D. M.; Ball, M. J.; Lukiw, W.; Hill, J. M. Senile plaques in Alzheimer's diseased brains: possible association of β -amyloid with herpes simplex virus type 1 (HSV-1) L-particles. *Med. Hypotheses* **2006**, *66*, 294-299.
291. Katan, M.; Moon, Y. P.; Paik, M. C.; Sacco, R. L.; Wright, C. B.; Elkind, M. S. Infectious burden and cognitive function: the Northern Manhattan Study. *Neurology* **2013**, *80*, 1209-1215.
292. Itzhaki, R. F.; Lin, W. R.; Shang, D.; Wilcock, G. K.; Faragher, B.; Jamieson, G. A. Herpes simplex virus type 1 in brain and risk of Alzheimer's disease. *Lancet* **1997**, *349*, 241-244.
293. Carter, C. J. Alzheimer's disease plaques and tangles: cemeteries of a pyrrhic victory of the immune defence network against herpes simplex infection at the expense of complement and inflammation-mediated neuronal destruction. *Neurochem. Int.* **2011**, *58*, 301-320.
294. Carter, C. J. APP, APOE, complement receptor 1, clusterin and PICALM and their involvement in the herpes simplex life cycle. *Neurosci. Lett.* **2010**, *483*, 96-100.

295. Wang, Z.; Zhang, X.; Wang, H.; Qi, L.; Lou, Y. Neuroprotective effects of icaritin against β amyloid-induced neurotoxicity in primary cultured rat neuronal cells via estrogen-dependent pathway. *Neuroscience* **2007**, *145*, 911-922.
296. Henderson, V. W. Estrogen-containing hormone therapy and Alzheimer's disease risk: Understanding discrepant inferences from observational and experimental research. *Neuroscience* **2006**, *138*, 1031-1039.
297. Yue, X.; Lu, M.; Lancaster, T.; Cao, P.; Honda, S.; Staufenbiel, M.; Harada, N.; Zhong, Z.; Shen, Y.; Li, R. Brain estrogen deficiency accelerates A β plaque formation in an Alzheimer's disease animal model. *Proc. Natl. Acad. Sci. U. S. A.* **2005**, *102*, 19198-19203.
298. Nilsen, J.; Chen, S.; Irwin, R. W.; Iwamoto, S.; Brinton, R. D. Estrogen protects neuronal cells from amyloid β -induced apoptosis via regulation of mitochondrial proteins and function. *BMC Neurosci.* **2006**, *7*, 74.
299. Xu, H.; Wang, R.; Zhang, Y. W.; Zhang, X. Estrogen, β -amyloid metabolism/trafficking, and Alzheimer's disease. *Ann. N. Y. Acad. Sci.* **2006**, *1089*, 324-342.
300. Selkoe, D. J. Soluble oligomers of the amyloid β -protein impair synaptic plasticity and behavior. *Behav. Brain Res.* **2008**, *192*, 106-113.
301. Arendt, T. Synaptic degeneration in Alzheimer's disease. *Acta Neuropathol.* **2009**, *118*, 167-179.
302. Armstrong, R. A. The spatial pattern of discrete β -amyloid deposits in Alzheimer's disease reflects synaptic disconnection. *Dementia* **1996**, *7*, 86-90.
303. Cirrito, J. R.; Yamada, K. A.; Finn, M. B.; Sloviter, R. S.; Bales, K. R.; May, P. C.; Schoepp, D. D.; Paul, S. M.; Mennerick, S.; Holtzman, D. M. Synaptic activity regulates interstitial fluid amyloid- β levels in vivo. *Neuron* **2005**, *48*, 913-922.
304. Lacor, P. N.; Buniel, M. C.; Furlow, P. W.; Clemente, A. S.; Velasco, P. T.; Wood, M.; Viola, K. L.; Klein, W. L. A β oligomer-induced aberrations in synapse composition, shape, and density provide a molecular basis for loss of connectivity in Alzheimer's disease. *J. Neurosci.* **2007**, *27*, 796-807.
305. Blenow, K.; Bogdanovic, N.; Alafuzoff, I.; Ekman, R.; Davidsson, P. Synaptic pathology in Alzheimer's disease: relation to severity of dementia, but not to senile plaques, neurofibrillary tangles, or the ApoE4 allele. *J. Neural Transm.* **1996**, *103*, 603-618.
306. Callahan, L. M.; Coleman, P. D. Neurons bearing neurofibrillary tangles are responsible for selected synaptic deficits in Alzheimer's disease. *Neurobiol. Aging* **1995**, *16*, 311-314.

307. Cerpa, W.; Dinamarca, M. C.; Inestrosa, N. C. Structure-function implications in Alzheimer's disease: effect of A β oligomers at central synapses. *Curr. Alzheimer Res.* **2008**, *5*, 233-243.
308. Evans, N. A.; Facci, L.; Owen, D. E.; Soden, P. E.; Burbidge, S. A.; Prinjha, R. K.; Richardson, J. C.; Skaper, S. D. A β ₁₋₄₂ reduces synapse number and inhibits neurite outgrowth in primary cortical and hippocampal neurons: a quantitative analysis. *J. Neurosci. Methods* **2008**, *175*, 96-103.
309. De Felice, F. G.; Vieira, M. N.; Bomfim, T. R.; Decker, H.; Velasco, P. T.; Lambert, M. P.; Viola, K. L.; Zhao, W. Q.; Ferreira, S. T.; Klein, W. L. Protection of synapses against Alzheimer's-linked toxins: insulin signaling prevents the pathogenic binding of A β oligomers. *Proc. Natl. Acad. Sci. U. S. A.* **2009**, *106*, 1971-1976.
310. Viola, K. L.; Velasco, P. T.; Klein, W. L. Why Alzheimer's is a disease of memory: the attack on synapses by A β oligomers (ADDLs). *J. Nutr. Health Aging* **2008**, *12*, 51S-7S.
311. Mandelkow, E. M.; Stamer, K.; Vogel, R.; Thies, E.; Mandelkow, E. Clogging of axons by tau, inhibition of axonal traffic and starvation of synapses. *Neurobiol. Aging* **2003**, *24*, 1079-1085.
312. Borlikova, G. G.; Trejo, M.; Mably, A. J.; Mc Donald, J. M.; Sala Frigerio, C.; Regan, C. M.; Murphy, K. J.; Masliah, E.; Walsh, D. M. Alzheimer brain-derived amyloid β -protein impairs synaptic remodeling and memory consolidation. *Neurobiol. Aging* **2013**, *34*, 1315-1327.
313. Du, H.; Guo, L.; Yan, S. S. Synaptic mitochondrial pathology in Alzheimer's disease. *Antioxid. Redox Signal.* **2012**, *16*, 1467-1475.
314. Selkoe, D. J. Alzheimer's disease is a synaptic failure. *Science* **2002**, *298*, 789-791.
315. Masliah, E. Alzheimer's in real time. *Nature* **2008**, *451*, 638-639.
316. Coleman, P. D.; Yao, P. J. Synaptic slaughter in Alzheimer's disease. *Neurobiol. Aging* **2003**, *24*, 1023-1027.
317. Miklossy, J. Chronic inflammation and amyloidogenesis in Alzheimer's disease -- role of Spirochetes. *J. Alzheimers Dis.* **2008**, *13*, 381-391.
318. Rojo, L. E.; Fernández, J. A.; Maccioni, A. A.; Jimenez, J. M.; Maccioni, R. B. Neuroinflammation: Implications for the Pathogenesis and Molecular Diagnosis of Alzheimer's Disease. *Arch. Med. Res.* **2008**, *39*, 1-16.
319. Eikelenboom, P.; van Gool, W. A. Neuroinflammatory perspectives on the two faces of Alzheimer's disease. *J. Neural Transm.* **2004**, *111*, 281-294.

320. Eikelenboom, P.; Rozemuller, J. M.; van Muiswinkel, F. L. Inflammation and Alzheimer's disease: relationships between pathogenic mechanisms and clinical expression. *Exp. Neurol.* **1998**, *154*, 89-98.
321. Sheng, J. G.; Bora, S. H.; Xu, G.; Borchelt, D. R.; Price, D. L.; Koliatsos, V. E. Lipopolysaccharide-induced-neuroinflammation increases intracellular accumulation of amyloid precursor protein and amyloid β peptide in APPswe transgenic mice. *Neurobiol. Dis.* **2003**, *14*, 133-145.
322. Morishima, Y.; Gotoh, Y.; Zieg, J.; Barrett, T.; Takano, H.; Flavell, R.; Davis, R. J.; Shirasaki, Y.; Greenberg, M. E. β -amyloid induces neuronal apoptosis via a mechanism that involves the c-Jun N-terminal kinase pathway and the induction of Fas ligand. *J. Neurosci.* **2001**, *21*, 7551-7560.
323. Mattson, M. P.; Partin, J.; Begley, J. G. Amyloid β -peptide induces apoptosis-related events in synapses and dendrites. *Brain Res.* **1998**, *807*, 167-176.
324. Forloni, G.; Bugiani, O.; Tagliavini, F.; Salmona, M. Apoptosis-mediated neurotoxicity induced by β -amyloid and PrP fragments. *Mol. Chem. Neuropathol.* **1996**, *28*, 163-171.
325. LeBlanc, A.; Liu, H.; Goodyer, C.; Bergeron, C.; Hammond, J. Caspase-6 role in apoptosis of human neurons, amyloidogenesis, and Alzheimer's disease. *J. Biol. Chem.* **1999**, *274*, 23426-23436.
326. Guo, H.; Albrecht, S.; Bourdeau, M.; Petzke, T.; Bergeron, C.; LeBlanc, A. C. Active caspase-6 and caspase-6-cleaved tau in neuropil threads, neuritic plaques, and neurofibrillary tangles of Alzheimer's disease. *Am. J. Pathol.* **2004**, *165*, 523-531.
327. Galli, C.; Piccini, A.; Ciotti, M. T.; Castellani, L.; Calissano, P.; Zaccheo, D.; Tabaton, M. Increased amyloidogenic secretion in cerebellar granule cells undergoing apoptosis. *Proc. Natl. Acad. Sci. U. S. A.* **1998**, *95*, 1247-1252.
328. Gervais, F. G.; Xu, D.; Robertson, G. S.; Vaillancourt, J. P.; Zhu, Y.; Huang, J.; LeBlanc, A.; Smith, D.; Rigby, M.; Shearman, M. S.; Clarke, E. E.; Zheng, H.; Van Der Ploeg, L. H.; Ruffolo, S. C.; Thornberry, N. A.; Xanthoudakis, S.; Zamboni, R. J.; Roy, S.; Nicholson, D. W. Involvement of caspases in proteolytic cleavage of Alzheimer's amyloid- β precursor protein and amyloidogenic A β peptide formation. *Cell* **1999**, *97*, 395-406.
329. Esposito, L.; Gan, L.; Yu, G. Q.; Essrich, C.; Mucke, L. Intracellularly generated amyloid- β peptide counteracts the antiapoptotic function of its precursor protein and primes proapoptotic pathways for activation by other insults in neuroblastoma cells. *J. Neurochem.* **2004**, *91*, 1260-1274.

330. Zhang, Y.; Goodyer, C.; LeBlanc, A. Selective and protracted apoptosis in human primary neurons microinjected with active caspase-3, -6, -7, and -8. *J. Neurosci.* **2000**, *20*, 8384-8389.
331. Li, Y. P.; Bushnell, A. F.; Lee, C. M.; Perlmutter, L. S.; Wong, S. K. β -amyloid induces apoptosis in human-derived neurotypic SH-SY5Y cells. *Brain Res.* **1996**, *738*, 196-204.
332. LaFerla, F. M.; Tinkle, B. T.; Bieberich, C. J.; Haudenschild, C. C.; Jay, G. The Alzheimer's A β peptide induces neurodegeneration and apoptotic cell death in transgenic mice. *Nat. Genet.* **1995**, *9*, 21-30.
333. Kienlen-Campard, P.; Miolet, S.; Tasiaux, B.; Octave, J. N. Intracellular amyloid- β_{1-42} , but not extracellular soluble amyloid- β peptides, induces neuronal apoptosis. *J. Biol. Chem.* **2002**, *277*, 15666-15670.
334. Behl, C.; Davis, J. B.; Klier, F. G.; Schubert, D. Amyloid β peptide induces necrosis rather than apoptosis. *Brain Res.* **1994**, *645*, 253-264.
335. Kang, J.; Lemaire, H. G.; Unterbeck, A.; Salbaum, J. M.; Masters, C. L.; Grzeschik, K. H.; Multhaup, G.; Beyreuther, K.; Muller-Hill, B. The precursor of Alzheimer's disease amyloid A4 protein resembles a cell-surface receptor. *Nature* **1987**, *325*, 733-736.
336. Konig, G.; Salbaum, J. M.; Wiestler, O.; Lang, W.; Schmitt, H. P.; Masters, C. L.; Beyreuther, K. Alternative splicing of the β A4 amyloid gene of Alzheimer's disease in cortex of control and Alzheimer's disease patients. *Brain Res. Mol. Brain Res.* **1991**, *9*, 259-262.
337. Sandbrink, R.; Masters, C. L.; Beyreuther, K. APP gene family: unique age-associated changes in splicing of Alzheimer's β A4-amyloid protein precursor. *Neurobiol. Dis.* **1994**, *1*, 13-24.
338. Panegyres, P. K. The functions of the amyloid precursor protein gene. *Rev. Neurosci.* **2001**, *12*, 1-39.
339. Wertkin, A. M.; Turner, R. S.; Pleasure, S. J.; Golde, T. E.; Younkin, S. G.; Trojanowski, J. Q.; Lee, V. M. Human neurons derived from a teratocarcinoma cell line express solely the 695-amino acid amyloid precursor protein and produce intracellular β -amyloid or A4 peptides. *Proc. Natl. Acad. Sci. U. S. A.* **1993**, *90*, 9513-9517.
340. Sandbrink, R.; Masters, C. L.; Beyreuther, K. Similar alternative splicing of a non-homologous domain in β A4-amyloid protein precursor-like proteins. *J. Biol. Chem.* **1994**, *269*, 14227-14234.

341. Beyreuther, K.; Pollwein, P.; Multhaup, G.; Monning, U.; König, G.; Dyrks, T.; Schubert, W.; Masters, C. L. Regulation and expression of the Alzheimer's β /A4 amyloid protein precursor in health, disease, and Down's syndrome. *Ann. N. Y. Acad. Sci.* **1993**, *695*, 91-102.
342. Mattson, M. P.; Cheng, B.; Culwell, A. R.; Esch, F. S.; Lieberburg, I.; Rydel, R. E. Evidence for excitoprotective and intraneuronal calcium-regulating roles for secreted forms of the β -amyloid precursor protein. *Neuron* **1993**, *10*, 243-254.
343. Small, D. H.; Nurcombe, V.; Reed, G.; Clarris, H.; Moir, R.; Beyreuther, K.; Masters, C. L. A heparin-binding domain in the amyloid protein precursor of Alzheimer's disease is involved in the regulation of neurite outgrowth. *J. Neurosci.* **1994**, *14*, 2117-2127.
344. Schubert, D.; Jin, L. W.; Saitoh, T.; Cole, G. The regulation of amyloid β protein precursor secretion and its modulatory role in cell adhesion. *Neuron* **1989**, *3*, 689-694.
345. Van Nostrand, W. E.; Schmaier, A. H.; Farrow, J. S.; Cunningham, D. D. Protease nexin-II (amyloid β -protein precursor): a platelet α -granule protein. *Science* **1990**, *248*, 745-748.
346. Van Nostrand, W. E. Zinc (II) selectively enhances the inhibition of coagulation factor XIa by protease nexin-2/amyloid β -protein precursor. *Thromb. Res.* **1995**, *78*, 43-53.
347. Smith, R. P.; Higuchi, D. A.; Broze, G. J., Jr Platelet coagulation factor XIa-inhibitor, a form of Alzheimer amyloid precursor protein. *Science* **1990**, *248*, 1126-1128.
348. Henry, A.; Li, Q. X.; Galatis, D.; Hesse, L.; Multhaup, G.; Beyreuther, K.; Masters, C. L.; Cappai, R. Inhibition of platelet activation by the Alzheimer's disease amyloid precursor protein. *Br. J. Haematol.* **1998**, *103*, 402-415.
349. White, A. R.; Reyes, R.; Mercer, J. F.; Camakaris, J.; Zheng, H.; Bush, A. I.; Multhaup, G.; Beyreuther, K.; Masters, C. L.; Cappai, R. Copper levels are increased in the cerebral cortex and liver of APP and APLP2 knockout mice. *Brain Res.* **1999**, *842*, 439-444.
350. Bentahir, M.; Nyabi, O.; Verhamme, J.; Tolia, A.; Horre, K.; Wiltfang, J.; Esselmann, H.; De Strooper, B. Presenilin clinical mutations can affect γ -secretase activity by different mechanisms. *J. Neurochem.* **2006**, *96*, 732-742.
351. Greenfield, J. P.; Tsai, J.; Gouras, G. K.; Hai, B.; Thinakaran, G.; Checler, F.; Sisodia, S. S.; Greengard, P.; Xu, H. Endoplasmic reticulum and trans-Golgi network generate distinct populations of Alzheimer β -amyloid peptides. *Proc. Natl. Acad. Sci. U. S. A.* **1999**, *96*, 742-747.
352. Bouwman, F. H.; Schoonenboom, N. S.; Verwey, N. A.; van Elk, E. J.; Kok, A.; Blankenstein, M. A.; Scheltens, P.; van der Flier, W. M. CSF biomarker levels in early and late onset Alzheimer's disease. *Neurobiol. Aging* **2008**.

353. Bateman, R. J.; Munsell, L. Y.; Morris, J. C.; Swarm, R.; Yarasheski, K. E.; Holtzman, D. M. Human amyloid- β synthesis and clearance rates as measured in cerebrospinal fluid in vivo. *Nat. Med.* **2006**, *12*, 856-861.
354. Zou, K.; Gong, J. S.; Yanagisawa, K.; Michikawa, M. A novel function of monomeric amyloid β -protein serving as an antioxidant molecule against metal-induced oxidative damage. *J. Neurosci.* **2002**, *22*, 4833-4841.
355. Kontush, A. Alzheimer's amyloid- β as a preventive antioxidant for brain lipoproteins. *Cell. Mol. Neurobiol.* **2001**, *21*, 299-315.
356. Atwood, C. S.; Bowen, R. L.; Smith, M. A.; Perry, G. Cerebrovascular requirement for sealant, anti-coagulant and remodeling molecules that allow for the maintenance of vascular integrity and blood supply. *Brain Res. Brain Res. Rev.* **2003**, *43*, 164-178.
357. Meier-Stephenson, V. C. Quantum Medicine: Novel Applications of Computational Chemistry to the Treatment of Neurological Diseases, Dalhousie University, Halifax, Nova Scotia, 2005.
358. Soccia, S. J.; Kirby, J. E.; Washicosky, K. J.; Tucker, S. M.; Ingelsson, M.; Hyman, B.; Burton, M. A.; Goldstein, L. E.; Duong, S.; Tanzi, R. E.; Moir, R. D. The Alzheimer's disease-associated amyloid β -protein is an antimicrobial peptide. *PLoS One* **2010**, *5*, e9505.
359. Nordstedt, C.; Naslund, J.; Tjernberg, L. O.; Karlstrom, A. R.; Thyberg, J.; Terenius, L. The Alzheimer A β peptide develops protease resistance in association with its polymerization into fibrils. *J. Biol. Chem.* **1994**, *269*, 30773-30776.
360. Shapira, R.; Austin, G. E.; Mirra, S. S. Neuritic plaque amyloid in Alzheimer's disease is highly racemized. *J. Neurochem.* **1988**, *50*, 69-74.
361. Roher, A. E.; Lowenson, J. D.; Clarke, S.; Woods, A. S.; Cotter, R. J.; Gowing, E.; Ball, M. J. β -Amyloid-(1-42) is a major component of cerebrovascular amyloid deposits: implications for the pathology of Alzheimer disease. *Proc. Natl. Acad. Sci. U. S. A.* **1993**, *90*, 10836-10840.
362. Roher, A. E.; Palmer, K. C.; Yurewicz, E. C.; Ball, M. J.; Greenberg, B. D. Morphological and biochemical analyses of amyloid plaque core proteins purified from Alzheimer disease brain tissue. *J. Neurochem.* **1993**, *61*, 1916-1926.
363. Vitek, M. P.; Bhattacharya, K.; Glendening, J. M.; Stopa, E.; Vlassara, H.; Bucala, R.; Manogue, K.; Cerami, A. Advanced glycation end products contribute to amyloidosis in Alzheimer disease. *Proc. Natl. Acad. Sci. U. S. A.* **1994**, *91*, 4766-4770.

364. Smith, M. A.; Taneda, S.; Richey, P. L.; Miyata, S.; Yan, S. D.; Stern, D.; Sayre, L. M.; Monnier, V. M.; Perry, G. Advanced Maillard reaction end products are associated with Alzheimer disease pathology. *Proc. Natl. Acad. Sci. U. S. A.* **1994**, *91*, 5710-5714.
365. Smith, M. A.; Sayre, L. M.; Monnier, V. M.; Perry, G. Radical AGEing in Alzheimer's disease. *Trends Neurosci.* **1995**, *18*, 172-176.
366. Atwood, C. S.; Huang, X.; Khatri, A.; Scarpa, R. C.; Kim, Y. S.; Moir, R. D.; Tanzi, R. E.; Roher, A. E.; Bush, A. I. Copper catalyzed oxidation of Alzheimer A β . *Cell. Mol. Biol. (Noisy-le-grand)* **2000**, *46*, 777-783.
367. Atwood, C. S.; Perry, G.; Zeng, H.; Kato, Y.; Jones, W. D.; Ling, K. Q.; Huang, X.; Moir, R. D.; Wang, D.; Sayre, L. M.; Smith, M. A.; Chen, S. G.; Bush, A. I. Copper mediates dityrosine cross-linking of Alzheimer's amyloid- β . *Biochemistry* **2004**, *43*, 560-568.
368. Chen, K.; Maley, J.; Yu, P. H. Potential implications of endogenous aldehydes in β -amyloid misfolding, oligomerization and fibrillogenesis. *J. Neurochem.* **2006**, *99*, 1413-1424.
369. Reddy, V. P.; Obrenovich, M. E.; Atwood, C. S.; Perry, G.; Smith, M. A. Involvement of Maillard reactions in Alzheimer disease. *Neurotox Res.* **2002**, *4*, 191-209.
370. Atwood, C. S.; Obrenovich, M. E.; Liu, T.; Chan, H.; Perry, G.; Smith, M. A.; Martins, R. N. Amyloid- β : a chameleon walking in two worlds: a review of the trophic and toxic properties of amyloid- β . *Brain Res. Brain Res. Rev.* **2003**, *43*, 1-16.
371. Araki, W.; Kitaguchi, N.; Tokushima, Y.; Ishii, K.; Aratake, H.; Shimohama, S.; Nakamura, S.; Kimura, J. Trophic effect of β -amyloid precursor protein on cerebral cortical neurons in culture. *Biochem. Biophys. Res. Commun.* **1991**, *181*, 265-271.
372. Takenouchi, T.; Munekata, E. Trophic effects of substance P and β -amyloid peptide on dibutyryl cyclic AMP-differentiated human leukemic (HL-60) cells. *Life Sci.* **1995**, *56*, PL479-84.
373. Halverson, K.; Fraser, P. E.; Kirschner, D. A.; Lansbury, P. T., Jr Molecular determinants of amyloid deposition in Alzheimer's disease: conformational studies of synthetic β -protein fragments. *Biochemistry* **1990**, *29*, 2639-2644.
374. Fraser, P. E.; Nguyen, J. T.; Inouye, H.; Surewicz, W. K.; Selkoe, D. J.; Podlisny, M. B.; Kirschner, D. A. Fibril formation by primate, rodent, and Dutch-hemorrhagic analogues of Alzheimer amyloid β -protein. *Biochemistry* **1992**, *31*, 10716-10723.
375. Soto, C.; Castano, E. M.; Kumar, R. A.; Beavis, R. C.; Frangione, B. Fibrillogenesis of synthetic amyloid- β peptides is dependent on their initial secondary structure. *Neurosci. Lett.* **1995**, *200*, 105-108.

376. Ma, K.; Clancy, E. L.; Zhang, Y.; Ray, D. G.; Wollenberg, K.; Zagorski, M. G. Residue-Specific pKa Measurements of the β -Peptide and Mechanism of pH-Induced Amyloid Formation. *J. Am. Chem. Soc.* **1999**, *121*, 8698-8706.
377. Crescenzi, O.; Tomaselli, S.; Guerrini, R.; Salvadori, S.; D'Ursi, A. M.; Temussi, P. A.; Picone, D. Solution structure of the Alzheimer amyloid β -peptide (1-42) in an apolar microenvironment. Similarity with a virus fusion domain. *Eur. J. Biochem.* **2002**, *269*, 5642-5648.
378. Giulian, D.; Haverkamp, L. J.; Yu, J.; Karshin, W.; Tom, D.; Li, J.; Kazanskaia, A.; Kirkpatrick, J.; Roher, A. E. The HHQK domain of β -amyloid provides a structural basis for the immunopathology of Alzheimer's disease. *J. Biol. Chem.* **1998**, *273*, 29719-29726.
379. Zagorski, M. G.; Barrow, C. J. NMR studies of amyloid β -peptides: proton assignments, secondary structure, and mechanism of an α -helix \rightarrow β -sheet conversion for a homologous, 28-residue, N-terminal fragment. *Biochemistry* **1992**, *31*, 5621-5631.
380. Tjernberg, L. O.; Callaway, D. J.; Tjernberg, A.; Hahne, S.; Lilliehook, C.; Terenius, L.; Thyberg, J.; Nordstedt, C. A molecular model of Alzheimer amyloid β -peptide fibril formation. *J. Biol. Chem.* **1999**, *274*, 12619-12625.
381. Fraser, P. E.; Nguyen, J. T.; Surewicz, W. K.; Kirschner, D. A. pH-dependent structural transitions of Alzheimer amyloid peptides. *Biophys. J.* **1991**, *60*, 1190-1201.
382. Finder, V. H.; Glockshuber, R. Amyloid- β aggregation. *Neurodegener Dis.* **2007**, *4*, 13-27.
383. Zhai, J.; Lee, T. H.; Small, D. H.; Aguilar, M. I. Characterization of early stage intermediates in the nucleation phase of A β aggregation. *Biochemistry* **2012**, *51*, 1070-1078.
384. Shankar, G. M.; Leissring, M. A.; Adame, A.; Sun, X.; Spooner, E.; Masliah, E.; Selkoe, D. J.; Lemere, C. A.; Walsh, D. M. Biochemical and immunohistochemical analysis of an Alzheimer's disease mouse model reveals the presence of multiple cerebral A β assembly forms throughout life. *Neurobiol. Dis.* **2009**, *36*, 293-302.
385. Selkoe, D. J. Cell biology of protein misfolding: the examples of Alzheimer's and Parkinson's diseases. *Nat. Cell Biol.* **2004**, *6*, 1054-1061.
386. Zhang, S.; Iwata, K.; Lachenmann, M. J.; Peng, J. W.; Li, S.; Stimson, E. R.; Lu, Y.; Felix, A. M.; Maggio, J. E.; Lee, J. P. The Alzheimer's peptide A β adopts a collapsed coil structure in water. *J. Struct. Biol.* **2000**, *130*, 130-141.
387. Barrow, C. J.; Zagorski, M. G. Solution structures of β peptide and its constituent fragments: relation to amyloid deposition. *Science* **1991**, *253*, 179-182.

388. Lazo, N. D.; Grant, M. A.; Condrón, M. C.; Rigby, A. C.; Teplow, D. B. On the nucleation of amyloid β -protein monomer folding. *Protein Sci.* **2005**, *14*, 1581-1596.
389. Xu, Y.; Shen, J.; Luo, X.; Zhu, W.; Chen, K.; Ma, J.; Jiang, H. Conformational transition of amyloid β -peptide. *Proc. Natl. Acad. Sci. U. S. A.* **2005**, *102*, 5403-5407.
390. Garzon-Rodriguez, W.; Sepulveda-Becerra, M.; Milton, S.; Glabe, C. G. Soluble amyloid A β -(1-40) exists as a stable dimer at low concentrations. *J. Biol. Chem.* **1997**, *272*, 21037-21044.
391. Roher, A. E.; Chaney, M. O.; Kuo, Y. M.; Webster, S. D.; Stine, W. B.; Haverkamp, L. J.; Woods, A. S.; Cotter, R. J.; Tuohy, J. M.; Krafft, G. A.; Bonnell, B. S.; Emmerling, M. R. Morphology and toxicity of A β -(1-42) dimer derived from neuritic and vascular amyloid deposits of Alzheimer's disease. *J. Biol. Chem.* **1996**, *271*, 20631-20635.
392. Podlisny, M. B.; Ostaszewski, B. L.; Squazzo, S. L.; Koo, E. H.; Rydell, R. E.; Teplow, D. B.; Selkoe, D. J. Aggregation of secreted amyloid β -protein into sodium dodecyl sulfate-stable oligomers in cell culture. *J. Biol. Chem.* **1995**, *270*, 9564-9570.
393. Hilbich, C.; Kisters-Woike, B.; Reed, J.; Masters, C. L.; Beyreuther, K. Substitutions of hydrophobic amino acids reduce the amyloidogenicity of Alzheimer's disease β A4 peptides. *J. Mol. Biol.* **1992**, *228*, 460-473.
394. Nakabayashi, J.; Yoshimura, M.; Morishima-Kawashima, M.; Funato, H.; Miyakawa, T.; Yamazaki, T.; Ihara, Y. Amyloid β -protein (A β) accumulation in the putamen and mammillary body during aging and in Alzheimer disease. *J. Neuropathol. Exp. Neurol.* **1998**, *57*, 343-352.
395. Lesne, S.; Koh, M. T.; Kotilinek, L.; Kaye, R.; Glabe, C. G.; Yang, A.; Gallagher, M.; Ashe, K. H. A specific amyloid- β protein assembly in the brain impairs memory. *Nature* **2006**, *440*, 352-357.
396. Townsend, M.; Shankar, G. M.; Mehta, T.; Walsh, D. M.; Selkoe, D. J. Effects of secreted oligomers of amyloid β -protein on hippocampal synaptic plasticity: a potent role for trimers. *J. Physiol.* **2006**, *572*, 477-492.
397. Chen, Y. R.; Glabe, C. G. Distinct early folding and aggregation properties of Alzheimer amyloid- β peptides A β ₄₀ and A β ₄₂: stable trimer or tetramer formation by A β ₄₂. *J. Biol. Chem.* **2006**, *281*, 24414-24422.
398. Kuo, Y. M.; Emmerling, M. R.; Vigo-Pelfrey, C.; Kasunic, T. C.; Kirkpatrick, J. B.; Murdoch, G. H.; Ball, M. J.; Roher, A. E. Water-soluble A β (N-40, N-42) oligomers in normal and Alzheimer disease brains. *J. Biol. Chem.* **1996**, *271*, 4077-4081.

399. McLean, C. A.; Cherny, R. A.; Fraser, F. W.; Fuller, S. J.; Smith, M. J.; Beyreuther, K.; Bush, A. I.; Masters, C. L. Soluble pool of A β amyloid as a determinant of severity of neurodegeneration in Alzheimer's disease. *Ann. Neurol.* **1999**, *46*, 860-866.
400. Bitan, G.; Kirkitadze, M. D.; Lomakin, A.; Vollers, S. S.; Benedek, G. B.; Teplow, D. B. Amyloid β -protein (A β) assembly: A β ₄₀ and A β ₄₂ oligomerize through distinct pathways. *Proc. Natl. Acad. Sci. U. S. A.* **2003**, *100*, 330-335.
401. Cleary, J. P.; Walsh, D. M.; Hofmeister, J. J.; Shankar, G. M.; Kuskowski, M. A.; Selkoe, D. J.; Ashe, K. H. Natural oligomers of the amyloid- β protein specifically disrupt cognitive function. *Nat. Neurosci.* **2005**, *8*, 79-84.
402. Chromy, B. A.; Nowak, R. J.; Lambert, M. P.; Viola, K. L.; Chang, L.; Velasco, P. T.; Jones, B. W.; Fernandez, S. J.; Lacor, P. N.; Horowitz, P.; Finch, C. E.; Krafft, G. A.; Klein, W. L. Self-Assembly of A₁₋₄₂ into Globular Neurotoxins. *Biochemistry* **2003**, *42*, 12749-12760.
403. Losic, D.; Martin, L. L.; Mechler, A.; Aguilar, M. I.; Small, D. H. High resolution scanning tunnelling microscopy of the β -amyloid protein (A β ₁₋₄₀) of Alzheimer's disease suggests a novel mechanism of oligomer assembly. *J. Struct. Biol.* **2006**, *155*, 104-110.
404. Nimmrich, V.; Grimm, C.; Draguhn, A.; Barghorn, S.; Lehmann, A.; Schoemaker, H.; Hillen, H.; Gross, G.; Ebert, U.; Bruehl, C. Amyloid β oligomers (A β ₁₋₄₂ globulomer) suppress spontaneous synaptic activity by inhibition of P/Q-type calcium currents. *J. Neurosci.* **2008**, *28*, 788-797.
405. Arimon, M.; Diez-Perez, I.; Kogan, M. J.; Durany, N.; Giralt, E.; Sanz, F.; Fernandez-Busquets, X. Fine structure study of A β ₁₋₄₂ fibrillogenesis with atomic force microscopy. *FASEB J.* **2005**, *19*, 1344-1346.
406. Gellermann, G. P.; Byrnes, H.; Striebinger, A.; Ullrich, K.; Mueller, R.; Hillen, H.; Barghorn, S. A β -globulomers are formed independently of the fibril pathway. *Neurobiol. Dis.* **2008**, *30*, 212-220.
407. Lashuel, H. A.; Hartley, D.; Petre, B. M.; Walz, T.; Lansbury, P. T., Jr Neurodegenerative disease: amyloid pores from pathogenic mutations. *Nature* **2002**, *418*, 291.
408. Quist, A.; Doudevski, I.; Lin, H.; Azimova, R.; Ng, D.; Frangione, B.; Kagan, B.; Ghiso, J.; Lal, R. Amyloid ion channels: a common structural link for protein-misfolding disease. *Proc. Natl. Acad. Sci. U. S. A.* **2005**, *102*, 10427-10432.
409. Kagan, B. L.; Hirakura, Y.; Azimov, R.; Azimova, R.; Lin, M. C. The channel hypothesis of Alzheimer's disease: current status. *Peptides* **2002**, *23*, 1311-1315.

410. Klein, W. L.; Stine, W. B., Jr; Teplow, D. B. Small assemblies of unmodified amyloid β -protein are the proximate neurotoxin in Alzheimer's disease. *Neurobiol. Aging* **2004**, *25*, 569-580.
411. Lambert, M. P.; Barlow, A. K.; Chromy, B. A.; Edwards, C.; Freed, R.; Liosatos, M.; Morgan, T. E.; Rozovsky, I.; Trommer, B.; Viola, K. L.; Wals, P.; Zhang, C.; Finch, C. E.; Krafft, G. A.; Klein, W. L. Diffusible, nonfibrillar ligands derived from $A\beta_{1-42}$ are potent central nervous system neurotoxins. *Proc. Natl. Acad. Sci. U. S. A.* **1998**, *95*, 6448-6453.
412. Harper, J. D.; Wong, S. S.; Lieber, C. M.; Lansbury, P. T., Jr Assembly of $A\beta$ amyloid protofibrils: an in vitro model for a possible early event in Alzheimer's disease. *Biochemistry* **1999**, *38*, 8972-8980.
413. Gong, Y.; Chang, L.; Viola, K. L.; Lacor, P. N.; Lambert, M. P.; Finch, C. E.; Krafft, G. A.; Klein, W. L. Alzheimer's disease-affected brain: presence of oligomeric $A\beta$ ligands (ADDLs) suggests a molecular basis for reversible memory loss. *Proc. Natl. Acad. Sci. U. S. A.* **2003**, *100*, 10417-10422.
414. Georganopoulou, D. G.; Chang, L.; Nam, J. M.; Thaxton, C. S.; Mufson, E. J.; Klein, W. L.; Mirkin, C. A. Nanoparticle-based detection in cerebral spinal fluid of a soluble pathogenic biomarker for Alzheimer's disease. *Proc. Natl. Acad. Sci. U. S. A.* **2005**, *102*, 2273-2276.
415. Harper, J. D.; Lansbury, P. T., Jr Models of amyloid seeding in Alzheimer's disease and scrapie: mechanistic truths and physiological consequences of the time-dependent solubility of amyloid proteins. *Annu. Rev. Biochem.* **1997**, *66*, 385-407.
416. Harper, J. D.; Wong, S. S.; Lieber, C. M.; Lansbury, P. T. Observation of metastable $A\beta$ amyloid protofibrils by atomic force microscopy. *Chem. Biol.* **1997**, *4*, 119-125.
417. Kheterpal, I.; Lashuel, H. A.; Hartley, D. M.; Walz, T.; Lansbury, P. T., Jr; Wetzel, R. $A\beta$ protofibrils possess a stable core structure resistant to hydrogen exchange. *Biochemistry* **2003**, *42*, 14092-14098.
418. Walsh, D. M.; Lomakin, A.; Benedek, G. B.; Condron, M. M.; Teplow, D. B. Amyloid β -protein fibrillogenesis. Detection of a protofibrillar intermediate. *J. Biol. Chem.* **1997**, *272*, 22364-22372.
419. Williams, A. D.; Segal, M.; Chen, M.; Kheterpal, I.; Geva, M.; Berthelie, V.; Kaleta, D. T.; Cook, K. D.; Wetzel, R. Structural properties of $A\beta$ protofibrils stabilized by a small molecule. *Proc. Natl. Acad. Sci. U. S. A.* **2005**, *102*, 7115-7120.
420. O'Quinn, P. R.; Koo, S. I.; Noh, S. K.; Nelssen, J. L.; Goodband, R. D.; Tokach, M. D. Effects of modified tall oil on body composition and serum and tissue levels of cholesterol, phospholipids, and α -tocopherol in adult ovariectomized rats. *Nutrition Research* **2003/4**, *23*, 549-566.

421. Hartley, D. M.; Walsh, D. M.; Ye, C. P.; Diehl, T.; Vasquez, S.; Vassilev, P. M.; Teplow, D. B.; Selkoe, D. J. Protofibrillar intermediates of amyloid β -protein induce acute electrophysiological changes and progressive neurotoxicity in cortical neurons. *J. Neurosci.* **1999**, *19*, 8876-8884.
422. Ward, R. V.; Jennings, K. H.; Jepras, R.; Neville, W.; Owen, D. E.; Hawkins, J.; Christie, G.; Davis, J. B.; George, A.; Karran, E. H.; Howlett, D. R. Fractionation and characterization of oligomeric, protofibrillar and fibrillar forms of β -amyloid peptide. *Biochem. J.* **2000**, *348 Pt 1*, 137-144.
423. Ban, T.; Morigaki, K.; Yagi, H.; Kawasaki, T.; Kobayashi, A.; Yuba, S.; Naiki, H.; Goto, Y. Real-time and single fibril observation of the formation of amyloid β spherulitic structures. *J. Biol. Chem.* **2006**, *281*, 33677-33683.
424. Mann, D. M.; Yates, P. O.; Marcyniuk, B.; Ravindra, C. R. The topography of plaques and tangles in Down's syndrome patients of different ages. *Neuropathol. Appl. Neurobiol.* **1986**, *12*, 447-457.
425. Shibata, C.; Kashima, T.; Ohuchi, K. Nonthermal Influence of Microwave Power on Chemical Reactions. *Jpn. J. Appl. Phys.* **1996**, *35*, 316-319.
426. Ross, C. A.; Poirier, M. A. Opinion: What is the role of protein aggregation in neurodegeneration? *Nat. Rev. Mol. Cell Biol.* **2005**, *6*, 891-898.
427. LeVine, H., 3rd Quantification of β -sheet amyloid fibril structures with thioflavin T. *Methods Enzymol.* **1999**, *309*, 274-284.
428. Klunk, W. E.; Jacob, R. F.; Mason, R. P. Quantifying amyloid β -peptide ($A\beta$) aggregation using the Congo red- $A\beta$ (CR- $A\beta$) spectrophotometric assay. *Anal. Biochem.* **1999**, *266*, 66-76.
429. Kirschner, D. A.; Inouye, H.; Duffy, L. K.; Sinclair, A.; Lind, M.; Selkoe, D. J. Synthetic peptide homologous to β protein from Alzheimer disease forms amyloid-like fibrils in vitro. *Proc. Natl. Acad. Sci. U. S. A.* **1987**, *84*, 6953-6957.
430. Stromer, T.; Serpell, L. C. Structure and morphology of the Alzheimer's amyloid fibril. *Microsc. Res. Tech.* **2005**, *67*, 210-217.
431. Luhrs, T.; Ritter, C.; Adrian, M.; Riek-Loher, D.; Bohrmann, B.; Dobeli, H.; Schubert, D.; Riek, R. 3D structure of Alzheimer's amyloid- β (1-42) fibrils. *Proc. Natl. Acad. Sci. U. S. A.* **2005**, *102*, 17342-17347.
432. Malinchik, S. B.; Inouye, H.; Szumowski, K. E.; Kirschner, D. A. Structural analysis of Alzheimer's β (1-40) amyloid: protofilament assembly of tubular fibrils. *Biophys. J.* **1998**, *74*, 537-545.

433. Lansbury, P. T., Jr Evolution of amyloid: what normal protein folding may tell us about fibrillogenesis and disease. *Proc. Natl. Acad. Sci. U. S. A.* **1999**, *96*, 3342-3344.
434. Terry, R. D.; Masliah, E.; Salmon, D. P.; Butters, N.; DeTeresa, R.; Hill, R.; Hansen, L. A.; Katzman, R. Physical basis of cognitive alterations in Alzheimer's disease: synapse loss is the major correlate of cognitive impairment. *Ann. Neurol.* **1991**, *30*, 572-580.
435. Muller-Hill, B.; Beyreuther, K. Molecular biology of Alzheimer's disease. *Annu. Rev. Biochem.* **1989**, *58*, 287-307.
436. Dickson, D. W.; Crystal, H. A.; Bevona, C.; Honer, W.; Vincent, I.; Davies, P. Correlations of synaptic and pathological markers with cognition of the elderly. *Neurobiol. Aging* **1995**, *16*, 285-98; discussion 298-304.
437. Wang, H. Y.; D'Andrea, M. R.; Nagele, R. G. Cerebellar diffuse amyloid plaques are derived from dendritic A β_{42} accumulations in Purkinje cells. *Neurobiol. Aging* **2002**, *23*, 213-223.
438. Armstrong, R. A.; Cairns, N. J.; Lantos, P. L. Spatial distribution of diffuse, primitive, and classic amyloid- β deposits and blood vessels in the upper laminae of the frontal cortex in Alzheimer disease. *Alzheimer Dis. Assoc. Disord.* **1998**, *12*, 378-383.
439. Nacula, M.; Breydo, L.; Milton, S.; Kaye, R.; van der Veer, W. E.; Tone, P.; Glabe, C. G. Methylene blue inhibits amyloid A β oligomerization by promoting fibrillization. *Biochemistry* **2007**, *46*, 8850-8860.
440. Nacula, M.; Kaye, R.; Milton, S.; Glabe, C. G. Small molecule inhibitors of aggregation indicate that amyloid β oligomerization and fibrillization pathways are independent and distinct. *J. Biol. Chem.* **2007**, *282*, 10311-10324.
441. Jarrett, J. T.; Lansbury, P. T., Jr Amyloid fibril formation requires a chemically discriminating nucleation event: studies of an amyloidogenic sequence from the bacterial protein OsmB. *Biochemistry* **1992**, *31*, 12345-12352.
442. Lomakin, A.; Chung, D. S.; Benedek, G. B.; Kirschner, D. A.; Teplow, D. B. On the nucleation and growth of amyloid β -protein fibrils: detection of nuclei and quantitation of rate constants. *Proc. Natl. Acad. Sci. U. S. A.* **1996**, *93*, 1125-1129.
443. Lomakin, A.; Teplow, D. B.; Kirschner, D. A.; Benedek, G. B. Kinetic theory of fibrillogenesis of amyloid β -protein. *Proc. Natl. Acad. Sci. U. S. A.* **1997**, *94*, 7942-7947.
444. Wogulis, M.; Wright, S.; Cunningham, D.; Chilcote, T.; Powell, K.; Rydel, R. E. Nucleation-dependent polymerization is an essential component of amyloid-mediated neuronal cell death. *J. Neurosci.* **2005**, *25*, 1071-1080.

445. Naiki, H.; Nagai, Y. Molecular Pathogenesis of Protein Misfolding Diseases: Pathological Molecular Environments versus Quality Control Systems against Misfolded Proteins. *J. Biochem.* **2009**.
446. Jarrett, J. T.; Costa, P. R.; Griffin, R. G.; Lansbury, P. T., Jr. Models of the β -Protein C-Terminus: Differences in Amyloid Structure May Lead to Segregation of "Long" and "Short" Fibrils. *J. Am. Chem. Soc.* **1994**, *116*, 9741-9742.
447. Naiki, H.; Nakakuki, K. First-order kinetic model of Alzheimer's β -amyloid fibril extension in vitro. *Lab. Invest.* **1996**, *74*, 374-383.
448. Morinaga, A.; Hasegawa, K.; Nomura, R.; Ookoshi, T.; Ozawa, D.; Goto, Y.; Yamada, M.; Naiki, H. Critical role of interfaces and agitation on the nucleation of A β amyloid fibrils at low concentrations of A β monomers. *Biochim. Biophys. Acta* **2010**, *1804*, 986-995.
449. Cannon, M. J.; Williams, A. D.; Wetzel, R.; Myszka, D. G. Kinetic analysis of β -amyloid fibril elongation. *Anal. Biochem.* **2004**, *328*, 67-75.
450. Esler, W. P.; Stimson, E. R.; Jennings, J. M.; Vinters, H. V.; Ghilardi, J. R.; Lee, J. P.; Mantyh, P. W.; Maggio, J. E. Alzheimer's disease amyloid propagation by a template-dependent dock-lock mechanism. *Biochemistry* **2000**, *39*, 6288-6295.
451. Hasegawa, K.; Ono, K.; Yamada, M.; Naiki, H. Kinetic modeling and determination of reaction constants of Alzheimer's β -amyloid fibril extension and dissociation using surface plasmon resonance. *Biochemistry* **2002**, *41*, 13489-13498.
452. Jarrett, J. T.; Berger, E. P.; Lansbury, P. T., Jr. The carboxy terminus of the β amyloid protein is critical for the seeding of amyloid formation: implications for the pathogenesis of Alzheimer's disease. *Biochemistry* **1993**, *32*, 4693-4697.
453. Hasegawa, K.; Yamaguchi, I.; Omata, S.; Gejyo, F.; Naiki, H. Interaction between A β (1-42) and A β (1-40) in Alzheimer's β -amyloid fibril formation in vitro. *Biochemistry* **1999**, *38*, 15514-15521.
454. Huang, T. H.; Yang, D. S.; Fraser, P. E.; Chakrabartty, A. Alternate aggregation pathways of the Alzheimer β -amyloid peptide. An in vitro model of preamyloid. *J. Biol. Chem.* **2000**, *275*, 36436-36440.
455. Yan, Y.; Wang, C. A β 40 Protects Non-toxic A β 42 Monomer from Aggregation. *Journal of Molecular Biology* **2007/6/15**, *369*, 909-916.
456. Wood, S. J.; Maleeff, B.; Hart, T.; Wetzel, R. Physical, morphological and functional differences between pH 5.8 and 7.4 aggregates of the Alzheimer's amyloid peptide A β . *J. Mol. Biol.* **1996**, *256*, 870-877.

457. Klug, G. M.; Losic, D.; Subasinghe, S. S.; Aguilar, M. I.; Martin, L. L.; Small, D. H. β -amyloid protein oligomers induced by metal ions and acid pH are distinct from those generated by slow spontaneous ageing at neutral pH. *Eur. J. Biochem.* **2003**, *270*, 4282-4293.
458. Yang, X. H.; Huang, H. C.; Chen, L.; Xu, W.; Jiang, Z. F. Coordinating to three histidine residues: Cu(II) promotes oligomeric and fibrillar amyloid- β peptide to precipitate in a non- β aggregation manner. *J. Alzheimers Dis.* **2009**, *18*, 799-810.
459. Yanagisawa, K.; Odaka, A.; Suzuki, N.; Ihara, Y. GM1 ganglioside-bound amyloid β -protein (A β): a possible form of preamyloid in Alzheimer's disease. *Nat. Med.* **1995**, *1*, 1062-1066.
460. Choo-Smith, L. P.; Surewicz, W. K. The interaction between Alzheimer amyloid β (1-40) peptide and ganglioside GM1-containing membranes. *FEBS Lett.* **1997**, *402*, 95-98.
461. Choo-Smith, L. P.; Garzon-Rodriguez, W.; Glabe, C. G.; Surewicz, W. K. Acceleration of amyloid fibril formation by specific binding of A β -(1-40) peptide to ganglioside-containing membrane vesicles. *J. Biol. Chem.* **1997**, *272*, 22987-22990.
462. Kakio, A.; Nishimoto, S. I.; Yanagisawa, K.; Kozutsumi, Y.; Matsuzaki, K. Cholesterol-dependent formation of GM1 ganglioside-bound amyloid β -protein, an endogenous seed for Alzheimer amyloid. *J. Biol. Chem.* **2001**, *276*, 24985-24990.
463. Yamamoto, N.; Matsubara, T.; Sato, T.; Yanagisawa, K. Age-dependent high-density clustering of GM1 ganglioside at presynaptic neuritic terminals promotes amyloid β -protein fibrillogenesis. *Biochim. Biophys. Acta* **2008**, *1778*, 2717-2726.
464. Ikeda, K.; Yamaguchi, T.; Fukunaga, S.; Hoshino, M.; Matsuzaki, K. Mechanism of amyloid β -protein aggregation mediated by GM1 ganglioside clusters. *Biochemistry* **2011**, *50*, 6433-6440.
465. Fukunaga, S.; Ueno, H.; Yamaguchi, T.; Yano, Y.; Hoshino, M.; Matsuzaki, K. GM1 cluster mediates formation of toxic A β fibrils by providing hydrophobic environments. *Biochemistry* **2012**, *51*, 8125-8131.
466. Yamamoto, N.; Fukata, Y.; Fukata, M.; Yanagisawa, K. GM1-ganglioside-induced A β assembly on synaptic membranes of cultured neurons. *Biochim. Biophys. Acta* **2007**, *1768*, 1128-1137.
467. Mochizuki, A.; Tamaoka, A.; Shimohata, A.; Komatsuzaki, Y.; Shoji, S. A β 42-positive non-pyramidal neurons around amyloid plaques in Alzheimer's disease. *Lancet* **2000**, *355*, 42-43.
468. Wilson, C. A.; Doms, R. W.; Lee, V. M. Intracellular APP processing and A β production in Alzheimer disease. *J. Neuropathol. Exp. Neurol.* **1999**, *58*, 787-794.

469. Iwatsubo, T.; Odaka, A.; Suzuki, N.; Mizusawa, H.; Nukina, N.; Ihara, Y. Visualization of A β 42(43) and A β 40 in senile plaques with end-specific A β monoclonals: evidence that an initially deposited species is A β 42(43). *Neuron* **1994**, *13*, 45-53.
470. Rogers, J.; Morrison, J. H. Quantitative morphology and regional and laminar distributions of senile plaques in Alzheimer's disease. *J. Neurosci.* **1985**, *5*, 2801-2808.
471. Pike, C. J.; Cummings, B. J.; Cotman, C. W. Early association of reactive astrocytes with senile plaques in Alzheimer's disease. *Exp. Neurol.* **1995**, *132*, 172-179.
472. Akiyama, H.; Barger, S.; Barnum, S.; Bradt, B.; Bauer, J.; Cole, G. M.; Cooper, N. R.; Eikelenboom, P.; Emmerling, M.; Fiebich, B. L.; Finch, C. E.; Frautschy, S.; Griffin, W. S.; Hampel, H.; Hull, M.; Landreth, G.; Lue, L.; Mrak, R.; Mackenzie, I. R.; McGeer, P. L.; O'Banion, M. K.; Pachter, J.; Pasinetti, G.; Plata-Salman, C.; Rogers, J. T.; Rydel, R.; Shen, Y.; Streit, W.; Strohmeyer, R.; Tooyoma, I.; Van Muiswinkel, F. L.; Veerhuis, R.; Walker, D.; Webster, S.; Wegrzyniak, B.; Wenk, G.; Wyss-Coray, T. Inflammation and Alzheimer's disease. *Neurobiol. Aging* **2000**, *21*, 383-421.
473. Tagliavini, F.; Giaccone, G.; Frangione, B.; Bugiani, O. Preamyloid deposits in the cerebral cortex of patients with Alzheimer's disease and nondemented individuals. *Neurosci. Lett.* **1988**, *93*, 191-196.
474. Yamaguchi, H.; Hirai, S.; Morimatsu, M.; Shoji, M.; Harigaya, Y. Diffuse type of senile plaques in the brains of Alzheimer-type dementia. *Acta Neuropathol.* **1988**, *77*, 113-119.
475. Spillantini, M. G.; Goedert, M.; Jakes, R.; Klug, A. Different configurational states of β -amyloid and their distributions relative to plaques and tangles in Alzheimer disease. *Proc. Natl. Acad. Sci. U. S. A.* **1990**, *87*, 3947-3951.
476. Armstrong, R. A. β -amyloid plaques: stages in life history or independent origin? *Dement. Geriatr. Cogn. Disord.* **1998**, *9*, 227-238.
477. Dickson, D. W. The pathogenesis of senile plaques. *J. Neuropathol. Exp. Neurol.* **1997**, *56*, 321-339.
478. Kuo, Y. M.; Kokjohn, T. A.; Beach, T. G.; Sue, L. I.; Brune, D.; Lopez, J. C.; Kalback, W. M.; Abramowski, D.; Sturchler-Pierrat, C.; Staufenbiel, M.; Roher, A. E. Comparative analysis of amyloid- β chemical structure and amyloid plaque morphology of transgenic mouse and Alzheimer's disease brains. *J. Biol. Chem.* **2001**, *276*, 12991-12998.
479. Veerhuis, R.; Van Breemen, M. J.; Hoozemans, J. M.; Morbin, M.; Ouladhadj, J.; Tagliavini, F.; Eikelenboom, P. Amyloid β plaque-associated proteins C1q and SAP enhance the A β ₁₋₄₂ peptide-induced cytokine secretion by adult human microglia in vitro. *Acta Neuropathol.* **2003**, *105*, 135-144.

480. Selkoe, D. J. Alzheimer's disease: genes, proteins, and therapy. *Physiol. Rev.* **2001**, *81*, 741-766.
481. Burns, M. P.; Noble, W. J.; Olm, V.; Gaynor, K.; Casey, E.; LaFrancois, J.; Wang, L.; Duff, K. Co-localization of cholesterol, apolipoprotein E and fibrillar A β in amyloid plaques. *Brain Res. Mol. Brain Res.* **2003**, *110*, 119-125.
482. Bronfman, F. C.; Garrido, J.; Alvarez, A.; Morgan, C.; Inestrosa, N. C. Laminin inhibits amyloid- β -peptide fibrillation. *Neurosci. Lett.* **1996**, *218*, 201-203.
483. Glenner, G. G.; Wong, C. W.; Quaranta, V.; Eanes, E. D. The amyloid deposits in Alzheimer's disease: their nature and pathogenesis. *Appl. Pathol.* **1984**, *2*, 357-369.
484. Haass, C.; Schlossmacher, M. G.; Hung, A. Y.; Vigo-Pelfrey, C.; Mellon, A.; Ostaszewski, B. L.; Lieberburg, I.; Koo, E. H.; Schenk, D.; Teplow, D. B. Amyloid β -peptide is produced by cultured cells during normal metabolism. *Nature* **1992**, *359*, 322-325.
485. Grundke-Iqbal, I.; Iqbal, K.; George, L.; Tung, Y. C.; Kim, K. S.; Wisniewski, H. M. Amyloid protein and neurofibrillary tangles coexist in the same neuron in Alzheimer disease. *Proc. Natl. Acad. Sci. U. S. A.* **1989**, *86*, 2853-2857.
486. Gouras, G. K.; Tsai, J.; Naslund, J.; Vincent, B.; Edgar, M.; Checler, F.; Greenfield, J. P.; Haroutunian, V.; Buxbaum, J. D.; Xu, H.; Greengard, P.; Relkin, N. R. Intraneuronal A β 42 accumulation in human brain. *Am. J. Pathol.* **2000**, *156*, 15-20.
487. D'Andrea, M. R.; Nagele, R. G.; Wang, H. Y.; Peterson, P. A.; Lee, D. H. Evidence that neurones accumulating amyloid can undergo lysis to form amyloid plaques in Alzheimer's disease. *Histopathology* **2001**, *38*, 120-134.
488. Nagele, R. G.; D'Andrea, M. R.; Anderson, W. J.; Wang, H. Y. Intracellular accumulation of β -amyloid₁₋₄₂ in neurons is facilitated by the α 7 nicotinic acetylcholine receptor in Alzheimer's disease. *Neuroscience* **2002**, *110*, 199-211.
489. Lee, S. J.; Liyanage, U.; Bickel, P. E.; Xia, W.; Lansbury, P. T., Jr; Kosik, K. S. A detergent-insoluble membrane compartment contains A β in vivo. *Nat. Med.* **1998**, *4*, 730-734.
490. Strandberg, Y.; Gray, C.; Vuocolo, T.; Donaldson, L.; Broadway, M.; Tellam, R. Lipopolysaccharide and lipoteichoic acid induce different innate immune responses in bovine mammary epithelial cells. *Cytokine* **2005**, *31*, 72-86.
491. Xu, H.; Sweeney, D.; Wang, R.; Thinakaran, G.; Lo, A. C.; Sisodia, S. S.; Greengard, P.; Gandy, S. Generation of Alzheimer β -amyloid protein in the trans-Golgi network in the apparent absence of vesicle formation. *Proc. Natl. Acad. Sci. U. S. A.* **1997**, *94*, 3748-3752.

492. Chui, D. H.; Dobo, E.; Makifuchi, T.; Akiyama, H.; Kawakatsu, S.; Petit, A.; Checler, F.; Araki, W.; Takahashi, K.; Tabira, T. Apoptotic neurons in Alzheimer's disease frequently show intracellular A β 42 labeling. *J. Alzheimers Dis.* **2001**, *3*, 231-239.
493. Busciglio, J.; Gabuzda, D. H.; Matsudaira, P.; Yankner, B. A. Generation of β -amyloid in the secretory pathway in neuronal and nonneuronal cells. *Proc. Natl. Acad. Sci. U. S. A.* **1993**, *90*, 2092-2096.
494. LeBlanc, A. C.; Xue, R.; Gambetti, P. Amyloid precursor protein metabolism in primary cell cultures of neurons, astrocytes, and microglia. *J. Neurochem.* **1996**, *66*, 2300-2310.
495. LeBlanc, A. C.; Papadopoulos, M.; Belair, C.; Chu, W.; Crosato, M.; Powell, J.; Goodyer, C. G. Processing of amyloid precursor protein in human primary neuron and astrocyte cultures. *J. Neurochem.* **1997**, *68*, 1183-1190.
496. Echeverria, V.; Ducatzenzeiler, A.; Alhonen, L.; Janne, J.; Grant, S. M.; Wandosell, F.; Muro, A.; Baralle, F.; Li, H.; Duff, K.; Szyf, M.; Cuelllo, A. C. Rat transgenic models with a phenotype of intracellular A β accumulation in hippocampus and cortex. *J. Alzheimers Dis.* **2004**, *6*, 209-219.
497. Oddo, S.; Caccamo, A.; Smith, I. F.; Green, K. N.; LaFerla, F. M. A dynamic relationship between intracellular and extracellular pools of A β . *Am. J. Pathol.* **2006**, *168*, 184-194.
498. Masliah, E.; Sisk, A.; Mallory, M.; Mucke, L.; Schenk, D.; Games, D. Comparison of neurodegenerative pathology in transgenic mice overexpressing V717F β -amyloid precursor protein and Alzheimer's disease. *J. Neurosci.* **1996**, *16*, 5795-5811.
499. Hsia, A. Y.; Masliah, E.; McConlogue, L.; Yu, G. Q.; Tatsuno, G.; Hu, K.; Kholodenko, D.; Malenka, R. C.; Nicoll, R. A.; Mucke, L. Plaque-independent disruption of neural circuits in Alzheimer's disease mouse models. *Proc. Natl. Acad. Sci. U. S. A.* **1999**, *96*, 3228-3233.
500. Bayer, T. A.; Breyhan, H.; Duan, K.; Rettig, J.; Wirths, O. Intraneuronal β -amyloid is a major risk factor--novel evidence from the APP/PS1KI mouse model. *Neurodegener Dis.* **2008**, *5*, 140-142.
501. Takahashi, R. H.; Milner, T. A.; Li, F.; Nam, E. E.; Edgar, M. A.; Yamaguchi, H.; Beal, M. F.; Xu, H.; Greengard, P.; Gouras, G. K. Intraneuronal Alzheimer A β 42 accumulates in multivesicular bodies and is associated with synaptic pathology. *Am. J. Pathol.* **2002**, *161*, 1869-1879.
502. Takahashi, R. H.; Almeida, C. G.; Kearney, P. F.; Yu, F.; Lin, M. T.; Milner, T. A.; Gouras, G. K. Oligomerization of Alzheimer's β -amyloid within processes and synapses of cultured neurons and brain. *J. Neurosci.* **2004**, *24*, 3592-3599.

503. LaFerla, F. M.; Troncoso, J. C.; Strickland, D. K.; Kawas, C. H.; Jay, G. Neuronal cell death in Alzheimer's disease correlates with apoE uptake and intracellular A β stabilization. *J. Clin. Invest.* **1997**, *100*, 310-320.
504. Cook, D. G.; Forman, M. S.; Sung, J. C.; Leight, S.; Kolson, D. L.; Iwatsubo, T.; Lee, V. M.; Doms, R. W. Alzheimer's A β (1-42) is generated in the endoplasmic reticulum/intermediate compartment of NT2N cells. *Nat. Med.* **1997**, *3*, 1021-1023.
505. Skovronsky, D. M.; Moore, D. B.; Milla, M. E.; Doms, R. W.; Lee, V. M. Protein kinase C-dependent α -secretase competes with β -secretase for cleavage of amyloid- β precursor protein in the trans-golgi network. *J. Biol. Chem.* **2000**, *275*, 2568-2575.
506. Perez, R. G.; Soriano, S.; Hayes, J. D.; Ostaszewski, B.; Xia, W.; Selkoe, D. J.; Chen, X.; Stokin, G. B.; Koo, E. H. Mutagenesis identifies new signals for β -amyloid precursor protein endocytosis, turnover, and the generation of secreted fragments, including A β 42. *J. Biol. Chem.* **1999**, *274*, 18851-18856.
507. Burdick, D.; Kosmoski, J.; Knauer, M. F.; Glabe, C. G. Preferential adsorption, internalization and resistance to degradation of the major isoform of the Alzheimer's amyloid peptide, A β 1-42, in differentiated PC12 cells. *Brain Res.* **1997**, *746*, 275-284.
508. Skovronsky, D. M.; Zhang, B.; Kung, M. P.; Kung, H. F.; Trojanowski, J. Q.; Lee, V. M. In vivo detection of amyloid plaques in a mouse model of Alzheimer's disease. *Proc. Natl. Acad. Sci. U. S. A.* **2000**, *97*, 7609-7614.
509. Knauer, M. F.; Soreghan, B.; Burdick, D.; Kosmoski, J.; Glabe, C. G. Intracellular accumulation and resistance to degradation of the Alzheimer amyloid A4/ β protein. *Proc. Natl. Acad. Sci. U. S. A.* **1992**, *89*, 7437-7441.
510. Bahr, B. A.; Hoffman, K. B.; Yang, A. J.; Hess, U. S.; Glabe, C. G.; Lynch, G. Amyloid β protein is internalized selectively by hippocampal field CA1 and causes neurons to accumulate amyloidogenic carboxyterminal fragments of the amyloid precursor protein. *J. Comp. Neurol.* **1998**, *397*, 139-147.
511. Glabe, C. Intracellular mechanisms of amyloid accumulation and pathogenesis in Alzheimer's disease. *J. Mol. Neurosci.* **2001**, *17*, 137-145.
512. Oddo, S.; Billings, L.; Kesslak, J. P.; Cribbs, D. H.; LaFerla, F. M. A β Immunotherapy Leads to Clearance of Early, but Not Late, Hyperphosphorylated Tau Aggregates via the Proteasome. *Neuron* **2004**, *43*, 321-332.
513. Reddy, P. H. Abnormal tau, mitochondrial dysfunction, impaired axonal transport of mitochondria, and synaptic deprivation in Alzheimer's disease. *Brain Res.* **2011**, *1415*, 136-148.

514. Manczak, M.; Reddy, P. H. Abnormal Interaction of Oligomeric Amyloid- β with Phosphorylated Tau: Implications to Synaptic Dysfunction and Neuronal Damage. *J. Alzheimers Dis.* **2013**, *36*, 285-295.
515. Takahashi, R. H.; Capetillo-Zarate, E.; Lin, M. T.; Milner, T. A.; Gouras, G. K. Co-occurrence of Alzheimer's disease ss-amyloid and tau pathologies at synapses. *Neurobiol. Aging* **2010**, *31*, 1145-1152.
516. Caspersen, C.; Wang, N.; Yao, J.; Sosunov, A.; Chen, X.; Lustbader, J. W.; Xu, H. W.; Stern, D.; McKhann, G.; Yan, S. D. Mitochondrial A β : a potential focal point for neuronal metabolic dysfunction in Alzheimer's disease. *FASEB J.* **2005**, *19*, 2040-2041.
517. Suh, Y. H.; Checler, F. Amyloid precursor protein, presenilins, and α -synuclein: molecular pathogenesis and pharmacological applications in Alzheimer's disease. *Pharmacol. Rev.* **2002**, *54*, 469-525.
518. Oda, T.; Wals, P.; Osterburg, H. H.; Johnson, S. A.; Pasinetti, G. M.; Morgan, T. E.; Rozovsky, I.; Stine, W. B.; Snyder, S. W.; Holzman, T. F. Clusterin (apoJ) alters the aggregation of amyloid β -peptide (A β ₁₋₄₂) and forms slowly sedimenting A β complexes that cause oxidative stress. *Exp. Neurol.* **1995**, *136*, 22-31.
519. Serpell, L. C. Alzheimer's amyloid fibrils: structure and assembly. *Biochim. Biophys. Acta* **2000**, *1502*, 16-30.
520. Stine, W. B., Jr; Dahlgren, K. N.; Krafft, G. A.; LaDu, M. J. In vitro characterization of conditions for amyloid- β peptide oligomerization and fibrillogenesis. *J. Biol. Chem.* **2003**, *278*, 11612-11622.
521. Okada, T.; Ikeda, K.; Wakabayashi, M.; Ogawa, M.; Matsuzaki, K. Formation of Toxic A β (1-40) Fibrils on GM1 Ganglioside-Containing Membranes Mimicking Lipid Rafts: Polymorphisms in A β (1-40) Fibrils. *J. Mol. Biol.* **2008**, *382*, 1066-1074.
522. Crowther, R. A.; Olesen, O. F.; Smith, M. J.; Jakes, R.; Goedert, M. Assembly of Alzheimer-like filaments from full-length tau protein. *FEBS Lett.* **1994**, *337*, 135-138.
523. Couchie, D.; Mavilia, C.; Georgieff, I. S.; Liem, R. K.; Shelanski, M. L.; Nunez, J. Primary structure of high molecular weight tau present in the peripheral nervous system. *Proc. Natl. Acad. Sci. U. S. A.* **1992**, *89*, 4378-4381.
524. Hasegawa, M.; Morishima-Kawashima, M.; Takio, K.; Suzuki, M.; Titani, K.; Ihara, Y. Protein sequence and mass spectrometric analyses of tau in the Alzheimer's disease brain. *J. Biol. Chem.* **1992**, *267*, 17047-17054.

525. Geula, C.; Wu, C. K.; Saroff, D.; Lorenzo, A.; Yuan, M.; Yankner, B. A. Aging renders the brain vulnerable to amyloid β -protein neurotoxicity. *Nat. Med.* **1998**, *4*, 827-831.
526. Breuzard, G.; Hubert, P.; Nouar, R.; De Bessa, T.; Devred, F.; Barbier, P.; Sturgis, J. N.; Peyrot, V. Molecular mechanisms of Tau binding to microtubules and its role in microtubule dynamics in live cells. *J. Cell. Sci.* **2013**, *126*, 2810-2819.
527. Siegel, G. J.; Chauhan, N.; Karczmar, A. G. In *Links Between Amyloid and Tau Biology in Alzheimer's Disease and Their Cholinergic Aspects*; Karczmar, A. G., Ed.; Exploring the Vertebrate Central Cholinergic Nervous System; Springer Science+Business Media, LLC: New York, NY, **2007**; pp. 597-656.
528. Karp, G. *Cell and molecular biology: concepts and experiments*; J. Wiley: New York, **2002**; , pp 785.
529. Billingsley, M. L.; Kincaid, R. L. Regulated phosphorylation and dephosphorylation of tau protein: effects on microtubule interaction, intracellular trafficking and neurodegeneration. *Biochem. J.* **1997**, *323 (Pt 3)*, 577-591.
530. Alonso, A. D.; Grundke-Iqbal, I.; Barra, H. S.; Iqbal, K. Abnormal phosphorylation of tau and the mechanism of Alzheimer neurofibrillary degeneration: sequestration of microtubule-associated proteins 1 and 2 and the disassembly of microtubules by the abnormal tau. *Proc. Natl. Acad. Sci. U. S. A.* **1997**, *94*, 298-303.
531. Alonso, A. D.; Di Clerico, J.; Li, B.; Corbo, C. P.; Alaniz, M. E.; Grundke-Iqbal, I.; Iqbal, K. Phosphorylation of tau at Thr212, Thr231, and Ser262 combined causes neurodegeneration. *J. Biol. Chem.* **2010**, *285*, 30851-30860.
532. Avila, J.; Santa-Maria, I.; Perez, M.; Hernandez, F.; Moreno, F. Tau phosphorylation, aggregation, and cell toxicity. *J. Biomed. Biotechnol.* **2006**, *2006*, 74539.
533. Avila, J.; Lim, F.; Moreno, F.; Belmonte, C.; Cuello, A. C. Tau function and dysfunction in neurons: its role in neurodegenerative disorders. *Mol. Neurobiol.* **2002**, *25*, 213-231.
534. Ballatore, C.; Lee, V. M.; Trojanowski, J. Q. Tau-mediated neurodegeneration in Alzheimer's disease and related disorders. *Nat. Rev. Neurosci.* **2007**, *8*, 663-672.
535. Hernandez, F.; Avila, J. Tau aggregates and tau pathology. *J. Alzheimers Dis.* **2008**, *14*, 449-452.
536. O'Brien, J.; Ames, D.; Burns, A., Eds.; In *Dementia*; Arnold: London, **2000**; pp. 940.
537. Perl, D. P. Neuropathology of Alzheimer's disease and related disorders. *Neurol. Clin.* **2000**, *18*, 847-864.

538. Hill, J. M.; Steiner, I.; Matthews, K. E.; Trahan, S. G.; Foster, T. P.; Ball, M. J. Statins lower the risk of developing Alzheimer's disease by limiting lipid raft endocytosis and decreasing the neuronal spread of Herpes simplex virus type 1. *Med. Hypotheses* **2005**, *64*, 53-58.
539. Halle, A.; Hornung, V.; Petzold, G. C.; Stewart, C. R.; Monks, B. G.; Reinheckel, T.; Fitzgerald, K. A.; Latz, E.; Moore, K. J.; Golenbock, D. T. The NALP3 inflammasome is involved in the innate immune response to amyloid- β . *Nat. Immunol.* **2008**, *9*, 857-865.
540. Udan, M. L.; Ajit, D.; Crouse, N. R.; Nichols, M. R. Toll-like receptors 2 and 4 mediate A β (1-42) activation of the innate immune response in a human monocytic cell line. *J. Neurochem.* **2008**, *104*, 524-533.
541. Gasque, P.; Dean, Y. D.; McGreal, E. P.; VanBeek, J.; Morgan, B. P. Complement components of the innate immune system in health and disease in the CNS. *Immunopharmacology* **2000**, *49*, 171-186.
542. McGeer, P. L.; McGeer, E. G. Inflammation, autotoxicity and Alzheimer disease. *Neurobiol. Aging* **2001**, *22*, 799-809.
543. Bsibsi, M.; Persoon-Deen, C.; Verwer, R. W.; Meeuwssen, S.; Ravid, R.; Van Noort, J. M. Toll-like receptor 3 on adult human astrocytes triggers production of neuroprotective mediators. *Glia* **2006**, *53*, 688-695.
544. Husemann, J.; Loike, J. D.; Anankov, R.; Febbraio, M.; Silverstein, S. C. Scavenger receptors in neurobiology and neuropathology: their role on microglia and other cells of the nervous system. *Glia* **2002**, *40*, 195-205.
545. Kielian, T.; Mayes, P.; Kielian, M. Characterization of microglial responses to *Staphylococcus aureus*: effects on cytokine, costimulatory molecule, and Toll-like receptor expression. *J. Neuroimmunol.* **2002**, *130*, 86-99.
546. Gaskin, F.; Finley, J.; Fang, Q.; Xu, S.; Fu, S. M. Human antibodies reactive with β -amyloid protein in Alzheimer's disease. *J. Exp. Med.* **1993**, *177*, 1181-1186.
547. Hyman, B. T.; Smith, C.; Buldyrev, I.; Whelan, C.; Brown, H.; Tang, M. X.; Mayeux, R. Autoantibodies to amyloid- β and Alzheimer's disease. *Ann. Neurol.* **2001**, *49*, 808-810.
548. Hershey, C. O.; Hershey, L. A.; Varnes, A.; Vibhakar, S. D.; Lavin, P.; Strain, W. H. Cerebrospinal fluid trace element content in dementia: clinical, radiologic, and pathologic correlations. *Neurology* **1983**, *33*, 1350-1353.
549. Ehmann, W. D.; Markesbery, W. R.; Alauddin, M.; Hossain, T. I.; Brubaker, E. H. Brain trace elements in Alzheimer's disease. *Neurotoxicology* **1986**, *7*, 195-206.

550. Thompson, C. M.; Markesbery, W. R.; Ehmann, W. D.; Mao, Y. X.; Vance, D. E. Regional brain trace-element studies in Alzheimer's disease. *Neurotoxicology* **1988**, *9*, 1-7.
551. Vance, D. E.; Ehmann, W. D.; Markesbery, W. R. A search for longitudinal variations in trace element levels in nails of Alzheimer's disease patients. *Biol. Trace Elem. Res.* **1990**, *26-27*, 461-470.
552. Basun, H.; Forssell, L. G.; Wetterberg, L.; Winblad, B. Metals and trace elements in plasma and cerebrospinal fluid in normal aging and Alzheimer's disease. *J. Neural Transm. Park. Dis. Dement. Sect.* **1991**, *3*, 231-258.
553. Samudralwar, D. L.; Diprete, C. C.; Ni, B. F.; Ehmann, W. D.; Markesbery, W. R. Elemental imbalances in the olfactory pathway in Alzheimer's disease. *J. Neurol. Sci.* **1995**, *130*, 139-145.
554. Cornett, C. R.; Markesbery, W. R.; Ehmann, W. D. Imbalances of trace elements related to oxidative damage in Alzheimer's disease brain. *Neurotoxicology* **1998**, *19*, 339-345.
555. Bush, A. I. Metals and neuroscience. *Curr. Opin. Chem. Biol.* **2000**, *4*, 184-191.
556. Hou, L.; Zagorski, M. G. NMR reveals anomalous copper(II) binding to the amyloid A β peptide of Alzheimer's disease. *J. Am. Chem. Soc.* **2006**, *128*, 9260-9261.
557. Atwood, C. S.; Scarpa, R. C.; Huang, X.; Moir, R. D.; Jones, W. D.; Fairlie, D. P.; Tanzi, R. E.; Bush, A. I. Characterization of copper interactions with Alzheimer amyloid β peptides: identification of an attomolar-affinity copper binding site on amyloid β 1-42. *J. Neurochem.* **2000**, *75*, 1219-1233.
558. Syme, C. D.; Viles, J. H. Solution ^1H NMR investigation of Zn^{2+} and Cd^{2+} binding to amyloid- β peptide (A β) of Alzheimer's disease. *Biochim. Biophys. Acta* **2006**, *1764*, 246-256.
559. Danielsson, J.; Pierattelli, R.; Banci, L.; Graslund, A. High-resolution NMR studies of the zinc-binding site of the Alzheimer's amyloid β -peptide. *FEBS J.* **2007**, *274*, 46-59.
560. Yang, D. S.; McLaurin, J.; Qin, K.; Westaway, D.; Fraser, P. E. Examining the zinc binding site of the amyloid- β peptide. *Eur. J. Biochem.* **2000**, *267*, 6692-6698.
561. Bin, Y.; Chen, S.; Xiang, J. pH-dependent kinetics of copper ions binding to amyloid- β peptide. *J. Inorg. Biochem.* **2013**, *119*, 21-27.
562. Strozyk, D.; Launer, L. J.; Adlard, P. A.; Cherny, R. A.; Tsatsanis, A.; Volitakis, I.; Blennow, K.; Petrovitch, H.; White, L. R.; Bush, A. I. Zinc and copper modulate Alzheimer A β levels in human cerebrospinal fluid. *Neurobiol. Aging* **2009**, *30*, 1069-1077.

563. Curtain, C. C.; Ali, F.; Volitakis, I.; Cherny, R. A.; Norton, R. S.; Beyreuther, K.; Barrow, C. J.; Masters, C. L.; Bush, A. I.; Barnham, K. J. Alzheimer's disease amyloid- β binds copper and zinc to generate an allosterically ordered membrane-penetrating structure containing superoxide dismutase-like subunits. *J. Biol. Chem.* **2001**, *276*, 20466-20473.
564. Bush, A. I. The metallobiology of Alzheimer's disease. *Trends Neurosci.* **2003**, *26*, 207-214.
565. Crapper, D. R.; Krishnan, S. S.; Dalton, A. J. Brain aluminum distribution in Alzheimer's disease and experimental neurofibrillary degeneration. *Science* **1973**, *180*, 511-513.
566. Crapper, D. R.; Krishnan, S. S.; Quittkat, S. Aluminium, neurofibrillary degeneration and Alzheimer's disease. *Brain* **1976**, *99*, 67-80.
567. Sparks, D. L.; Friedland, R.; Petanceska, S.; Schreurs, B. G.; Shi, J.; Perry, G.; Smith, M. A.; Sharma, A.; Derosa, S.; Ziolkowski, C.; Stankovic, G. Trace copper levels in the drinking water, but not zinc or aluminum influence CNS Alzheimer-like pathology. *J. Nutr. Health Aging* **2006**, *10*, 247-254.
568. Zatta, P. Aluminum and Alzheimer's disease: a Vexata Questio between uncertain data and a lot of imagination. *J. Alzheimers Dis.* **2006**, *10*, 33-37.
569. Drago, D.; Bettella, M.; Bolognin, S.; Cendron, L.; Scancar, J.; Milacic, R.; Ricchelli, F.; Casini, A.; Messori, L.; Tognon, G.; Zatta, P. Potential pathogenic role of β -amyloid₁₋₄₂-aluminum complex in Alzheimer's disease. *Int. J. Biochem. Cell Biol.* **2008**, *40*, 731-746.
570. Banks, W. A.; Niehoff, M. L.; Drago, D.; Zatta, P. Aluminum complexing enhances amyloid β protein penetration of blood-brain barrier. *Brain Res.* **2006**, *1116*, 215-221.
571. Bush, A. I.; Huang, X.; Fairlie, D. P. The possible origin of free radicals from amyloid β peptides in Alzheimer's disease. *Neurobiol. Aging* **1999**, *20*, 335-7; discussion 339-42.
572. Huang, X.; Moir, R. D.; Tanzi, R. E.; Bush, A. I.; Rogers, J. T. Redox-active metals, oxidative stress, and Alzheimer's disease pathology. *Ann. N. Y. Acad. Sci.* **2004**, *1012*, 153-163.
573. Verdier, Y.; Penke, B. Binding sites of amyloid β -peptide in cell plasma membrane and implications for Alzheimer's disease. *Curr. Protein Pept. Sci.* **2004**, *5*, 19-31.
574. Verdier, Y.; Zarandi, M.; Penke, B. Amyloid β -peptide interactions with neuronal and glial cell plasma membrane: binding sites and implications for Alzheimer's disease. *J. Pept. Sci.* **2004**, *10*, 229-248.
575. Shao, H.; Jao, S.; Ma, K.; Zagorski, M. G. Solution structures of micelle-bound amyloid β -(1-40) and β -(1-42) peptides of Alzheimer's disease. *J. Mol. Biol.* **1999**, *285*, 755-773.

576. Kisilevsky, R.; Lemieux, L. J.; Fraser, P. E.; Kong, X.; Hultin, P. G.; Szarek, W. A. Arresting amyloidosis in vivo using small-molecule anionic sulphonates or sulphates: implications for Alzheimer's disease. *Nat. Med.* **1995**, *1*, 143-148.
577. Carter, D. B.; Chou, K. C. A model for structure-dependent binding of Congo red to Alzheimer β -amyloid fibrils. *Neurobiol. Aging* **1998**, *19*, 37-40.
578. Kuner, P.; Bohrmann, B.; Tjernberg, L. O.; Naslund, J.; Huber, G.; Celenk, S.; Gruninger-Leitch, F.; Richards, J. G.; Jakob-Roetne, R.; Kemp, J. A.; Nordstedt, C. Controlling polymerization of β -amyloid and prion-derived peptides with synthetic small molecule ligands. *J. Biol. Chem.* **2000**, *275*, 1673-1678.
579. Talafous, J.; Marcinowski, K. J.; Klopman, G.; Zagorski, M. G. Solution structure of residues 1-28 of the amyloid β -peptide. *Biochemistry* **1994**, *33*, 7788-7796.
580. Salomon, A. R.; Marcinowski, K. J.; Friedland, R. P.; Zagorski, M. G. Nicotine inhibits amyloid formation by the β -peptide. *Biochemistry* **1996**, *35*, 13568-13578.
581. Fonnum, F.; Myhrer, T.; Paulsen, R. E.; Wangen, K.; Oksengard, A. R. Role of glutamate and glutamate receptors in memory function and Alzheimer's disease. *Ann. N. Y. Acad. Sci.* **1995**, *757*, 475-486.
582. Kar, S.; Slowikowski, S. P.; Westaway, D.; Mount, H. T. Interactions between β -amyloid and central cholinergic neurons: implications for Alzheimer's disease. *J. Psychiatry Neurosci.* **2004**, *29*, 427-441.
583. Hasselmo, M. E.; Stern, C. E. Mechanisms underlying working memory for novel information. *Trends Cogn. Sci.* **2006**, *10*, 487-493.
584. Li, S.; Hong, S.; Shepardson, N. E.; Walsh, D. M.; Shankar, G. M.; Selkoe, D. Soluble oligomers of amyloid β protein facilitate hippocampal long-term depression by disrupting neuronal glutamate uptake. *Neuron* **2009**, *62*, 788-801.
585. Courtney, C.; Farrell, D.; Gray, R.; Hills, R.; Lynch, L.; Sellwood, E.; Edwards, S.; Hardyman, W.; Raftery, J.; Crome, P.; Lendon, C.; Shaw, H.; Bentham, P.; AD2000 Collaborative Group Long-term donepezil treatment in 565 patients with Alzheimer's disease (AD2000): randomised double-blind trial. *Lancet* **2004**, *363*, 2105-2115.
586. Vardy, E. R.; Hussain, I.; Hooper, N. M. Emerging therapeutics for Alzheimer's disease. *Expert Rev. Neurother* **2006**, *6*, 695-704.
587. Hardy, J. A.; Higgins, G. A. Alzheimer's disease: the amyloid cascade hypothesis. *Science* **1992**, *256*, 184-185.

588. Golde, T. E.; Dickson, D.; Hutton, M. Filling the gaps in the A β cascade hypothesis of Alzheimer's disease. *Curr. Alzheimer Res.* **2006**, *3*, 421-430.
589. Beckerman, M. In *Alzheimer's Disease; Cellular Signaling in Health and Disease*; Springer US: **2009**; pp. 369-389.
590. De Felice, F. G.; Ferreira, S. T. β -amyloid production, aggregation, and clearance as targets for therapy in Alzheimer's disease. *Cell. Mol. Neurobiol.* **2002**, *22*, 545-563.
591. Skovronsky, D. M.; Lee, V. M.; Trojanowski, J. Q. Neurodegenerative diseases: new concepts of pathogenesis and their therapeutic implications. *Annu. Rev. Pathol.* **2006**, *1*, 151-170.
592. Lee, V. M.; Trojanowski, J. Q. The disordered neuronal cytoskeleton in Alzheimer's disease. *Curr. Opin. Neurobiol.* **1992**, *2*, 653-656.
593. Iqbal, K.; Liu, F.; Gong, C. X.; Alonso Adel, C.; Grundke-Iqbal, I. Mechanisms of tau-induced neurodegeneration. *Acta Neuropathol.* **2009**, *118*, 53-69.
594. Rodríguez-Martín, T.; Cuchillo-Ibáñez, I.; Noble, W.; Nyenya, F.; Anderton, B. H.; Hanger, D. P. Tau phosphorylation affects its axonal transport and degradation. *Neurobiol. Aging* **2013**, *34*, 2146-2157.
595. Kowall, N. W.; Kosik, K. S. Axonal disruption and aberrant localization of tau protein characterize the neuropil pathology of Alzheimer's disease. *Ann. Neurol.* **1987**, *22*, 639-643.
596. Patterson, K. R.; Ward, S. M.; Combs, B.; Voss, K.; Kanaan, N. M.; Morfini, G.; Brady, S. T.; Gamblin, T. C.; Binder, L. I. Heat shock protein 70 prevents both tau aggregation and the inhibitory effects of preexisting tau aggregates on fast axonal transport. *Biochemistry* **2011**, *50*, 10300-10310.
597. Mattson, M. P.; Cheng, B.; Davis, D.; Bryant, K.; Lieberburg, I.; Rydel, R. E. β -Amyloid peptides destabilize calcium homeostasis and render human cortical neurons vulnerable to excitotoxicity. *J. Neurosci.* **1992**, *12*, 376-389.
598. LaFerla, F. M. Calcium dyshomeostasis and intracellular signalling in Alzheimer's disease. *Nat. Rev. Neurosci.* **2002**, *3*, 862-872.
599. Paschen, W. Mechanisms of neuronal cell death: diverse roles of calcium in the various subcellular compartments. *Cell Calcium* **2003**, *34*, 305-310.
600. Bush, A. I.; Tanzi, R. E. Therapeutics for Alzheimer's disease based on the metal hypothesis. *Neurotherapeutics* **2008**, *5*, 421-432.
601. Exley, C. Aluminum and Alzheimer's disease. *J. Alzheimers Dis.* **2001**, *3*, 551-552.

602. Exley, C.; Birchall, J. D. Aluminium and Alzheimer's disease. *Age Ageing* **1993**, *22*, 391-392.
603. Exley, C. Aluminium, tau and Alzheimer's disease. *J. Alzheimers Dis.* **2007**, *12*, 313-5; author reply 317-8.
604. Jaeger, L. B.; Dohgu, S.; Hwang, M. C.; Farr, S. A.; Murphy, M. P.; Fleegal-DeMotta, M. A.; Lynch, J. L.; Robinson, S. M.; Niehoff, M. L.; Johnson, S. N.; Kumar, V. B.; Banks, W. A. Testing the neurovascular hypothesis of Alzheimer's disease: LRP-1 antisense reduces blood-brain barrier clearance, increases brain levels of amyloid- β protein, and impairs cognition. *J. Alzheimers Dis.* **2009**, *17*, 553-570.
605. Robinson, S. R.; Bishop, G. M. A β as a bioflocculant: implications for the amyloid hypothesis of Alzheimer's disease. *Neurobiol. Aging* **2002**, *23*, 1051-1072.
606. Swerdlow, R. H.; Khan, S. M. The Alzheimer's disease mitochondrial cascade hypothesis: an update. *Exp. Neurol.* **2009**, *218*, 308-315.
607. Arispe, N.; Rojas, E.; Pollard, H. B. Alzheimer disease amyloid β protein forms calcium channels in bilayer membranes: blockade by tromethamine and aluminum. *Proc. Natl. Acad. Sci. U. S. A.* **1993**, *90*, 567-571.
608. Pollard, H. B.; Arispe, N.; Rojas, E. Ion channel hypothesis for Alzheimer amyloid peptide neurotoxicity. *Cell. Mol. Neurobiol.* **1995**, *15*, 513-526.
609. Arispe, N.; Pollard, H. B.; Rojas, E. β -Amyloid Ca²⁺-channel hypothesis for neuronal death in Alzheimer disease. *Mol. Cell. Biochem.* **1994**, *140*, 119-125.
610. Shirwany, N. A.; Payette, D.; Xie, J.; Guo, Q. The amyloid β ion channel hypothesis of Alzheimer's disease. *Neuropsychiatr. Dis. Treat.* **2007**, *3*, 597-612.
611. Strandberg, T. E.; Aiello, A. E. Is the microbe-dementia hypothesis finally ready for a treatment trial? *Neurology* **2013**, *80*, 1182-1183.
612. Robinson, S. R.; Dobson, C.; Lyons, J. Challenges and directions for the pathogen hypothesis of Alzheimer's disease. *Neurobiol. Aging* **2004**, *25*, 629-637.
613. Lee, H. G.; Zhu, X.; Nunomura, A.; Perry, G.; Smith, M. A. Amyloid β : the alternate hypothesis. *Curr. Alzheimer Res.* **2006**, *3*, 75-80.
614. Lee, H. G.; Casadesus, G.; Zhu, X.; Takeda, A.; Perry, G.; Smith, M. A. Challenging the amyloid cascade hypothesis: senile plaques and amyloid- β as protective adaptations to Alzheimer disease. *Ann. N. Y. Acad. Sci.* **2004**, *1019*, 1-4.

615. Small, S. A.; Duff, K. Linking A β and Tau in Late-Onset Alzheimer's Disease: A Dual Pathway Hypothesis. *Neuron* **2008**, *60*, 534-542.
616. Ittner, L. M.; Gotz, J. Amyloid- β and tau--a toxic pas de deux in Alzheimer's disease. *Nat. Rev. Neurosci.* **2011**, *12*, 65-72.
617. Li, B.; Chohan, M. O.; Grundke-Iqbal, I.; Iqbal, K. Disruption of microtubule network by Alzheimer abnormally hyperphosphorylated tau. *Acta Neuropathol.* **2007**, *113*, 501-511.
618. Gustke, N.; Trinczek, B.; Biernat, J.; Mandelkow, E. M.; Mandelkow, E. Domains of tau protein and interactions with microtubules. *Biochemistry* **1994**, *33*, 9511-9522.
619. Gustke, N.; Steiner, B.; Mandelkow, E. M.; Biernat, J.; Meyer, H. E.; Goedert, M.; Mandelkow, E. The Alzheimer-like phosphorylation of tau protein reduces microtubule binding and involves Ser-Pro and Thr-Pro motifs. *FEBS Lett.* **1992**, *307*, 199-205.
620. Weingarten, M. D.; Lockwood, A. H.; Hwo, S. Y.; Kirschner, M. W. A protein factor essential for microtubule assembly. *Proc. Natl. Acad. Sci. U. S. A.* **1975**, *72*, 1858-1862.
621. Sloboda, R. D.; Rudolph, S. A.; Rosenbaum, J. L.; Greengard, P. Cyclic AMP-dependent endogenous phosphorylation of a microtubule-associated protein. *Proc. Natl. Acad. Sci. U. S. A.* **1975**, *72*, 177-181.
622. Iqbal, K.; Grundke-Iqbal, I.; Zaidi, T.; Merz, P. A.; Wen, G. Y.; Shaikh, S. S.; Wisniewski, H. M.; Alafuzoff, I.; Winblad, B. Defective brain microtubule assembly in Alzheimer's disease. *Lancet* **1986**, *2*, 421-426.
623. Lindwall, G.; Cole, R. D. Phosphorylation affects the ability of tau protein to promote microtubule assembly. *J. Biol. Chem.* **1984**, *259*, 5301-5305.
624. Goedert, M.; Hasegawa, M.; Jakes, R.; Lawler, S.; Cuenda, A.; Cohen, P. Phosphorylation of microtubule-associated protein tau by stress-activated protein kinases. *FEBS Lett.* **1997**, *409*, 57-62.
625. Chevalier-Larsen, E.; Holzbaur, E. L. F. Axonal transport and neurodegenerative disease. *Biochimica et Biophysica Acta (BBA) - Molecular Basis of Disease* **2006**, *1762*, 1094-1108.
626. Goldstein, L. S. B. In *Axonal Transport and Alzheimer's Disease*; Editor-in-Chief: Larry R. Squire, Ed.; Encyclopedia of Neuroscience; Academic Press: Oxford, 2009; pp. 1189-1194.
627. Alonso, A. C.; Zaidi, T.; Grundke-Iqbal, I.; Iqbal, K. Role of abnormally phosphorylated tau in the breakdown of microtubules in Alzheimer disease. *Proc. Natl. Acad. Sci. U. S. A.* **1994**, *91*, 5562-5566.

628. Alonso, A. C.; Grundke-Iqbal, I.; Iqbal, K. Alzheimer's disease hyperphosphorylated tau sequesters normal tau into tangles of filaments and disassembles microtubules. *Nat. Med.* **1996**, *2*, 783-787.
629. Grundke-Iqbal, I.; Iqbal, K.; Quinlan, M.; Tung, Y. C.; Zaidi, M. S.; Wisniewski, H. M. Microtubule-associated protein tau. A component of Alzheimer paired helical filaments. *J. Biol. Chem.* **1986**, *261*, 6084-6089.
630. Grundke-Iqbal, I.; Iqbal, K.; Tung, Y. C.; Quinlan, M.; Wisniewski, H. M.; Binder, L. I. Abnormal phosphorylation of the microtubule-associated protein tau (tau) in Alzheimer cytoskeletal pathology. *Proc. Natl. Acad. Sci. U. S. A.* **1986**, *83*, 4913-4917.
631. Goedert, M.; Spillantini, M. G.; Jakes, R.; Rutherford, D.; Crowther, R. A. Multiple isoforms of human microtubule-associated protein tau: sequences and localization in neurofibrillary tangles of Alzheimer's disease. *Neuron* **1989**, *3*, 519-526.
632. Brion, J. P.; Hanger, D. P.; Bruce, M. T.; Couck, A. M.; Flament-Durand, J.; Anderton, B. H. Tau in Alzheimer neurofibrillary tangles. N- and C-terminal regions are differentially associated with paired helical filaments and the location of a putative abnormal phosphorylation site. *Biochem. J.* **1991**, *273(Pt 1)*, 127-133.
633. Seino, Y.; Kawarabayashi, T.; Wakasaya, Y.; Watanabe, M.; Takamura, A.; Yamamoto-Watanabe, Y.; Kurata, T.; Abe, K.; Ikeda, M.; Westaway, D.; Murakami, T.; Hyslop, P. S.; Matsubara, E.; Shoji, M. Amyloid β accelerates phosphorylation of tau and neurofibrillary tangle formation in an amyloid precursor protein and tau double-transgenic mouse model. *J. Neurosci. Res.* **2010**, *88*, 3547-3554.
634. Alonso, A.; Zaidi, T.; Novak, M.; Grundke-Iqbal, I.; Iqbal, K. Hyperphosphorylation induces self-assembly of tau into tangles of paired helical filaments/straight filaments. *Proc. Natl. Acad. Sci. U. S. A.* **2001**, *98*, 6923-6928.
635. Delacourte, A.; Sergeant, N.; Champain, D.; Wattez, A.; Maurage, C. A.; Lebert, F.; Pasquier, F.; David, J. P. Nonoverlapping but synergetic tau and APP pathologies in sporadic Alzheimer's disease. *Neurology* **2002**, *59*, 398-407.
636. Ghetti, B.; Murrell, J.; Spillantini, M. G. Mutations in the Tau gene cause frontotemporal dementia. *Brain Res. Bull.* **1999**, *50*, 471-472.
637. Spillantini, M. G.; Bird, T. D.; Ghetti, B. Frontotemporal dementia and Parkinsonism linked to chromosome 17: a new group of tauopathies. *Brain Pathol.* **1998**, *8*, 387-402.
638. Goate, A. Segregation of a missense mutation in the amyloid β -protein precursor gene with familial Alzheimer's disease. *J. Alzheimers Dis.* **2006**, *9*, 341-347.

639. Sherrington, R.; Rogaev, E. I.; Liang, Y.; Rogaeva, E. A.; Levesque, G.; Ikeda, M.; Chi, H.; Lin, C.; Li, G.; Holman, K.; Tsuda, T.; Mar, L.; Foncin, J. F.; Bruni, A. C.; Montesi, M. P.; Sorbi, S.; Rainero, I.; Pinessi, L.; Nee, L.; Chumakov, I.; Pollen, D.; Brookes, A.; Sanseau, P.; Polinsky, R. J.; Wasco, W.; Da Silva, H. A.; Haines, J. L.; Perkicak-Vance, M. A.; Tanzi, R. E.; Roses, A. D.; Fraser, P. E.; Rommens, J. M.; St George-Hyslop, P. H. Cloning of a gene bearing missense mutations in early-onset familial Alzheimer's disease. *Nature* **1995**, *375*, 754-760.
640. Hutton, M.; Lendon, C. L.; Rizzu, P.; Baker, M.; Froelich, S.; Houlden, H.; Pickering-Brown, S.; Chakraverty, S.; Isaacs, A.; Grover, A.; Hackett, J.; Adamson, J.; Lincoln, S.; Dickson, D.; Davies, P.; Petersen, R. C.; Stevens, M.; de Graaff, E.; Wauters, E.; van Baren, J.; Hillebrand, M.; Joosse, M.; Kwon, J. M.; Nowotny, P.; Che, L. K.; Norton, J.; Morris, J. C.; Reed, L. A.; Trojanowski, J.; Basun, H.; Lannfelt, L.; Neystat, M.; Fahn, S.; Dark, F.; Tannenberg, T.; Dodd, P. R.; Hayward, N.; Kwok, J. B.; Schofield, P. R.; Andreadis, A.; Snowden, J.; Craufurd, D.; Neary, D.; Owen, F.; Oostra, B. A.; Hardy, J.; Goate, A.; van Swieten, J.; Mann, D.; Lynch, T.; Heutink, P. Association of missense and 5'-splice-site mutations in tau with the inherited dementia FTDP-17. *Nature* **1998**, *393*, 702-705.
641. Götz, J.; David, D. C.; Ittner, L. M. In *Impact of β -Amyloid on the Tau Pathology in Tau Transgenic Mouse and Tissue Culture Models*; Barrow, C. J., Small, D. H., Eds.; A β peptide and Alzheimer's disease - Celebrating a century of research; Springer: London, 2007; pp. 198-215.
642. Götz, J.; Chen, F.; van Dorpe, J.; Nitsch, R. M. Formation of neurofibrillary tangles in P301L tau transgenic mice induced by A β 42 fibrils. *Science* **2001**, *293*, 1491-1495.
643. Lewis, J.; Dickson, D. W.; Lin, W. L.; Chisholm, L.; Corral, A.; Jones, G.; Yen, S. H.; Sahara, N.; Skipper, L.; Yager, D.; Eckman, C.; Hardy, J.; Hutton, M.; McGowan, E. Enhanced neurofibrillary degeneration in transgenic mice expressing mutant tau and APP. *Science* **2001**, *293*, 1487-1491.
644. De Felice, F. G.; Wu, D.; Lambert, M. P.; Fernandez, S. J.; Velasco, P. T.; Lacor, P. N.; Bigio, E. H.; Jerecic, J.; Acton, P. J.; Shughrue, P. J.; Chen-Dodson, E.; Kinney, G. G.; Klein, W. L. Alzheimer's disease-type neuronal tau hyperphosphorylation induced by A β oligomers. *Neurobiology of Aging* **2008**, *29*, 1334-1347.
645. Jin, M.; Shepardson, N.; Yang, T.; Chen, G.; Walsh, D.; Selkoe, D. J. Soluble amyloid β -protein dimers isolated from Alzheimer cortex directly induce Tau hyperphosphorylation and neuritic degeneration. *Proc. Natl. Acad. Sci. U. S. A.* **2011**, *108*, 5819-5824.
646. Roberson, E. D.; Scarce-Levie, K.; Palop, J. J.; Yan, F.; Cheng, I. H.; Wu, T.; Gerstein, H.; Yu, G. Q.; Mucke, L. Reducing endogenous tau ameliorates amyloid β -induced deficits in an Alzheimer's disease mouse model. *Science* **2007**, *316*, 750-754.

647. Ittner, L. M.; Ke, Y. D.; Delerue, F.; Bi, M.; Gladbach, A.; van Eersel, J.; Wolfing, H.; Chieng, B. C.; Christie, M. J.; Napier, I. A.; Eckert, A.; Staufenbiel, M.; Hardeman, E.; Gotz, J. Dendritic function of tau mediates amyloid- β toxicity in Alzheimer's disease mouse models. *Cell* **2010**, *142*, 387-397.
648. Jack, C. R., Jr; Knopman, D. S.; Jagust, W. J.; Petersen, R. C.; Weiner, M. W.; Aisen, P. S.; Shaw, L. M.; Vemuri, P.; Wiste, H. J.; Weigand, S. D.; Lesnick, T. G.; Pankratz, V. S.; Donohue, M. C.; Trojanowski, J. Q. Tracking pathophysiological processes in Alzheimer's disease: an updated hypothetical model of dynamic biomarkers. *Lancet Neurol.* **2013**, *12*, 207-216.

CHAPTER II.

ALZHEIMER'S DISEASE AS AN AUTOIMMUNE DISEASE OF THE INNATE IMMUNE SYSTEM

1. Introduction

Despite over 100 years of research, there is still no truly comprehensive theory of AD. As the incidence of AD will increase with the aging of our population, there is a pressing need for disease-modifying agents that can replace the symptomatic drugs currently available. To enable the development of such a drug, a rigorous knowledge of the pathologic mechanism is necessary that must be based on an understanding of all processes and factors involved.

The goal of the research for this thesis was to develop a new theory of Alzheimer's Disease (AD) that is based on the notion that *Alzheimer's Disease is an autoimmune disease of the innate immune system*. Starting from the theoretical work by VC Meier-Stephenson, this hypothesis was expanded and supporting experimental evidence was obtained. Predicated on all currently implicated processes and factors, and including this new experimental evidence, the 'Vicious Cycle of Alzheimer's Disease' was devised, which proposes a physiological function for the A β peptide as an antimicrobial peptide of the innate immune system of the brain, and fills in the gaps in current hypotheses to explain why AD is a chronic and progressive disease. This theory

will provide further scientific insights and enable further development into what are currently limited therapeutic interventions, in particular, the development of potentially curative drugs.

2. The Physiologic Function of β -Amyloid: **A β as an Antimicrobial Peptide**

2.1. Introduction

Throughout evolution there has been a struggle of multicellular organisms to defend themselves against invading microorganisms. Over time, mammals developed two strategies for this purpose, the innate immune system and the adaptive immune system.

The innate immune system, being evolutionary older, is more 'primitive' and found in all classes of life. It relies on a number of agents, such as the complement system and antimicrobial peptides (AMPs) (1). The adaptive immune system is the more advanced and only found in vertebrates (2). Initiated by components of the innate immune system (3, 4), it provides cell-mediated immunity, which is based on the specific detection of invading species such as bacteria and viruses (so-called 'antigens'), by specialized proteins, the antibodies. It also features a 'memory', which allows for a quicker response to an antigen that has already been encountered in the past.

Both these systems have to be able to distinguish between 'self' and 'non-self' to avoid an attack on the own organism. 'Self' includes all healthy cells as well as symbiotic microorganisms and harmless/useful chemicals; 'non-self' comprises all harmful invading species such as bacteria, viruses, parasites, fungi and toxins as well as diseased cells like transformed or cancerous cells. Consequently, these systems are strictly regulated. However, a number of autoimmune diseases have been described, where this regulation fails and parts of the 'self' are targeted by the adaptive immune system; notably, no innate autoimmune disease has been

described to date. A few examples include Guillain-Barré syndrome, rheumatoid arthritis, Crohn's disease, systemic lupus erythematosus, and multiple sclerosis (5).

In this chapter, I will explore the concept that AD is an autoimmune disorder of the innate immune system.

2.2. Innate vs. Acquired Immunity

The innate immune system, as compared to the adaptive immune system, is the evolutionary older one. It is present in all classes of plants and animals (6, 7), and considered the first line of defense (8). It relies on a number of agents, such as the complement system and antimicrobial peptides (AMPs) (1, 9, 10). The complement system consists of a series of 20 peptides that control neutrophils (the most abundant type of leukocytes) and facilitate target identification (11, 12). AMPs are potent, relatively non-discriminative broad-spectrum antibiotics (13-16) that also seem to function as immunomodulators, thus enhancing immunity and connecting the innate to the adaptive immune system (17-23). It is now being recognised that not only does the innate immune system control the adaptive immune system (3, 4, 24), but the latter also has some control over the former (25, 26), and there is tightly regulated cross-talk between these two systems (27-30)

2.3. Effectors of the Innate Immune System

Contrary to early conceptions, the innate immune system is capable of detecting microbial intruders and cell damage specifically (31, 32). Pathogen recognition receptors (PRRs) have

evolved to detect conserved molecular motifs of pathogens referred to as pathogen-associated molecular patterns (PAMPs) (33, 34), such as lipids, lipoproteins, proteins and nucleic acids originating from wide range of microbes, e.g., bacteria, viruses, parasites, and fungi (33, 35-37). Three families of PRRs have been identified so far (6, 38, 39), Toll-like receptors (TLRs) (33, 37, 40-42), RIG I¹-like receptors (RLRs) (43-47), and NOD²-like receptors (NLRs) (48-50), that are expressed by many cell types, including nonimmune cells (31). Upon activation, PRRs oligomerize to assemble large complexes comprised of multiple subunits that initiate signaling cascades which ultimately recruit cells of the adaptive immune system to the affected tissue. As the most important family of PRRs, TLRs mediate the recognition of PAMPs; in humans the presence of 10 different TLRs has been established, each with distinct functions in terms of PAMP recognition and immune response (6, 31). Recognition of PAMPs by TLRs occurs in various cellular compartments, including the plasma membrane, endoplasmic reticulum, endosomes, lysosomes and endolysosomes (6). Besides their intended role in mediating immunity against pathogens, misguided TLR reactions lead to acute and chronic inflammation, and are involved in systemic autoimmune diseases (31).

2.3.1. Bacteria

Bacteria can be grouped roughly into two classes, Gram-positive and Gram-negative bacteria, which are distinguished by the structure and components of their cell walls (Figure II-1). The cell wall of Gram-positive bacteria consists of a cytoplasmic membrane made of phospholipids and a surrounding cell wall constructed from numerous dense layers of

¹ RIG I: retinoic acid-inducible gene 1

² NOD: Nucleotide-binding oligomerization domain containing protein

peptidoglycans³. Lipoteichoic acids (LTAs)⁴ anchored in the cytoplasmic membrane protrude through the cell wall, thus attaching it to the membrane, and reach into the extracellular space (Figure II-1). Gram-negative bacteria have a thinner cell wall than Gram-positive microorganisms, but possess an additional outer membrane that is attached to the cell wall through lipoproteins. The outer membrane consists of mostly lipoproteins on the inside and mainly lipopolysaccharides (LPS; also known as endotoxin) on the outside of the bilayer (Figure II-1).

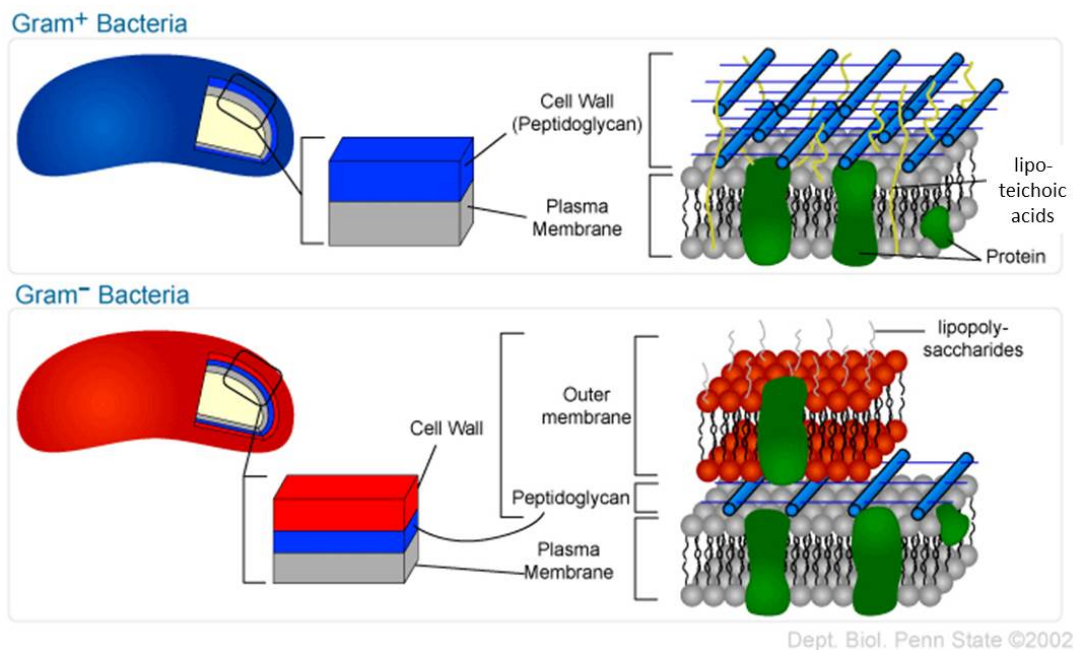


Figure II-1 Schematic of Gram-positive and Gram-negative bacterial cell walls.

In Gram-positive bacteria, the plasma membrane is surrounded by the cell wall made of peptidoglycans; lipoteichoic acids (LTAs) are anchored in the cell membrane and reach through the well wall into the extracellular space. In Gram-negative bacteria, the cell wall is significantly thinner, but is itself surrounded by a second, outer membrane consisting of lipoproteins and lipopolysaccharides (LPS).

Adapted from <https://wikispaces.psu.edu/display/110Master/Prokaryotes+II+-+Structure+and+Function>

³ These are also called mureins, from Latin 'murus' = wall

⁴ From Greek 'teichos' = city wall

Four types of LTA are known so far; in general, they consist of a polyglycerophosphate chain attached to a diglucosyl moiety which is bound to the lipid tail made up of two fatty acids. Since two *S. aureus* strains are used in this thesis, the chemical structure of its LTA is given in Figure II-2. A more detailed discussion of the structural differences between the four types of LTA is beyond the scope of this thesis but has been reviewed in the pertinent literature, e.g., in References (51-54).

Almost every structure of LPS characterised to date conforms to a common general structure. It typically consists of three regions, a lipid anchor termed 'lipid A', a core region (which itself is divided into the inner and outer core), and an O-polysaccharide chain. Lipid A consists of a highly conserved di-glucosamine backbone and acyl chains of varying number and length. The inner core is also highly conserved and contains a high proportion of the unusual sugars 3-deoxy-D-manno-octulosonic acid and L-glycero-D-manno heptose; the outer core usually contains more common sugars such as hexoses or hexosamines. Attached to the outer core is, in most cases, the O-polysaccharide, with repeating units of one to eight glycosyl residues. As these repeating O-oligosaccharides differ between strains in the type of sugars, sequence, chemical linkage, substitution, and ring forms utilised, they provide an enormous diversity. Furthermore, the number of monomers in the chain ranges from 0 to ~50 in a single bacterium due to incomplete synthesis of the chain, leading to an almost unlimited diversity among the different organisms. As an example, the structure of the lipid A portion of *E. coli* LPS is given in Figure II-2, but again, a more in depth discussion of specific structures of the different strains is beyond the scope of this thesis, but has been reviewed in the pertinent literature, e.g., in References (55-57).

The most potent effectors of PRRs are LTA in Gram-positive bacteria (6, 58-61), and LPS in Gram-negative bacteria (6, 59, 62, 63) (Figure II-2). LTA activates the immune cells via the

TLR2/TLR6 heterodimer (58, 64-67). In LPS, the part termed “lipid A” causes most of the pathogenic phenomena associated with infections by Gram-negative bacteria such as endotoxin shock (6). LPS recognition is among the most sensitive systems in biology; LPS can induce direct responses from cells in subpicomolar concentrations. It involves TLR4 in concert with LPS-binding protein (LBP), myeloid differentiation-2 (MD-2) and CD14 (63, 68-75).

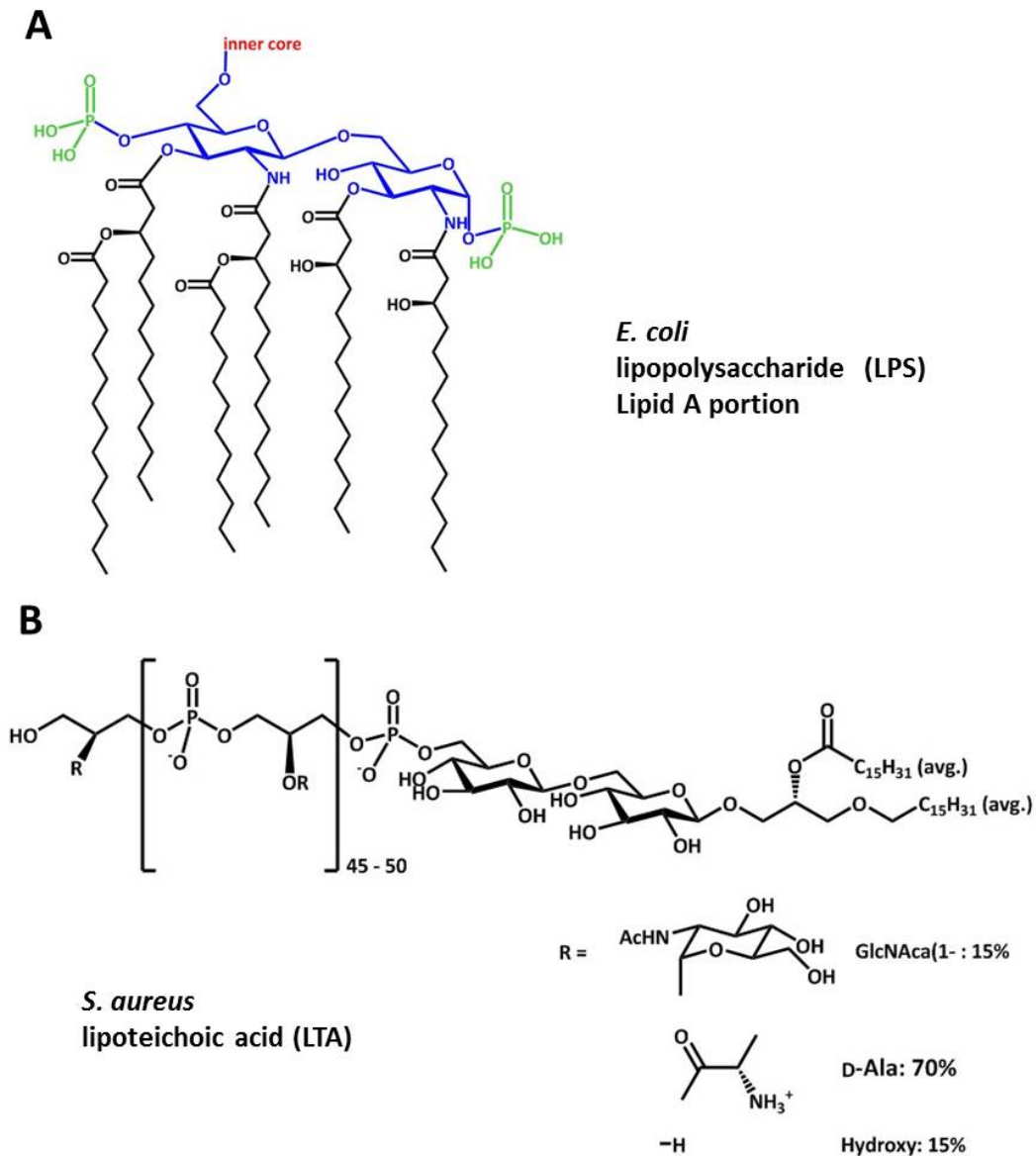


Figure II-2 Chemical structures of lipid A portion of lipopolysaccharide (LPS) and lipoteichoic acid (LTA). Displayed are the chemical structures of the Lipid A portion of *E. coli* LPS (A) (56), and *S. aureus* LTA (B) (54).

2.3.2. Viruses

Subsequent to endocytosis or fusion at the plasma membrane, viruses enter the cytoplasm and initiate replication. PRRs recognize virus-associated molecules, such as DNA or RNA in a replication-independent (TLR7, TLR8, TLR9) or replication-dependent (TLR3, RNA helicases) manner. Upon activation by viral components, these PRRs initiate production of a variety of cytokines and induce an inflammatory and adaptive immune responses (6, 34-37, 76, 77).

2.3.3. Trauma

In addition to PAMPs, innate immune system cells also detect damage-associated molecular patterns (DAMPs). These are endogenous molecules found under physiological conditions inside cells that get released during injury or necrosis, or by tumor cells and induce sterile inflammation. Examples for DAMPs are degradation products of the extracellular matrix, heat shock proteins, adenosine triphosphate (ATP), the cytokine IL1 α , uric acid, the calcium-binding cytoplasmic proteins S100A8 and S100A9, and the DNA-binding nuclear protein high mobility group box 1 (HMGB1).

Injury, and even sterile wounding induces an epidermal innate immune response during wound healing (78, 79) that is thought to increase resistance to overt infection and microbial colonization. Interestingly, in AD the A β peptide is recognized in a TLR4/TLR6 dimer-dependent manner and triggers sterile inflammation (80-83).

2.3.4. AMPs

Once microorganisms are detected, antimicrobial peptides (AMPs) are produced to help fight the intruders. AMPs are potent, relatively non-discriminative broad-spectrum antibiotics

with activity against Gram-negative and Gram-positive bacteria (including antibiotic-resistant strains), mycobacteria, enveloped viruses, fungi and even transformed or cancerous cells (18, 20, 84). They are expressed in a wide range of tissues, e.g., skin, airways, mouth, stomach, intestine, liver, genital tract (85, 86), i.e., tissue that is likely to encounter bacteria.

Recently, besides directly killing intruding microorganisms, AMPs have been shown to also possess immunomodulatory activity (87-90). They were found to induce or modulate chemokine and cytokine production, to alter gene expression in host cells, and inhibit proinflammatory responses of host cells to bacterial endotoxins in vitro and in vivo (18, 89, 91-94).

2.4. Evolutionary Connections between AMPs and β -Amyloid

Over millions of years, evolution has optimized organisms for the never-ending battle for survival. In the evolutionary process, unnecessary functions were lost to save energy for more important ones. Therefore it is sensible to assume that A β is not just waste of a process involving APP, but has a function of its own.

Being the barrier between an organism and the outside world, the skin is known to produce a range of AMPs in order to prevent a penetration of potentially pathogenic microorganisms (13, 85, 95). Examples are the two AMP families, cathelicidins (96) and dermaseptins (97). Since brain cells and skin cells are of the same developmental origin (endoderm layer of the gastrula) it is reasonable that cells of both tissues can express similar proteins, such as AMPs, as part of the defense mechanisms (98-100). Although the brain is normally well protected against any microbial invasion by the blood-brain barrier (BBB), it is also separated from the immune system guarding the rest of the body. It is logical that such a crucial

organ would not rely solely upon this mechanical barrier for its protection. Thus it is not surprising that AMPs, albeit only a very small number, have actually been found in brain tissue. For example, in mice embryos, the antimicrobial peptide LANCL1 is expressed in the brain upon formation of the blood-brain barrier (101). Another example is human β -defensin 2, which was found to be expressed in human astrocytes (102). The fact that only very few examples of AMPs are known to exist in the brain suggests the possibility that there may still be more yet to be identified.

2.5. Structural Comparison of β -Amyloid to AMPs

To date, over 4650 different antimicrobial peptides have been identified and sequenced; furthermore, some additional 860 sequences are predicted to have antimicrobial activity (LAMP database; accessed: March 2014) (103). AMPs are small peptides with a length of about 10 – 50 amino acids, although shorter and longer peptides with antimicrobial activity have been found (with the upper end being a matter of definition). Typically, AMPs possess a positive net charge due to an excess of basic residues compared to the number of acidic residues. This feature causes a strong attraction to the negatively charged membranes of bacteria, and at the same time prevents them from attacking 'self' cells (104). They do not exhibit a preferential type of secondary structure, in fact there are examples for each structural category (Figure II-3). For example, LL-37 (human) is α -helical; β -defensin-1 (human, hBD-1) is mainly β -sheet; and indolicidin (bovine) is found as an extended coil. Furthermore, some AMPs show increased activity when they are bound to a metal ion (105-109), e.g., psoriasin bound to Zn^{2+} (110). They can be classified into four broad structural categories: α -helical with amphipathic region, β -sheet

with disulfide linkages, high content of a certain amino acid, and others which include loop peptides, fragment peptides, and anionic surfactant associated peptides (7, 18).

Despite their vastly different secondary structures, AMPs seem to adopt one of two general three-dimensional conformations; an amphipathic structure where hydrophobic amino acid residues are present preferentially on one face, and polar/cationic residues on the other face of a (helical) secondary structure; and a cationic double-wing structure with a hydrophobic core bracketed by two regions of positive charge (111). A number of databases for AMPs are available, e.g., the *Antimicrobial Peptides Database* (APD; <http://aps.unmc.edu/AP/main.php>) (112), the *Antimicrobial Sequences Database* (AMSDb; <http://www.bbcm.units.it/~tossi/pag1.htm>) (113), *Yet Another Database of Antimicrobial Peptides* (YADAMP; <http://www.yadamp.unisa.it/>) (114), and *LAMP: A database linking antimicrobial peptide*, (<http://biotechlab.fudan.edu.cn/database/lamp/index.php>) (103).

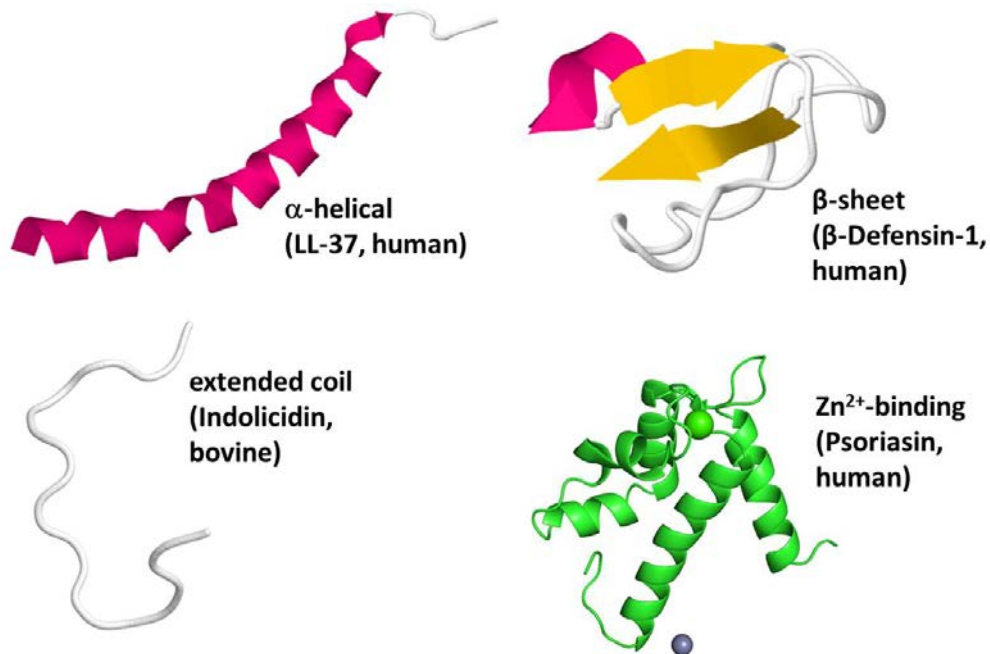


Figure II-3 Examples of AMPs with different secondary structures.

PDB IDs: LL-37: 2K6O(115); β -Defensin: 1KJ5 (116); Indolicidin: 1G89 (117); Psoriasin: 2PSR (green sphere: Zn²⁺, blue sphere: Ca²⁺) (110).

2.5.1. A β Sequence, Constituent Amino Acid Residues & Charge State

The primary structure of A β ₁₋₄₂ (Figure II-4) exhibits features that are typically also found in AMPs. Both basic (H, K, and R) and acidic (D,E), as well as hydrophobic residues (A, C, F, I, L, M, V, W) are present. As most α -helical AMPs, A β has an equal number of acidic and basic amino acids present leading to an overall charge of zero (Figure II-5). Furthermore, the percentage of hydrophobic residues (19 residues; 45.2 %) lies close to the average value for other α -helical AMPs (Figure II-5) (118).

DAEFRHDSGY¹⁰EVHHQKLVFF²⁰AEDVGSNKG³⁰IIGLMVGGVV⁴⁰IA

Figure II-4 Amino acid sequence of A β ₁₋₄₂.

Red: negatively charged residues; blue: positively charged residues; underscored: hydrophobic residues

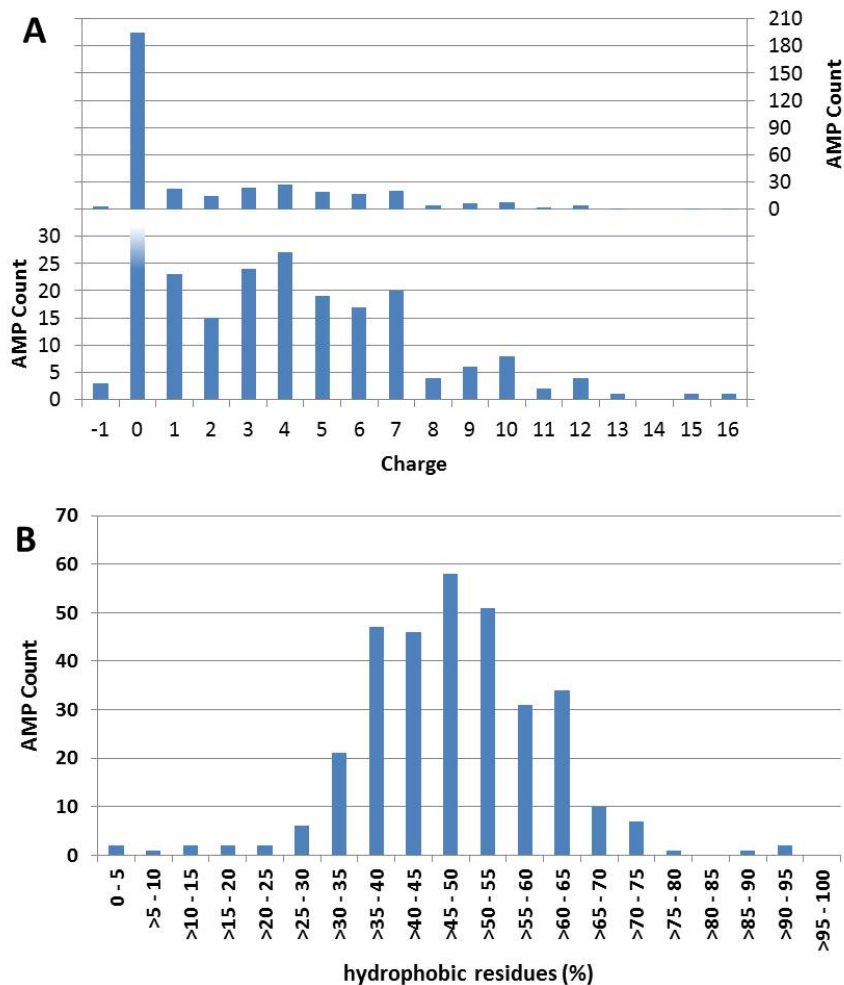


Figure II-5 Distribution of charged and hydrophobic residues in α -helical AMPs.

The sequences of all exclusively α -helical AMPs contained in the APD2 (112) (<http://aps.unmc.edu/AP/main.php>; accessed: July 24, 2013; 324⁵ of a total of 2253 AMPs contained in the database) were analyzed for their charge (at neutral pH) (A) and their content of hydrophobic amino acid residues (B). (A) Top shows complete AMP count, bottom shows “zoom in” on lower counts (i.e., charge ‘0’ is cut off).

2.5.2. Amphipathicity & Schiffer-Edmundson Helical Wheel

The amphipathicity of a peptide is a measure for the anisotropic distribution of charges on different sides of a helix. A convenient visualization of this property is the Schiffer-Edmundson

⁵ These contain 14 synthetic peptides (4.3%), none of them with charge ‘0’

helical wheel (119). It arranges the residues in a pattern that would be observable when looking down the core axis of the helix from N- to C-terminus.

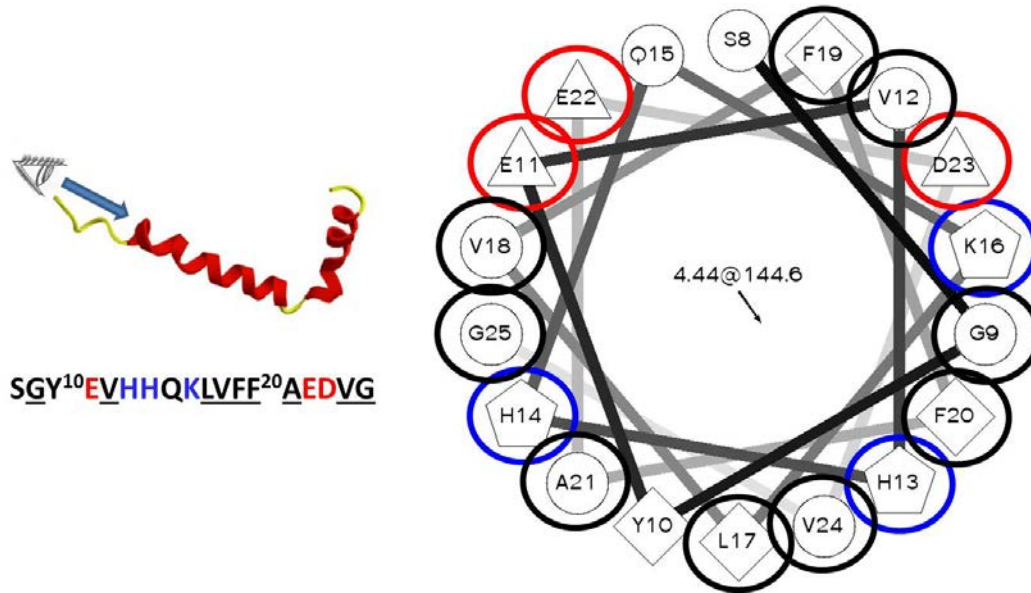


Figure II-6 Helical wheel of the N-terminal helix ($A\beta_{8-25}$).

Red: acidic, blue, basic, black: hydrophobic, unmarked: polar, uncharged. In the centre the hydrophobic

moment @ angle is displayed. Helical wheel produced with script available at:

<http://r2lab.ucr.edu/scripts/wheel/wheel.cgi>

The helical wheel projection was developed by Schiffer and Edmundson (119)

α -helical AMPs in particular often contain an amphipathic region allowing them to interact directly with microbial membranes, which they can rapidly permeabilize (118). Figure II-6 depicts a helical wheel representation of $A\beta_{8-25}$, the first α -helical segment in the full sequence (Figure II-4). The amphipathicity of $A\beta$ can be clearly seen, with the positively charged residues (blue circles) mainly on the right-hand side, the negatively charge amino acids (red circles) predominantly on the left, and the hydrophobic residues (black circles) mainly on the bottom right.

2.5.3. Boman Index

Another piece of the puzzle is given by the Boman index (BI), which allows the calculation of the binding potential of the interaction between a peptide and bacterial membranes based on the amino acid side chain amphipathicity according to the following Equation (II-1):

$$BI = \frac{\sum_n(\Delta G_{chx \rightarrow water})}{n} \quad (II-1)$$

Here, $\Delta G_{chx \rightarrow water}$ is the solvation free energy for an amino acid side chain of n residues to transfer from cyclohexane (chx) to water (120). A high BI indicates a strong binding potential, but also the potential for unspecific binding and thus greater side effects. One example of such a peptide is the vaso-active intestinal peptide. It has a BI of 10.38 kJ/mol (2.48 kcal/mol) and acts as both a neurotransmitter and an antibacterial agent. A low BI, in contrast, suggests a more specific antibacterial activity as exemplified by the natural peptide magainin 2, which has a BI of 1.72 kJ/mol (0.41 kcal/mol). The BI for A β_{1-40} is 4.10 kJ/mol (0.98 kcal/mol)⁶, and for A β_{1-42} 3.22 kJ/mol (0.77 kcal/mol), falling well within the range of already established AMPs, thus indicating the potential for binding to bacterial membranes.

2.5.4. Heparin Affinity

Interestingly, Andersson *et al.* reported that structural motifs associated with heparin affinity, such as cationicity, amphipathicity, and consensus regions may confer antimicrobial properties to a given peptide (121); a result confirmed in studies by Lu *et al.* (122). As has been illustrated in the previous sections, all of these features are actually present in A β .

⁶ Both values were calculated with the Antimicrobial Peptide Predictor available at: http://aps.unmc.edu/AP/prediction/prediction_main.php

2.5.5. AMP Activity Prediction

Finally, there are now prediction tools available online that calculate, based on structural similarity to known AMPs, whether a peptide sequence potentially has antimicrobial activity. The prediction tool available on the Antimicrobial Peptides Databank (APD) website (123) predicts for the sequence of A β ₁₋₄₀ that the “[...] peptide may interact with membranes and has a chance to be an antimicrobial peptide” (see Appendix A).

2.6. Mechanism of Action

An important point to consider in the comparison of A β with known AMPs is the mechanism of action. AMPs have been shown to act through a number of different mechanisms. The following section will describe the different types that are distinguished and discuss the mechanism proposed for A β .

2.6.1. Mechanisms of Action of Known AMPs

Most AMPs are thought to kill microorganisms *via* a non-receptor-mediated mechanism with in vitro activity at micromolar concentrations, which is comparable to their biological concentration at the site of infection (124). The few examples of AMPs believed to act through receptor-mediated mechanisms are active at much lower concentrations, in the nanomolar range (124).

2.6.1.1. Non-Receptor Mediated AMPs

AMPs falling into the first group are far more abundant and exhibit a broad spectrum of amino acid composition, length and structure. A few examples are mellitin (125), cecropin (126), magainin (127), and androctonin (128). Their non-receptor-mediated action is aimed, as the term implies, not at a specific but rather a more general target, the bacterial membrane. The outer surface of Gram-negative bacteria contains lipopolysaccharides (LPS), whereas that of Gram-positive bacteria contains acidic polysaccharides (teichoic acids), thus giving the surface of both Gram-positive and -negative bacteria a net negative charge (104). Furthermore, the inner membrane of Gram-negative bacteria and the single membrane of Gram-positive bacteria are composed of negatively charged phospholipids. To the contrary, the phospholipids comprising the membrane of normal mammalian cells are asymmetrically distributed, where the outer leaflet is composed predominantly of zwitterionic phosphatidylcholine (PC) and sphingomyelin phospholipids, while the inner leaflet is composed of negatively charged phosphatidylserine (PS) (104). Therefore, the net positive charge, which is the most preserved property of antimicrobial peptides, allows preferential binding to the negatively charged outer surface of bacteria (118, 129-133). Support for the notion that bacterial membranes are the non-specific target of this group of AMPs comes from a few studies, which showed that all-D-enantiomers of a number of lytic peptides exhibit the exact same biological activity as their natural (all-L) parent molecules (134-137). However, a specific target would not interact with the enantiomer of the substrate. Furthermore, the all-D-enantiomers adopted an exact mirror image structure of their parent compound. Therefore it was concluded that the amphipathic structure of these AMPs is essential for the antimicrobial activity.

2.6.1.2. Receptor Mediated AMPs

AMPs that act *via* a receptor-mediated mechanism are typically compiled of two regions, a receptor-binding domain and a pore-forming domain. In this group only a few examples are described in the literature, e.g., nisin Z (124) and mesentericin Y (138). Typically, these AMPs show a significant degree of stereospecificity, which is necessary to bind specifically to a certain receptor (139). Moreover, removing the receptor-binding domain leads to a decreased activity in the micromolar range, comparable to AMPs in the first group (140).

2.6.1.3. AMP Mechanisms of Action

The peptides of the first group are believed to cause damage to the bacterial membrane by forming pores or disintegrating the membrane, which results in the collapse of the transmembrane electrochemical gradients (92, 118, 129, 133, 141-145). Due to the collapse of the electrochemical gradient, the microorganisms lose their source of energy, allowing increased water and ion flow across the membrane, ultimately resulting in cell swelling and osmolysis. Three different mechanisms for the formation of pores have been proposed, the barrel-stave pore formation model, the carpet-like destruction model, and the toroidal pore formation model (146).

(a) Barrel-Stave Pore Formation Model

In the barrel-stave pore formation model, the peptides attached to the membrane aggregate and integrate into the membrane bilayer such that the hydrophobic peptide regions align with the lipid tails and the hydrophilic peptide regions form the interior region of the water-filled pore (Figure II-7) (132).

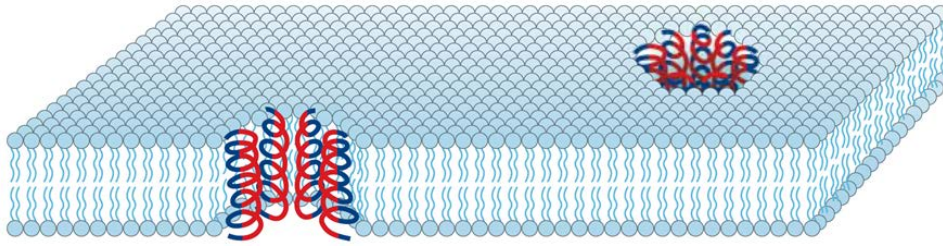


Figure II-7 The barrel-stave model of AMP-induced killing.
 Reprinted by permission from Macmillan Publishers Ltd. [Ref. (146)], © 2005.

(b) Carpet-like Destruction Model

In the carpet-like destruction model, the peptides disrupt the membrane by orienting parallel to the surface and, once it is saturated, collapsing the integrity of the membrane leading to abrupt lysis of the cell (Figure II-8) (132).

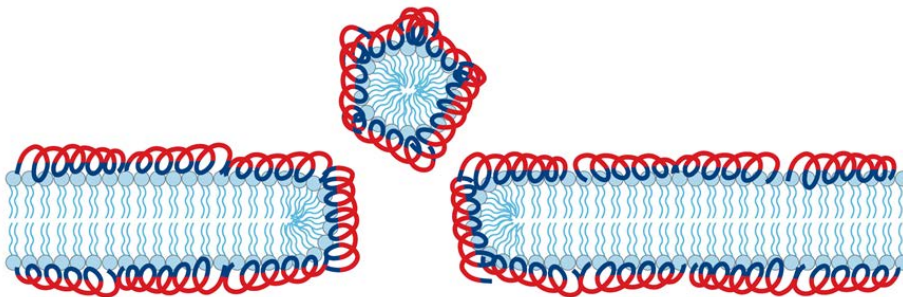


Figure II-8 The carpet model of AMP-induced killing.
 Reprinted by permission from Macmillan Publishers Ltd. [Ref. (146)], © 2005.

(c) Toroidal Pore Formation Model

In the toroidal pore formation model, aggregation of the peptides induces the lipid monolayers to bend continuously through the pore so that the water-filled core is lined by the inserted peptides, as well as the lipid head groups (Figure II-9) (147). The latter two models are sometimes considered as one (148).

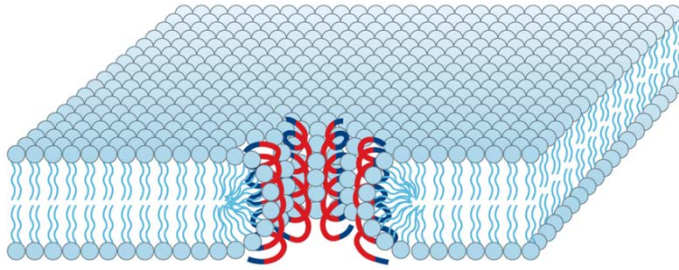


Figure II-9 The torroidal pore model of AMP-induced killing.

Reprinted by permission from Macmillan Publishers Ltd. [Ref. (146)], © 2005.

(d) Aggregate Channel Model

After results from some AMPs pointed to a mechanism that does not involve the destruction of the membrane, the aggregate channel model was proposed (149). There, the peptides, after binding to the phospholipid head groups, insert into the membrane and cluster into unstructured aggregates, which span the entire membrane (Figure II-10). These aggregates are proposed to contain water molecules providing channels for leakage of ions and possibly larger molecules through the membrane. Furthermore, the aggregates are thought to exist only for a short time, but permit the peptides to cross the membrane without causing significant damage. Subsequently they can reach their intracellular target to kill the microorganism. Intracellular targets that have been identified are for example, stimulation of autolytic enzymes (150), interference with bacterial DNA and/or protein synthesis (151-156), inhibition of cell-wall synthesis (157), and enzymatic activity (84, 158), binding to and inhibition of cellular nucleic acids (159-163), alteration of cytoplasmic membrane septum formation (152, 157, 164), and flocculation of intracellular contents (165).

This last mechanism has a great advantage in that it neither releases potentially toxic contents of the microorganisms nor breaks the bacterial membrane into pieces (LPS contamination is the major cause of bacterial sepsis).

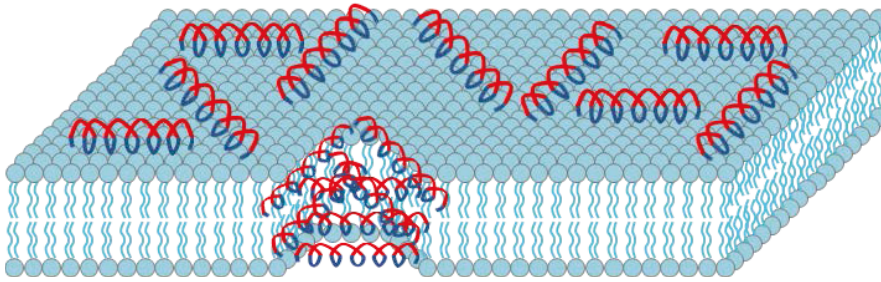


Figure II-10 The aggregate channel model of AMP-induced killing.

2.6.1.4. Connection of Antibacterial and Immunomodulatory Effects

Connecting the antibacterial with the immunomodulatory effect of AMPs, Otvos *et al.* proposed a link between the innate and the adaptive immune system in that the cell-penetrating fragments of AMPs are located at one terminus, while the protein-binding domains responsible for the activation of the adaptive immune system are found on the other terminus (166).

2.6.2. Effect of Metal Cations on the Activity of AMPs

Some AMPs have been shown to have an antimicrobial activity dependent on binding to a third species. In the literature most prominently represented are cholesterol and metal cations.

For example, Rydengard *et al.* found that Zn^{2+} potentiates the antibacterial effects of histidine-rich peptides against *Enterococcus faecalis* (108). In particular, Histatin 3 and Histatin 5 were demonstrated to bind Zn^{2+} resulting in increased activity (105, 167). Similar results were found for Kappacin upon binding of divalent metal cations (Zn^{2+} , Ca^{2+}) (107). Furthermore, McEntire demonstrated a synergy between nisin and select lactates against *Listeria monocytogenes*, which was caused by Zn^{2+} cations (168).

2.6.3. Effect of Cholesterol on the Activity of AMPs

An entire class of AMPs, the cholesterol-dependent cytolysins (CDCs), contain in their name the importance of binding to cholesterol (169). CDCs are bacterial protein toxins, which bind to cholesterol-containing membranes to form oligomeric complexes and then insert into the bilayer to create large aqueous pores. Ramachandran *et al.* found that membrane-dependent structural rearrangements are required to initiate the oligomerization of perfringolysin O monomers (169). Giddings and co-workers reported that depletion of membrane cholesterol prevents the insertion of the transmembrane β -barrel and pore formation of CDCs (170). Cholesterol was also found to attenuate the interaction of the AMP gramicidin S (171) and granulysin (172) with phospholipid bilayer membranes.

2.6.4. β -Amyloid's Mechanism of Action

Based on computational studies, VC Meier-Stephenson proposed that A β may act through three distinct mechanisms, depending on the secondary structure it adopts at the moment of interaction (173). If A β were to adopt a β -sheet conformation, the most likely mechanism of action would be through a barrel-stave mechanism whereby the monomers pre-assemble to form structured fibrils, which then insert into the membrane causing leakage. However, if A β were to adopt an α -helical conformation, two possible mechanisms were proposed. Firstly, A β could act through a carpet-type destruction mechanism, with the peptide anchored onto the membrane surface by the charged helix arranged parallel to the membrane surface, thus allowing the hydrophobic helix to insert into the membrane. And secondly, a flip-flop mechanism was suggested, where A β , similar to other AMPs, induces increased flip-flop rates of membrane lipids due to pore formation (174-176). In the process it would get transferred across the membrane and subsequently attack intracellular targets, such as mitochondria (177-181).

A number of AMPs have been found that contain a “hinge” between two α -helices, which is proposed to facilitate the insertion into the membrane. First, one of the helices anchors the peptide by electrostatic interactions onto the surface of the membrane (182). This gives the second helix enough leverage to insert itself into the membrane, allowing it to attain the proper orientation for pore formation. Some examples for such peptides are cecropins (183), melittins (184), PMAP37 (118, 185), and caerin-1 (118, 186). Some A β secondary structures, obtained by NMR experiments, have been shown to exhibit comparable structural features (187, 188), possibly enabling a similar mechanism (Figure II-11).

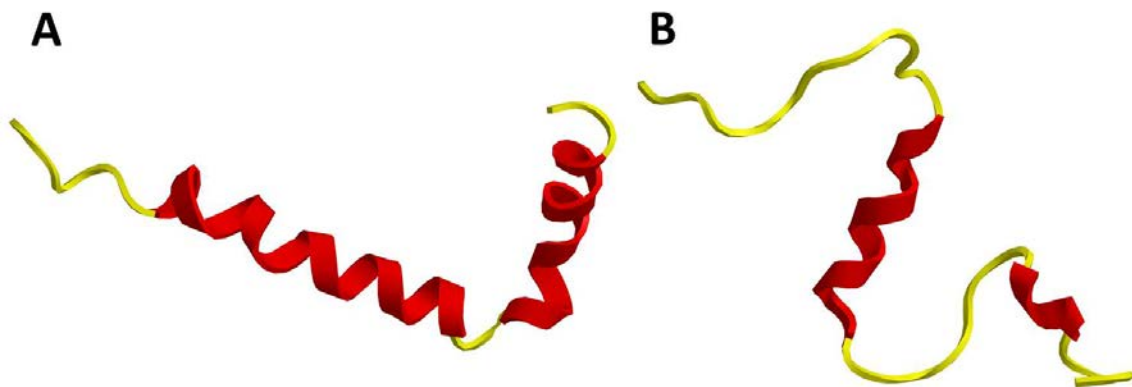


Figure II-11 A β secondary structures containing a flexible “hinge” region between two α -helices.
PDB files: A: 1IYT (187), B: 1AML (188).

Early on, it was noticed that A β seems to disrupt Ca²⁺ homeostasis (189); Arispe *et al.* suggested that A β might form cation (Ca²⁺)-selective ion channels in lipid bilayers (190). Subsequent atomic force microscopy studies on solid supported bilayers by Lin *et al.* have shown that the interactions of A β peptides result in the formation of conducting ion channels that have rectangular or hexagonal shapes containing four or six subunits, are 80-120 Å in diameter and protrude ~10 Å from the bilayer surface (191). This gives further experimental support for the role and mechanism of A β 's action on cellular membranes.

2.7. β -Amyloid is Produced in Response to Infection

2.7.1. Introduction

Providing further support for the hypothesis of A β as an AMP in the brain, experimental evidence is presented here that A β is produced in response to the presence of bacteria, i.e., that the peptide production is upregulated by neurons in an attempt to protect themselves from the invading organisms.

To show this, experiments incubating two types of neuronal cells—neuroblastoma cells and primary rat neurons, with various types of pathogenic bacteria—*Escherichia coli* (*E. coli*), *Serratia marcescens* (*S. marcescens*), *Klebsiella pneumoniae* (*K. pneumoniae*), and methicillin-resistant and methicillin-sensitive *Staphylococcus aureus* (MRSA and MSSA, respectively) were performed and their products analysed. A schematic of the overall approach (Figure II-12) and summary of the experimental evidence is presented below.

For ease of understanding the derivation of evidence, Figure II-12 describes the workflow of the experiment. First, a bacterial culture was grown and autoclaved to kill the bacteria. After isolation of the bacterial fragments, neuronal cells were incubated with those fragments. Next, the supernatant and neuronal cells from that incubation were separated. The supernatant was analysed directly using an enzyme-linked immunosorbent assay (ELISA) to determine the amount of A β *excreted from* the neuronal cells; the neuronal cells underwent a lysis step before their contents were analysed by ELISA in the same manner, to determine the amount of A β *produced internally*.

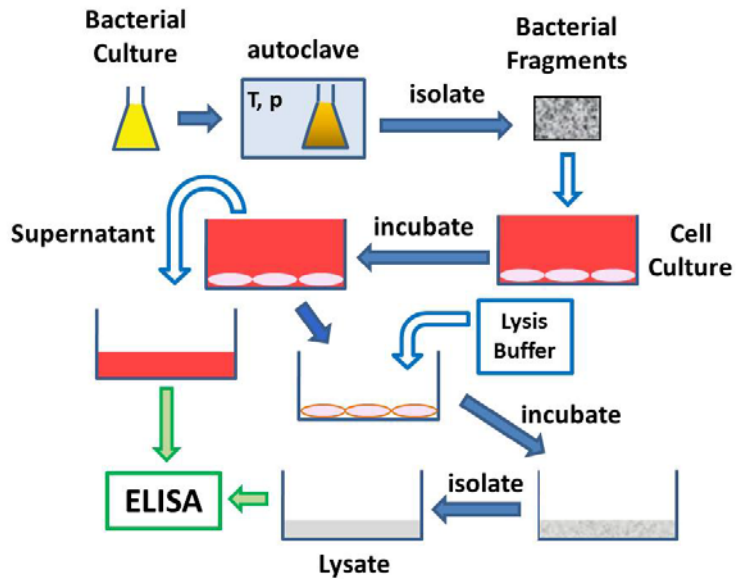


Figure II-12 Schematic of experimental procedure for A β production by neuronal cells.

A bacterial culture was autoclaved to produce bacterial fragments. Cells were then incubated with the bacterial fragments overnight; A β concentrations in supernatant and cell lysate were determined by ELISA (for details see text).

2.7.2. Materials

2.7.2.1. Biological Materials

(a) Bacteria

The following bacterial strains, unless otherwise noted kindly provided by Dr. A. Henneberry of DeNovaMed, Inc., were used in the experiments.

Gram-negative strains:

- *Escherichia coli* BL21; ATCC #BAA-1025; (*E. coli*); Risk Group: 1
- *Serratia marcescens*; ATCC #13880; (*S. marcescens*); Risk Group: 1
- *Klebsiella pneumoniae*; ATCC #13883; (*K. pneumoniae*); Risk Group: 2

Gram-positive strains:

- methicillin-susceptible *Staphylococcus aureus* (MSSA); clinical isolate; Risk Group: 1
- methicillin-resistant *Staphylococcus aureus* (MRSA); clinical isolate; Risk Group: 2

(b) Mammalian Cells

Furthermore, the following mammalian cell lines were used:

- SH-SY5Y; human neuroblastoma; ATCC #CRL-2266; Risk Group: 1
(a kind gift by Dr. D. Byers of Dalhousie's Atlantic Research Centre and Department of Biochemistry & Molecular Biology)
- SK-N-AS, human neuroblastoma, ATCC # CRL-2137, Risk Group: 1 (American Type Culture Collection (ATCC), Manassas, VA, USA)

As well, primary neuronal rat cells were used, kindly provided by Dr. B. Karten (Department of Biochemistry & Microbiology, Dalhousie University)

2.7.2.2. Chemicals

Some experiments also required use of specially prepared solutions and other chemicals including the following:

Ultra-purified water (Millipore system); Luria-Bertoni (LB) broth, Miller; LB agar; phosphate-buffered saline (PBS)(192); Dulbecco/Vogt modified Eagle's minimal essential medium (DMEM; with and without phenol red); fetal bovine serum (FBS); penicillin-streptomycin solution; L-glutamine; sodium pyruvate; CO₂ medical grade; Trypsin-EDTA 1× (Gibco, Cat.# 25200-072), TrypLE Select 10× (Invitrogen, Cat.#A1217701); lipopolysaccharide (LPS) from *E.coli*

(a kind gift by Dr. T. B. Grindley, Dalhousie University, Department of Chemistry); LPS from *E. coli* O111:B4 (Sigma-Aldrich, Cat.# L3024); lipoteichoic acid (LTA) from *S. aureus* (Sigma; Cat.# L2515); Triton X-100; A β ₁₋₄₀ ELISA kit (Signet, Cat.# 8940, Lot# 05LK02508); A β ₁₋₄₀ ELISA kit (Cat.# hAmyloid β 40 Elisa (HS), Lot# 3_022); A β ₁₋₄₂ ELISA kit (Cat.# hAmyloid β 42 Elisa (HS), Lot# 4_020); A β ₁₋₄₀ (AnaSpec, Inc., Cat.# 24236); A β ₁₋₄₂ (AnaSpec, Inc., Cat.# 20276); Tris base; anti-A β antibody 6E10 (193) (Covance, Cat.# SIG-39320); biotinylated anti-A β antibody 6E10 (Covance, Cat.# SIG-39340); anti-A β antibody 4G8 (194) (Covance, Cat.# 39220); biotinylated anti-A β antibody 4G8 (Covance, Cat.# SIG-39240); Tween-20; bovine serum albumin (BSA) ; horseradish peroxidase (HRP)-streptavidin; 3,3',5,5'-tetramethylbenzidine (TMB); hydrogen peroxide; citric acid, monohydrate; potassium citrate, tribasic, monohydrate; tetrabutylammonium borohydrate; dimethylacetamide; sulfuric acid; Hank's Balanced Salt Solution (HBSS).

2.7.2.3. Instrumentation

For bacterial cultures, a Labnet 311DS Shaking incubator was used; for mammalian cell cultures, a CO₂ incubator (HERAcell 150, Heraeus). To determine the optical density of bacterial cultures, a Waters 2487 Dual Wavelength absorbance detector was used. Microplates were read in a Genios or an Infinite 200 microplate reader (both Tecan), which were both equipped with optical filters for the appropriate wavelengths.

2.7.3. Methods

2.7.3.1. Preparation of β -Amyloid Stock Solutions

A β is a peptide with a high propensity to aggregate, making it inherently difficult⁷ to prepare consistent solutions. Great care has to be taken in its handling. Accordingly, the protocol for the preparation of stock solutions evolved over time as new information became available from the literature and through our own experimentation.

Initially, A β was dissolved in 20 mM Tris Base (pH ~10.4), sonicated for 10 - 15 minutes; the pH was adjusted to 7.4 with concentrated HCl, the volume adjusted with 20 mM Tris/HCl pH 7.4 to gain the desired concentration and the solution filtered through a 0.2 μ m PVDF syringe filter. Stock solutions were stored in the refrigerator at 4°C for up to two weeks.

Since it had been reported that the toxic species of A β might actually be small oligomers, “aged” A β solutions were produced by shaking for 24 hours at ~400 rpm at room temperature.

It later became clear that the former treatment may not completely disassemble all aggregates present in the lyophilised peptide. Complete disassembly of aggregates is an essential step to achieve a consistent and reproducible starting point for any further treatment of the A β . Thus, A β was dissolved in 1,1,1,3,3,3-hexafluoroisopropanol (HFIP), vortexed and sonicated for 10 minutes. The solution was aliquoted and the HFIP evaporated overnight; to remove residual HFIP, the tubes were placed under high-vacuum for three hours. The resulting wax was frozen and stored at -80°C in the freezer. Eventually, the overnight evaporation was replaced by blowing off the HFIP with a gentle stream of inert gas (nitrogen or argon) for about half an hour.

⁷ A β has actually been termed the “peptide from hell” since it is so tricky to work with (323).

To obtain small toxic oligomers, 10 μL of DMSO were added to 50 μg A β wax. After vortexing for 30 seconds, the solution was sonicated for 10 minutes. Addition of 300 μL of PBS was followed by vortexing for 30 s. Finally, the solution was stored in the refrigerator at 4°C overnight (for at least twelve hours).

To obtain dodecameric A β , 10 μL of DMSO were added to 50 μg A β wax. After vortexing for 30 seconds, the solution was sonicated for 10 minutes. Addition of 300 μL of PBS with 0.2% SDS was followed by vortexing for 30 s. Finally, the solution was stored in the refrigerator at 4°C overnight (for at least twelve hours).

An even more thorough de-aggregation procedure was adopted towards the end since some literature suggested that a single treatment with HFIP might not be enough to achieve complete dissociation of all aggregates. 1 mL of distilled HFIP was added into the original glass vial; after vortexing for 1 minute the solution was sonicated at room temperature for 15 minutes. The HFIP was removed in a dessicator under high vacuum for about 45 minutes. 1 mL of trifluoroethanol (TFE) or trifluoroacetic acid (TFA) was added to the glass vial, vortexed for 30 seconds, and sonicated for 15 minutes. The solution was aliquoted into microcentrifuge tubes, and the solvent removed under high vacuum as above. 200 μL HFIP were added into each tube, which were then vortexed for 30 seconds, sonicated for 15 minutes and incubated overnight at room temperature. The following morning, HFIP was removed under high vacuum for about 90 minutes; the dessicator was purged with ultrahigh purity argon, and put under high vacuum for another 2 hours. Unused aliquots were stored at -80°C in a chest freezer.

2.7.3.2. β -Amyloid Quantitation by BCA Assay

After our supplier of A β told us partway through this work that the peptide content was not 100%, and since a filtration step was often required in the preparation of the A β stock

solution, the bicinchoninic acid (BCA) assay (195) was introduced for the determination of the peptide content of our peptide stock solutions.

(a) Standard Assay (100 – 1000 µg/mL total protein)

The assay was essentially performed as described in (196), but Na_2CO_3 was used in place of $\text{Na}_2\text{CO}_3 \cdot \text{H}_2\text{O}$, and volumes were adjusted for the use in 96-well plates. To prepare the working solution, 100 parts of reagent A (sodium bicinchoninate (0.1 g), Na_2CO_3 (1.49 g), sodium tartrate dihydrate) (0.16 g), NaOH (0.4 g), NaHCO_3 (0.95 g), made up to 100 mL with HPLC-grade water, pH adjusted to 11.25 with 10 M NaOH) were mixed with 2 parts reagent B ($\text{CuSO}_4 \cdot 5 \text{H}_2\text{O}$ (0.4 g) in 10 mL of HPLC-grade water). 95 µL/well of working solution were added to 5 µL/well of sample and mixed by gentle shaking, the covered plate was incubated at 60°C for 30 minutes in a drybath, and after cooling to room temperature, absorbance was read in a plate reader at 540 nm.

(b) Microassay (0.5 – 10 µg/mL total protein)

The assay was essentially performed as described in (196), but Na_2CO_3 was used in place of $\text{Na}_2\text{CO}_3 \cdot \text{H}_2\text{O}$. To prepare the working solution, 1 part of reagent C ($\text{CuSO}_4 \cdot 5 \text{H}_2\text{O}$ (0.4 g) in 10 mL of HPLC-grade water) was first mixed with 25 parts reagent B (sodium bicinchoninate (1.994 g) made up to 50 mL with HPLC-grade water), and then with 26 parts of reagent A (Na_2CO_3 (0.597 g), sodium tartrate (dihydrate) (1.6 g), NaOH (1.6 g), pH adjusted to 11.25 with 10 M NaOH). 50 µL/well of working solution were added to 50 µL/well of sample and mixed by gentle shaking, the covered plate was incubated at 60°C for 60 minutes in a drybath, and after cooling to room temperature absorbance was read in a plate reader at 540 nm.

(c) Microwave Assay (0.5 – 10 µg/mL total protein)

A protocol was found in the literature (197) that promised a 20 s BCA assay using a regular household microwave. This protocol was attempted for use in the 96-well plate format, with the goal of developing a procedure that could be completed in less than 10 minutes.

Reagents and samples were prepared as described above; however, to ensure reproducible heating conditions, empty wells were filled with water. The 96-well plate was placed in the centre of the microwave turning table (Danby, Model # DMW799W), and two 100 mL Erlenmeyer flasks containing 50 mL of tap water were put on either (long) side. Various microwave heating times, energy settings and cooling conditions were explored, but with less than ideal results, in regards to both, time goal and compromise of the microplate shape; therefore, the procedure was aborted.

2.7.3.3. *β*-Amyloid Quantitation by ELISA

(a) Determination of A β ₁₋₄₀ and A β ₁₋₄₂ content

For the determination of the A β ₁₋₄₀ and A β ₁₋₄₂ content, the respective ELISA test kits by The Genetics Company were used according to their protocol. In short, standards and samples were prepared according to an appropriate scheme, 50 µL of antibody conjugate solution and 50 µL of standard or sample solution were added to each well of the supplied ELISA microwell plates. The plates were covered with a cover seal, thoroughly mixed in a microplate reader and incubated overnight in the refrigerator at 4°C. The following day, the plates were washed 5 times with 300 µL of washing solution per well and incubated with 100 µL of enzyme conjugate solution per well for 30 minutes in a microplate reader at 800 rpm. Subsequently, the plates were again washed 5 times with washing solution, followed by the addition of 100 µL of

substrate solution and 30 minutes incubation at room temperature in the dark (plates wrapped in aluminum foil). After adding 50 μ L of stop solution per well, the absorption at 450 nm was read in a microplate reader against a reference wavelength of 620 nm.

(b) Determination of oligomeric and total A β content

A protocol developed by Levine (198) to detect oligomeric or total A β was used (see Figure II-13). It makes use of the fact that an antibody cannot attach to an antigen (on a peptide monomer) that is already occupied by another antibody of the same type; however, a second antibody can bind to a different molecule in an oligomer, if the binding site has not been buried in the process of oligomerisation (see Figure II-14).

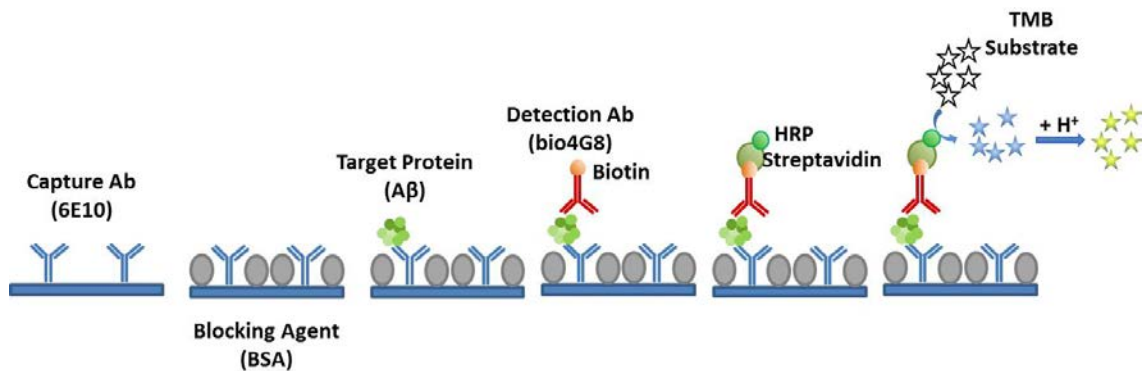


Figure II-13 ELISA workflow.

Pictorial description of the workflow of the A β ELISA assay described above (198) (Ab: antibody; BSA: bovine serum albumin; HRP: horseradish peroxidase; TMB: 3,3',5,5'-Tetramethylbenzidine). 6E10 epitope: A β ₃₋₈; 4G8 epitope: A β ₁₇₋₂₄

The 96-well plates were prepared using 50 μ L/well of a solution containing 2 μ g/mL of capture antibody (oligomers: 4G8; total: 6E10) in 10 mM sodium phosphate, pH 7.5. The plate was covered, sealed with parafilm and incubated overnight at 4°C. The following morning the plate was emptied and washed three times with washing solution (TBST: 20 mM Tris-HCl, 34 mM NaCl, pH 7.5, 0.1 % v/v Tween 20), with vigorous blotting in between steps. To block the plate,

200 μL /well of blocking buffer (TBST + 2 mg/mL fatty-acid free BSA) were added, the plate was covered, sealed with parafilm and incubated for two hours at room temperature. After washing the plate four times as above, 50 μL /well of standards or sample was added. Standards were made either from leftover stock from the kit by The Genetics Company described above or made from $\text{A}\beta$ purchased from Anaspec, Inc. and prepared as described in Section 2.7.3.1. The plate was covered, sealed with parafilm and incubated for two hours at room temperature.

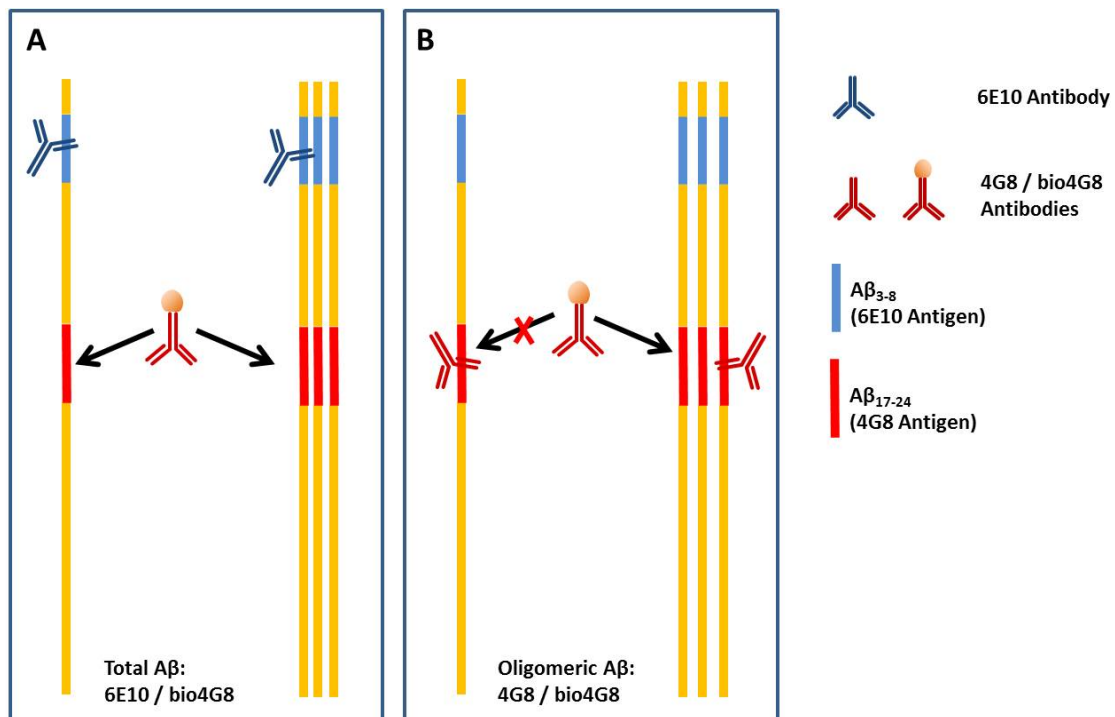


Figure II-14 Oligomeric $\text{A}\beta$ ELISA principle.

The principle of the oligomeric $\text{A}\beta$ ELISA developed by LeVine is depicted (192). A: Total $\text{A}\beta$ is determined by capturing monomers and oligomers of $\text{A}\beta$ with the 6E10 antibody, followed by detection with the bio4G8 antibody; both monomers (left) and oligomers (right) are detected. B: Determination of oligomeric $\text{A}\beta$ makes use of the fact that an antibody cannot attach to an antigen (on a monomer) that is already occupied by another antibody of the same type (left), i.e., only oligomers (right) are detected with the 4G8/bio4G8 antibody pair. The 4G8 antibody captures both, monomer and oligomers, however, only oligomers can be detected by the bio4G8 antibody, since in monomers the epitope is already occupied by the capture 4G8 antibody.

Subsequent to washing the plate five times as above, 50 μL /well of a solution containing 1 $\mu\text{g}/\text{mL}$ of detection antibody (oligomers & total: biotinylated 4G8 (bio4G8)) dissolved in

blocking buffer (TBST + 0.2% BSA) were added, the plate was covered, sealed with parafilm and incubated for one hour at room temperature. After washing the plate five times as above, 50 μ L/well of a solution containing 50 ng/mL HRP-streptavidin dissolved in blocking buffer (TBST + 0.2% BSA) were added, the plate was covered, sealed with parafilm and incubated for one hour at room temperature in the dark (wrapped in aluminum foil). Washing the plate five times as above, was followed by addition of 100 μ L/well of a solution containing a mixture of substrate reagents A and B (3,3',5,5'-Tetramethylbenzidine/H₂O₂). The plate covered, sealed with parafilm and incubated with gentle shaking (~20 rpm) for 2 – 30 minutes at room temperature in the dark (wrapped in aluminum foil). Development of the blue colour was checked regularly, and at an appropriate time, 100 μ L/well of stop solution (0.118 M H₂SO₄) was added which resulted in a colour change to yellow. After five minutes the OD was read at 450 nm.

It should be noted that the assay developed by LeVine (198) cannot distinguish between A β ₁₋₄₀ and A β ₁₋₄₂, since both the antibodies are directed at N-terminal epitopes (6E10: A β ₃₋₈; 4G8: A β ₁₇₋₂₄) and not at a C-terminal epitope, where these two A β isoforms differ.

2.7.3.4. Bacterial Cell Culture

Bacteria were originally received on streaked agar plates and stored at 4°C in the refrigerator. 30 mL LB broth were inoculated with a carefully selected colony (of average size and appearance) and incubated overnight at 37°C and 180 rpm. Bacterial cells were harvested by centrifugation for 10 minutes at 200 \times g and resuspended in fresh LB broth containing 15 % glycerol. 1 mL aliquots were frozen immediately at -80°C in a chest freezer.

The protocol to maintain bacterial cell cultures evolved over the span of the project. Originally, bacterial cell cultures were maintained in LB broth by inoculating 20 – 30 mL of LB broth with 1 mL of the last available culture and incubating overnight at 37°C and 180 rpm.

After discussions with Dr. William Wong (Treventis Corp.), the protocol was changed to maintain the bacterial cell cultures on LB agar plates, subculturing them on a weekly schedule. To start a bacterial cell culture, originally, a 1 mL aliquot was thawed at 37°C in a water bath and transferred to 20 – 30 mL of LB broth for overnight incubation at 37°C and 180 rpm. On the following day, a 1 µL loop was used to streak the LB agar plate. After one week, a new LB agar plate was produced by suspending one colony in 20 – 30 mL of LB broth and overnight incubation at 37°C and 180 rpm. A sample was streaked on a new LB agar plate with a 1 µL loop, and the plate was incubated overnight at 37°C. Subsequently, the agar plate was stored in the refrigerator at 4°C for one week.

After a suggestion from Yanfei Wang (a technician in our group), to start a new culture, a sample of bacteria was taken directly from the frozen tube with a 1 µL loop, suspended in 100 µL LB broth, and streaked with a new 1 µL loop on an LB agar plate, which was incubated overnight as before. To produce a new agar plate, one colony from the plate from the previous week was suspended in 100 µL LB broth and streaked with a new 1 µL loop on an LB agar plate, which was incubated overnight as the thawed sample.

2.7.3.5. Preparation of Bacterial Cell Cultures for Assays

To prepare a bacterial cell culture for an assay, a single colony was harvested from an agar plate with a sterile needle and transferred to a culture flask containing 20 - 30 mL of growth medium. Bacterial cultures were grown in a LabNet 311DS shaking incubator at 37°C and 180 rpm. Normal growth media were 2.5 % (w/v) LB broth or 3 % (w/v) TSB, autoclaved for

15 minutes at 121°C and 1 bar positive pressure. Next, a second sub-culture was prepared by inoculating 25-30 mL of growth medium with 1 mL of the first and incubated at 37°C and 180 rpm until the log-phase was reached ($OD_{600} = 0.6$; ca. 3.5 – 4 hours). Growth of the bacterial culture was followed by measuring the optical density at 600 nm (OD_{600}) with a Waters 2487 Dual Wavelength absorbance detector using disposable polystyrene UV cuvettes (Fisher Scientific).

2.7.3.6. Preparation of Bacterial Membrane Fragments

Initial experiments involved incubation of live bacterial and neuronal cells in the same culture. Unfortunately, the rapid rate of bacterial growth would consistently overwhelm and kill the neuronal cells. After several failed attempts to produce meaningful results by this co-incubation method, it was decided to use killed bacteria or bacterial fragments instead. Because of the concerns of interference with the downstream cell assays, chemical killing of the bacteria was avoided. Instead, repeated freeze-thaw cycles were first tried in order to kill the bacteria. Cultures of *E. coli*, *S. marcescens*, *K. pneumonia*, MSSA, and MRSA were grown as described above (Section 2.7.3.5). To wash the cells, 10 mL of a culture were centrifuged for 10 minutes at $900 \times g$, the supernatant was discarded and the pellet resuspended in 10 mL of cold (4°C) PBS; this washing cycle was repeated twice. After resuspending the cells in cold (4°C) PBS they were frozen at -80°C for ~30 minutes and then thawed in a 37°C water bath; the freeze-thaw cycle was repeated eight more times to yield a suspension of bacterial membrane fragments.

Since the above procedure failed to kill all bacteria (as indicated by bacterial growth in co-incubation experiments with BV-2 cells), an alternative procedure was used for subsequent

experiments. Bacterial cultures were again grown as described above (see Section 2.7.3.4) and then autoclaved for 15 minutes at 121°C (liquids program). 11 mL of the vortexed cultures were centrifuged for 10 minutes at 3716 × g, the supernatant was discarded and the pellet resuspended in 11 mL PBS. Killing efficiency was tested by spreading 100 µL of the suspension on an agar plate and incubation overnight at 37°C. Since some of the plates showed growth, the samples were autoclaved again as above. Killing efficiency testing still yielded growth on some plates, therefore the samples were autoclaved for a third time as above. This finally gave total bacteria killing, as evidenced by subsequent test agar plates. For all subsequent experiments requiring this type of sample, the bacterial samples were autoclaved once for 45 minutes. This gave equivalent killing efficiency and testing never showed any growth with this approach.

2.7.3.7. Mammalian Cell Culture

SH-SY5Y, and SK-N-AS cells were grown in high-glucose DMEM growth medium, supplemented with 10 % FBS, and containing 100,000 IU/L penicillin G⁸ and 100 mg/L streptomycin at 37°C in a water-saturated atmosphere with 5 % CO₂. Cells were grown in T-25 cell culture flasks containing 10 mL of growth medium. For subculturing, cells were dissociated with 500 µL of 0.25% trypsin, or TrypLE Select.

2.7.3.8. Preparation of Mammalian Cell Cultures for Assays

To prepare a mammalian cell culture for an assay, leftover cells from subculturing were seeded typically at 10,000 cells/well in 96-well plates with a total volume of 200 µL cell culture

⁸ For penicillin G: 1 IU (international unit) = 0.6 µg

medium. After 24 hours incubation at 37°C in a water-saturated atmosphere with 5 % CO₂, each well was checked by phase-contrast light microscopy to confirm that confluency was reached (around 20,000 cells/well) and thus the cells were ready for the assay.

2.7.3.9. Preparation of primary rat neurons

Primary hippocampal rat neurons were prepared by Dr. Barbara Karten (Department of Biochemistry & Molecular Biology, Dalhousie University) as described in (199) and according to protocols approved by Dalhousie University's research ethics board. In short, timed pregnant Sprague-Dawley rats (E17) were terminated with an overdose of halothane and cervical dislocation to remove embryos. Hippocampi were dissected and placed in Hank's Balanced Salt Solution (HBSS) on ice. They were digested with 0.25 mg/mL trypsin in HBSS for 10 min at 37°C, and after washing twice with HBSS dissociated by trituration through a flame-polished Pasteur pipette. Cells were counted and the cell suspension was diluted to the appropriate cell density in Neurobasal medium (supplemented with B27, 0.5 mM glutamine, 0.25 µM glutamate, antibiotics, and 7% heat-inactivated FBS) for plating at a density of 15,000 cells/well in a 96-well plate, which had been coated with 0.1% (w/v) poly-D-lysine and conditioned in MEM medium with 7% FBS. After 3 h, Neurobasal medium was replaced with phenol-red free medium with the same additives except serum. Neurons were grown for 14-16 days before being used in experiments.

2.7.3.10. Aβ production in mammalian cells induced by infection

As noted earlier (in Section 2.7.3.6), co-incubation of mammalian cells with live bacteria (to simulate an infection in the cell culture) did not produce any meaningful results, secondary

to bacterial overgrowth and neuronal demise. Therefore, an alternate approach to simulate an infection was attempted by incubating cell cultures with bacterial fragments produced by autoclaving (see Section 2.7.3.6). Human neuroblastoma cell cultures and primary rat neurons were grown as described above (see Sections 2.7.3.7 - 2.7.3.9). Mammalian cell cultures were incubated with 20 μL /well (96-well plates; total volume: 200 μL /well) of bacterial fragment suspension for 18 – 24 hours. The supernatant was carefully transferred to a microcentrifuge tube, and centrifuged for 10 minutes at 3716 \times g; then the supernatant was transferred to a cryovial (leaving about 50 μL in the tube to avoid disturbing the pellet) and stored at -80°C in a chest freezer for later analysis. 200 μL /well of cell extraction buffer (50 mM Tris, pH 8.0; 2 mM CaCl_2 ; 80 mM NaCl; 1 % Triton X-100) were added to the plate and it was incubated for one hour in the CO_2 incubator at 37°C with shaking once at about half-time. After the lysis was completed, the well contents were collected by first vigorously pipetting the lysis buffer and then transferring the entire contents to a microcentrifuge tube. After centrifugation for 10 minutes at 3,716 \times g, the supernatant lysate was transferred to a cryovial (leaving about 50 μL in the tube to avoid disturbing the pellet) and frozen at -80°C in a chest freezer for later analysis.

The $\text{A}\beta$ content was determined by ELISA as described in Section 2.7.3.3 above. For samples produced from human neuroblastoma cells (SH-SY-5Y and SK-N-AS), the capture antibody was 6E10 and the detection antibody bio4G8, as this pair had been shown to produce significantly less background compared to the reverse configuration of 4G8/bio6E10 (198). For samples produced from primary rat neurons, the configuration 4G8/bio4G8 had to be employed, since rodent $\text{A}\beta$ (R5G, Y10F, H13R) has a mutation within the 6E10 epitope at position 5.

2.7.4. Results & Discussion

As shown in Figure II-15, $A\beta_{1-40}$ was produced intracellularly by SK-N-AS neuroblastoma cells in response to co-incubation with fragments of a number of the investigated bacterial strains (simulated infection) as well as LPS, however, no $A\beta_{1-40}$ was found in the supernatant. $A\beta_{1-42}$ levels were below the lowest standard in both, supernatant and lysate (not shown).

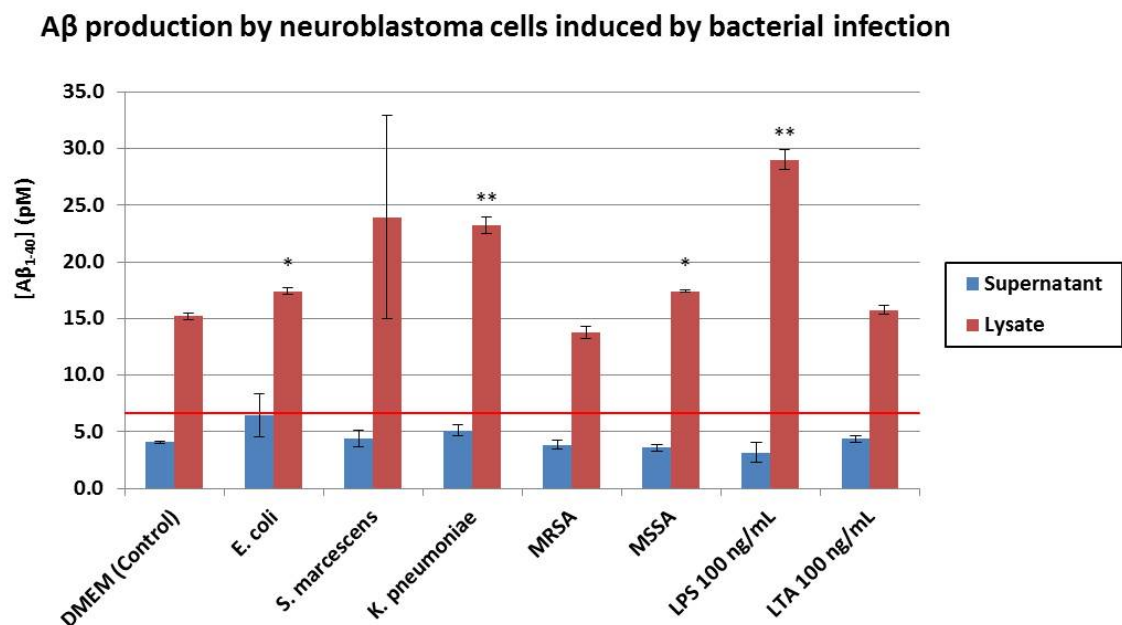


Figure II-15 $A\beta$ production by neuroblastoma cells induced by bacterial infection.

SK-N-AS neuroblastoma cells were incubated with fragments of different bacterial strains, as well as lipopolysaccharide (LPS) and lipoteichoic acid (LTA); extracellular and intracellular $A\beta$ production was analysed by ELISA (for details see text). $A\beta_{1-42}$ levels were below the lowest standard in both, supernatant and lysate (not shown); significant increases of $A\beta_{1-40}$ production compared to PBS control were detected only in the lysate, but were below the lowest standard in the supernatant (5.8 pM, nominally 4 pM; red line). Error Bars: \pm S.E.M.; *: $P < 0.05$; **: $P < 0.01$ ($n = 2$; two-tailed Student's t-test).

The same experiment was conducted with primary rat neurons, using the ELISA procedure described by LeVine. Since rodent $A\beta$ (R5G, Y10F, H13R) has a mutation within the 6E10 epitope at position 5, the antibody configuration 4G8/bio4G8 had to be employed (see Figure II-16). Of

course, this means that only oligomeric A β species were detected (also see Figure II-14), and one expected a lower signal compared to samples from neuroblastoma cells.

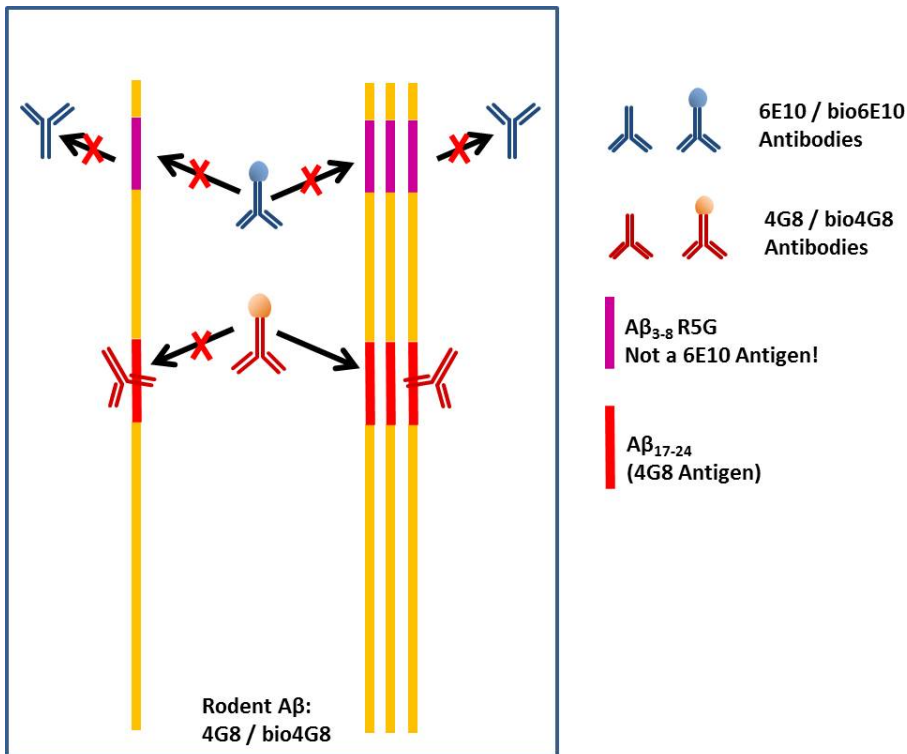


Figure II-16 ELISA of rodent A β .

Rodent A β is not bound by the 6E10 antibody due to a mutation (R5G) in the antigen region. The 4G8/bio4G8 antibody pair has to be utilised for the ELISA assay, which only detects oligomeric A β .

As expected, results for primary rat neurons showed considerably lower values as compared to the neuroblastoma cells, in fact, all values were below the blank (nominally 0 nM; back-calculated from the calibration curve as 0.33 nM). Attempts to concentrate the samples by lyophilisation by a factor of up to five were unsuccessful and did not lead to higher values.

The fact that the 4G8/bio4G8 antibody pair only detects oligomers, lead to a number of issues causing lower signals. Since only oligomers are detected, a potentially sizable portion of monomeric A β goes undetected. Of significance is also the fact that rodent A β shows a

considerable lower propensity to aggregate compared to human A β (200). It also leads to a lower sensitivity of the calibration curve, since again only oligomers in the standards are detected; e.g., in the experiment discussed here, the slopes of the calibration curves for SK-N-AS neuroblastoma cells and for primary rat neurons were 0.0509 and 0.0380 a.u./nM (a.u.: absorbance units), respectively. Furthermore, results are valid only under the assumption that the same fraction of A β is in the (detectable) oligomeric state in the standards and samples.

The assay kits by The Genetics Company used to distinguish A β ₁₋₄₀ and A β ₁₋₄₂ could not be employed for this assay, since the capture antibody W0-2 recognises the epitope A β ₄₋₁₀ (201) and therefore has the same issues as described above for the 6E10 antibody. Ideally, an antibody that recognises an epitope in the C-terminal region of rodent A β that does not interfere with the binding of 4G8 would have been used in this experiment.

In order to further examine the effect of LPS and LTA as the active compounds in gram-negative and gram-positive bacteria, respectively, SK-N-AS neuroblastoma cells were incubated at a higher concentration (1 μ g/mL) and the production of A β after 1, 2, and 3 hours was analysed (see Figure II-17).

In just 1 hour, a significant increase in A β production was detected, which further increased over the next 2 hours. This shows the fast response of neuronal cells upon encountering bacteria, as is expected for an activation of the innate immune system to prevent spread of the invading microbial species.

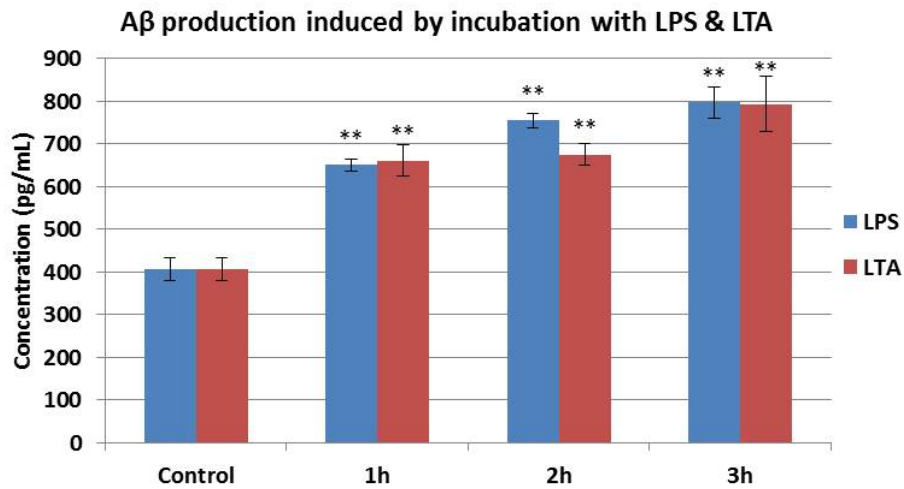


Figure II-17 Time series of A β production by neuroblastoma cells induced by incubation with LPS and LTA.

SK-N-AS neuroblastoma cells were incubated with 1 μ g/mL of lipopolysaccharide (LPS) and lipoteichoic acid (LTA), respectively, and samples were taken after 1, 2, and 3 hours; A β production in the cell lysate was analysed by ELISA. Error Bars: \pm S.E.M.; **: P < 0.01 (compared to Control; n = 8; two-tailed Student's t-test)

2.7.5. Summary

Historically, the central nervous system (CNS) has been considered an immune-privileged site, with microglia acting independently as the macrophages of the brain. However, it is now being recognised that neurons are not merely passive targets of infections, but can mount an immune response of their own and activate microglia through bidirectional communication with these brain immune cells (202-206).

Our experiments also show the neurons' ability to act in response to invasion. When an infection is simulated in neuronal cells, as with the use of bacterial fragments, the cells will produce A β in response. Similarly, when the major antigenic species of bacteria membranes, LPS and LTA, are used, a similar response is found, suggesting these as the likely candidate entity for inducing this response.

2.8. Antibacterial Activity of β -Amyloid

2.8.1. Introduction

In the previous series of experiments (Section 2.7), it has been shown that $A\beta$ is produced in response to bacterial exposure. The next logical step is to show that $A\beta$ is actually toxic to bacteria.

Since it is a well-known fact that the activity of some AMPs is increased by metal binding (see Chapter I, Section 2.3.4), and since it is known that $A\beta$ has a number of metal binding sites (see Chapter I, Section 1.4.1), it was decided to include copper and zinc in the form of Cu^{2+} and Zn^{2+} in the experiments described in this section.

Furthermore, the pH in brain tissue has been shown to be decreased in individuals with AD (207) or traumatic brain injury (208-210). Since the pH directly controls the protonation state of basic and acidic peptide side chains, which has a major influence on metal ion binding, the antimicrobial activity of $A\beta$ was also evaluated at three different pH values, 7.3, 7.0 and 6.5.

And finally, because *in silico* calculations in our lab, as well as experimental evidence from the literature suggest that cholesterol is involved in the insertion of $A\beta$ into a membrane (see Chapter I, Section 1.3.4.1), cholesterol was included as another variable in these experiments. Although cholesterol is conventionally considered absent from bacterial membranes (211) (because bacteria lack the biochemical pathways to produce cholesterol), it is hypothesised here, that cholesterol would insert into the membranes of bacteria present in the blood of a mammal, based on the polarity of cholesterol and its presence in serum (in human serum cholesterol content typically ranges from 2.5 – 7.5 mM).

2.8.2. Materials

2.8.2.1. *Biological Materials*

To explore the activity of A β as AMP, the same bacterial strains as in the previous section were used in the experiments. The bacterial strains used in this study were chosen based on their Risk Group rating of not higher than level 2, and their availability, as well as their cell wall and cell membrane characteristic. As opposed to mammalian cells, bacteria also possess, in addition to their cell membrane, a cell wall that mainly consists of peptidoglycans. Gram-positive bacteria differ from Gram-negative in that they are enclosed by a very thick layer of cross-linked peptidoglycans. When tested via the Gram staining method, Gram-positive bacteria are able to retain the Crystal Violet stain, hence the 'positive'. Gram-negative bacteria, on the other hand, possess only a thin peptidoglycan layer, which is not able to retain Crystal violet. This type of organism, however, has an additional outer membrane that covers this peptidoglycan layer. These differences in cell wall construction are the reason for their distinct susceptibilities to antimicrobial agents.

For experiments to determine the minimum inhibitory concentration (MIC) of A β , the following bacterial strains were used in addition to the ones already mentioned:

Gram-negative strain:

- *Pseudomonas aeruginosa*; Strain Boston 41501; ATCC #27853; (*P. aeruginosa*); Risk Group: 2 (purchased from ATCC)

Gram-positive strain:

- *Staphylococcus epidermidis*; ATCC #12228; (*S. epidermidis*); Risk Group: 1 (purchased from ATCC)

2.8.2.2. Chemicals

In addition to the materials mentioned in the previous section, the following materials were used:

CuCl₂·2H₂O; ZnCl₂·H₂O; cholesterol; methyl-β-cyclodextrin (Sigma-Aldrich, Cat.# C4555); low-electroendosmosis (EEO) agarose, tryptone soy broth (TSB).

2.8.3. Methods

2.8.3.1. Bacterial Cell Culture

Bacterial cell cultures were grown as described in the previous section (see 2.7.3.4 & 2.7.3.5). For media containing cholesterol, the tip of a spatula of cholesterol was added to the broth before autoclaving. After sterilization, the warm solutions were sterile-filtered with a 0.2 μm PVDF syringe filter to obtain a sterile, particle-free cholesterol-saturated solution.

2.8.3.2. Radial Diffusion Assay

The Radial Diffusion Assay (RDA) was adapted from the method first published by Lehrer *et al.* (212). Petri dishes were each blocked with 12 mL of 0.5 % casein in PBS for 1 h and subsequently dried under UV light ($\lambda = 254$ nm) for 4 h in the biosafety laminar flow hood. For the underlay agar, 2 × 200 mL of 0.03 % TSB (60 mg/200 mL) were prepared in Milli-Q water, the

tip of a spatula of cholesterol was added to one, and the media were autoclave for 15 min at 121°C and 1 bar positive pressure. After autoclaving, the solution with cholesterol was filtered with a sterile 0.2 µm PVDF syringe filter to obtain a particle-free cholesterol-saturated solution. The 2 solutions were both split into three aliquots (~65 mL), the pH of one aliquot each was adjusted with 10 M NaOH or 10 M HCl to 7.4, 7.0, or 6.5, respectively. 600 mg of low-EEO agarose were added to 60 mL of each solution, and all solutions were autoclaved for 15 min at 121°C and 1 bar positive pressure. For each Petri dish, 50 µL of the respective bacterial culture (in exponential growth phase) were added into a culture tube. 10 mL of warm (~50°C), autoclaved TSB agar were added to each tube individually, which was vortexed for 10 s to disperse the culture and the gel immediately poured into the Petri dish on a level platform in the laminar flow biosafety hood. The gel was allowed to solidify for 1 h, before 12 punch holes per Petri dish were made with a sterile glass pipette with 4 mm diameter tip; the centers of the punch holes were removed with a sterile Pasteur pipette that was attached to a vacuum line. 5-10 µL of test solution were added to three wells each (i.e., tested in triplicate), and incubated for 3 h at 37°C. The overlay agar was prepared analogously to the underlay agar, but as 6 % TSB solution. After incubation of the samples, 10 mL of the warm (~50°C), autoclaved overlay agar was added to each Petri dish and left to set. To prevent bacterial growth on the overlay agar surface, which interferes with accurate measurement of the inhibition zones, 3 mL of Pen-Strep solution (in PBS) was spread on the surface and removed immediately by decanting and shaking, two plates at a time. No interference of this procedure with the assay was detected in control experiments. Finally, the agar plates were incubated upside-down overnight at 37°C. The clear areas of inhibition were measured with a ruler with a precision of 0.5 mm.

2.8.3.3. Micro-Gel Well Diffusion Assay

The Micro-Gel Well Diffusion Assay (MWDA) was adapted from (213). Bacteria were grown overnight in 3% TSB at 37°C; in the morning, the bacteria were subcultured and grown to $OD_{620} = 0.6$. A sample was centrifuged for 10 minutes at $900 \times g$, the supernatant discarded and the cells washed with 10 mL cold Dulbecco's PBS (8.0 g NaCl, 0.2 g KCl, 1.15 g Na_2HPO_4 , 0.2 g KH_2PO_4 dissolved in 800 mL H_2O ; 0.1 g $CaCl_2$ dissolved in 100 mL H_2O ; 0.1 g $MgCl_2 \cdot 6 H_2O$ dissolved in 100 mL H_2O ; autoclaved separately and mixed after cooling). After centrifugation for 10 minutes at $900 \times g$, the supernatant was discarded and the cells diluted to $OD_{620} = 0.6$ with cold Dulbecco's PBS.

To prepare the gel, 1% (w/v) TSB, 1% (w/v) low-EEO agarose, and 0.02% (v/v) Tween-20 in Dulbecco's PBS were autoclaved. After cooling to 50°C, 10 mL portions were aliquoted into sterile tubes, 1 mL bacterial suspension were added and dispersed by vortexing for 10 seconds. 70 μ L/well of gel or gel-bacteria suspension were added to the 96-well plate column-wise according to the layout, and the gel was allowed to set for 30 minutes. 30 μ L/well of sample were applied directly onto the gel, the plate was covered and incubated for 17 hours at 37°C. Finally, the light dispersion at 620 nm was determined in a plate reader without cover.

2.8.3.4. Bacterial Growth Curve Assay (incl. CFU/time curves)

For the bacterial growth curve assay (GCA), reagents were prepared in ultra-purified water (18.2 M Ω) and pipetted into a 96-well microtiter plate according to an appropriate scheme. Bacterial cultures were incubated in solutions containing a range of concentrations of $A\beta_{1-40}$, $A\beta_{1-42}$, Cu^{2+} and Zn^{2+} , as well as combinations of $A\beta_{1-40}/A\beta_{1-42}$ with Cu^{2+} and Zn^{2+} , respectively, in the presence and absence of cholesterol and at three different pH values (7.3 / 7.0 / 6.5). 1 μ L of

bacterial culture (in exponential phase) was added to each well. The microtiter plates were incubated in a Tecan Genios or a Tecan Infinite 200 microplate reader at 37°C with intermittent shaking. Growth was followed over 24 hours by measuring the optical density at 595 nm (OD_{595} , optical filter: 595 ± 20 nm) or 620 nm (OD_{620} , optical filter: 620 ± 20 nm) of the sample in each well in constant time intervals (5 min).

2.8.3.5. Broth Microdilution Assay

To determine the minimum inhibitory concentration (MIC) of A β , the respective protocol from the *Manual of Clinical Microbiology* was adopted (214). An overnight culture of the organism to be tested was prepared in 2 mL LB broth, and incubated at 35 C and 220 rpm. 90 μ L Mueller Hinton II Cation Adjusted (MHIICA) broth were pipetted into each well of a 96-well plate, with an extra 85 μ L MHIICA in column 1. An aliquot of the overnight culture was adjusted to $OD_{600} = 0.132$ (0.5 McFarland Standard [$\sim 1 \times 10^8$ CFU/mL]) with MHIICA broth. 1.0 mL of the adjusted culture was added to a sterile reservoir containing 19.0 mL sterile H₂O, and mixed thoroughly ([$\sim 5 \times 10^6$ CFU/mL]). 5 μ L of A β solution (2 mg/mL; determined by Micro-BCA, and adjusted accordingly to give a final concentration of 50 μ g/mL) were added into column 1 according to the prepared plan. 90 μ L were serial-diluted (1:1) across the plate to column 10 (column 11 was for 0 μ g/mL, column 12 for controls), and 90 μ L discarded from column 10. If included in the experiment, 1 μ L/well of Cu²⁺ or Zn²⁺ solution and 1 μ L/well of cholesterol solution were added. The prepared testing plate was inoculated with 10 μ L/well ($\sim 5 \times 10^5$ CFU/mL) of the diluted culture and incubated approximately 20 hours at 35°C in a non-sealed plastic bag. After centrifuging the plate for 5 minutes at 3000 \times g, the lowest A β concentration with no visible pellet was determined as the MIC. Samples were typically analysed in duplicate.

2.8.4. Results & Discussion

2.8.4.1. Radial Diffusion Assay (RDA)

The Radial Diffusion Assay (RDA) is a widely used assay in the study of the antimicrobial activity of AMPs. It relies on diffusion of an antibiotic compound out of an impregnated disk or well to inhibit a bacterial culture. The diameter of the inhibition zone directly relates to the inhibitory ability of an antibiotic. For the assessment of the RDA, only experiments with *E. coli* were conducted. Results for a representative experiment are presented here (see Table II-1, Table II-2, and Figure II-18).

Table II-1 Results of RDA with *E. coli* on TSB agar without cholesterol.

Volume: 5 µL/well	Final concentration in well	Average inhibition zone diameter (mm) (well diameter: 4.0 mm)		
		pH 7.4	pH 7.0	pH 6.5
Tris, pH 7.4	18 mM	4.0	4.0	4.0
Cu ²⁺	1 mM	6.8	5.8	5.0
Zn ²⁺	1 mM	5.8	5.7	5.0
Aβ ₁₋₄₀ (90)	90 µM	4.0	4.0	4.0
Aβ ₁₋₄₀ (50)	50 µM	5.5	5.5	4.7
Aβ ₁₋₄₀ (90)+ Cu ²⁺	90 µM / 1 mM	4.03	4.3	4.2
Aβ ₁₋₄₀ (50)+ Zn ²⁺	50 µM / 1 mM	4.0	4.0	4.0
Pen-Strep	1x	16.3	17.0	17.5

Table II-2 Results of RDA with *E. coli* on TSB agar with cholesterol.

Volume: 5 µL/well	Final concentration in well	Average inhibition zone diameter (mm) (well diameter: 4.0 mm)		
		pH 7.4	pH 7.0	pH 6.5
Tris, pH 7.4	18 mM	4.0	4.0	4
Cu ²⁺	1 mM	5.2	6.0	5.5
Zn ²⁺	1 mM	6.7	4.7	6.0
Aβ ₁₋₄₀ (90)	90 µM	4.0	4.0	4.0
Aβ ₁₋₄₀ (50)	50 µM	5.2	4.0	4.7
Aβ ₁₋₄₀ (90)+ Cu ²⁺	90 µM / 1 mM	4.0	4.0	4.8
Aβ ₁₋₄₀ (50)+ Zn ²⁺	50 µM / 1 mM	4.0	4.0	4.0
Pen-Strep	1x	17.0	15.3	15.8

Influence of A β ₁₋₄₀ on viability of *E. coli* (Radial Diffusion Assay)

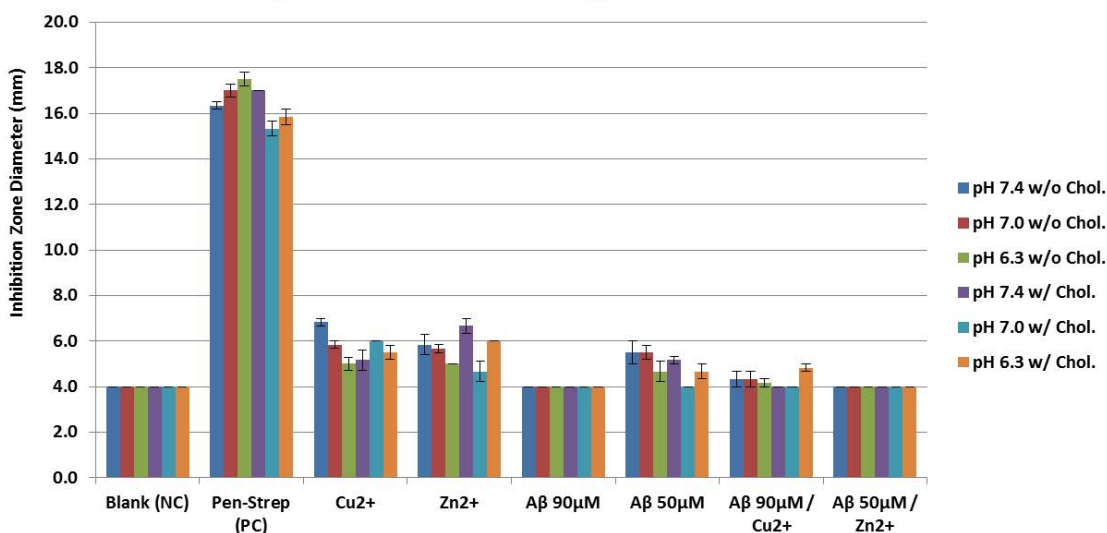


Figure II-18 Influence of A β ₁₋₄₀ on viability of *E. coli* assessed by the Radial Diffusion Assay.

The influence on the viability of *E. coli* of two different concentrations of A β ₁₋₄₀ in absence or presence of cholesterol, and Cu²⁺ or Zn²⁺ (1 mM) at three different pH (7.3 / 7.0 / 6.5) was analysed with the RDA Assay. The inhibitory effects seen are only minor, in particular in relation to the positive control Penicillin-Streptomycin (Pen-Strep); the pH did not have an obvious effect. Note that the well diameter, i.e., the lowest possible value, was 4 mm. Error Bars: \pm S.E.M.; n = 3.

Inspection of the data shows that A β ₁₋₄₀ (50 and 90 μ M), Cu²⁺ and Zn²⁺, as well as the combination of A β ₁₋₄₀ with Cu²⁺ and Zn²⁺, respectively, exhibit only minor inhibitory effects on colony growth of *E. coli* compared to the control Penicillin-Streptomycin (Pen-Strep). The pH had a significant effect only on Cu²⁺ (without cholesterol), decreasing the inhibition zone diameter with increasing acidity, and on the Pen-Strep control (without cholesterol), increasing the inhibition zone diameters with increasing acidity of the medium. A more thorough statistical analysis is given in Appendix B.

To explain the failure of the RDA assay in the assessment of A β 's antimicrobial activity, it was planned to analyse by mass spectrometry how far away from the wells A β would diffuse. This would provide insight into whether there were issues with the diffusion or the activity of A β . However, these experiments were not performed.

Interestingly, much later Soscia *et al.* mentioned, consistent with the results presented here, that in their hands RDAs were unreliable for testing the antimicrobial activity of A β (215). They posited that the peptide failed to diffuse away from the wells, however, without showing any data. They argued that the aggregation propensity of A β solutions, especially in the presence of even trace amounts of metal, and interaction with the media matrix or contaminants may lead to rapid precipitation of the peptide within the agar and thus prevent diffusion and activity.

2.8.4.2. Micro-gel Well Diffusion Assay

Due to the cost of materials, labour-intensity and lack of reliability of the Radial Diffusion Assay, an alternative was sought to streamline the assessment of the antimicrobial effect of A β . The Micro-gel Well Diffusion Assay (MWDA) (213) promised to achieve just that with the use of standard 96-well microplates.

When the first batch of plates was ready to be analysed in the plate reader, it was noticed on visual inspection, that a majority of the wells did not appear uniform. Therefore, the dispersion was determined at 16 locations in each well, distributed in a regular 4 \times 4 pattern; the average value of each well was used in subsequent data analyses.

As it turned out, the most common spread frequency ΔOD_{620} over the three plates of the first batch was $>1.0 - 1.05$ (see Figure II-19), calculated according to Equation (II-2):

$$\Delta OD_{620} = \text{max. OD}_{620} - \text{min. OD}_{620} \quad \text{(II-2)}$$

where ΔOD_{620} is the spread frequency, and max. OD_{620} and min. OD_{620} the maximum and minimum OD_{620} of a well, respectively. This analysis of the spread frequency confirmed the non-uniformity of the majority of the wells that was noticed during the visual inspection of the microplates.

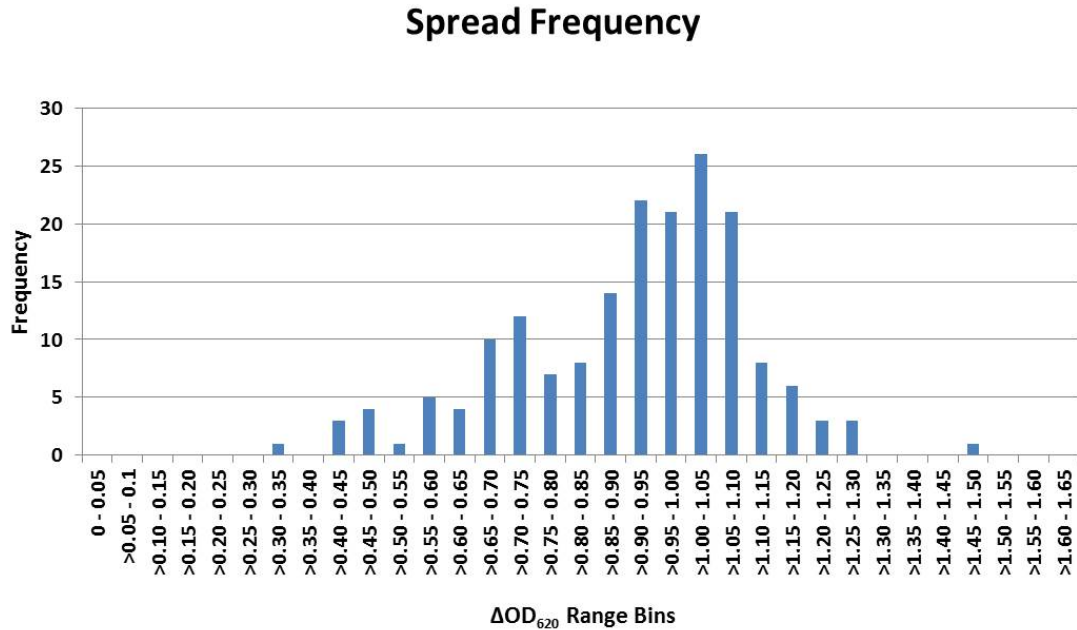


Figure II-19 Spread frequency in the Micro-gel Well Diffusion Assay.

The spread frequency of all sample wells of the three plates (60 wells each; 16 reads per well) of the first batch of the MWDA was calculated according to Equation (II-2) to examine the uniformity of the wells.

The results of the first Micro-well Gel Diffusion Assay revealed no significant reduction of the viability of *E. coli* caused by $A\beta_{1-42}$ or the presence of cholesterol (see Figure II-20). The only significant reductions were caused by Cu^{2+} and Zn^{2+} in the presence of cholesterol; however, they showed no dependence on the $A\beta$ concentration and were only minor (max. $\Delta OD = 0.0538$). Furthermore, the significance might actually be an artifact, caused by a slightly increased viability of *E. coli* in controls samples with cholesterol for all $A\beta$ concentrations (significant only for 1 μM and 5 μM).

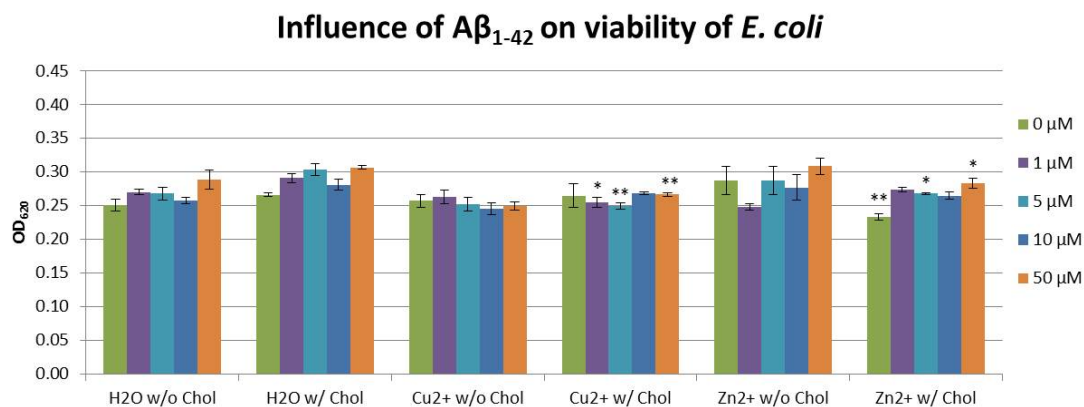


Figure II-20 Influence of A β ₁₋₄₂ on the viability of *E. coli* determined by Micro-gel Well Diffusion Assay. The influence of different concentrations of A β ₁₋₄₂ in absence or presence of cholesterol, and Cu²⁺ or Zn²⁺ (1 mM) on the viability of *E. coli* was analysed with the MWDA. Cu²⁺ and Zn²⁺ caused a minor decrease in viability of *E. coli* only in the presence of cholesterol; however, this effect was not observed consistently for all A β concentrations. Error Bars: \pm S.E.M.; *: P < 0.05, **: P < 0.01 (comparing samples with Cu²⁺/Zn²⁺ to controls (H₂O); n = 3; two-tailed Student's t-test).

A β ₁₋₄₂ caused a statistically significant albeit minor decrease in viability of *MRSA* in presence of H₂O and Zn²⁺, but not Cu²⁺ (Figure II-21); however, this effect was not observed consistently for all A β concentrations (blue */**): compared to 0 μ M A β ₁₋₄₂). Cu²⁺ caused a minor decrease in viability of *MRSA*; however, this effect was again not observed consistently for all A β concentrations (black *: Cu²⁺/Zn²⁺ compared to H₂O) (max. Δ OD = 0.0566).

In the Micro-gel Well Diffusion Assay (MWDA), 96 samples per microplate could be analysed as opposed to only 12 samples per Petri dish as in the Radial Diffusion Assay. Since neither the overlay agar nor time intensive preparations associated with the RDA were required, and because of the speed of automated reading of the microplates, the MWDA protocol lead to considerable time (and material) savings over the Radial Diffusion Assay. An additional advantage of the MWDA was that a microplate could easily be fixed and stored for later re-analysis, if so desired.

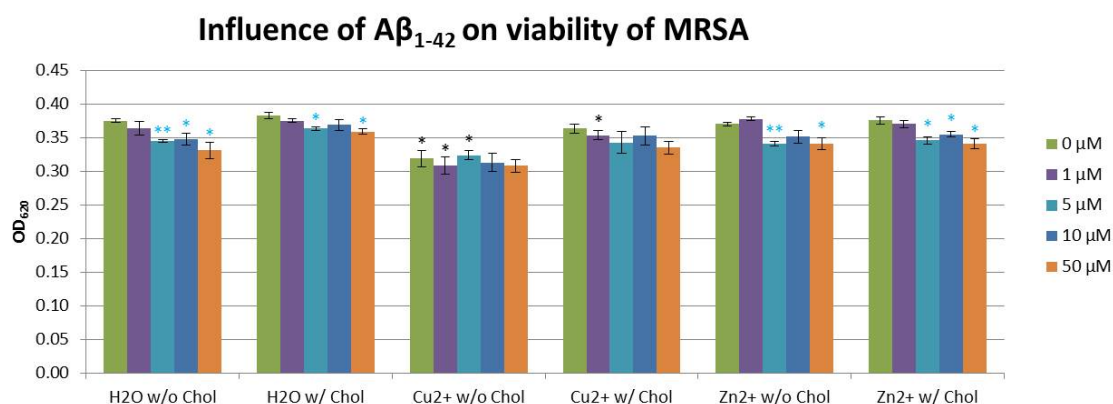


Figure II-21 Influence of Aβ₁₋₄₂ on the viability of MRSA determined by Micro-gel Well Diffusion Assay. The influence of different concentrations of Aβ₁₋₄₂ in absence or presence of cholesterol, and Cu²⁺ or Zn²⁺ (1 mM) on the viability of MRSA was analysed with the MWDA. Aβ₁₋₄₂ caused a significant but only minor decrease in viability of MRSA only for H₂O and Zn²⁺, but not for Cu²⁺; however, this effect was not observed consistently for all Aβ concentrations (blue */**): compared to 0 μM Aβ₁₋₄₂). Cu²⁺ caused a minor decrease in viability of MRSA; however, this effect was again not observed consistently for all Aβ concentrations (black *: Cu²⁺/Zn²⁺ compared to H₂O). (Error Bars: ± S.E.M.; *: P < 0.05, **: P < 0.01; n = 3; two-tailed Student's t-test)

Compared with the Growth Curve Assay (GCA) (see next section), however, the hands-on time for the MWDA was still considerably longer and the amount of material use higher due to the use of agar gels instead of broth. Furthermore, like the RDA, the MWDA gives only one time point, whereas the GCA returns the complete growth profile of a sample, which allows a much more detailed analysis of the influence of an agent on the microorganism; therefore it was decided to abandon the MWDA and rather improve the GCA.

2.8.4.3. Bacterial Growth Curve Assay

(a) Development of the Growth Curve Assay (GCA)

Bacterial growth, when measured by various viability methods, can usually be summarised in a typical graph of their growth (Figure II-22). The growth curve can be divided into four phases: the *lag phase*, where the bacteria are adapting to their new environment and preparing to multiply; the *exponential phase*, where the bacteria are undergoing rapid growth and the

slope of the line when plotted as a natural logarithm represents their actual growth rate; the *stationary phase*, where the bacteria have depleted nearly all the nutrients in their accessible environment and their growth and death rates are equal; and the *death phase*, where the bacteria have run out of nutrients and die.

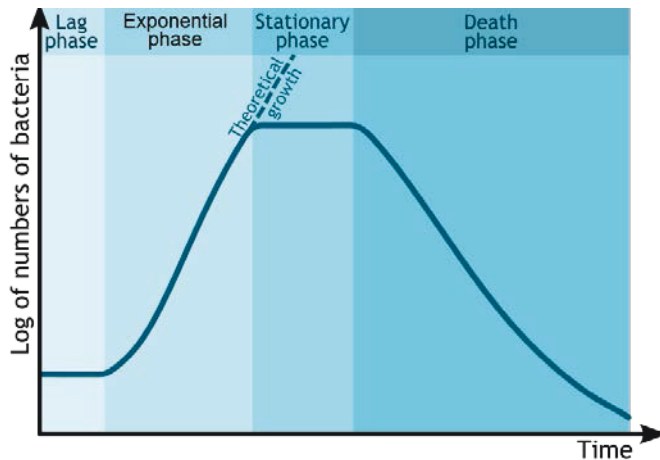


Figure II-22 Idealised bacterial growth curve and growth phases.

Bacterial growth in the most commonly used batch culture can be described by four different phases: **lag phase**, **log phase** (or exponential phase), **stationary phase**, and **death phase**. For details see text. From: http://en.wikipedia.org/wiki/File:Bacterial_growth_en.svg

More typically, and what has also been observed in this work, the growth curves tend to show a slightly different trajectory, with less well-defined stationary and death phases (Figure II-23). As an example, in Figure II-24 the growth curves of *E. coli* cultures incubated in LB broth (pH 6.5) containing cholesterol and various additives are displayed in one graph. A few effects become obvious at once; addition of Cu^{2+} delays bacterial growth in the exponential phase by about 30 minutes, addition of Zn^{2+} not only delays the growth in the exponential phase by about 120 minutes, but also decreases the OD_{595} value of the endpoint of the exponential phase by $\sim 30\%$. If at all, $\text{A}\beta_{1-40}$ seems to have only a minor decreasing effect on the growth of the bacteria.

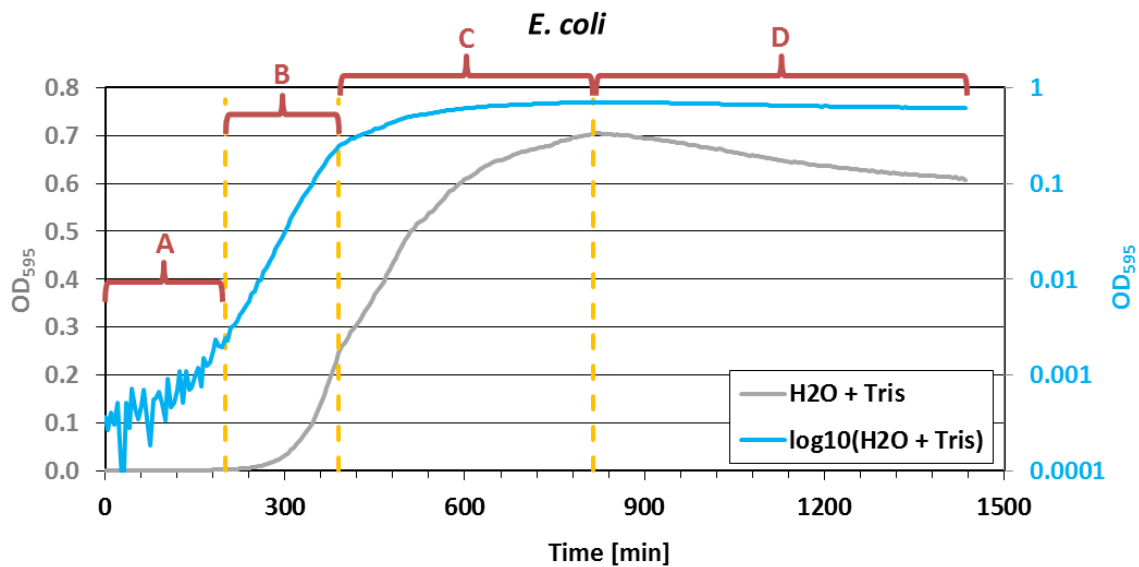


Figure II-23 Typical growth curve of a bacterial culture.

Typical growth curve of *E. coli* incubated in LB broth (grey); the logarithmic transformation is shown on the secondary vertical axis (blue). The four characteristic phases of bacterial growth are clearly discernible, the 'lag phase' (<math>< 200\text{ min}</math>, A), the 'exponential (or log) phase' (200 – 390 min, B), the 'stationary phase' (390 – 815 min, C), and the 'death phase' (> 815 min, D); however, in particular phases A, C, and D are not as clear-cut as in the idealised growth curve shown above (Figure II-22).

Figure II-24 also showcases a number of issues related to the interpretation of the data.

Traditionally, the OD₅₉₅ value after 24 hours of incubation is considered a good measure of the effect of a substance on bacterial growth. However, inspection of Figure II-24 reveals that this parameter may not accurately reflect the effect of a substance on the growth of bacteria. For example, in the case of added Zn²⁺ the curves without and with Aβ₁₋₄₀ reach about the same maximum OD₅₉₅ value (although the sample with Aβ₁₋₄₀ is delayed), however, the curves cross over during the death phase and at the endpoint (24 h = 1440 min) the respective values differ by 0.02 units (~3.5%).

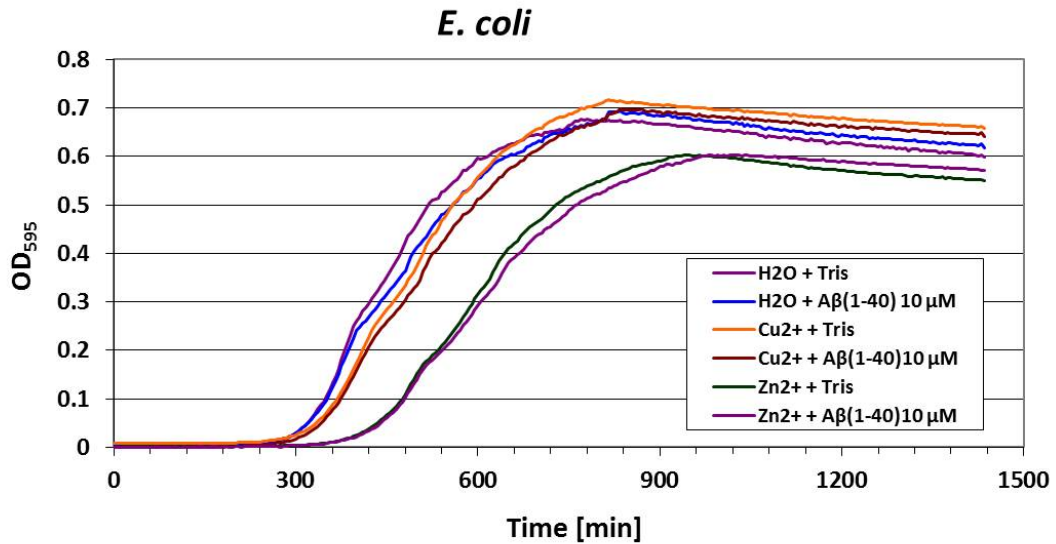


Figure II-24 Influence of different additives on bacterial growth.

E. coli incubated in LB broth (pH 6.5) containing cholesterol. Aβ concentration: 10 μM, Cu²⁺/Zn²⁺ concentration: 1 mM, Tris and H₂O are controls for Aβ and metal ion solutions, respectively; incubation temperature: 37°C. Data acquired on Tecan Genios microplate reader; curves show average of 3 samples per condition.

For the GCA a number of parameters for the evaluation of growth data were evaluated

(see Figure II-25):

- the maximum slope during the exponential phase ($Slope_{max}$),
- the time of $Slope_{max}$ ($t_{Slopemax}$)
- the OD₅₉₅ value at $t_{Slopemax}$ ($OD_{Slopemax}$)
- the doubling time in the exponential phase (t_{2x})
- the onset time of the exponential phase (t_{onset}),
- the OD₅₉₅ value at 12 hours (before the death phase) (OD_{12h}),
- the maximum OD₅₉₅ value (OD_{max}),
- the time point of OD_{max} (t_{ODmax}),
- the difference between t_{ODmax} and t_{onset} (Δt_{max}), and
- the difference between OD_{max} and the last OD₅₉₅ value (ΔOD_{final}).

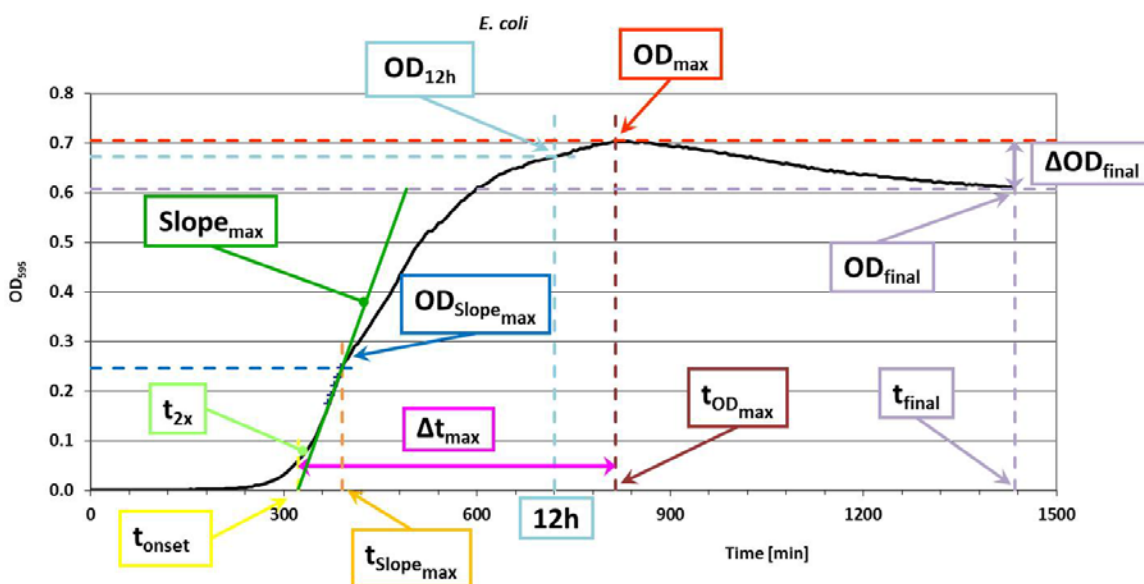


Figure II-25 The bacterial Growth Curve Assay.

For the bacterial GCA, the bacteria were incubated in a 96-well plate at 37°C in a microplate reader. The optical density at 595 nm was read every 5 minutes for about 24 h with intermittent shaking. To determine the influence of different conditions, the following data were extracted from the growth curves: maximum slope of exponential growth phase ($Slope_{max}$; the slope was calculated as the slope of a straight line through 5 consecutive data points); the time of the last of the five points used in determining $Slope_{max}$ ($t_{Slope_{max}}$); the OD_{595} value at $t_{Slope_{max}}$ ($OD_{Slope_{max}}$); the onset time of growth, defined as the intersection of the straight line with maximum slope with the x-axis (t_{onset}); the doubling time in the last hour of the exponential phase (t_{2x}); the optical density at 12 h (OD_{12h}); the maximum optical density (OD_{max}); the time of maximum optical density ($t_{OD_{max}}$); the time difference between t_{onset} and $t_{OD_{max}}$ (Δt_{max}); and the difference between the maximum optical density and the OD value of the last time point ($\Delta OD_{final} = OD_{max} - OD_{final}$).

The slope of the growth curve was calculated for a moving window of five consecutive time points using a least square fit; the resulting values were multiplied by a factor of 100 to make data handling easier. The use of a window of five data points was found to be the best compromise between smoothing of the slope and accuracy of detecting the actual point of maximum slope (see Figure II-26). The maximum slope at the end of the exponential phase was taken as $Slope_{max}$. $Slope_{max}$, i.e., the maximum growth rate of the bacteria in the exponential phase, is a measure for how fast the bacteria are replicating. The time point of the last of the five data points from the calculation of $Slope_{max}$ was taken as $t_{Slope_{max}}$. It is dependent, among other factors, on the initial number of bacteria and the growth rate. The OD_{595} for that point is

$OD_{Slope_{max}}$, which is dependent on the growth rate and factors impacting continued bacterial growth. The doubling time in the exponential phase, t_{2x} , was calculated for the 60 minute period ending at $t_{Slope_{max}}$. t_{2x} is, like $Slope_{max}$, a measure for how fast the bacteria are replicating. The onset time of the exponential growth phase, t_{onset} , was defined as the intercept of the line of maximum slope with the time axis (see Figure II-25 & Figure II-26). It is dependent, e.g., on the initial number of bacteria and factors retarding processes taking place in the lag phase. In combination with $Slope_{max}$ and t_{2x} , t_{onset} allows the identification of factors impacting bacterial replication. The OD_{595} value at 12 hours, OD_{12h} , is dependent on the initial number of bacteria, as well as factors slowing their growth. The maximum OD_{595} value, OD_{max} , is impacted by factors that prevent bacterial growth and accelerate death. The time point of OD_{max} , $t_{OD_{max}}$, depends on factors that delay growth and accelerate death of bacteria.

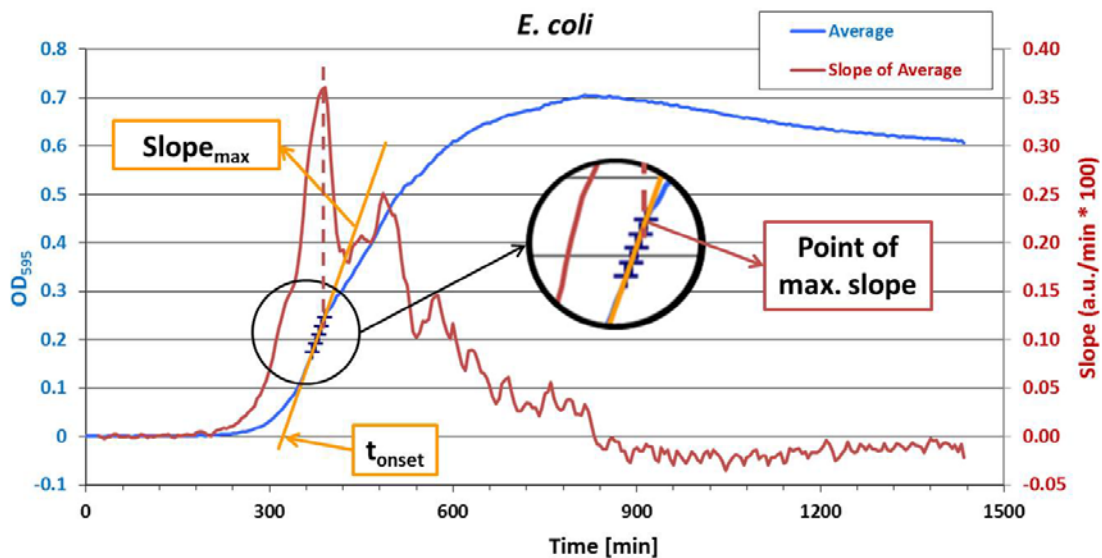


Figure II-26 Bacterial Growth Curve Assay – $Slope_{max}$ and t_{onset} .

To determine the $Slope_{max}$, the slope (dark red; on the secondary vertical axis) was calculated for a moving window of five points. The orange line shows the one with maximum slope; the insert zooms in to show the five points used for the calculation of the slope, and the point of maximum slope. t_{onset} was defined as the intercept of the line of $Slope_{max}$ with the time axis.

Δt_{max} , the difference between t_{ODmax} and t_{onset} , is a measure for factors that delay or decrease bacterial growth. The difference between OD_{max} and the last OD_{595} value, ΔOD_{final} , captures factors that accelerate bacterial death after the stationary phase.

For clarity, only results for the four most important of these parameters are presented in this section (t_{onset} , t_{2x} , OD_{max} , Δt_{max}). After an analysis of their correlation, four of these parameters were chosen based on their average correlation and mechanistic considerations (see Appendix C).

Results for incubation of five bacterial strains (*E. coli*, *S. marcescens*, *K. pneumoniae*, MRSA, MSSA) with 10 μM $\text{A}\beta_{1-40}$ and 1 mM Cu^{2+} or Zn^{2+} in the absence and presence of cholesterol at three pH values (7.3 / 7.0 / 6.5) are shown in Figure II-27 – Figure II-31. To facilitate analysis of the various incubation conditions employed in these experiments, tables containing the data used to produce these figures can be found in Appendix C. These tables also compare bacterial growth under conditions with and without $\text{A}\beta$, with and without cholesterol, and with and without Cu^{2+} or Zn^{2+} (see Appendix C) to facilitate analysis of the influence of these different incubation conditions. In a few instances parameters could not be determined due to the very noisy data of the growth curves. In Table II-3, results are summarized for addition of $\text{A}\beta$, metal ions, and cholesterol. The scale ranges from very strong decrease (----) to very strong increase (++++); in some instances the results varied widely such that a range had to be given. In all experiments involving MRSA and MSSA, the addition of Zn^{2+} at a concentration of 1 mM resulted in complete suppression of growth; therefore, determination of any of the parameters was not possible.

Table II-3 Result summary of the influence of A β ₁₋₄₀, Cu²⁺, Zn²⁺, and cholesterol on the viability of *E. coli*, *S. marcescens*, *K. pneumoniae*, MRSA, and MSSA as determined by the Growth Curve Assay. The scale ranges from very strong decrease (----) to very strong increase (++++); in some instances the results varied widely such that a range had to be given.

Bacterial Strain	A β ₁₋₄₀ (10 μ M)				Cholesterol			
	t _{onset}	t _{2x}	OD _{max}	Δ t _{max}	t _{onset}	t _{2x}	OD _{max}	Δ t _{max}
<i>E. coli</i>	(+)	(+)	(+)	(++) - (+++)	(--)	(--)- (++)	(+)	(--)- (+)
<i>S. marcescens</i>	(-/+)- (---)	(---)- (++++)	(+)	(++)	(++)	(-/+)	(+)	(+)- (++)
<i>K. pneumoniae</i>	(+)	(+)- (+++)	(-)	(+)- (++)	(-)- (--)	(-/+)	(-)- (---)	(--)- (+++)
MRSA	(+)	(-/+)	(-/+)	(-/+)	(+)- (++)	(-/+)	(+)	(-/+)
MSSA	(-/+)	(-/+)	(-/+)	(-/+)	(-/+)	(-/+)	(+)	(-/+)

Bacterial Strain	Cu ²⁺ (1 mM)				Zn ²⁺ (1 mM)			
	t _{onset}	t _{2x}	OD _{max}	Δ t _{max}	t _{onset}	t _{2x}	OD _{max}	Δ t _{max}
<i>E. coli</i>	(-)	(+++)	(-/+)	(--)- (+++)	(+)- (+++)	(+++)	(-)	(--)- (+++)
<i>S. marcescens</i>	(+)	(---)- (++++)	(+)	(+)- (++)	(++++)	(++++)	(--)	(--)
<i>K. pneumoniae</i>	(-/+)	(+)- (++)	(-)	(----)	(++++)	(+++)- (++++)	(---)	(--)- (++)
MRSA	(++)- (+++)	(-/+)	(+)	(----)	*	*	*	*
MSSA	(+)- (++)	(+)- (++)	(+)- (++)	(+)- (++)	*	*	*	*

*: In all experiments, the addition of Zn²⁺ at a concentration of 1 mM resulted in complete suppression of growth of MRSA and MSSA; therefore, determination of any of the parameters was not possible.

(a) Incubation of *E. coli*

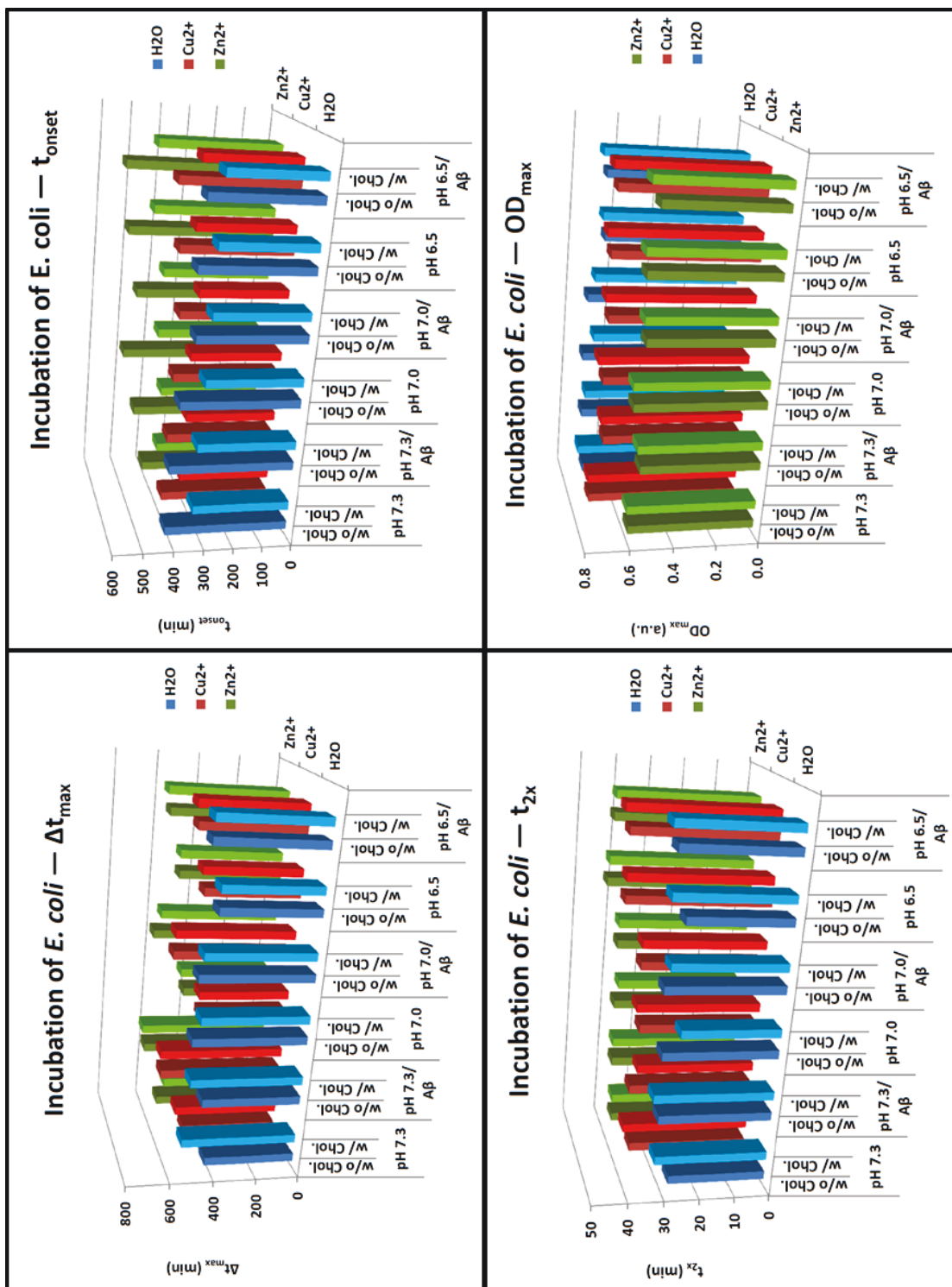


Figure II-27 Growth Curve Assay results for incubation of *E. coli*.

Results for the four most important parameters determined in the Growth Curve Assay are displayed. For details see text and Appendix C.

(b) Incubation of *S. marcescens*

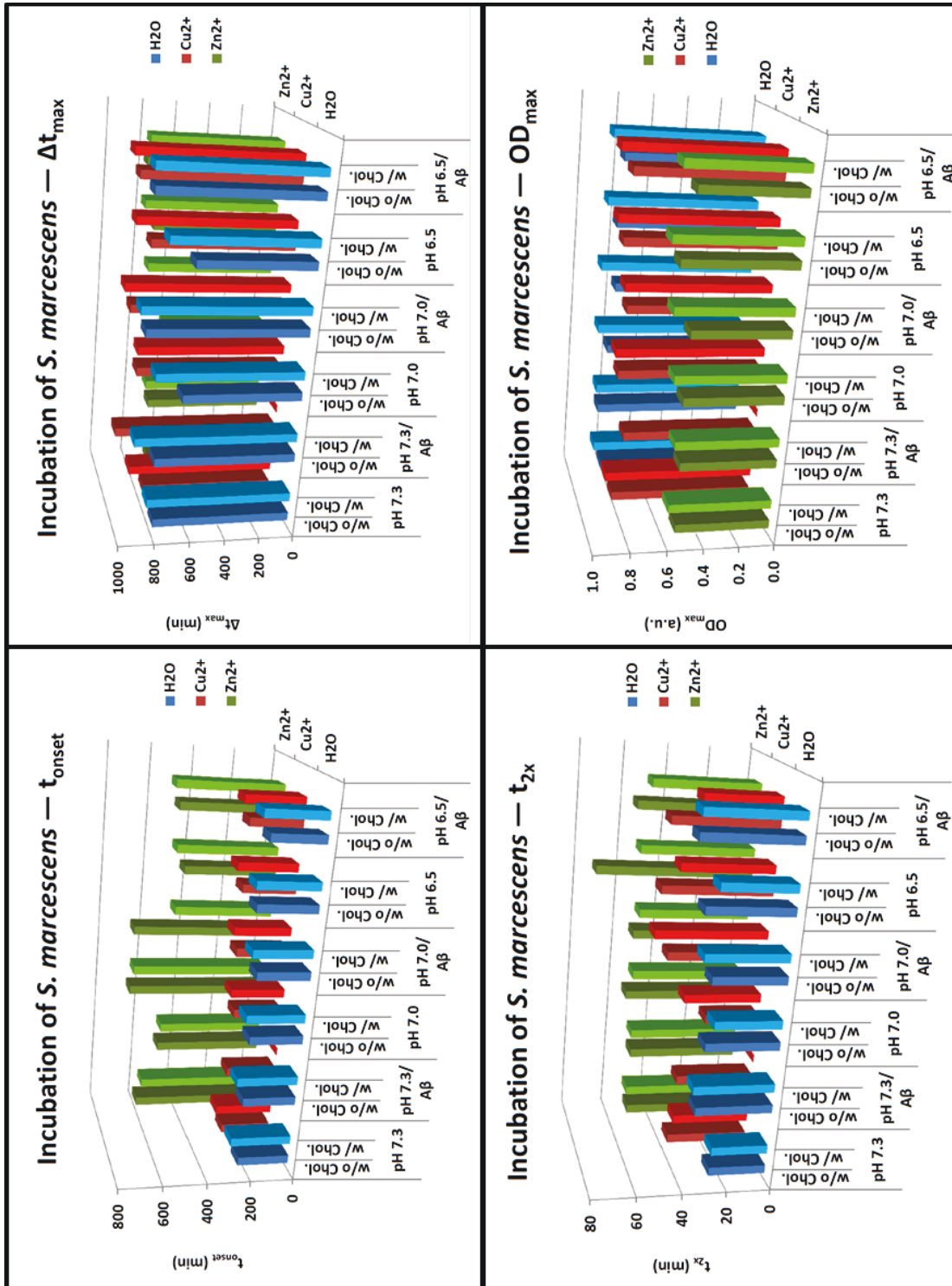


Figure II-28 Growth Curve Assay results for incubation of *S. marcescens*. Results for the four most important parameters determined in the Growth Curve Assay are displayed. For details see text and Appendix C.

(c) Incubation of *K. pneumoniae*

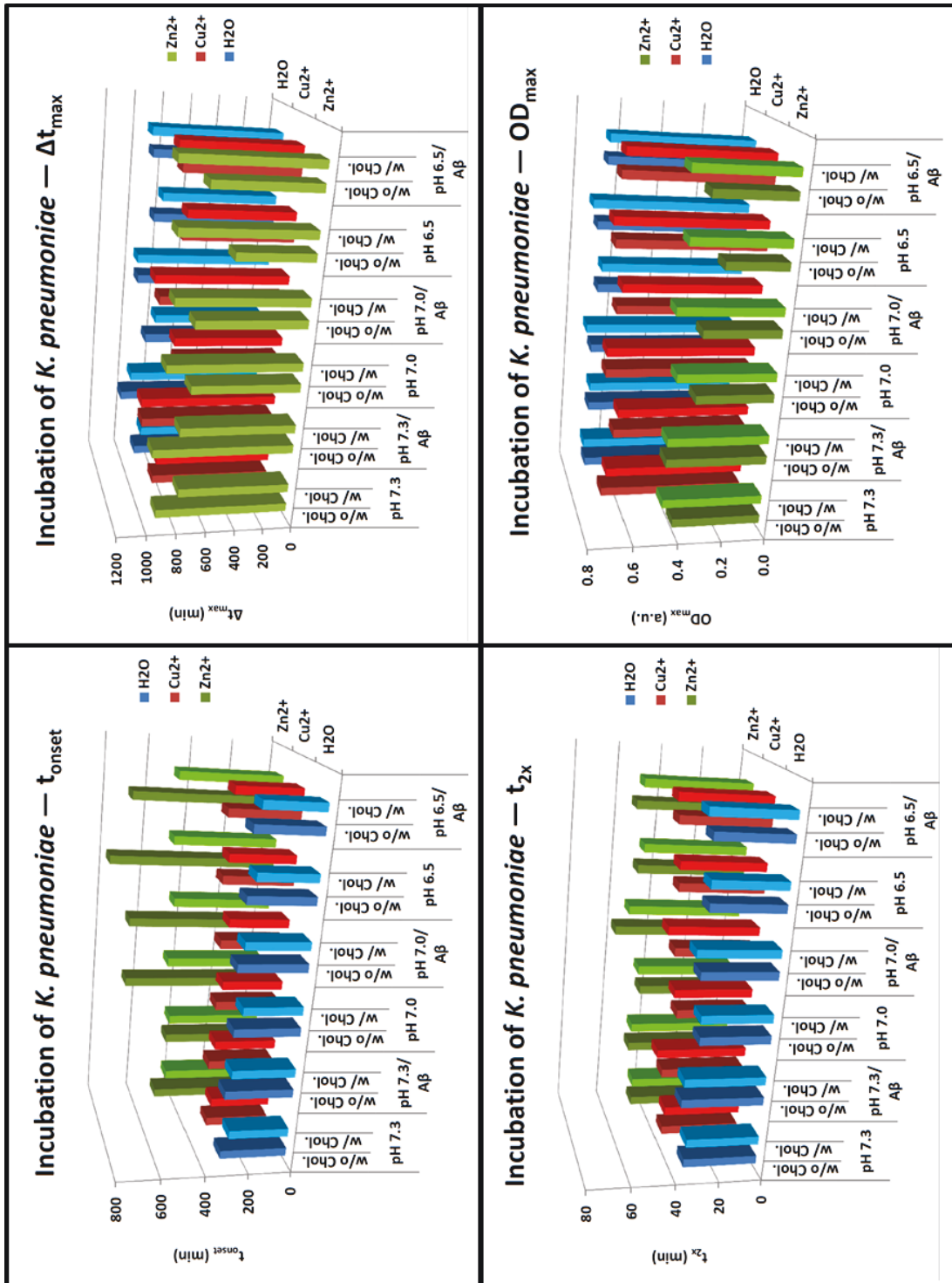


Figure II-29 Growth Curve Assay results for incubation of *K. pneumoniae*.

Results for the four most important parameters determined in the Growth Curve Assay are displayed. For details see text and Appendix C.

(d) Incubation of methicillin-resistant *S. aureus* (MRSA)

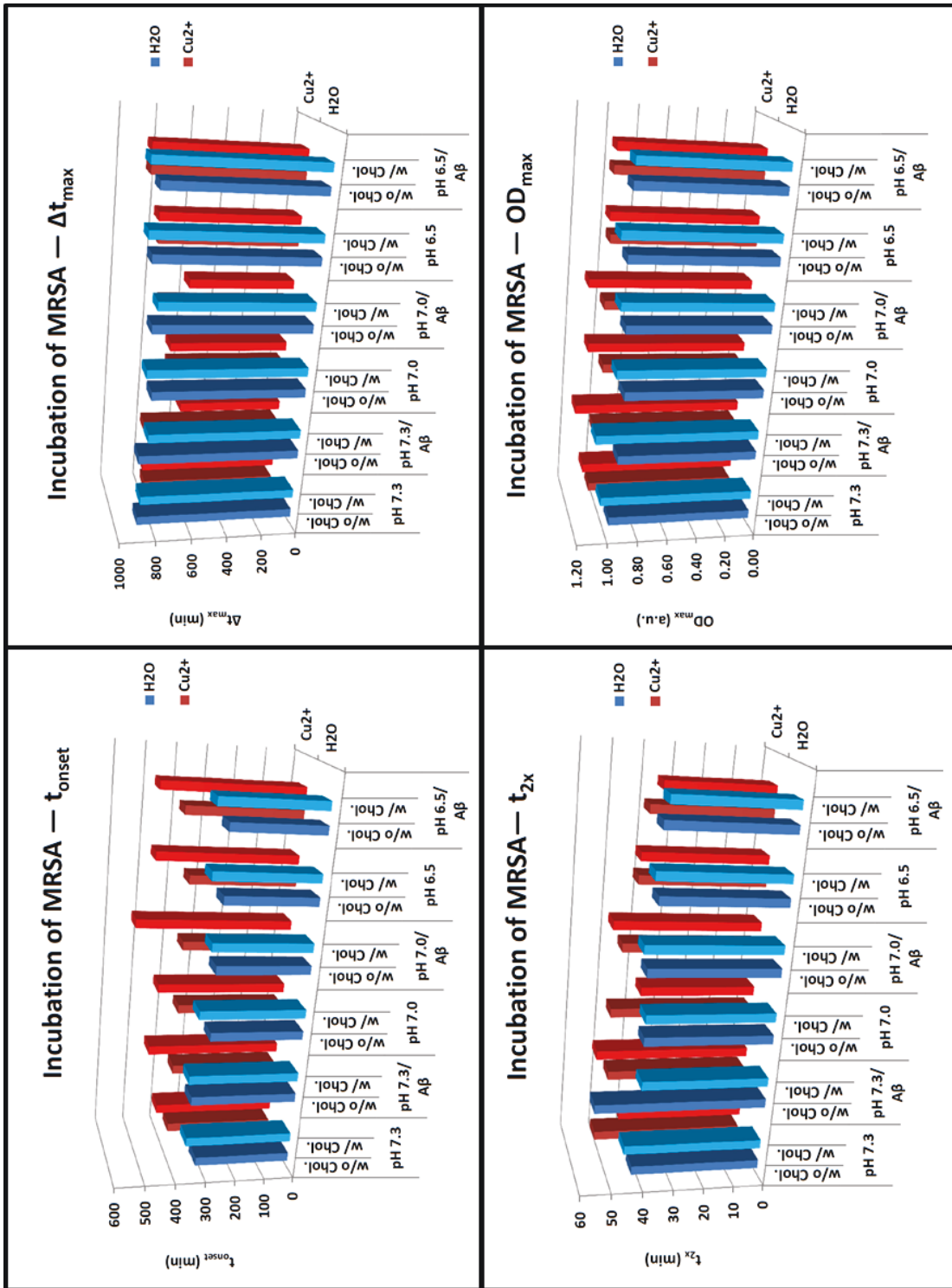


Figure II-30 Growth Curve Assay results for incubation of MRSA.
 Results for the four most important parameters determined in the Growth Curve Assay are displayed. For details see text and Appendix C.

(e) Incubation of methicillin-susceptible *S. aureus* (MSSA)

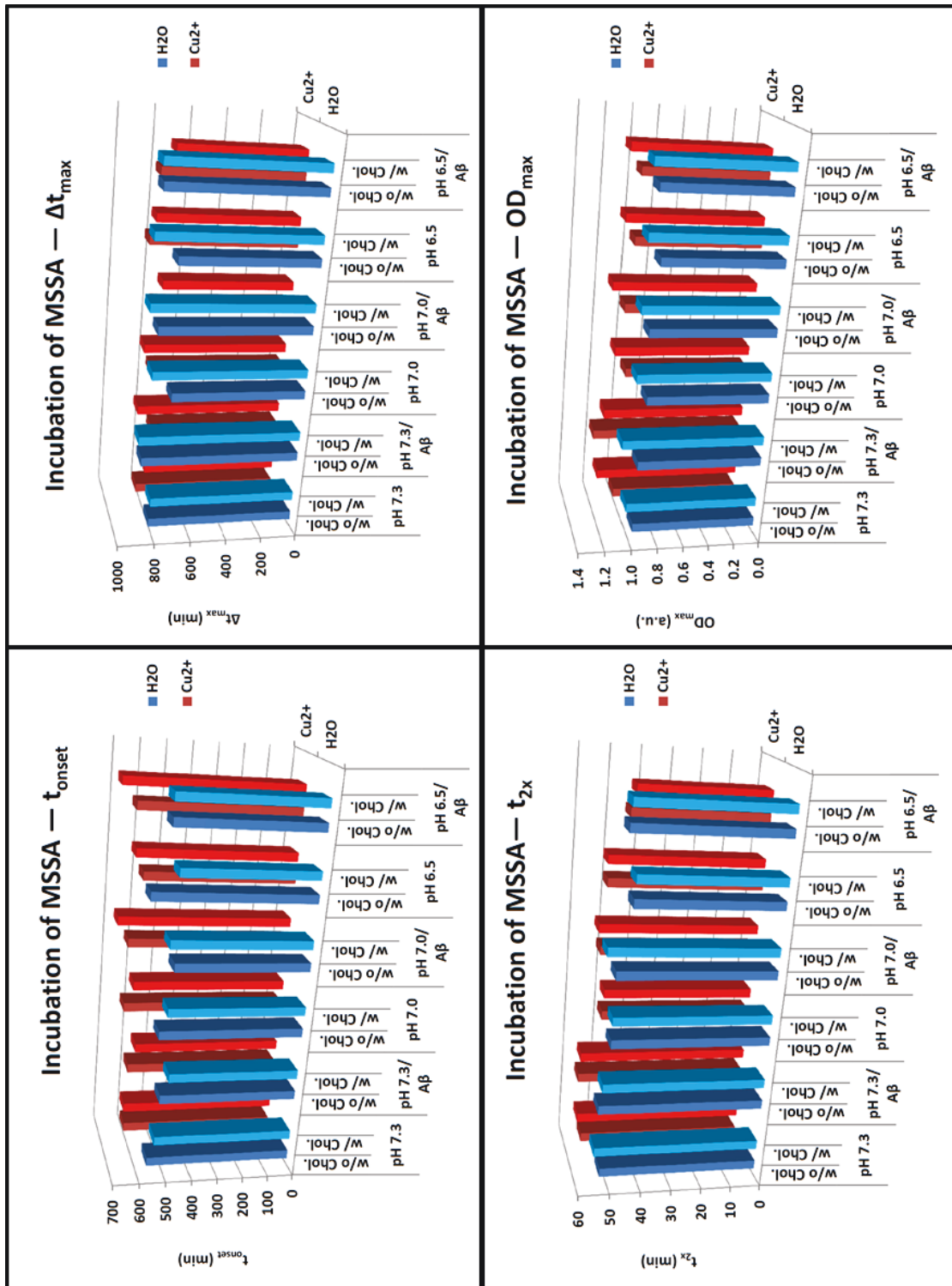


Figure II-31 Growth Curve Assay results for incubation of MSSA.

Results for the four most important parameters determined in the Growth Curve Assay are displayed. For details see text and Appendix C.

(f) Summary of parameters for all bacterial strains

In comparing the influence of the different incubation conditions between the bacterial strains, one notices that some of the parameter – incubation condition pairs show relatively constant results or trends for all bacterial strains, whereas others vary widely without any discernible trend. Especially in cases with only small changes, the relative errors were quite large, in some instances well over 100%.

A β typically had a small effect on t_{onset} , both positive and negative. Cu^{2+} had only a small effect on t_{onset} for Gram-negative bacteria, both positive and negative, but caused a medium to large increase for Gram-positive strains. With the exception of *E. coli* at pH 7.4, Zn^{2+} caused a moderate to very large increase of t_{onset} . The effect of cholesterol on t_{onset} strongly depended on the bacterial strain, as it showed a small to medium decrease of t_{onset} for *E. coli* and *K. pneumoniae*, and a small to medium increase for *S. marcescens*, MRSA, and MSSA.

A β mainly caused small to medium decreases of t_{2x} . Cu^{2+} and Zn^{2+} also caused decreases in t_{2x} — the effect of Cu^{2+} varied from small to large, whereas that of Zn^{2+} from medium to very large. pH trends were present but not the same for all bacterial strains. The presence of A β typically reduced the effect of the metal ions. Cholesterol addition in most cases showed no discernible trends.

With regards to the Δt_{max} , addition of A β led to small to large increases for gram negative bacteria, but did not show any clear trends for gram positive strains. Metal ions caused small to medium increases or decreases of Δt_{max} , dependent on the type of bacterial strain, pH and presence of A β , but with no clear trends. Cholesterol addition tended to caused small to medium increases of Δt_{max} .

Addition of A β , as well as Cu²⁺ mainly caused small effects on OD_{max}, both positive and negative with no clear trends discernible. Addition of Zn²⁺ caused medium to large decreases of OD_{max}, whereas addition of cholesterol led to small to large increases of OD_{max}.

In summary, for this series of experiments the biggest effects were typically seen with Zn²⁺, however, synergistic effects with A β were seen in more instances in its combination with Cu²⁺ (albeit minimal). If at all, cholesterol tended to have a trophic effect on the bacterial growth (i.e., earlier t_{onset}, shorter t_{2x}, longer Δ t_{max}, or higher OD_{max}). This result is contrary to the hypothesis proposed at the outset of this section that cholesterol was necessary for insertion of A β into the bacterial membrane and therefore its antimicrobial activity.

2.8.4.4. Growth Curve Assays of A β dilution series

Since the effects described in the results above were not of the desired magnitude, it was decided to do dilution series of A β in order to determine whether higher A β concentrations would reveal an antibacterial effect for the different bacterial strains.

Bacteria were incubated with varying concentrations of A β in presence of Cu²⁺, Zn²⁺ and cholesterol as before. The A β ₁₋₄₀ used in this series of experiments had been synthesised and purified by the author (see Chapter IV); A β ₁₋₄₂ was from Anaspec, Inc. The concentration of metal ions was decreased to 300 μ M to avoid the negative effects seen with gram positive bacteria in earlier experiments (see section 2.8.4.3). The OD_{12h} was chosen as parameter for comparison of the different samples. The averages for each sample were normalised based on the initial value, to ensure the first value was always equal to zero.

(a) $A\beta_{1-40}$

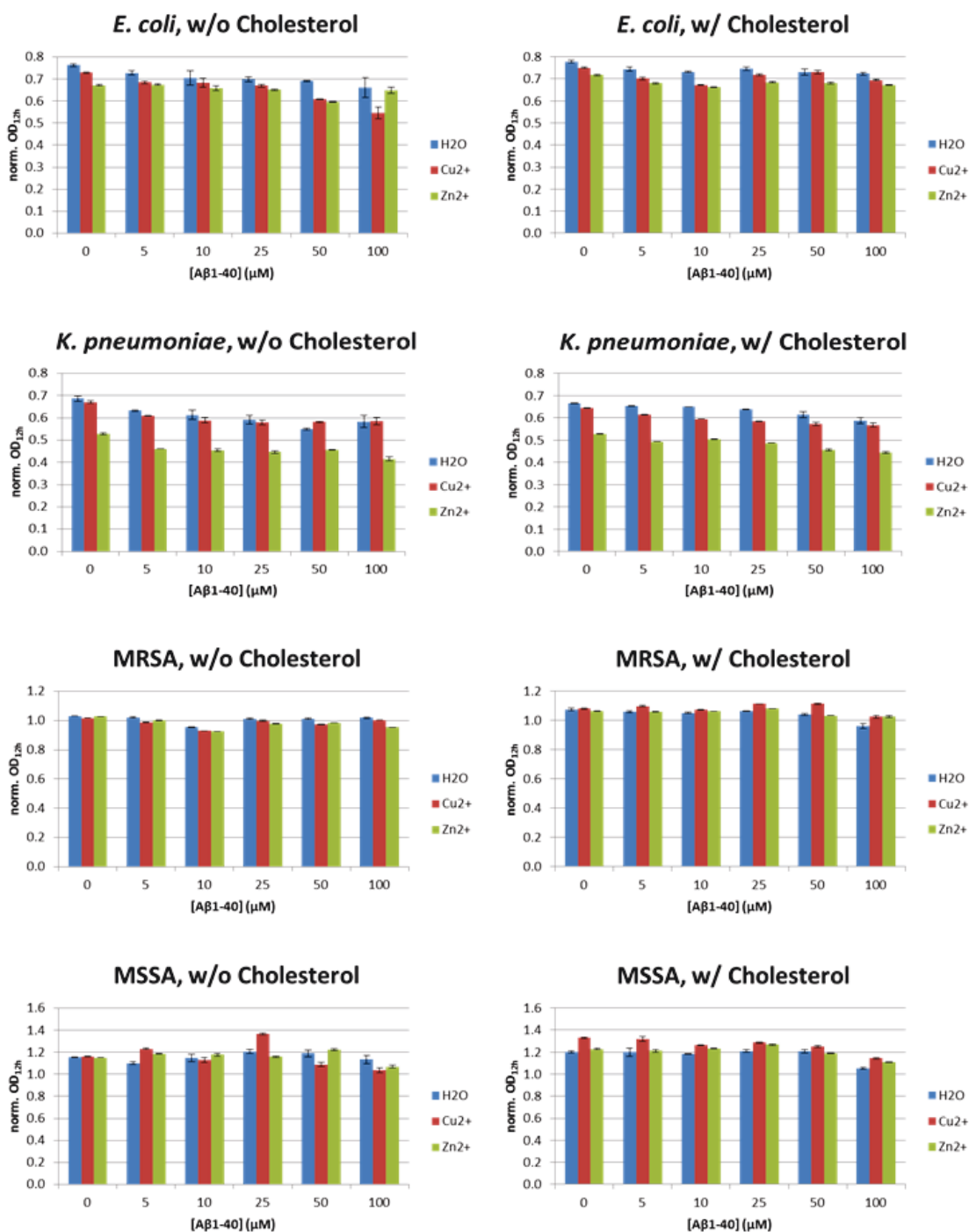


Figure II-32 Dilution series of $A\beta_{1-40}$ to determine its activity against different bacterial strains. Bacteria were incubated with varying concentrations of $A\beta$ in presence of Cu^{2+} , Zn^{2+} (both 300 μM) and cholesterol as before. The $\text{OD}_{12\text{h}}$ was chosen as parameter for comparison of the different samples. The averages for each sample were normalised by subtracting the first value from all other time points, resulting in the first value always equalling zero. Note that the scale of the vertical axis is not the same for all bacterial strains. Error Bars: \pm S.E.M. (n = 3).

Inspecting the graphs in Figure II-32, it becomes obvious that none of the experimental conditions had a major impact on bacterial viability. A β exerts its largest effect on *E. coli* in the presence of Cu²⁺, reducing the viability to 75%. The biggest overall effect was seen in *K. pneumoniae*, where for 100 μ M A β_{1-40} the OD_{12h} dropped to 71% of the H₂O control upon addition of Zn²⁺. As seen in the previous section (see 2.8.4.3), cholesterol mainly exerted a protective effect on the bacteria, increasing viability by up to 27% (*E. coli* at 100 μ M A β_{1-40} in presence of Cu²⁺).

In addition to the four bacterial strains shown in Figure II-32, *S. marcescens* was also tested, but an instrument failure produced growth curves that could not be analysed with the GCA procedures; however, the same apparent trends as shown for the other bacterial strains were obvious, i.e., A β_{1-40} did not exhibit any considerable antimicrobial activity at concentrations up to 100 μ M.

(b) A β_{1-42}

Since A β_{1-42} has been shown to be considerably more toxic in cell culture experiments than A β_{1-40} , it was decided to test its antibacterial activity, as well. *E. coli* was incubated with a dilution series of A β_{1-42} as above for A β_{1-40} and the OD_{12h} determined for each sample. The averages for each sample were again normalised based on the first value. Using Microsoft Excel®, a sigmoidal curve was fitted to the data (Figure II-33) and the IC₅₀ values⁹ were calculated according to Equation (II-3):

$$y = d + \frac{a - d}{1 + (x/c)^b} \quad \text{(II-3)}$$

⁹ Calculation of the IC₅₀ values was done in hindsight (since information from Robert Moir about the narrow time window to detect an antibacterial effect of A β became available (see p. 162) and OD_{12h} was considered a valid parameter for its detection) and in the process of writing this thesis.

where a is the value of the top plateau, b is the slope factor, c is the IC_{50} value, and d is the value of the bottom plateau. Fitting was done by varying the slope factor b and the IC_{50} value c , while the top plateau value a was kept constant at the respective value for '0 μM $A\beta$ ' (since that value cannot be displayed on a logarithmically scaled axis and is supposedly the maximum possible value), and the bottom plateau value d at '0' (since the data had been normalised to '0').

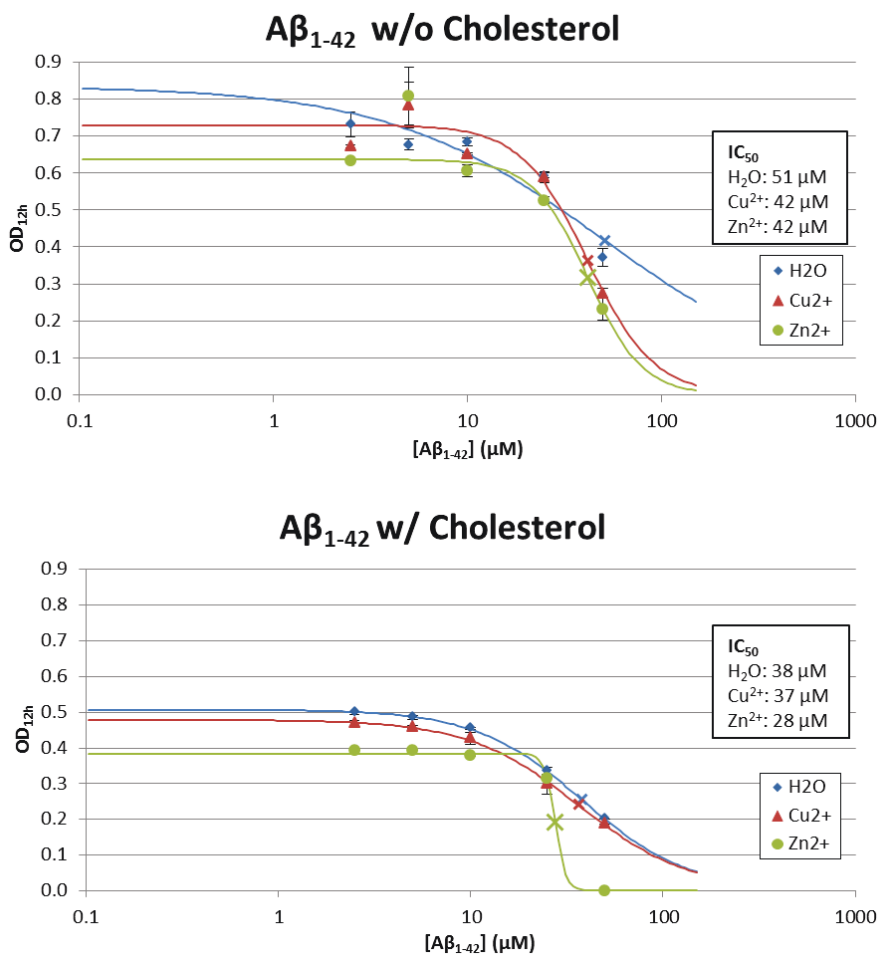


Figure II-33 Dose-response curves and IC_{50} values for incubation of *E. coli* with $A\beta_{1-42}$. *E. coli* bacteria were incubated with varying concentrations of $A\beta_{1-42}$ in presence of Cu^{2+} , Zn^{2+} (both 300 μM) and cholesterol. The OD_{12h} was chosen as parameter for comparison of the different samples. The averages for each sample were normalised by subtracting the first value from all other time points, resulting in the first value always equalling zero. Using Microsoft Excel®, a sigmoidal line (H₂O: blue line, Cu²⁺: red line, Zn²⁺: green line) was fitted to the data (H₂O: blue diamonds, Cu²⁺: red triangles, Zn²⁺: green circles) and the IC_{50} values were calculated (H₂O: blue x, Cu²⁺: red x, Zn²⁺: green x); for details about the fitting see text. Error Bars: \pm S.E.M. ($n = 3$).

These results show an antibacterial effect of A β ₁₋₄₂ against *E. coli* with an IC₅₀ of 51 μ M. Added Cu²⁺ and Zn²⁺ ions reduce the IC₅₀ value to 42 μ M; presence of cholesterol further reduces the IC₅₀ values to 38 μ M, 37 μ M, and 28 μ M for H₂O, Cu²⁺, and Zn²⁺, respectively. Considering the IC₅₀ values obtained for A β ₁₋₄₂ in these experiments here, it is not surprising that only minor effects were seen in a previous section (2.8.4.3), where the less potent A β ₁₋₄₀ at a concentration of 10 μ M was used to determine the influence on bacterial viability in presence of metal ions and cholesterol at three different pH, and in the dilution series of A β ₁₋₄₀, even though a higher maximum concentration of 100 μ M was used for those experiments. These results also point to an enhanced activity of A β ₁₋₄₂ induced by Cu²⁺ and Zn²⁺, and suggest an involvement of cholesterol in the antibacterial mechanism of A β .

2.8.4.5. Growth Curve Assays of LL-37

To put the results obtained for the antibacterial activity of A β in context with other known AMPs, *E. coli* bacteria were subjected to the GCA with a dilution series of LL-37. An LL-37 stock solution was prepared as recommended by the manufacturer by dissolution in DMSO (~10 mg/mL), followed by dilution in Tris buffer (20 mM, pH 7.4) to a concentration of 200 μ g/mL. After normalisation of the data, a sigmoidal curve was fitted to the OD_{12h} values as above for A β ₁₋₄₂, except the bottom plateau value was set to the value of the highest sample instead of '0'. The IC₅₀ value for LL-37 was calculated to be 12 μ M (see Figure II-34).

Under the experimental conditions used here, LL-37 appears about four times more potent than A β ₁₋₄₂. However, the A β experiments described in this section were performed before the supplier provided information about the actual peptide content of their product. Therefore, it can be presumed that the potency of A β is likely greater than the IC₅₀ values calculated here would suggest. However, even taking the lower actual peptide content into

account, LL-37 would still be at least two times as potent as A β (A β peptide contents of batches received since this information became available varied between 65-88% according to their certificate of analysis).

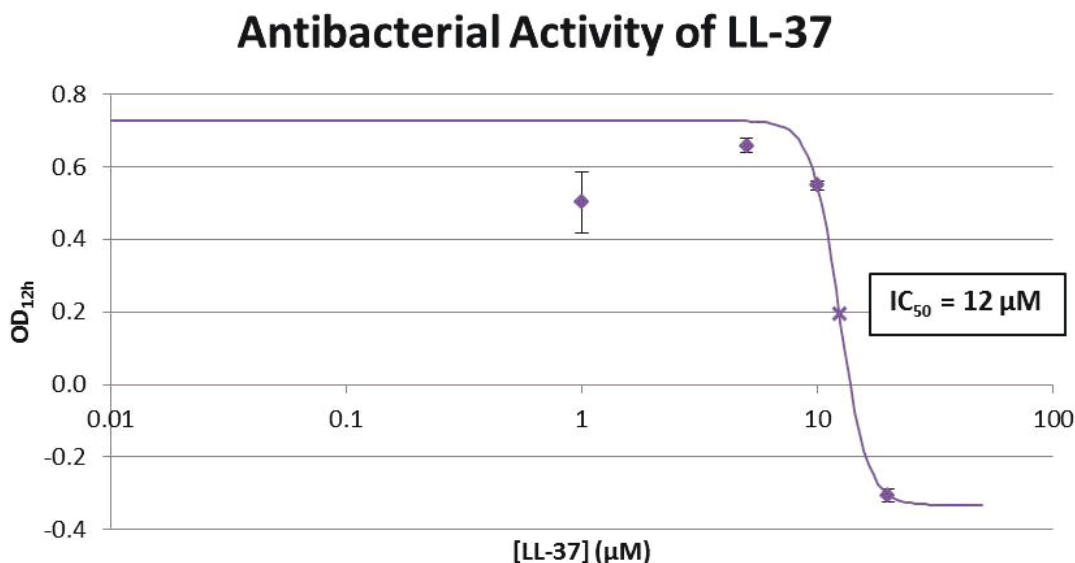


Figure II-34 Antibacterial activity of LL-37 against *E. coli*.

The antibacterial activity of LL-37 against *E. coli* was determined as described above for A β ₁₋₄₂. Diamonds: data points; solid line: sigmoidal line fitted to data points; \times : IC₅₀. Error Bars: \pm S.E.M. (n = 3).

2.8.4.6. Minimum Inhibitory Concentration (MIC)

After a paper was published by Soccia et al. (215) that showed that A β has antimicrobial activity, it was attempted to reproduce their results and also investigate the effect that Cu²⁺ and Zn²⁺, as well as cholesterol have in these experiments. Since their experiments were based on the determination of the minimum inhibitory concentration (MIC), the broth microdilution assay was adopted. At first, microplates were prepared as for the GCA, but then incubated in the shaking incubator (without shaking) rather than directly in the microplate reader; assay conditions are given in Table II-4.

Table II-4 MIC Assay conditions for experiments using the GCA preparation protocol.

Aβ Isoform	[Aβ]	Bacterial strains	Additives	Incubation Time	Comments
A β ₁₋₄₀	0/5/10/25/5 0/100 μ M	<i>E. coli</i>	Cu ²⁺ /Zn ²⁺ 0.3 mM	~24h	A β synthesised by author; see Chapter IV
A β ₁₋₄₂	0/5/10/25/5 0 μ M	MRSA	Cu ²⁺ /Zn ²⁺ 0.3 mM	~29h	compares incubation in plate reader vs. incubator
A β ₁₋₄₂	0/5/10/25/5 0 μ M	<i>S. marcescens</i>	Cu ²⁺ /Zn ²⁺ 0.3 mM	~20h	compares incubation in plate reader vs. incubator
A β ₁₋₄₂	0/5/10/25/5 0 μ M	<i>K. pneumoniae</i>	Cu ²⁺ /Zn ²⁺ 0.3 mM	~22h	compares incubation in plate reader vs. incubator

Since these experiments all failed, subsequent assays were prepared according to a literature protocol as described in the methods section (see Section 2.8.3.5); in Table II-5, a list of all the variations of experimental conditions for those assays is given.

After both, A β ₁₋₄₀ and A β ₁₋₄₂ showed no effect in the first two experiments, it was investigated whether oligomers, which are supposedly more toxic than monomers, would elicit antibacterial activity, but without success. Neither addition of cholesterol (dissolved in 2-propanol or solubilised with methyl- β -cyclodextrin) nor silanisation of the microplates to reduce peptide binding changed the results. Inspired by a paper that showed synergetic effects between kanamycin and certain AMPs in the killing of *E. coli* (216), a checkerboard assay, where the concentration of one compound increases column-wise, while the concentration of the second compound increases row-wise, was tried but failed. Finally, it was attempted to produce a toxic A β species by coating the microplates with GM₁ (and sphingomyelin and cholesterol; for details see Chapter V), but again to no avail.

Table II-5 MIC assay conditions for experiments using MIC preparation protocol.

Aβ Species [Aβ] (μg/mL)	Bacterial strains	Additives	Incubation Time	Comments
A β ₁₋₄₀ 50/25/12.5/6.25/3.13/1.56/0.78/ 0.39/0.20/0.10/0	<i>E. coli</i> , <i>S. marcescens</i> , <i>K. pneumoniae</i> , <i>P. aeruginosa</i> , <i>S. epidermidis</i> , MRSA, MSSA	n/a	~20h	[A β] adjusted according to BCA assay results; CFU determination of inoculum
A β ₁₋₄₀ & A β ₁₋₄₂ 50/25/12.5/6.25/3.13/1.56/0.78/ 0.39/0.20/0.10/0	<i>E. coli</i> , <i>S. marcescens</i> , <i>K. pneumoniae</i> , <i>P. aeruginosa</i> , <i>S. epidermidis</i> , MRSA, MSSA	n/a	~20h	[A β] adjusted according to BCA assay results; CFU determination of inoculum
A β ₁₋₄₀ & A β ₁₋₄₂ : both monomeric & oligomeric 50/25/12.5/6.25/3.13/1.56/0.78/ 0.39/0.20/0.10/0	<i>E. coli</i> , <i>S. marcescens</i> , <i>K. pneumoniae</i> , <i>P. aeruginosa</i> , <i>S. epidermidis</i> , MRSA, MSSA	n/a	~20h	[A β] adjusted according to CoA* peptide content
A β ₁₋₄₂ monomeric 50/25/12.5/6.25/3.13/1.56/0.78/ 0.39/0.20/0.10/0	<i>E. coli</i> , <i>S. marcescens</i> , <i>S. epidermidis</i> , MSSA	w/o & w/ cholesterol (200 μ g/mL [stock 20 mg/mL in 2-PROH])	~20h	[A β] adjusted according to CoA* peptide content; untreated vs. silanised plates
A β ₁₋₄₂ monomeric 50/25/12.5/6.25/3.13/1.56/0.78/ 0.39/0.20/0.10/0	<i>E. coli</i> , <i>S. marcescens</i> , <i>S. epidermidis</i> , MSSA	w/o & w/ cholesterol (5 mM M β CD*, saturated w/ cholesterol [\sim 0.625 mM])	~20h	[A β] adjusted according to CoA* peptide content
A β ₁₋₄₀ 50/25/12.5/6.25/3.13/1.56/0.78/ 0.39/0.20/0.10/0	<i>E. coli</i> , MSSA	Cu ²⁺ /Zn ²⁺ (both 0.3 mM); w/o & w/ cholesterol (5 mM M β CD*, saturated w/ cholesterol [\sim 0.625 mM])	~23h	[A β] adjusted according to CoA* peptide content
A β ₁₋₄₀ 50/25/12.5/6.25/3.13/1.56/0.78/ 0.39/0.20/0.10/0	<i>E. coli</i>	Cu ²⁺ /Zn ²⁺ (both 0.3 mM); w/o & w/ cholesterol (5 mM M β CD*, saturated w/ cholesterol [\sim 0.625 mM])	5h/~20h	[A β] adjusted according to CoA* peptide content; addition of resazurin after 5h incubation
A β ₁₋₄₀ 25/12.5/6.25/3.13/1.56/0.78/0	<i>E. coli</i>	Zn ²⁺ (0.3 mM); Kanamycin: 25/5/1/ 0.2/0.04/0 μ g/mL (checkerboard assay)	~27h	[A β] & [Kanamycin] adjusted according to CoA* peptide content/activity
A β ₁₋₄₀ 25/12.5/6.25/3.13/1.56/0.78/0	<i>E. coli</i>	plate coated with GM ₁ /sphingomyelin/ cholesterol (1:0.75:0.75), [GM ₁] 3.16/1/0.316/0.1/0.0316/0.01/0.0001/0 nmole/well (checkerboard assay)	~17h	[A β] adjusted according to CoA* peptide content; CFU determination of inoculum
A β ₁₋₄₂ 50/0	<i>E. coli</i>	plate coated with GM ₁ /sphingomyelin/ cholesterol (1:0.75:0.75), [GM ₁] 0.01/0 nmole/well; w/o & w/ cholesterol (5 mM M β CD*, saturated w/ cholesterol [\sim 0.625 mM])	~19h	[A β] adjusted according to CoA* peptide content; A β pre-incubated in plate for 8/4/2/1.5/1./ 0.5/0h

* : Abbreviations/acronyms: CoA = Certificate of Analysis; M β CD = methyl- β -cyclodextrin

Comparing the antibacterial activity of A β as determined here with the values obtained by Soscia et al. (215) (see Table II-6), it became obvious that some experimental conditions must have been different causing the experiments described here to show a much lower activity of A β .

Table II-6 Select MICs of A β determined by Soscia et al. (215).

MICs of different A β isoforms and LL-37 against the bacterial strains investigated in this thesis as published in (215). Rodent A β : R5G, Y10F, H13R.

Organism	MIC ($\mu\text{g/ml}$)					
	A β_{1-42}	A β_{1-40}	rodent A β_{1-42}	LL-37	reverse A β_{1-42}	scrambled A β_{1-42}
<i>E. coli</i>	1.56	1.56	3.13	1.56	>50	>50
<i>S. epidermidis</i>	3.13	50	3.13	25	>50	>50
<i>S. aureus</i>	6.25	25	12.5	6.25	>50	>50
<i>P. aeruginosa</i>	>50	>50	>50	6.25	>50	>50

Personal communication with Robert Moir, whose lab performed the MIC experiments published in Ref. (215), revealed a number of key issues that led to their successful experiments. Firstly, preparation of A β solutions was crucial to their success; they had to develop a special protocol to reliably form monomeric A β as a consistent starting point, however, oligomers seem to be the active species (unpublished results). Secondly, the strain of bacteria had a major influence, as different strains showed widely varying susceptibility to A β (a phenomenon also known for other AMPs). Thirdly, the culture broth and in particular its salt content greatly affected AMP activity. And finally, the time window to see an effect was often quite small, which was attributed to degradation of A β (a bacterial defense mechanism) when an assay was run too long.

This information about the narrow time window for detecting the antibacterial effect of A β showcases again the superiority of the GCA over other assays that just determine an endpoint. The possibility of retrospective analysis for any time point allows discovery of effects

not initially detected. This was done during writing this thesis in the calculation of IC_{50} values based on the OD_{12h} for $A\beta_{1-42}$ and LL-37, where initially the activity of $A\beta$ was underestimated because no total killing was seen at the 24h time point.

2.8.5. Summary

A central point of this work is the hypothesis that $A\beta$'s physiological function is as an antimicrobial peptide of the brain. In this section a number of different assays adopted from literature protocols were employed to investigate the antibacterial activity of $A\beta$ against a range of bacterial strains and their performance was compared. Both, the Radial Diffusion Assay (RDA) and the Micro-gel Well Diffusion Assay (MWDA) employed initially failed to show an antibacterial effect of $A\beta$; however, the MWDA was faster to perform, required less hands-on time by the experimenter and needed fewer materials leading to significant time and cost savings compared to the RDA.

Since both these assays failed, the Growth Curve Assay (GCA) was developed which allows a much more detailed analysis of the effect a compound has on bacterial growth. The GCA revealed a low activity of $A\beta_{1-42}$ against *E. coli* ($IC_{50} = 51 \mu M$); the activity of $A\beta_{1-40}$ was too low to afford the calculation of an IC_{50} value. Addition of metal ions (Cu^{2+} and Zn^{2+}) decreased bacterial growth, but it seemed to be mainly an additive, rather than a synergistic effect. Addition of cholesterol led to a decrease of the IC_{50} value of $A\beta_{1-42}$ by about 25%; however, for $A\beta_{1-40}$ cholesterol showed a protective effect and even increased bacterial growth, a result contrary to the hypothesis proposed at the outset of this section that cholesterol was necessary for insertion of $A\beta$ into the bacterial membrane and therefore its antimicrobial activity.

Attempts to reproduce the results of another research group that had published the antimicrobial activity of $A\beta$ (215) (Table II-6) using a broth microdilution assay to determine the

minimum inhibitory concentration (MIC) of A β for a number of bacterial strains failed. Personal communication revealed a number of factors that possibly contributed to the failure to reproduce those results; the preparation of A β , the choice of bacterial strain, the type of broth, and the narrow time window for reading of the assay.

In conclusion, experimental results presented here and published in the recent literature confirm the antibacterial activity of A β . Going forward, the opportunity afforded by the GCA that combines a number of parameters allowing a much more comprehensive evaluation of the influence of a range of factors on bacterial growth in a single experiment than all the other assays used during this project should be seized. After validation of a protocol to reliably produce oligomeric A β , more experiments should be done that take into account the choice of bacterial strain and the type of broth. Furthermore, it might be interesting to revisit the addition of cholesterol, as essentially only one concentration ('cholesterol-saturated' broth) was used here. As mentioned in Table II-5, methyl- β -cyclodextrin (M β CD) was used (unsuccessfully) in trying to see an antibacterial effect of A β with increased cholesterol concentration. However, a number of issues arise from the use of M β CD that could give rise to artifacts. Firstly, M β CD has been shown to promote A β aggregation and increase its toxicity towards neuroblastoma cells (217). Secondly, free M β CD might not be a valid blank sample since it could lead to extraction of other lipids from the bacterial membrane¹⁰ and distort results obtained that way. One way around this problem may be preloading the blank M β CD with lipids previously extracted from bacteria of the respective strain. It might also be of interest to determine whether cholesterol actually inserts into the bacterial membrane as posited at the outset of this section. Preliminary

¹⁰ Free M β CD has been used to extract cholesterol from cell membranes, while cholesterol-preloaded M β CD has been used to increase the cholesterol content in cell membranes (324, 325). Binding of hydrophobic molecules other than cholesterol, e.g., phospholipids, and of hydrophobic domains of proteins has been observed (325).

experiments at visualising cholesterol in bacterial membranes by staining with filipin (218) were unsuccessful. Experiments to determine the cholesterol content by an enzymatic assay of extracts (chloroform:2-propanol:Triton X-100 = 7:11:0.1) obtained from bacteria that had been incubated in cholesterol-containing broth showed some promising results, but could not be reproduced due to time restrictions.

2.9. Antiviral activity

2.9.1. Introduction

In addition to antibacterial activity, A β may also have antiviral activity. Numerous research groups have investigated a possible link of viral infections to AD (219). Gadjusek was the first to suggest that, in analogy to Kuru, a viral infection might have a role in the aetiology of familial AD (220). This notion was later disproved with the discovery of several mutations found in the genes of AD-affected individuals (221-223), and the discovery of prions instead of viruses as the cause of Kuru (224, 225). In 1982, Ball proposed the herpes virus as a likely candidate (226).

Very recently, Katan et al. evaluated data from the Northern Manhattan Study and found a link between AD cognitive function and infectious burden in the patients (227). Infectious burden was defined as a composite serologic measure of exposure to common pathogens (i.e., *Chlamydia pneumoniae*, *Helicobacter pylori*, cytomegalovirus, and herpes simplex virus 1 and 2). In an exploratory analysis they discovered that the associations of cognitive function with viral burden only were almost identical to those using a combined viral and bacterial score, supporting the notion that most of the effect of the infectious burden on cognition is mediated through mechanisms involving viruses rather than bacteria.

A number of AMPs possess not only antibacterial, but also antiviral activity, as for example LL-37 (228, 229), α -defensins (230, 231), polyphemusins (232), tachyplesin I (233), mellitin (234), and cecropin A (235). AMPs can act on viruses in three ways (84): direct action due to binding of the AMP to the virus particle; inhibition of virion production; and mimicry of viral infective processes, e.g., by perturbation of virus assembly or blockage of virus — cell fusion. Therefore, we propose that A β as an AMP may have not only antibacterial, but also antiviral activity.

In our experiments, we intended to gather preliminary evidence confirming whether A β is able to reduce the infectivity of enveloped viruses, specifically herpes simplex virus 1 (HSV-1) and vesicular stomatitis virus (VSV). As this idea was conceived very late in the project, further investigations are planned in the future. All experiments in this section, except the pre-treatment of A β , were performed by Dr. Ryan Noyce, a postdoctoral fellow in Christopher Richardson's (Department of Microbiology and Immunology, Dalhousie University, Halifax, Nova Scotia, Canada) laboratory in their facilities at the IWK Health Care Centre.

2.9.2. Results & Discussion

In a preliminary experiment, both HSV-1-GFP and VSV-GFP were pre-incubated with A β ₁₋₄₂ for 18 h at 37°C. The pre-treatment at 37°C had a negative effect on the stability of HSV-1-GFP, as only a very limited number of plaques were detected in all of the samples and controls, even after extended incubation up to 72 h. There was a trend to lower plaque numbers with increasing A β concentration, but the results were deemed not reliable due to the strong effect of the pre-treatment on the virus. VSV-GFP on the other hand clearly showed a dose-dependent response to the A β treatment; however, a negative impact of the pre-treatment on the virus was noticeable as well as seen in the lower number of plaques in the pre-treated control versus the

untreated control (see Figure II-35, bottom two rows; plaques are dark-grey spots in column A, green spots in column B).

Given the decreased infectivity of HSV-1 in the control plate compared to cells infected with the same amount of virus without pre-incubation at 37°C, we decreased the pre-treatment time from 18 h to 2.5 h at 37°C to maintain viability of HSV during pre-incubation with A β . Vero cells were subsequently infected with HSV-1-GFP or VSV-GFP and the effect of A β was observed 48 h post infection.

In shortening the pre-treatment of virus with A β , the antiviral effect seen with VSV was lost, presumably because this virus is much more cytopathic and replicates faster than HSV-1. However, shortening the pre-treatment of HSV with A β resulted in a dose-dependent decrease in virus production (see Table II-7 and Figure II-36). An A β_{1-42} concentration of 20 $\mu\text{g}/\text{mL}$ (= 4.4 μM) reduced the viral load 26-fold (viral inhibition: 96.2%). Fitting a sigmoidal curve to the average data (using Microsoft Excel®) resulted in the following Equation (II-4):

$$y = 1.03 \times 10^8 + \frac{2.60 \times 10^9}{1 + (x/1.01)^{1.77}} \quad (\text{II-4})$$

with a correlation coefficient $R^2 = 0.9996$.

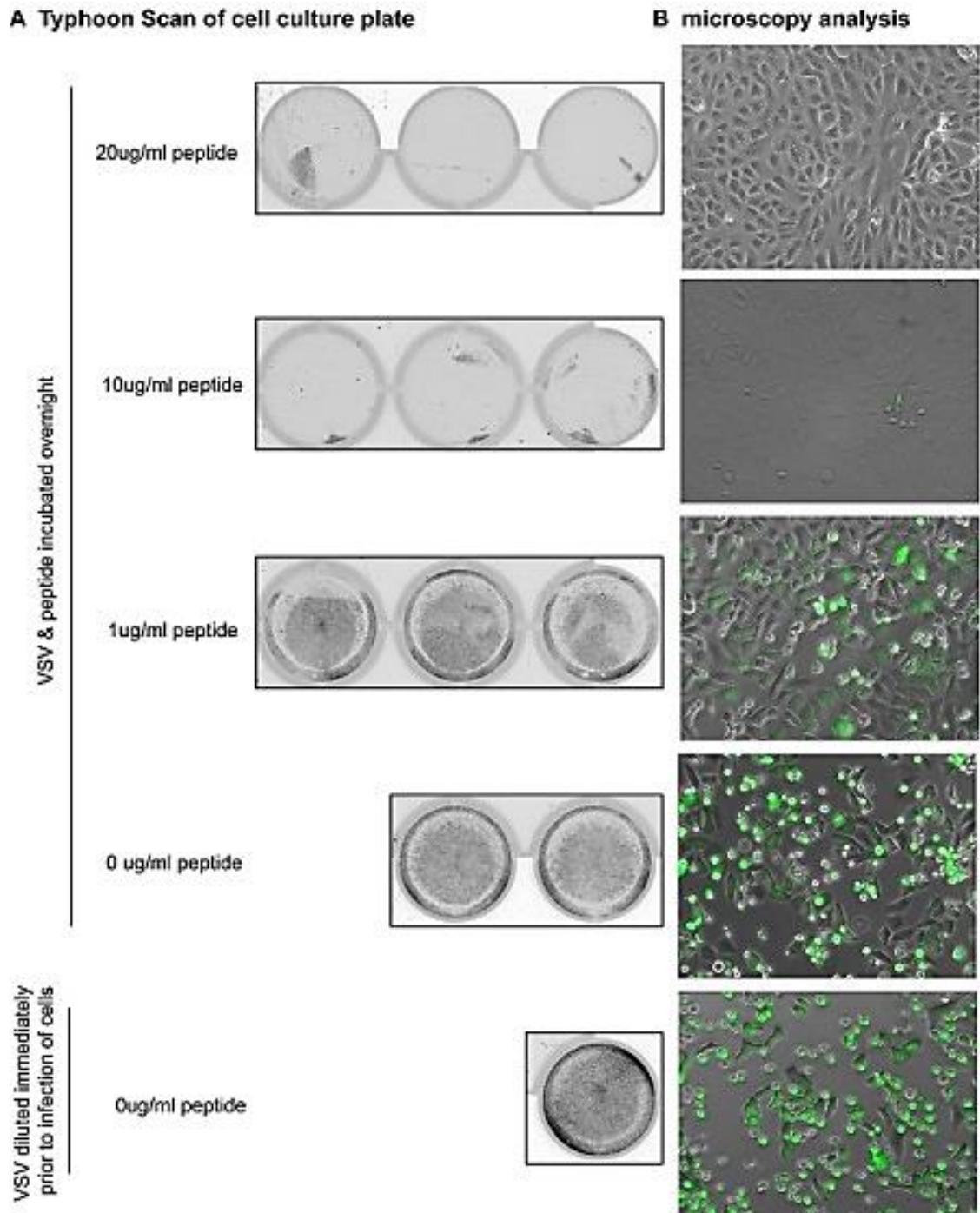


Figure II-35 Effect of $A\beta_{1-42}$ pretreatment on VSV-GFP.

Vesicular stomatitis virus tagged with green fluorescent protein (VSV-GFP) was pre-treated with $A\beta_{1-42}$ overnight before infection of Vero cells. 24 h after the infection, the plates were analysed by (A) Typhoon scan of the cell culture plates, and (B) fluorescence microscopy (for details see text). In (A) plaques are visible as dark-grey spots, in (B) as green spots, taking advantage of the GFP tag. A dose-dependent response is clearly noticeable, as well as the negative effect of the pre-treatment on the virus.

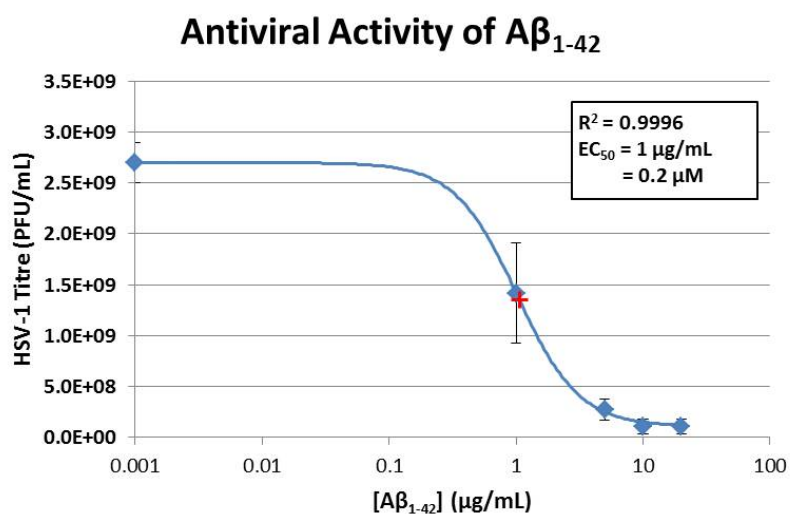


Figure II-36 Antiviral activity of A β ₁₋₄₂ against HSV-1-GFP.

A β ₁₋₄₂ shows a dose-dependent effect on HSV-1-GFP. The graph shows the averages of three independent experiments; error bars: \pm S.E.M. The EC₅₀ (+) was calculated by fitting a sigmoidal curve to the average data. Note that the data point at 0.001 μ g/mL is actually for 0 μ g/mL, however, the value '0' cannot be displayed on a logarithmic scale; therefore the value '0.001' was chosen instead as reasonable approximation for the purpose of display. For experimental details see text.

With an EC₅₀ of 1 μ g/mL (0.2 μ M), the activity of A β ₁₋₄₂ seems quite significant. Furman *et al.* determined the EC₅₀ value for the antiviral agent acyclovir (the gold standard for anti-HSV therapy) to be about 0.7 μ M for KOS HSV-1 in Vero cells (236). It should be pointed out, though, that A β was only effective when the virus was pre-treated before infecting the cells. When cells were incubated simultaneous with A β and virus, no reduction in plaque numbers was seen. This finding points to a mechanism of action where A β either destroys the virions, or prevents attachment to or entry into the host cells. Acyclovir, on the other hand, shows no effect when used as pre-treatment for virions (237), since its mechanism of action is based on selective inhibition of the viral DNA synthesis, i.e., acyclovir prevents replication of the virus inside the host cell, but not attachment to or entry of the virus particles into the host cell. Therefore, one has to be cautious in comparing these two EC₅₀ values. Furthermore, A β would not be a good antiviral drug since it would have to be administered before the infection occurred, although it

might be able to reduce or prevent secondary infection and could possibly be used as part of a combination therapy¹¹.

Table II-7 Antiviral activity of A β ₁₋₄₂ against HSV-1-GFP.

[A β ₁₋₄₂]		Viral Load (PFU/mL)		Viral Inhibition
(μ g/mL)	(μ M)	Average	S.E.M.	
0	0	2.70×10^9	1.98×10^8	0%
1	0.22	1.42×10^9	4.89×10^8	47.6%
5	1.11	2.70×10^8	1.03×10^8	90.0%
10	2.22	1.03×10^8	7.42×10^7	96.2%
20	4.43	1.03×10^8	6.84×10^7	96.2%

Epidemiologic evidence points to a role of viral and in particular HSV infections in the development of dementia (227). Recently, many failures of AD drugs in clinical trials have been blamed on the fact that the treated patients were already showing some signs of dementia, a point when the disease apparently had already progressed too far for an effective therapeutic treatment (238, 239). The fact that most HSV-1 infections occur in early childhood (240) and that in the U.S.A. HSV-1 seroprevalence was found to reach majority (56%) already by age 30 and rise to >90% in the age group >70 years (240) indicates that the causative event for AD might occur even earlier than thought currently (up to 20 years before the onset of symptoms (241)), and stresses the importance of an early intervention to the prevention or treatment of AD.

If A β was produced by the body as an AMP to control or fight a latent (HSV) infection contracted in early childhood, it also would explain why A β is found in healthy (in regards to dementia) individuals in low nanomolar concentrations (CSF concentration 700-860 pg/mL) (242), and why A β has high synthesis and clearance rates (243).

¹¹ A β would not be a good drug in general for other reasons, e.g., low metabolic stability as linear peptide, and high aggregation propensity.

2.9.3. Summary

Here we showed for the first time that A β ₁₋₄₂ has antiviral activity. Our data support the notion of A β as AMP in the brain, active not only against bacteria, but also against viruses. The activity seems to be quite significant, considering that it is well within the range of the established antiviral agent acyclovir. However, comparison of these two agents has to be done with caution as they have (likely) different mechanisms of action; acyclovir inhibits viral DNA synthesis, whereas A β acts further upstream. Since A β , due to its mechanism of action affecting the early life-cycle of the virus, would have to be administered before an infection occurred, it would not make for a good antiviral drug. However, a scenario is imaginable, where A β (or rather a drug-like analog) could be given as part of a combination therapy to reduce or prevent secondary infection.

Given the high HSV-1 seroprevalence in the general population, A β 's role as AMP may explain its presence even in the CSF of healthy individuals as well as the correlation of the viral infectious burden with dementia.

As this concept of A β possessing antiviral activity was conceived so late into my project, these experiments have to be seen as the starting point for a more thorough investigation in the future. For example, the antiviral mechanism of action of A β should be determined, whether A β attacks virus particles directly, or if it inhibits the attachment to or entry into the host cells. Also of interest would be the activity spectrum, whether it is active only against enveloped viruses (like HSV and VSV chosen for our experiments), or also against non-enveloped viruses. Furthermore, it should be confirmed, first in cell culture, and then in animal models, that a viral infection (of the brain) can induce the production of A β . Transgenic models could be used to find out if a viral infection leads to earlier and/or increased symptoms of AD.

2.10. Summary

In this section, the idea of A β 's physiologic function as an antimicrobial peptide was developed including a mechanism of action. Experimental evidence showing activity of A β against bacteria and viruses was presented. The influence of cholesterol and metal ions (Cu²⁺ and Zn²⁺) on the antibacterial activity was investigated to evaluate the proposed mechanism of action requiring cholesterol for membrane insertion of A β , and its enhancement by presence of Cu²⁺ or Zn²⁺.

3. Why A β Attacks Neurons

3.1. Introduction

With the more clearly defined role of A β as an antimicrobial peptide in the brain attempting to ward off invading organisms, the next question would then be why A β would attack the body's own neuronal cells? This question may be more readily answered if one looks at the structural characteristics of neurons. Because of their unique functionality, neurons exhibit features that are distinct from most other mammalian cells. Their membrane composition, including lipids and cholesterol, as well as their transmembrane potential is very different from that of a typical mammalian cell. Interestingly enough, however, the features that set them apart from other mammalian cells makes them quite similar to those of bacteria.

3.2. Comparison of Mammalian and Bacterial Membranes

For the immune system to function effectively, it needs to be able to distinguish between 'self' and 'non-self' that it attacks only invading species but not cells of the own organism. Two main factors have been identified that distinguish bacterial from mammalian cell membranes, the lipid composition and the magnitude of the transmembrane potential (143, 244-246). For example, the outer leaflets of human erythrocyte bilayers are composed exclusively of zwitterionic, i.e., electrically neutral phospholipids (104), the main species being phosphatidylcholine and sphingomyelin. Acidic phospholipids, like phosphatidylserine, are sequestered in the inner leaflets. In contrast, bacterial membranes contain large amounts of

acidic phospholipids (211), such as phosphatidylglycerol and phosphatidylethanolamine, about a third of which is located in the outer monolayers of the bilayer membranes (247, 248).

Both, the negatively charged acidic lipid head groups of bacterial membranes and the highly-negative internal potential of bacterial cells attract the positively charged basic residues on one face of an amphipathic α -helix or β -sheet that comprises an AMP. Thus, binding of the AMP to the membrane is facilitated, leading to insertion and ultimately destruction of the bacterium (84). The neutrality of (most) mammalian outer membrane leaflets results in a much lower propensity to interact with AMPs (249), still, some AMPs have shown lytic activity towards mammalian cells, as well (250, 251). Interestingly, the high cholesterol content typical for mammalian cells has been demonstrated by multiple research groups to ameliorate or even prevent this lytic activity (244, 246, 252).

Cholesterol is very abundant in erythrocyte membranes (253), but considered absent in bacterial cell membranes (211). Interactions of cholesterol with the AMP are thought to inhibit the formation of peptide structures capable of cell lysis (252, 254), although some AMPs show cholesterol-dependent activity (169-172).

The transmembrane potential has also been shown to affect peptide-lipid interactions (255-257), e.g., by facilitating ion channel formation by peptide self-assembly. Erythrocytes exhibit a different magnitude of the transmembrane potential compared to energised bacterial cells. For normal human erythrocytes, the membrane potential in standard media is about -9 mV (258) while respiring bacterial cells have inside-negative potentials of 100-150 mV (259, 260). Furthermore, bacterial cells that were artificially depolarised, have been shown to be less susceptible to the antibacterial actions of magainin and melittin (261, 262). A table comparing bacterial with mammalian and neuronal membranes is given in the next section (Table II-8)

3.3. Comparison of Neuronal and Bacterial Membranes

Among mammalian cells, neurons take somewhat of an outsider role and exhibit a number of features different from other types of mammalian cells. The defining features of neurons being their electrical excitability and the presence of synapses, these exceptional characteristics are due to their functional difference, i.e., the task of transmitting an electrical signal along the cell membrane surface. The two most prominent differences are the negatively charged outer leaflet of neuronal cell membranes, and the inside-negative resting potential of -70 mV in neurons (263). The negative charge on the extracellular leaflet is caused by the presence of acidic phospholipids, such as glycerophospholipid, and phosphatidylethanolamine.

Table II-8 Similarities and differences between bacterial, mammalian neuronal and other mammalian cells.

Cell Type	Bacterial cells	Mammalian neuronal cells	Mammalian cells (e.g., erythrocytes)
Membrane lipid composition	Acidic phospholipids (negative), e.g., phosphatidylglycerol, phosphatidylethanolamine	Zwitterionic or acidic phospholipids, e.g., glycerophospholipid, sphingomyelin, gangliosides (GM ₁)	Zwitterionic phospholipids (neutral), e.g., phosphatidylcholine sphingomyelin
Membrane cholesterol	No	Yes	Yes
Transmembrane potential*	-100 to -150 mV	-70 mV (resting)	- 9 mV

*As per references (258-260, 263).

3.4. Neurotoxicity of β -Amyloid

3.4.1. Introduction

The neurotoxicity of $A\beta$ is a well-known fact and has been established over 20 years ago (264, 265). However, since $A\beta$ is inherently difficult to work with (as already experienced in the experiments of the previous sections) and in order to establish a baseline allowing comparison to the neurotoxicity of AMPs discussed below (see Section 3.5), experiments aimed at quantifying the neurotoxicity of $A\beta$ were performed.

3.4.2. Materials

3.4.2.1. *Biological Materials*

The following mammalian cell lines, already described previously, were used:

- SK-N-AS, human neuroblastoma, ATCC # CRL-2137, Risk Group: 1 (American Type Culture Collection (ATCC), Manassas, VA, USA)
- primary neuronal rat cells, kindly provided by Dr. B. Karten (Department of Biochemistry & Microbiology, Dalhousie University)

3.4.2.2. *Chemicals*

In addition to materials related to mammalian cell culture already mentioned in previous sections, the following chemicals were used:

$A\beta_{1-40}$; $A\beta_{1-42}$ (both Anaspec, Inc.); 3-(4,5-Dimethylthiazol-2-yl)-2,5-diphenyltetrazolium bromide (MTT)

3.4.3. Methods

In addition to methods related to mammalian cell culture already described in previous sections, the following procedures were employed:

3.4.3.1. MTT Cell Viability Assay

The MTT assay developed by Mosman (266, 267) is a commonly used cell viability assay based on the metabolic activity of the analysed cells. Metabolically active cells will reduce the yellow MTT (3-(4,5-Dimethylthiazol-2-yl)-2,5-diphenyltetrazolium bromide) to the corresponding purple formazan (see Figure II-37); damaged or dead cells will show much less or no formazan formation at all.

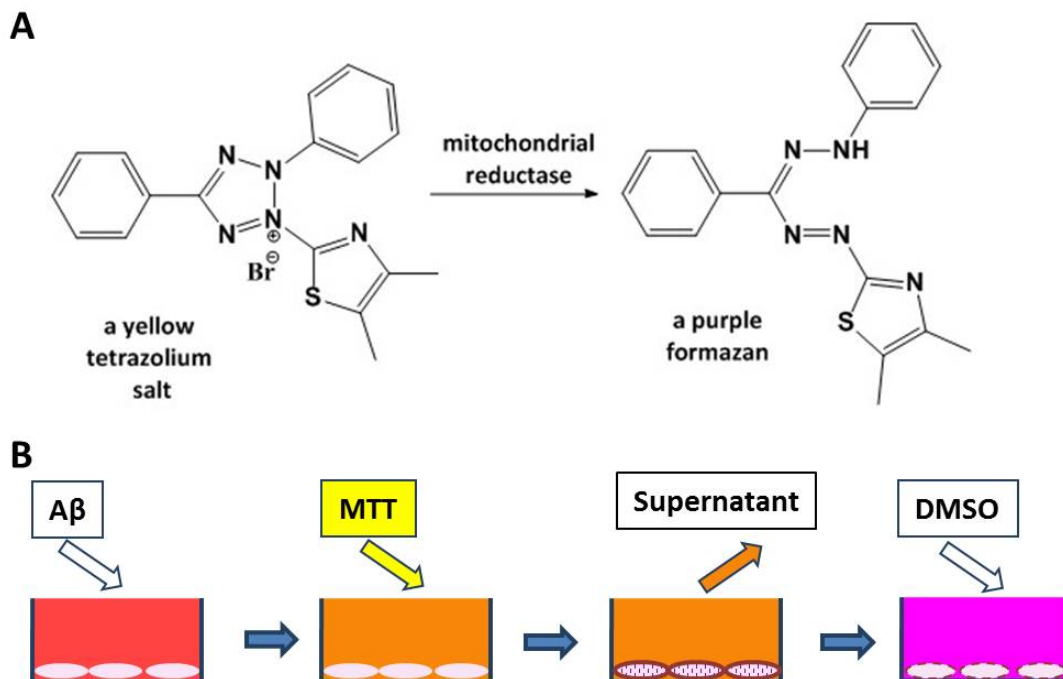


Figure II-37 MTT assay.

In metabolically active cells, MTT (3-(4,5-Dimethylthiazol-2-yl)-2,5-diphenyltetrazolium bromide; yellow) is reduced intracellularly to the corresponding purple formazan (A). After incubation of cells with $A\beta$, they are further incubated with MTT; removal of the supernatant is necessary to allow solubilisation of the purple formazan with solvent, e.g., DMSO or 2-propanol (B).

A 96-well plate with SK-N-AS neuroblastoma cells or primary rat neuronal cells was prepared as described previously (see Sections 2.7.3.7 - 2.7.3.9); after 24 hours, cells were washed twice with warm (37°C) PBS, supplied with fresh growth medium without phenol red, and incubated with A β prepared in phenol red-free medium for 4 hours at 37°C in a water-saturated atmosphere with 5 % CO₂. After 4 hours, the cells were inspected visually by light microscopy for any signs of toxicity. Then, 20 μ L/well of MTT solution (5 mg/mL) were added to the plate, which was incubated for another two hours at the same conditions to allow for the reduction to take place. After inspecting the cells under the microscope for differences in formation of formazan crystals, the medium was removed, while taking care that no formazan crystals were discarded inadvertently. The cells were lysed and the formazan crystals dissolved in 100 μ L/well DMSO by gently shaking the plate for about one minute. After checking for complete dissolution of all crystals, the absorbance was read at 540 nm in a microplate reader.

3.4.4. Results & Discussion

The MTT assay is a well-established method to determine cell viability, or more precisely metabolic activity of cells. It was utilised here to determine the neurotoxic activity of A β in order to establish a baseline for further experiments (described in Section 3.5), and to confirm that the protocol for preparation of A β actually yielded a toxic species.

Results for incubation of SK-N-AS neuroblastoma cells (Graph A) and primary rat neuronal cells (Graph B) with both, A β ₁₋₄₀ and A β ₁₋₄₂ are displayed in Figure II-38. The IC₅₀ value could only be calculated for A β ₁₋₄₀ in primary rat neurons, it was 14 μ M; due to the shape of the other curves, the iteration would never converge to a reasonable value.

For both cell lines, the two A β species show similar trends; as the concentration of A β increased, initially the cell viability dropped considerably, however, after reaching a

concentration of 5 μM , the decline was strongly attenuated or even reversed. The reversal effect was more pronounced for $\text{A}\beta_{1-42}$. This somewhat unexpected result may be explained by aggregation of $\text{A}\beta$. As the concentration of $\text{A}\beta$ increases, more and more (non-toxic) higher aggregates are formed, which removes molecules from the pool of active species. Since $\text{A}\beta_{1-42}$ has a higher aggregation propensity, this effect is more pronounced as compared to $\text{A}\beta_{1-40}$.

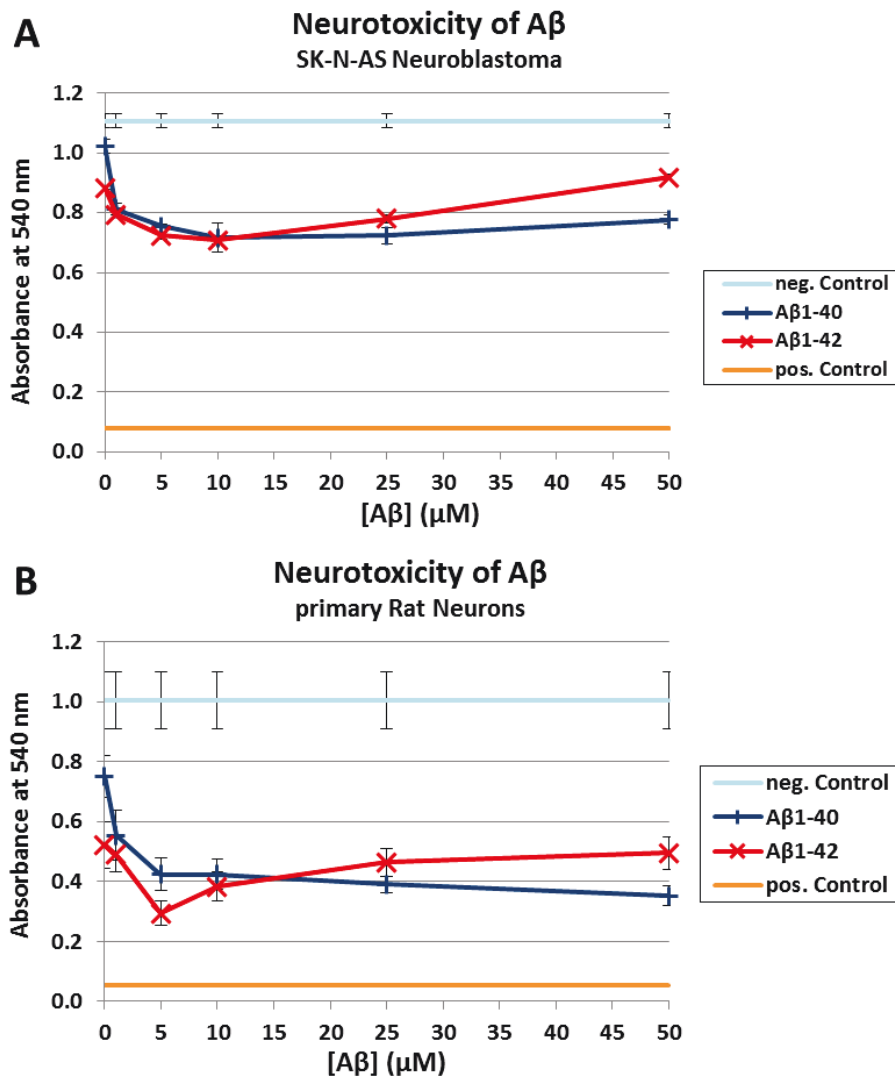


Figure II-38 Toxicity of $\text{A}\beta_{1-40}$ and $\text{A}\beta_{1-42}$ against SK-N-AS neuroblastomas and primary rat neurons. SK-N-AS neuroblastoma cells (A) and primary rat neuronal cells (B) were incubated with dilution series of $\text{A}\beta_{1-40}$ and $\text{A}\beta_{1-42}$ in order to establish the neurotoxicity of $\text{A}\beta$. Cell viability was determined by MTT assay; neg. Control: Growth Medium, pos. Control: 1% Triton X-100. Error Bars: \pm S.E.M.; $n = 2$ for SK-N-AS; $n = 4$ for rat neurons. Error bars for pos. Control are present but too small to be visible.

The results encountered here would seem to contradict results obtained for A β 's antibacterial activity discussed earlier (see Section 2.8), which did not show attenuation at higher concentrations of A β . However, it is conceivable that mammalian neurons possess molecules in their membranes (that are not present in bacteria) that increase A β aggregation in order to protect themselves from its toxic effects.

One mechanism by which AMPs may exert neurotoxic properties is through damage to mitochondria. Mitochondria are a type of organelle that exists in the cytoplasm of cells and provides the cell's energy. If AMPs were to cross the membrane without actually disrupting it (i.e., "flip-flop" mechanism), they would gain access to this essential cellular component causing mitochondrial damage. This anti-mitochondrial effect has been previously demonstrated in vitro for a number of AMPs, e.g., histatin 5 (268), or lactoferricin B (269). It was ascribed to the evolutionary origin of mitochondria, which are assumed to have developed from engulfed, symbiotic bacteria (endosymbiont theory) (270-272). VC Meier-Stephenson proposed in her thesis that neurons may be susceptible to the actions of A β (as AMP) in addition to its membrane-disrupting properties, based on the mitochondria's similarity to bacteria (173).

The involvement of mitochondria in the process of AD has been known since the 1980s and numerous effects of A β on mitochondria have been described, such as inhibition of key mitochondrial enzymes, impact on mitochondrial respiration, and oxidative damage to mitochondrial DNA (181, 273-286).

3.4.5. Summary

In this series of experiments, neurotoxicity of A β_{1-40} and A β_{1-42} was established in SK-N-AS neuroblastoma and primary rat neuronal cells using the MTT cell viability assay. Neurotoxicity

was attenuated or even reversed at higher concentrations of A β , possibly due to its aggregation forming non-toxic species. As another possible mechanism besides membrane disruption, mitochondrial toxicity was discussed in analogy to known AMPs.

3.5. Neurotoxicity of Known AMPs

3.5.1. Introduction

After considering the similarities of A β with AMPs, it was decided to explore whether AMPs have properties that A β is known for, specifically, its neurotoxicity. Under the pretense that A β 's neurotoxic activity is due to it being an AMP charging a misdirected attack on 'self' neurons, AMPs should elicit comparable neurotoxic effects. Indeed, there is literature precedence for cytotoxic activity of the AMP lactoferricin B towards neuroblastoma cells (269). In order to establish the effect of AMPs on neurons, two well-known AMPs, LL-37 and cecropin A (see Figure II-39), were incubated with neuroblastoma, as well as primary neuronal cells. These two AMPs were chosen based on their secondary structure, the defining features being α -helices, just like in A β .

3.5.2. Materials

3.5.2.1. Biological Materials

The following mammalian cell lines, already described previously, were used:

- SK-N-AS, human neuroblastoma, ATCC # CRL-2137, Risk Group: 1 (American Type Culture Collection (ATCC), Manassas, VA, USA)

- primary neuronal rat cells, kindly provided by Dr. B. Karten (Department of Biochemistry & Microbiology, Dalhousie University)

3.5.2.2. Chemicals

In addition to materials related to mammalian cell culture already mentioned in previous sections, the following chemicals were used:

A β ₁₋₄₀; A β ₁₋₄₂; LL-37; Cecropin A (all Anaspec, Inc.); MTT

LL-37:

LLG**D****F****F****R****K****S****K**¹⁰**E****K****I****G****K****E****F****K****R****I**²⁰**V****Q****R****I****K****D****F****L****R****N**³⁰**L****V****P****R****T****E****S**

Cecropin A:

K**W****K****L****F****K****K****I****E**¹⁰**V****G****Q****N****I****R****D****G****I**²⁰**K****A****G****P****A****V****A****V****V****G**³⁰**Q****A****T****Q****I****A****K**

Figure II-39 Primary sequences of known AMPs LL-37 and cecropin A.

The primary sequences of LL-37 and cecropin A are given. Basic residues (positively charged): blue; acidic residues (negatively charged): red; hydrophobic residues: underscored. The overall charge at physiologic pH of both LL-37 and cecropin A is '+6'.

3.5.3. Methods

SK-N-AS neuroblastoma and primary rat neuronal cells were grown and prepared for the assay as described in Section 2.5.3. Neurotoxicity was evaluated by the MTT assay as described in Section 3.4.3.

3.5.4. Results & Discussion

SK-AN-AS neuroblastoma cells (Graph A) and primary rat neuronal cells (Graph B) were incubated with dilution series of LL-37, and cecropin A in order to establish the neurotoxicity of AMPs (see Figure II-40); results for A β ₁₋₄₀ and A β ₁₋₄₂ were already presented in Section 3.4 and are included for comparison (the assays were performed in the same plates). The IC₅₀ values for

LL-37 were 4 μM and 34 μM for primary rat neurons and SK-N-AS neuroblastomas, respectively; for cecropin A, they were 12 μM and 116 μM , respectively. As already mentioned in Section 3.4, the IC_{50} value for $\text{A}\beta$ could only be calculated for one curve, $\text{A}\beta_{1-40}$ in primary rat neurons; it was 14 μM .

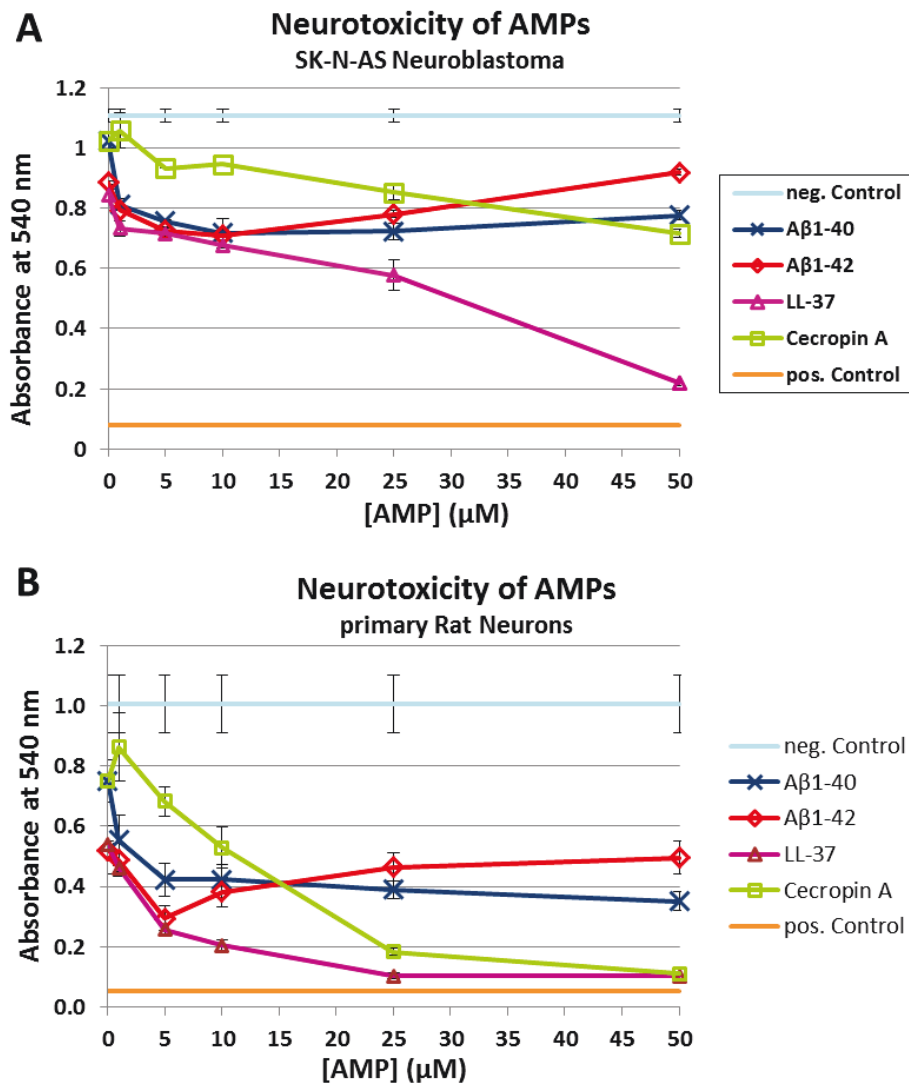


Figure II-40 Toxicity of AMPs against SK-N-AS neuroblastomas and primary rat neurons. SK-N-AS neuroblastoma cells (A) and primary rat neuronal cells (B) were incubated with dilution series of LL-37, and cecropin A in order to establish the neurotoxicity of AMPs; $\text{A}\beta_{1-40}$ and $\text{A}\beta_{1-42}$ were included for comparison. Cell viability was determined by MTT assay; neg. Control: Growth Medium, pos. Control: 1% Triton X-100. Error Bars: \pm S.E.M.; $n = 2$ for SK-N-AS; $n = 4$ for rat neurons. Error bars for pos. Control are present but too small to be visible.

The results obtained in this series of experiments clearly demonstrate a toxic effect of two AMPs (LL-37 & cecropin A) against both, neuroblastoma and primary rat neuronal cells, with a higher activity against primary neurons as evidenced by the lower IC₅₀ values. While activity against neuroblastoma cells is not surprising in the light of previously reported activity against other cancer cells (287-290), toxicity against primary neurons has not been reported for either molecule to date. Interestingly, the selectivity of AMPs towards cancer vs. normal cells is mainly ascribed to a higher than normal expression of anionic molecules such as phosphatidylserine and *O*-glycosylated mucins in cancer cells (288), and their negative membrane potential (261) — the same mechanisms proposed here being responsible for the toxicity of A β against neuronal cells. The reason essentially no neurotoxicity of AMPs in vivo is reported in the literature likely is due to the blood-brain barrier preventing passive diffusion of these highly charged peptides across its membranes, thus preventing exposure of neurons to these molecules.

3.5.5. Summary

Results presented in this section demonstrate a toxic effect of two (α -helical) AMPs, L-37 and cecropin A, against neuroblastoma and primary rat neuronal cells with activity comparable to A β . This is the first report about neurotoxic activity of these two molecules. Demonstrating neurotoxic activity of AMPs adds to the growing list of similarities of A β to AMPs and further supports the notion of A β actually being an AMP.

3.6. Summary

Investigations in this section dealt with answering the question why A β attacks neurons. It was proposed that similarities of neuronal and bacterial cells, i.e., the negative charges on the outside and a negative transmembrane potential, are the reason for the misdirected attack of A β on neurons. To establish a baseline, the neurotoxicity of A β was reproduced, followed by a discussion about toxicity of A β against mitochondria, thus providing another mechanism (besides membrane disruption) for its toxic effects on neurons. Finally, the concept of similarity between A β and AMPs was extended and reversed; while experiments described in previous sections showed similarities of A β to other AMPs, here similarity of AMPs to A β was revealed. For the first time, toxicity of two AMPs, LL-37 and cecropin A, against primary neurons was demonstrated experimentally in vitro.

4. Why AD is Progressive and Chronic

AD, like many other autoimmune diseases, is a chronic process where the health of affected individuals progressively deteriorates over time. For this last piece of the puzzle, evidence has been gathered to give further description of the underlying mechanism of the progressive and chronic nature of AD.

4.1. Mechanism for Progression and Chronicity of AD

There are two generally accepted mechanisms by which cell death can occur, necrosis and apoptosis (291), although more recently, necroptosis as a process with features of both has been described (292).

Apoptosis, also called 'programmed cell death', involves the degradation of cells in a controlled manner in order to minimize a possible inflammatory response. Apoptosis is involved in a variety of physiological and pathological events, e.g., normal fetal development, cancer, organ failure and neurodegenerative diseases. It is a tightly controlled process that can be induced by a number of extracellular or intracellular triggers, for example toxins, hormones, cytokines, heat, radiation, and nutrient deprivation (293). These signals trigger a cascade of signalling events, in most cases leading to the activation of caspase-3 and caspase-7, which is considered the 'point of no return' *en route* to cell death. The initiated process of programmed cell death through the organized degradation of cellular organelles by activated proteolytic caspases leads to changes in cellular morphology such as blebbing, cell shrinkage, nuclear fragmentation, chromatin condensation, and chromosomal DNA fragmentation. In the end

stage of apoptosis, the cell breaks apart into several vesicles, so-called apoptotic bodies, which are subsequently phagocytosed. Since apoptosis progresses quickly and its products are quickly removed, detection or visualisation is difficult.

In necrosis, cell death is caused by traumatic injury due to mechanical or chemical insult, infection or toxins. Cell death occurs by autolysis resulting in the unregulated digestion of cell components. The uncontrolled spillage of the cell contents into the surrounding tissue induces a strong inflammatory response that often causes further damage to the surrounding tissue.

Although necrosis has been implicated in AD (294), most of the research on processes of cell death in AD has focussed on apoptosis (295-298). Experiments in this section are aimed toward determining whether apoptosis or necrosis is responsible for the *progression* of AD, and establishing a mechanism for the propagation of cell death from one neuron to the next. Additional focus has also been given to GM₁, the major ganglioside in (human) neuronal membranes, as it was identified as a candidate component released from the membrane of necrosed cells that might be involved in this process. Previous research has shown that GM₁ can bind A β , both specifically and tightly, to form seeds that promote further aggregation and formation of toxic A β species (299, 300). An in-depth discussion of the connection of A β to GM₁, their interaction and involvement in AD is given in Chapter V.

4.1.1. Materials

4.1.1.1. Biological Materials

The following mammalian cell lines, already described previously, were used:

- SK-N-AS, human neuroblastoma, ATCC # CRL-2137, Risk Group: 1 (American Type Culture Collection (ATCC), Manassas, VA, USA)

- primary neuronal rat cells, kindly provided by Dr. B. Karten (Department of Biochemistry & Microbiology, Dalhousie University)

4.1.1.2. Chemicals

In addition to materials related to mammalian cell culture already mentioned in previous sections, the following chemicals were used:

SensoLyte Homogeneous AMC Caspase-3/7 Assay Kit (Anaspec, Cat.# 71118, San Jose, CA, USA); HiLyteFluor™ 555-A β ₁₋₄₀ (both Anaspec, Inc.); carboxyfluoresceine (FAM)-A β ₁₋₄₂; Monosialoganglioside 1 (GM₁) (Genway Biotech, Inc.);

4.1.2. Methods

The overall design of the experiment was as follows: apoptosis and necrosis were induced in cells by UV irradiation and mechanical damage, respectively; their supernatants and cell lysates were isolated and tested for caspase-3/-7 activity (i.e., the marker for apoptosis); the isolated supernatants and cell lysates were incubated with new cell cultures in an attempt to see how the products of ill-fated cells affected undamaged ones; finally, A β production in the supernatants and cell lysates of these cell cultures was determined.

In addition, cells were incubated with A β and GM₁/A β ¹² for comparison and isolation of effect in the necrosis arm.

¹² GM₁/A β : Monosialoganglioside 1 – β -amyloid complex (292, 293)

4.1.2.1. Preparation of Apoptotic and Necrotic Cell Supernatants and Lysates

SK-N-AS neuroblastoma and primary neuronal rat cells were seeded in 96-well plates at 10,000 cells/well and grown to confluence. To collect a 'Control' sample, supernatants were transferred to a microcentrifuge tube combining wells 3-10 of row B and C in one tube each, and centrifuged for 10 minutes at $3,716 \times g$; then the supernatant was transferred to a cryovial (leaving about 100 μL in the tube to avoid disturbing the pellet) and frozen at -80°C in a chest freezer. 200 μL /well of cell lysis buffer provided with the Caspase-3/7 kit (Anaspec; see Section 0 below) were added to the plate and it was incubated for one hour in the CO_2 incubator at 37°C with shaking once at about half-time. After the lysis was completed, the well contents were collected by first vigorously mixing the lysis buffer with the pipette and then transferring the entire contents to a microcentrifuge tube combining wells 3-10 of each row in one tube. After centrifugation for 10 minutes at $3,716 \times g$, the supernatant lysate was transferred to a cryovial (leaving about 100 μL in the tube to avoid disturbing the pellet) and frozen at -80°C in a chest freezer.

To induce necrosis, about half the area in each well of rows D and E was scraped with the tip of a pipette. After taking micrographs, the plate was incubated for one hour in the CO_2 incubator at 37°C . Then supernatants and lysates were collected as described above for the 'Control Treatment' samples.

To induce apoptosis, a UV lamp (UVG-54, UVP, LLC, Upland, CA, USA) that had been sterilized by wiping it down with 70% 2-propanol was positioned under sterile conditions about 7 cm above the plate without cover in a biosafety cabinet. The plate was irradiated for 10 minutes with 254 nm light, and then incubated for one hour in the CO_2 incubator at 37°C . Finally, supernatants and lysates were collected from rows F and G as described above for the 'Control Treatment' samples.

4.1.2.2. Caspase-3/-7 Assay

To confirm that the UV-irradiated cells were indeed undergoing apoptosis, the caspase-3/7 activity was assayed with the SensoLyte Homogeneous AMC Caspase-3/7 Assay Kit. The assay is based on the strongly increased fluorescence of 7-amino-4-methylcoumarin (AMC) upon cleavage from the assay substrate Ac-DEVD-AMC, which shows only a weak fluorescence (see Figure II-41); the substrate for both, caspase-3 and caspase-7 is the DEVD motif with cleavage occurring after the second D residue. It was performed as described in the manufacturer's instructions. Samples were prepared as described above (see Section 4.1.2.1), and 150 μL /well of samples and controls pipetted into a 96-well plate. The caspase-3/7 substrate solution was prepared with the reagents provided in the kit according to the manual. 50 μL /well of the substrate solution was added to the plate followed by mixing in the plate reader at 200 rpm for 60 seconds. Bubbles formed in the pipetting and mixing step were removed with a sterile inoculation needle. The measurement of the fluorescence signal was started immediately and read every five minutes for one hour with excitation at 360 nm and emission at 450 nm.

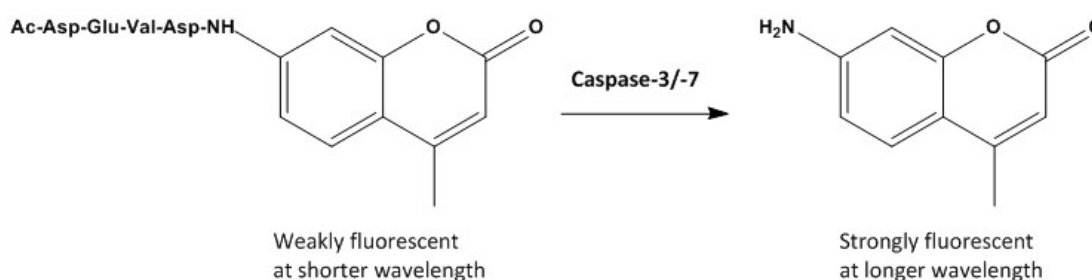


Figure II-41 Caspase-3/-7 assay principle.

The assay is based on the strongly increased fluorescence of 7-amino-4-methylcoumarin (AMC) upon cleavage from the assay substrate, Ac-DEVD-AMC, which shows only a weak fluorescence; the substrate for both caspase-3 and caspase-7 is the DEVD motif with cleavage occurring after the second D residue.

For data analysis, the fluorescence reading of cells with growth medium was subtracted from all other samples to obtain the relative fluorescence units (RFU). The range of initial time points during which the reaction is linear was determined and the initial reaction velocity, i.e., the slope of the linear portion in RFU/min was calculated.

4.1.2.3. Simulating the propagation of AD

After determining the caspase-3/-7 activity in the supernatant and lysate samples, new SK-N-AS neuroblastoma or primary neuronal rat cell cultures were prepared in 96-well plates as previously described. Cells were incubated with 20 μL of these samples (total volume: 200 μL /well), as well as A β alone (final concentration: 10 μM) and A β /GM1 mixtures (final concentrations: 10 μM A β /5 μM GM1) for about 24 hours. The A β species used were fluorescently labeled forms, HiLyteFluor™ 555-A β ₁₋₄₀ and FAM-Abeta₁₋₄₂, respectively, in order to allow distinction of A β added to the culture from A β produced by the cells. Again, supernatant and lysate samples were collected, and production of A β induced by incubation with apoptotic or necrotic supernatant and lysate, as well as A β and A β /GM₁ mixtures was quantified by ELISA as described in Section 2.7.3.3(b).

4.1.3. Results & Discussion

4.1.3.1. Apoptosis

Primary neuronal rat cells did not show significant increases in caspase-3/-7 activity in any of the samples (data not shown). This is possibly due to the considerably lower number of cells per well in these experiments (primary neuronal cells do not proliferate).

For SK-N-AS neuroblastoma cells, the results for the lysate samples were as expected; only the apoptotic sample showed strongly increased caspase activity with basically no activity in the necrotic or control sample. However, in the supernatant both the necrotic and the apoptotic sample showed an increased caspase-3/-7 activity, albeit not statistically significant when compared to the high background signal in the control (see Figure II-42).

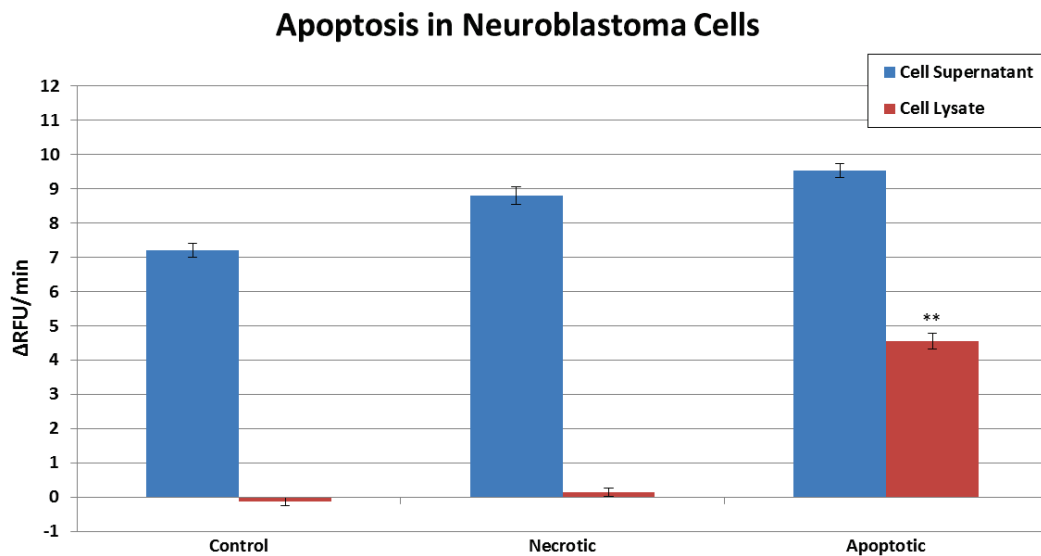


Figure II-42 Apoptosis in differently treated SK-N-AS neuroblastoma cells.

SK-N-AS neuroblastoma cells were treated to induce apoptosis and necrosis, respectively. Supernatants and lysates were harvested, and caspase-3/-7 activity was determined (for details see text). **: significantly different from 'Control'. Error Bars: \pm 95% confidence interval; *: $P < 0.05$; **: $P < 0.01$ ($n = 2$; one-tailed Student's t-test).

4.1.3.1. β -Amyloid production induced by apoptosis and necrosis

For the primary neuronal rat cells, all samples showed values smaller than the lowest standard (data not shown). Like in the case of the caspase-3/-7 assay, this is likely due to the considerably lower number of cells/well for the rat neurons.

Figure II-43 shows the results for A β production by SK-N-AS neuroblastoma cells in response to apoptosis and necrosis. The only sample that caused a statistically significant increased A β production was the lysate of cells treated with the supernatant of necrotic cells. These results imply that necrosis, but not apoptosis of one cell can induce intracellular A β production in a neighbouring cell, which could go on to kill that cell as well. This provides a mechanism for the spread of neuronal death in AD.

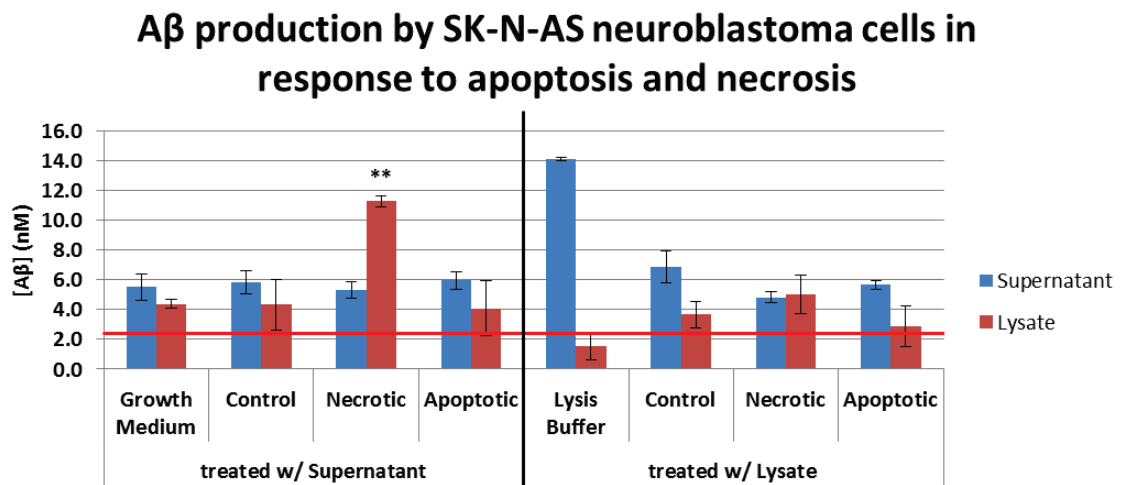


Figure II-43 A β production by SK-N-AS neuroblastoma cells in response to apoptosis and necrosis. Cells were incubated with the supernatants (left) and lysates (right) obtained from SK-N-AS cells cultures treated to induce apoptosis and necrosis, respectively. A β content of the supernatants (blue bars) and lysates (red bars) was determined by ELISA. The red line shows the concentration of the lowest A β standard (2.4 nM; nominally 2 nM). Error Bars: \pm S.E.M.; *: P < 0.05; **: P < 0.01 (n = 2; one-tailed Student's t-test).

Most cells in AD undergo apoptosis, while only a small number necrose. The proposition that necrosis but not apoptosis is responsible for the propagation of neuronal cell death in AD is well-supported here. It is through this mechanism that A β can form the first seeds to propagate the process — i.e., complexation with GM1, a neuronal membrane component that is released only via necrosis.

It has been shown here that one possible mechanism for the progressive nature of AD may be that necrotic death of one neuron spreads to neighbouring neurons by release of GM1 and/or A β . Spread to more than one neuron would result in a snowball effect causing an ever increasing number of lost neurons. In order to estimate how many neurons would have to die by necrosis and 'infect' a neighbouring neuron to cause the neuron losses seen in AD, a simple model was devised.

The number of neurons in the neocortex alone is estimated to be about 20 billion (301, 302), the average total number of neurons 100 billion (303). It has also been found that at gross examination, the Alzheimer's brain shows severe atrophy and a reduction in brain weight of usually more than 35 % (304). Neuron loss is estimated to contribute 20-30% of cerebral weight loss in individuals afflicted with AD (305, 306).

Assuming that all neurons are of equal mass, that only neurons are lost, that all neurons are equally susceptible, and that the 'spread rate' is constant, one may model the decrease of number of neurons according to Equation (II-5):

$$N_n = N_0 - r^n \quad \text{(II-5)}$$

with N_n as number of neurons remaining n years after loss of first neuron, N_0 as number of neurons at the onset of disease, and r as 'effective spread rate'.

For the following calculation it was assumed that the affected individual lost the first neuron at age 20 ($N_0 = 1 \times 10^{11}$), and succumbed to AD 60 years ($n = 60$) later at age 80. At that time he had lost 25% of his neurons ($N_n = N_0 \cdot (100\% - 25\%) = N_0 \cdot 0.75 = 7.5 \times 10^{10}$). Table II-9 and Figure II-44 show results obtained by fitting the data in Microsoft Excel® to Equation (II-5). The effective spread rate, r , was calculated to be 1.490/yr.

Table II-9 Simulated neuron loss in AD.

Years after loss of first neuron	# of neurons remaining	# of neurons lost
0	1.0000E+11	1
1	1.0000E+11	1.490
2	1.0000E+11	2.221
3	1.0000E+11	3.311
4	1.0000E+11	4.934
5	1.0000E+11	7.354
10	1.0000E+11	54.07
15	1.0000E+11	397.6
20	1.0000E+11	2924
25	1.0000E+11	2.1502E+04
30	1.0000E+11	1.5811E+05
35	9.9999E+10	1.1627E+06
40	9.9991E+10	8.5499E+06
45	9.9937E+10	6.2872E+07
50	9.9538E+10	4.6233E+08
55	9.6600E+10	3.3997E+09
60	7.5000E+10	2.5000E+10

Simulated Neuronal Loss in AD

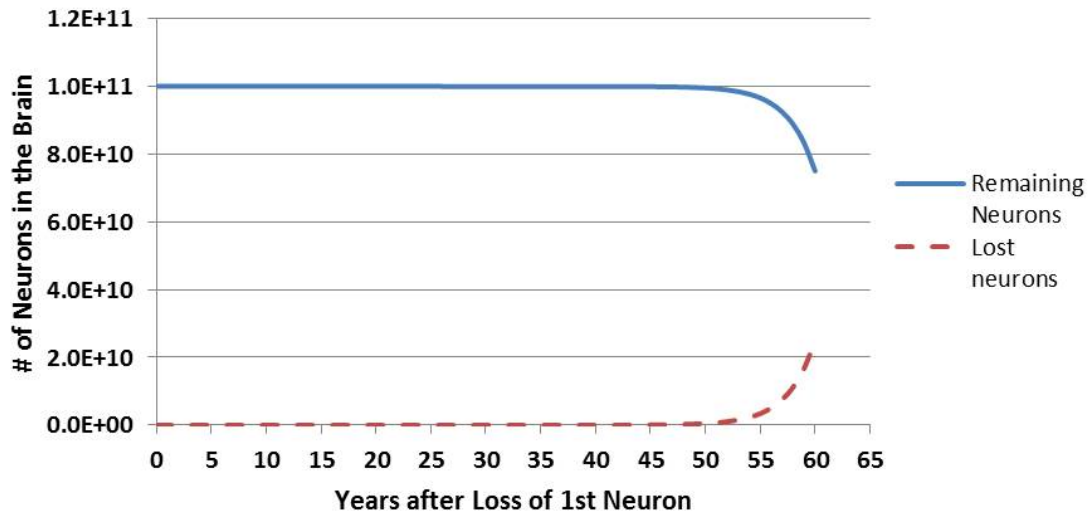


Figure II-44 Simulated neuronal loss in AD.

The neuronal loss seen in AD was modelled by Equation (II-5) to demonstrate how a small effective spread rate (rooted in necrotic neuronal cell death) is sufficient to cause extensive damage over the course of decades now recognised as probable time frame for the development of (late onset) AD. For details see text.

Based on the above assumptions, necrotic cell death needs to spread from one neuron only to 1.490 other neurons over the span of an entire year to lead to the massive neuronal losses seen in AD. To further put this into perspective, each neuron is surrounded by hundreds of neurons and connected to about seven thousand other neurons via its synapses (307). In normal aging, the average loss of neocortical neurons between ages 20 – 90 has been estimated at about 10%, which amounts to about 85,000 per day, approximately 1 per second (302) (= 31 million per year). This estimate may also explain why the influence of necrosis on AD has been neglected in favour of apoptosis so far in the literature.

To further delineate the role of GM₁ in the spread of cell death caused by Aβ, SK-N-AS neuroblastoma cells were incubated with Aβ alone and Aβ/GM₁ mixtures, and intracellular Aβ production was determined by ELISA (Figure II-45). This experiment was performed only with the neuroblastoma cells since neither the caspase-3/-7 assay nor the treatment with apoptotic and necrotic samples had yielded appreciable signals for the primary rat neurons.

Results show that only Aβ₁₋₄₂/GM₁ caused an increased Aβ production compared to incubation with Aβ alone, but not Aβ₁₋₄₀/GM₁. The intended purpose for using fluorescently labeled forms of Aβ, HiLyteFluor™ 555-Aβ₁₋₄₀ and FAM-Aβ₁₋₄₂, respectively, was to allow distinction of Aβ added to the culture from Aβ produced by the cells. However, problems with the calibration curves led to a failure of this part of the experiment.

These results imply that only incubation with Aβ₁₋₄₂ (the most toxic Aβ isoform) complexed with GM₁ is able to induce a production increase of Aβ by exposed cells, thus providing evidence for another route for Aβ₁₋₄₂ to exert its toxicity.

A β production by neuroblastoma cells induced by incubation with A β & GM₁/A β

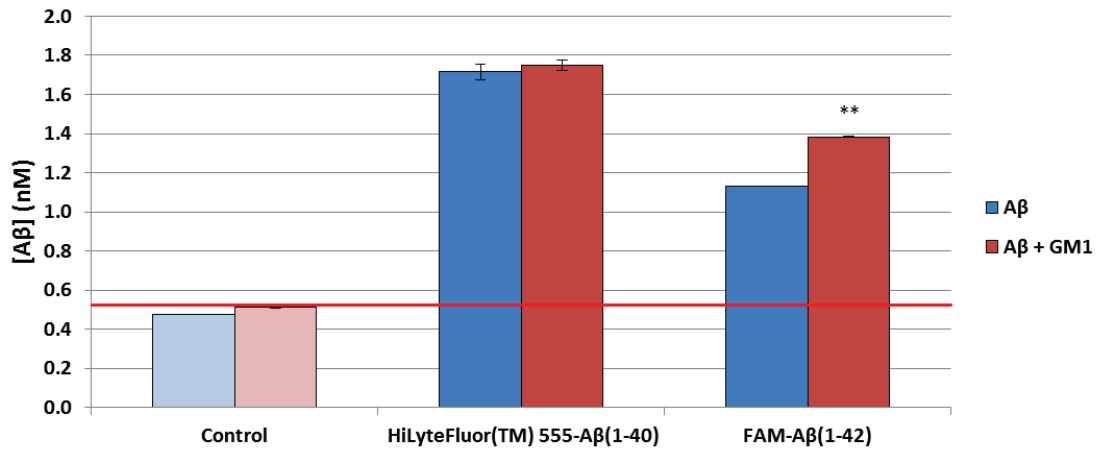


Figure II-45 A β production by SK-N-AS neuroblastoma cells induced by incubation with GM₁ and GM₁/A β .

Cells were incubated with fluorescently labeled A β ₁₋₄₀ and A β ₁₋₄₂ in the absence (blue bars) and presence (red bars) of GM₁. A β content of the lysates was determined by ELISA. Controls were PBS buffer (blue) and GM₁+PBS buffer (red). The red line shows the back-calculated concentration of the lowest standard (0.52 nM; nominally 0.5 nM). Error Bars: \pm S.E.M.; *: P < 0.05; **: P < 0.01 (for comparing samples with and without GM₁; n = 2; one-tailed Student's t-test).

A β may also influence the brain's recovery process in a threatened/'attacked' situation.

Neuron loss is estimated to contribute 20-30% of cerebral weight loss in individuals afflicted with AD (305, 306). For quite some time it was thought that neuronal renewal (or neurogenesis) ceases with the end of embryonic development; however, current research has found that at least two areas of the adult CNS continuously produce new neuronal and glial cells (308-310). Evidence from AD animal models suggests that impaired neurogenesis in these areas may be at least partially responsible for progressive memory loss and reduced capability for learning and processing of new information so characteristic of AD (311). Newly formed neurons have been implicated in the strengthening of memory circuits related to new stimuli (312, 313). Many studies have found that A β ₁₋₄₂ seems to compromise the survival and differentiation of

progenitor cells, although there is some variability in the results reported in the literature, possibly owing to differences in A β preparation (314-318).

Based on this evidence it may be plausible to hypothesise that A β , and in particular A β_{1-42} , is (at least partially) responsible for the chronicity of AD by first killing neurons and then preventing recovery by impairing neurogenesis.

4.2. Summary

Experimental evidence presented here provides insights into a possible mechanism responsible for the progressive nature of AD. Although most research implicates apoptosis in AD, and in most cases, neurons attacked and damaged by A β *do* undergo apoptosis (319), this concept lacks the supportive mechanistic drive for the process. Here, it is shown that it is the process and products of necrosis, which actually lead to the propagation of neuronal cell death that characterises the disease. Neurons damaged through necrosis release the ganglioside GM $_1$ which complexes with A β_{1-42} , creating the first seeds of toxic A β species that can lead to the death of neighbouring neurons. A simple model of neuron loss in AD was devised demonstrating how a small effective spread rate (rooted in necrotic neuronal cell death) is sufficient to cause extensive damage over the course of decades now recognised as probable time frame for the development of AD. This is the first time a clear mechanism of propagation has been put forth.

Additionally, as A β_{1-42} impairs neurogenesis, it prevents the brain's recovery from the insult of A β thus causing the well-described progression in AD. Since necrosis (primary or secondary) occurs in only a low percentage of attacked neurons, spread of the disease is slow, making the process a chronic one.

5. How it all fits together

To date, no truly comprehensive theory of Alzheimer's disease has been developed. The experimental evidence obtained in this project challenges our current thinking of AD and allows for the creation of a new model and thus a new comprehensive theory with which to explain the complex aetiology and pathogenesis of Alzheimer's Disease.

5.1. AD is an autoimmune disease of the innate immune system

5.1.1. What is an autoimmune disease?

Autoimmune diseases are classically defined as organ- or tissue-specific disorders that are the result of multi-factorial processes involving dysregulation of the adaptive immune system leading to an attack of the immune system against the body's own tissue (320). They are typically chronic and often characterised by debilitating, and life-threatening symptoms that aggravate as the disease progresses. According to the most recent version of *Witebsky's postulates*, first formulated by Ernst Witebsky *et al.* in 1957 (321), a disease can be considered an autoimmune disease if there is direct evidence from transfer of pathogenic T cells or pathogenic antibodies; or if indirect evidence is provided by reproduction in animal models; or based on circumstantial evidence from clinical clues (322). Distinct mechanisms that silence self-reactive cells of the adaptive immune system have evolved to avoid the development of autoimmune diseases.

5.1.2. An autoimmune disease of the innate immune system?

To date, there has been no autoimmune disease described in the literature that is caused by an AMP, i.e., an effector molecule of the innate immune system. Evidence obtained for this thesis, however, points to a role of A β , the central molecule of AD, as an AMP in the brain and provides a process by which this AMP can propagate neuronal cell death, a hallmark of AD. Here, the antimicrobial activity of A β against both bacteria and viruses was demonstrated; another research group has shown activity against both bacteria and fungi (215). The antibacterial activity of A β is thought to be at the root of its neurotoxicity — through the similarities of bacterial and neuronal cells in regards to membrane composition and the transmembrane potential, A β leads a misdirected attack on neurons instead of invading microorganisms. Stated differently, a part of the immune system leads a misdirected attack against “self” cells, resulting in inflammation and ultimately destruction of the wrongly targeted tissue.

Because of the many similarities of AD to other conventional autoimmune diseases, and because of the increasingly recognised interconnections between the innate and acquired immune systems, it is suggested here, that the definition for autoimmune diseases should be expanded to allow inclusion of effectors of the innate immune system such as AMPs in addition to effectors of the acquired immune system as for example antibodies.

5.2. The Vicious Cycle of Alzheimer's Disease

5.2.1. A mechanism for the propagation of cell death in AD

Evidence gathered for this thesis suggests a cyclical rather than linear mechanism as the cause for AD. Accordingly, the Vicious Cycle of AD (see Figure II-46) was developed to replace the (linear) amyloid cascade hypothesis.

Necrosis, with its uncontrolled spillage of membrane fragments and cell contents, was identified as the mechanism likely responsible for the spread of cell death. This is not to suggest that apoptosis is not involved in AD, however, since apoptosis keeps potentially harmful cell contents contained (thus reducing inflammation), it is, according to the data obtained here, not involved in the *propagation* of cell death to neighbouring neurons.

Entry into the vicious cycle occurs, when neuronal trauma-induced necrosis or infection leads to the release of damage-associated molecular patterns (DAMPs) or pathogen-associated molecular patterns (PAMPs), respectively. The intracellular production of A β (being an AMP and innate immune system effector) is upregulated in response to this insult. Upon excretion of A β , it binds to GM1 present in the membrane or released during necrosis resulting in the formation of toxic A β oligomers. These toxic oligomers, acting as AMP, can either kill microorganisms that are at the root of the infection, or cause damage to the membrane and ultimately necrosis of the neuronal cell. Either pathway completes the cycle to form a positive (self-enhancing) feedback loop, the *Vicious Cycle of Alzheimer's Disease*.

The Vicious Cycle of AD

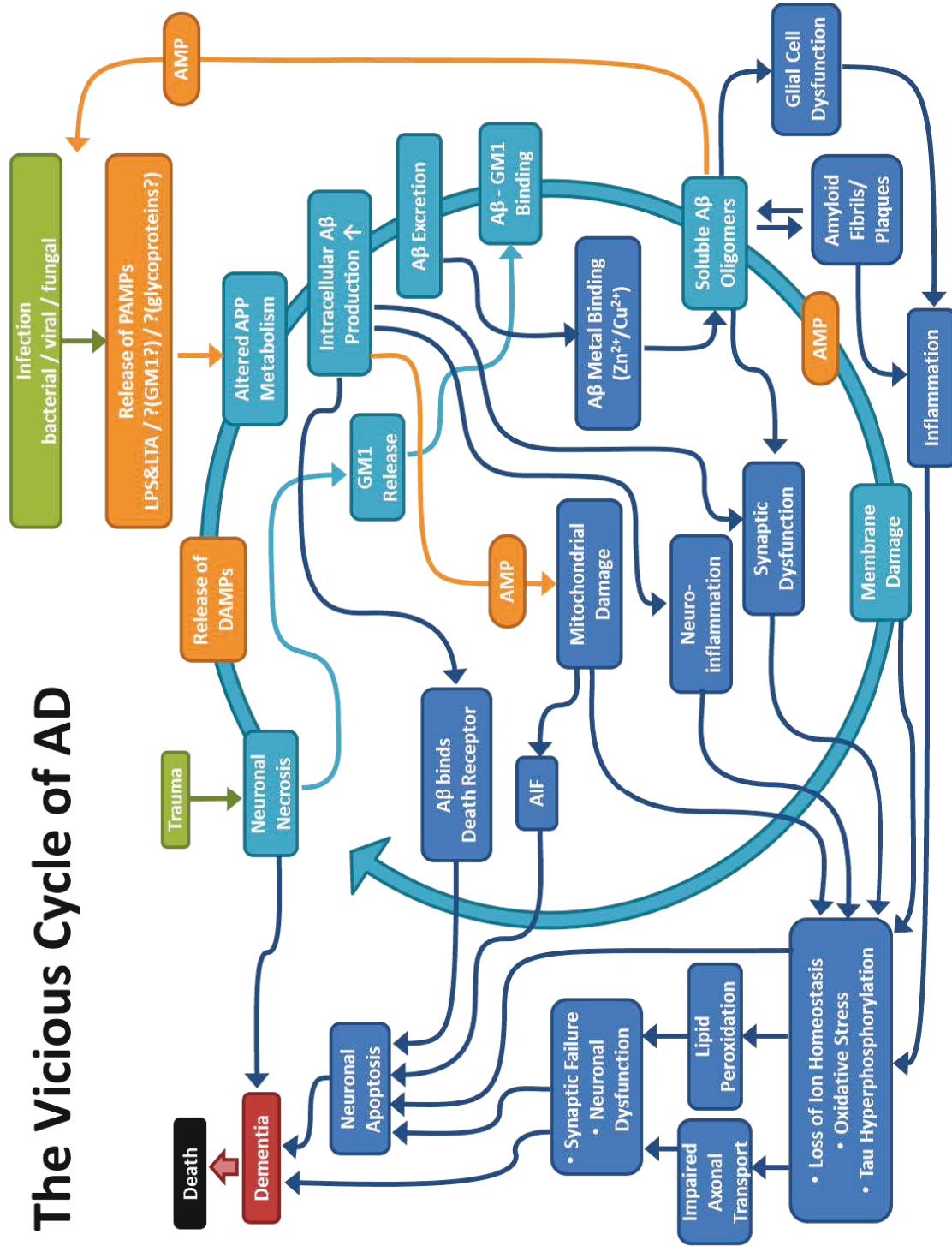


Figure II-46 The Vicious Cycle of Alzheimer’s Disease.

The Vicious Cycle of AD replaces the amyloid cascade hypothesis (for details see text). DAMPs/PAMPs: damage-/pathogen-associated molecular patterns; LPS: lipopolysaccharide; LTA: lipoteichoic acid; GM1: monosialoganglioside 1; AMP: antimicrobial peptide; APP: amyloid precursor protein; Aβ: beta-amyloid peptide; AIF: apoptosis-inducing factor. Green: original insult leading to cycle entry; orange: involvement of the innate immune system; light blue: vicious cycle responsible for the propagation of neuronal cell death; dark blue: other processes involved in AD; red/black: clinical manifestation and end result of AD.

5.3. Addressing gaps in current AD hypotheses

In Chapter I, a number of questions arising from gaps in current AD hypotheses were posed (Chapter I, Section 1.5.3). With the knowledge gained here it is now possible to address them.

1. What is the underlying physiologic role of A β ?

A β is an antimicrobial peptide and an effector of the innate immune system.

2. Why would A β attack neurons?

The similarity of neuronal and bacterial cells in terms of membrane composition and transmembrane potential leads to the misdirected attack of A β on neurons.

3. Why does AD get worse over time?

The breakdown products from necrotic neurons induce production of A β which in turn may kill more neurons. A β also impairs neurogenesis thus preventing repair of the damage it already caused.

4. Why is AD chronic?

The low percentage of cell death by necrosis makes the process slow.

5. How is it all connected?

Neuronal trauma or brain infection are the entry points into a vicious cycle.

Neuronal necrosis or microbial activators of the innate immune system induce A β production that leads to formation of toxic A β oligomers, which may cause necrosis in neighbouring neurons, thus creating the *Vicious Cycle of Alzheimer's Disease*.

5.4. Summary

Here, new evidence has been combined with the work of many different research groups in an attempt to explain the complex underlying processes of Alzheimer's disease and the very nature of its existence. The Vicious Cycle of AD, borne from the concept of Alzheimer's disease as an autoimmune disease of the innate immune system explains many of the underlying questions of A β 's role, why it attacks neurons and links the progressive and chronic nature with a more comprehensive self-perpetuating mechanism.

6. Conclusions

Alzheimer's disease is a chronic progressive condition. Attempts to understand its underlying mechanisms have only been able to detail smaller components of the process without tying all aspects together. AD cannot be explained by a simple linear model like the β -amyloid cascade.

This work integrates new experimental evidence with research and data from many research groups across many branches of science to challenge our previous thinking of AD. Traditionally, AD was considered a type of protein folding disorder. Here, it is proposed that AD is actually an autoimmune disease — one of the innate immune system, based on experimental evidence in support of each of the aspects of this novel idea. Such a concept has never before been proposed in AD, nor has such a concept been proposed for AMPs. The *Vicious Cycle of Alzheimer's Disease* is put forward as a mechanism accounting for the previously unexplained progression and chronicity of the disease.

This work has the potential to open whole new areas of research into Alzheimer's disease that were previously never considered.

7. References

1. Tosi, M. F. Innate immune responses to infection. *J. Allergy Clin. Immunol.* **2005**, *116*, 241-9; quiz 250.
2. Pancer, Z.; Cooper, M. D. The evolution of adaptive immunity. *Annu. Rev. Immunol.* **2006**, *24*, 497-518.
3. Iwasaki, A.; Medzhitov, R. Regulation of adaptive immunity by the innate immune system. *Science* **2010**, *327*, 291-295.
4. Schenten, D.; Medzhitov, R. The control of adaptive immune responses by the innate immune system. *Adv. Immunol.* **2011**, *109*, 87-124.
5. National Library of Medicine Autoimmune Diseases. http://www.nlm.nih.gov/cgi/mesh/2011/MB_cgi?mode=&term=Autoimmune+Diseases (accessed 02/10, 2014).
6. Akira, S.; Uematsu, S.; Takeuchi, O. Pathogen Recognition and Innate Immunity. *Cell* **2006**, *124*, 783-801.
7. Hancock, R. E.; Scott, M. G. The role of antimicrobial peptides in animal defenses. *Proc. Natl. Acad. Sci. U. S. A.* **2000**, *97*, 8856-8861.
8. Yoshio, H.; Lagercrantz, H.; Gudmundsson, G. H.; Agerberth, B. First line of defense in early human life. *Semin. Perinatol.* **2004**, *28*, 304-311.
9. Turvey, S. E.; Broide, D. H. Innate immunity. *J. Allergy Clin. Immunol.* **2010**, *125*, S24-32.
10. Beutler, B. Innate immunity: an overview. *Mol. Immunol.* **2004**, *40*, 845-859.
11. Nonaka, M.; Yoshizaki, F. Evolution of the complement system. *Mol. Immunol.* **2004**, *40*, 897-902.
12. Trouw, L. A.; Daha, M. R. Role of complement in innate immunity and host defense. *Immunol. Lett.* **2011**, *138*, 35-37.
13. Braff, M. H.; Bardan, A.; Nizet, V.; Gallo, R. L. Cutaneous defense mechanisms by antimicrobial peptides. *J. Invest. Dermatol.* **2005**, *125*, 9-13.

14. Bulet, P.; Stocklin, R.; Menin, L. Anti-microbial peptides: from invertebrates to vertebrates. *Immunol. Rev.* **2004**, *198*, 169-184.
15. De Smet, K.; Contreras, R. Human antimicrobial peptides: defensins, cathelicidins and histatins. *Biotechnol. Lett.* **2005**, *27*, 1337-1347.
16. Jenssen, H.; Hamill, P.; Hancock, R. E. Peptide antimicrobial agents. *Clin. Microbiol. Rev.* **2006**, *19*, 491-511.
17. Durr, M.; Peschel, A. Chemokines meet defensins: the merging concepts of chemoattractants and antimicrobial peptides in host defense. *Infect. Immun.* **2002**, *70*, 6515-6517.
18. Kamysz, W.; Okroj, M.; Lukasiak, J. Novel properties of antimicrobial peptides. *Acta Biochim. Pol.* **2003**, *50*, 461-469.
19. Barlow, P. G.; Li, Y.; Wilkinson, T. S.; Bowdish, D. M.; Lau, Y. E.; Cosseau, C.; Haslett, C.; Simpson, A. J.; Hancock, R. E.; Davidson, D. J. The human cationic host defense peptide LL-37 mediates contrasting effects on apoptotic pathways in different primary cells of the innate immune system. *J. Leukoc. Biol.* **2006**, *80*, 509-520.
20. Bowdish, D. M.; Davidson, D. J.; Hancock, R. E. A re-evaluation of the role of host defence peptides in mammalian immunity. *Curr. Protein Pept. Sci.* **2005**, *6*, 35-51.
21. Beisswenger, C.; Bals, R. Functions of antimicrobial peptides in host defense and immunity. *Curr. Protein Pept. Sci.* **2005**, *6*, 255-264.
22. Oppenheim, J. J.; Biragyn, A.; Kwak, L. W.; Yang, D. Roles of antimicrobial peptides such as defensins in innate and adaptive immunity. *Ann. Rheum. Dis.* **2003**, *62 Suppl 2*, ii17-21.
23. Brown, K. L.; Hancock, R. E. Cationic host defense (antimicrobial) peptides. *Curr. Opin. Immunol.* **2006**, *18*, 24-30.
24. Iwasaki, A.; Medzhitov, R. Toll-like receptor control of the adaptive immune responses. *Nat. Immunol.* **2004**, *5*, 987-995.
25. Shanker, A. Adaptive control of innate immunity. *Immunol. Lett.* **2010**, *131*, 107-112.
26. Zhao, J.; Yang, X.; Auh, S. L.; Kim, K. D.; Tang, H.; Fu, Y. Do adaptive immune cells suppress or activate innate immunity? *Trends Immunol.* **2009**, *30*, 8-12.
27. Kabelitz, D.; Medzhitov, R. Innate immunity — cross-talk with adaptive immunity through pattern recognition receptors and cytokines. *Curr. Opin. Immunol.* **2007**, *19*, 1-3.

28. Abdelsadik, A.; Trad, A. Toll-like receptors on the fork roads between innate and adaptive immunity. *Hum. Immunol.* **2011**, *72*, 1188-1193.
29. McGonagle, D.; Savic, S.; McDermott, M. The NLR network and the immunological disease continuum of adaptive and innate immune-mediated inflammation against self. *Seminars in Immunopathology* **2007**, *29*, 303-313.
30. Goldstein, D. R. Toll-like receptors and other links between innate and acquired alloimmunity. *Curr. Opin. Immunol.* **2004**, *16*, 538-544.
31. Kawai, T.; Akira, S. The role of pattern-recognition receptors in innate immunity: update on Toll-like receptors. *Nat. Immunol.* **2010**, *11*, 373-384.
32. O'Neill, L. Specificity in the innate response: pathogen recognition by Toll-like receptor combinations. *Trends Immunol.* **2001**, *22*, 70.
33. Akira, S.; Takeda, K.; Kaisho, T. Toll-like receptors: critical proteins linking innate and acquired immunity. *Nat. Immunol.* **2001**, *2*, 675.
34. Janeway, C. A., Jr; Medzhitov, R. Innate immune recognition. *Annu. Rev. Immunol.* **2002**, *20*, 197-216.
35. Theofilopoulos, A. N.; Baccala, R.; Beutler, B.; Kono, D. H. Type I interferons (alpha/beta) in immunity and autoimmunity. *Annu. Rev. Immunol.* **2005**, *23*, 307-336.
36. Takeda, K.; Akira, S. Toll-like receptors in innate immunity. *Int. Immunol.* **2005**, *17*, 1-14.
37. Takeda, K.; Kaisho, T.; Akira, S. Toll-like receptors. *Annu. Rev. Immunol.* **2003**, *21*, 335-376.
38. Creagh, E. M.; O'Neill, L. A. J. TLRs, NLRs and RLRs: a trinity of pathogen sensors that cooperate in innate immunity. *Trends Immunol.* **2006**, *27*, 352-357.
39. Newton, K.; Dixit, V. M. Signaling in innate immunity and inflammation. *Cold Spring Harb Perspect. Biol.* **2012**, *4*, 10.1101/cshperspect.a006049.
40. Medzhitov, R.; Preston-Hurlburt, P.; Janeway, C. A., Jr A human homologue of the *Drosophila* Toll protein signals activation of adaptive immunity. *Nature* **1997**, *388*, 394-397.
41. Rock, F. L.; Hardiman, G.; Timans, J. C.; Kastelein, R. A.; Bazan, J. F. A family of human receptors structurally related to *Drosophila* Toll. *Proc. Natl. Acad. Sci. U. S. A.* **1998**, *95*, 588-593.
42. Kumar, H.; Kawai, T.; Akira, S. Toll-like receptors and innate immunity. *Biochem. Biophys. Res. Commun.* **2009**, *388*, 621-625.

43. Onoguchi, K.; Yoneyama, M.; Fujita, T. Retinoic acid-inducible gene-I-like receptors. *J. Interferon Cytokine Res.* **2011**, *31*, 27-31.
44. Yoneyama, M.; Fujita, T. Structural Mechanism of RNA Recognition by the RIG-I-like Receptors. *Immunity* **2008**, *29*, 178-181.
45. Li, X.; Lu, C.; Stewart, M.; Xu, H.; Strong, R. K.; Igumenova, T.; Li, P. Structural basis of double-stranded RNA recognition by the RIG-I like receptor MDA5. *Arch. Biochem. Biophys.* **2009**, *488*, 23-33.
46. Li, X.; Ranjith-Kumar, C. T.; Brooks, M. T.; Dharmiah, S.; Herr, A. B.; Kao, C.; Li, P. The RIG-I-like Receptor LGP2 Recognizes the Termini of Double-stranded RNA. *Journal of Biological Chemistry* **2009**, *284*, 13881-13891.
47. Takahashi, K.; Kumeta, H.; Tsuduki, N.; Narita, R.; Shigemoto, T.; Hirai, R.; Yoneyama, M.; Horiuchi, M.; Ogura, K.; Fujita, T.; Inagaki, F. Solution Structures of Cytosolic RNA Sensor MDA5 and LGP2 C-terminal Domains: Identification of the RNA Recognition Loop in RIG-I-like Receptors. *Journal of Biological Chemistry* **2009**, *284*, 17465-17474.
48. Ting, J. P. -.; Lovering, R. C.; Alnemri, E. S.; Bertin, J.; Boss, J. M.; Davis, B. K.; Flavell, R. A.; Girardin, S. E.; Godzik, A.; Harton, J. A.; Hoffman, H. M.; Hugot, J.; Inohara, N.; MacKenzie, A.; Maltais, L. J.; Nunez, G.; Ogura, Y.; Otten, L. A.; Philpott, D.; Reed, J. C.; Reith, W.; Schreiber, S.; Steimle, V.; Ward, P. A. The NLR Gene Family: A Standard Nomenclature. *Immunity* **2008**, *28*, 285-287.
49. Shaw, M. H.; Reimer, T.; Kim, Y.; Nuñez, G. NOD-like receptors (NLRs): bona fide intracellular microbial sensors. *Curr. Opin. Immunol.* **2008**, *20*, 377-382.
50. Franchi, L.; Warner, N.; Viani, K.; Nunez, G. Function of Nod-like receptors in microbial recognition and host defense. *Immunol. Rev.* **2009**, *227*, 106-128.
51. Greenberg, J. W.; Fischer, W.; Joiner, K. A. Influence of lipoteichoic acid structure on recognition by the macrophage scavenger receptor. *Infect. Immun.* **1996**, *64*, 3318-3325.
52. Fischer, W. Pneumococcal lipoteichoic and teichoic acid. *Microb. Drug Resist.* **1997**, *3*, 309-325.
53. Xia, G.; Kohler, T.; Peschel, A. The wall teichoic acid and lipoteichoic acid polymers of *Staphylococcus aureus*. *International Journal of Medical Microbiology* **2010**, *300*, 148-154.
54. Schmidt, R. R.; Pedersen, C. M.; Qiao, Y.; Zahring, U. Chemical synthesis of bacterial lipoteichoic acids: an insight on its biological significance. *Org. Biomol. Chem.* **2011**, *9*, 2040-2052.

55. Erridge, C.; Bennett-Guerrero, E.; Poxton, I. R. Structure and function of lipopolysaccharides. *Microb. Infect.* **2002**, *4*, 837-851.
56. Raetz, C. R.; Whitfield, C. Lipopolysaccharide endotoxins. *Annu. Rev. Biochem.* **2002**, *71*, 635-700.
57. Caroff, M.; Karibian, D. Structure of bacterial lipopolysaccharides. *Carbohydr. Res.* **2003**, *338*, 2431-2447.
58. Ozinsky, A.; Underhill, D. M.; Fontenot, J. D.; Hajjar, A. M.; Smith, K. D.; Wilson, C. B.; Schroeder, L.; Aderem, A. The repertoire for pattern recognition of pathogens by the innate immune system is defined by cooperation between toll-like receptors. *Proc. Natl. Acad. Sci. U. S. A.* **2000**, *97*, 13766-13771.
59. Takeuchi, O.; Hoshino, K.; Kawai, T.; Sanjo, H.; Takada, H.; Ogawa, T.; Takeda, K.; Akira, S. Differential roles of TLR2 and TLR4 in recognition of gram-negative and gram-positive bacterial cell wall components. *Immunity* **1999**, *11*, 443-451.
60. Takeuchi, O.; Hoshino, K.; Akira, S. TLR2-deficient and MyD88-deficient mice are highly susceptible to *Staphylococcus aureus* infection. *J. Immunol.* **2000**, *165*, 5392-5396.
61. Yoshimura, A.; Lien, E.; Ingalls, R. R.; Tuomanen, E.; Dziarski, R.; Golenbock, D. Recognition of Gram-positive bacterial cell wall components by the innate immune system occurs via Toll-like receptor 2. *J. Immunol.* **1999**, *163*, 1-5.
62. Ulevitch, R. J.; Tobias, P. S. Recognition of Gram-negative bacteria and endotoxin by the innate immune system. *Curr. Opin. Immunol.* **1999**, *11*, 19-22.
63. Shimazu, R.; Akashi, S.; Ogata, H.; Nagai, Y.; Fukudome, K.; Miyake, K.; Kimoto, M. MD-2, a molecule that confers lipopolysaccharide responsiveness on Toll-like receptor 4. *J. Exp. Med.* **1999**, *189*, 1777-1782.
64. Alexopoulou, L.; Holt, A. C.; Medzhitov, R.; Flavell, R. A. Recognition of double-stranded RNA and activation of NF-kappaB by Toll-like receptor 3. *Nature* **2001**, *413*, 732-738.
65. Takeuchi, O.; Kawai, T.; Muhlradt, P. F.; Morr, M.; Radolf, J. D.; Zychlinsky, A.; Takeda, K.; Akira, S. Discrimination of bacterial lipoproteins by Toll-like receptor 6. *Int. Immunol.* **2001**, *13*, 933-940.
66. Yamamoto, M.; Sato, S.; Mori, K.; Hoshino, K.; Takeuchi, O.; Takeda, K.; Akira, S. Cutting edge: a novel Toll/IL-1 receptor domain-containing adapter that preferentially activates the IFN-beta promoter in the Toll-like receptor signaling. *J. Immunol.* **2002**, *169*, 6668-6672.

67. Takeuchi, O.; Sato, S.; Horiuchi, T.; Hoshino, K.; Takeda, K.; Dong, Z.; Modlin, R. L.; Akira, S. Cutting edge: role of Toll-like receptor 1 in mediating immune response to microbial lipoproteins. *J. Immunol.* **2002**, *169*, 10-14.
68. Tobias, P. S.; Soldau, K.; Ulevitch, R. J. Isolation of a lipopolysaccharide-binding acute phase reactant from rabbit serum. *J. Exp. Med.* **1986**, *164*, 777-793.
69. Schumann, R. R.; Leong, S. R.; Flaggs, G. W.; Gray, P. W.; Wright, S. D.; Mathison, J. C.; Tobias, P. S.; Ulevitch, R. J. Structure and function of lipopolysaccharide binding protein. *Science* **1990**, *249*, 1429-1431.
70. Wright, S. D.; Tobias, P. S.; Ulevitch, R. J.; Ramos, R. A. Lipopolysaccharide (LPS) binding protein opsonizes LPS-bearing particles for recognition by a novel receptor on macrophages. *J. Exp. Med.* **1989**, *170*, 1231-1241.
71. Wright, S. D.; Ramos, R. A.; Tobias, P. S.; Ulevitch, R. J.; Mathison, J. C. CD14, a receptor for complexes of lipopolysaccharide (LPS) and LPS binding protein. *Science* **1990**, *249*, 1431-1433.
72. Miyake, K. Innate recognition of lipopolysaccharide by CD14 and toll-like receptor 4-MD-2: unique roles for MD-2. *Int. Immunopharmacol.* **2003**, *3*, 119-128.
73. Jiang, Q.; Akashi, S.; Miyake, K.; Petty, H. R. Lipopolysaccharide induces physical proximity between CD14 and toll-like receptor 4 (TLR4) prior to nuclear translocation of NF-kappa B. *J. Immunol.* **2000**, *165*, 3541-3544.
74. Akashi, S.; Saitoh, S.; Wakabayashi, Y.; Kikuchi, T.; Takamura, N.; Nagai, Y.; Kusumoto, Y.; Fukase, K.; Kusumoto, S.; Adachi, Y.; Kosugi, A.; Miyake, K. Lipopolysaccharide interaction with cell surface Toll-like receptor 4-MD-2: higher affinity than that with MD-2 or CD14. *J. Exp. Med.* **2003**, *198*, 1035-1042.
75. Fitzgerald, K. A.; Rowe, D. C.; Golenbock, D. T. Endotoxin recognition and signal transduction by the TLR4/MD2-complex. *Microbes Infect.* **2004**, *6*, 1361-1367.
76. Kawai, T.; Akira, S. Innate immune recognition of viral infection. *Nat. Immunol.* **2006**, *7*, 131-137.
77. Saito, T.; Gale Jr, M. Principles of intracellular viral recognition. *Curr. Opin. Immunol.* **2007**, *19*, 17-23.
78. Hartmann, T.; Bieger, S. C.; Bruhl, B.; Tienari, P. J.; Ida, N.; Allsop, D.; Roberts, G. W.; Masters, C. L.; Dotti, C. G.; Unsicker, K.; Beyreuther, K. Distinct sites of intracellular production for Alzheimer's disease A beta40/42 amyloid peptides. *Nat. Med.* **1997**, *3*, 1016-1020.

79. Sorensen, O. E.; Thapa, D. R.; Roupe, K. M.; Valore, E. V.; Sjobring, U.; Roberts, A. A.; Schmidtchen, A.; Ganz, T. Injury-induced innate immune response in human skin mediated by transactivation of the epidermal growth factor receptor. *J. Clin. Invest.* **2006**, *116*, 1878-1885.
80. Tahara, K.; Kim, H. D.; Jin, J. J.; Maxwell, J. A.; Li, L.; Fukuchi, K. Role of toll-like receptor signalling in Abeta uptake and clearance. *Brain* **2006**, *129*, 3006-3019.
81. Stewart, C. R.; Stuart, L. M.; Wilkinson, K.; van Gils, J. M.; Deng, J.; Halle, A.; Rayner, K. J.; Boyer, L.; Zhong, R.; Frazier, W. A.; Lacy-Hulbert, A.; El Khoury, J.; Golenbock, D. T.; Moore, K. J. CD36 ligands promote sterile inflammation through assembly of a Toll-like receptor 4 and 6 heterodimer. *Nat. Immunol.* **2010**, *11*, 155-161.
82. El Khoury, J. B.; Moore, K. J.; Means, T. K.; Leung, J.; Terada, K.; Toft, M.; Freeman, M. W.; Luster, A. D. CD36 mediates the innate host response to beta-amyloid. *J. Exp. Med.* **2003**, *197*, 1657-1666.
83. Moore, K. J.; El Khoury, J.; Medeiros, L. A.; Terada, K.; Geula, C.; Luster, A. D.; Freeman, M. W. A CD36-initiated signaling cascade mediates inflammatory effects of beta-amyloid. *Biol. Chem.* **2002**, *277*, 47373-47379.
84. Andreu, D.; Rivas, L. Animal antimicrobial peptides: an overview. *Biopolymers* **1998**, *47*, 415-433.
85. Huttner, K. M.; Bevins, C. L. Antimicrobial peptides as mediators of epithelial host defense. *Pediatr. Res.* **1999**, *45*, 785-794.
86. Devine, D. A.; Hancock, R. E. Cationic peptides: distribution and mechanisms of resistance. *Curr. Pharm. Des.* **2002**, *8*, 703-714.
87. Bowdish, D. M.; Davidson, D. J.; Scott, M. G.; Hancock, R. E. Immunomodulatory activities of small host defense peptides. *Antimicrob. Agents Chemother.* **2005**, *49*, 1727-1732.
88. Steinstraesser, L.; Kraneburg, U.; Jacobsen, F.; Al-Benna, S. Host defense peptides and their antimicrobial-immunomodulatory duality. *Immunobiology* **2011**, *216*, 322-333.
89. Bowdish, D. M.; Davidson, D. J.; Hancock, R. E. Immunomodulatory properties of defensins and cathelicidins. *Curr. Top. Microbiol. Immunol.* **2006**, *306*, 27-66.
90. Kolls, J. K.; McCray, P. B., Jr; Chan, Y. R. Cytokine-mediated regulation of antimicrobial proteins. *Nat. Rev. Immunol.* **2008**, *8*, 829-835.
91. Hancock, R. E. Cationic peptides: effectors in innate immunity and novel antimicrobials. *Lancet Infect. Dis.* **2001**, *1*, 156-164.

92. Hancock, R. E.; Diamond, G. The role of cationic antimicrobial peptides in innate host defences. *Trends Microbiol.* **2000**, *8*, 402-410.
93. Legrand, D.; Mazurier, J. A critical review of the roles of host lactoferrin in immunity. *Biometals* **2010**, *23*, 365-376.
94. Bowdish, D. M.; Davidson, D. J.; Lau, Y. E.; Lee, K.; Scott, M. G.; Hancock, R. E. Impact of LL-37 on anti-infective immunity. *J. Leukoc. Biol.* **2005**, *77*, 451-459.
95. Braff, M. H.; Gallo, R. L. Antimicrobial peptides: an essential component of the skin defensive barrier. *Curr. Top. Microbiol. Immunol.* **2006**, *306*, 91-110.
96. Bals, R.; Wilson, J. M. Cathelicidins--a family of multifunctional antimicrobial peptides. *Cell Mol. Life Sci.* **2003**, *60*, 711-720.
97. Mor, A.; Nguyen, V. H.; Delfour, A.; Migliore-Samour, D.; Nicolas, P. Isolation, amino acid sequence, and synthesis of dermaseptin, a novel antimicrobial peptide of amphibian skin. *Biochemistry* **1991**, *30*, 8824-8830.
98. Shinnar, A. E.; Butler, K. L.; Park, H. J. Cathelicidin family of antimicrobial peptides: proteolytic processing and protease resistance. *Bioorg. Chem.* **2003**, *31*, 425-436.
99. Nizet, V.; Gallo, R. L. Cathelicidins and innate defense against invasive bacterial infection. *Scand. J. Infect. Dis.* **2003**, *35*, 670-676.
100. Niyonsaba, F.; Hirata, M.; Ogawa, H.; Nagaoka, I. Epithelial cell-derived antibacterial peptides human beta-defensins and cathelicidin: multifunctional activities on mast cells. *Curr. Drug Targets Inflamm. Allergy* **2003**, *2*, 224-231.
101. Nielsen, J. E.; Hansen, M. A.; Jorgensen, M.; Tanaka, M.; Almstrup, K.; Skakkebaek, N. E.; Leffers, H. Germ cell differentiation-dependent and stage-specific expression of LANCL1 in rodent testis. *Eur. J. Histochem.* **2003**, *47*, 215-222.
102. Hao, H. N.; Zhao, J.; Lotoczky, G.; Grever, W. E.; Lyman, W. D. Induction of human beta-defensin-2 expression in human astrocytes by lipopolysaccharide and cytokines. *J. Neurochem.* **2001**, *77*, 1027-1035.
103. Zhao, X.; Wu, H.; Lu, H.; Li, G.; Huang, Q. LAMP: A Database Linking Antimicrobial Peptides. *PLoS One* **2013**, *8*, e66557.
104. Verkleij, A. J.; Zwaal, R. F.; Roelofsen, B.; Comfurius, P.; Kastelijn, D.; van Deenen, L. L. The asymmetric distribution of phospholipids in the human red cell membrane. A combined study using phospholipases and freeze-etch electron microscopy. *Biochim. Biophys. Acta* **1973**, *323*, 178-193.

105. Brewer, D.; Lajoie, G. Evaluation of the metal binding properties of the histidine-rich antimicrobial peptides histatin 3 and 5 by electrospray ionization mass spectrometry. *Rapid Commun. Mass Spectrom.* **2000**, *14*, 1736-1745.
106. Edstrom, A. M.; Malm, J.; Frohm, B.; Martellini, J. A.; Giwercman, A.; Morgelin, M.; Cole, A. M.; Sorensen, O. E. The major bactericidal activity of human seminal plasma is zinc-dependent and derived from fragmentation of the semenogelins. *J. Immunol.* **2008**, *181*, 3413-3421.
107. Dashper, S. G.; O'Brien-Simpson, N. M.; Cross, K. J.; Paolini, R. A.; Hoffmann, B.; Catmull, D. V.; Malkoski, M.; Reynolds, E. C. Divalent metal cations increase the activity of the antimicrobial Peptide kappacin. *Antimicrob. Agents Chemother.* **2005**, *49*, 2322-2328.
108. Rydengard, V.; Andersson Nordahl, E.; Schmidtchen, A. Zinc potentiates the antibacterial effects of histidine-rich peptides against *Enterococcus faecalis*. *FEBS J.* **2006**, *273*, 2399-2406.
109. Wang, M.; Liu, L. H.; Wang, S.; Li, X.; Lu, X.; Gupta, D.; Dziarski, R. Human peptidoglycan recognition proteins require zinc to kill both gram-positive and gram-negative bacteria and are synergistic with antibacterial peptides. *J. Immunol.* **2007**, *178*, 3116-3125.
110. Brodersen, D. E.; Nyborg, J.; Kjeldgaard, M. Zinc-binding site of an S100 protein revealed. Two crystal structures of Ca²⁺-bound human psoriasin (S100A7) in the Zn²⁺-loaded and Zn²⁺-free states. *Biochemistry* **1999**, *38*, 1695-1704.
111. Hancock, R. E.; Lehrer, R. I. Cationic peptides: a new source of antibiotics. *Trends Biotechnol.* **1998**, *16*, 82-88.
112. Wang, G.; Li, X.; Wang, Z. APD2: the updated antimicrobial peptide database and its application in peptide design. *Nucleic Acids Res.* **2009**, *37*, D933-7.
113. Tossi, A.; Sandri, L. Molecular diversity in gene-encoded, cationic antimicrobial polypeptides. *Curr. Pharm. Des.* **2002**, *8*, 743-761.
114. Piotto, S. P.; Sessa, L.; Concilio, S.; Iannelli, P. YADAMP: yet another database of antimicrobial peptides. *Int. J. Antimicrob. Agents* **2012**, *39*, 346-351.
115. Wang, G. Structures of human host defense cathelicidin LL-37 and its smallest antimicrobial peptide KR-12 in lipid micelles. *J. Biol. Chem.* **2008**, *283*, 32637-32643.
116. Schibli, D. J.; Hunter, H. N.; Aseyev, V.; Starner, T. D.; Wiencek, J. M.; McCray, P. B.; Tack, B. F.; Vogel, H. J. The Solution Structures of the Human β -Defensins Lead to a Better Understanding of the Potent Bactericidal Activity of HBD3 against *Staphylococcus aureus*. *Journal of Biological Chemistry* **2002**, *277*, 8279-8289.

117. Rozek, A.; Friedrich, C. L.; Hancock, R. E. Structure of the bovine antimicrobial peptide indolicidin bound to dodecylphosphocholine and sodium dodecyl sulfate micelles. *Biochemistry* **2000**, *39*, 15765-15774.
118. Tossi, A.; Sandri, L.; Giangaspero, A. Amphipathic, alpha-helical antimicrobial peptides. *Biopolymers* **2000**, *55*, 4-30.
119. Schiffer, M.; Edmundson, A. B. Use of helical wheels to represent the structures of proteins and to identify segments with helical potential. *Biophys. J.* **1967**, *7*, 121-135.
120. Boman, H. G. Antibacterial peptides: basic facts and emerging concepts. *J. Intern. Med.* **2003**, *254*, 197-215.
121. Andersson, E.; Rydengard, V.; Sonesson, A.; Morgelin, M.; Bjorck, L.; Schmidtchen, A. Antimicrobial activities of heparin-binding peptides. *Eur. J. Biochem.* **2004**, *271*, 1219-1226.
122. Lu, X.; Wang, M.; Qi, J.; Wang, H.; Li, X.; Gupta, D.; Dziarski, R. Peptidoglycan recognition proteins are a new class of human bactericidal proteins. *J. Biol. Chem.* **2006**, *281*, 5895-5907.
123. Wang, Z.; Wang, G. APD: the Antimicrobial Peptide Database. *Nucleic Acids Res.* **2004**, *32*, D590-2.
124. Breukink, E.; Wiedemann, I.; van Kraaij, C.; Kuipers, O. P.; Sahl, H.; de Kruijff, B. Use of the cell wall precursor lipid II by a pore-forming peptide antibiotic. *Science* **1999**, *286*, 2361-2364.
125. Terwilliger, T. C.; Eisenberg, D. The structure of melittin. I. Structure determination and partial refinement. *J. Biol. Chem.* **1982**, *257*, 6010-6015.
126. Holak, T. A.; Engstrom, A.; Kraulis, P. J.; Lindeberg, G.; Bennich, H.; Jones, T. A.; Gronenborn, A. M.; Clore, G. M. The solution conformation of the antibacterial peptide cecropin A: a nuclear magnetic resonance and dynamical simulated annealing study. *Biochemistry* **1988**, *27*, 7620-7629.
127. Zasloff, M. Magainins, a class of antimicrobial peptides from *Xenopus* skin: isolation, characterization of two active forms, and partial cDNA sequence of a precursor. *Proc. Natl. Acad. Sci. U. S. A.* **1987**, *84*, 5449-5453.
128. Mandard, N.; Sy, D.; Maufrais, C.; Bonmatin, J. M.; Bulet, P.; Hetru, C.; Vovelle, F. Androctonin, a novel antimicrobial peptide from scorpion *Androctonus australis*: solution structure and molecular dynamics simulations in the presence of a lipid monolayer. *J. Biomol. Struct. Dyn.* **1999**, *17*, 367-380.

129. Shai, Y. Mechanism of the binding, insertion and destabilization of phospholipid bilayer membranes by alpha-helical antimicrobial and cell non-selective membrane-lytic peptides. *Biochim. Biophys. Acta* **1999**, *1462*, 55-70.
130. Wu, M.; Maier, E.; Benz, R.; Hancock, R. E. Mechanism of interaction of different classes of cationic antimicrobial peptides with planar bilayers and with the cytoplasmic membrane of *Escherichia coli*. *Biochemistry* **1999**, *38*, 7235-7242.
131. Matsuzaki, K.; Sugishita, K.; Ishibe, N.; Ueha, M.; Nakata, S.; Miyajima, K.; Epand, R. M. Relationship of membrane curvature to the formation of pores by magainin 2. *Biochemistry* **1998**, *37*, 11856-11863.
132. Oren, Z.; Shai, Y. Mode of action of linear amphipathic alpha-helical antimicrobial peptides. *Biopolymers* **1998**, *47*, 451-463.
133. Bulet, P.; Hetru, C.; Dimarcq, J. L.; Hoffmann, D. Antimicrobial peptides in insects; structure and function. *Dev. Comp. Immunol.* **1999**, *23*, 329-344.
134. Wade, D.; Boman, A.; Wahlin, B.; Drain, C. M.; Andreu, D.; Boman, H. G.; Merrifield, R. B. All-D amino acid-containing channel-forming antibiotic peptides. *Proc. Natl. Acad. Sci. U. S. A.* **1990**, *87*, 4761-4765.
135. Merrifield, R. B.; Juvvadi, P.; Andreu, D.; Ubach, J.; Boman, A.; Boman, H. G. Retro and retroenantio analogs of cecropin-melittin hybrids. *Proc. Natl. Acad. Sci. U. S. A.* **1995**, *92*, 3449-3453.
136. Bessalle, R.; Kapitkovsky, A.; Gorea, A.; Shalit, I.; Fridkin, M. All-D-magainin: chirality, antimicrobial activity and proteolytic resistance. *FEBS Lett.* **1990**, *274*, 151-155.
137. Hetru, C.; Letellier, L.; Oren, Z.; Hoffmann, J. A.; Shai, Y. Androctonin, a hydrophilic disulphide-bridged non-haemolytic anti-microbial peptide: a plausible mode of action. *Biochem. J.* **2000**, *345 Pt 3*, 653-664.
138. Fleury, Y.; Dayem, M. A.; Montagne, J. J.; Chaboisseau, E.; Le Caer, J. P.; Nicolas, P.; Delfour, A. Covalent structure, synthesis, and structure-function studies of mesentericin Y 105(37), a defensive peptide from gram-positive bacteria *Leuconostoc mesenteroides*. *J. Biol. Chem.* **1996**, *271*, 14421-14429.
139. Cudic, M.; Otvos, L., Jr Intracellular targets of antibacterial peptides. *Curr. Drug Targets* **2002**, *3*, 101-106.
140. Feder, R.; Dagan, A.; Mor, A. Structure-activity relationship study of antimicrobial dermaseptin S4 showing the consequences of peptide oligomerization on selective cytotoxicity. *J. Biol. Chem.* **2000**, *275*, 4230-4238.

141. Lehrer, R. I.; Ganz, T. Antimicrobial peptides in mammalian and insect host defence. *Curr. Opin. Immunol.* **1999**, *11*, 23-27.
142. Hancock, R. E.; Rozek, A. Role of membranes in the activities of antimicrobial cationic peptides. *FEMS Microbiol. Lett.* **2002**, *206*, 143-149.
143. Matsuzaki, K. Why and how are peptide–lipid interactions utilized for self-defense? Magainins and tachyplesins as archetypes. *Biochimica et Biophysica Acta (BBA) - Biomembranes* **1999/12/15**, *1462*, 1-10.
144. Bechinger, B. The structure, dynamics and orientation of antimicrobial peptides in membranes by multidimensional solid-state NMR spectroscopy. *Biochim. Biophys. Acta* **1999**, *1462*, 157-183.
145. Shai, Y. From innate immunity to de-novo designed antimicrobial peptides. *Curr. Pharm. Des.* **2002**, *8*, 715-725.
146. Brogden, K. A. Antimicrobial peptides: pore formers or metabolic inhibitors in bacteria? *Nat. Rev. Microbiol.* **2005**, *3*, 238-250.
147. Huang, H. W.; Chen, F. Y.; Lee, M. T. Molecular mechanism of Peptide-induced pores in membranes. *Phys. Rev. Lett.* **2004**, *92*, 198304.
148. van 't Hof, W.; Veerman, E. C.; Helmerhorst, E. J.; Amerongen, A. V. Antimicrobial peptides: properties and applicability. *Biol. Chem.* **2001**, *382*, 597-619.
149. Hancock, R. E.; Chapple, D. S. Peptide antibiotics. *Antimicrob. Agents Chemother.* **1999**, *43*, 1317-1323.
150. Chitnis, S. N.; Prasad, K. S.; Bhargava, P. M. Isolation and characterization of autolysis-defective mutants of *Escherichia coli* that are resistant to the lytic activity of seminalplasmin. *J. Gen. Microbiol.* **1990**, *136*, 463-469.
151. Boman, H. G.; Agerberth, B.; Boman, A. Mechanisms of action on *Escherichia coli* of cecropin P1 and PR-39, two antibacterial peptides from pig intestine. *Infect. Immun.* **1993**, *61*, 2978-2984.
152. Subbalakshmi, C.; Sitaram, N. Mechanism of antimicrobial action of indolicidin. *FEMS Microbiol. Lett.* **1998**, *160*, 91-96.
153. Skerlavaj, B.; Romeo, D.; Gennaro, R. Rapid membrane permeabilization and inhibition of vital functions of gram-negative bacteria by bactenecins. *Infect. Immun.* **1990**, *58*, 3724-3730.

154. Xiong, Y. Q.; Yeaman, M. R.; Bayer, A. S. In vitro antibacterial activities of platelet microbicidal protein and neutrophil defensin against *Staphylococcus aureus* are influenced by antibiotics differing in mechanism of action. *Antimicrob. Agents Chemother.* **1999**, *43*, 1111-1117.
155. Lehrer, R. I.; Barton, A.; Daher, K. A.; Harwig, S. S.; Ganz, T.; Selsted, M. E. Interaction of human defensins with *Escherichia coli*. Mechanism of bactericidal activity. *J. Clin. Invest.* **1989**, *84*, 553-561.
156. Patrzykat, A.; Friedrich, C. L.; Zhang, L.; Mendoza, V.; Hancock, R. E. Sublethal concentrations of pleurocidin-derived antimicrobial peptides inhibit macromolecular synthesis in *Escherichia coli*. *Antimicrob. Agents Chemother.* **2002**, *46*, 605-614.
157. Brotz, H.; Bierbaum, G.; Leopold, K.; Reynolds, P. E.; Sahl, H. G. The lantibiotic mersacidin inhibits peptidoglycan synthesis by targeting lipid II. *Antimicrob. Agents Chemother.* **1998**, *42*, 154-160.
158. Otvos, L., Jr.; O, I.; Rogers, M. E.; Consolvo, P. J.; Condie, B. A.; Lovas, S.; Bulet, P.; Blaszczyk-Thurin, M. Interaction between heat shock proteins and antimicrobial peptides. *Biochemistry* **2000**, *39*, 14150-14159.
159. Park, C. B.; Kim, H. S.; Kim, S. C. Mechanism of action of the antimicrobial peptide buforin II: buforin II kills microorganisms by penetrating the cell membrane and inhibiting cellular functions. *Biochem. Biophys. Res. Commun.* **1998**, *244*, 253-257.
160. Park, C. B.; Yi, K. S.; Matsuzaki, K.; Kim, M. S.; Kim, S. C. Structure-activity analysis of buforin II, a histone H2A-derived antimicrobial peptide: the proline hinge is responsible for the cell-penetrating ability of buforin II. *Proc. Natl. Acad. Sci. U. S. A.* **2000**, *97*, 8245-8250.
161. Kobayashi, S.; Takeshima, K.; Park, C. B.; Kim, S. C.; Matsuzaki, K. Interactions of the novel antimicrobial peptide buforin 2 with lipid bilayers: proline as a translocation promoting factor. *Biochemistry* **2000**, *39*, 8648-8654.
162. Zhang, L.; Benz, R.; Hancock, R. E. Influence of proline residues on the antibacterial and synergistic activities of alpha-helical peptides. *Biochemistry* **1999**, *38*, 8102-8111.
163. Yonezawa, A.; Kuwahara, J.; Fujii, N.; Sugiura, Y. Binding of tachyplesin I to DNA revealed by footprinting analysis: significant contribution of secondary structure to DNA binding and implication for biological action. *Biochemistry* **1992**, *31*, 2998-3004.
164. Shi, J.; Ross, C. R.; Chengappa, M. M.; Sylte, M. J.; McVey, D. S.; Blecha, F. Antibacterial activity of a synthetic peptide (PR-26) derived from PR-39, a proline-arginine-rich neutrophil antimicrobial peptide. *Antimicrob. Agents Chemother.* **1996**, *40*, 115-121.

165. Brogden, K. A.; Ackermann, M.; Huttner, K. M. Detection of anionic antimicrobial peptides in ovine bronchoalveolar lavage fluid and respiratory epithelium. *Infect. Immun.* **1998**, *66*, 5948-5954.
166. Otvos, L., Jr Antibacterial peptides and proteins with multiple cellular targets. *J. Pept. Sci.* **2005**, *11*, 697-706.
167. Gusman, H.; Lendenmann, U.; Grogan, J.; Troxler, R. F.; Oppenheim, F. G. Is salivary histatin 5 a metallopeptide? *Biochim. Biophys. Acta* **2001**, *1545*, 86-95.
168. McEntire, J. C.; Montville, T. J.; Chikindas, M. L. Synergy between nisin and select lactates against *Listeria monocytogenes* is due to the metal cations. *J. Food Prot.* **2003**, *66*, 1631-1636.
169. Ramachandran, R.; Tweten, R. K.; Johnson, A. E. Membrane-dependent conformational changes initiate cholesterol-dependent cytolysin oligomerization and intersubunit beta-strand alignment. *Nat. Struct. Mol. Biol.* **2004**, *11*, 697-705.
170. Giddings, K. S.; Johnson, A. E.; Tweten, R. K. Redefining cholesterol's role in the mechanism of the cholesterol-dependent cytolysins. *Proc. Natl. Acad. Sci. U. S. A.* **2003**, *100*, 11315-11320.
171. Prenner, E. J.; Lewis, R. N.; Jelokhani-Niaraki, M.; Hodges, R. S.; McElhaney, R. N. Cholesterol attenuates the interaction of the antimicrobial peptide gramicidin S with phospholipid bilayer membranes. *Biochim. Biophys. Acta* **2001**, *1510*, 83-92.
172. Barman, H.; Walch, M.; Latinovic-Golic, S.; Dumrese, C.; Dolder, M.; Groscurth, P.; Ziegler, U. Cholesterol in negatively charged lipid bilayers modulates the effect of the antimicrobial protein granulysin. *J. Membr. Biol.* **2006**, *212*, 29-39.
173. Meier-Stephenson, V. C. Quantum Medicine: Novel Applications of Computational Chemistry to the Treatment of Neurological Diseases, Dalhousie University, Halifax, Nova Scotia, 2005.
174. Matsuzaki, K.; Murase, O.; Fujii, N.; Miyajima, K. An antimicrobial peptide, magainin 2, induced rapid flip-flop of phospholipids coupled with pore formation and peptide translocation. *Biochemistry* **1996**, *35*, 11361-11368.
175. Zhang, L.; Rozek, A.; Hancock, R. E. Interaction of cationic antimicrobial peptides with model membranes. *J. Biol. Chem.* **2001**, *276*, 35714-35722.
176. Matsuzaki, K.; Murase, O.; Fujii, N.; Miyajima, K. Translocation of a channel-forming antimicrobial peptide, magainin 2, across lipid bilayers by forming a pore. *Biochemistry* **1995**, *34*, 6521-6526.

177. Yan, S. D.; Fu, J.; Soto, C.; Chen, X.; Zhu, H.; Al-Mohanna, F.; Collison, K.; Zhu, A.; Stern, E.; Saïdo, T.; Tohyama, M.; Ogawa, S.; Roher, A.; Stern, D. An intracellular protein that binds amyloid-beta peptide and mediates neurotoxicity in Alzheimer's disease. *Nature* **1997**, *389*, 689-695.
178. Abramov, A. Y.; Canevari, L.; Duchen, M. R. Beta-amyloid peptides induce mitochondrial dysfunction and oxidative stress in astrocytes and death of neurons through activation of NADPH oxidase. *J. Neurosci.* **2004**, *24*, 565-575.
179. Huang, H. M.; Fowler, C.; Xu, H.; Zhang, H.; Gibson, G. E. Mitochondrial function in fibroblasts with aging in culture and/or Alzheimer's disease. *Neurobiol. Aging* **2005**, *26*, 839-848.
180. Canevari, L.; Abramov, A. Y.; Duchen, M. R. Toxicity of amyloid beta peptide: tales of calcium, mitochondria, and oxidative stress. *Neurochem. Res.* **2004**, *29*, 637-650.
181. Casley, C. S.; Canevari, L.; Land, J. M.; Clark, J. B.; Sharpe, M. A. Beta-amyloid inhibits integrated mitochondrial respiration and key enzyme activities. *J. Neurochem.* **2002**, *80*, 91-100.
182. Bonev, B.; Watts, A.; Bokvist, M.; Gröbner, G. Electrostatic peptide-lipid interactions of amyloid-beta peptide and pentyllysine with membrane surfaces monitored by ³¹P MAS NMR. *Phys. Chem. Chem. Phys.* **2001**, *3*, 2904-2910.
183. Saberwal, G.; Nagaraj, R. Cell-lytic and antibacterial peptides that act by perturbing the barrier function of membranes: facets of their conformational features, structure-function correlations and membrane-perturbing abilities. *Biochim. Biophys. Acta* **1994**, *1197*, 109-131.
184. Levy, O. Antibiotic proteins of polymorphonuclear leukocytes. *Eur. J. Haematol.* **1996**, *56*, 263-277.
185. Tossi, A.; Scocchi, M.; Zanetti, M.; Storici, P.; Gennaro, R. PMAP-37, a novel antibacterial peptide from pig myeloid cells. cDNA cloning, chemical synthesis and activity. *Eur. J. Biochem.* **1995**, *228*, 941-946.
186. Wong, H.; Bowie, J. H.; Carver, J. A. The solution structure and activity of caerin 1.1, an antimicrobial peptide from the Australian green tree frog, *Litoria splendida*. *Eur. J. Biochem.* **1997**, *247*, 545-557.
187. Crescenzi, O.; Tomaselli, S.; Guerrini, R.; Salvadori, S.; D'Ursi, A. M.; Temussi, P. A.; Picone, D. Solution structure of the Alzheimer amyloid beta-peptide (1-42) in an apolar microenvironment. Similarity with a virus fusion domain. *Eur. J. Biochem.* **2002**, *269*, 5642-5648.

188. Sticht, H.; Bayer, P.; Willbold, D.; Dames, S.; Hilbich, C.; Beyreuther, K.; Frank, R. W.; Rosch, P. Structure of amyloid A4-(1-40)-peptide of Alzheimer's disease. *Eur. J. Biochem.* **1995**, *233*, 293-298.
189. Mattson, M. P.; Cheng, B.; Davis, D.; Bryant, K.; Lieberburg, I.; Rydel, R. E. beta-Amyloid peptides destabilize calcium homeostasis and render human cortical neurons vulnerable to excitotoxicity. *J. Neurosci.* **1992**, *12*, 376-389.
190. Arispe, N.; Pollard, H. B.; Rojas, E. beta-Amyloid Ca(2+)-channel hypothesis for neuronal death in Alzheimer disease. *Mol. Cell. Biochem.* **1994**, *140*, 119-125.
191. Lin, H.; Bhatia, R.; Lal, R. Amyloid beta protein forms ion channels: implications for Alzheimer's disease pathophysiology. *FASEB J.* **2001**, *15*, 2433-2444.
192. Dulbecco, R.; Vogt, M. Plaque formation and isolation of pure lines with poliomyelitis viruses. *J. Exp. Med.* **1954**, *99*, 167-182.
193. Fonnum, F.; Myhrer, T.; Paulsen, R. E.; Wangen, K.; Oksengard, A. R. Role of glutamate and glutamate receptors in memory function and Alzheimer's disease. *Ann. N. Y. Acad. Sci.* **1995**, *757*, 475-486.
194. Demuro, A.; Parker, I.; Stutzmann, G. E. Calcium signaling and amyloid toxicity in Alzheimer disease. *J. Biol. Chem.* **2010**, *285*, 12463-12468.
195. Smith, P. K.; Krohn, R. I.; Hermanson, G. T.; Mallia, A. K.; Gartner, F. H.; Provenzano, M. D.; Fujimoto, E. K.; Goeke, N. M.; Olson, B. J.; Klenk, D. C. Measurement of protein using bicinchoninic acid. *Anal. Biochem.* **1985**, *150*, 76-85.
196. Walker, J. M., Ed.; In *The Protein Protocols Handbook*; Humana Press: Totowa, NJ, USA, **2002**; pp. 1146.
197. Akins, R. E.; Tuan, R. S. Measurement of protein in 20 seconds using a microwave BCA assay. *BioTechniques* **1992**, *12*, 496-499.
198. LeVine, H., 3rd Alzheimer's beta-peptide oligomer formation at physiologic concentrations. *Anal. Biochem.* **2004**, *335*, 81-90.
199. Brewer, G. J.; Torricelli, J. R.; Evege, E. K.; Price, P. J. Optimized survival of hippocampal neurons in B27-supplemented Neurobasal, a new serum-free medium combination. *J. Neurosci. Res.* **1993**, *35*, 567-576.
200. Otvos, L., Jr; Szendrei, G. I.; Lee, V. M.; Mantsch, H. H. Human and rodent Alzheimer beta-amyloid peptides acquire distinct conformations in membrane-mimicking solvents. *Eur. J. Biochem.* **1993**, *211*, 249-257.

201. Jensen, M.; Hartmann, T.; Engvall, B.; Wang, R.; Uljon, S. N.; Sennvik, K.; Naslund, J.; Muehlhauser, F.; Nordstedt, C.; Beyreuther, K.; Lannfelt, L. Quantification of Alzheimer amyloid beta peptides ending at residues 40 and 42 by novel ELISA systems. *Mol. Med.* **2000**, *6*, 291-302.
202. Neumann, H.; Wekerle, H. Neuronal control of the immune response in the central nervous system: linking brain immunity to neurodegeneration. *J. Neuropathol. Exp. Neurol.* **1998**, *57*, 1-9.
203. Cho, H.; Prohl, S. C.; Szretter, K. J.; Katze, M. G.; Gale, M., Jr; Diamond, M. S. Differential innate immune response programs in neuronal subtypes determine susceptibility to infection in the brain by positive-stranded RNA viruses. *Nat. Med.* **2013**, *19*, 458-464.
204. Hung, J.; Chansard, M.; Ousman, S. S.; Nguyen, M. D.; Colicos, M. A. Activation of microglia by neuronal activity: Results from a new in vitro paradigm based on neuronal-silicon interfacing technology. *Brain Behav. Immun.* **2010**, *24*, 31-40.
205. Butovsky, O.; Talpalar, A. E.; Ben-Yaakov, K.; Schwartz, M. Activation of microglia by aggregated β -amyloid or lipopolysaccharide impairs MHC-II expression and renders them cytotoxic whereas IFN- γ and IL-4 render them protective. *Molecular and Cellular Neuroscience* **2005**, *29*, 381-393.
206. Biber, K.; Neumann, H.; Inoue, K.; Boddeke, H. W. Neuronal 'On' and 'Off' signals control microglia. *Trends Neurosci.* **2007**, *30*, 596-602.
207. Yates, C. M.; Butterworth, J.; Tennant, M. C.; Gordon, A. Enzyme activities in relation to pH and lactate in postmortem brain in Alzheimer-type and other dementias. *J. Neurochem.* **1990**, *55*, 1624-1630.
208. Clausen, T.; Khaldi, A.; Zauner, A.; Reinert, M.; Doppenberg, E.; Menzel, M.; Soukup, J.; Alves, O. L.; Bullock, M. R. Cerebral acid-base homeostasis after severe traumatic brain injury. *J. Neurosurg.* **2005**, *103*, 597-607.
209. Timofeev, I.; Carpenter, K. L.; Nortje, J.; Al-Rawi, P. G.; O'Connell, M. T.; Czosnyka, M.; Smielewski, P.; Pickard, J. D.; Menon, D. K.; Kirkpatrick, P. J.; Gupta, A. K.; Hutchinson, P. J. Cerebral extracellular chemistry and outcome following traumatic brain injury: a microdialysis study of 223 patients. *Brain* **2011**, *134*, 484-494.
210. DeSalles, A. A.; Kontos, H. A.; Becker, D. P.; Yang, M. S.; Ward, J. D.; Moulton, R.; Gruemer, H. D.; Lutz, H.; Maset, A. L.; Jenkins, L. Prognostic significance of ventricular CSF lactic acidosis in severe head injury. *J. Neurosurg.* **1986**, *65*, 615-624.
211. Ratledge, C.; Wilkinson, S. G. *Microbial lipids*; Academic Press: London ; Toronto, 1988; .

212. Lehrer, R. I.; Rosenman, M.; Harwig, S. S.; Jackson, R.; Eisenhauer, P. Ultrasensitive assays for endogenous antimicrobial polypeptides. *J. Immunol. Methods* **1991**, *137*, 167-173.
213. du Toit, E. A.; Rautenbach, M. A sensitive standardised micro-gel well diffusion assay for the determination of antimicrobial activity. *Journal of Microbiological Methods* **2000/10**, *42*, 159-165.
214. Patel, J. P.; Tenover, F. C.; Turnidge, J. D.; Jorgenson, J. H. In *Susceptibility Test Methods - Dilution and Disk Diffusion Methods*; Versalovic, J., Carroll, K. C., Funke, G., Jorgensen, J. H., Landry, M. L. and Warnock, D. W., Eds.; Manual of Clinical Microbiology; ASM Press: Washington, DC, USA, 2011; Vol. 1, pp. 1122-1143.
215. Soscia, S. J.; Kirby, J. E.; Washicosky, K. J.; Tucker, S. M.; Ingelsson, M.; Hyman, B.; Burton, M. A.; Goldstein, L. E.; Duong, S.; Tanzi, R. E.; Moir, R. D. The Alzheimer's disease-associated amyloid beta-protein is an antimicrobial peptide. *PLoS One* **2010**, *5*, e9505.
216. Anantharaman, A.; Rizvi, M. S.; Sahal, D. Synergy with rifampin and kanamycin enhances potency, kill kinetics, and selectivity of de novo-designed antimicrobial peptides. *Antimicrob. Agents Chemother.* **2010**, *54*, 1693-1699.
217. Wang, M. S.; Boddapati, S.; Sierks, M. R. Cyclodextrins promote protein aggregation posing risks for therapeutic applications. *Biochem. Biophys. Res. Commun.* **2009**, *386*, 526-531.
218. Hassall, D. G.; Graham, A. Changes in free cholesterol content, measured by filipin fluorescence and flow cytometry, correlate with changes in cholesterol biosynthesis in THP-1 macrophages. *Cytometry* **1995**, *21*, 352-362.
219. Dobson, C. B.; Itzhaki, R. F. Herpes simplex virus type 1 and Alzheimer's disease. *Neurobiol. Aging* **1999**, *20*, 457-465.
220. Gajdusek, D. C. Unconventional viruses and the origin and disappearance of kuru. *Science* **1977**, *197*, 943-960.
221. Heston, L. L.; Mastri, A. R. The genetics of Alzheimer's disease: associations with hematologic malignancy and Down's syndrome. *Arch. Gen. Psychiatry* **1977**, *34*, 976-981.
222. Schellenberg, G. D. Early Alzheimer's disease genetics. *J. Alzheimers Dis.* **2006**, *9*, 367-372.
223. Bertram, L.; Tanzi, R. E. The genetics of Alzheimer's disease. *Prog. Mol. Biol. Transl. Sci.* **2012**, *107*, 79-100.
224. Wadsworth, J. D.; Joiner, S.; Linehan, J. M.; Asante, E. A.; Brandner, S.; Collinge, J. Review. The origin of the prion agent of kuru: molecular and biological strain typing. *Philos. Trans. R. Soc. Lond. B. Biol. Sci.* **2008**, *363*, 3747-3753.

225. Wadsworth, J. D.; Joiner, S.; Linehan, J. M.; Desbruslais, M.; Fox, K.; Cooper, S.; Cronier, S.; Asante, E. A.; Mead, S.; Brandner, S.; Hill, A. F.; Collinge, J. Kuru prions and sporadic Creutzfeldt-Jakob disease prions have equivalent transmission properties in transgenic and wild-type mice. *Proc. Natl. Acad. Sci. U. S. A.* **2008**, *105*, 3885-3890.
226. Ball, M. J. "Limbic predilection in Alzheimer dementia: is reactivated herpesvirus involved?". *Can. J. Neurol. Sci.* **1982**, *9*, 303-306.
227. Katan, M.; Moon, Y. P.; Paik, M. C.; Sacco, R. L.; Wright, C. B.; Elkind, M. S. Infectious burden and cognitive function: the Northern Manhattan Study. *Neurology* **2013**, *80*, 1209-1215.
228. Howell, M. D.; Jones, J. F.; Kisich, K. O.; Streib, J. E.; Gallo, R. L.; Leung, D. Y. Selective killing of vaccinia virus by LL-37: implications for eczema vaccinatum. *J. Immunol.* **2004**, *172*, 1763-1767.
229. Gordon, Y. J.; Huang, L. C.; Romanowski, E. G.; Yates, K. A.; Proske, R. J.; McDermott, A. M. Human cathelicidin (LL-37), a multifunctional peptide, is expressed by ocular surface epithelia and has potent antibacterial and antiviral activity. *Curr. Eye Res.* **2005**, *30*, 385-394.
230. Daher, K. A.; Selsted, M. E.; Lehrer, R. I. Direct inactivation of viruses by human granulocyte defensins. *J. Virol.* **1986**, *60*, 1068-1074.
231. Lehrer, R. I.; Daher, K.; Ganz, T.; Selsted, M. E. Direct inactivation of viruses by MCP-1 and MCP-2, natural peptide antibiotics from rabbit leukocytes. *J. Virol.* **1985**, *54*, 467-472.
232. Tamamura, H.; Murakami, T.; Masuda, M.; Otaka, A.; Takada, W.; Ibuka, T.; Nakashima, H.; Waki, M.; Matsumoto, A.; Yamamoto, N. Structure-activity relationships of an anti-HIV peptide, T22. *Biochem. Biophys. Res. Commun.* **1994**, *205*, 1729-1735.
233. Murakami, T.; Niwa, M.; Tokunaga, F.; Miyata, T.; Iwanaga, S. Direct virus inactivation of tachyplesin I and its isopeptides from horseshoe crab hemocytes. *Chemotherapy* **1991**, *37*, 327-334.
234. Wachinger, M.; Saermark, T.; Erfle, V. Influence of amphipathic peptides on the HIV-1 production in persistently infected T lymphoma cells. *FEBS Lett.* **1992**, *309*, 235-241.
235. Wachinger, M.; Kleinschmidt, A.; Winder, D.; von Pechmann, N.; Ludvigsen, A.; Neumann, M.; Holle, R.; Salmons, B.; Erfle, V.; Brack-Werner, R. Antimicrobial peptides melittin and cecropin inhibit replication of human immunodeficiency virus 1 by suppressing viral gene expression. *J. Gen. Virol.* **1998**, *79* (Pt. 4), 731-740.

236. Furman, P. A.; Coen, D. M.; St Clair, M. H.; Schaffer, P. A. Acyclovir-resistant mutants of herpes simplex virus type 1 express altered DNA polymerase or reduced acyclovir phosphorylating activities. *J. Virol.* **1981**, *40*, 936-941.
237. Uribe, L. H.; Olarte, E. C.; Castillo, G. T. In vitro antiviral activity of *Chamaecrista nictitans* (Fabaceae) against herpes simplex virus: Biological characterization of mechanisms of action. *Rev. Biol. Trop.* **2004**, *52*, 807-816.
238. Cummings, J. L. Alzheimer's disease clinical trials: changing the paradigm. *Curr. Psychiatry Rep.* **2011**, *13*, 437-442.
239. Mullane, K.; Williams, M. Alzheimer's therapeutics: continued clinical failures question the validity of the amyloid hypothesis-but what lies beyond? *Biochem. Pharmacol.* **2013**, *85*, 289-305.
240. Schillinger, J. A.; Xu, F.; Sternberg, M. R.; Armstrong, G. L.; Lee, F. K.; Nahmias, A. J.; McQuillan, G. M.; Louis, M. E.; Markowitz, L. E. National seroprevalence and trends in herpes simplex virus type 1 in the United States, 1976-1994. *Sex. Transm. Dis.* **2004**, *31*, 753-760.
241. Sperling, R. A.; Aisen, P. S.; Beckett, L. A.; Bennett, D. A.; Craft, S.; Fagan, A. M.; Iwatsubo, T.; Jack Jr., C. R.; Kaye, J.; Montine, T. J.; Park, D. C.; Reiman, E. M.; Rowe, C. C.; Siemers, E.; Stern, Y.; Yaffe, K.; Carrillo, M. C.; Thies, B.; Morrison-Bogorad, M.; Wagster, M. V.; Phelps, C. H. Toward defining the preclinical stages of Alzheimer's disease: Recommendations from the National Institute on Aging-Alzheimer's Association workgroups on diagnostic guidelines for Alzheimer's disease. *Alzheimer's and Dementia* **2011**, *7*, 280-292.
242. Bouwman, F. H.; Schoonenboom, N. S.; Verwey, N. A.; van Elk, E. J.; Kok, A.; Blankenstein, M. A.; Scheltens, P.; van der Flier, W. M. CSF biomarker levels in early and late onset Alzheimer's disease. *Neurobiol. Aging* **2009**, *30*, 1895-1901.
243. Bateman, R. J.; Munsell, L. Y.; Morris, J. C.; Swarm, R.; Yarasheski, K. E.; Holtzman, D. M. Human amyloid-beta synthesis and clearance rates as measured in cerebrospinal fluid in vivo. *Nat. Med.* **2006**, *12*, 856-861.
244. Matsuzaki, K.; Sugishita, K.; Fujii, N.; Miyajima, K. Molecular basis for membrane selectivity of an antimicrobial peptide, magainin 2. *Biochemistry* **1995**, *34*, 3423-3429.
245. Dathe, M.; Wieprecht, T. Structural features of helical antimicrobial peptides: their potential to modulate activity on model membranes and biological cells. *Biochim. Biophys. Acta* **1999**, *1462*, 71-87.

246. Glukhov, E.; Stark, M.; Burrows, L. L.; Deber, C. M. Basis for selectivity of cationic antimicrobial peptides for bacterial versus mammalian membranes. *J. Biol. Chem.* **2005**, *280*, 33960-33967.
247. Duckworth, D. H.; Bevers, E. M.; Verkleij, A. J.; Op den Kamp, J. A.; van Deenen, L. L. Action of phospholipase A2 and phospholipase C on *Escherichia coli*. *Arch. Biochem. Biophys.* **1974**, *165*, 379-387.
248. Rothman, J. E.; Kennedy, E. P. Asymmetrical distribution of phospholipids in the membrane of *Bacillus megaterium*. *J. Mol. Biol.* **1977**, *110*, 603-618.
249. Neville, F.; Cahuzac, M.; Konovalov, O.; Ishitsuka, Y.; Lee, K. Y.; Kuzmenko, I.; Kale, G. M.; Gidalevitz, D. Lipid headgroup discrimination by antimicrobial peptide LL-37: insight into mechanism of action. *Biophys. J.* **2006**, *90*, 1275-1287.
250. Helmerhorst, E. J.; Reijnders, I. M.; van 't Hof, W.; Veerman, E. C.; Nieuw Amerongen, A. V. A critical comparison of the hemolytic and fungicidal activities of cationic antimicrobial peptides. *FEBS Lett.* **1999**, *449*, 105-110.
251. Hong, J.; Oren, Z.; Shai, Y. Structure and organization of hemolytic and nonhemolytic diastereomers of antimicrobial peptides in membranes. *Biochemistry* **1999**, *38*, 16963-16973.
252. Tytler, E. M.; Anantharamaiah, G. M.; Walker, D. E.; Mishra, V. K.; Palgunachari, M. N.; Segrest, J. P. Molecular basis for prokaryotic specificity of magainin-induced lysis. *Biochemistry* **1995**, *34*, 4393-4401.
253. Turner, J. D.; Rouser, G. Precise quantitative determination of human blood lipids by thin-layer and triethylaminoethylcellulose column chromatography. I. Erythrocyte lipids. *Anal. Biochem.* **1970**, *38*, 423-436.
254. Sal-Man, N.; Oren, Z.; Shai, Y. Preassembly of membrane-active peptides is an important factor in their selectivity toward target cells. *Biochemistry* **2002**, *41*, 11921-11930.
255. de Kroon, A. I.; de Gier, J.; de Kruijff, B. The effect of a membrane potential on the interaction of mastoparan X, a mitochondrial presequence, and several regulatory peptides with phospholipid vesicles. *Biochim. Biophys. Acta* **1991**, *1068*, 111-124.
256. Sansom, M. S. The biophysics of peptide models of ion channels. *Prog. Biophys. Mol. Biol.* **1991**, *55*, 139-235.
257. Vaz Gomes, A.; de Waal, A.; Berden, J. A.; Westerhoff, H. V. Electric potentiation, cooperativity, and synergism of magainin peptides in protein-free liposomes. *Biochemistry* **1993**, *32*, 5365-5372.

258. Rink, T. J.; Hladky, S. B. In Ellory, J. C., Young, J. D., Eds.; *Red Cell Membranes - A Methodological Approach*; Academic Press: London, 1982; pp. 321-334.
259. Laris, P. C.; Pershadsingh, H. A. Estimations of membrane potentials in *Streptococcus faecalis* by means of a fluorescent probe. *Biochem. Biophys. Res. Commun.* **1974**, *57*, 620-626.
260. Zilberstein, D.; Schuldiner, S.; Padan, E. Proton electrochemical gradient in *Escherichia coli* cells and its relation to active transport of lactose. *Biochemistry* **1979**, *18*, 669-673.
261. Cruciani, R. A.; Barker, J. L.; Zasloff, M.; Chen, H. C.; Colamonici, O. Antibiotic magainins exert cytolytic activity against transformed cell lines through channel formation. *Proc. Natl. Acad. Sci. U. S. A.* **1991**, *88*, 3792-3796.
262. Diaz-Achirica, P.; Ubach, J.; Guinea, A.; Andreu, D.; Rivas, L. The plasma membrane of *Leishmania donovani* promastigotes is the main target for CA(1-8)M(1-18), a synthetic cecropin A-melittin hybrid peptide. *Biochem. J.* **1998**, *330* (Pt. 1), 453-460.
263. Karp, G. *Cell and molecular biology: concepts and experiments*; J. Wiley: New York, 2002; , pp 785.
264. Yankner, B. A.; Dawes, L. R.; Fisher, S.; Villa-Komaroff, L.; Oster-Granite, M. L.; Neve, R. L. Neurotoxicity of a fragment of the amyloid precursor associated with Alzheimer's disease. *Science* **1989**, *245*, 417-420.
265. Pike, C. J.; Walencewicz, A. J.; Glabe, C. G.; Cotman, C. W. In vitro aging of beta-amyloid protein causes peptide aggregation and neurotoxicity. *Brain Res.* **1991**, *563*, 311-314.
266. Mosmann, T. Rapid colorimetric assay for cellular growth and survival: application to proliferation and cytotoxicity assays. *J. Immunol. Methods* **1983**, *65*, 55-63.
267. Berridge, M. V.; Tan, A. S. Characterization of the cellular reduction of 3-(4,5-dimethylthiazol-2-yl)-2,5-diphenyltetrazolium bromide (MTT): subcellular localization, substrate dependence, and involvement of mitochondrial electron transport in MTT reduction. *Arch. Biochem. Biophys.* **1993**, *303*, 474-482.
268. Helmerhorst, E. J.; Breeuwer, P.; van't Hof, W.; Walgreen-Weterings, E.; Oomen, L. C.; Veerman, E. C.; Amerongen, A. V.; Abee, T. The cellular target of histatin 5 on *Candida albicans* is the energized mitochondrion. *J. Biol. Chem.* **1999**, *274*, 7286-7291.
269. Eliassen, L. T.; Berge, G.; Leknessund, A.; Wikman, M.; Lindin, I.; Lokke, C.; Ponthan, F.; Johnsen, J. I.; Sveinbjornsson, B.; Kogner, P.; Flaegstad, T.; Rekdal, O. The antimicrobial peptide, lactoferricin B, is cytotoxic to neuroblastoma cells in vitro and inhibits xenograft growth in vivo. *Int. J. Cancer* **2006**, *119*, 493-500.

270. Mereschkowsky, K. Theorie der zwei Plasmaarten als Grundlage der Symbiogenesis, einer neuen Lehre von der Entstehung der Organismen. *Biol. Centralbl.* **1910**, *30*, 353-367.
271. Wallin, I. E. The Mitochondria Problem. *The American Naturalist* **1923**, *57*, 255-261.
272. Wallin, I. E. *Symbiogenesis and the Origin of Species*; The Williams & Wilkins Company: Baltimore, MD, U.S.A., 1927; , pp 171.
273. Lustbader, J. W.; Cirilli, M.; Lin, C.; Xu, H. W.; Takuma, K.; Wang, N.; Caspersen, C.; Chen, X.; Pollak, S.; Chaney, M.; Trinchese, F.; Liu, S.; Gunn-Moore, F.; Lue, L. F.; Walker, D. G.; Kuppusamy, P.; Zewier, Z. L.; Arancio, O.; Stern, D.; Yan, S. S.; Wu, H. ABAD directly links Abeta to mitochondrial toxicity in Alzheimer's disease. *Science* **2004**, *304*, 448-452.
274. Manczak, M.; Anekonda, T. S.; Henson, E.; Park, B. S.; Quinn, J.; Reddy, P. H. Mitochondria are a direct site of A beta accumulation in Alzheimer's disease neurons: implications for free radical generation and oxidative damage in disease progression. *Hum. Mol. Genet.* **2006**, *15*, 1437-1449.
275. Swerdlow, R. H.; Khan, S. M. A "mitochondrial cascade hypothesis" for sporadic Alzheimer's disease. *Med. Hypotheses* **2004**, *63*, 8-20.
276. Swerdlow, R. H.; Burns, J. M.; Khan, S. M. The Alzheimer's disease mitochondrial cascade hypothesis. *J. Alzheimers Dis.* **2010**, *20 Suppl 2*, S265-79.
277. Wang, X.; Perry, G.; Smith, M. A.; Zhu, X. Amyloid-beta-derived diffusible ligands cause impaired axonal transport of mitochondria in neurons. *Neurodegener Dis.* **2010**, *7*, 56-59.
278. Eckert, A.; Schulz, K. L.; Rhein, V.; Gotz, J. Convergence of amyloid-beta and tau pathologies on mitochondria in vivo. *Mol. Neurobiol.* **2010**, *41*, 107-114.
279. Eckert, A.; Schmitt, K.; Gotz, J. Mitochondrial dysfunction - the beginning of the end in Alzheimer's disease? Separate and synergistic modes of tau and amyloid-beta toxicity. *Alzheimers Res. Ther.* **2011**, *3*, 15.
280. Keil, U.; Hauptmann, S.; Bonert, A.; Scherping, I.; Eckert, A.; Muller, W. E. Mitochondrial dysfunction induced by disease relevant AbetaPP and tau protein mutations. *J. Alzheimers Dis.* **2006**, *9*, 139-146.
281. Atamna, H.; Frey, W. H., 2nd Mechanisms of mitochondrial dysfunction and energy deficiency in Alzheimer's disease. *Mitochondrion* **2007**, *7*, 297-310.
282. Davis, J. N.; Hunnicutt Jr, E. J.; Chisholm, J. C. A mitochondrial bottleneck hypothesis of Alzheimer's disease. *Mol. Med. Today* **1995**, *1*, 240-247.

283. Gibson, G. E.; Starkov, A.; Blass, J. P.; Ratan, R. R.; Beal, M. F. Cause and consequence: Mitochondrial dysfunction initiates and propagates neuronal dysfunction, neuronal death and behavioral abnormalities in age-associated neurodegenerative diseases. *Biochimica et Biophysica Acta (BBA) - Molecular Basis of Disease* **2010**, *1802*, 122-134.
284. Dragicevic, N.; Mamcarz, M.; Zhu, Y.; Buzzeo, R.; Tan, J.; Arendash, G. W.; Bradshaw, P. C. Mitochondrial amyloid-beta levels are associated with the extent of mitochondrial dysfunction in different brain regions and the degree of cognitive impairment in Alzheimer's transgenic mice. *J. Alzheimers Dis.* **2010**, *20 Suppl 2*, S535-50.
285. Hsu, M. J.; Sheu, J. R.; Lin, C. H.; Shen, M. Y.; Hsu, C. Y. Mitochondrial mechanisms in amyloid beta peptide-induced cerebrovascular degeneration. *Biochim. Biophys. Acta* **2010**, *1800*, 290-296.
286. Riemer, J.; Kins, S. Axonal Transport and Mitochondrial Dysfunction in Alzheimer's Disease. *Neurodegener Dis.* **2012**.
287. Ceron, J. M.; Contreras-Moreno, J.; Puertollano, E.; de Cienfuegos, G. A.; Puertollano, M. A.; de Pablo, M. A. The antimicrobial peptide cecropin A induces caspase-independent cell death in human promyelocytic leukemia cells. *Peptides* **2010**, *31*, 1494-1503.
288. Hoskin, D. W.; Ramamoorthy, A. Studies on anticancer activities of antimicrobial peptides. *Biochim. Biophys. Acta* **2008**, *1778*, 357-375.
289. Schweizer, F. Cationic amphiphilic peptides with cancer-selective toxicity. *Eur. J. Pharmacol.* **2009**, *625*, 190-194.
290. Bhutia, S. K.; Maiti, T. K. Targeting tumors with peptides from natural sources. *Trends Biotechnol.* **2008**, *26*, 210-217.
291. Han, S. I.; Kim, Y. S.; Kim, T. H. Role of apoptotic and necrotic cell death under physiologic conditions. *BMB Rep.* **2008**, *41*, 1-10.
292. Wiechelman, K. J.; Braun, R. D.; Fitzpatrick, J. D. Investigation of the bicinchoninic acid protein assay: identification of the groups responsible for color formation. *Anal. Biochem.* **1988**, *175*, 231-237.
293. Ray, S. D.; Mehendale, H. M. In *Apoptosis*; Editor-in-Chief: Philip Wexler, Ed.; Encyclopedia of Toxicology (Second Edition); Elsevier: New York, 2005; pp. 153-167.
294. Behl, C.; Davis, J. B.; Klier, F. G.; Schubert, D. Amyloid beta peptide induces necrosis rather than apoptosis. *Brain Res.* **1994**, *645*, 253-264.

295. Loo, D. T.; Copani, A.; Pike, C. J.; Whittemore, E. R.; Walencewicz, A. J.; Cotman, C. W. Apoptosis is induced by beta-amyloid in cultured central nervous system neurons. *Proc. Natl. Acad. Sci. U. S. A.* **1993**, *90*, 7951-7955.
296. LaFerla, F. M.; Tinkle, B. T.; Bieberich, C. J.; Haudenschild, C. C.; Jay, G. The Alzheimer's A beta peptide induces neurodegeneration and apoptotic cell death in transgenic mice. *Nat. Genet.* **1995**, *9*, 21-30.
297. Kienlen-Campard, P.; Miolet, S.; Tasiaux, B.; Octave, J. N. Intracellular amyloid-beta 1-42, but not extracellular soluble amyloid-beta peptides, induces neuronal apoptosis. *J. Biol. Chem.* **2002**, *277*, 15666-15670.
298. Cha, M. Y.; Han, S. H.; Son, S. M.; Hong, H. S.; Choi, Y. J.; Byun, J.; Mook-Jung, I. Mitochondria-specific accumulation of amyloid beta induces mitochondrial dysfunction leading to apoptotic cell death. *PLoS One* **2012**, *7*, e34929.
299. Yanagisawa, K.; Odaka, A.; Suzuki, N.; Ihara, Y. GM1 ganglioside-bound amyloid beta-protein (A beta): a possible form of preamyloid in Alzheimer's disease. *Nat. Med.* **1995**, *1*, 1062-1066.
300. Yanagisawa, K. GM1 ganglioside and the seeding of amyloid in Alzheimer's disease: endogenous seed for Alzheimer amyloid. *Neuroscientist* **2005**, *11*, 250-260.
301. Pakkenberg, B.; Gundersen, H. J. Neocortical neuron number in humans: effect of sex and age. *J. Comp. Neurol.* **1997**, *384*, 312-320.
302. Pakkenberg, B.; Pelvig, D.; Marnier, L.; Bundgaard, M. J.; Gundersen, H. J.; Nyengaard, J. R.; Regeur, L. Aging and the human neocortex. *Exp. Gerontol.* **2003**, *38*, 95-99.
303. Chudler, E. H. Brain Facts and Figures. <http://faculty.washington.edu/chudler/facts.html> (accessed 02/08, 2014).
304. Farfara, D.; Lifshitz, V.; Frenkel, D. Neuroprotective and Neurotoxic Properties of Glial Cells in the Pathogenesis of Alzheimer's Disease. *J. Cell. Mol. Med.* **2008**, *12*, 762-780.
305. LaFerla, F. M.; Green, K. N.; Oddo, S. Intracellular amyloid-beta in Alzheimer's disease. *Nat. Rev. Neurosci.* **2007**, *8*, 499-509.
306. Vina, J.; Lloret, A.; Valles, S. L.; Borrás, C.; Badia, M. C.; Pallardo, F. V.; Sastre, J.; Alonso, M. D. Effect of gender on mitochondrial toxicity of Alzheimer's A beta peptide. *Antioxid. Redox Signal.* **2007**, *9*, 1677-1690.
307. Tang, Y.; Nyengaard, J. R.; De Groot, D. M.; Gundersen, H. J. Total regional and global number of synapses in the human brain neocortex. *Synapse* **2001**, *41*, 258-273.

308. Alvarez-Buylla, A.; Lim, D. A. For the long run: maintaining germinal niches in the adult brain. *Neuron* **2004**, *41*, 683-686.
309. Alvarez-Buylla, A.; Seri, B.; Doetsch, F. Identification of neural stem cells in the adult vertebrate brain. *Brain Res. Bull.* **2002**, *57*, 751-758.
310. Zhao, C.; Deng, W.; Gage, F. H. Mechanisms and Functional Implications of Adult Neurogenesis. *Cell* **2008**, *132*, 645-660.
311. Demars, M.; Hu, Y. S.; Gadadhar, A.; Lazarov, O. Impaired neurogenesis is an early event in the etiology of familial Alzheimer's disease in transgenic mice. *J. Neurosci. Res.* **2010**, *88*, 2103-2117.
312. Trouche, S.; Bontempi, B.; Rouillet, P.; Rampon, C. Recruitment of adult-generated neurons into functional hippocampal networks contributes to updating and strengthening of spatial memory. *Proc. Natl. Acad. Sci. U. S. A.* **2009**, *106*, 5919-5924.
313. Aimone, J. B.; Wiles, J.; Gage, F. H. Potential role for adult neurogenesis in the encoding of time in new memories. *Nat. Neurosci.* **2006**, *9*, 723-727.
314. Haughey, N. J.; Nath, A.; Chan, S. L.; Borchard, A. C.; Rao, M. S.; Mattson, M. P. Disruption of neurogenesis by amyloid beta-peptide, and perturbed neural progenitor cell homeostasis, in models of Alzheimer's disease. *J. Neurochem.* **2002**, *83*, 1509-1524.
315. Millet, P.; Lages, C. S.; Haik, S.; Nowak, E.; Allemand, I.; Granotier, C.; Boussin, F. D. Amyloid-beta peptide triggers Fas-independent apoptosis and differentiation of neural progenitor cells. *Neurobiol. Dis.* **2005**, *19*, 57-65.
316. McLaurin, J.; Chakrabartty, A. Membrane disruption by Alzheimer beta-amyloid peptides mediated through specific binding to either phospholipids or gangliosides. Implications for neurotoxicity. *J. Biol. Chem.* **1996**, *271*, 26482-26489.
317. Lopez-Toledano, M. A.; Shelanski, M. L. Neurogenic effect of beta-amyloid peptide in the development of neural stem cells. *J. Neurosci.* **2004**, *24*, 5439-5444.
318. Lazarov, O.; Marr, R. A. Neurogenesis and Alzheimer's disease: At the crossroads. *Exp. Neurol.* **2010**, *223*, 267-281.
319. Estus, S.; Tucker, H. M.; van Rooyen, C.; Wright, S.; Brigham, E. F.; Wogulis, M.; Rydel, R. E. Aggregated amyloid-beta protein induces cortical neuronal apoptosis and concomitant "apoptotic" pattern of gene induction. *J. Neurosci.* **1997**, *17*, 7736-7745.
320. Waldner, H. The role of innate immune responses in autoimmune disease development. *Autoimmun. Rev.* **2009**, *8*, 400-404.

321. Witebsky, E.; Rose, N. R.; Terplan, K.; Paine, J. R.; Egan, R. W. Chronic thyroiditis and autoimmunization. *J. Am. Med. Assoc.* **1957**, *164*, 1439-1447.
322. Rose, N. R.; Bona, C. Defining criteria for autoimmune diseases (Witebsky's postulates revisited). *Immunol. Today* **1993**, *14*, 426-430.
323. Zagorski, M. G.; Yang, J.; Shao, H.; Ma, K.; Zeng, H.; Hong, A. Methodological and chemical factors affecting amyloid beta peptide amyloidogenicity. *Methods Enzymol.* **1999**, *309*, 189-204.
324. Christian, A. E.; Haynes, M. P.; Phillips, M. C.; Rothblat, G. H. Use of cyclodextrins for manipulating cellular cholesterol content. *J. Lipid Res.* **1997**, *38*, 2264-2272.
325. Zidovetzki, R.; Levitan, I. Use of cyclodextrins to manipulate plasma membrane cholesterol content: Evidence, misconceptions and control strategies. *Biochim. Biophys. Acta - Biomembranes* **2007**, *1768*, 1311-1324.

CHAPTER III.

PENICILLIN AS A RISK FACTOR FOR ALZHEIMER'S DISEASE

1. Introduction

The incidence and prevalence of Alzheimer's Disease has continued to increase over the past 60-70 years. Interestingly, whether causal or coincidental, this is approximately the same time frame as the discovery and introduction of many new medications. In this chapter it is explored whether the introduction of penicillin may have a role to play in the increased incidence of AD over the course of the 20th century.

Penicillin was first introduced in the 1940's, after discovery in the laboratory of Sir Alexander Fleming. Since that time, penicillin and its derivatives have undergone widespread use, saving innumerable lives and preventing significant morbidity. The drug itself acts to inhibit cell wall synthesis through binding of penicillin-binding proteins (PBPs) to prevent the formation of the stabilizing cross-linking reaction in the peptidoglycan layer (1). This is ultimately lethal to the bacterium, causing it to lyse.

By virtue of their mechanism, penicillin and other antibiotics that act to disrupt and fragment the bacterial cell wall also expose the hosts' cells to toxic fragments released from the lysed bacterial wall, namely the bacterial endotoxins (2). Lipopolysaccharide (LPS) is released in the case of Gram-negative bacteria (3, 4), and lipoteichoic acid (LTA), or peptidoglycan in the

case of Gram-positive bacteria (5-7). These endotoxins stimulate the body's immune system and inflammatory response (8-11), which may lead to sepsis, and in extreme cases death through septic shock (2, 12). Release of endotoxins caused by treatment with antibiotics has been identified as one factor that might aggravate these serious effects of a systemic infection (2, 7, 13-15). However, even if the patient survives because of these antibiotics, their use may have unanticipated long-term effects.

In the previous chapter, the role of A β was described as an antimicrobial peptide with capabilities of killing bacteria through membrane disruption and how the release of bacterial membrane components can result in the formation of neurotoxic A β species that are the root cause of Alzheimer's Disease.

Here, we pose an interesting, albeit provocative question: If an antibiotic, such as penicillin, that kills bacteria by membrane destruction was given to a patient, could this in turn set the *Vicious Cycle of AD* into motion? Could the use of penicillin be an unrecognized risk factor for Alzheimer's Disease?

2. Penicillin as a Risk Factor for AD

2.1. Classes of Antibiotics and their Mechanism of Action

Since the introduction of penicillin into the general medical practice in the early 1940s, new antibiotic classes had to be developed to overcome resistance by various bacterial strains. Because several different antibiotics were used in the experiments described in this chapter, a brief summary of the different antibiotic classes and their mechanisms are described — namely, the β -lactams, sulfonamides, quinolones, macrolides, tetracyclines, aminoglycosides, and

glycopeptides. The chemical structures of used antibiotics are given in Figure III-1. Information was obtained from the Manual of Clinical Microbiology (16) unless otherwise referenced.

2.1.1. β -Lactam Antibiotics

Penicillin is the prototype of a class of antibiotics containing a β -lactam ring; these include the penicillins, cephalosporins, monobactams, carbapenems, and β -lactamase inhibitors.

Typically, this class of bactericidal antibiotics acts by inhibiting a number of bacterial enzymes called penicillin-binding proteins (PBPs) that are essential for synthesis of peptidoglycans, components of the bacterial cell wall. Binding of PBPs triggers membrane-associated autolytic enzymes that destroy the cell wall. Other, minor mechanisms include the inhibition of bacterial endopeptidases and glycosidases. Their activity spectrum includes most Gram-positive, and many Gram-negative and anaerobic organisms.

2.1.2. Sulfonamides & Trimethoprim

Sulfonamides are folate synthesis inhibitors. They inhibit bacterial modification of *p*-aminobenzoic acid into dihydrofolate by competitively binding to the enzyme dihydropteroate synthetase; trimethoprim (TMP) inhibits bacterial dihydrofolate reductase. This sequential inhibition of folate metabolism ultimately prevents the synthesis of bacterial DNA. Since mammalian cells do not synthesize folic acid, human purine synthesis is not affected significantly by sulfonamides or TMP. They are inhibitory to a variety of Gram-positive and Gram-negative bacteria, fungi and parasites.

2.1.3. Quinolones

Quinolones are a bactericidal class of antibiotic. Their primary bacterial target is DNA gyrase, a type II DNA topoisomerase enzyme essential for DNA replication, recombination and repair; some newer quinolones also inhibit Topoisomerase IV, thus inhibiting DNA replication and transcription. Their activity spectrum varies widely, with first generation compounds being inactive against Gram-positive cocci, while the latest generation shows extended activity against both Gram-negative and Gram-positive bacteria.

2.1.4. Macrolides

Macrolides inhibit RNA-dependent bacterial protein synthesis by binding reversibly to the 23S rRNA of the 50S ribosomal subunits of susceptible organisms, thereby blocking the translocation reaction of peptidyl tRNA. The reversible nature of this interaction renders them bacteriostatic rather than bactericidal. Their activity spectrum includes Gram-positive and some Gram-negative bacteria, mycoplasmas, chlamydiae, treponemes, and rickettsiae.

2.1.5. Tetracyclines & Glycylcyclines

Tetracyclines are bacteriostatic antibiotics with broad spectrum activity. They enter bacteria by an energy-dependent process and inhibit bacterial protein synthesis by binding reversibly to the 30S ribosomal subunit, thus preventing the attachment of aminoacyl-tRNA to the ribosomal acceptor A-site in the RNA-ribosome complex. Their activity spectrum includes many Gram-positive and Gram-negative bacteria, mycoplasmas, chlamydiae, rickettsiae, as well as some protozoa.

2.1.6. Aminoglycosides & Aminocyclitols

Aminoglycosides are another bactericidal class of antibiotics. They inhibit bacterial protein synthesis by binding irreversibly to the bacterial 30S ribosomal subunit, which becomes unavailable for the translation of mRNA during protein synthesis. They can also cause misreading of the genetic code leading to production of nonsense proteins. An aerobic energy-dependent process is necessary for penetration of the bacterial inner cell membrane. Their activity spectrum is primarily aerobic, Gram-negative bacilli, and *S. aureus*.

Aminocyclitols inhibit bacterial protein synthesis through the same route, however, they are not bactericidal, and do not cause misreading of mRNA.

2.1.7. Glycopeptides

Glycopeptides inhibit peptidoglycan synthesis of Gram-positive strains in the bacterial cell wall by complexing with the D-alanyl-D-alanine portion of the cell wall precursor. They are active mainly against aerobic and anaerobic Gram-positive species.

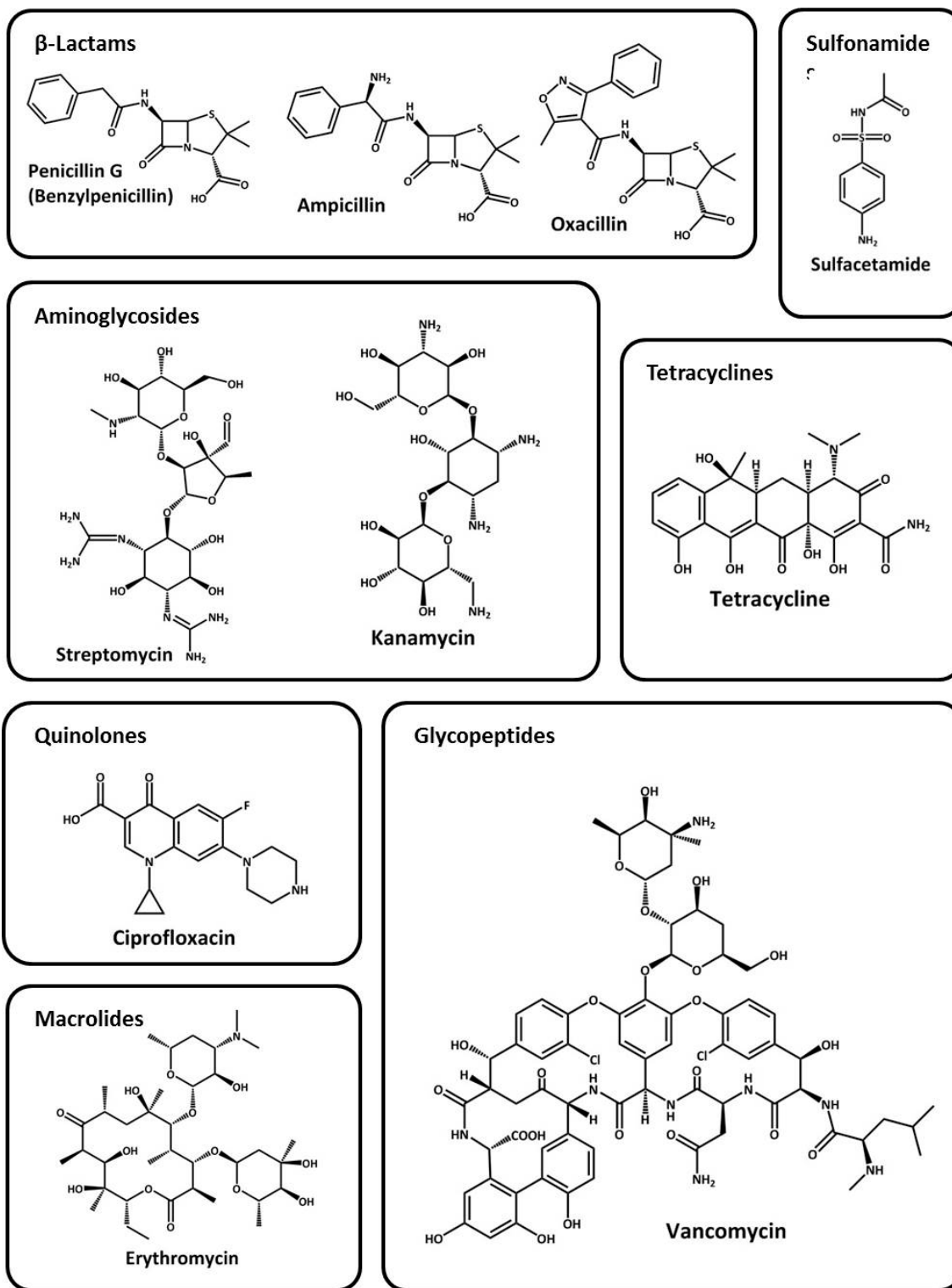


Figure III-1 Chemical structures of used antibiotics.

The chemical structures of the antibiotics used in this chapter are given. They include the β-lactam antibiotics penicillin G, ampicillin, and oxacillin; the sulfonamide sulfacetamide; the aminoglycosides streptomycin and kanamycin; tetracycline; the quinolone ciprofloxacin; the macrolide erythromycin; and the glycopeptide vancomycin.

2.2. Materials

2.2.1. Biological Materials

2.2.1.1. Bacteria

The following, previously described bacterial strains were used in these experiments.

Gram-negative strains:

- *Escherichia coli* BL21; ATCC #BAA-1025; (*E. coli*); Risk Group: 1

Gram-positive strains:

- methicillin-susceptible *Staphylococcus aureus* (MSSA); clinical isolate; Risk Group:
1

2.2.1.2. Mammalian Cells

The following mammalian cell line was used:

- SK-N-AS, human neuroblastoma, ATCC # CRL-2137, Risk Group: 1 (American Type Culture Collection (ATCC), Manassas, VA, USA)

2.2.2. Chemicals

Some experiments also required use of specially prepared solutions and other chemicals including the following:

Ampicillin; Kanamycin; Penicillin G; Tetracycline; Oxacillin (all Sigma-Aldrich); Sulfacetamide; Vancomycin (both Alfa-Aesar); Ciprofloxacin (Enzo Life Sciences, Inc.); Erythromycin; Streptomycin (Amresco, LLC).

2.3. Methods

2.3.1. Killing bacteria

Bacterial cell cultures were grown as described in Chapter II, Section 2.7.3.4.

In preliminary experiments, bacteria were killed through different means. The methods and agents for killing bacteria selected for this series of experiments are either established methods of sterilisation (γ -radiation, autoclave), antibiotics in clinical use (penicillin, ampicillin, kanamycin), or used to break bacterial cell walls in order to allow isolation of cytosolic proteins (French press). Therefore, one would expect total or at the very least high bacteria killing efficacies.

These different approaches could be divided into methods that either cause cell wall damage – i.e., an 18-h incubation with antibiotic classes like β -lactams or glycopeptides (penicillin, vancomycin, etc.), autoclaving for 45 min at 121°C, and one pass-through with a French press; or left it intact — i.e., incubation with antibiotic classes like aminoglycosides or quinolones (kanamycin, ciprofloxacin, etc.), and γ -irradiation. Subsequently, killing success was checked by plating samples on agar plates. Dead bacteria or bacterial fragments were isolated by centrifugation for 10 minutes at $3,716 \times g$ and washing once with PBS; the growth medium (supernatant) and wash solution were saved.

For the last experiment (see section 2.4.1.4), *E. coli* and MSSA bacterial cultures were incubated with dilution series of penicillin, kanamycin, or sulfacetamide (final concentration: 100/10/1/0 $\mu\text{g}/\text{mL}$) for 24 hours. Then, bacterial fragments were again isolated by centrifugation for 10 minutes at $3,716 \times g$ and washing once with PBS; the supernatant and wash solution were saved. Bacterial fragments were re-suspended in PBS (original volume) for incubation with neuroblastoma cell cultures.

2.3.2. Resazurin Cell Viability Assay

To further test the effect on bacterial viability of the different treatments described above, the Resazurin Cell Viability Assay was used (17-19) (Figure III-2). Resazurin (see Figure III-2 has a number of advantages over MTT ((3-(4,5-Dimethylthiazol-2-yl)-2,5-diphenyltetrazolium bromide); see Chapter II, Section 3.4.3.1). Firstly, the formazan formed by reduction (resorufin) is water-soluble, thus avoiding washing and extraction steps necessary with MTT. Secondly, its redox potential ($E_0 = +380$ mV (pH 7.0/25°C)) allows it to be reduced by cytochromes (typically $E_0 = +290 - +80$ mV (pH 7.0/25°C)), whereas MTT ($E_0 = -110$ mV (pH 7.0/25°C)) is not; this prevents possible interference with the flow of electrons through the electron transport chain and blockage of the respiratory chain. And thirdly, its reduction can be detected by both, fluorescence- and absorbance-based methods.

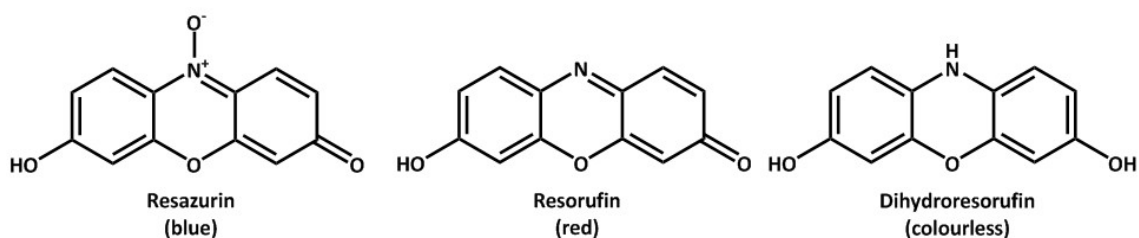


Figure III-2 Resazurin and related compounds.

Reduction of the non-fluorescent, blue resazurin in metabolically active cells yields the fluorescent red resorufin, which may be further reduced to the non-fluorescent, uncoloured dihydroresorufin (19).

For the assay, a 100 × resazurin stock solution (5 mg/mL in HPLC-grade water) was diluted 1:10 and a volume equal to 10% of the well content was added to the wells. Bacterial cultures in 96-well plates were then incubated directly in the microplate reader at 37°C, with a reading of the OD_{595} taken every 10 minutes for one hour.

2.3.3. Testing the Hypothesis

In order to evaluate the hypothesis that penicillin may be a risk factor for AD, neuroblastoma cells were seeded at 10,000 cells/well into 96-well plates and incubated for 24 hours until confluency was reached (as described in Chapter II, Section 2.7.3.7). Then, used growth medium was replaced with 180 μL /well fresh growth medium. 20 μL /well of the supernatant of bacteria killed by different means as described in section 2.3.1 were added immediately (24 h sample), after 16 hours (8 h sample), and after 24 hours (0 h sample). Immediately after the last addition of killed bacteria (0 h sample), supernatant and cell lysate samples were taken as described in Chapter II, Section 2.7.3.10. Finally, A β production by neuroblastoma cells induced by incubation with these different samples was determined by ELISA as described in Chapter II, Section 2.7.3.3 (b) with 6E10 capture antibody and bio4G8 detection antibody.

In order to estimate effects of antibiotic-treated bacteria on the growth and proliferation of the neuroblastoma cells, total protein content of SK-N-AS cells that had been incubated for 24 hours with the supernatant of MSSA bacteria treated for 24 hours with a dilution series (100 / 50 / 25 / 10 / 5 / 0 $\mu\text{g}/\text{mL}$) of ten different antibiotics (Ampicillin, Ciprofloxacin, Erythromycin, Kanamycin, Oxacillin, Penicillin G, Streptomycin, Sulfacetamide, Tetracycline, Vancomycin) was determined with the BCA Assay as described in Chapter II, Section 2.7.3.2 (b).

2.4. Results & Discussion

Since this is an ongoing project that is still in the early stages, only preliminary results can be presented in some instances, and some experiments will need to be repeated with optimised conditions.

2.4.1. Preliminary Experiments

Originally, it was planned to incubate the neuroblastoma cells directly with suspensions of dead bacteria (to avoid losses of any potentially active component); however, after considering problems encountered previously during co-incubation of “killed” bacteria¹ with mammalian cell cultures (see Chapter II, Section 2.7.3.6), it was decided to first check the killing efficacy of the methods utilised here.

2.4.1.1. Bacteria killing efficacy

With the concern that the antibiotics may not give complete killing of the culture, it was planned to γ -irradiate the bacteria samples if they were to still show growth after antibiotic treatment. γ -Irradiation was chosen because it does not damage the bacterial cell walls thus preventing alteration of the nature of the respective samples.

To establish the bacteria killing efficacy of γ -irradiation, *E. coli* and MSSA bacterial cultures were grown until they reached the log phase ($OD_{595} \sim 0.5$); 1 mL of sample were then irradiated with γ -radiation from a Co-60 source (located in the Tupper Building, Dalhousie University) for 10 minutes (= 100 Gy²). Plating of the γ -irradiated sample proved that this radiation dose was not sufficient to achieve complete killing of the bacteria. Irradiation for 6 hours (= 1500 Gy) was enough to kill 100 % of *E. coli* bacteria, however, MSSA samples had to be diluted at least 1:6 to achieve complete killing with that dose of radiation.

Following these first experiments, the other killing methods were tested; results are summarised in Table III-1. None of the antibiotics achieved total killing, the autoclaving

¹ 100% killing is required for co-incubation (longer than a couple of hours) of bacteria with mammalian cell cultures in order to avoid that the bacteria overgrown the culture.

² Gy = gray: SI derived unit of absorbed dose of ionising radiation; defined as absorption of 1 J of such energy per 1 kg of matter (20).

conditions established earlier (see Chapter II, Section 2.7.3.6) were repeated to confirm them. One pass-through with the French press of the samples did not completely kill the bacteria; however, for protein isolation, typically at least three pass-throughs are performed to achieve efficient lysis.

Table III-1 Comparison of the efficacy of methods to kill bacteria.

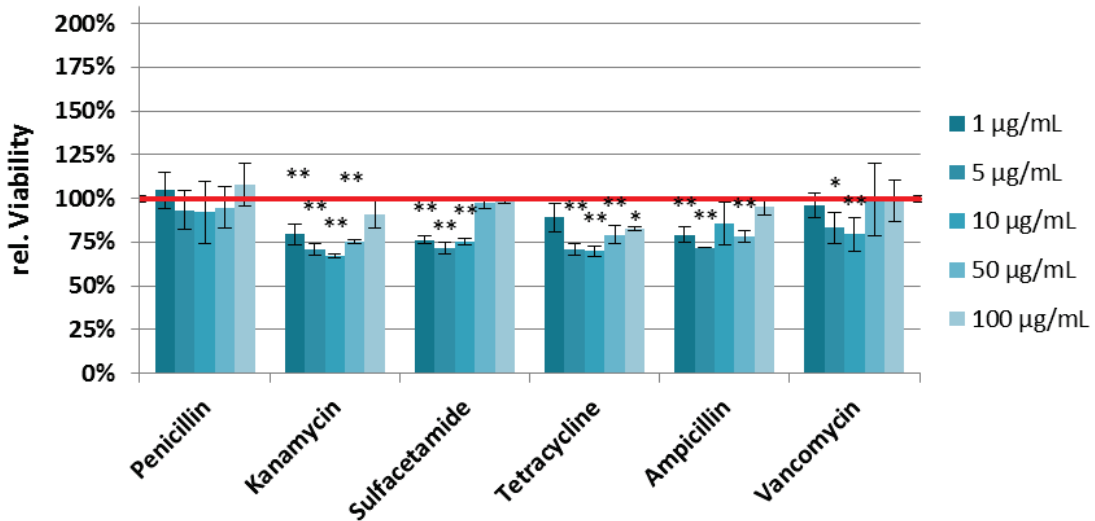
Bacteria treatment	<i>E. coli</i> (Gram-negative)	MSSA (Gram-positive)	Compromise of cell wall integrity
γ-Radiation (1500 Gy / 6 hours)	+	+	N
Ampicillin (50 µg/mL)	-	-	Y
Kanamycin (10 g/mL)	-	-	N
Penicillin (100 IU/mL)	-	-	Y
Autoclave (121°C / 45 min)	+	+	Y
French Press (1 pass-through)	-	-	Y

In a related experiment, the bacterial toxicity of six antibiotics — penicillin, kanamycin, sulfacetamide, tetracycline, ampicillin, and vancomycin — was determined. *E. coli* was incubated with a dilution series of each of these antibiotics (100 / 50 / 10 / 5 / 1 µg/mL), and bacterial viability was determined after 30 and 60 minutes by the Resazurin assay (see Figure III-3).

As expected, penicillin and vancomycin exhibited little to no activity against *E. coli*, a Gram-negative rod-shaped bacterium, while kanamycin, sulfacetamide, tetracycline, and ampicillin were more active. A curious observation for all antibiotics is that the activity, after reaching a maximum at 5 – 10 µg/mL, seems to decrease again with increasing antibiotic

concentration. Furthermore, that activity seems to decrease with longer incubation, possibly an artifact of bacterial cultures with lower than standard dilutions for the experiment.

Bacterial Viability (30 min)



Bacterial Viability (60 min)

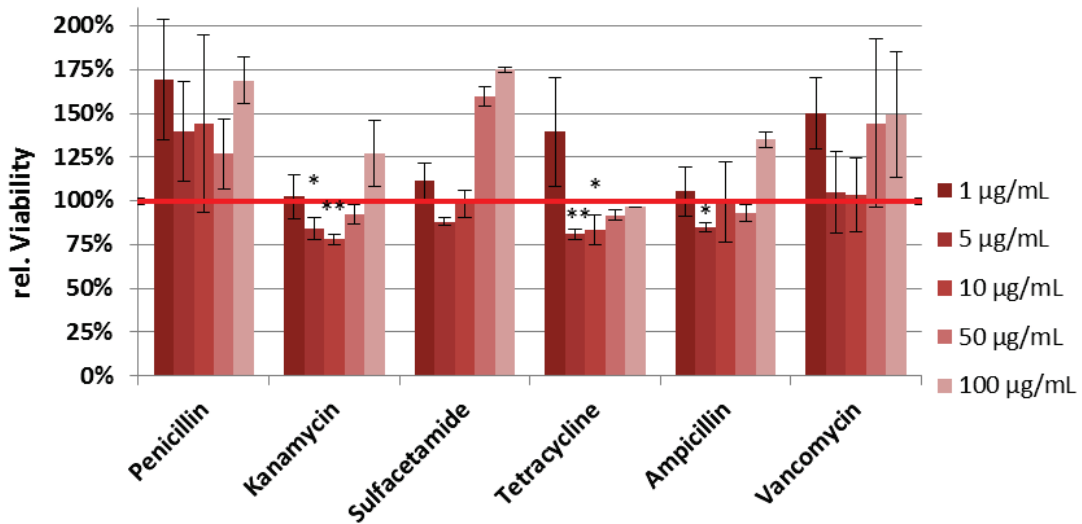


Figure III-3 Bacterial toxicity of antibiotics.

To determine the bacterial toxicity of six antibiotics (Penicillin, Kanamycin, Sulfacetamide, Tetracycline, Ampicillin, Vancomycin), *E. coli* was incubated with a dilution series of each of these antibiotics (100 / 50 / 10 / 5 / 1 µg/mL); bacterial viability was determined by the Resazurin assay after 30 and 60 minutes. The relative bacterial viability is calculated in relation to incubation of bacteria without antibiotics (control, red line; note the error bars on either side). Error Bars: ± S.E.M.; *: P < 0.05, **: P < 0.01 (two-tailed Student's t-test), n = 2, for control n = 16.

2.4.1.2. A β production induced by bacterial fragments and medium

To find out whether the active agents (supposedly LPS and LTA) that induce A β production in the neuroblastoma cells are released into the growth medium or stay in the membrane fragments, SK-N-AS neuroblastoma cells were incubated for 18 hours with fragments and medium of *E. coli* and MSSA bacteria killed by autoclaving. Subsequently, A β production in the supernatant and cell lysate was determined by ELISA.

Inspection of the results (see Figure III-4) reveals a clear difference; while incubation with the bacterial growth medium did not cause production of appreciable amounts of A β (less than the lowest standard), incubation with bacterial fragments did. Furthermore, for both *E. coli* and MSSA only the amount of A β secreted into the supernatant was significantly higher than control, but not the amount found in the cell lysate.

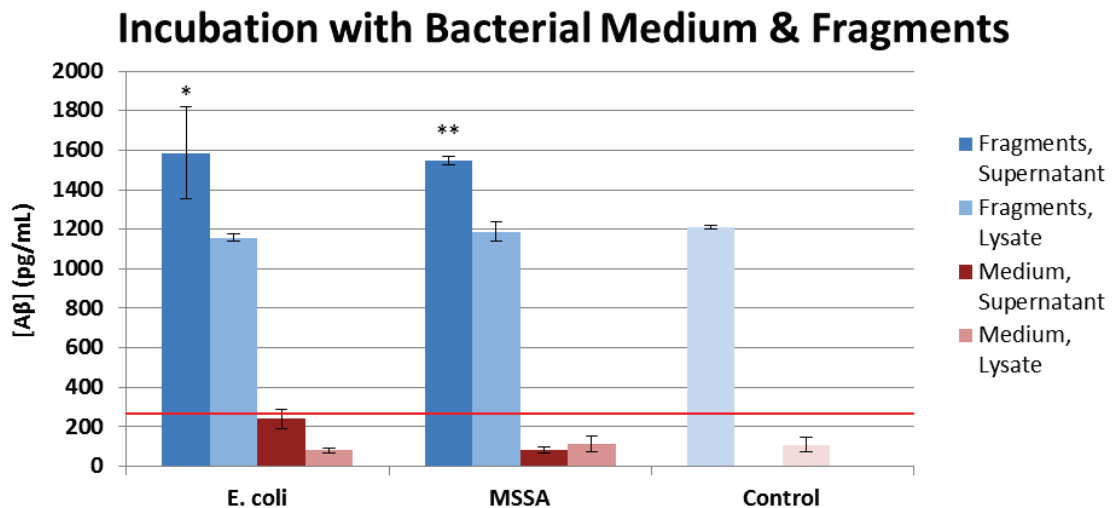


Figure III-4 A β production in SK-N-AS neuroblastoma cells induced by incubation with bacterial medium and fragments.

SK-N-AS neuroblastoma cells were incubated with the medium and fragments of *E. coli* and MSSA bacteria killed by autoclaving. A β production in the supernatant and cell lysate was determined by ELISA. The red line shows the concentration of the lowest A β standard (266 pM; nominally 187.5 pM). Error Bars: \pm S.E.M.; *: $P < 0.05$, **: $P < 0.01$ (compared to Control); $n = 3$; two-tailed Student's t-test.

2.4.1.3. A β production induced by bacterial fragments obtained through γ -irradiation and autoclaving

In a next step, it was investigated what difference the bacteria killing method and the incubation time makes for the induced A β production. *E. coli* and MSSA bacteria were killed by γ -irradiation and autoclaving, and fragments were isolated; SK-N-AS neuroblastoma cell cultures were incubated with the isolated bacterial fragments for 3 or 24 hours; A β production in the supernatant was determined by ELISA.

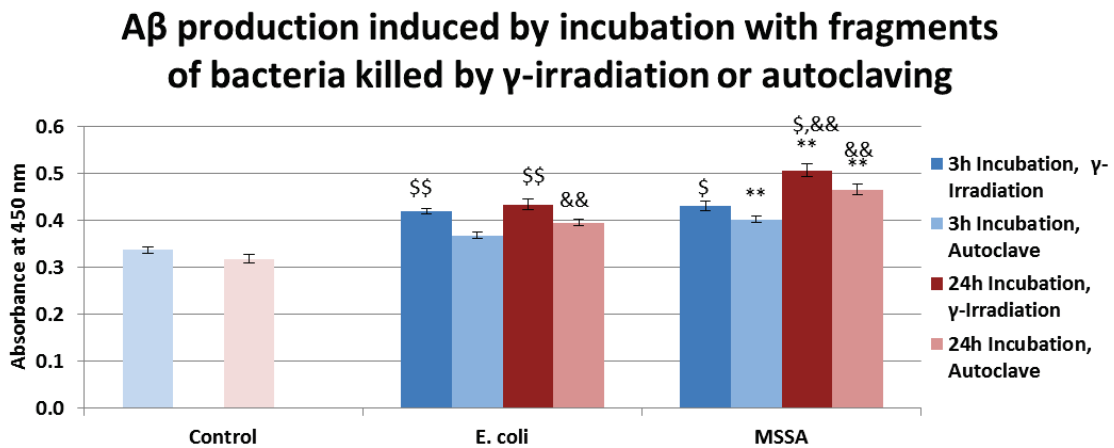


Figure III-5 A β production in SK-N-AS neuroblastoma cells induced by incubation with fragments of bacteria killed by γ -irradiation or autoclaving.

SK-N-AS neuroblastoma cells were incubated for 3 or 24 hours with the fragments of *E. coli* and MSSA bacteria obtained through either γ -irradiation or autoclaving. A β production in the supernatant was determined by ELISA. Error Bars: \pm S.E.M.; \$: P < 0.05, \$\$: P < 0.01 (comparing killing methods); *: P < 0.05, **: P < 0.01 (comparing bacterial strains); &: P < 0.05, &&: P < 0.01 (comparing incubation times); n = 8; two-tailed Student's t-test.

As can be seen in Figure III-5, for both bacterial strains, both killing methods led to significantly increased A β production, with fragments from bacteria killed by γ -irradiation inducing a significantly higher production of A β than those from bacteria killed by autoclaving.

MSSA fragments caused in most cases a significantly higher A β production than *E. coli* fragments, as did a longer incubation time.

The result that samples from γ -irradiated bacteria induce a higher production of A β compared to those obtained by autoclaving is somewhat unexpected. It was thought that γ -radiation would leave the cell wall of the bacteria intact, whereas autoclaving would destroy it, thus leading to a higher A β production induced by the active compound released from the compromised cell wall. One explanation might be that the heat from the autoclaving process inactivated some of the active compounds thereby leading to a reduced response by the neuroblastoma cells.

2.4.1.4. A β production induced by bacterial fragments obtained through treatment with antibiotics

Initially, experiments were performed using three antibiotics. Cultures of *E. coli* and MSSA were incubated with ampicillin (50 μ g/mL), penicillin (100 IU/mL), and kanamycin (10 μ g/mL) for 5 hours. Supernatants were isolated; then, SK-N-AS neuroblastoma cells cultures were incubated with 20 μ L/ well (total volume: 200 μ L/ well) of these supernatants for 3 hours. This short incubation time was chosen to prevent bacteria that had not been killed by the antibiotic from overpowering the cell culture. γ -Irradiation had not been performed since the previous experiment did not show conclusively that it would not have an influence on the induced A β production. Furthermore, time series experiments with LPS and LTA had shown a significantly increased A β production already after 1 hour (see Chapter II, Section 2.7.4).

The results show an increased A β production upon incubation with the bacterial supernatants (see Figure III-6), however, since it did not reach statistical significance, not much can be said about any trends or comparisons. In a repeat experiment, longer incubation time

and more samples per condition may lead to a higher production of A β and smaller error bars in order to reach statistical significance.

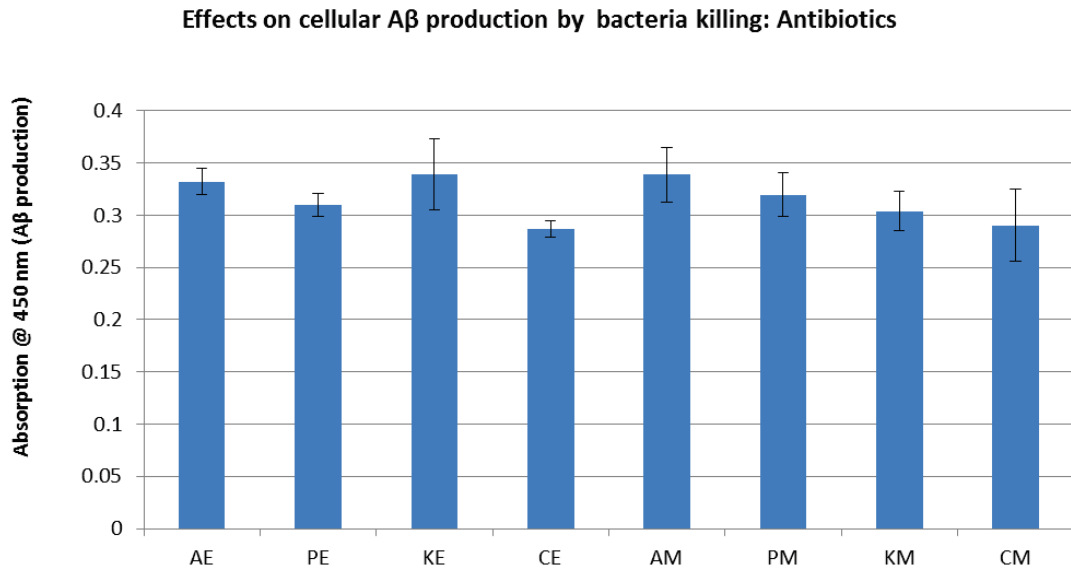
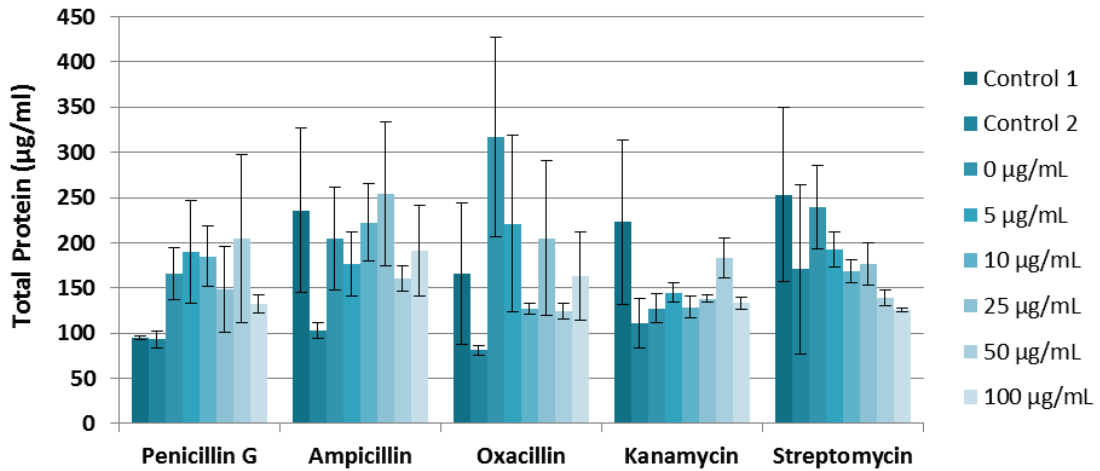


Figure III-6 A β production in SK-N-AS neuroblastoma cells induced by incubation with fragments of bacteria killed by different antibiotics.

SK-N-AS neuroblastoma cells were incubated for 3 hours with the fragments of *E. coli* (E) and MSSA (M) bacteria obtained through treatment with different antibiotics (A: ampicillin; P: penicillin; K: kanamycin). A β production in the supernatant was determined by ELISA. Error Bars: \pm S.E.M.; *: $P < 0.05$ (compared to respective controls (CE & CM)); $n = 4$; two-tailed Student's *t*-test.

In order to estimate effects of antibiotic-treated bacteria on the growth and proliferation of the neuroblastoma cells, total protein content of SK-N-AS cells that had been incubated for 24 hours with the supernatant of MSSA bacteria treated for 24 hours with a dilution series (100 / 50 / 25 / 10 / 5 / 0 $\mu\text{g}/\text{mL}$) of ten different antibiotics (Ampicillin, Ciprofloxacin, Erythromycin, Kanamycin, Oxacillin, Penicillin G, Streptomycin, Sulfacetamide, Tetracycline, Vancomycin) was determined with the BCA Assay (see Figure III-7).

Effect of antibiotic-treated MSSA on total protein production by SK-N-AS



Effect of antibiotic-treated MSSA on total protein production by SK-N-AS

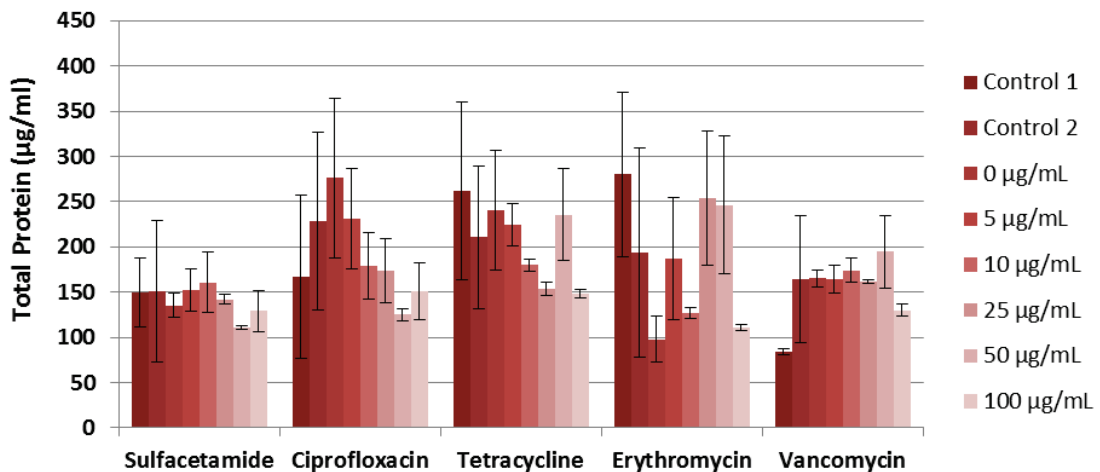


Figure III-7 Effect of antibiotic-treated MSSA on total protein production by SK-N-AS neuroblastoma cells.

SK-N-AS neuroblastoma cells were incubated with the supernatant of MSSA treated with a dilution series of 10 different antibiotics. Total protein production was determined by BCA assay. Control was incubation of antibiotic and bacteria without SK-N-AS. Error Bars: \pm S.E.M.; n = 2.

Unfortunately, results were not interpretable due to the large error bars. A repetition of this experiment might be able to show some differences caused by the different classes of antibiotics. It should also include controls for the effect of the antibiotic alone on protein

production by the SK-N-AS cells, since the antibiotics are still present, albeit diluted, in the supernatant of the bacteria added to the growth medium of the neuroblastoma cells.

Finally, a large experiment was conducted, where SK-N-AS neuroblastoma cells were incubated for different time intervals (0 / 8 / 24 hours) with supernatants from *E. coli* and MSSA treated with dilution series (0 / 1 / 10 / 100 $\mu\text{g}/\text{mL}$) of three antibiotics (kanamycin, penicillin, sulfacetamide); then A β production in the supernatant and cell lysate was determined by ELISA (Figure III-8 and Figure III-9).

Again, due to large error bars for most samples interpretation of the data was practically impossible. For *E. coli*, no trends were discernible and most values were at or below controls. For MSSA, A β production in the supernatant generally seemed to be higher than in the cell lysate. In a repeat experiment, care should be taken with pipetting to reduce the size of the error bars. Along the same line, the number of samples per condition should be increased.

Aβ production in SK-N-AS induced by incubation with *E. coli* fragments

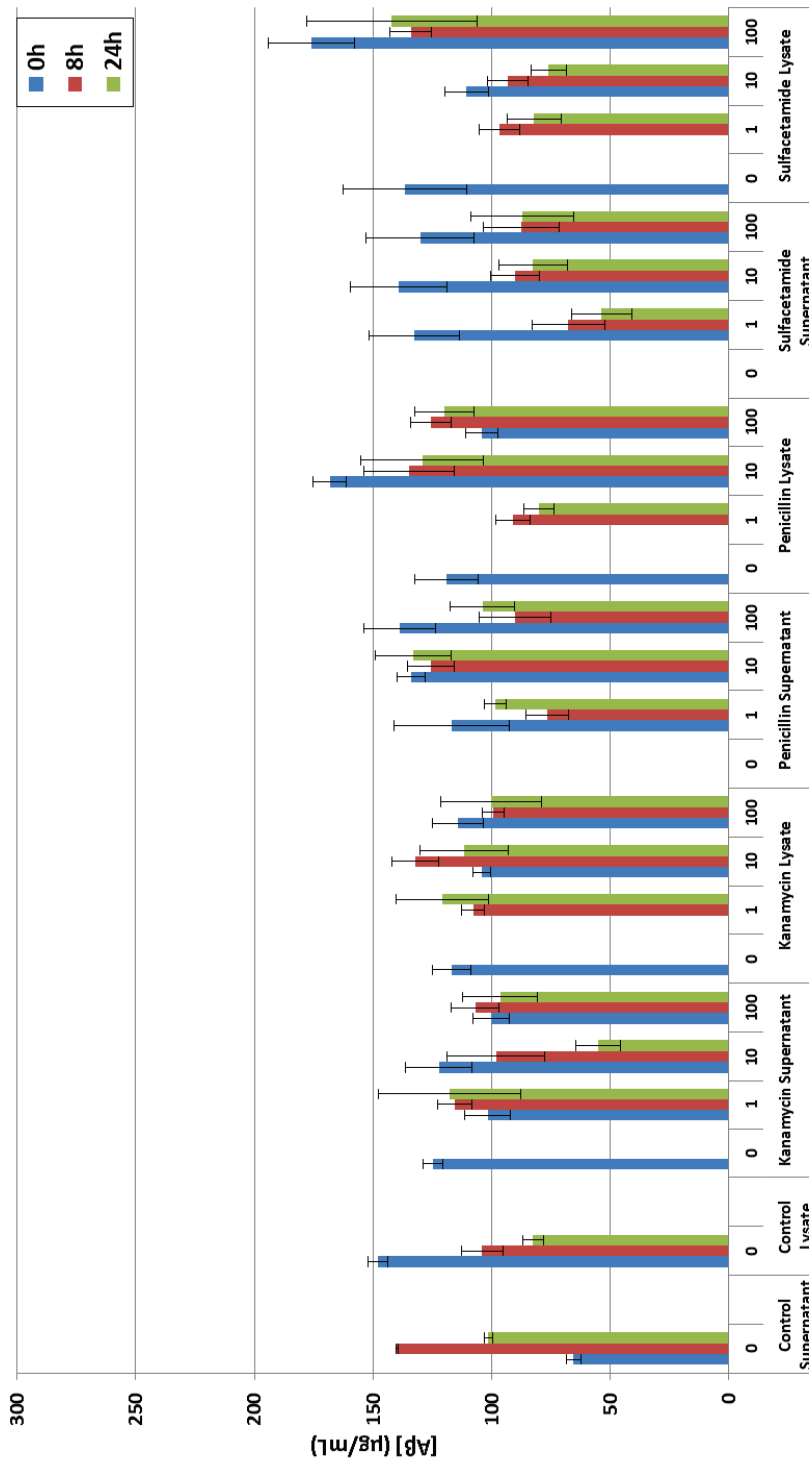


Figure III-8 Aβ production in SK-N-AS induced by incubation with *E. coli* fragments.

SK-N-AS neuroblastoma cells were incubated for 0, 8, and 24 hours with the supernatants of *E. coli* treated with dilution series of three antibiotics (kanamycin, penicillin, sulfacetamide); Aβ production in the supernatant and lysate of the cells was then determined by ELISA. Values are average of two independent experiments determined in duplicate; error bars: ± S.E.M.; n = 2.

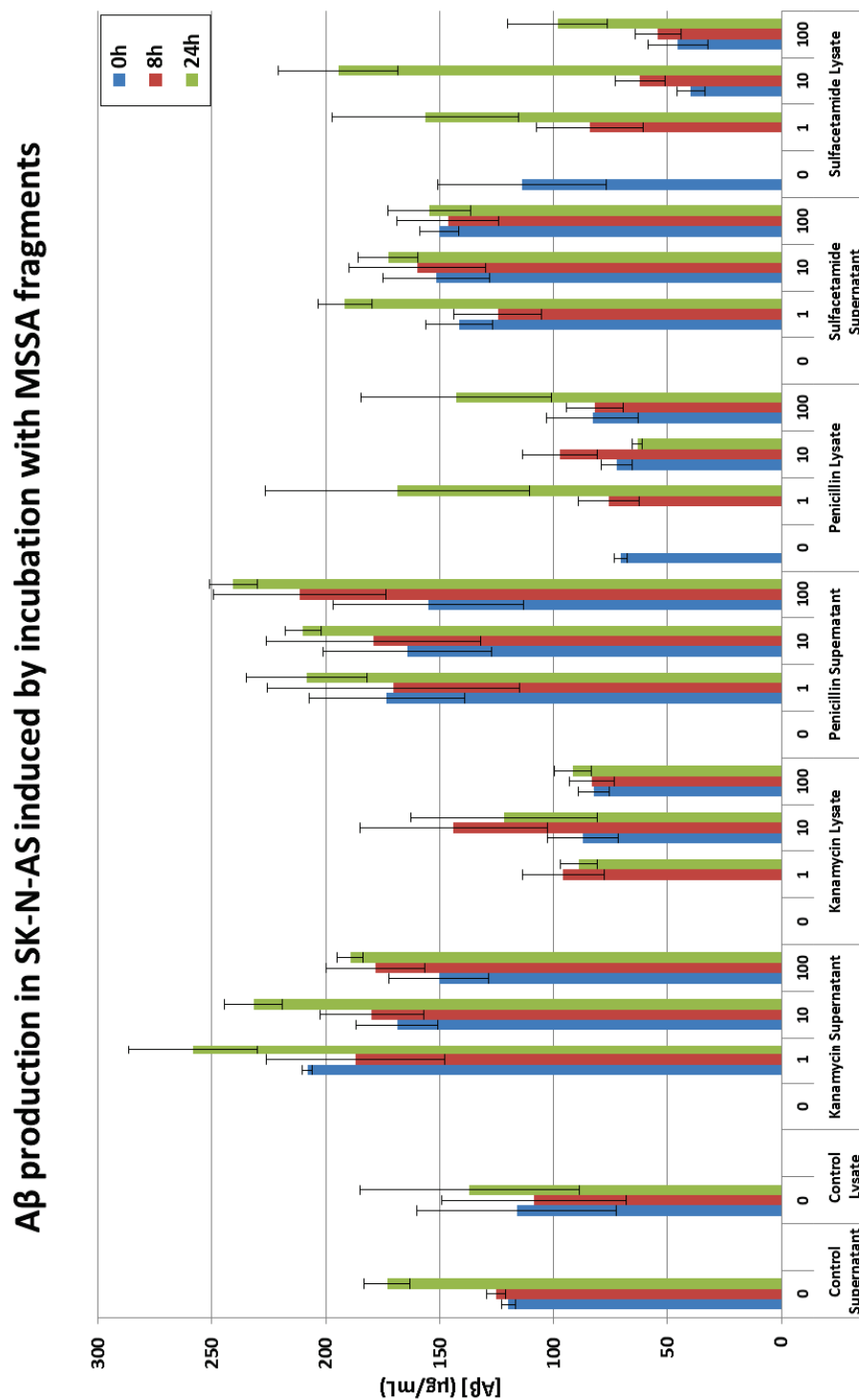


Figure III-9 Aβ production in SK-N-AS induced by incubation with MSSA fragments.

SK-N-AS neuroblastoma cells were incubated for 0, 8, and 24 hours with the supernatants of MSSA treated with dilution series of three antibiotics (kanamycin, penicillin, sulfacetamide); Aβ production in the supernatant and lysate of the cells was then determined by ELISA. Values are average of two independent experiments determined in duplicate; error bars: ± S.E.M.; n = 2.

3. Conclusion & Future Work

Bacterial cell components can be potent stimulators of the immune system. As shown in the previous chapter, their specific membrane lipids are able to bind with A β to form the toxic form that initiates and enters the Vicious Cycle of AD. We provide evidence here that bacteria killed by cell wall/cell membrane-active agents can induce the production of A β . This then raises the possibility of an antibiotic's link with the development of Alzheimer's disease.

While the experiments performed here certainly provide plausibility to this hypothesis, it would be necessary to do further research into this area to draw more definitive conclusions. Besides repetition of some of these experiments as mentioned in the discussion, some suggested experiments would include incubations with antibiotics of other classes; determining cell wall integrity after killing bacteria, e.g., by Trypan Blue or Live/Dead[®] stain; quantitating how much LPS or LTA is released by each killing method using mass spectrometry or ELISA; test dilution series of LPS/LTA and bacterial fragments for concentration dependence of the induced A β production; and determining the influence of added A β ₁₂₋₁₇ (VHHQKL \rightarrow BBXB is binding motif for LPS (LTA?)) on the induced A β production.

An animal trial is in the planning stage pending the outcome of further in vitro test results. Performed by Kurt Stover, a Ph.D. student working under the supervision of Dr. Richard Brown at Dalhousie's Department of Psychology, it is intended to infect AD transgenic mice with bacteria, treat them with different antibiotics, and determine behaviour and brain pathology changes (in particular plaque load) over a time period of about six months in order to evaluate the influence that different classes of antibiotics may have on the progression of AD.

4. References

1. Tomasz, A.; Waks, S. Mechanism of action of penicillin: triggering of the pneumococcal autolytic enzyme by inhibitors of cell wall synthesis. *Proc. Natl. Acad. Sci. U. S. A.* **1975**, *72*, 4162-4166.
2. Nau, R.; Eiffert, H. Modulation of release of proinflammatory bacterial compounds by antibacterials: potential impact on course of inflammation and outcome in sepsis and meningitis. *Clin. Microbiol. Rev.* **2002**, *15*, 95-110.
3. Goto, H.; Nakamura, S. Liberation of endotoxin from *Escherichia coli* by addition of antibiotics. *Jpn. J. Exp. Med.* **1980**, *50*, 35-43.
4. Crosby, H. A.; Bion, J. F.; Penn, C. W.; Elliott, T. S. Antibiotic-induced release of endotoxin from bacteria in vitro. *J. Med. Microbiol.* **1994**, *40*, 23-30.
5. Soto, A.; Evans, T. J.; Cohen, J. Proinflammatory cytokine production by human peripheral blood mononuclear cells stimulated with cell-free supernatants of Viridans streptococci. *Cytokine* **1996**, *8*, 300-304.
6. van Langevelde, P.; van Dissel, J. T.; Ravensbergen, E.; Appelmelk, B. J.; Schrijver, I. A.; Groeneveld, P. H. Antibiotic-induced release of lipoteichoic acid and peptidoglycan from *Staphylococcus aureus*: quantitative measurements and biological reactivities. *Antimicrob. Agents Chemother.* **1998**, *42*, 3073-3078.
7. Mattie, H.; Stuertz, K.; Nau, R.; van Dissel, J. T. Pharmacodynamics of antibiotics with respect to bacterial killing of and release of lipoteichoic acid by *Streptococcus pneumoniae*. *J. Antimicrob. Chemother.* **2005**, *56*, 154-159.
8. Heumann, D.; Barras, C.; Severin, A.; Glauser, M. P.; Tomasz, A. Gram-positive cell walls stimulate synthesis of tumor necrosis factor α and interleukin-6 by human monocytes. *Infect. Immun.* **1994**, *62*, 2715-2721.
9. Heumann, D.; Roger, T. Initial responses to endotoxins and Gram-negative bacteria. *Clinica Chimica Acta* **2002**, *323*, 59-72.
10. Heumann, D.; Glauser, M. P.; Calandra, T. Molecular basis of host-pathogen interaction in septic shock. *Curr. Opin. Microbiol.* **1998**, *1*, 49-55.

11. Elson, G.; Dunn-Siegrist, I.; Daubeuf, B.; Pugin, J. Contribution of Toll-like receptors to the innate immune response to Gram-negative and Gram-positive bacteria. *Blood* **2007**, *109*, 1574-1583.
12. Ginsburg, I. The role of bacteriolysis in the pathophysiology of inflammation, infection and post-infectious sequelae. *APMIS* **2002**, *110*, 753-770.
13. Kirikae, T.; Nakano, M.; Morrison, D. C. Antibiotic-induced endotoxin release from bacteria and its clinical significance. *Microbiol. Immunol.* **1997**, *41*, 285-294.
14. Bucklin, S. E.; Fujihara, Y.; Leeson, M. C.; Morrison, D. C. Differential antibiotic-induced release of endotoxin from gram-negative bacteria. *Eur. J. Clin. Microbiol. Infect. Dis.* **1994**, *13 Suppl 1*, S43-51.
15. Utsui, Y.; Ohya, S.; Takenouchi, Y.; Tajima, M.; Sugawara, S.; Deguchi, K.; Suginaka, H. Release of lipoteichoic acid from *Staphylococcus aureus* by treatment with cefmetazole and other β -lactam antibiotics. *J. Antibiot. (Tokyo)* **1983**, *36*, 1380-1386.
16. Yao, J. D. C.; Moellering, J., Robert C. In *Antibacterial Agents*; Versalovic, J., Carroll, K. C., Funke, G., Jorgensen, J. H., Landry, M. L. and Warnock, D. W., Eds.; Manual of Clinical Microbiology; ASM Press: Washington, DC, USA, 2011; Vol. 1, pp. 1043-1081.
17. Page, B.; Page, M.; Noel, C. A new fluorometric assay for cytotoxicity measurements in-vitro. *Int. J. Oncol.* **1993**, *3*, 473-476.
18. Ahmed, S. A.; Gogal, R. M., Jr; Walsh, J. E. A new rapid and simple non-radioactive assay to monitor and determine the proliferation of lymphocytes: an alternative to [³H]thymidine incorporation assay. *J. Immunol. Methods* **1994**, *170*, 211-224.
19. O'Brien, J.; Wilson, I.; Orton, T.; Pognan, F. Investigation of the Alamar Blue (resazurin) fluorescent dye for the assessment of mammalian cell cytotoxicity. *Eur. J. Biochem.* **2000**, *267*, 5421-5426.
20. International Bureau of Weights and Measures. The International System of Units (SI). **2006**, 88.

CHAPTER IV.

Microwave-Assisted Solid-Phase Peptide Synthesis

1. Introduction

Peptides and proteins are involved in virtually every biological process. Consequently, research in this field has grown enormously in recent years, producing over 20,000 publications annually (1). It has been established that peptides are involved in as diverse biochemical processes as cell-cell communication, metabolism, immune response and reproduction. As well, their functions as hormones and neurotransmitters are extensively documented. With their importance in so many biochemical and physiological processes, peptides have also received considerable attention as potential drug candidates. Although there are definite problems associated with peptide drugs, some advancement has been made in terms of peptidic drug delivery systems, such as PEGylation, and pulmonary delivery (2, 3). Furthermore, because facile ways for their syntheses are available, they can be used as prototype for the development of small molecule drugs.

Chemical synthesis has several advantages over the recombinant production of peptides and proteins. Firstly, it enables site-specific control of backbone and side-chain modifications that are not available through recombinant methods. Secondly, it offers rapid synthesis of a product that is free from DNA impurities or endotoxins that may be produced during

recombinant synthesis. To date, small proteins with up to 200 amino acid residues have been produced by a combination of different chemical synthetic strategies.

However, there are also a few disadvantages connected with the chemical synthesis approach. This strategy requires the use of toxic reagents, as well as significant amounts of expensive chemicals. It also often suffers from incomplete reactions leading to reduced final product purity and yield.

Solution-phase, solid-phase and combination strategies have been developed for the chemical synthesis of peptides. For large-scale preparations, solution-phase has been the preferred strategy; however, recently some solid-phase methods were developed for this application. For small-scale syntheses of peptides with a chain length of up to 50 amino acid residues, solid-phase peptide synthesis (SPPS) (4) has superseded solution-phase methods.

2. Solid-Phase Peptide Synthesis

2.1. Principles of Solid-Phase Peptide Synthesis

The problems associated with classical solution-phase peptide synthesis (SPPS), namely the extremely time consuming purification and characterization at each step, fuelled the search for an alternative method. In 1963, Merrifield developed a method based on the use of solid resin beads as an anchor for the growing peptide chain (5). Unlike the natural enzymatic peptide synthesis, which is performed from the N- to the C-terminus, in Merrifield's method the peptide is assembled starting from the C-terminus and growing the peptide chain towards the N-terminus (see Figure IV-1). The carboxylate group of the C-terminal amino acid is attached to the resin *via* a linker. The N-terminus carries a temporary protecting group, while side chains are protected permanently if necessary. After removal of the N- α -protecting group, the second amino acid (with N- α - and side chain protecting groups) is added to the reaction in excess, and the C-terminus is activated *in situ* to generate an activated ester thus enabling amide bond formation. Excess reagents and side products are removed by filtration, followed by multiple washing steps with solvent. The N-terminal protecting group of the dipeptide, which is attached to the resin, is removed subsequently to start the next cycle. This procedure is repeated until the desired peptide is assembled. Once the last amino acid (the peptide's N-terminus) is attached, its N- α -protecting group is removed, and simultaneously the peptide is cleaved from the resin and the permanent side chain protecting groups are removed.

Some excellent reviews and books are available discussing in detail the intricacies of SPPS, e.g., Refs. (6-8).

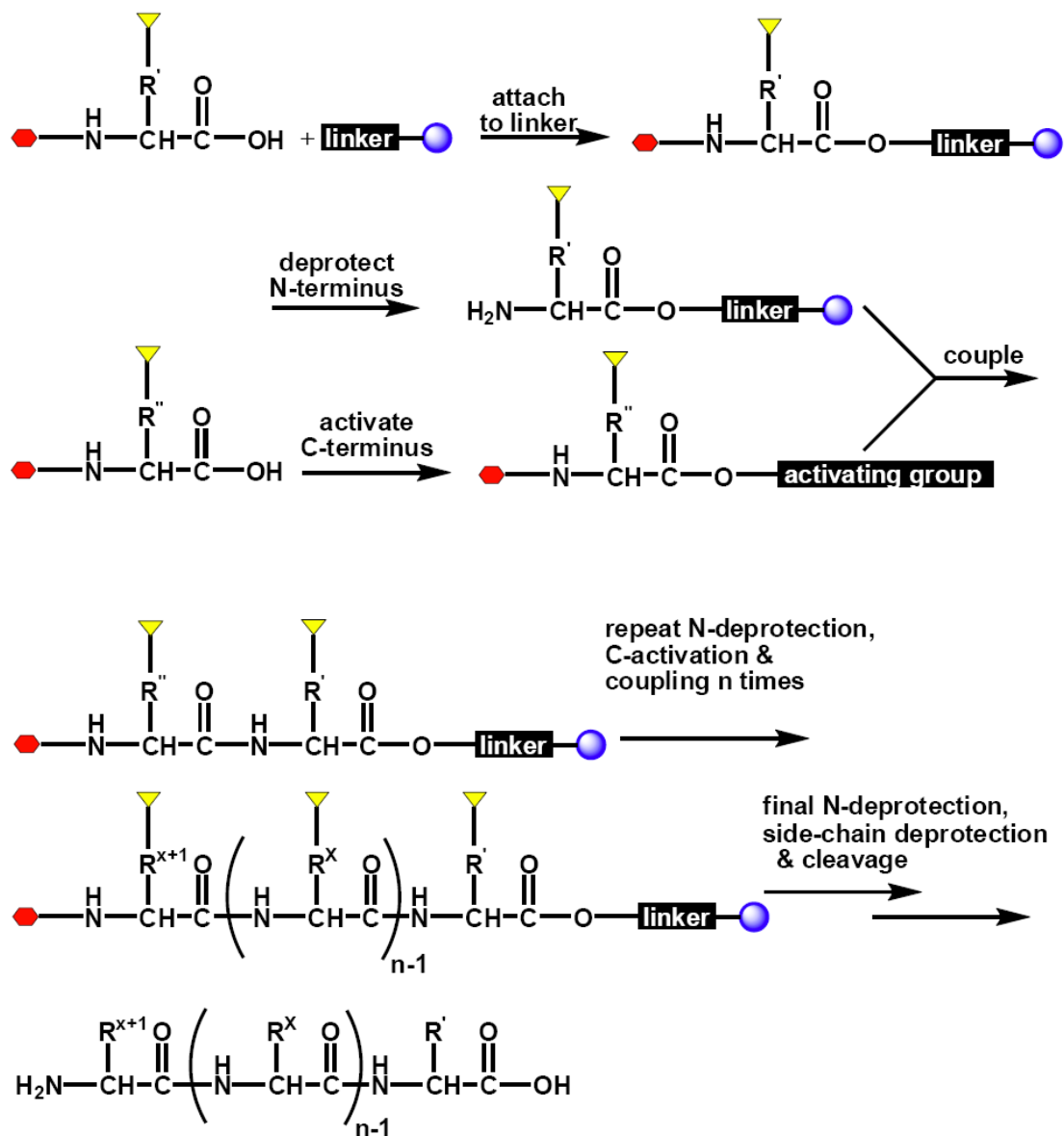


Figure IV-1 General reaction scheme of SPPS.

To begin, the first, N-terminally protected amino acid (C-terminus) is attached via the linker to the resin. After deprotection, it is reacted with the second, (*in situ*) activated amino acid. Deprotection of the last attached amino acid, C-activation of the next amino acid, and coupling are repeated until the sequence is completed. After N-deprotection of the last amino acid (N-terminus), side chains are deprotected simultaneously with cleavage of the peptide from the resin. Red hexagon: N-terminal protecting group; yellow triangle: side-chain protecting group; blue circle: polymer support.

2.2. Principles of Microwave-Assisted Organic Synthesis

2.2.1. Background

The use of microwaves for the purpose of heating was discovered in the 1940s by Percy Spencer (9); the first commercial microwave ovens became available shortly after (in 1947). Microwave ovens have since found widespread use in industrial as well as in domestic settings. In organic synthesis, however, microwave heating was first applied only in the mid-1980s (10, 11), but quickly received widespread attention in the scientific community with over 2,500 publications to date.

2.2.2. Microwaves

Microwaves are a form of electromagnetic radiation that is located between radio and IR frequencies in the electromagnetic spectrum ($\lambda = 1\text{cm} - 1\text{m}$) (see Figure IV-2). Virtually all commercially available microwave ovens (domestic and laboratory) operate at a frequency of $\nu = 2.45\text{ GHz}$ ($\lambda = 12.25\text{ cm}$), one of the five ISM frequencies assigned for the use in industrial, scientific, and medical microwave ovens.

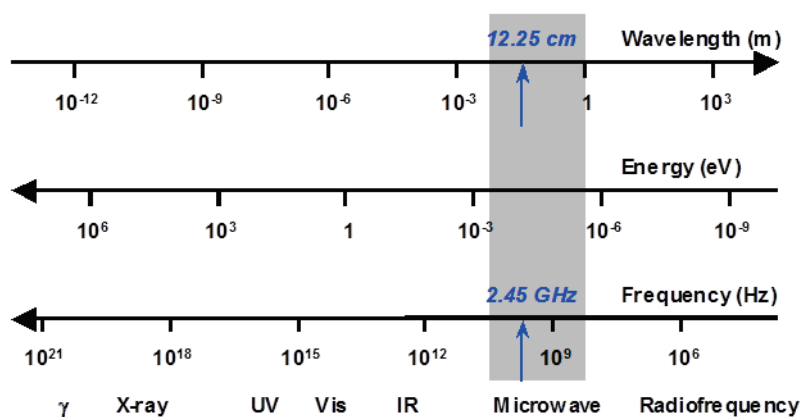


Figure IV-2 The electromagnetic spectrum. Wavelength, energy and frequency of the electromagnetic spectrum are given. The range for microwaves is highlighted in grey, with the approximate location of the frequency of the used instrument indicated by blue arrows.

As becomes evident from comparing the data in Table IV-1, the energy of a microwave photon is too small to cleave any molecular bonds, and is even lower than Brownian motion. Thus, as opposed to ultraviolet and visible radiation, microwaves cannot induce a chemical reaction by direct absorption of their electromagnetic energy. However, microwave dielectric heating was found to be an efficient way of heating reaction mixtures.

Table IV-1 Comparison of frequency and quantum energy of a range of radiation types with the bond energy of select bond types (12-14).

Radiation Type	Frequency (MHz)	Quantum energy (eV)	Bond type	Bond energy (eV)
γ rays	3.0×10^{14}	1.24×10^6	C-C single bond	3.61
X-rays	3.0×10^{13}	1.24×10^5	C=C double bond	6.35
Ultraviolet	1.0×10^9	4.1	C-O single bond	3.74
Visible light	6.0×10^8	2.5	C=O double bond	7.71
Infrared light	3.0×10^6	0.012	C-H bond	4.28
Microwaves	2450	0.0016	O-H bond	4.80
Radiofrequencies	1	4.0×10^{-9}	Hydrogen bond	0.04 – 0.44
Brownian motion		0.017 (200K)		

2.2.3. Microwave Dielectric Heating

Microwave dielectric heating effects are the basis for the efficient heating of materials. They depend on the ability of a material (solvent, reagent, catalyst) to absorb microwave energy and convert it into heat. Of the two components of electromagnetic microwave radiation (see Figure IV-3), the electric component is the most important for the interaction of microwaves with matter. It causes heating by two main mechanisms, dipolar polarization and ionic conduction. Possession of a dipole moment is the prerequisite for a substance to be able to generate heat when irradiated with microwaves. Microwave radiation causes the dipoles to align in the applied electric field. Since the electric field of the microwaves oscillates, the dipole field attempts to realign itself with the alternating electric field thereby converting electromagnetic energy into heat through molecular friction and dielectric loss.

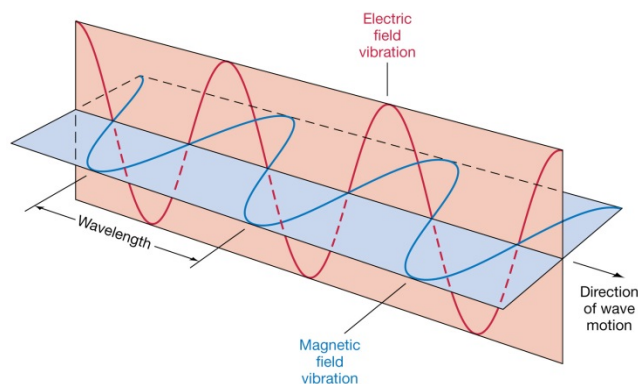


Figure IV-3 Electric and magnetic field components in microwaves.
 (From: <http://www2.astro.psu.edu/users/cpalma/astro10/class5.html>).

The amount of heat generated is directly related to ability of the matrix molecules to align themselves with the frequency of the applied field. No heating occurs in high frequency fields, where the dipoles do not have enough time to realign themselves with the external electric field, as well as in low-frequency fields where they reorient too quickly. In medium-frequency fields, dipoles have enough time to align with the field, but not to follow the alternating field precisely. This creates a phase difference between the orientation of the field and that of the dipole, which leads to loss of energy from the dipole by molecular friction and collisions resulting in dielectric heating. It has to be emphasized that in the condensed phase, this interaction is not a quantum mechanical resonance phenomenon. There, transitions between rotational quantum excitation states are not involved, i.e., the energy transfer is not a property of individual molecules, but rather the result of a collective phenomenon involving the bulk (15, 16). Furthermore, it should be mentioned that gases cannot be heated by microwaves. In the gas phase, the rotation of molecules is quantized (which allows for microwave spectroscopy), but since the mean free paths between individual molecules are too big for molecular friction to occur, heating of gases by microwave radiation cannot be achieved. On the other end of the scale, e.g., ice is (nearly) microwave transparent, since the water dipoles are constraint in the crystal lattice and cannot move as freely as in solution.

During ionic conduction the ions dissolved in a sample oscillate back and forth under the influence of the microwave field and collide with neighboring atoms or molecules ultimately creating heat. For that reason, tap water for example, heats up much faster than distilled water because of the dissolved ions.

Comparing these two effects with regards to their heat-generating capacity, ionic conduction displays a much stronger effect than the dipolar rotation mechanism.

2.2.4. Dielectric Properties

The heating characteristics of a material under microwave irradiation depend on its dielectric properties and are determined by the loss factor, or loss-tangent, $\tan \delta$ (Equation (IV-1))

$$\tan \delta = \frac{\epsilon''}{\epsilon'} \quad \text{(IV-1)}$$

where ϵ'' is the dielectric loss (a measure for efficiency with which electromagnetic radiation is converted into heat), and ϵ' is the dielectric constant (a description of the polarizability of the molecules in an electric field). A high $\tan \delta$ is required for efficient absorption which leads to rapid heating, however, materials with a high dielectric constant ϵ' may not necessarily also have a high $\tan \delta$ value (Table IV-2). Typically, solvents are classified as high ($\tan \delta > 0.5$), medium ($\tan \delta = 0.1-0.5$), or low microwave-absorbing ($\tan \delta < 0.1$) media.

Other common organic solvents without a permanent dipole moment, such as benzene, carbon tetrachloride, or dioxane, are more or less microwave transparent; however, this fact does not preclude their use in microwave-heated reactions. In most cases, as long as the substrate or at least some of the reagents or catalysts are polar, sufficient heating by

microwaves can be attained. Another option would be the use of polar additives like alcohols or ionic liquids in order to increase the capacity of the medium to absorb microwave radiation.

Table IV-2 Dielectric constants, dielectric losses and loss tangent ($\tan \delta$) of various solvents (2.45 GHz, 20°C) (17, 18).

Solvent	ϵ'	ϵ''	$\tan \delta$	Solvent	ϵ'	ϵ''	$\tan \delta$
Ethylene glycol	37.0	49.950	1.350	N,N-dimethyl-formamide (DMF)	37.7	6.070	0.161
Ethanol	24.3	22.866	0.941	1,2-dichloroethane	10.3	1.308	0.127
Dimethyl sulfoxide	45.0	37.125	0.825	Water	80.4	9.889	0.123
2-propanol	20.2	16.124	0.799	Chlorobenzene	5.6	0.566	0.101
Formic acid	58.5	42.237	0.722	Chloroform	4.8	0.437	0.091
Methanol	32.6	21.483	0.659	Acetonitrile	37.5	2.325	0.062
Nitrobenzene	34.8	20.497	0.589	Ethyl acetate	6.0	0.324	0.059
1-butanol	17.8	10.164	0.571	Acetone	20.7	1.118	0.054
2-butanol	17.3	7.733	0.447	Tetrahydrofuran	7.4	0.348	0.047
1,2-dichlorobenzene	9.9	2.772	0.280	Dichloromethane	9.1	0.382	0.042
1-methyl-2-pyrrolidone (NMP)	32.2	8.855	0.275	Toluene	2.4	0.096	0.040
Acetic acid	6.2	1.079	0.174	Hexane	2.0	0.040	0.020

The penetration depth of microwave radiation is *per definitionem* the point in the medium where $1/e$ (~37 %) of the initially applied microwave power is still present (Equation (IV-2))

$$D_p \propto \sqrt{e'/e''} \quad \text{(IV-2)}$$

where D_p is the penetration depth, and λ_0 the wavelength of microwave radiation. Since the penetration depth is inversely proportional to the loss tangent it is critically dependent on factors such as the frequency of the microwave radiation and the temperature of the reaction medium.

2.2.5. Conventional vs. Microwave Heating

Conventional heating is typically carried out by conductive heating with an external heat source such as an oil bath or a heating mantle. Since it depends mainly on convective currents and the thermal conductivity of the various materials that must be penetrated it leads to the temperature of the reaction vessel walls being higher than that of the reaction mixture. As well, a temperature gradient can develop within the sample and local overheating may result in decomposition of substrate, catalyst, reagent or product. Microwave radiation, on the other hand, produces internal heating within the core of the sample rather leading to an inverted temperature gradient (Figure IV-4) (19). Because microwave dielectric heating and conventional thermal heating by convection are totally different processes, any comparison of results acquired by these two methods is inherently difficult and has to be thoroughly validated.

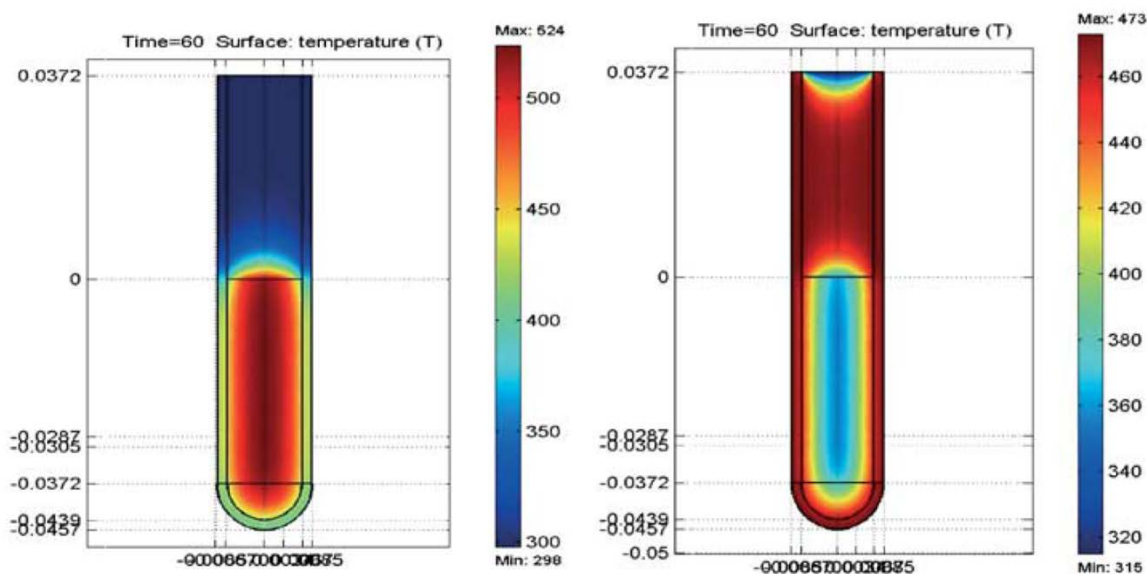


Figure IV-4 Modelling of inverted temperature gradients in microwave versus normal in oil-bath heating.

Temperature profiles (obtained by finite element modeling) after 1 min as affected by microwave irradiation (left) compared to treatment in an oil bath (right). Microwave irradiation raises the temperature of the whole volume simultaneously (bulk heating), whereas in the oil-heated tube the reaction mixture in contact with the vessel wall is heated first. (Reproduced with permission from Ref. (19)).

2.2.6. Microwave Effects

Currently, the exact mechanisms by which microwaves enhance chemical reactions are still not completely understood. Several groups proposed the existence of so-called 'microwave effects' which are thought to be the consequence of specific wave-material interactions. Orientation effects of polar species in an electromagnetic field could decrease the activation energy or increase in the pre-exponential factor in the Arrhenius law (20, 21). However, other researchers dismiss the idea of the existence of non-thermal effects and reason that all rate enhancements are the result of rapid heating and the high temperatures that are achieved in microwave-heated chemical reactions (22, 23), the formation of microscopic or macroscopic hotspots, or the selective heating of a specific component in the reaction mixture (24). Three possibilities have been put forward for the rationalization of the rate enhancements that are observed in microwave-assisted chemical reactions, thermal (kinetic) effects, specific microwave effects, and non-thermal (athermal) microwave effects (25).

2.2.6.1. Thermal Effects (Kinetics)

In many cases the observed rate enhancements can be ascribed to purely thermal/kinetic effects, i.e., they are a result of the high reaction temperatures, which can rapidly be attained when polar materials are irradiated in a microwave field (22, 23). Even solvents that absorb microwave radiation only moderately, e.g., dichlorobenzene (Table IV-2) can be heated very rapidly in a microwave reactor.

Under sealed-vessel conditions in a single-mode microwave (high power density) a rapid increase in temperature leading to super-heating can be achieved. When using media with extreme loss tangents, such as ionic liquids, temperature jumps of 200 K within a few seconds

are not uncommon. Obviously, it is very difficult, or even not at all possible to reproduce such temperature profiles by conventional thermal heating. This fact, of course, reduces the comparability of results obtained by those two methods.

2.2.6.2. Specific Microwave Effects

The term 'specific microwave effects' is used to describe microwave effects that are caused by the unique nature of the microwave dielectric heating mechanism. These effects are defined as “[...] accelerations of chemical transformations in a microwave field that cannot be achieved or duplicated by conventional heating, but essentially are still thermal effects” (26). One example for such an effect is superheating of solvents at atmospheric pressure (27-29). Since both the rate of evaporation and the temperature at the interface of vapor and liquid strongly depend on the experimental conditions (22, 23) microwave-heated liquids can boil at temperatures above the equilibrium boiling point at atmospheric pressure (27, 28). This effect occurs, because the microwave power is dissipated over the whole volume of the solvent, which may allow some solvents to reach temperatures up to 40 K above the classical boiling point (29). For a heated solvent the most significant way to lose excess thermal energy is by boiling. However, while in a thermally heated solvent boiling typically occurs at nucleation points on the hot glass reactor surface, in microwave heated solvents it will occur only at the existing liquid-gas interfaces (27). In addition, Chemat and co-workers found that the kinetics of homogeneous organic reactions show Arrhenius behaviour extended into the superheated temperature region (29). Therefore, reaction rate enhancements of the order of 10-100 may be achieved, which is normally only possible under increased pressure.

Wall effects that occur in conventional heating are eliminated due to the inverted temperature gradient that results from the unique mechanism of microwave heating

(Figure IV-4, left). The reactor material is generally not heated but rather the energy is dissipated inside the bulk liquid. It can be assumed that while in a conventional oil-bath experiment (Figure IV-4, right) temperature-sensitive species, for example catalysts, may decompose at the hot reactor surface (wall effects), the elimination of such a hot surface when using microwave heating will increase the lifetime of the catalyst and therefore will lead to better conversions in a microwave-heated as compared to a conventionally heated process.

In the end, all rate enhancements falling under the category of specific microwave effects are essentially still a result of thermal effects, i.e., an increased heating rate and a change in the temperature profile compared to heating by standard convection methods.

2.2.6.3. Non-Thermal Microwave Effects

In contrast to the specific microwave effects described in the previous section, some authors have proposed the existence of non-thermal microwave effects (also referred to as athermal effects). These were defined as “[...] *accelerations of chemical transformations in a microwave field that cannot be rationalized in terms of either purely thermal/kinetic or specific microwave effects*” (26). They were thought to result from a proposed direct interaction of the microwave electric field with specific molecules in the reaction medium. One conception was, for example that the presence of an electric field would lead to orientation effects of dipolar molecules thus changing the pre-exponential factor A (30-32) or the activation energy E_a (entropy term) (33, 34) in the Arrhenius equation (Equation (IV-3))

$$k = A * e^{\left(\frac{-E_a}{k*T}\right)} \quad \text{(IV-3)}$$

where k is the rate constant, A the pre-exponential factor, E_a the activation energy (kJ/mol), k the Boltzmann constant ($k = 1.38 \times 10^{-23}$ J/K), and T the absolute temperature (K). Moreover, a

comparable effect should be observed for polar reaction mechanisms, where the polarity is increased on going from the ground state to the transition state, resulting in an enhanced reactivity by decreasing the activation energy.

However, other scientists denounce the existence of such dipolar orientation effects in the electric fields, arguing that disorientation phenomena such as thermal agitation, would supersede those effects and thus prevent any statistically significant orientation of dipolar molecules (14, 17, 22, 23).

Regardless of the rationalization, in many cases one can observe a change in selectivity (chemo-, regio-, and stereoselectivity) when comparing microwave irradiation to conventional heating (35). However, currently microwave effects are still the subject of considerable debate and controversy in the scientific community, and there is no agreement on the role that they might play in chemical reactions.

2.3. Microwaves in SPPS

Concerns about side-reactions and the lack of proper tools prohibited the use of microwaves in SPPS for another two decades after their introduction to organic synthesis. Several side-reactions are known to occur in SPPS, e.g., aspartimide and oxazolone formation, and racemisation. Since microwaves have been shown to increase reaction rates, microwave heating was expected to accelerate these side-reactions, as well. A few publications reported the use of domestic microwave ovens for the enhancement of the deprotection. However, it was not until 2003 that the first synthesis of a deca-meric peptide (ACP₆₅₋₇₄), was performed exclusively in a single-mode microwave generator (36, 37). Since deprotection was completed in 2 minutes and coupling in 3 minutes, the complete synthesis took only 4.5 hours. Furthermore,

it also resulted in higher product purity compared to conventional automated SPPS. Since then, the number of reports mentioning microwave-assisted SPPS is steadily increasing.

Microwaves are thought to influence the reaction rate mainly in two ways. Firstly, the solvents commonly used all absorb microwaves, thus leading to an increased temperature causing acceleration of the reaction. And secondly, since both the N-terminal amine group and the backbone of the peptide chain are polar, they constantly try to align with the alternating electric field of the microwave. This motion can help break up chain aggregation (another problem known to occur in SPPS), thus enabling better solvation and easier access of reagents to the growing peptide chain. This becomes particularly important in the synthesis of longer or difficult sequences.

A few reports show improved reaction rates, when the reaction was cooled simultaneously with microwave irradiation (38-40). This strategy allowed greater amounts of microwave energy to be delivered to the reaction vessel while reducing the temperature of the bulk solution.

3. Peptide Synthesis and Purification

3.1. Background

As detailed in the previous section, the use of microwaves in SPPS offers a number of advantages over conventional methods, namely faster reaction times, and often higher purity of the products. Since this research project involved a number of different peptides involved in AD, it was decided to synthesise them on the automated synthesiser available in this laboratory, a CEM Liberty Microwave peptide synthesiser.

3.2. Materials

For the synthesis of peptides, the following chemicals were used: N,N-dimethylformamide (DMF); dichloromethane; trifluoroacetic acid (TFA) (all EMD Chemicals, Gibbstown, NJ, USA); Wang resins with the first Fmoc-protected amino acid residue already attached; Fmoc-protected amino acid residues (both SynBioSci, Livermore, CA, USA & Novabiochem, Läufelfingen, Switzerland); N,N,N',N'-tetramethyl-O-(1H-benzotriazol-1-yl)uronium hexafluorophosphate (HBTU); 1-[bis(dimethylamino)methylene]-1H-1,2,3-triazolo[4,5-b]pyridinium 3-oxid hexafluorophosphate (HATU) (both Aroz Technologies, Cincinnati, OH, USA); diisopropylethylamine (DIEA); N-methyl-pyrrolidone (NMP); piperidine; 1,8-diazabicyclo[5.4.0]undec-7-ene (DBU); triisopropylsilane (TIS) (all Alfa Aesar, Ward Hill, MA, USA); HOBt; piperazine; *t*-butyl-methyl ether, acetic anhydride (all Sigma-Aldrich, St. Louis, MO, USA); Chemicals, Gibbstown, NJ, USA); ultrapurified water (Millipore, Billerica, MA, USA); diethyl

ether (Fisher Scientific, Fair Lawn, NJ, USA & EMD Chemicals, Gibbstown, NJ, USA); molecular trap with amine scavenger (Biolytic Lab Performance, Inc., Fremont, CA, USA).

3.3. Methods

3.3.1. Peptide Synthesis Instrumentation

For peptide synthesis, the CEM Liberty system was employed. It enables the automated sequential synthesis of up to twelve peptides at a time in a microwave reactor. The standard reaction vessel allows synthesis scales of 0.1-1.0 mmol; additionally, a large reaction vessel is available for syntheses of up to 5.0 mmol of peptide. The system uses nitrogen pressure for transfer of all reagents and to provide an inert environment during synthesis. Nitrogen-bubbling is used for the mixing during deprotection, coupling and cleavage reactions. Metered sample loops are employed for precise delivery of all amino acid, activator and cleavage solutions. The polymer support resin is typically weighed into a 50 mL centrifuge tube, which is attached to one of the twelve ports of resin tube manifold. To collect the final product, the same type of tube is attached to the respective port of the product tube manifold. A 20 L liquid level-controlled carboy serves as waste container.

3.3.2. Peptide Synthesis Methods

The automated synthesis of a peptide on the CEM Liberty is performed by consecutive execution of a number of protocols termed 'cycles'. These typically include a resin cycle, multiple repetitions of amino acid cycles, followed by the final deprotection cycle and if desired

the cleavage cycle. Each cycle consists of multiple steps and includes the appropriate microwave and washing (with DMF) steps. Examples for each of the cycles are given in Appendix E.

The resin cycle consists of transfer of the resin from the resin tube to the reaction vessel, and swelling of the resin. The first step is optional; if only one peptide is synthesized, the resin may be weighed in directly into the reaction vessel to avoid any losses. Swelling of the resin is necessary to ensure optimal access of all reagents to the functionalized sites on the resin surface; for Wang-resins, which were used in the majority of syntheses, it was being done in a 1:1 mixture of DMF and dichloromethane.

The amino acid cycle includes the deprotection, as well as the addition and *in situ* activation of the amino acid residue and the subsequent coupling. The cycle in Appendix E is for the coupling of a non-problematic amino acid at a 0.1 mM scale. Special cycles are available for amino acid residues that are prone to side reactions, as well as for amino acids that are known to react slowly. Coupling of the amino acid residues (Cys, His) is performed at 50°C; for slow reacting amino acid residues (Arg), a double-coupling is performed, where addition of the residue, activation and coupling is repeated after a washing step and without prior deprotection. Fmoc-protected amino acids were used as 0.2 M solutions in DMF. The standard activator was 0.5 M HBTU in DMF, although for some syntheses of the full length A β the stronger HATU was employed instead. To avoid side-reactions of the activator before addition to the amino acid, the activator base was prepared separately and added immediately prior to the reaction step into the reaction vessel. The standard activator base solution was 2 M DIEA in NMP. Originally, the deprotection solution used was 20 % piperidine in DMF containing 0.1 M HOBt; however, problems with the availability, as well as with the purity of some peptides led to the decision to switch to a solution of 5% piperazine in DMF with 0.1 M HOBt (41). Later on, a solution of 2% DBU in DMF was also employed in the synthesis of full-length A β (42, 43).

After the last amino acid residue has been attached, its Fmoc protecting group has to be removed in a final deprotection cycle to avoid problems in the subsequent cleavage and side-chain deprotection.

In one instance, the last amino acid of a peptide (BBXB IL_4b) had to be acetylated in order to prevent cyclisation. This was achieved by including a capping reaction using neat acetic anhydride in the final deprotection cycle.

The cleavage cycle allows for the automated cleavage of the final product from the resin after which the product is transferred to the product tube followed by neutralization and cleaning of the reaction vessel to prepare it for the synthesis of the next peptide. This last cycle may be omitted; the resin with the attached peptide is then transferred to the original resin tube instead of the product tube. After a number of problems and on recommendation of the service technician, this step was being skipped and cleavage was performed manually in the fume hood (see 3.3.3). In both instances, washing of the resin-attached peptide before cleavage was done with dichloromethane. The used cleavage cocktail consisted of 95 % TFA, 2.5 % TIS, and 2.5 % ultrapurified water. Ice-cold diethyl ether or *t*-butyl-methyl ether were used for precipitation of the crude peptides.

3.3.3. Manual Peptide Cleavage

Manual cleavage of the peptide from the resin was performed in a fume hood. The contents of the resin tube (resin suspension in DMF/dichloromethane) were poured into a cleavage filter (see Figure IV-5) to wash the resin. The cleavage filter had been designed to have a minimal dead volume below the glass frit to reduce the needed volume of cleavage cocktail; it was custom-made by Jürgen Müller (Chemistry Department, Dalhousie University). A water-jet

vacuum pump was used to remove the solvents under vacuum. The resin was washed 5 × with the appropriate volume of dichloromethane (see Table IV-3).

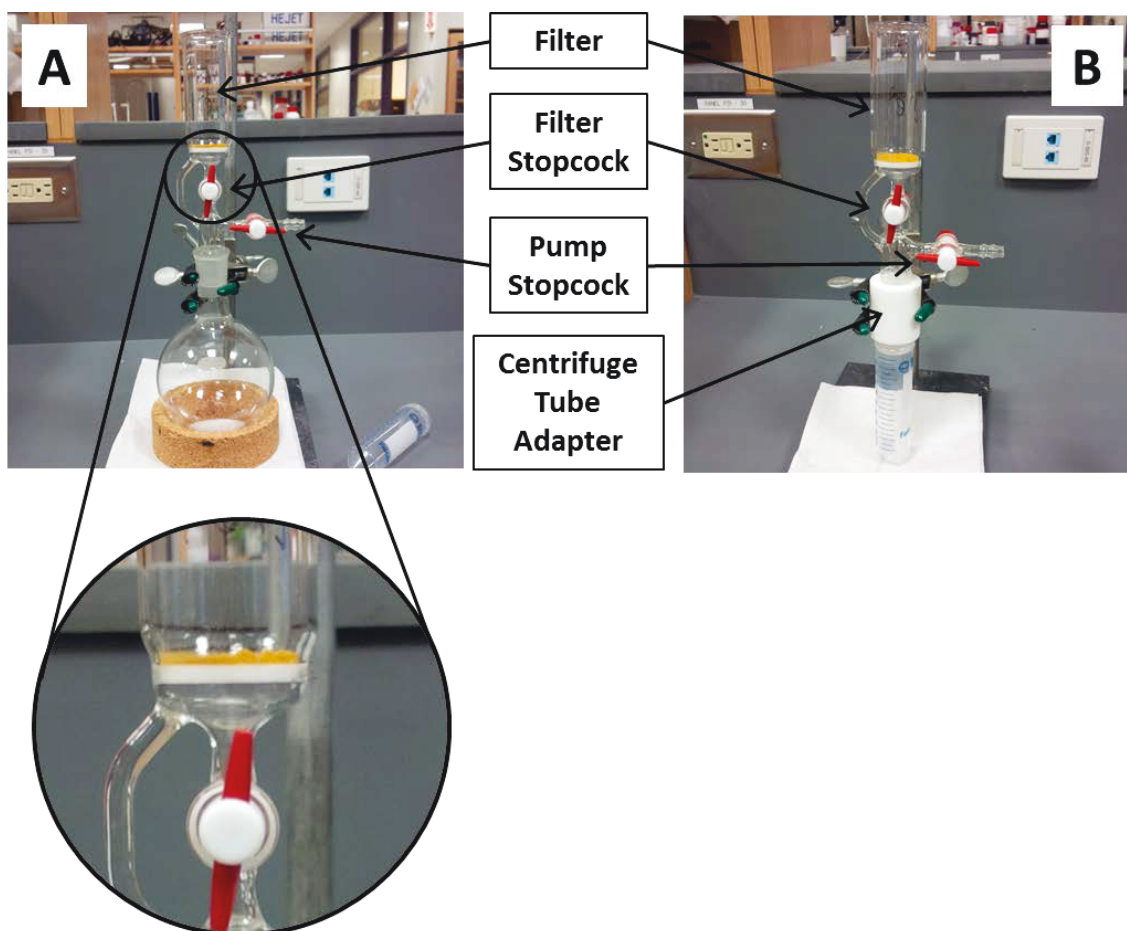


Figure IV-5 Manual peptide cleavage filter.

The manual peptide cleavage filter was designed to have a minimal dead volume below the glass frit (see zoom-in, (A)) to reduce the needed volume of cleavage cocktail; it was hand-made by Jürgen Müller (Chemistry Department, Dalhousie University). (B) shows it attached to the PTFE centrifuge tube adapter, which was made to avoid transfer of the cleaved and filtered peptide from a round-bottom flask to a centrifuge tube thus reducing peptide loss.

Table IV-3 Volume chart for the different steps of manual peptide cleavage.

Peptide Synthesis Scale (mM)	0.1	0.25	0.5	1.0
Wash Solvent Volume (mL)	5-7	13-18	25-30	50-60
Cleavage Cocktail Volume (mL)	10	15	20	30
Ether Precipitation Volume (mL)	40	80	160	320
# of 50 mL Centrifuge Tubes	1	2	4	8
mL Ether / tube	40	40	40	40

After closing the filter stopcock, the cleavage cocktail was added to the resin (see Table IV-3). The vessel was covered with parafilm and the left to react for 3-4 hours at RT. The reaction mixture was swirled intermittently, about once every hour.

Subsequently, the cleavage filter was inserted into the PTFE centrifuge tube adapter, which itself was inserted into a 50 mL polypropylene centrifuge tube. After removal of the parafilm, the cleavage reaction mixture was filtered with the help of a water-jet vacuum pump into the centrifuge tube. Finally, the resin was washed 2 × with a small amount of cleavage cocktail. The filtered cleavage reaction solution was aliquoted into the appropriate number of tubes (see Table IV-3) and the appropriate volume of ice-cold (~ -20°C) diethyl ether or *t*-butylmethyl ether (see Table IV-3) was added to the solution in the centrifuge tube and mixed. The tubes were centrifuged for 5 minutes at 3,716 × *g* to precipitate the peptide.

After decanting off the solution into a round-bottom flask, the precipitates were washed one more time with the same volume of ice-cold ether and centrifuged as before. The ether was again decanted into the same flask. Finally, the peptide was either analyzed directly or lyophilized to obtain a dry powder form. To recover more of the crude peptide, the decanted ether/TFA solution was evaporated to dryness in a rotary evaporator.

3.3.4. Peptide Purification Instrumentation and Materials

Purification of the crude peptides can be a major challenge in the process of peptide synthesis. Particularly peptides with longer sequences may contain a multitude of more or less easily detectable and separable side-products. Due to its unsurpassed flexibility provided by the wide range of stationary and mobile phases available, high-pressure liquid chromatography (HPLC) has become the standard method for this task.

The separation station used was comprised of the following modules, Dionex Ultimate LPG-3400A Analytical Pump (quaternary low-pressure gradient, pressures: ≤ 400 bars (4.00×10^7 Pa), flow rates: ≤ 10 mL/min); Dionex Ultimate HPG-3200P Semipreparative Pump (binary high-pressure gradient; pressures: ≤ 150 bars (3.5×10^7 Pa); flow rates: ≤ 50 mL/min, with double flow ≤ 100 mL/min; manual injector, injection loops available: 20 μ L, 100 μ L, 500 μ L, 1 mL); Dionex Ultimate WPS-3000TSL, Analytical Autosampler (temperature-range: 4-45°C; injection volume: ≤ 100 μ L); Dionex Ultimate TCC-3100, 6P Column Compartment (temperature range: 4-85°C; 6-port-2-position switching valve; capacity: 4 columns); Dionex Ultimate VWD-3400 Variable Wavelength UV/Vis detector (detects 4 different wavelengths simultaneously; wavelength range: 190-900 nm); Dionex RF-2000 Fluorescence Detector (excitation & emission wavelength range: 200-900 nm); Teledyne Isco Foxy Jr.® Fraction Collector; and Dionex UCI-50 Universal Chromatography Interface. Analytical runs were performed on a Dionex Acclaim® 120 reversed-phase column (C-18, 5 μ m, 120 Å, 4.6 x 150 mm), semipreparative runs on a Restek Ultra C18 reversed-phase column (C-18, 5 μ m, 100 Å, 21.2 x 150 mm).

Initially, the gradient for peptide purification consisted of the following mobile phases, A: ultrapurified water containing 0.05 % TFA, B: acetonitrile (MeCN) containing 0.05 % TFA. Mobile phases were degassed by applying ultrasound for 10 minutes. On recommendation from the service technician, they were switched to A: ultrapurified water containing 5% MeCN and 0.05% TFA (v/v/v), and B: MeCN containing 5% ultrapurified water and 0.05 % TFA (v/v/v); HPLC methods were switched to reflect the changed concentrations. Because the price for MeCN increased about five-fold partway through this project (in 2009), it was substituted for MeOH. Conversion of the gradients to reflect the eluotropic differences between MeOH and MeCN was

based on data obtained from Ref. (44) (Table IV-4), which was fitted in Microsoft Excel® with a second order polynomial curve given in Equation (IV-4)).

Table IV-4 Equal solvent strength mixtures of MeOH/H₂O and MeCN/H₂O. Data from Ref. (44).

% MeOH in H₂O (v/v)	% MeCN in H₂O (v/v)
0	0
10	5
20	14
30	22
40	32
50	40
60	50
70	60
80	73
90	86
100	100

$$\% \text{ MeOH in H}_2\text{O} = -0.003756x^2 + 1.359134x + 1.312083 \quad (\text{IV-4})$$

with x being the % MeCN in H₂O in the previously used gradients. After the prices for acetonitrile decreased about one year later, MeCN was used again as the solvent of choice for the organic modifier.

3.3.5. Peptide Purification Conditions

Crude peptides were initially analyzed with the following gradient on the analytical column at a flow rate of 1 mL/min and at 23°C: 0-2 min: 5 % B, 30 min: 95 % B (linear), 32 min: 95 % B, 34 min: 5 % B, 40 min: 5 % B. Based on the chromatogram, the conditions for each peptide were individually optimized by adjusting gradient steepness and temperature. Scale-up conditions for semipreparative purification of the peptides were calculated with the Waters Prep Calculator

software (Waters, Milford, MA, USA). The required flow rate was calculated to be 21.24 mL/min.

3.3.6. Mass Spectrometry

Samples were submitted to Dalhousie's mass spectrometry facility; analysis was performed by Mr. Xiao Feng on a Bruker microTOF with an attached electrospray ion source in positive ion mode.

3.4. Results & Discussion

A number of peptides have been synthesized to date. In the following section they are put into the context of this project and a few details about their synthesis are given. The respective HPLC chromatograms and mass spectra are compiled in Appendix F.

3.4.1. β -Amyloid-related peptides

3.4.1.1. $A\beta_{1-40}$

$A\beta_{1-40}$ is one of the two major forms of $A\beta$ involved in AD. Many researches prefer to use it in their assays over $A\beta_{1-42}$ because of its slower aggregation kinetics. Since many experiments for this project required $A\beta_{1-40}$, and because $A\beta_{1-40}$ is quite expensive (~200 \$US/mg) it was attempted to develop a protocol enabling the reliable synthesis of $A\beta_{1-40}$.

Full-length $A\beta_{1-40}$ is known to be a problematic peptide to synthesize, the major issue being its propensity to aggregate. To avoid these problems, two pseudoproline dipeptides (45,

46) (see Figure IV-6) were incorporated in the sequence, where pseudoproline 1 substituted an Asp-Ser dipeptide, and pseudoproline 2 a Gly-Ser dipeptide (highlighted in blue):

DAEFRH1GYEVHHQKLVFFAEDV2NKGAIIGLMVGGVV

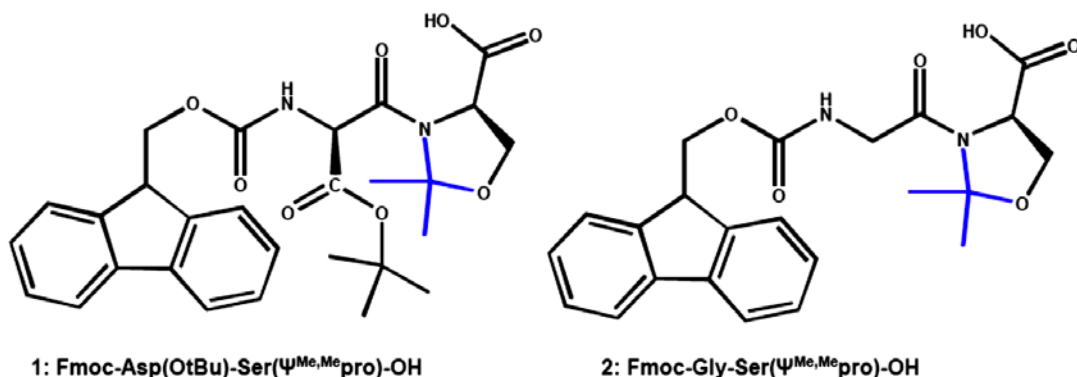


Figure IV-6 Pseudoproline dipeptides for difficult Aβ_{1-40/42} synthesis. The pseudoproline bridge is highlighted in blue.

Since further study of the literature revealed that these pseudoproline dipeptides are most effective when spaced 5 – 6 residues apart in regions with mainly nonpolar amino acid residues (47), pseudoproline 1 was omitted in the synthesis of batch #3. Furthermore, to improve the purity and overall yield of the final product, 1,8-Diazabicyclo[5.4.0]undec-7-ene (DBU) was used as the base for the deprotection cocktail (2% DBU/0.1M HOBt in 90% dichloromethane/10%DMF) up to residue Ser8; piperazine (5% piperazine/0.1M HOBt in 90% dichloromethane/10%DMF) was then used for the synthesis of the remainder of the sequence (42, 43).

$$M_{\text{avg}}^1 = 4,329.8646 \text{ g/mol}, M_{\text{mono}} = 4,327.1483 \text{ g/mol}$$

¹ Molecular weights (M_{avg}) and monoisotopic masses (M_{mono}) of all peptides mentioned in this section were calculated with the script available at: http://immweb.vet.uu.nl/P&P_fac/pepcalc.htm (accessed: Jan 20 & 21, 2014)

Table IV-5 Synthesis of A β ₁₋₄₀

Batch #	Synthesis Scale (mmol)	Theoretical Yield (mg)	Crude Yield (mg)	Crude Yield (%)	Pure Yield (mg)	Pure Yield (%)	MS ID	
							Base Peak m/z	theor. m/z Ion
1	0.1	433.0	275.3	63.6	N/D	N/D	1083.3	1082.7948 [M+4H] ⁴⁺
2 ^a	1.0	4,329.8	628.0	14.5	75.0	1.7	1083.2925	1082.7948 [M+4H] ⁴⁺
3 ^b	1.0	4,329.8	503.4	11.6	28.0 ^c	4.3 ^c (0.6)	1083.2931 866.8306 ^d	1082.7948 [M+4H] ⁴⁺ 866.4374 [M+5H] ⁵⁺

^a synthesis was interrupted a number of times due to instrument failure.

^b: some tubes containing the collected fractions broke in the freezer; recovery was only partially successful.

^c: not the entire batch was purified; pure yield relative to crude was calculated for 5 semiprep HPLC runs (3.75 mL @ 50.875 mg/mL → 190.8 mg crude, 8.3 mg yield = 4.35%); in parentheses the overall yield (rel. to theoretical) is given.

^d: base peaks vary, probably due to slightly different acidity of the samples which causes different protonation states to be dominant.

Despite the use of microwave irradiation and a number of other measures to address the difficulties associated with the synthesis of A β ₁₋₄₀, results were not as successful as anticipated. Although purity of the crude seemed to be somewhat improved by the use of DBU as base in the deprotection cocktail, in particular the yield was lower than desired. One factor that reduced the yield was the automated fraction collection, since the collector would redirect the flow to waste when moving the drop head from one tube to the next one. Another one might be that delays caused by instrument failure led to degradation of reagents or the unfinished peptide thus causing decreased yields of the desired product. And a third reason might be the potential presence of amines in the DMF used as solvent for most reagents and as main washing solvent (it had not been of 'peptide synthesis grade'). Only towards the end of the project, the pouches containing molecular trap with amine scavenger mentioned in the Materials section were used, however no new batch of A β ₁₋₄₀ (or any other previously synthesised peptide) had been synthesised since, precluding conclusions about their effectiveness.

On the other hand, material costs for synthesis and purification of a 1 mmol batch of A β ₁₋₄₀ were calculated to be about \$1,300 CAD (based on the cost of raw materials and solvents at the time of synthesis). Therefore, even a very moderate yield of 28 mg would provide considerable savings compared to the commercial product (~\$5,600 US).

Comparison of the yields achieved here to literature values is more difficult than one would expect, since these values are often completely omitted or rather vague. For example, Tickler *et al.* state in regards to their synthesis of A β ₁₋₄₀ and A β ₁₋₄₂ using DBU for the deprotection step that “[B]oth peptides could be readily purified by conventional RP-HPLC in overall yields of 24 and 17%, respectively, relative to starting crude peptide” (43), however, without mentioning at all the amount of crude obtained or yield relative to the theoretical amount (scale: 0.1 mmol).

Furthermore, it should be noted in hindsight that yields actually should have been based on results from amino acid analysis. This was realised only after most of these peptides were synthesised (and used up in experiments), and after information was provided from Anaspec about the peptide content of their products (see Chapter II), typically ranging anywhere from 60 - 80%. According to communication with their technical service, the rest is made up primarily of water and TFA.

In the end, the A β ₁₋₄₀ that had been obtained was used in some of the experiments related to the antimicrobial activity of A β (see Chapter II), and also by other members of this research group in their experiments.

3.4.1.2. A β ₁₋₄₂

A β ₁₋₄₂ is the other of the two main forms of A β implicated in AD. Considering that A β ₁₋₄₂ is even more expensive than A β ₁₋₄₀ (~230 \$US/mg), it was attempted to develop a protocol for its reliable synthesis, as well.

The full-length A β ₁₋₄₂ is even more prone to aggregation than A β ₁₋₄₀ and also known to be a problematic peptide to synthesize. To avoid these problems, again a pseudoproline dipeptide (45, 46) (see Figure IV-6) was incorporated in the sequence; pseudoproline 2 being a Gly-Ser dipeptide (highlighted in blue):

DAEFRHDSGYEVHHQKLVFFAEDV2NKGAIIGLMVGGVVIA

As for the later batches of A β ₁₋₄₀, up to Ser8 the deprotection cocktail contained DBU, while piperazine was used for synthesis of the remainder of the sequence.

$$M_{\text{avg}} = 4,514.1029 \text{ g/mol}, M_{\text{mono}} = 4,511.2694 \text{ g/mol}$$

Table IV-6 Synthesis of A β ₁₋₄₂.

Batch #	Synthesis Scale (mmol)	Theoretical Yield (mg)	Crude Yield (mg)	Crude Yield (%)	Pure Yield (mg)	Pure Yield (%)	MS ID	
							Base Peak m/z	theor. m/z Ion
1	0.5	2,257.1	275.3	63.6	N/D	N/D	N/D	N/D

Both, yield and purity of this synthesis were insufficient to warrant efforts for purification. Rather it was intended to resynthesize this peptide under optimised conditions, a plan that never materialised.

3.4.1.3. A β ₁₋₄₀ K28A Mutant

This A β mutant was synthesized to help in experimentally validating a computational model of the formation of A β oligomers developed in this laboratory. Alanine mutations or alanine scans are common tools to determine key residues in a sequence. Unlike glycine, they preserve the stereochemistry, but introduce an only marginally larger (than a hydrogen) nonpolar methyl residue. Since the same problem of aggregation as in the native A β ₁₋₄₀ was expected, both pseudoproline were incorporated (pseudoproline in blue, mutation in green):



$$M_{\text{avg}} = 4,272.7692 \text{ g/mol}, M_{\text{mono}} = 4,270.0904 \text{ g/mol}$$

Table IV-7 Synthesis of A β ₁₋₄₀ K28A mutant.

Batch #	Synthesis Scale (mmol)	Theoretical Yield (mg)	Crude Yield (mg)	Crude Yield (%)	Pure Yield (mg)	Pure Yield (%)	MS ID	
							Base Peak m/z	theor. m/z Ion
1	0.1	427.3	418.5	97.9	10.0 ^a	10.2 ^a (2.3)	1069.0391	1068.5299 [M+4H] ⁴⁺

^a: not the entire batch was purified; pure yield calculated for 4 semiprep HPLC runs (92.6 mg crude peptide).

Although the yield was not high, the amount obtained was enough to perform the experiments needed for the evaluation of the computational model (done by Michael Carter, a former postdoctoral fellow in this lab); results are not included in this thesis.

3.4.1.4. A β ₁₂₋₁₇

The HHQK motif in A β has been identified as a key sequence for the interaction with a multitude of molecules, e.g., metal ions (48-50), lipids (51, 52), and glycosaminoglycans (53). In order to study the importance of this motif for the interaction of A β with other molecules, it was

decided to synthesis A β ₁₂₋₁₇, the A β fragment that contains the HHQK motif plus one more residue on either end.

The sequence of A β ₁₂₋₁₇ (VHHQKL) does not contain any synthetically challenging residues. However, the analysis of the crude product of the first batch showed a number of deletion side-products, notably HHQKL and HQKL (Appendix F). Therefore in subsequent syntheses, the coupling of the second His (from the C-terminus) and of the Val residue were performed with a double coupling cycle.

$$M_{\text{avg}} = 760.8947 \text{ g/mol}; M_{\text{mono}} = 760.4343 \text{ g/mol}$$

Table IV-8 Synthesis of A β ₁₂₋₁₇.

Batch #	Synthesis Scale (mmol)	Theoretical Yield (mg)	Crude Yield (mg)	Crude Yield (%)	Pure Yield (mg)	Pure Yield (%)	MS ID	
							Base Peak m/z	theor. m/z Ion
1	0.25	190.2	40.2	21.1	N/D	N/D	381.2215	381.2250 [M+2H] ²⁺
2 ^a	1.0	760.9	688.9	90.5	180.3	23.7	761.4404	761.4422 [M+H] ⁺

^a: Identity was confirmed by 1H-NMR and DOSY-NMR; see Appendix F.4.2.

It had been planned to crystallise this A β fragment alone and in presence of nicotinic acid and nicotinamide in order to obtain a crystal structure of that part of A β , which is thought to play a key role in many of its interactions with other molecules. It was also meant to guide the development of A β antiaggregants by other researchers in this group. Efforts to obtain any crystals were unsuccessful, so far, and are not included in this thesis.

Some of this product was used by Gordon Simms, a doctoral student in this research group, in his project about the interaction of anthranilates with A β .

3.4.1.5. VHHQKLAAAA

In order to investigate the binding of small molecules to the HHQK motif of A β , the VHHQKLAAAA peptide was designed. The idea behind this design was to immobilise the HHQK motif — with one more residue on either side and four alanine residues as spacer— onto a resin or silica gel particles, thus enabling the determination of parameters related to the binding of these small molecules to the HHQK motif. Upon proof of concept, it was planned to synthesise two more peptides — KLVFFAAAAA, which includes the LVFF motif (A β ₁₇₋₂₀), another potential drug binding site of A β , and GAIIGLAAAA (GAIIGL motif, A β ₂₉₋₃₄) as negative control.

$$M_{\text{avg}} = 1,045.2099 \text{ g/mol}, M_{\text{mono}} = 1,044.5828 \text{ g/mol}$$

Table IV-9 Synthesis of VHHQKLAAAA.

Batch #	Synthesis Scale (mmol)	Theoretical Yield (mg)	Crude Yield (mg)	Crude Yield (%)	Pure Yield (mg)	Pure Yield (%)	MS ID	
							Base Peak m/z	theor. m/z Ion
1	0.1	104.5	522.9	500	0 ^a	0 ^a		

^a: the intended product was undetectable in any of the fractions of the crude peptide analysed (see Appendix F).

Since none of the peptide could be isolated, this project lost its priority status and unfortunately was never completed due to time issues. Suggested improvements would be the use of a different resin, in particular the HMPB-ChemMatrix resin, which has shown superior results in the synthesis of difficult peptides (54, 55). Furthermore, it allows cleavage of the peptide from the resin without prior deprotection of the side chains, thus avoiding an extra step to re-protect side chains and N-terminus for the attachment to the solid matrix.

3.4.2. BBXB Series

VC Meier-Stephenson identified the BBXB motif — where ‘B’ is any basic amino acid residue and ‘X’ any non-basic residue — as common receptor of a large number of proteins implicated in AD (56). It was planned to experimentally investigate commonalities between these different peptides. To make the problem at hand more manageable, it was decided to synthesize decameric fragments centered on the BBXB motif of the respective protein (see Table IV-11). Upon examination of the sequences it became obvious that some proteins contain more than one BBXB motif, and furthermore, in some proteins these motifs overlap. In the latter case, the fragment was chosen that contains all overlapping BBXB motifs plus three amino acid residues on either side. For example, in ApoE4 there are three BBXB/BXBB motifs, HLRK, RKLK and KLRK which all overlap with each other. Therefore the fragment chosen for synthesis was LASHLRKLRKLL, with LAS added at the N-terminus of the overlapping HLRKLRK, and RLL added at the C-terminus. Furthermore, in cases where the BBXB motif was too close to either end of the sequence, the decamer that comes closest to this concept was chosen. A complete list of the peptides included in this series is shown in Table IV-11. Nine of these were selected and synthesized on a scale of 0.25 mM (see Table IV-12).

Table IV-10 BBXB series peptides.

Original Protein	PDB ID ^a	BBXB / BXBB	Position in sequence ^b	decamer	x-mer to synthesise
Aβ	1IYT	HHQK	13	YEVHHQKLVF	YEVHHQKLVF
Tau	Ref. (57)	KKAK	141	SDDKKAKGAD	SDDKKAKGAD
S100β	1MQ1 (A Chain)	HKLK	25	GDKHKLKKSE	GDKHKLKKSEL
		KLKK	26	DKHKLKKSEL	--
C1qA	1PK6 (A Chain)	KKGH	111	KDPKKGHIYQ	KDPKKGHIYQ
IFN-γ	1FYH (A Chain)	KKKR	87 & 211 ^d	NSNKKKRDDF	NSNKKKRDDF
		KRKR	253	KTGKRKRSQM	KTGKRKRSQM
AChE	1EEA	RFRR	44	GNMRFRRPEP	GNMRFRRPEP
ApoE4	1B68	HLRK	140	LASHLRKLRK	LASHLRKLRKLL

Original Protein	PDB ID ^a	BBXB / BXBB	Position in sequence ^b	decamer	x-mer to synthesise
		RKLR KLRK	142 143	SHLRKLRKRL HLRKLKRLL	--
IL-1R1	1ITB (B chain)	HQHK HKEK	58 60	SRIHQHKEKL IHQHKEKLWF	SRIHQHKEKLWF
IL-1βCE	1BMQ (B chain)	KKAH RKVR	3 55	AIKKAHIEKD EIFRKVRFSF	AIKKAHIEKD EIFRKVRFSF
IL3^c	1JLI	HHLK HLKR	12 13	EIIHHLKRPP IIHHLKRPPN	EIIHHLKRPPN --
IL4	1ITI	HHEK HRHK	62 78	FYSHHEKDTR QQFHRHKQLI	FYSHHEKDTR QQFHRHKQLI
IL6	1P9M (B Chain)	KKAK	130	FLQKKAKNLD	FLQKKAKNLD
IL-6Rβ	1P9M (A Chain)	KKMR	118	NEGKKMRCEW	NEGKKMRCEW
IL-6Rβ		KAKR	151	ADCKAKRDTP	ADCKAKRDTP

Continued on next page.

Original Protein	PDB ID ^a	BBXB / BXBB	Position in sequence ^b	decamer	x-mer to synthesise
IL-10R1 α Chain	1LQS (R & S Chains)	KKVK KVKH	162 163	FTHKKVKHEQ THKKVKHEQF	FTHKKVKHEQF --
IL-10 like protein (HHV-5)	1LQS (L & M Chains)	HRVK	36	VFHHRVKPTL	VFHHRVKPTL
IL-12 subunit β	3HMX (A Chain)	HCLK KSKR KREK REKK KKDR	194 258 260 261 263	DAVHCLKYEN VQGKSKREKK GKSKREKKDR KSKREKKDRV KREKKDRVFT	DAVHCLKYEN VQGKSKREKKDRVFT -- --
IL13	1IJZ	HLKK	102	LLLHLKCLFR	LLLHLKCLFR
α1-ACT	2ACH (A Chain)	KRWR	274	ETLKRWRDSL	ETLKRWRDSL
BHMT	1LT8 (A Chain)	RARK	346	VRARARKEYW	VRARARKEYW
B7-1	1I8L (A Chain)	KREH	93	DAFKREHLAE	DAFKREHLAE
ICAM-1	1IC1 (A & B Chains, identical) 1IC1	RRDH RDHH	149 150	VLVRRDHHGA LVRRDHHGAN	VLVRRDHHGAN --
MIP-1α	3H44 (C & D Chains)	KRSR	45	FLTKRSRQVC	FLTKRSRQVC
MIP-1β	1JE4	KRSK	45	FQTKRSKQVC	FQTKRSKQVC
SDF-1	1SDF	KHLK	24	ANVKHLKILN	ANVKHLKILN
Neprilysin	1R1H	KKLR HCRK KKCR	470 680 691	KQLKKLREKV EAFHCRKNSY MNPEK <u>KCR</u> VW	KQLKKLREKV EAFHCRKNSY MNPEK <u>KCR</u> VW
Transferrin	1D3K	RGKK	111	NQLRGKKSCH	NQLRGKKSCH
RANTES	1HRJ (A & B Chains, identical)	RKNR	44	FVTRKNRQVC	FVTRKNRQVC

Original Protein	PDB ID ^a	BBXB / BXBB	Position in sequence ^b	decamer	x-mer to synthesise
HFE	1A6Z	HKIR	150	WERHKIRARQ	WERHKIRARQ
MHC(CII)	1FNG (A Chain)	RKFH	146	HLFRKFHYLT	HLFRKFHYLT

^a Protein Data Bank ID, obtained from: <http://www.rcsb.org/pdb/home/home.do>

^b designates position within complete protein sequence of the first B of the respective BBXB/BXBB motif

^c mutated form of IL3: Del(1-13), V14A, N18I, T25H, Q29R, L32N, F37P, G42S, Q45M, N51R, R55T, E59L, N62V, S67H, Q69E, Del(126-133) → native form does not contain a BBXB/BXBB motif

^d: identical decamers

HHV-5: Human Herpesvirus 5

Table IV-11 Synthesized BBXB series peptides.

Protein	Synthesis Scale (mM)	Avg. Mol. Mass (g/mol)	Theoretical Yield (mg)	Crude Yield (mg)	Crude Yield (%)	Pure Yield (mg)	MS ID	
							Peak m/z	theor. m/z Ion
Aβ	0.25	1299.476	324.8	240.9	74.2	N/D	1299.6929 ^a	1299.6844 [M+H] ⁺
Tau	0.25	1034.073	258.5	331.6	128.3	N/D	N/D	N/D
S100β	0.25	1282.487	320.5	443.4	138.3	N/D	1282.7493 ^a	1282.7478 [M+H] ⁺
C1qA	0.25	1213.383	303.3	268.7	88.6	N/D	1213.6722 ^a	1213.6688 [M+H] ⁺
IL4_a	0.25	1319.380	329.8	265.5	80.5	N/D	660.3138 ^b	660.3100 [M+2H] ²⁺
IL4_b [§]	0.25	1376.565	344.3	475.1	138.0	N/D	N/D	N/D
IL6_a	0.25	1204.417	301.0	283.1	94.1	N/D	N/D	N/D
IL6_b	0.25	1104.232	276.0	150.2	54.4	N/D	N/D	N/D
IL6_c	0.25	1280.471	320.0	228.8	71.5	N/D	N/D	N/D

[§]: Q at N-terminus was acetylated after final deprotection to prevent cyclization.

^a: accurate mass for base peak was not determined

^b: base peak

3.4.2.1. BBXB Aβ

BBXB Aβ was obtained in good purity; however two contaminants — deletion peptides missing the last residue (ΔY) and the two last residues (ΔYE), respectively — overlapped with the product peak and could not be removed. One way to avoid or remove these contaminants may

be the use of capping agents in the synthesis of this peptide. An intriguing method was published by Montanari and Kumar (57), which prevents formation of deletion peptides by capping in the coupling step unreacted N-termini of the growing peptide chain and allows removal of essentially all unwanted shorter fragments by the use of specially designed fluororous capping agents (57).

3.4.2.2. BBXB Tau

For BBXB Tau, the purity seemed quite good in the first chromatograms; however, even an isocratic run at only 5% organic modifier did not move the main peak away from the injection peak (although they revealed a major peak that came out with the column cleaning ramp). The fact that there were still some (small) peaks overlapping meant that separation could not be achieved by reversed-phase HPLC. Since normal phase semiprep HPLC was not available, this peptide was put to the back of the list and in the end never purified.

3.4.2.3. BBXB S100 β , BBXB C1qA, BBXB IL4_a & BBXB IL6_a

All of BBXB S100 β , BBXB C1qA, BBXB IL4_a, and BBXB IL6_a were purified and identified by mass spectrometry. Unfortunately, after purification and lyophilisation all tubes were lost in an accident; no product could be recovered.

3.4.2.4. BBXB IL4_b, BBXB IL6_b & BBXB IL6_c

BBXB IL4_b, BBXB IL6_b, and BBXB IL6_c were all deemed too 'dirty' to warrant efforts to purify them; it was rather planned to optimise conditions for their synthesise, but that was never accomplished due to time restrictions.

4. Conclusions

Despite the use of microwave irradiation and a number of other measures undertaken to address the difficulties associated with the synthesis of $A\beta_{1-40}$, $A\beta_{1-42}$, and other peptides produced here, production of these peptides is still not a trivial task and each one needs careful consideration of the specific issues that arise for each one of them. Individual optimisation of reaction conditions is mostly required. In the majority of cases purity of the crude peptide was at acceptable levels; however, overall yields were in general quite low. A number of issues related to these low yields were identified; in addition to well-known 'difficult sequences' as in $A\beta_{1-42}$ and $A\beta_{1-40}$ (58), the automated fraction collection, instrument failure causing lengthy interruptions that could possibly lead to degradation of used reactants, and potential presence of amines in the used DMF.

The peptides that were successfully isolated and purified were used in experiments related to this thesis and the work of other members of this research group.

In going forward, two things that would make peptide synthesis a more accessible part of research for this group would be easy access to LC-MS equipment (ideally also coupled to the semiprep HPLC), and adoption of amino acid analysis protocols for the HPLC already present or access to a dedicated instrument. The former would accelerate the optimisation of gradients for the purification tremendously; the latter would enable taking quality control of the produced peptides to the next level.

5. References

1. Sewald, N.; Jakubke, H., Eds.; In *Peptides: Chemistry and Biology*; Wiley-VCH: Weinheim, Germany, **2002**.
2. Delgado, C.; Francis, G. E.; Fisher, D. The uses and properties of PEG-linked proteins. *Crit. Rev. Ther. Drug Carrier Syst.* **1992**, *9*, 249-304.
3. Pettit, D. K.; Bonnert, T. P.; Eisenman, J.; Srinivasan, S.; Paxton, R.; Beers, C.; Lynch, D.; Miller, B.; Yost, J.; Grabstein, K. H.; Gombotz, W. R. Structure-function studies of interleukin 15 using site-specific mutagenesis, polyethylene glycol conjugation, and homology modeling. *J. Biol. Chem.* **1997**, *272*, 2312-2318.
4. Barany, G.; Kneib-Cordonier, N.; Mullen, D. G. Solid-phase peptide synthesis: a silver anniversary report. *Int. J. Pept. Protein Res.* **1987**, *30*, 705-739.
5. Merrifield, R. B. Solid Phase Peptide Synthesis. I. The Synthesis of a Tetrapeptide. *J. Am. Chem. Soc.* **1963**, *85*, 2149-2154.
6. Fields, G. B., Ed.; In *Solid-phase Peptide Synthesis*; **1997**; Vol. 289, pp. 780.
7. Howl, J., Ed.; In *Peptide Synthesis and Application*; Humana Press: Totowa, NJ, USA, **2005**; Vol. 298, pp. 262.
8. Bodanzky, M. *Principles of Peptide Synthesis*; Springer-Verlag: Berlin; New York, **1993**; pp. 329.
9. Spencer, P. L. Patent: US2495429 A, **1950**.
10. Gedye, R.; Smith, F.; Westaway, K.; Ali, H.; Baldisera, L.; Laberge, L.; Rousell, J. The use of microwave ovens for rapid organic synthesis. *Tetrahedron Letters*, **1986**, *27*, 279-282.
11. Giguere, R. J.; Bray, T. L.; Duncan, S. M.; Majetich, G. Application of commercial microwave ovens to organic synthesis. *Tetrahedron Letters*, **1986**, *27*, 4945-4948.
12. Nuechter, M.; Ondruschka, B.; Bonrath, W.; Gumb, A. Microwave assisted synthesis - a critical technology overview. *Green Chem.* **2004**, *6*, 128-141.
13. Neas, E.; Collins, M. In Kingston, H. M., Jassie, L. B., Eds.; Introduction to Microwave Sample Preparation: Theory and Practice; American Chemical Society: Washington, DC, 1988; .

14. Stuerge, D.; Delmotte, M. In *Wave-Material Interactions, Microwave Technology and Equipment*; Loupy, A., Ed.; Microwaves in Organic Synthesis; Wiley-VCH: Weinheim, **2002**; Vol. 1, pp. 1-33.
15. Mingos, D. M. P.; Baghurst, D. A. Applications of Microwave Dielectric Heating Effects to Synthetic Problems in Chemistry. *Chem. Soc. Rev.* **1991**, *20*, 1-47.
16. Gabriel, C.; Gabriel, S.; Grant, E. H.; Halstead, B. S. J.; Mingos, D. M. P. Dielectric parameters relevant to microwave dielectric heating. *Chem. Soc. Rev.* **1998**, *27*, 213-224.
17. Hayes, B. L. *Microwave Synthesis: Chemistry at the Speed of Light*; CEM Publishing: Matthews, NC, **2002**; pp. 289.
18. Lide, D. R. CRC Handbook of Chemistry and Physics: A Ready-Reference Book of Chemical and Physical Data. **2003**.
19. Schanche, J. S. Microwave synthesis solutions from Personal Chemistry. *Mol. Divers.* **2003**, *7*, 293-300.
20. de la Hoz, A.; Diaz-Ortiz, A.; Moreno, A. Microwaves in organic synthesis. Thermal and non-thermal microwave effects. *Chem. Soc. Rev.* **2005**, *34*, 164-178.
21. Perreux, L.; Loupy, A. A tentative rationalization of microwave effects in organic synthesis according to the reaction medium, and mechanistic considerations. *Tetrahedron*, **2001**, *57*, 9199-9223.
22. Kuhnert, N. Microwave-Assisted Reactions in Organic Synthesis - Are There Any Nonthermal Microwave Effects? *Angew. Chem. Int. Ed. Engl.* **2002**, *41*, 1863-1866.
23. Strauss, C. R. Microwave-Assisted Reactions in Organic Synthesis - Are There Any Nonthermal Microwave Effects? Response to the Highlight by N. Kuhnert. *Angew. Chem. Int. Ed. Engl.* **2002**, *41*, 3589-3591.
24. Hajek, M. In *Microwave Catalysis in Organic Synthesis*; Loupy, A., Ed.; Microwaves in Organic Synthesis; Wiley-VCH: Weinheim, Germany, **2002**; pp. 345-378 (Chapter 10).
25. Kappe, C. O. Controlled microwave heating in modern organic synthesis. *Angew. Chem. Int. Ed. Engl.* **2004**, *43*, 6250-6284.
26. Kappe, O. C.; Stadler, A., Eds.; In *Microwaves in Organic and Medicinal Chemistry*; Mannhold, R., Kubinyi, H. and Folkers, G., Eds.; Methods and Principles in Medicinal Chemistry; Wiley-VCH Verlag GmbH Co. KGaA: Weinheim, **2005**; Vol. 25, pp. 410.
27. Baghurst, D. A.; Mingos, D. M. P. Superheating effects associated with microwave dielectric heating. *J. Chem. Soc., Chem. Commun.* **1992**, 674-677.

28. Saillard, R.; Poux, M.; Berlan, J.; Audhuy-Peaudecerf, M. Microwave heating of organic solvents: Thermal effects and field modelling. *Tetrahedron*, **1995**, *51*, 4033-4042.
29. Chemat, F.; Esveld, E. Microwave Super-Heated Boiling of Organic Liquids: Origin, Effect and Application. *Chem. Eng. Technol.* **2001**, *24*, 735-744.
30. Shibata, C.; Kashima, T.; Ohuchi, K. Nonthermal Influence of Microwave Power on Chemical Reactions. *Jpn. J. Appl. Phys.* **1996**, *35*, 316-319.
31. Jacob, J.; Chia, L. H. L.; Boey, F. Y. C. *J. Mater. Sci.* **1995**, *301*, 5322-5327.
32. Binner, J. G. P.; Hassine, N. A.; Cross, T. E. *J. Mater. Sci.* **1955**, *30*, 5289-5322.
33. Berlan, J.; Giboreau, P.; Lefeuvre, S.; Marchand, C. Synthèse organique sous champ microondes : premier exemple d'activation spécifique en phase homogène. *Tetrahedron Lett.* **1991**, *32*, 2363-2366.
34. Lewis, D. A.; Summers, J. D.; Ward, T. C.; McGrath, J. E. Accelerated imidization reactions using microwave radiation. *J. Polym. Sci. Part A* **1992**, *30*, 1647-1653.
35. de La Hoz, A.; Díaz-Ortiz, A.; Moreno, A. Selectivity in Organic Synthesis Under Microwave Irradiation. *Curr. Org. Chem.* **2004**, *8*, 903-918.
36. Yu, H. M.; Chen, S. T.; Wang, K. T. Enhanced coupling efficiency in solid-phase peptide synthesis by microwave irradiation. *J. Org. Chem.* **1992**, *57*, 4781-4784.
37. Erdélyia, M.; Gogoll, A. Rapid Microwave-Assisted Solid Phase Peptide Synthesis. *Synthesis* **2002**, *2002*, 1592-1596.
38. Katritzky, A. R.; Zhang, Y.; Singh, S. K.; Steelb, P. J. 1,3-Dipolar cycloadditions of organic azides to ester or benzotriazolylcarbonyl activated acetylenic amides. *ARKIVOC* **2003**, 47-64.
39. Chen, J. J.; Deshpande, S. V. Rapid synthesis of α -ketoamides using microwave irradiation—simultaneous cooling method. *Tetrahedron Lett.* **2003**, *44*, 8873-8876.
40. Humphrey, C. E.; Easson, M. A. M.; Tierney, J. P.; Turner, N. J. Solid-Supported Cyclohexane-1,3-dione (CHD): A "Capture and Release" Reagent for the Synthesis of Amides and Novel Scavenger Resin. *Org. Lett.* **2003**, *5*, 849-852.
41. Hachmann, J.; Lebl, M. Alternative to piperidine in Fmoc solid-phase synthesis. *J. Comb. Chem.* **2006**, *8*, 149.
42. Wade, J. D.; Bedford, J.; Sheppard, R. C.; Tregear, G. W. DBU as an N^α-Deprotecting Reagent for the Fluorenylmethoxycarbonyl Group in Continuous Flow Solid-Phase Peptide Synthesis. *Pept. Res.* **1991**, *4*, 194-199.

43. Tickler, A. K.; Barrow, C. J.; Wade, J. D. Improved Preparation of Amyloid- β Peptides Using DBU as N^α-Fmoc Deprotection Reagent. *J. Pept. Sci.* **2001**, *7*, 488-494.
44. GraceVydac HPLC Catalog. **2008**, p. 208.
45. Mutter, M.; Nefzi, A.; Sato, T.; Sun, X.; Wahl, F.; Wohr, T. Pseudo-prolines (psi Pro) for accessing "inaccessible" peptides. *Pept. Res.* **1995**, *8*, 145-153.
46. Haack, T.; Mutter, M. Serine derived oxazolidines as secondary structure disrupting, solubilizing building blocks in peptide synthesis. *Tetrahedron Lett.* **1992**, *33*, 1589-1592.
47. Novabiochem Synthesis design using pseudoproline dipeptides. *Novabiochem innovations* **2004**, *4*.
48. Syme, C. D.; Viles, J. H. Solution ¹H NMR investigation of Zn²⁺ and Cd²⁺ binding to amyloid- β peptide (A β) of Alzheimer's disease. *Biochim. Biophys. Acta* **2006**, *1764*, 246-256.
49. Danielsson, J.; Pierattelli, R.; Banci, L.; Graslund, A. High-resolution NMR studies of the zinc-binding site of the Alzheimer's amyloid β -peptide. *FEBS J.* **2007**, *274*, 46-59.
50. Yang, D. S.; McLaurin, J.; Qin, K.; Westaway, D.; Fraser, P. E. Examining the zinc binding site of the amyloid- β peptide. *Eur. J. Biochem.* **2000**, *267*, 6692-6698.
51. Ariga, T.; Yu, R. K. GM1 inhibits amyloid β -protein-induced cytokine release. *Neurochem. Res.* **1999**, *24*, 219-226.
52. Williamson, M. P.; Suzuki, Y.; Bourne, N. T.; Asakura, T. Binding of amyloid β -peptide to ganglioside micelles is dependent on histidine-13. *Biochem. J.* **2006**, *397*, 483-490.
53. Brunden, K. R.; Richter-Cook, N. J.; Chaturvedi, N.; Frederickson, R. C. pH-dependent binding of synthetic β -amyloid peptides to glycosaminoglycans. *J. Neurochem.* **1993**, *61*, 2147-2154.
54. Garcia-Martin, F.; Quintanar-Audelo, M.; Garcia-Ramos, Y.; Cruz, L. J.; Gravel, C.; Furic, R.; Cote, S.; Tulla-Puche, J.; Albericio, F. ChemMatrix, a poly(ethylene glycol)-based support for the solid-phase synthesis of complex peptides. *J. Comb. Chem.* **2006**, *8*, 213-220.
55. Garcia-Martin, F.; White, P.; Steinauer, R.; Cote, S.; Tulla-Puche, J.; Albericio, F. The synergy of ChemMatrix resin and pseudoproline building blocks renders RANTES, a complex aggregated chemokine. *Biopolymers* **2006**, *84*, 566-575.
56. Stephenson, V. C.; Heyding, R. A.; Weaver, D. F. The "promiscuous drug concept" with applications to Alzheimer's disease. *FEBS Lett.* **2005**, *579*, 1338-1342.

57. Montanari, V.; Kumar, K. Just add water: a new fluororous capping reagent for facile purification of peptides synthesized on the solid phase. *J. Am. Chem. Soc.* **2004**, *126*, 9528-9529.
58. Sohma, Y.; Hayashi, Y.; Kimura, M.; Chiyomori, Y.; Taniguchi, A.; Sasaki, M.; Kimura, T.; Kiso, Y. The 'O-acyl isopeptide method' for the synthesis of difficult sequence-containing peptides: application to the synthesis of Alzheimer's disease-related amyloid β peptide (A β) 1-42. *J. Pept. Sci.* **2005**, *11*, 441-451.

CHAPTER V.

β -Amyloid Interaction Assays

1. Introduction

A β has been shown to interact with many different classes of molecules and ions, like peptides/proteins (including itself) (1-10), metal cations (11-19), GAGs(20-24), membrane lipids (25-29), and others (30-35) (see Chapter I, Section 1.4). These interactions are not only problematic, being implicated in the disease process of AD, but may also be utilised to one's advantage, e.g., for A β analysis (ELISA, ThT assay (see 3.4.5)). Herein, a number of projects are combined that are based on the interaction of A β with itself or other molecules.

2. Peptide binding to sample vessels

2.1. Background

Because peptide content has been a persistent problem throughout the course of this research programme, it was decided to investigate another possible source of peptide loss, binding of peptide to the walls of vessels commonly used in the preparation and execution of an assay, like microcentrifuge tubes, 96-well plates, or glass vials.

2.2. Materials

For the experiments, the following materials were used:

A β ₁₋₄₂ (Anaspec), QuantiPro BCA Assay Kit (Sigma-Aldrich).

The following sample vessels were tested:

- 1.5 mL Microcentrifuge Tubes (Axygen; Clear Homo-Polymer, Boil Proof Tubes); VWR Cat #: 10011-700
- 2.0 mL Eppendorf Protein LoBind Tube (Cat #: 022431102)
- 0.5 mL Fisherbrand Microcentrifuge tubes, polypropylene (PP) (Cat #: 02681248)
- 0.5 mL Fisherbrand Microcentrifuge tubes, PP; blocked with 1% BSA in PBS overnight, washed with PBS, blown dry with compressed air
- 0.5 mL Fisherbrand Microcentrifuge tubes, PP; blocked with dichlorodimethylsilane
- 96 Well Suspension Culture Plate, sterile U-bottom, with lid (CellStar DNase, RNase free, Cat #: 650 185)
- 96 Well Falcon Microtest Flat Bottom Polystyrene Plate (sterile); BD Falcon Cat #: 353072
- 96-well black Costar plate, Corning; Fisher Cat #: 07-200-590
- 96-well black Costar half-area plate, Corning; Fisher Cat #: 7-200-340
- 384-well Greiner Plate, clear; Greiner Cat #: M3311
- Fisherbrand screw cap Glass Sample Vial (Cat#: 03-338-E)

2.3. Methods

2.3.1. Coating glassware and plasticware

2.3.1.1. Silanisation

Silanisation is a common method to prevent binding of hydrophilic compounds to sample vials, e.g., in HPLC. Based on protocols found in References (36, 37), the following method was employed:

In a fume hood, a 50 mL beaker filled with 5 mL 50% dichlorodimethylsilane in chloroform was placed in the bottom of a large dessicator. The grate was inserted and the plasticware to be silanised was loosely stacked on top. After closing the dessicator, a vacuum was applied for ~5 minutes until the dimethylsilane solution started to boil; the connection to the pump was closed, and the dessicator left under vacuum until the liquid was completely evaporated (~3 - 4 hours). Then, the dessicator was opened in the fumehood and left uncovered for ~5 minutes to allow the vapors to disperse. Finally, the plasticware was thoroughly washed with ultrapurified water and air-dried overnight.

2.3.1.2. Blocking with BSA

Blocking of plastic surfaces with bovine serum albumin (BSA) is a commonly employed method to prevent unwanted binding of proteins. BSA binds well to most plastics used in biochemical applications, but shows only low binding of other proteins, which makes it ideal in biochemical assays, such as ELISAs, where it prevents nonspecific binding of the antibodies thus reducing the background signal (38).

Here, sample vessels were filled completely with 1% BSA in PBS and incubated overnight at room temperature. The following day, the BSA solution was discarded, and tubes and plates were washed with PBS and air-dried.

2.3.2. Determination of protein binding

To determine protein binding to the sample vessels, the BSA protein standard contained in the BCA Assay Kit was diluted to 20 $\mu\text{g}/\text{mL}$ (the concentration range of the kit is 0.5 – 30 $\mu\text{g}/\text{mL}$). 50 μL aliquots were added to each tested sample vessel; after the specified incubation time (30 minute or 24 hours), 40 μL aliquots of the samples and fresh standard were transferred into a 384-well plate, and the protein concentration determined with the BCA kit according to the manufacturer's instructions. To prepare the Working Reagent, 25 parts of Reagent QA were mixed with 25 parts Reagent QB, then 1 part of Reagent QC was added and the solution mixed until homogeneous. 40 μL of Working Reagent were added to each sample in the 384-well plate and mixed, followed by incubation for 1 hour at 60°C in a dry-bath. Finally, after cooling to room temperature, absorbance was read in a plate reader at 540 nm. Each plate was read three times and the averages for each well were used in subsequent calculations.

2.4. Results and Discussion

2.4.1. Time dependence of protein binding

In the first set of experiments, the time dependence of the binding of BSA was explored (see Table V-1 and Figure V-1). Sample vessels were incubated with BSA (20 $\mu\text{g}/\text{mL}$) for 30 minutes (at room temperature) or 24 hours (at 4°C); then, the BSA concentration was

determined with the BCA Assay. The experiment was repeated independently three times for each incubation time with samples determined in quintuplicate.

Table V-1 Recovery of BSA (20 µg/mL) after incubation for 30 minutes and 24 hours.

Type of Sample Vessel	Recovery of BSA	
	BSA / 30 min (RT)	BSA / 24 h (4°C)
1.5 mL Microcentrifuge Tube - Axygen	92.3%	80.1%
2.0 mL Protein LoBind Tube - Eppendorf	104.9%	102.5%
0.5 mL Microcentrifuge Tube - Fisher	93.5%	85.7%
0.5 mL Microcentrifuge Tube/BSA - Fisher	97.1%	97.9%
0.5 mL Microcentrifuge Tube/silanised - Fisher	92.4%	83.0%
96-well Suspension Culture Plate - CellStar	94.0%	74.7%
96-well Microtest Plate - Falcon	90.5%	77.5%
96-well Plate, black - Corning	89.6%	78.8%
96-well Plate, half-area, black - Corning	91.3%	87.9%
384-well Plate - Greiner	87.4%	80.4%
Glass Sample Vial - Fisher	68.6%	51.2%

As expected, the recovery was equal or smaller for all samples after incubation for 24 hours compared to 30 minutes. Best results were seen with the Protein LoBind microcentrifuge tubes manufactured by Eppendorf, which afforded complete recovery of the protein, followed by PP tubes previously blocked with BSA (about 90% recovery after 24 hours). The glass sample vial had the lowest recovery, reduced to about half after 24 hours. This result that may be explained by the presence of hydrophilic silyl groups at the glass surface, and is the reason why surface treatment of glass and plastic ware is recommended for a range of biochemical (hydrophilic) analytes (36, 37). The other sample vessels all allow recovery of about 80% of BSA protein after 24 hours incubation. Interestingly, and contrary to common conception (39), silanisation of polypropylene tubes did not improve protein recovery; an observation made previously by Goebel-Stengel, *et al.* (40). One reason might be the use of different silanes for the coating of the sample vessels. A reason for the differences between

uncoated PP vessels (Protein LoBind vs. 0.5 mL Microcentrifuge Tube Fisher) might be different grades of PP used in the production of the microcentrifuge tubes (41).

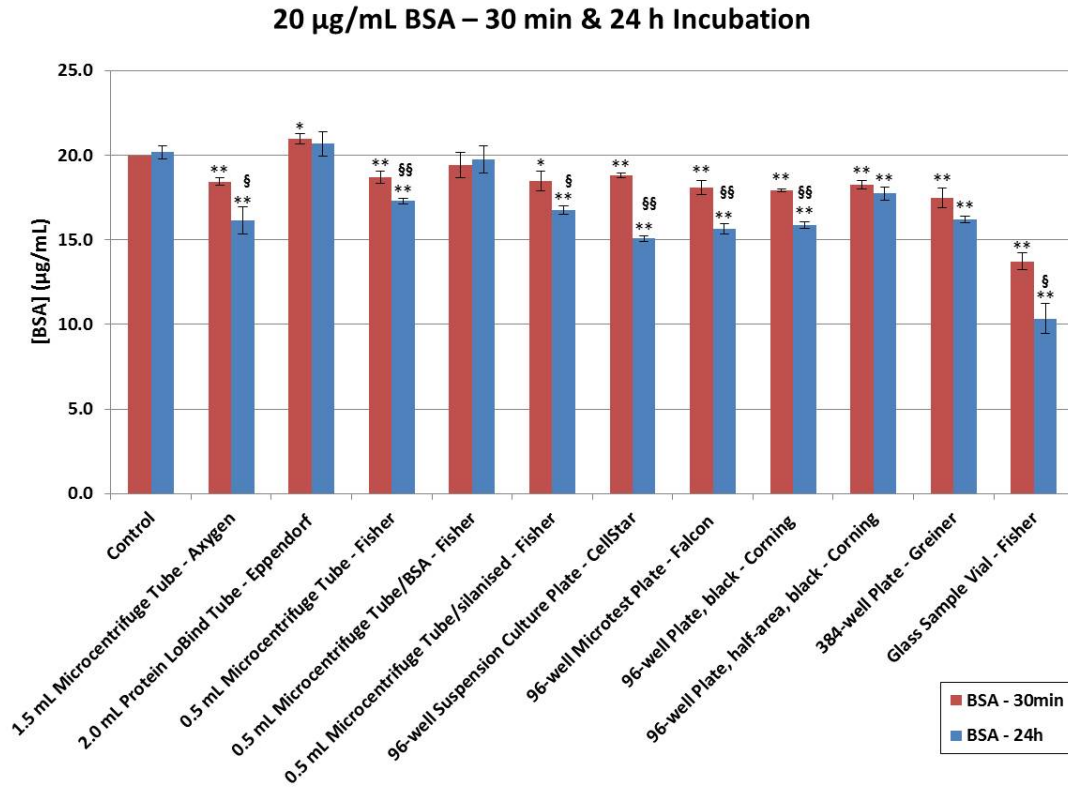


Figure V-1 Recovery of BSA after incubation for 30 minutes and 24 hours.

Sample vessels were incubated with BSA (20 µg/mL) for 30 minutes at RT (red bars) or 24 hours at 4°C (blue bars); then, the BSA concentration was determined with the BCA Assay. The assay was repeated independently three times for each incubation time with samples determined in quintuplicate. Here, results for one representative experiment are shown. Error Bars: ± S.E.M. (n = 5); *: P < 0.05; **: P < 0.01 (compared to respective control; two-tailed Student's t-test); §: P < 0.05; §§: P < 0.01 (comparison 30 min vs. 24 h; two-tailed Student's t-test).

2.4.2. Concentration dependence of protein binding

Next, the concentration dependence of the protein binding was investigated. Sample vessels were incubated with BSA (2 µg/mL) for 30 minutes; then, the BSA concentration was determined with the BCA Assay. The experiment was again repeated independently three times for each incubation time with samples determined in quintuplicate. Results were compared to

those obtained from the 30 minute incubation described in the previous section (see Figure V-2 and Table V-2).

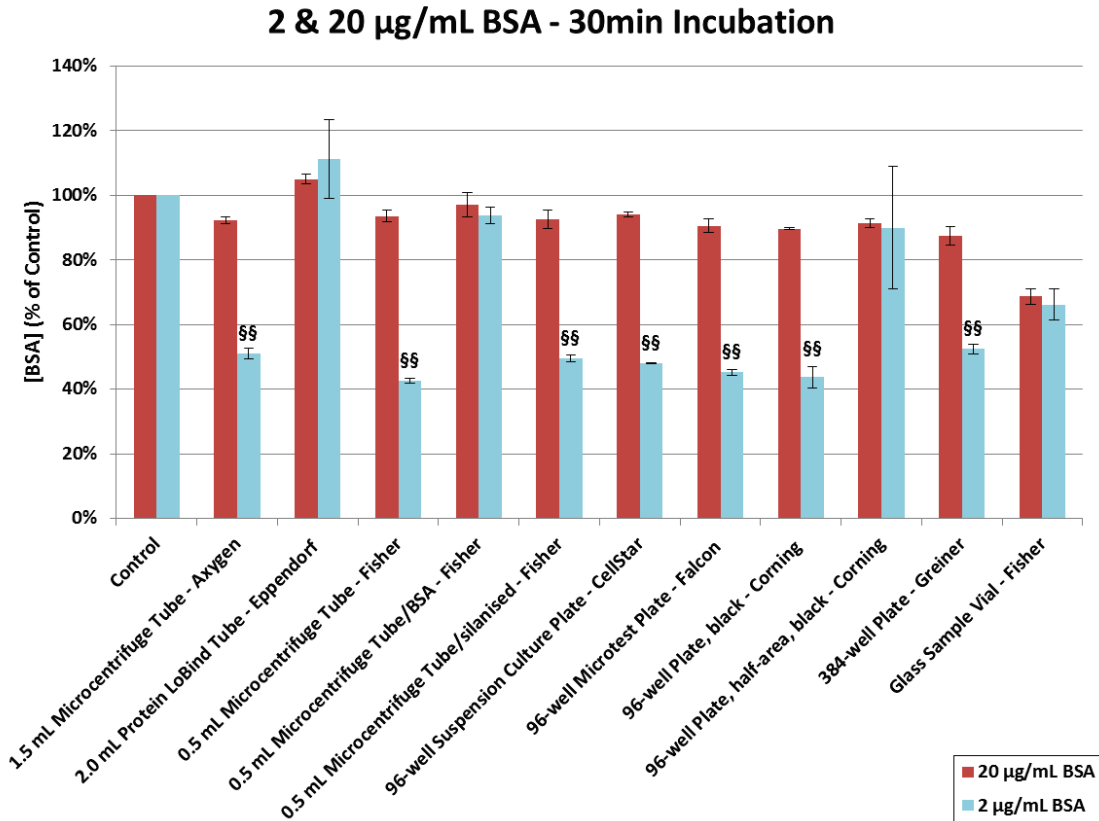


Figure V-2 Recovery of protein after incubation of different concentrations of BSA (2 and 20 µg/mL) for 30 minutes.

Sample vessels were incubated with BSA (2 µg/mL; light blue bars) for 30 minutes; then, the BSA concentration was determined with the BCA Assay. Results were compared to those obtained for 20 µg/mL BSA (red bars) from the 30 minute incubation described in the previous section. The experiment was repeated independently three times, with samples determined in quintuplicate. Here, results for one representative experiment are shown. Error Bars: ± S.E.M. (n = 5); [§]: P < 0.05; ^{§§}: P < 0.01 (comparison 2 µg/mL vs. 20 µg/mL BSA; two-tailed Student's t-test).

Recovery of BSA depended strongly on the sample concentration, with recovery values decreased by about 50% for some of the samples. Again, best results were seen with the Protein LoBind microcentrifuge tubes, which afforded complete recovery of the protein, followed by PP tubes previously blocked with BSA (about 94% recovery at 2µg/mL), and the Corning half-area

96-well plates (about 90% recovery at 2 μ g/mL). Silanisation did again not hold its promise of reducing protein binding showing recovery values only marginally better than the untreated tubes (~50% vs. ~43% recovery at 2 μ g/mL).

Table V-2 Recovery of protein after incubation of different concentrations of BSA (2 μ g/mL and 20 μ g/mL) for 30 minutes.

Type of Sample Vessel	Recovery of BSA	
	BSA 2 μ g/mL 30 min	BSA 20 μ g/mL 30 min
1.5 mL Microcentrifuge Tube - Axygen	51.1%	92.3%
2.0 mL Protein LoBind Tube - Eppendorf	111.1%	104.9%
0.5 mL Microcentrifuge Tube - Fisher	42.5%	93.5%
0.5 mL Microcentrifuge Tube/BSA - Fisher	93.8%	97.1%
0.5 mL Microcentrifuge Tube/silanised - Fisher	49.5%	92.4%
96-well Suspension Culture Plate - CellStar	47.9%	94.0%
96-well Microtest Plate - Falcon	45.2%	90.5%
96-well Plate, black - Corning	43.7%	89.6%
96-well Plate, half-area, black - Corning	89.9%	91.3%
384-well Plate - Greiner	52.4%	87.4%
Glass Sample Vial - Fisher	66.2%	68.6%

2.4.3. Dependence of protein binding on type of protein

Finally, the dependence of protein binding on the type of protein was probed. Since A β is being used in many experiments in this research group, A β ₁₋₄₂ samples (5 μ g/mL) were incubated for 30 minutes in the examined sample vessels, and protein recovery determined with the BCA Assay (see Table V-3 and Figure V-3). This experiment was performed only once; samples were analysed in quintuplicate.

Table V-3 Recovery of protein after incubation of A β ₁₋₄₂ (5 μ g/mL) samples for 30 minutes.

Type of Sample Vessel	Recovery of A β ₁₋₄₂ A β ₁₋₄₂ 5 μ g/mL 30 min
1.5 mL Microcentrifuge Tube - Axygen	76.5%
2.0 mL Protein LoBind Tube - Eppendorf	101.2%
0.5 mL Microcentrifuge Tube - Fisher	81.3%
0.5 mL Microcentrifuge Tube/BSA - Fisher	92.6%
0.5 mL Microcentrifuge Tube/silanised - Fisher	78.3%
96-well Suspension Culture Plate - CellStar	93.5%
96-well Microtest Plate - Falcon	73.9%
96-well Plate, black - Corning	53.3%
96-well Plate, half-area, black - Corning	71.3%
384-well Plate - Greiner	82.4%
Glass Sample Vial - Fisher	75.8%

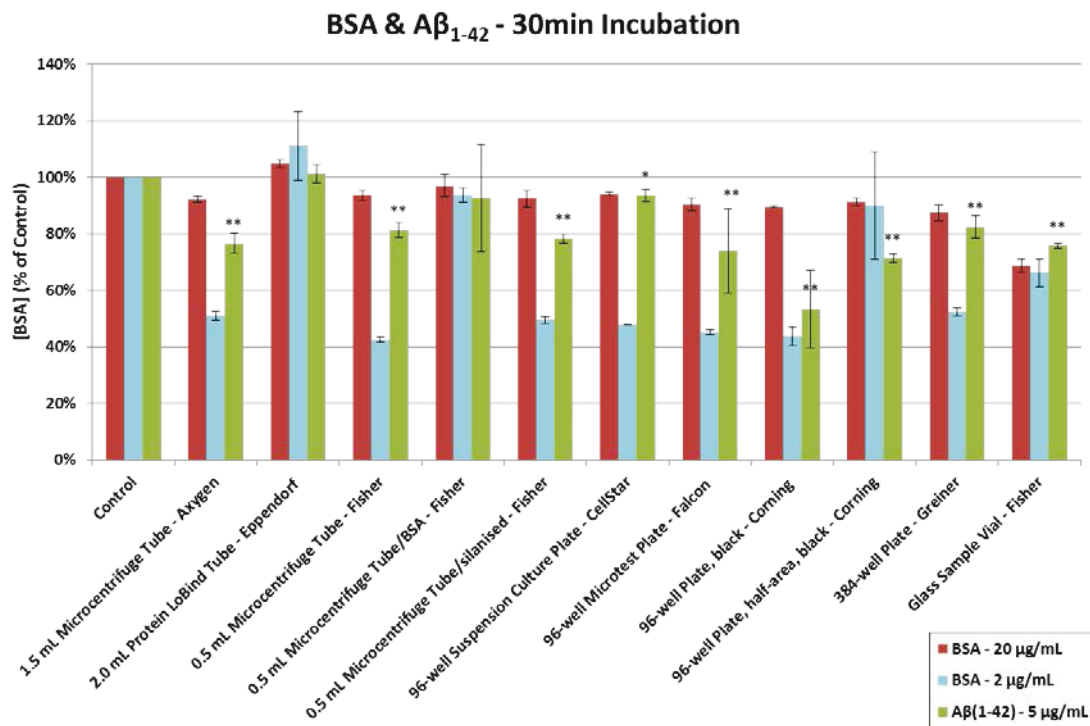


Figure V-3 Recovery of protein after incubation of A β ₁₋₄₂ (5 μ g/mL) for 30 minutes.

Sample vessels were incubated with A β ₁₋₄₂ (5 μ g/mL, green bars) for 30 minutes; then, the BSA concentration was determined with the BCA Assay. Results for protein recovery from 20 μ g/mL BSA (red bars) and 2 μ g/mL BSA (light blue bars) samples described in the previous section are included for comparison. For A β ₁₋₄₂ (green bars), the experiment was performed once, with samples determined in quintuplicate. Error Bars: \pm S.E.M. (n = 5); * : P < 0.05; ** : P < 0.01 (compared to control; two-tailed Student's t-test).

Results obtained here indicate that A β ₁₋₄₂ shows higher recovery than BSA. Again, the Protein LoBind tubes gave the best results allowing complete recovery of A β , with the BSA-blocked tubes coming in second. A truly quantitative comparison is difficult, since unfortunately not the same concentrations were used. Taking the concentration effect found in the previous section into account, one would expect the recovery of A β (5 μ g/mL) to be closer to the values for 2 μ g/mL BSA than those for 20 μ g/mL BSA; however, for most samples the opposite is true with some variation depending on the sample vessel. One may speculate about the reasons for the different adsorption properties; a few coming to mind are obviously the large difference in size and hence molecular weight, and the different pI values (see Table V-4).

Table V-4 Comparison of physical parameters for A β ₁₋₄₂ and BSA.

Parameter	A β ₁₋₄₂	BSA
# of AA residues	42	583
MW	4514.1 g/mol	66,463 g/mol
Size	0.9 \pm 0.1 nm (hydrodynamic radius) (42)	3.48 nm (Stokes radius r_s) (43)
Dimensions	n/d	140 \times 40 \times 40 \AA^3 (44)
pI (isoelectric point)	5.2 – 5.6 ¹	4.7 (in water at 25°C) (45)

Furthermore, the molar concentration differences might play a role, as well (A β ₁₋₄₂: 5 μ g/mL = 1.1 μ M; BSA: 2 μ g/mL = 0.03 μ M; 20 μ g/mL = 0.3 μ M).

One issue regarding comparison of different sample vessel that has to be considered is the different surface area exposed to a sample of equal volume; a conical microcentrifuge tube will

¹ Calculated with different scripts available online; e.g., <http://www.bioinformatics.org/JaMBW//3/1/6/index.html>, <http://mobylye.pasteur.fr/cgi-bin/MobylyePortal/portal.py?form=pepstats>, <http://www.scripps.edu/cgi-bin/cdputnam/protcalc3>, http://ca.expasy.org/tools/pi_tool.html

have a different wetted surface area, than a 96-well plate and a glass vial. This might be one explanation for the low recovery values found for the glass sample vials.

2.5. Summary

Protein binding to sample vessels may have a significant influence on the outcome of an experiment. Here, depending on the type of vessel, protein recovery was reduced by > 50%. Essentially complete recovery in all experiments was only found for the Protein LoBind microcentrifuge tubes manufactured by Eppendorf. Factors determining the protein binding were incubation time (longer incubation reduced recovery), protein concentration (lower concentration led to lower recovery), and type of protein.

3. GM1 Assay

3.1. Background

3.1.1. Current Aggregation Assays

Long before characterisation of its amino acid sequence, binding of A β to certain benzothiazole dyes, in particular Thioflavin S and Thioflavin T (6, 46-48), had been used in histopathology to image the A β fibrils that are one of the hallmarks of AD. Today, Thioflavin T (ThT) and the diazobenzidine sulfonate dye Congo Red (CR) (see Figure V-4) are probably the most commonly used dyes to assess activity of A β antiaggregants. Both, ThT and CR, experience characteristic spectral changes upon binding to a variety of amyloid fibrils (not just A β), which are not seen for interactions with the precursor peptides, monomers or amorphous aggregates (49-51).

However, a number of problems with these two (and other similar) dyes have been noticed over the years. Both, ThT and CR bind competitively to growing A β fibrils, thus causing an antiaggregant effect themselves (52-57); in fact, both have been used as leads for the development of dedicated antiaggregants (58, 59). In addition, binding of the dye to a tested compound may also interfere with these assays (60). Quenching of the fluorescence signal by tested molecules is another concern, especially with some highly coloured compounds (60). Since generally rather high concentrations of A β are needed in the aggregation assays to obtain a sufficient fluorescence signal (~25 - 50 μ M), cost becomes an issue, too, considering the commercial price of A β (~\$200-\$250 US/mg peptide). And finally, batch-to-batch variability of the A β peptide leads to variations in its aggregation behaviour, sometimes even necessitating repetition of an experiment.

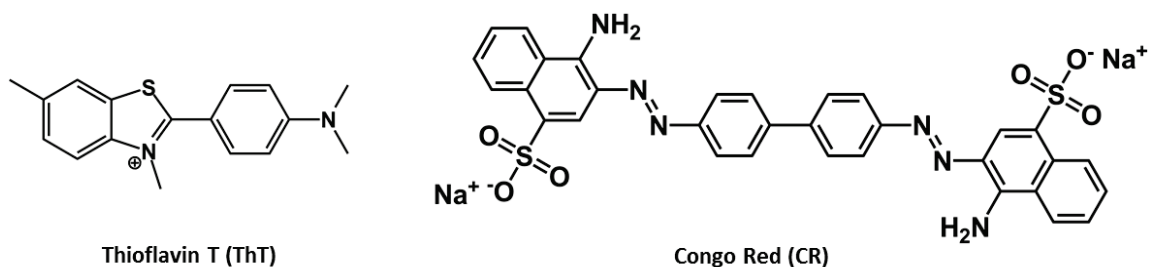


Figure V-4 Chemical structures of Thioflavin T and Congo Red.

The chemical structures of the two most commonly used dyes for in vitro detection of A β aggregation, Thioflavin T (ThT) and Congo Red (CR), are displayed.

3.1.2. Monosialoganglioside GM1 – A β Interactions

Gangliosides are membrane-bound, sialic acid-containing glycosphingolipids which are expressed ubiquitously in vertebrate cells. They reside predominantly on the extracellular side of the cellular membrane and are mainly found in neuronal cells (20-25% of the lipids of the outer membrane leaflet (61)). As mentioned in the introduction (see Chapter I, Section 1.3.4.1), the monosialoganglioside GM1 (structure displayed in Figure V-5) has been shown to bind A β in the brains of AD patients (3343,3082) and that through this specific binding, the process of amyloid fibril formation is accelerated (3082,3080, 2537, 3314). GM1 interacts with A β through its sialic acid residue, binding to A β in the region of amino acid residues 13-17 (62), and more specifically His-13 (63). Once bound, the GM1-A β species can act as a seed for the aggregation and formation of toxic fibrils (64). This formation of toxic fibrils (or a toxic species) requires the presence of cholesterol and sphingomyelin (4:3:3 GM1:Chol.:SM) (64). Ikeda *et al.* suggested a mechanism of A β aggregation mediated by GM1 clusters on raft-like lipid bilayers composed of GM1, cholesterol, and sphingomyelin, where, depending on the A β /GM1 ratio, A β assumes different secondary structures (65).

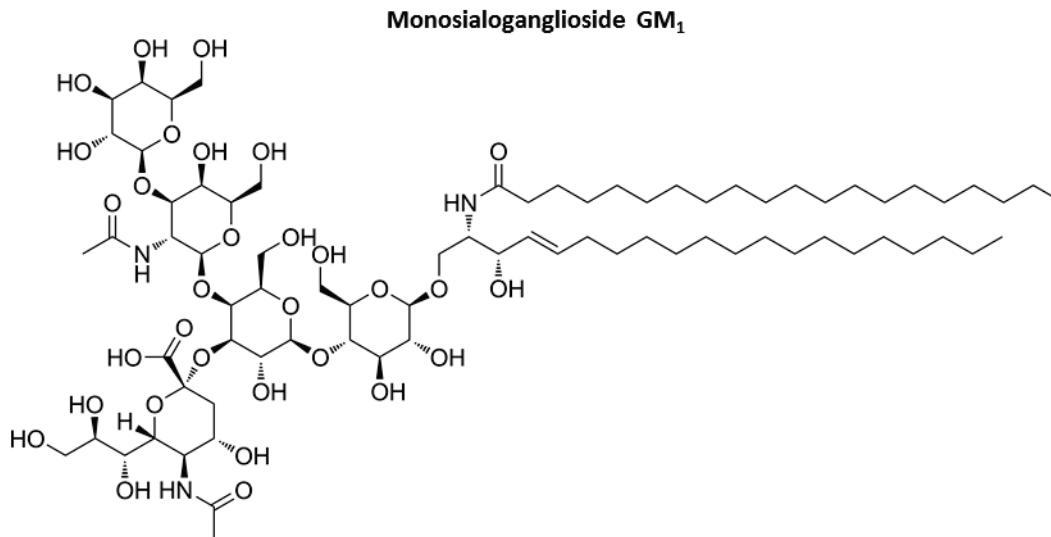


Figure V-5 Chemical structure of monosialoganglioside GM1.

The chemical structure of GM1 is displayed; the sialic acid residue on the bottom left is responsible for the binding to A β (63).

Here, an assay was developed to probe potential drug molecules for their ability to prevent the binding of A β to GM1. It is based on the assertion that interference with this interaction of GM1 with A β may prevent the formation of a toxic, disease-relevant A β species and thus provide a way helping to identify a curative drug for AD.

3.2. GM1 Assay Principle

The GM1 Assay is based on a microplate-based experiment by Yanagisawa *et al.* which solely demonstrated the physical interaction between GM1 and A β ₁₋₄₀ (66). The GM1 Assay is a ligand binding assay; its principle is shown in the schematic depicted in Figure V-6. Microplates are coated with GM1 / cholesterol / sphingomyelin (4:3:3), and subsequently blocked with BSA. After a wash, fluorescently labelled A β (in this example, FAM-A β) is added, which leads to the formation of GM1-A β seeds. During the following incubation, A β aggregates bound to the plate

are formed. After a final washing step, the fluorescence signal is read (here: excitation: 485 nm, emission: 535 nm). The presence of A β antiaggregants during the incubation step will diminish or prevent the formation of GM1-A β seeds and/or the subsequent A β aggregation ultimately leading to a lower fluorescence signal.

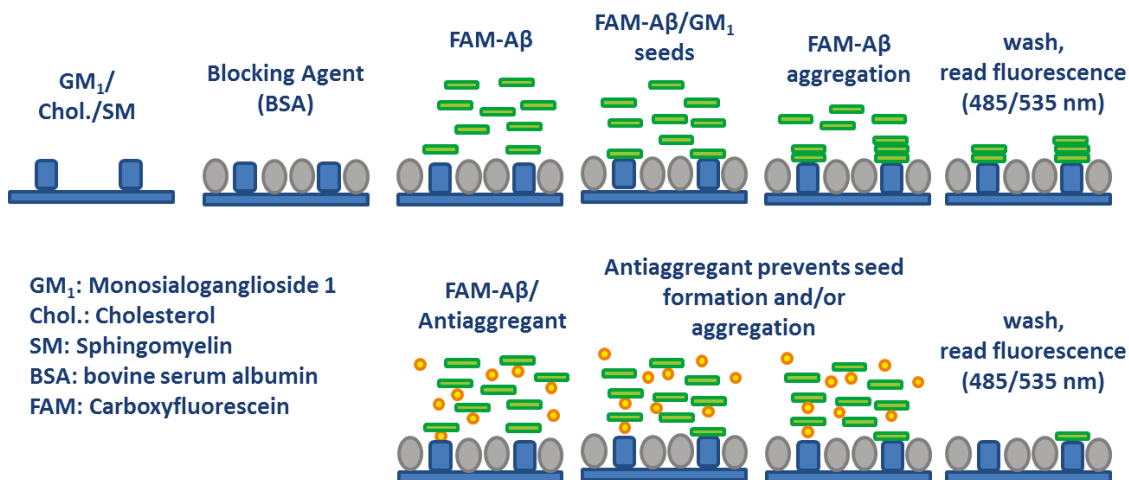


Figure V-6 Schematic of the GM1 Assay principle.

The GM1 Assay is essentially a ligand binding assay. Microplates are coated with GM1 / Cholesterol / Sphingomyelin (4:3:3), and subsequently blocked with BSA. After a wash, fluorescently labeled A β (in this example, FAM-A β) is added, which leads to the formation of GM1-A β seeds. During the following incubation, A β aggregates bound to the plate are formed. After a final washing step, the fluorescence signal is read (here: excitation: 485 nm, emission: 535 nm). Presence of A β antiaggregants during the incubation step will diminish or prevent the formation of GM1-A β seeds and/or the subsequent aggregation ultimately leading to a lower fluorescence signal.

This assay addresses a number of problems associated with the ThT or the CR assays. The use of a (fluorescently) labelled form of A β circumvents the necessity for addition of a dye which may inhibit the aggregation or bind to the tested compound. Labelling at the N-terminus of A β is thought to not interfere with the aggregation due to its distance from the residues involved in that process and the flexibility of the N-terminal tail. Furthermore, quenching of the fluorescence signal by the tested antiaggregant is avoided, since a number of washing steps are included after incubation with the tested compound.

3.3. Materials

The following materials were used in the development and application of the GM1 Assay: black, flat-bottom 96-well plates, regular and half area (Corning); Protein LoBind microcentrifuge tubes (Eppendorf); monosialoganglioside GM1 (GenWay Biotech); cholesterol; bovine serum albumin (BSA); Tween-20; Thioflavin T (ThT); Ultra-low Range Molecular Weight Marker (all Sigma-Aldrich); Sphingomyelin (SM) (Enzo Life Sciences); Methanol (MeOH), HPLC grade (EMD); PBS tablets (Amresco); FAM-A β ₁₋₄₀ (AnaSpec, Cat. # 23513-05); FAM-A β ₁₋₄₂ (AnaSpec, Cat. # 23525-05); CuCl₂; ZnCl₂; resveratrol; curcumin; HFIP; Cholera toxin subunit B, HRP conjugate (CtxB-HRP) (Invitrogen); TMB Substrate (Sigma); Tris(2,2'-bipyridyl)dichlororuthenium(II) hexahydrate ([Ru(Bpy)₃]Cl₂ · 6 H₂O) (Sigma-Aldrich); ammonium persulfate (APS); dithiothreitol (DTT); SDS-PAGE sample buffer (Invitrogen); tricine; sodium dodecyl sulfate (SDS); 10-20% Tris-Tricine gradient gel (NuSep, Cat.# NH31-1020); AquaStain (D-Mark Biosciences); methanol; acetic acid; sodium thiosulfate ; silver nitrate; formaldehyde; sodium carbonate; A β antiaggregants NCE-105, NCE-164, NCE-217; NCE-238; NCE-276; NCE-370; NCE-371; NCE-1027; NCE-1140 (for structures see Figure V-20).

3.4. Methods

3.4.1. Preparation of GM1 Assay 96-well plates

A black, flat-bottom 96-well plate ('Assay Plate') was coated with GM1/cholesterol/SM (ratio 4:3:3; most commonly used were 0.01/0.0075/0.0075 nmol/well) by adding 10 μ L/well of an appropriately concentrated solution (here: 1/0.75/0.75 μ M) in MeOH. After evaporation of the MeOH in a BSC or fume hood (~ 0.5 h), the plate was blocked by addition of 200 μ L/well of

0.1% BSA in PBST (0.01M PBS, pH 7.4; 0.05 % Tween-20), followed by incubation for 2 h at room temperature, or overnight at 4°C. Subsequent to washing the plate 3 × with 200 µL/well PBS, an appropriate volume of compound to be tested was added, followed by addition of an appropriate volume of fluorescently labeled Aβ (typically FAM-Aβ1-40 or FAM-Aβ1-42) to bring the total volume to 50 µL/well (a BSA-blocked pipetting trough was used for steps involving multichannel pipettes). After incubation for the desired time (typically overnight, ca. 18 h) in the dark (wrapped in aluminum foil), 25 µL/well of supernatant were transferred to a new BSA-blocked 96-well plate ('Supernatant Plate') and 25 µL/well PBST were added to the Supernatant Plate. The remaining solution was removed from the Assay Plate; it was washed 3 × with PBS, and 50 µL/well of PBS were added to the Assay Plate. Finally, the fluorescence intensity of both plates was read at 535 nm with excitation at 485 nm in a plate reader.

3.4.2. FAM-Aβ Preparation

Since fluorescently labelled Aβ species are light-sensitive, exposure to light was minimised by covering vials and tubes with aluminum foil. To prepare fluorescently labelled Aβ for the GM1 Assay, in the original vial the purchased peptide was dissolved in distilled HFIP at a concentration of nominally 1 mg/mL, vortexed for 30 s, sonicated for 15 min, and then incubated in HFIP for at least 1 hour. Subsequently, aliquots were transferred into 0.5 mL Eppendorf Protein LoBind tubes, and the HFIP removed under high vacuum in a dessicator for >= 1 h; aliquots were stored at -80 °C in a chest freezer.

To reconstitute aliquots, 1 % NH₄OH was added to obtain a concentration of 80 µL/mg using the NH₄OH that was provided with the peptide. The peptide was immediately diluted with 10 mM PBS to the desired stock concentration.

3.4.1. GM1 Coating Variability

In order to investigate the variability of the GM1 coating of the 96-well plates, a protocol for the (semi-quantitative) determination of amount of GM₁ bound to microplate was developed, based on a procedure published by Dawson (67). It relies on the specific binding of GM1 to the non-toxic subunit B of cholera toxin (CtxB).

All incubations for this assay were performed at room temperature (~21°C).

A 96-well plate was coated with a dilution series of GM1 (0.05/0.01/0.005/0.001/0 nmol/well); samples were pipetted in quintuplicate in a randomised pattern covering the full plate. Randomisation was done to minimise the influence of non-random effects like uneven heating of the plate. To achieve a random distribution of samples, in Microsoft Excel column A was filled with 96 random numbers generated with the built-in formula ("RAND()"); these values were then copied to column B. Column C was filled with five values (quintuplicate) for each of the five GM1 concentrations, as well as five times 'no CtxB'; the remaining cells were filled with 'x' for empty wells. Columns B and C were sorted in ascending order of Column B, and Column D was filled with the well labels (A1, A2, A3, ... , H11, H12). Finally, values were transferred to a 12 × 8 matrix (plate layout) to facilitate pipetting of the samples. After pipetting the samples according to the random layout and evaporation of the methanol, the plate was washed 3 × with 200 µL/well PBST and then incubated with 300 µL/well blocking buffer for 1 hour. After again washing 3 × with 200 µL/well PBST, the appropriate wells were incubated with 100 µL/well of Ctx B-HRP (100 ng/mL; diluted immediately prior to assay with PBST from stock (0.5 mg/ml in 0.01 M Na-phosphate, pH 7.5)) for 2 hours in the dark with gentle shaking. After washing 3 × with 200 µL/well PBST, and 1 × with 200 µL/well ultra-purified water, 100 µL/well TMB substrate solution were added and development of the assay was monitored by reading the absorbance at

620 nm in 2.5 minute intervals for 17.5 minutes. Finally, 50 μL /well Stop Solution were added and after 5 minutes absorbance was read at 450 nm.

3.4.2. Limits of Detection and Quantitation of FAM-A β

In order to determine the limit of detection (LoD) and limit of quantitation (LoQ) for FAM-A β , a black 96-well plate was blocked overnight with 1% BSA in PBS at 4°C in the fridge. After washing the plate 5 \times with PBS, 100 μL /well of dilution series of FAM-A β_{1-40} and FAM-A β_{1-42} (10 / 3.16 / 1 / 0.316 / 0.1 / 0.0316 / 0.01 / 0.00316 / 0.001 / 0.000316 / 0.0001 μM , which corresponds to 1 / 0.316 / 0.1 / 0.0316 / 0.01 / 0.00316 / 0.001 / 0.000316 / 0.0001 / 0.0000316 / 0.00001 nmol/well) were added to the plate in triplicate, as well as 30 control samples (PBS). Finally, the fluorescence signal was read at 535 nm with excitation at 485 nm in a plate reader. The gain factor, a parameter for the sensitivity of the instrument's detector, was initially set to 'optimal', for the second reading to '50', and then increased in intervals of 20 units up to '150'; in addition, the gain factor '100' was included, as well.

The Limit of Detection (LoD) was calculated according to Equation (V-1):

$$\mathbf{LoD = \bar{x} + 3 * s^2} \quad \mathbf{(V-1)}$$

where \bar{x} is the average fluorescence intensity of the control samples and s^2 their standard deviation.

Since there are generally two accepted levels for the Limit of Quantitation (LoQ), both were calculated according to the following equations (V-2) and (V-3):

$$\mathbf{LoQ_6 = \bar{x} + 6 * s^2} \quad \mathbf{(V-2)}$$

and

$$\text{LoQ}_{10} = \bar{x} + 10 * s^2 \quad (\text{V-3})$$

3.4.3. Plate Washing and Sensitivity

One part of developing a ligand binding assay is to determine how many washing steps are necessary to minimise non-specific binding and therefore background signal, while also avoiding signal reduction due to excessive washing. Another part is to establish the sensitivity of the assay. To that end, the first 6 columns of a 96-well plate were coated with a GM1 dilution series (0.1 / 0.0316 / 0.01 / 0.00316 / 0.001 / 0.000316 / 0.0001 nmol/well) as described previously; subsequently, the full plate and three additional plates were blocked overnight with BSA. After washing 5 × with PBS and drying, the GM1-coated wells were incubated with 40 µL/well of FAM-Aβ₁₋₄₀ (columns 1-3) and FAM-Aβ₁₋₄₂ (columns 4-6) dilution series (0.1 / 0.0316 / 0.01 / 0.00316 / 0.001 / 0.000316 / 0.0001 nmol/well = 2.5 / 0.79 / 0.25 / 0.079 / 0.025 / 0.0079 / 0.0025 µM) for 18 hours at 4°C in the dark. Then, 25 µL/well were transferred to the first blocked 96-well plate (in columns 1-6), and brought to 50 µL/well with PBS.

To determine the sensitivity of the assay, the assay plate was completely emptied by blotting, and the fluorescence intensity of the dry plate was read at 535 nm with excitation at 485 nm in a plate reader. After addition of 250 µL/well PBS and gentle shaking for about 30 seconds, samples (50 µL/well) of the washing buffer were transferred to the remaining wells of the first blocked 96-well plate (columns 7-12). Washing and fluorescence reading of the dry assay plate was repeated four more times, with transfer of washing buffer samples to the remaining two blocked 96-well plates. Finally, the fluorescence intensity of the 96-well plates was read at 535 nm with excitation at 485 nm in a plate reader. As a last step for

the assay plate, 50 μL /well PBS were added and the fluorescence intensity read one more time, to see if there is a difference between a dry and a liquid-filled plate.

To confirm the optimal number of washing steps, in a second experiment, a 96-well plate was coated with GM1 (0.01 nmol/well; 3 columns), and, along with two uncoated plates, blocked with BSA (0.1 % in PBST) overnight. After washing 5 \times with PBST (instead of PBS as in the first experiment) and drying, the GM1-coated wells were incubated with 100 μL /well of FAM-A β_{1-40} dilution series samples (2.5 / 1.25 / 0.625 / 0.313 / 0.156 / 0.078 / 0.039 μM) for 18 hours at 4°C in the dark. Then, 50 μL /well were transferred to the first supernatant plate (in columns 1 - 3). The assay plate was completely emptied by blotting, and 50 μL /well PBS were added.

To determine the sensitivity of the assay, the fluorescence intensity of the assay plate was read at 535 nm with excitation at 485 nm in a plate reader; then, an additional 150 μL /well PBS were added to the plate. After gently shaking for about 30 seconds, samples (50 μL /well) of the washing buffer were transferred to the first supernatant plate (columns 4-6). Washing and reading of the assay plate was repeated six more times, with transfer of washing buffer samples to the remaining supernatant plates. Finally, the fluorescence intensity of the supernatant plates was read at 535 nm with excitation at 485 nm in a plate reader.

To evaluate the use of half-area plates, the last experiment was repeated in a half-area plate with reduced volumes, 25 μL /well FAM-A β_{1-40} , 75 μL /well PBS (since the PBST washes showed considerable losses; see results) for washing, and 25 μL /well for plate reading.

3.4.4. Competitive Binding Assays

For competitive binding experiments, 96-well plates were coated with 0.1 nmol/well GM1 as described previously that were then incubated with FAM-A β in presence of a number of competitors, e.g., metal cations (Cu²⁺, Zn²⁺), or A β aggregation inhibitors in a range of appropriate conditions.

3.4.5. Thioflavin T Assay

In order to evaluate results from the GM1 Assay for the antiaggregant activity of tested compounds with a standard assay, they were compared to results obtained with the Thioflavin T (ThT) assay. HFIP-pretreated A β ₁₋₄₀ was dissolved in Tris base (20 mM), pH-adjusted to 7.4 with conc. HCl, filtered through a 0.2 μ m PVDF membrane filter and the volume adjusted to the desired concentration. This solution was mixed 1:1 (v/v) with ThT buffer (8 μ M ThT, 20 mM Tris, 0.3 M NaCl, pH 7.4) and pipetted into a black 96-well half-area plate. Finally, the anti-aggregants dissolved in DMSO were added to the plate and the ThT signal was followed by reading its fluorescence emission at 480 nm with excitation at 450 nm in 15 minute time intervals.

3.4.6. PICUP Assay

To perform a PICUP assay, A β samples in the concentration range of 20 – 100 μ M were treated as required for the experiment; then, 18 μ L were transferred into a clear 0.5 mL PCR tube or a 1 mm pathlength quartz microcuvette. After addition of 1 μ L of [Ru(Bpy)₃]²⁺ (typically at a concentration to achieve a 2:1 molar ratio to A β ; in 10 mM sodium phosphate buffer, pH 7.4) and 1 μ L APS (at a concentration to achieve a 20:1 molar ratio to [Ru(Bpy)₃]²⁺), the mixture was homogenised by aspiration and expelling from a pipette tip and irradiated in the LED irradiator described below (3.5.5) for an appropriate time interval. Finally, excess reagents were

quenched by the addition of DTT (1 M in ultrapurified water) or β -mercaptoethanol (4% (v/v) in tricine sample buffer).

3.4.7. Tricine-SDS-PAGE

To analyse samples obtained through PICUP, Tricine-SDS-PAGE (Tricine – sodium dodecyl sulfate – polyacrylamide gel electrophoresis) was employed, a method developed by Schägger and von Jagow for the separation of smaller proteins in the mass range 1 – 100 kDa (68, 69). Samples were mixed 1:1 (v/v) with SDS-PAGE sample buffer and heated in a boiling water bath to $\sim 95^{\circ}\text{C}$ for 5 minutes. After cooling to room temperature, 10 μL samples were loaded onto a 10 – 20% Tris-Tricine gradient gel. The gel was run on a Protean II vertical gel electrophoresis system (Bio-Rad) placed inside a tub filled with ice-water at 100 V for 1 – 1.5 hours; cathode buffer was 0.1 M Tris, 0.0225 M HCl in ultrapurified water, pH adjusted to 8.9; anode buffer was 0.1 M Tris, 0.1 M tricine, 1.0% SDS in ultrapurified water, pH ~ 8.25 (not adjusted).

After development, the gel was stained either with AcquaStain for 30 minutes, followed by three 10 minute washes in 50 mL ultrapurified water, or with a silver stain. For silver staining, the gel was first fixed for 1 hour in 50% methanol, 10% acetic acid, 100 mM ammonium acetate dissolved in ultrapurified water, followed by two washes in ultrapurified water for 1 hour each. Then, the gel was sensitised by incubation in 0.005% sodium thiosulfate for 1 hour, and stained in 0.1 % silver nitrate (in ultrapurified water) for 1 hour. After a short wash with ultrapurified water (a few seconds), the stain was developed by incubation in developer (0.036% formaldehyde, 2% sodium carbonate) for about 1 – 2 minutes. The developing was stopped by incubation in 50 mM EDTA for 1 hour, followed by two more washes in ultrapurified water.

3.5. Results and Discussion

In the process of developing this assay a number of parameters were determined to optimise several of the key steps involved.

3.5.1. Limits of Detection and Quantitation of FAM-A β

In a first step, the Limit of Detection and the Limit of Quantitation were determined to establish a concentration and amount range for the assay. Fluorescence intensity of dilution series samples of FAM-A β ₁₋₄₀ and FAM-A β ₁₋₄₂ along with Control samples was read in a plate reader at different gain factor settings. Results for three gain factor settings are displayed in Figure V-7.

Since the dilution series spanned five orders of magnitude starting at a relatively high amount of 1 nmol/well, the 'optimal' gain factor setting determined automatically by the instrument was quite low at a value of '37' (range: 1 – 150). When the instrument determines the optimal gain factor setting, it first scans the entire plate and then adjusts the gain factor such that the highest reading is within its scale (<65,000 a.u.). Increasing the gain factor setting yields higher fluorescence intensity values for the lower amounts of A β , but also pushes the highest values off the scale. It also increases the background noise, leading to higher absolute fluorescence intensity values for the LoD and LoQ. Besides the first read with the 'optimal' gain factor setting, which is optimised for the maximum fluorescence intensity values (but not the small values, which are relevant for LoD/LoQ), A β amounts down to 0.1 pmol/well were above the LoQ₁₀, the more conservative of the commonly accepted limits of quantitation. Furthermore, for gain factor settings of '50' and higher, all fluorescence intensity values were above the respective LoD. Table V-5 summarises the results for LoD, LoQ₆, and LoQ₁₀ for both

A β forms. The amount values were calculated based on linear regressions for the dilution series of FAM-A β_{1-40} and FAM-A β_{1-42} .

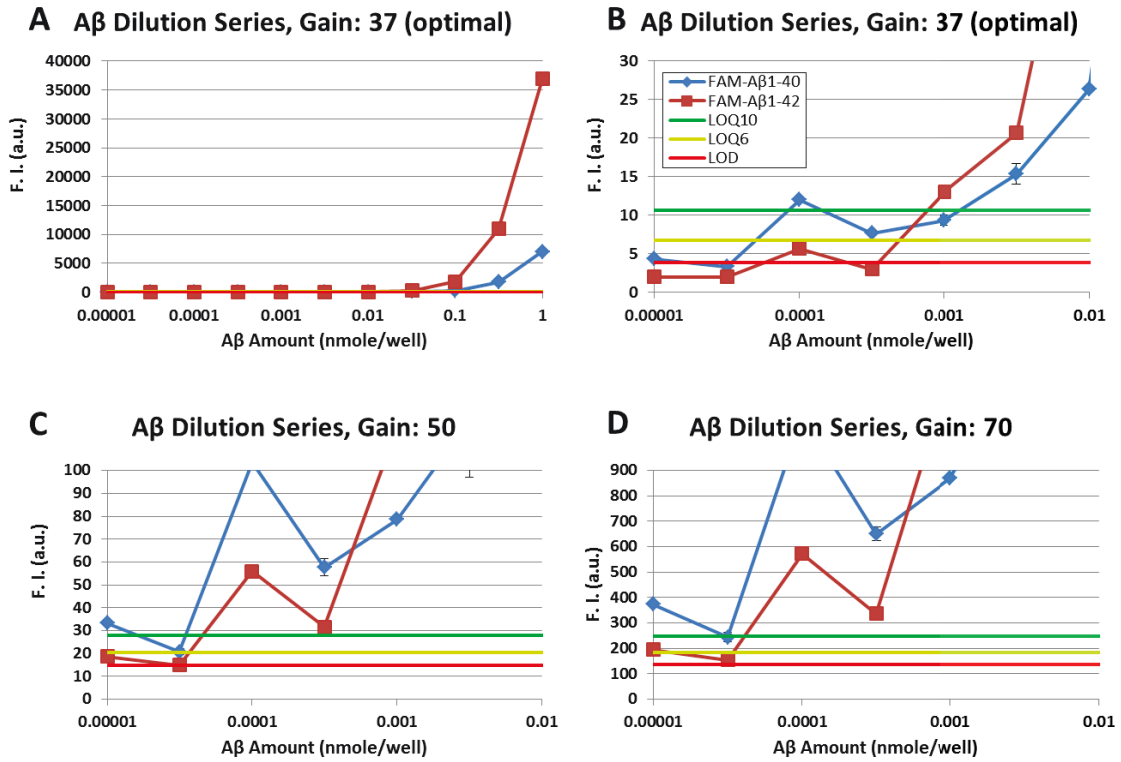


Figure V-7 Limit of Detection and Limit of Quantitation for FAM-A β .

To determine the Limit of Detection (LoD) and Limit of Quantitation (LoQ) for FAM-A β , dilution series (1 - 0.00001 nmol/well) of FAM-A β_{1-40} (blue line) and FAM-A β_{1-42} (dark red line) were added to a BSA-blocked 96-well plate, along with appropriate Control samples (PBS). The fluorescence signal at 535 nm was read with excitation at 485 nm; gain factor settings were adjusted to different values (see text). The LoD (bright red line), LoQ₆ (light green line) and LoQ₁₀ (green line) were calculated from the Control sample values according to Equations $LoD = \bar{x} + 3*s^2$ (V-1) - $LoQ_{10} = \bar{x} + 10*s^2$ (V-3) (for details see text). Panel A and B show graphs for the gain factor setting 'optimal', where A shows the complete A β amount and fluorescence intensity range, and B zooms into the lower amount/fluorescence intensity regions to allow distinction of LoD, LoQ₆ and LoQ₁₀. Graphs for gain factor settings '50' and '70' are shown in panel C and D, respectively (note the different vertical scales). Graphs for gain factor settings '90', '100', '110', '130', and '150' are not displayed since no more qualitative changes (fluorescence intensity values vs. LoD/LoQ) occurred. Error Bars: \pm S.E.M. (n = 3; for Control: n = 30). F.I.: fluorescence intensity; a.u.: arbitrary units.

Table V-5 Limit of Detection and Limit of Quantitation for FAM-A β .

The fluorescence intensity (F.I.) values for the Limit of Detection (LoD) and Limit of Quantitation (LoQ) were determined as described in the text. The LoD and LoQ for FAM-A β were calculated based on linear regressions for the dilution series of FAM-A β_{1-40} and FAM-A β_{1-42} . a.u. = arbitrary units; n/d: not determined, since there were too few points in the calibration curves (dilution series).

Gain Factor Setting	LoD			LoQ ₆			LoQ ₁₀		
	F.I. (a.u.)	FAM-A β_{1-40}	FAM-A β_{1-42}	F.I. (a.u.)	FAM-A β_{1-40}	FAM-A β_{1-42}	F.I. (a.u.)	FAM-A β_{1-40}	FAM-A β_{1-42}
Optimal (37)	3.8	1.3E-2	1.0E-2	6.7	1.4E-2	1.0E-2	10.7	1.4E-2	1.2E-2
50	14.8	1.1E-2	2.2E-3	20.5	1.1E-2	2.2E-3	28.1	1.1E-2	2.3E-3
70	135.6	-2.9E-3	3.0E-4	184.1	-2.7E-3	3.5E-4	248.8	-2.4E-3	4.3E-4
90	783.4	-1.7E-3	-2.4E-4	1066	-1.5E-3	-1.6E-4	1443	-1.2E-3	-5.3E-5
100	1,659	-2.5E-3	-3.5E-4	2,257	-2.2E-3	-2.6E-4	3,055	-1.9E-3	-1.3E-4
110	3,339	-2.4E-3	-3.5E-4	4,541	-2.2E-3	-2.6E-4	6,143	-1.9E-3	-1.4E-4
130	11,950	-1.3E-4	-2.5E-4	16,310	-8.3E-5	-1.5E-4	22,130	-2.3E-5	-7.6E-6
150	37,350	n/d	n/d	50,970	n/d	n/d	69,130	n/d	n/d

3.5.1. GM1 Coating Variability

To assess the variability of coating of 96-well plates with GM1, the amount of GM1 attached to the plate was determined by an assay that is based on the specific binding of the non-toxic cholera toxin subunit B to GM1. In order to minimise the influence of non-random effects like uneven heating of the plate, distribution of the samples was randomised over the entire plate.

Inspection of the results (see Figure V-8 and Table V-6) first of all revealed a dose-dependent detection of the binding of CtxB to GM1, which also confirmed a dose-dependent immobilisation of GM1 on the 96-well plates, i.e., the validity of the GM1 Assay principle.

In terms of variability of the GM1 plate coating, besides the highest GM1 amount (S.E.M.: 8.7%), standard errors were below 2%, i.e., well within an acceptable range for such an assay.

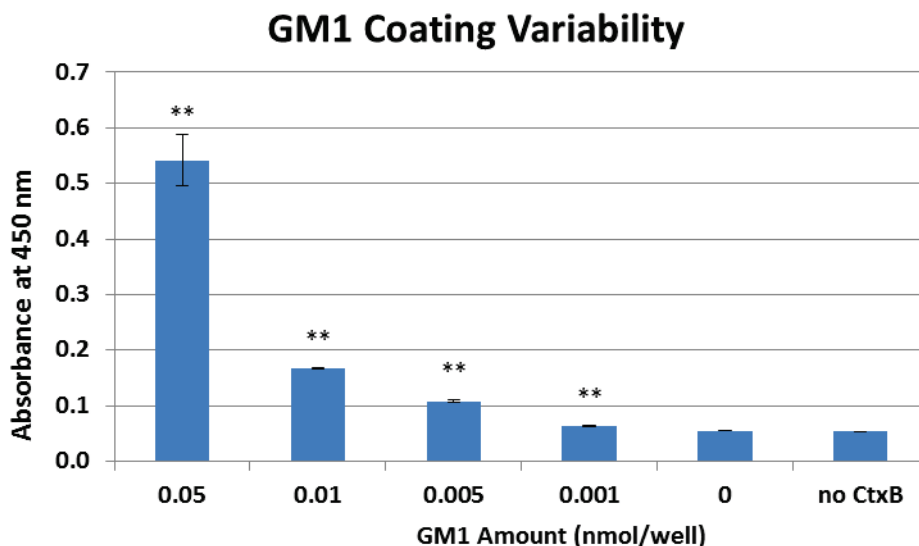


Figure V-8 GM1 plate coating variability.

To assess variability of coating plates with GM1, a 96-well plate was coated with four different concentrations of GM1 in a randomised pattern. Specific binding of HRP-labeled cholera toxin subunit B (CtxB) to GM1 allowed analysis of the variability of GM1 binding to the 96-well plate surface. Significance is shown for difference to next smaller GM1 amount; there was no significant difference between '0' and 'no CtxB'; *: $P < 0.05$; **: $P < 0.01$ ($n = 5$; two-tailed Student's t-test).

Table V-6 GM1 plate coating variability.

Data for GM1 plate coating variability results depicted in Figure V-8.

GM1 Amount (nmol/well)	Average Absorbance	S.E.M.	S.E.M. %
0.05	0.5420	0.0471	8.7%
0.01	0.1675	0.0016	1.0%
0.005	0.1077	0.0018	1.7%
0.001	0.0636	0.0007	1.0%
0 ^a	0.0552	0.0006	1.2%
no CtxB	0.0531	0.0006	1.2%

^a: one outlier (confirmed by Grubb's Test) was removed.

3.5.2. Plate Washing

In order to determine how many washing steps after incubation with FAM-A β are optimal, a 96-well plate was prepared and incubated with FAM-A β_{1-40} and FAM-A β_{1-42} as described in the methods section.

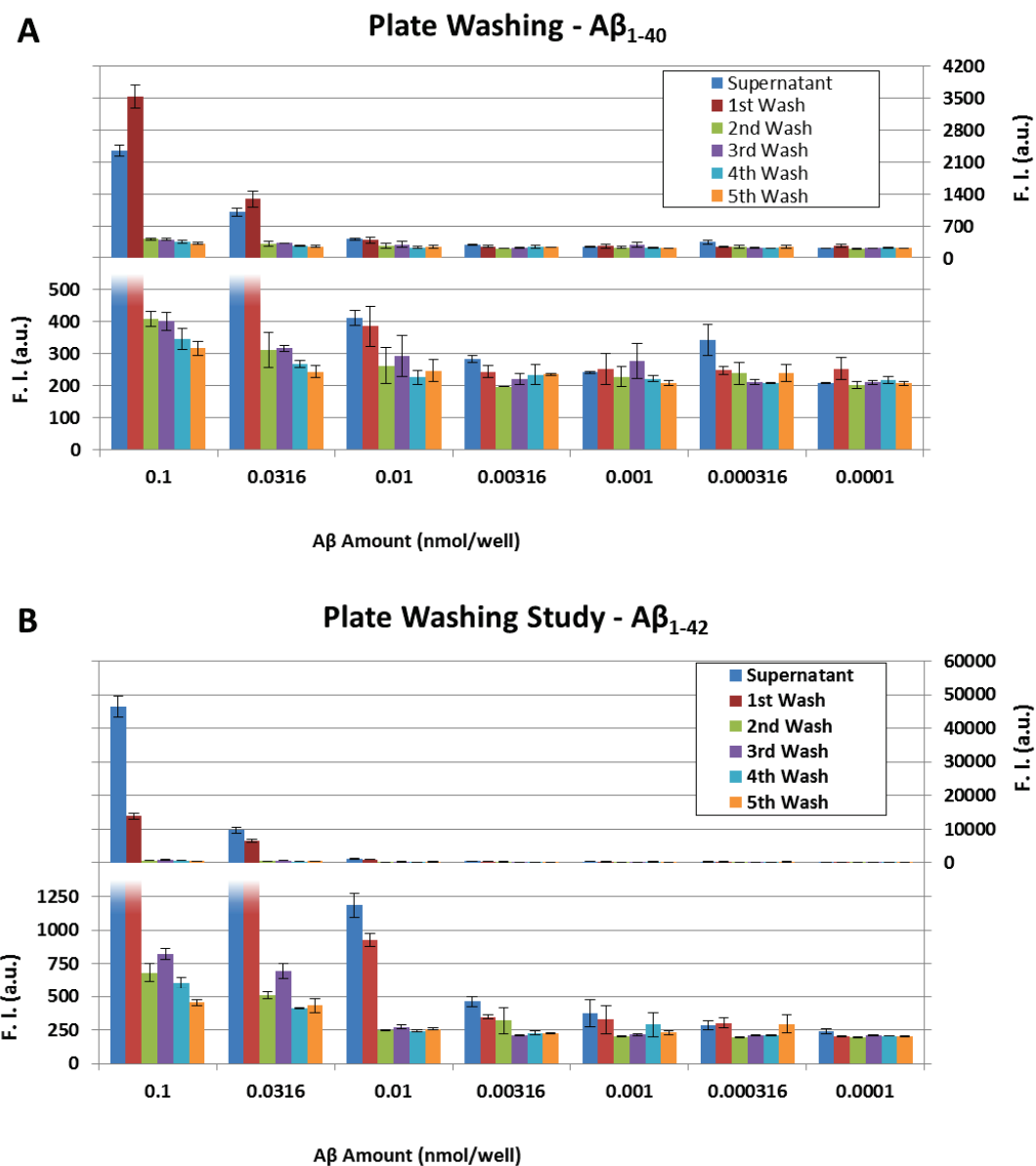


Figure V-9 GM1 Assay plate washing study – experiment 1.

To determine how many washing steps after incubation with FAM-A β are optimal, a 96-well plate was prepared and incubated with FAM-A β ₁₋₄₀ and FAM-A β ₁₋₄₂ as described in the methods section. Samples of the supernatant and washing buffers were transferred to BSA-blocked 96-well plates and their fluorescence intensity read in a plate reader (Gain Factor setting: 80). Panel A shows results for A β ₁₋₄₀, panel B for A β ₁₋₄₂. In each panel, the top graph shows complete results, while the bottom graph zooms into the lower F.I. regions. Error Bars: \pm S.E.M. (n = 3). F.I.: fluorescence intensity; a.u.: arbitrary units.

Inspecting the results (see Figure V-9), one striking observation is that the fluorescence intensity of the FAM-A β ₁₋₄₂ samples is much higher than for A β ₁₋₄₀; for the highest amount (0.1 nmol/well) of supernatant by almost 20-fold. One possible reason may be that the

FAM-A β ₁₋₄₂ had a higher peptide content than the FAM-A β ₁₋₄₀. According to the supplier (Anaspec), it is not possible to determine the peptide content of a fluorescently labeled peptide by amino acid analysis, the gold standard to determine peptide content of a sample. Therefore, the amounts and concentrations given here are only nominal values. A low FAM-A β ₁₋₄₀ concentration may not only exhibit a lower fluorescence intensity due to the lower concentration to begin with, but may also lead to considerable depletion, where the majority of the peptide is bound to the GM1, and therefore to a lower than expected signal.

In regards to the optimal number of washes, after 4 washes the fluorescence intensity of all samples except the highest concentration reaches essentially base levels, indicative of absence of free peptide to be washed away. Therefore, three washes were deemed optimal and used in all subsequent experiments.

For the second washing experiment, the plates were coated with 0.01 nmol/well of GM1, the optimum amount determined in the first sensitivity test (see Section 3.5.3 below); only the FAM-A β amount was varied.

This second experiment confirmed that three washes are sufficient to remove any free FAM-A β ₁₋₄₀ from the assay plate (see Figure V-10); actually here already the third wash showed no signal significantly higher than the background. One reason might be that in the second experiment with the regular plates a detergent, the non-ionic Tween-20, was included in the washing buffer (PBST). Comparing the results of the regular to the half-area plate, the effect of the missing detergent (in the half-area plate washes) can be seen in the more gradual decline of the signal with consecutive washes, in particular for the higher FAM-A β ₁₋₄₀ concentrations.

Another observation is the lower fluorescence signal for the half-area plate as indicated by the higher Gain Factor setting ('80' vs. '101'). One explanation may be that the material of the

plates was not exactly the same and different relative amounts of GM1 were bound to the well bottoms.

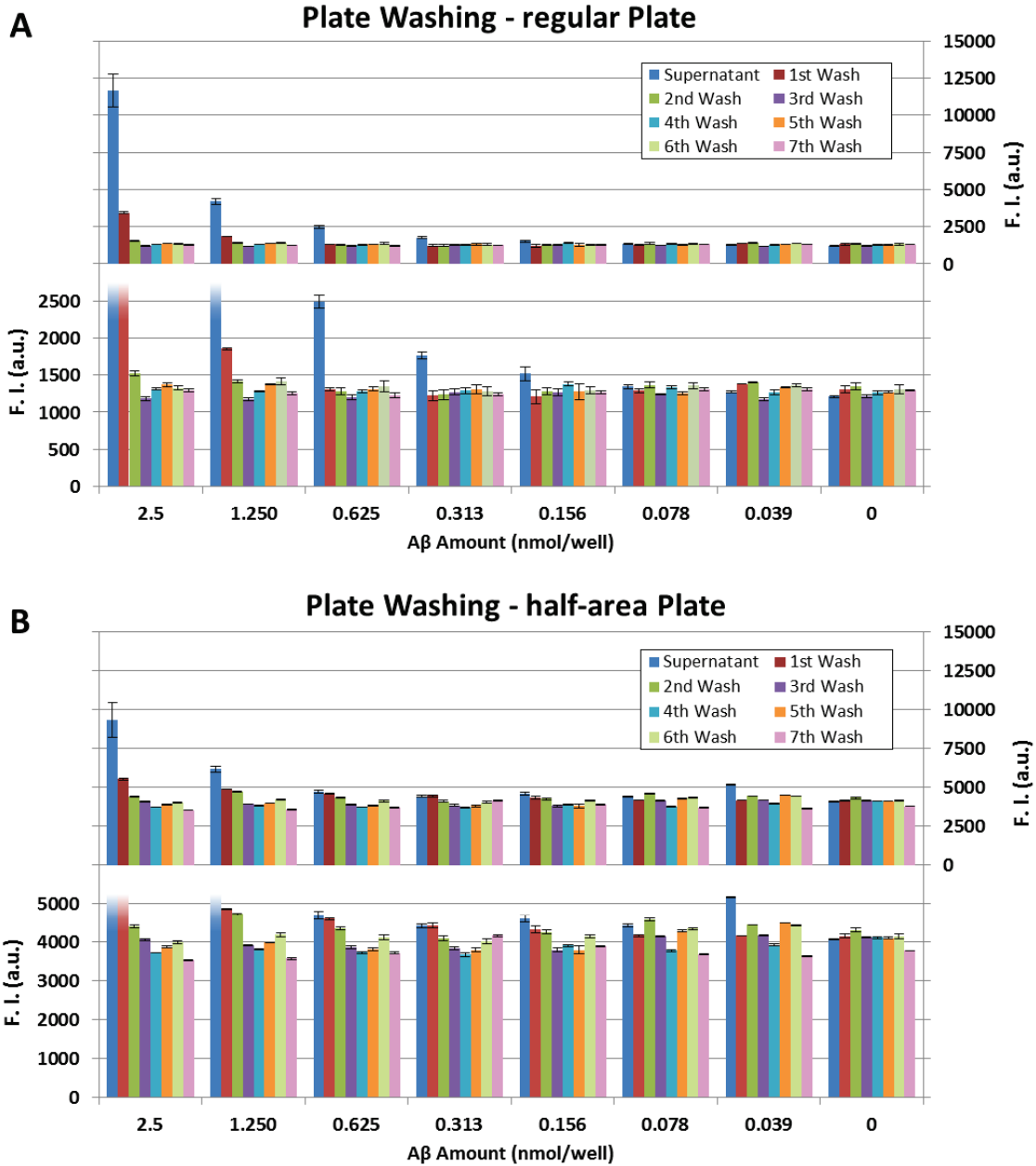


Figure V-10 GM1 Assay plate washing study – experiment 2.

To confirm in a second experiment how many washing steps after incubation with FAM-Aβ are optimal, a 96-well plate was prepared and incubated with FAM-Aβ₁₋₄₀ as described in the methods section. Samples of the supernatant and washing buffers were again transferred to BSA-blocked 96-well plates and their fluorescence intensity read in a plate reader (Gain Factor settings: 80 (regular) and 101 (half-area)). Panel A shows results for regular-sized wells, panel B for half-area wells. In each panel, the top graph shows complete results, while the bottom graph zooms into the lower F.I. regions. Error Bars: ± S.E.M. (n = 3). F.I.: fluorescence intensity; a.u.: arbitrary units.

3.5.3. Sensitivity

In order to determine the sensitivity of the GM1 Assay, i.e., the lowest amount/concentration of (FAM-)A β detectable by the assay, in a first experiment, a 96-well plate was coated with a dilution series of GM1 (see Section 3.4.3), and then incubated with equal amounts of FAM-A β ₁₋₄₀ and FAM-A β ₁₋₄₂. Subsequently, the fluorescence intensity was read of the (transferred) supernatant and of the assay plate after each washing step to simultaneously determine the optimal number of washing steps (see previous section).

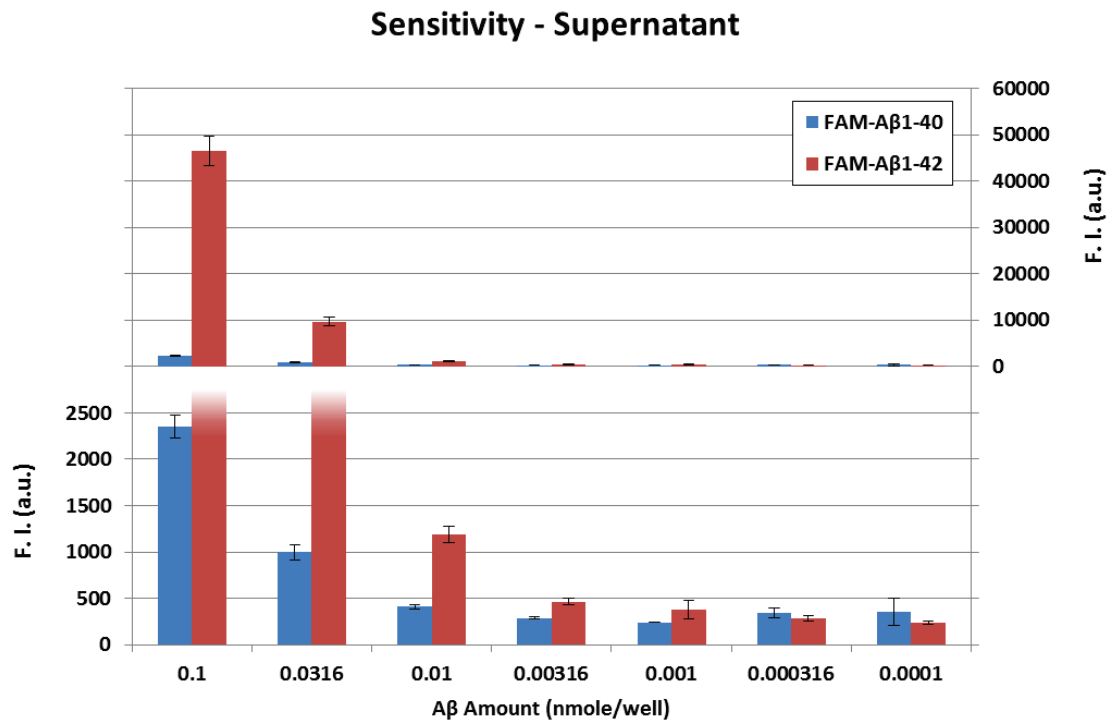


Figure V-11 Sensitivity of the GM1 Assay - experiment 1 – supernatant.

To determine the sensitivity of the GM1 Assay, a 96-well plate was prepared and incubated with FAM-A β ₁₋₄₀ and FAM-A β ₁₋₄₂ as described in the methods section. Samples of the supernatant were transferred to BSA-blocked 96-well plates and their fluorescence intensity read in a plate reader (Gain Factor setting: 80). The top graph shows complete results, while the bottom graph zooms into the lower F.I. regions. Error Bars: \pm S.E.M. (n = 3). F.I.: fluorescence intensity; a.u.: arbitrary units.

As already mentioned in the previous section, the two forms of FAM-A β show very different fluorescence intensity levels in the supernatant (see Figure V-9 and Figure V-11). One possible reason mentioned was different actual peptide contents of the two FAM-A β forms. However, comparing the fluorescence signals from the assay plates, they differ only by a factor of about two (see Figure V-12). Taken together, this might imply a higher affinity of FAM-A β_{1-40} to GM1 compared with FAM-A β_{1-42} ; however, affinities for binding of diethylaminocoumarin-3-carbonyl-labeled A β_{1-40} and A β_{1-42} to liposomes (GM1 : cholesterol : SM = 1 : 1 : 1) were reported to be very similar for both forms (70).

Furthermore, comparison of the intensities of supernatant and assay plates shows a higher signal for the supernatant (Gain Factor settings are '80' and '120' for supernatant and assay plate, respectively), indicating that most of the FAM-A β is not bound to GM1 (molar ratio of added FAM-A β : GM1 = 1 : 1).

Inspection of the graphs in Figure V-12 reveals that each washing step reduces the signal, although in most cases not statistically significant. This result is also reflected in the graphs for the washing solutions (see Figure V-9) where subsequently lower fluorescence signals are detected with each washing step.

The lower limit of sensitivity for FAM-A β_{1-40} is 0.0316 nmol/well, since the fluorescence intensity for that amount is, after three washes, statistically significant larger than the next one (0.01 nmol/well), which is not statistically significant larger than all of the following amounts. For FAM-A β_{1-42} , the lower limit of sensitivity is 0.00316 nmol/well.

Finally, addition of PBS enhanced the fluorescence signal by up to over 100%; however, this enhancement seemed to depend on the concentration in a non-linear fashion with a smaller effect at lower amounts of FAM-A β . Furthermore, samples generally showed a larger absolute as well as relative error.

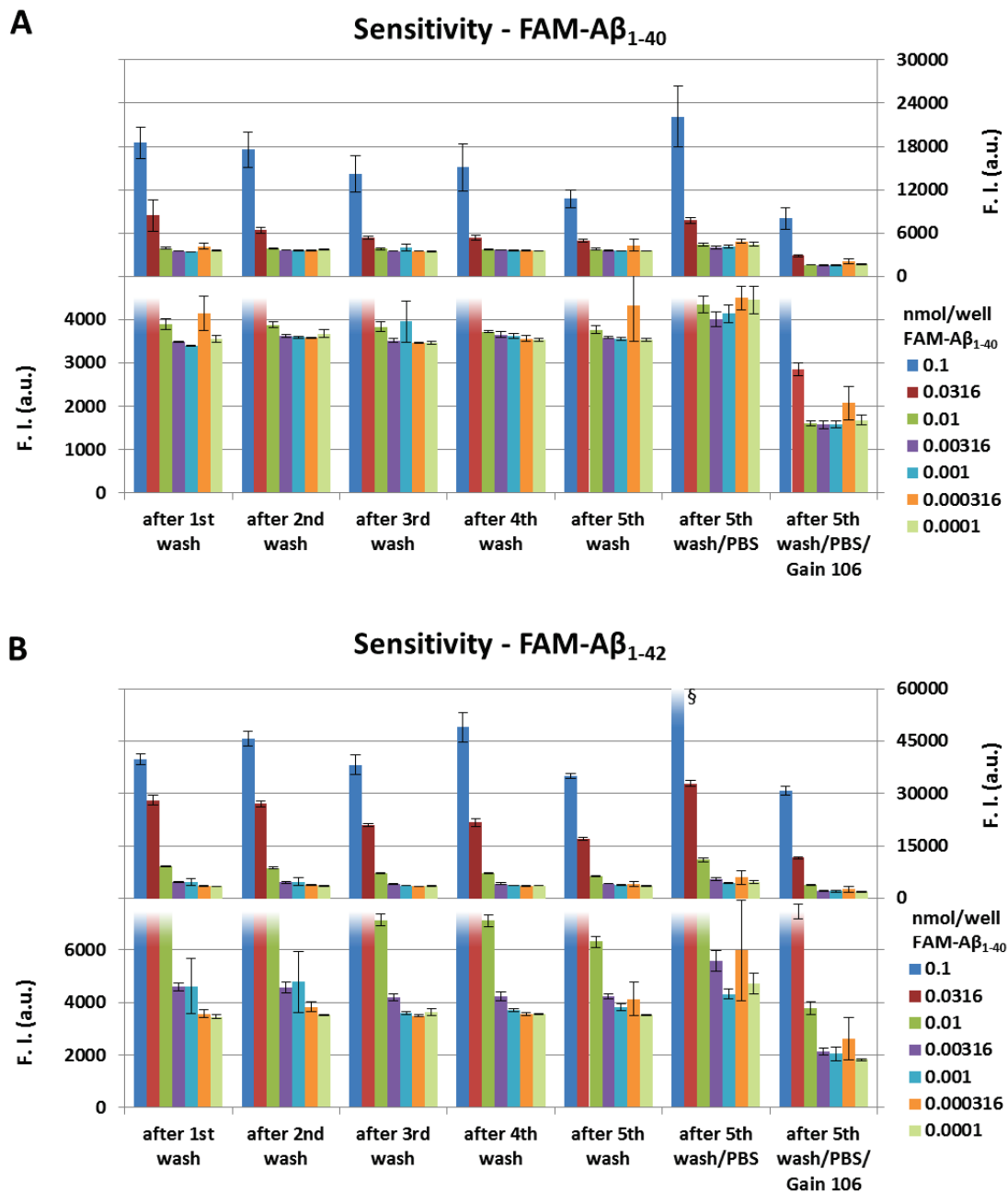


Figure V-12 Sensitivity of the GM1 Assay - experiment 1 – assay plate.

To determine the sensitivity of the GM1 Assay, a 96-well plate was prepared and incubated with FAM-A β ₁₋₄₀ (A) and FAM-A β ₁₋₄₂ (B) as described in the methods section. After each of 5 washes, the fluorescence intensity was read in a plate reader (Gain Factor setting: 120 ('optimal' setting for „after 1st wash“)). After the last wash, 50 μ L/well PBS were added and the plate was read again. Since the '0.1 nmol/well' value for A β ₁₋₄₂ was out of range for the instrument (§), the optimal gain setting was determined again; it was '106' and the plate read at that setting. Error Bars: \pm S.E.M. (n = 3). F.I.: fluorescence intensity; a.u.: arbitrary units.

For a second experiment, the plates were coated with 0.01 nmol/well of GM1; only the FAM- $\text{A}\beta_{1-40}$ amount was varied.

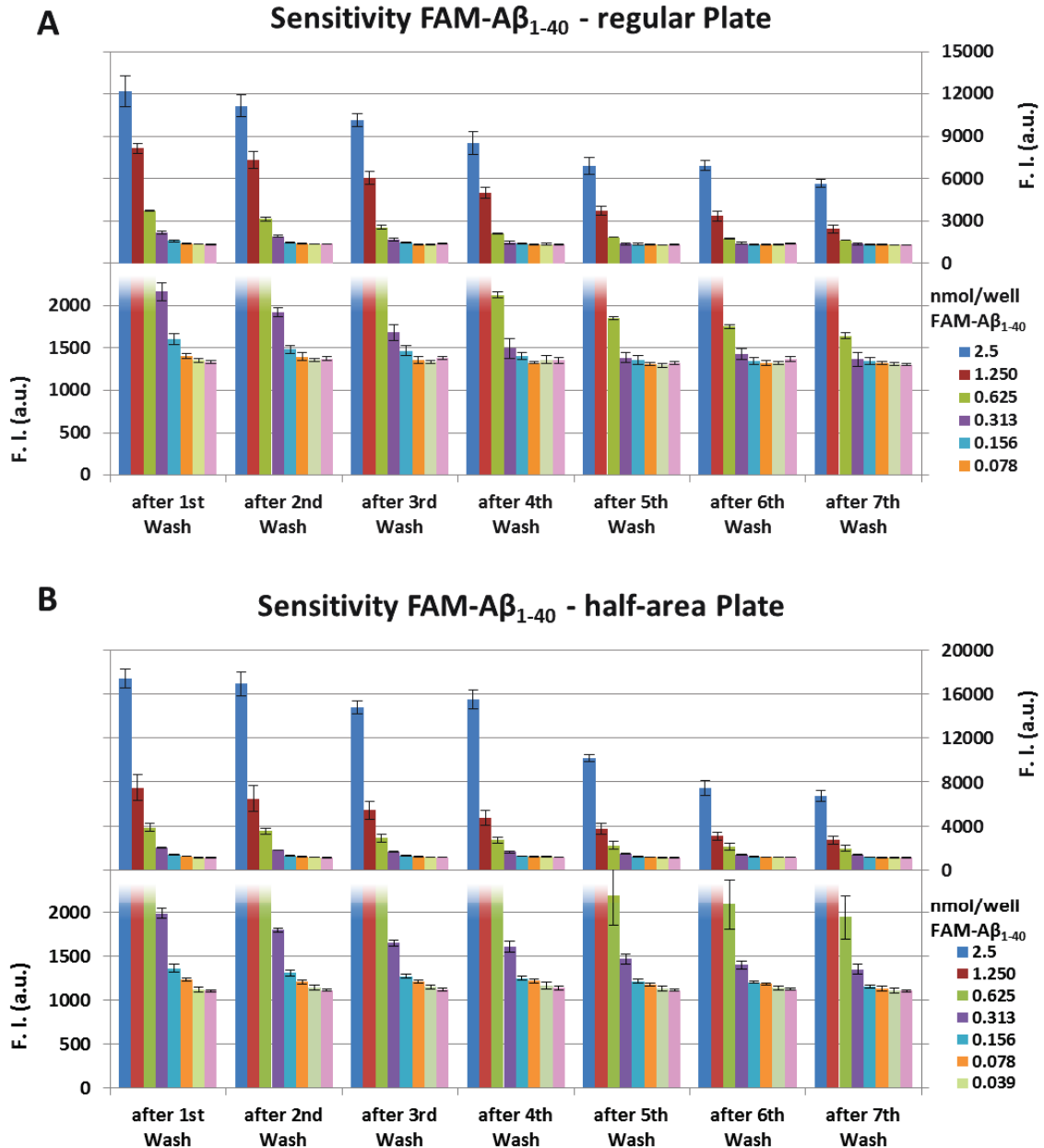


Figure V-13 Sensitivity of the GM1 Assay - experiment 2 – assay plate.

To further investigate the sensitivity of the GM1 Assay, a regular and a half-area 96-well plate were prepared and incubated with FAM- $\text{A}\beta_{1-40}$ as described in the methods section. Before, and after each of 7 washes, the fluorescence intensity was read in a plate reader (Gain Factor settings: 85 (regular) and 101 (half-area)). Panel A shows results for regular-sized wells, panel B for half-area wells; the top graph shows complete results, while the bottom graph zooms into the lower F.I. regions. Error Bars: \pm S.E.M. (n = 3). F.I.: fluorescence intensity; a.u.: arbitrary units.

In the second experiment (see Figure V-13), again the fluorescence intensity decreases with each consecutive washing step until it reached background levels. The limit of sensitivity was 0.625 μM for the regular plate, and 0.313 μM for the half-area plate.

In subsequent experiments requiring only one GM1 concentration, in order to allow detecting a fluorescence signal decrease caused by an investigated sample treatment without getting too close to the sensitivity limit, plates were coated with 0.1 nmol/well GM1.

3.5.4. Competitive Binding Assays

In order to showcase the utility of the GM1 Assay, the influence of a number of different competitors on the binding and aggregation of FAM-A β on GM1 were investigated.

3.5.4.1. Influence of Metal Ions

Since copper and zinc ions had been shown to bind to A β (in the same region as GM1) and to modulate the aggregation of A β , their influence on the fluorescence signal of the GM1 Assay was determined. GM1-coated plates (0.1 nmol/well) were incubated with FAM-A β_{1-40} and FAM-A β_{1-42} (0.25 and 2.5 μM) in presence of a dilution series of Cu²⁺ and Zn²⁺ (0.1 / 1 / 10 / 100 / 316 / 1000 μM in PBS) overnight (for 15.5 hours). Supernatant and assay plates were treated and read in a plate reader as described previously; results for FAM-A β_{1-40} are shown in Figure V-14, those for FAM-A β_{1-42} in Figure V-15.

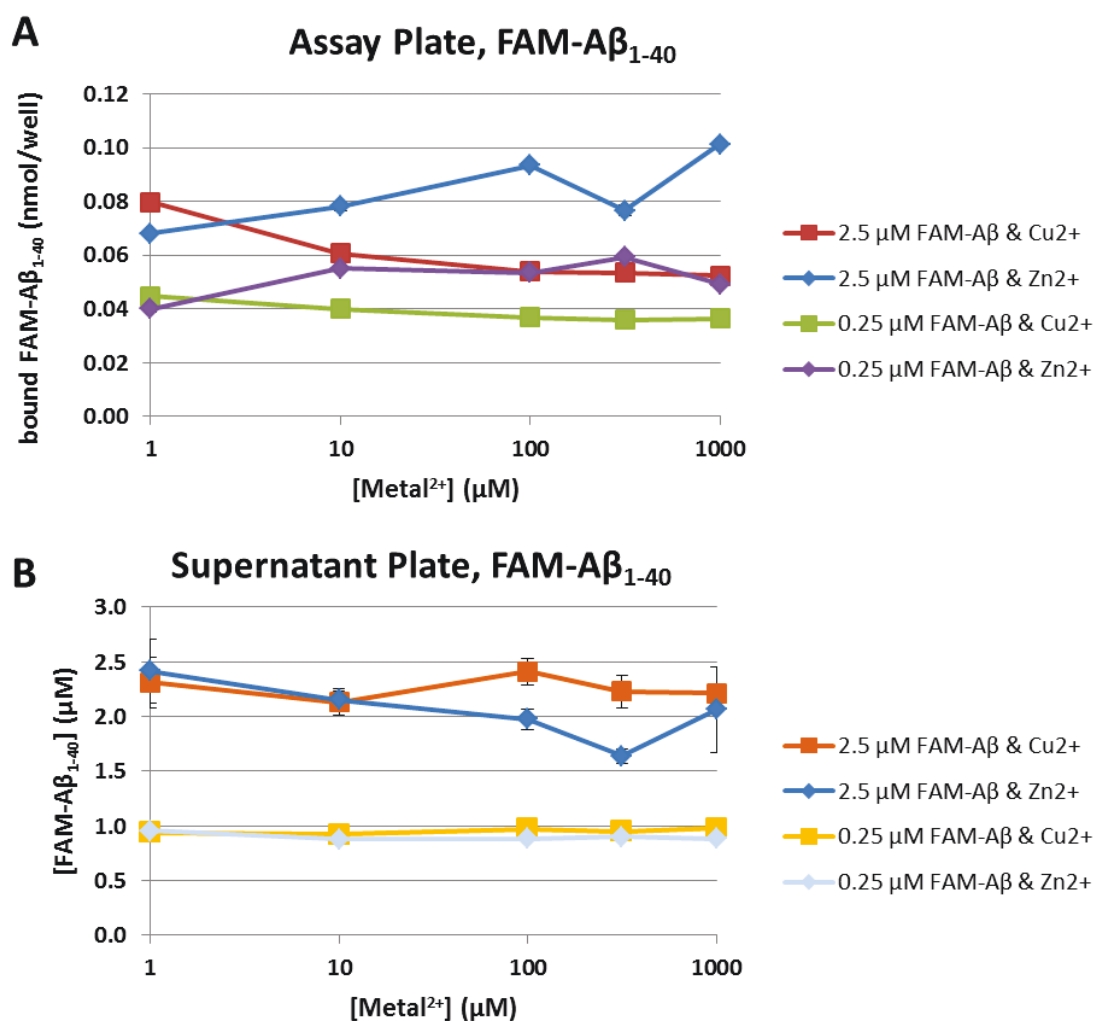


Figure V-14 Influence of Cu²⁺ and Zn²⁺ on GM1 – Aβ₁₋₄₀ binding and aggregation. GM1-coated plates (0.1 nmol/well) were incubated with FAM-Aβ₁₋₄₀ (0.25 and 2.5 μM) in presence of dilution series of Cu²⁺ and Zn²⁺ (0.1 / 1 / 10 / 100 / 316 / 1000 μM in PBS) overnight (for 15.5 hours); then the amount of bound (A) and free (B) FAM-Aβ₁₋₄₀ was determined as described previously (Gain Factor setting: 100). Error Bars: ± S.E.M. (n = 3); where invisible, error bars are smaller than marker.

Incubation with Cu²⁺ and Zn²⁺ had an opposing effect; while Cu²⁺ caused a decrease in bound FAM-Aβ₁₋₄₀, Zn²⁺ induced an increase, with a more pronounced effect for higher FAM-Aβ₁₋₄₀ concentrations. In the supernatant, only Zn²⁺ exhibited an effect when incubated with the higher concentration of FAM-Aβ₁₋₄₀ leading to a decrease in FAM-Aβ₁₋₄₀.

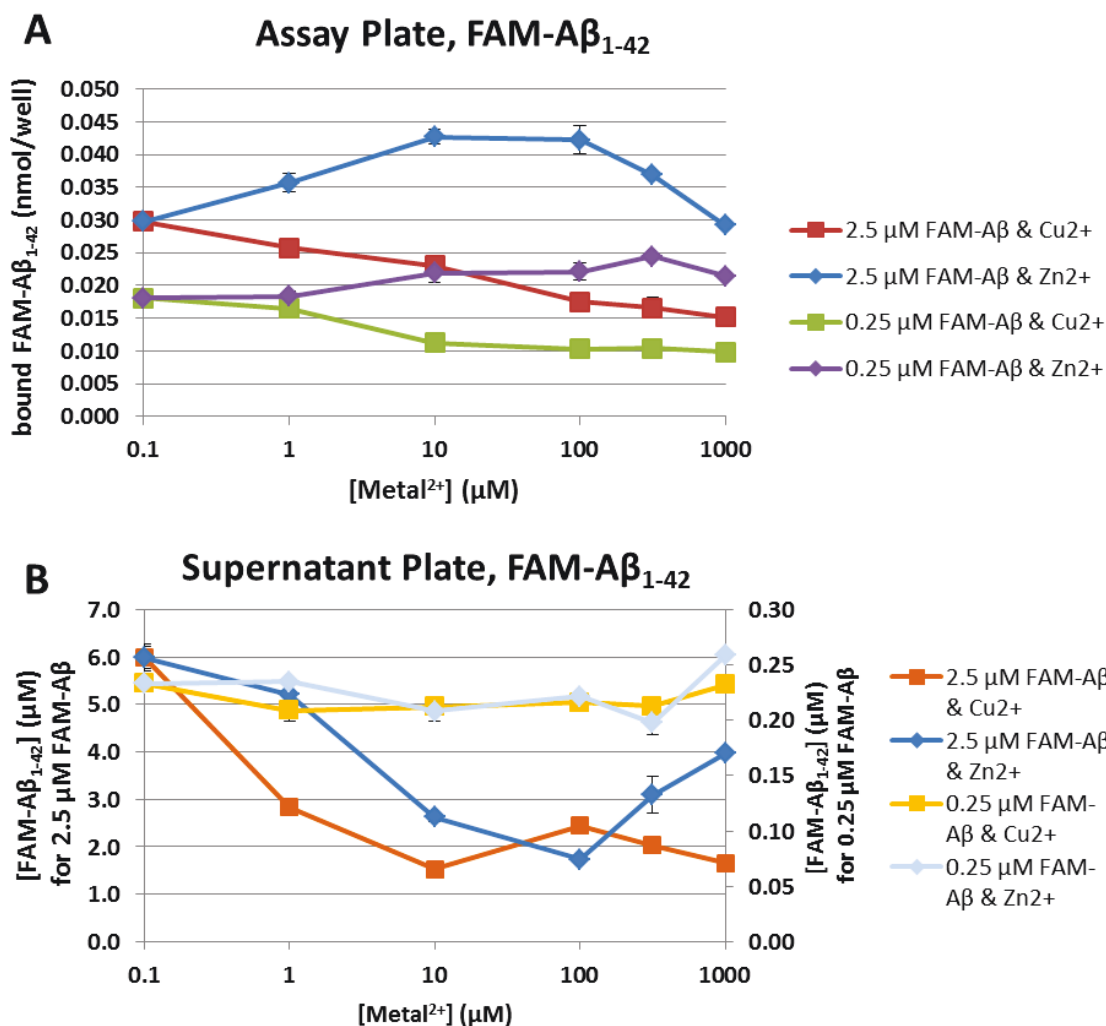


Figure V-15 Influence of Cu²⁺ and Zn²⁺ on GM1 – A β ₁₋₄₂ binding and aggregation. GM1-coated plates (0.1 nmol/well) were incubated with FAM-A β ₁₋₄₂ (0.25 and 2.5 μM) in presence of dilution series of Cu²⁺ and Zn²⁺ (0.1 / 1 / 10 / 100 / 316 / 1000 μM in PBS) overnight (for 15.5 hours); then the amount of bound (A) and free (B) FAM-A β ₁₋₄₂ was determined as described previously (Gain Factor setting: 75). Note secondary vertical axis for 0.25 μM FAM-A β ₁₋₄₂. Error Bars: \pm S.E.M. (n = 3); where invisible, error bars are smaller than marker.

For FAM-A β ₁₋₄₂, similar effects were seen for the bound portion in the presence of Cu²⁺ and for Zn²⁺ at 0.25 μM FAM-A β ₁₋₄₂; albeit at lower bound amounts of FAM-A β ₁₋₄₂. However, at 2.5 μM FAM-A β ₁₋₄₂, Zn²⁺ first led to an increase in the amount of FAM-A β ₁₋₄₂ bound to the plate (up to 10 μM Zn²⁺), but then caused a decrease in the bound amount. In the supernatant, Cu²⁺ and Zn²⁺ showed no or only a minor effect at the lower FAM-A β ₁₋₄₂ concentration, however, at

2.5 μM FAM- $\text{A}\beta_{1-42}$, in presence of Cu^{2+} the free amount of FAM- $\text{A}\beta_{1-42}$ first decreased (up to 10 μM Cu^{2+}), but then levelled off. In presence of Zn^{2+} , the free amount of FAM- $\text{A}\beta_{1-42}$ showed a complimentary effect to the bound amount, i.e., it first decreased (up to 10 μM Zn^{2+}), but then increased again. Drawing straight lines through the increasing (0.1 – 10 μM Zn^{2+}) and decreasing (100 – 1000 μM Zn^{2+}) portions of the graphs allows calculation of the point where these lines intersect (see Figure V-16); for the bound FAM- $\text{A}\beta$ they intersect at 9.5 μM Zn^{2+} , and for the free FAM- $\text{A}\beta$ at 12.1 μM Zn^{2+} , i.e., at values very close to each other.

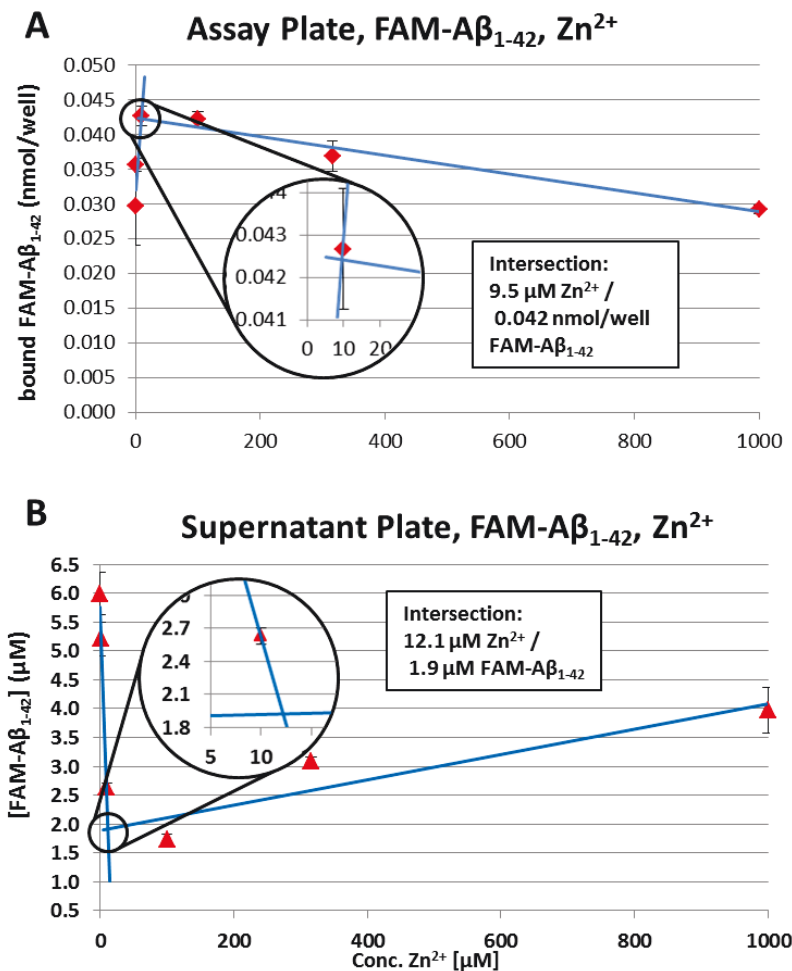


Figure V-16 Influence of Zn^{2+} on GM1 – $\text{A}\beta_{1-42}$ binding and aggregation.

At 2.5 μM FAM- $\text{A}\beta_{1-42}$, the influence of Zn^{2+} shows two distinct phases; up to 10 μM it first leads to a sharp increase in the amount of FAM- $\text{A}\beta_{1-42}$ that is bound to the plate (A), and then to a more gradual decrease of the bound amount. The supernatant (B) shows a complimentary shape of the curve that closely mirrors this effect as indicated by the intersection values. Note the non-logarithmic scale on the x-axis (as opposed to Figure V-15). Error Bars: \pm S.E.M. (n = 3); where invisible, error bars are smaller than marker.

One explanation for this effect may be that at lower concentrations, Zn^{2+} just increases the aggregation of $A\beta$ onto the pre-existing GM1 – $A\beta$ seeds, however, at higher concentrations, it also promotes the formation of seeds within the supernatant thus decreasing the amount of $A\beta$ that is available to attach to GM1 or grow GM1-bound aggregates.

3.5.4.2. Time Dependence of Zinc Effect

To further investigate this effect, a time series experiment was performed, where a GM1-coated plate (0.1 nmol/well) was incubated with 2.5 μM FAM- $A\beta_{1-42}$ in the presence of a dilution series of Zn^{2+} (0.1 / 1 / 10 / 31.6 / 100 / 1000 μM in PBS) for 0.5 h, 2 h, 4 h, and 18 h (see Figure V-17).

The results clearly show a time-dependent pattern of the zinc effect. At 0.5 hours, the amount of GM1-bound FAM- $A\beta_{1-42}$ only slightly increased with increasing Zn^{2+} concentration, but already after 2 hours a 'bump' appeared with a maximum at 31.6 μM Zn^{2+} (this data point was included, to allow more accurate determination of the Zn^{2+} concentration with maximal effect compared to the previous experiment). This maximum increased further through the next two time points. In the supernatant, a 'dip' (the inverse of a 'bump') was detectable only after 4 hours, with the minimum at 31.6 μM Zn^{2+} , and increasing values at 100 and 1000 μM Zn^{2+} upon further incubation. For the 18 hour experiment, the intersections of the straight lines drawn through the increasing (0.1 – 31.6 μM Zn^{2+}) and decreasing (31.6 – 1000 μM Zn^{2+}) portions of the graphs were at 15.6 μM Zn^{2+} , and at 20.5 μM Zn^{2+} for bound and free FAM- $A\beta$, respectively, i.e., at values again quite close to each other, as well as close to the results from the previous experiment.

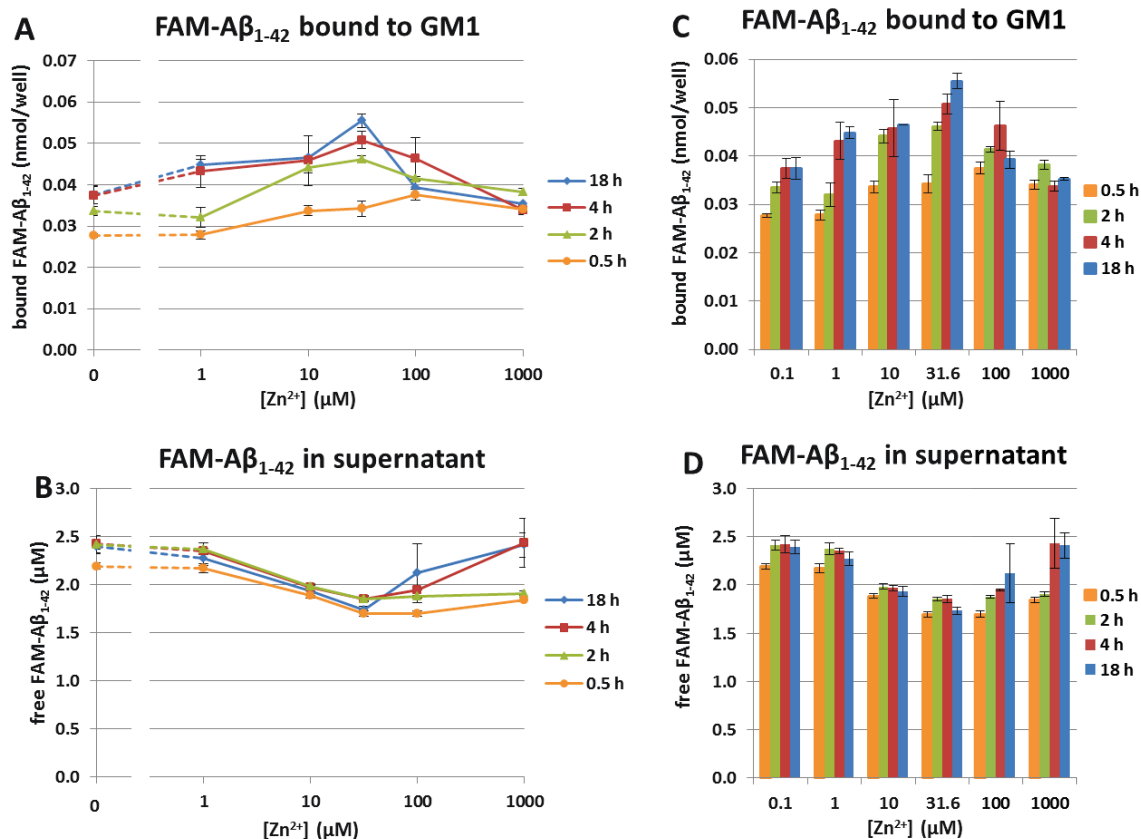


Figure V-17 Time dependence of zinc effect.

A GM1-coated plate (0.1 nmol/well) was incubated with FAM-Aβ₁₋₄₂ (2.5 μM) in presence of dilution series of Zn²⁺ (0 / 0.1 / 1 / 10 / 31.6 / 100 / 1000 μM in PBS); then the amount of bound (A and C) and free (B and D) FAM-Aβ₁₋₄₂ was determined as described previously after 0.5 h, 2 h, 4 h, and 18 h (Gain Factor settings: 100 (assay plate), 75 (supernatant plate)). Error Bars: ± S.E.M. (n = 3); where invisible, error bars are smaller than marker.

3.5.4.3. Influence of Aβ Antiaggregants

(a) Aβ Antiaggregants and Metals

Next, the response of the GM1 Assay to incubation in the presence of both, metal cations and Aβ antiaggregants, was tested. GM1-coated plates (0.1 nmol/well) were incubated with FAM-Aβ₁₋₄₀ and FAM-Aβ₁₋₄₂ (2.5 μM) in presence of a dilution series of three Aβ antiaggregants developed in this lab, NCE-217, NCE-370, and NCE-371 (0.001 / 0.1 / 0.316 / 1 / 3.16 / 10 / 100 μM), and two concentrations of Cu²⁺ and Zn²⁺ (31.6 / 1000 μM in PBS) overnight (for

18 hours). Assay plates were treated and read in a plate reader as described previously; results are shown in Figure V-18 and Figure V-19; IC_{50} values are compiled in Table V-7. Chemical structures for the A β aggregation inhibitors can be found in Figure V-20 (see p. 349).

Inspection of the results reveals a number of trends. For A β_{1-40} , increasing concentrations of Cu^{2+} caused a decrease in the amount of bound FAM-A β ; this effect was consistent for all inhibitor concentrations. Zn^{2+} had an opposite effect with increasing amounts of FAM-A β bound at higher concentrations of metal ion; however, this difference disappeared for higher concentrations of inhibitor. For A β_{1-42} , the effect of Cu^{2+} was stronger; Zn^{2+} on the other hand showed no effect. The results obtained here agree with those obtained earlier for Cu^{2+} (see Section 3.5.4.1), however, for Zn^{2+} one would have expected a higher amount of bound A β at 31.6 μ M than at 0 and 1000 μ M.

Another effect the metal ions exerted was on the elevation of the bottom plateau of the binding curves, i.e., the maximum inhibition of A β aggregation by an antiaggregant. This effect was particularly pronounced for the influence of Cu^{2+} on the activity of NCE-370 and NCE-371 against GM1-binding of FAM-A β_{1-42} , where an increase in the Cu^{2+} concentration led to an increase in the maximum aggregation inhibition by these antiaggregants. As this effect was not seen for all compounds it must be dependent on the chemical structure of the respective inhibitor and may involve binding of the metal ion to the antiaggregant.

A β ₁₋₄₀

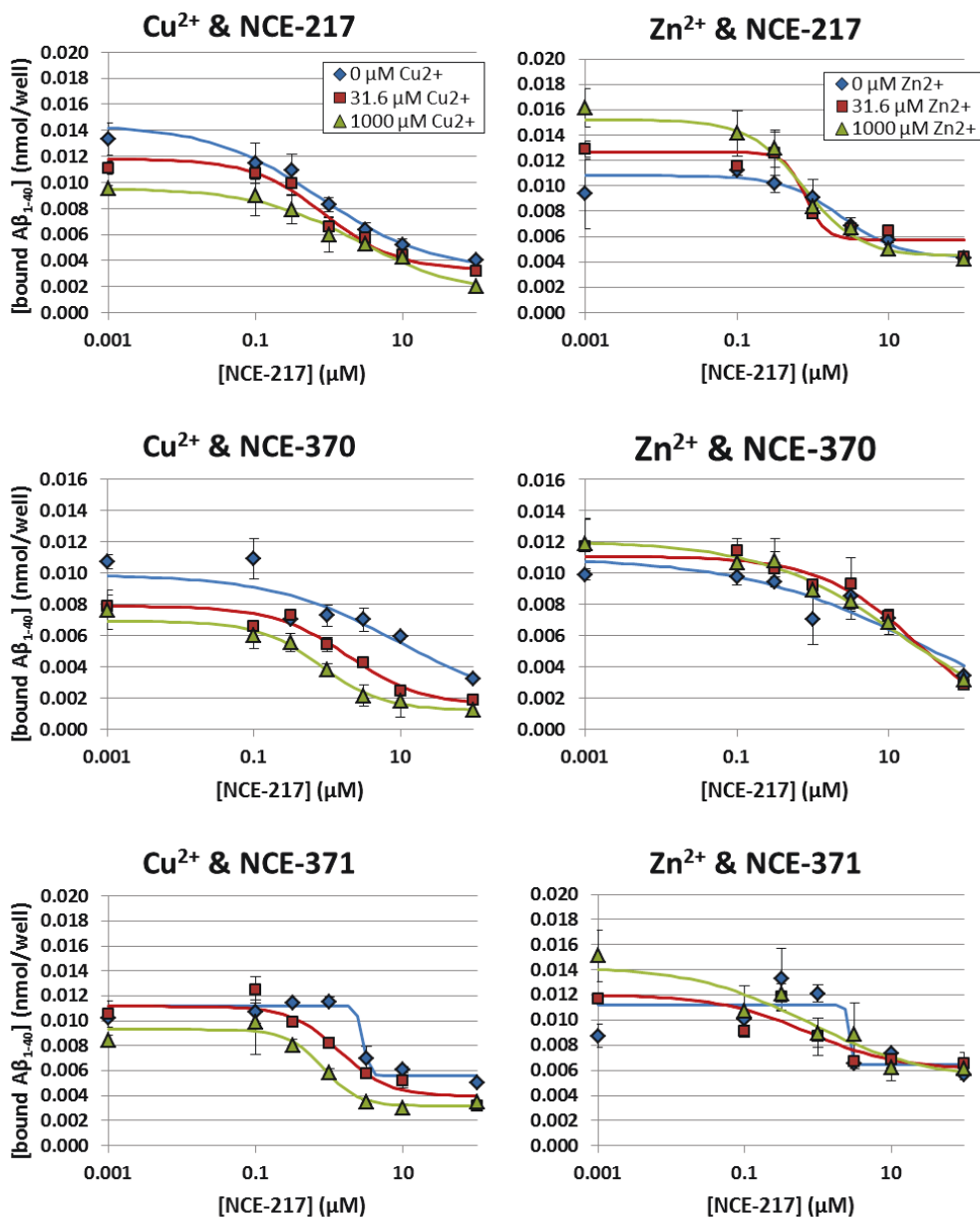


Figure V-18 Influence of metal ions and A β antiaggregants on GM1-binding by FAM-A β ₁₋₄₀. GM1-coated plates (0.1 nmol/well) were incubated with FAM-A β ₁₋₄₀ (2.5 μ M) in presence of a dilution series of three A β antiaggregants (NCE-217, NCE-370, and NCE-371; 0.001 / 0.1 / 0.316 / 1 / 3.16 / 10 / 100 μ M), and of two concentrations of Cu²⁺ (graphs on left) and Zn²⁺ (graphs on right) (31.6 / 1000 μ M in PBS) for 18 hours; then the amount of GM1-bound FAM-A β ₁₋₄₀ was determined as described previously (Gain Factor setting: 110). Data (markers: blue diamonds: 0 μ M Me²⁺, red squares: 31.6 μ M Me²⁺, green triangles: 1000 μ M Me²⁺) were fitted with a full 4-parameter fit to a sigmoidal curve (solid lines: blue: 0 μ M Me²⁺, red: 31.6 μ M Me²⁺, green: 1000 μ M Me²⁺) as described previously (see Chapter II, Section 2.7.4.4); fitting included the values for 0 μ M inhibitor, which could not be displayed on the logarithmically scaled x-axis, but were typically very close to the 0.001 μ M inhibitor values. Calculated IC₅₀ values are compiled in Table V-7. Error Bars: \pm S.E.M. (n = 3); where invisible, error bars are smaller than marker.

A β ₁₋₄₂

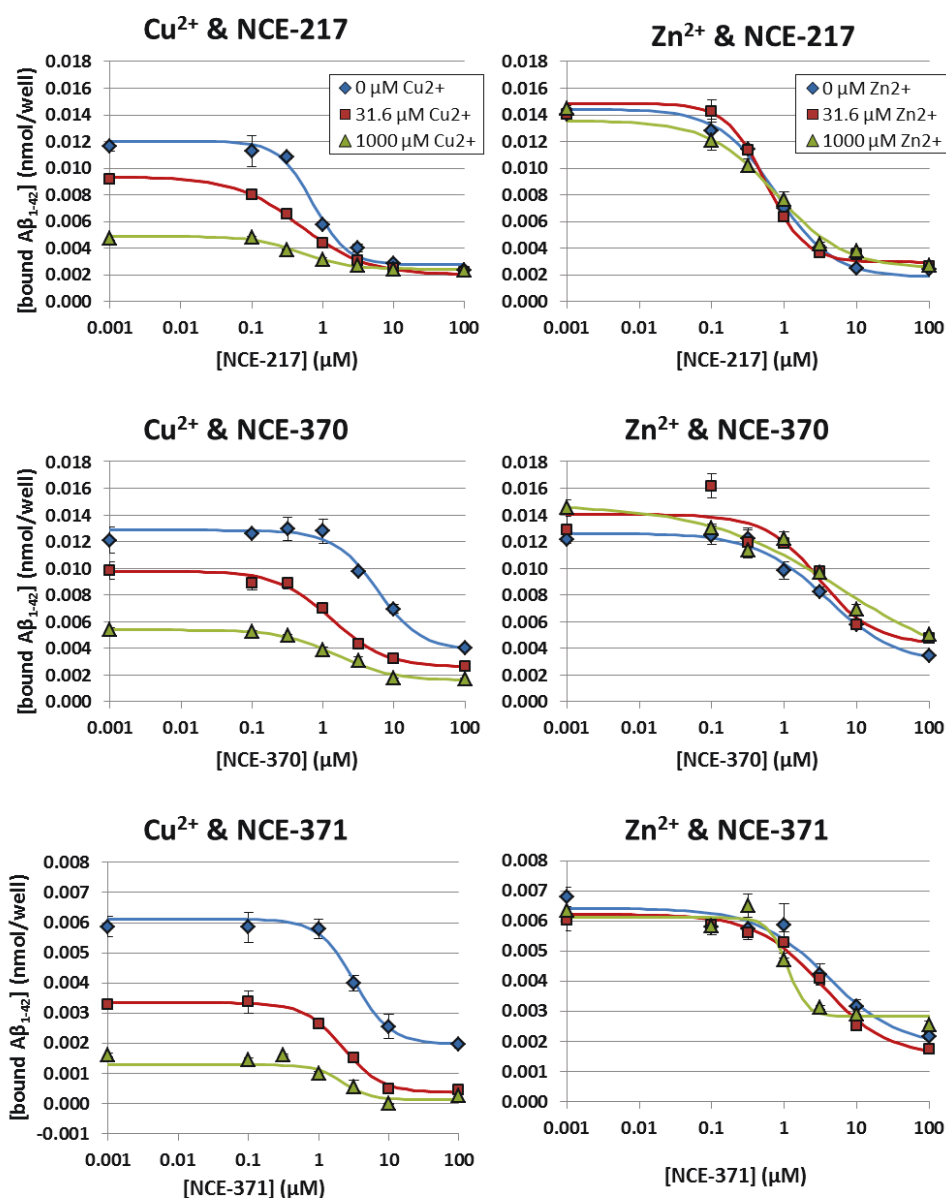


Figure V-19 Influence of metal ions and A β antiaggregants on GM1-binding by FAM-A β ₁₋₄₂. GM1-coated plates (0.1 nmol/well) were incubated with FAM-A β ₁₋₄₂ (2.5 μM) in presence of a dilution series of three A β antiaggregants (NCE-217, NCE-370, and NCE-371; 0.001 / 0.1 / 0.316 / 1 / 3.16 / 10 / 100 μM), and of two concentrations of Cu²⁺ (graphs on left) and Zn²⁺ (graphs on right) (31.6 / 1000 μM in PBS) for 18 hours; then the amount of GM1-bound FAM-A β ₁₋₄₂ was determined as described previously (Gain Factor setting: 95). Sigmoidal curves (solid lines: blue: 0 μM Me²⁺, red: 31.6 μM Me²⁺, green: 1000 μM Me²⁺) were fitted with a full 4-parameter fit to the data (markers: blue diamonds: 0 μM Me²⁺, red squares: 31.6 μM Me²⁺, green triangles: 1000 μM Me²⁺) as described previously (see Chapter II, Section 2.7.4.4); fitting included the values for 0 μM inhibitor, which could not be displayed on the logarithmically scaled x-axis, but were typically very close to the 0.001 μM inhibitor values. Calculated IC₅₀ values are compiled in Table V-7. Error Bars: ± S.E.M. (n = 3); where invisible, error bars are smaller than marker.

Table V-7 GM1 Assay IC₅₀ values for FAM-Aβ₁₋₄₀ and FAM-Aβ₁₋₄₂ of NCE-217, NCE-370 and NCE-371 in presence of Cu²⁺ and Zn²⁺.

IC₅₀ values for the data displayed in Figure V-18 and Figure V-19.

Incubation Additives	IC ₅₀ (μM) for FAM-Aβ ₁₋₄₀			IC ₅₀ (μM) for FAM-Aβ ₁₋₄₂		
	NCE-217	NCE-370	NCE-371	NCE-217	NCE-370	NCE-371
Cu ²⁺ , 0 μM	0.76	8.82*	2.83*	0.73	5.88*	3.21
Cu ²⁺ , 31.6 μM	0.89	1.94	1.37	0.49	1.31	2.21
Cu ²⁺ , 1000 μM	2.56	0.81	0.81	0.51	1.58	2.19
Zn ²⁺ , 0 μM	2.40	24.35*	2.65*	0.77	3.90*	4.04
Zn ²⁺ , 31.6 μM	0.78	23.21	0.72*	0.56	3.09	3.30
Zn ²⁺ , 1000 μM	0.77	14.23*	0.77	0.79	6.32	1.12

*: Curves seem to not have reached the bottom plateau, thus increasing the uncertainty in the calculated IC₅₀ values.

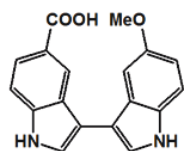
At first glance, one of the conditions is singled out with IC₅₀ values considerably elevated compared to the rest — co-incubation of Zn²⁺ and NCE-370 with FAM-Aβ₁₋₄₂. However, upon closer inspection of the binding curves, it becomes obvious that these (and a few others) did not reach the bottom plateau and therefore bear an increased uncertainty in the calculated IC₅₀ values. Otherwise, there were no major changes of the IC₅₀ values caused by addition of metal ions.

(b) Aβ Aggregation Inhibitors

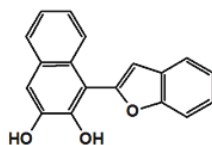
Finally, a number of Aβ aggregation inhibitors (see Figure V-20) developed in this lab were tested in the GM1 Assay to allow comparison to the standard ThT assay. As the ThT assay and the GM1 Assay are based on different mechanisms of detecting aggregation, and capture different pools of aggregated species, comparison of values obtained with these two assays might yield further insight not available through testing by ThT assay alone.

A β Aggregation Inhibitors

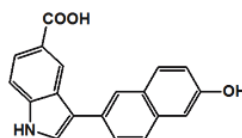
Bisindoles Series:



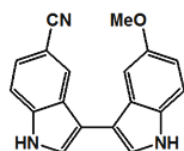
NCE-105 (M. Carter)



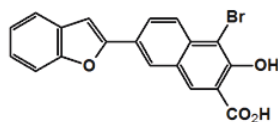
NCE-164 (S. Jacobo)



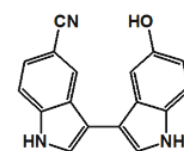
NCE-217 (E. Lu)



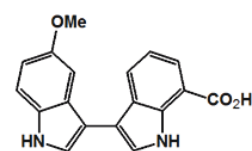
NCE-238 (E. Lu)



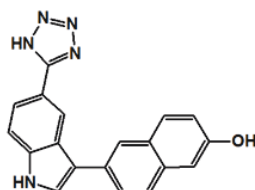
NCE-244 (S. Jacobo)



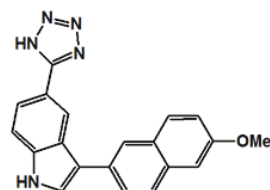
NCE-276 (E. Lu)



NCE-289 (E. Lu)

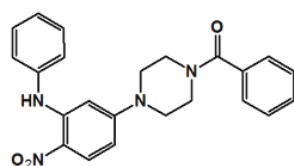


NCE-370 (A. McGrath)

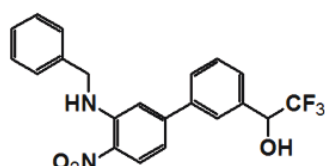


NCE-371 (A. McGrath)

Biaromatics Series:

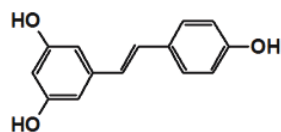


NCE-1027 (M. Reed)

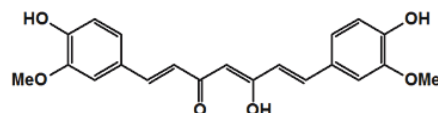


NCE-1140 (A. Yadav)

Natural Products:



Resveratrol



Curcumin

Figure V-20 Chemical structures of A β aggregation inhibitors.

Chemical structures of A β aggregation inhibitors tested in the GM1 Assay. Names in parentheses are of the researchers that synthesised the respective compound. Names of series reflect commonalities between compounds synthesised early on in the programme but do not necessarily apply literally to all compounds within a series. Both, resveratrol and curcumin, have been implicated in protection from dementia and their A β anti-amyloidogenic activity has been reported (71-74).

The compounds were chosen from two drug compound series that are based on different molecular scaffolds and A β binding sites; the bisindole series compounds were modelled to bind to the HHQK motif of A β (residues 12-17), whereas the biaromatics were designed to bind to the LVFF motif (residues 18-21). Furthermore, two natural products (resveratrol and curcumin) were included, because they had been implicated in protection from dementia and their A β anti-amyloidogenic activity had been reported (71-74).

GM1-coated plates (0.1 nmol/well) were incubated with FAM-A β ₁₋₄₀ (2.5 μ M) in presence of a dilution series of A β antiaggregants (0.0005 / 0.05 / 0.158 / 0.5 / 1.58 / 5 / 15.8 / 50 μ M) for 18 hours; then the amount of GM1-bound FAM-A β ₁₋₄₀ was determined as described previously. Sigmoidal curves (solid lines) were fitted with a full 4-parameter fit to the data (markers) as described previously (see Chapter II, Section 2.7.4.4); fitting included the values for 0 μ M inhibitor, which could not be displayed on the logarithmically scaled x-axis, but were typically very close to the 0.001 μ M inhibitor values. Binding curves are displayed in Figure V-21; calculated IC₅₀ values are compiled in Table V-8.

Inspection of the graphs shows a range of activities for the different compounds. These compounds were chosen deliberately with widely varying activity (based on ThT assay results) to see whether the GM1 assay can discriminate between them and if there are differences compared to the ThT assay.

A closer look reveals that the computer-generated values for the fitting parameters for three of the compounds (NCE-244, NCE-1027, resveratrol) did not yield realistic results due to the lack of data for the bottom plateau. Manually adjusting the parameters with an assumed bottom plateau at 0.008 nmol/well of GM1-bound FAM-A β ₁₋₄₀ (the background signal) gave binding curves (dashed lines) that appear more realistic; however, thus obtained IC₅₀ values still carry a considerable degree of uncertainty, since they assume total aggregation inhibition by

higher concentrations of these compounds, an assumption not necessarily valid as seen in the previous section.

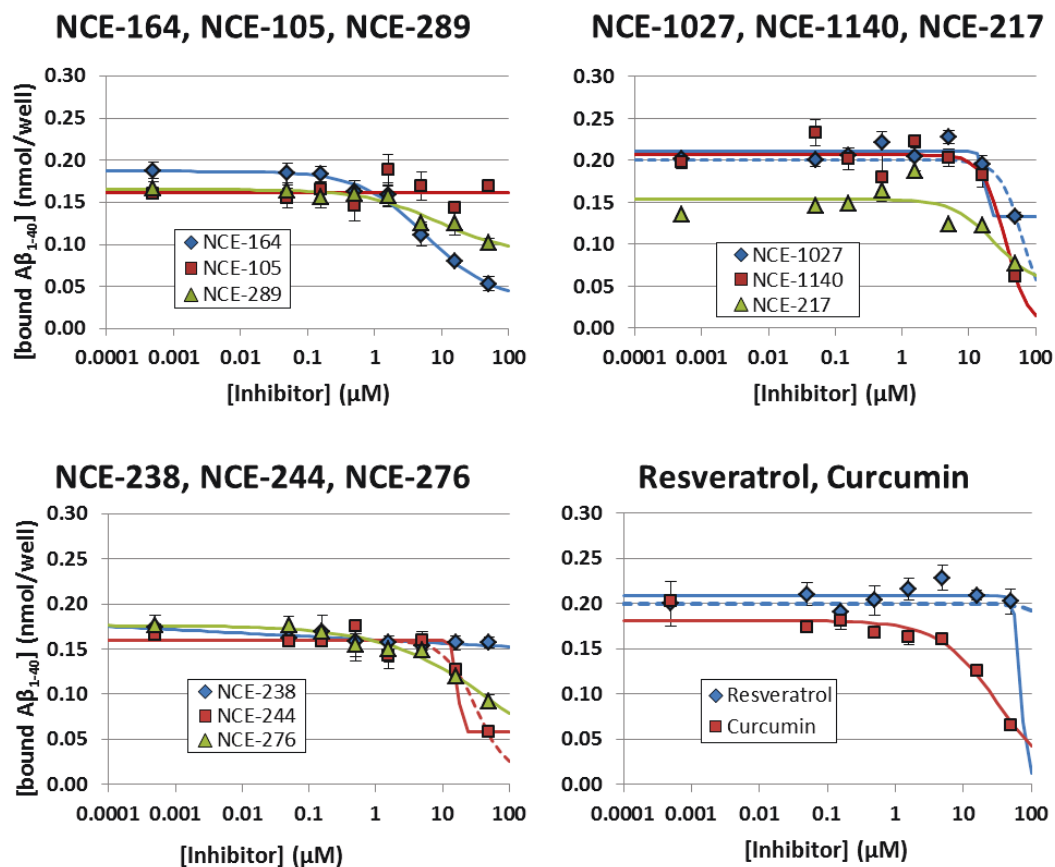


Figure V-21 Dose-response curves for Aβ aggregation inhibitors determined by GM1 Assay. GM1-coated plates (0.1 nmol/well) were incubated with FAM-Aβ₁₋₄₀ (2.5 μM) in presence of a dilution series of Aβ antiaggregants (0.0005 / 0.05 / 0.158 / 0.5 / 1.58 / 5 / 15.8 / 50 μM) for 18 hours; then the amount of GM1-bound FAM-Aβ₁₋₄₀ was determined as described previously (Gain Factor setting: 95). Sigmoidal curves (solid lines) were fitted with a full 4-parameter fit to the data (markers) as described previously (see Chapter II, Section 2.7.4.4); fitting included the values for 0 μM inhibitor, which could not be displayed on the logarithmically scaled x-axis, but were typically very close to the 0.001 μM inhibitor values. Dashed lines (NCE-244, NCE-1027, resveratrol) show curves obtained by manually adjusting the parameters to fit the data, which was done since the computer-generated fitting produced unrealistic curves due to the lack of data for the bottom plateau. Calculated IC₅₀ values are compiled in Table V-8. Error Bars: ± S.E.M. (n = 3); where invisible, error bars are smaller than marker.

IC₅₀ values obtained from the fitted curves as well as values gathered from ThT assays are compiled in Table V-8. Comparison of these results reveals that the GM1 assay in all cases yielded higher IC₅₀ values than the ThT assay while relative trends were conserved. IC₅₀ (GM1)

values for the bisindoles were in general closer to the IC₅₀ (ThT) values than those for the biaromatics, with bisindoles IC₅₀ (GM1) values being about 2 – 5 times larger than IC₅₀ (ThT) values, and biaromatics IC₅₀ (GM1) values being about 10 – 20 times larger. One reason may be the different (putative) binding sites of these two compound series. As mentioned previously, the bisindoles were modelled to bind to the HHQK motif of Aβ (residues 12-17) and would thus compete with GM1 binding of Aβ (which involves H-13) as well as Aβ aggregation, whereas the biaromatics were designed to bind to the neighbouring LVFF motif (residues 18-21), thus only preventing aggregation of Aβ but not its binding to GM1.

Table V-8 ThT assay and GM1 Assay IC₅₀ values for three series of Aβ aggregation inhibitors.

Inhibitor Series	Compound	IC ₅₀ (ThT)	Qual. Result (ThT)	IC ₅₀ (GM ₁)	Qual. Result (GM ₁)
Bisindoles	NCE-105	50.4 ± 7.3	-	** (>100)	-
	NCE-164	3.0 ± 1.6	+	5.82	+
	NCE-217	7.5 ± 1.2	+	24.67	o
	NCE-238	20.9 ± 8.1	o	** (>100)	-
	NCE-244	5.6 ± 0.1	+	16.75 [§] (32)	+ (o)
	NCE-276	16.5 ± 6.9	+	65.72 [§] (50)	-
	NCE-289	n/d	(+) *	8.83	+
Biaromatics	NCE-1027	0.85 ± 0.12	+	17.36 [§] (65)	+ (-)
	NCE-1140	3.09 ± 0.21	+	35.48	o
Natural Products	Resveratrol	32.1 ± 6.6	o	** (>100)	-
	Curcumin	n/d	n/d	31.37	o

Qualitative results were classified as follows: + (IC₅₀ < 20 μM); o (20 μM ≤ IC₅₀ < 50 μM); - (IC₅₀ > 50 μM). Values in parentheses were obtained from manually adjusted fitting of curve parameters. n/d: not determined.

*: from ThT assay with too few concentrations to calculate an IC₅₀ value. **: Iteration did not converge to a consistent value due to the lack of values for the sloped portion and the bottom plateau of the curve. §: Iteration did not yield realistic IC₅₀ values due to the lack of data for the bottom plateau. Values given in parentheses were obtained by manually adjusting parameters to fit the sigmoidal curve to the data; the bottom plateau was set to a value of 0.008 nmol/well (the background signal).

The results presented here clearly show the potential of the GM1 Assay in the evaluation of drug candidate molecules. However, in future work a number of issues should be addressed in order to completely validate the assay and realise its full potential.

A number of parameters related to the kinetic and thermodynamic characteristics of the GM1 Assay should be determined. Examples include association and dissociation rate constants (k_{on} and k_{off}) for the former, and the binding constant (affinity constant, K , or dissociation constant K_d) and the specificity of the GM1-A β binding for the latter (75). In the literature, a range of different systems and detection methods have already been used to obtain some of these values (64, 70, 76, 77); however, since none used the exact setup described and used here, one may expect some deviation in the results obtained through a different method. One may also want to investigate the differences for these constants between the initial binding of A β to GM1, i.e., the seed formation, and the subsequent attachment of further A β monomers as the oligomers grow in size.

Another aspect of the GM1 assay that should be investigated is the question of distinguishing a drug that prevents the initial binding of A β to GM1 from one that prevents A β aggregation, as both would lower the signal measured in the assay. One idea to address this question is to employ photo-induced cross-linking of unmodified proteins (PICUP) to determine the A β species (monomers or oligomers) bound to the assay plate and present in the supernatant as described in the next section.

3.5.5. PICUP Assay

One method that has been proven useful in the analysis of A β oligomers is the photo-induced cross-linking of unmodified proteins (PICUP) (78). This method was originally developed to resolve a number of problems associated with the chemical cross-linking of proteins (79, 80),

which had been used previously to investigate protein - protein interactions. The idea behind cross-linking of closely associated proteins is to introduce a covalent bond between these proteins that can withstand denaturing conditions used in analytical methods, such as SDS-PAGE (sodium dodecyl sulfate – polyacrylamide gel electrophoresis). The problems related to the chemical cross-linking of proteins are inherent to the method, where typically bifunctional crosslinkers comprised of two electrophiles connected by a linker arm are used to cross-link closely associated proteins. Most of these crosslinkers are inherently reactive and cannot be “switched on” to react at a certain time. Furthermore, some unintended modifications of nucleophilic side chains, like the acylation of lysines, on surface residues occurring during the prolonged incubation times often necessary for these reagents have been connected to artifactual results caused by structural destabilisation.

The PICUP process is based on the photolysis of certain metal complexes, e.g., tris-bipyridylruthenium(II) dication, with visible light in the presence of an electron acceptor, such as ammonium persulfate, and the proteins of interest. Besides avoiding use of a linker through direct cross-linking of proteins, use of visible instead of UV light in the PICUP process also reduces the chance of damage to proteins and other biomolecules that may be inflicted by UV light. Another advantage, particularly in relation to the study of oligomers with their short lifetimes and dynamic equilibria, is its short irradiation time of at the most a few seconds as compared to classical biophysical approaches, which may require up to 30 minutes.

A number of research groups have used PICUP successfully to investigate A β oligomers (81-85). However, their experimental setup has never left the initial stages where an SLR camera body is used to control the sample irradiation time (see Figure V-22).

Here, a new irradiator utilising an LED as light source was designed; it was then built by Brian Millier (Department of Chemistry, Dalhousie University) (see Figure V-23). Based on the absorption maximum in the visible range of the $[\text{Ru}(\text{Bpy})_3]^{2+}$ complex (for chemical structure and absorption spectrum see Figure V-23), the Luxeon V Star Royal Blue LED (Model LXHL-LR5C) was chosen as the light source. With an emission maximum at 455 nm, this LED closely matches the absorption maximum of the ruthenium complex in water at 452 nm (78). The LED is driven by a constant current source at 660 mA, providing a typical luminous flux of 500 mW. The sample holder places the sample at a reproducible distance of less than 1 cm from the LED (typical distances for the traditional setup are 10 – 15 cm).

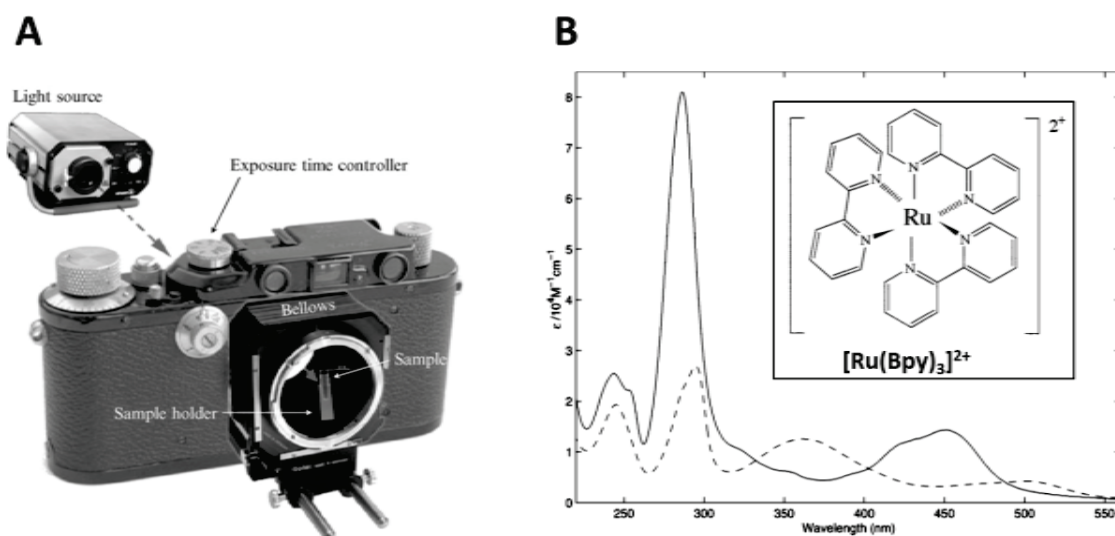


Figure V-22 Experimental configurations for the PICUP assay and $[\text{Ru}(\text{Bpy})_3]^{2+}$ absorbance spectrum.

In the traditional setup (A), a light source (150 – 200 W incandescent or xenon lamp) is connected to the open film chamber of an SLR camera body, and the sample tube is inserted in a bellows attached to the lens aperture. After capping the end of the bellows, the sample is irradiated upon shutter release for a precisely controlled time interval set by the camera body's exposure time mechanism. Reprinted from Ref. (78); copyright 2006, with permission from Elsevier.

The absorption spectrum (B) in acetonitrile of $[\text{Ru}(\text{bpy})_3]^{2+}$ in the ground state (solid line) (dashed line is for $[\text{Ru}(\text{bpy})(\text{py})_4]^{2+}$). The absorption maximum at 452 nm ($\epsilon \approx 14,700 \text{ M}^{-1}$) (86) is related to the metal-to-ligand charge transfer transitions that are utilised in the PICUP process. The insert shows the chemical structure of the ruthenium complex. Absorbance spectrum reprinted with permission from Ref. (87); copyright 2005, American Chemical Society.

Considering that the efficiency of incandescent light bulbs is typically less than 5% (88), and that the light intensity is inversely proportional to the square of the distance from the light source, this LED should actually provide a higher irradiance than the light sources used in the traditional setup. The irradiation time is adjusted with a microcontroller-based timer providing precise LED light exposures up to 9.99 seconds long, with a resolution of 0.01 second. The metal housing provides shielding of the sample from ambient light, as well as protection of the operator from the bright blue light emitted by the LED. A number of sample holders are available to accommodate different size PCR and microcentrifuge tubes, as well as quartz microcuvettes with a path length of 1 mm.

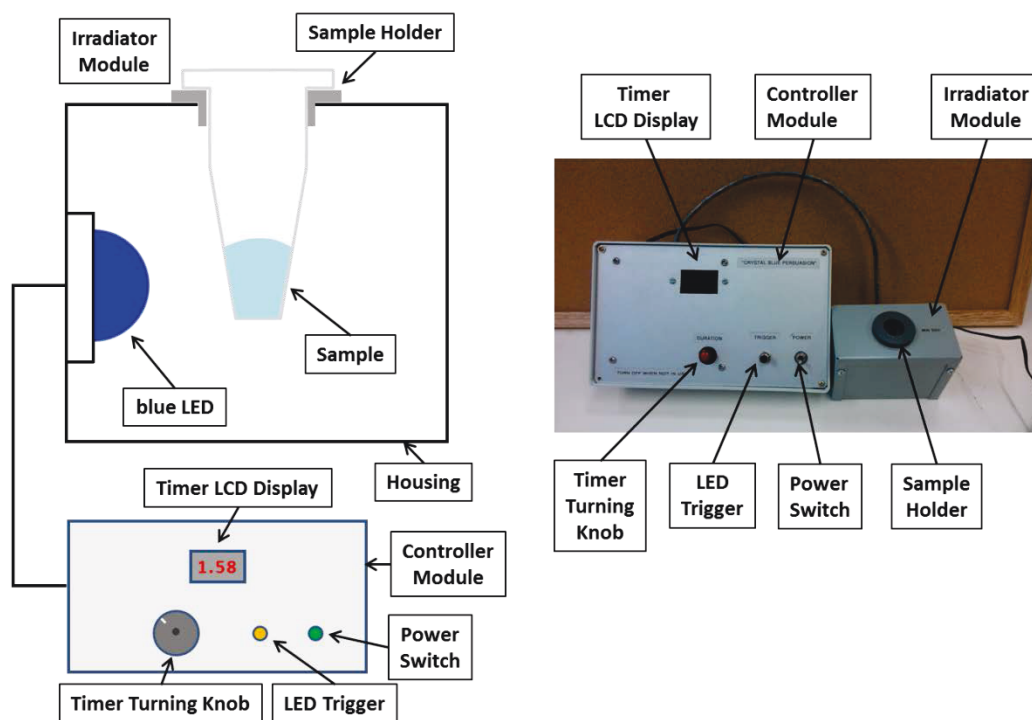


Figure V-23 The new PICUP LED Irradiator.

In the new PICUP LED Irradiator, the sample is placed inside a sample holder and inserted into the housing, thus ensuring a reproducible LED – sample distance. On the controller, the irradiation time is set with a turning knob; irradiation is then started by a trigger button.

In order to test the new irradiator, A β ₁₋₄₀ (100 μ M) was incubated for 24 h at 37°C with DMSO control or test compounds (NCE-1271, NCE-1273, NCE-1277, NCE-1284, NCE-1293, NCE-1310; 50 and 250 μ M). Samples were prepared on ice and as described in the Methods section with an irradiation time of 2 s. After developing the gel, peptides were visualised by silver staining (see Figure V-24).

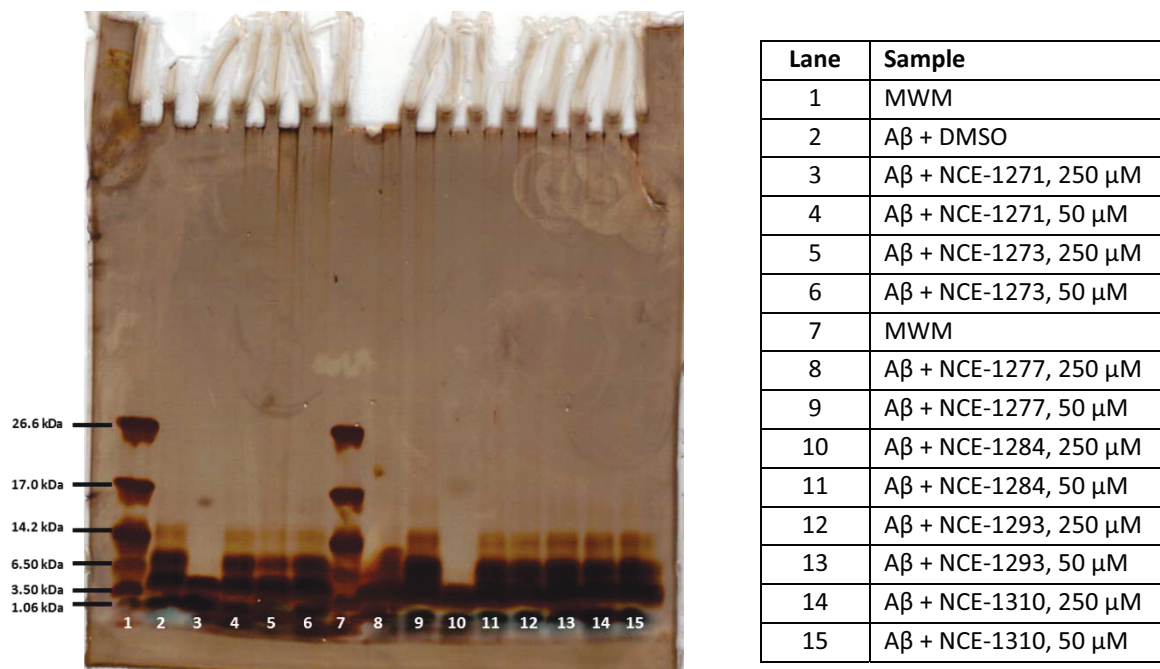


Figure V-24 Tris-Tricine SDS-PAGE gel of PICUP assay.

Six putative A β antiaggregants were incubated for 24 h with A β at 37°C and then subjected to the PICUP assay (2 s irradiation time). MWM: molecular weight markers (Bradikinin, 1,060 Da; Insulin Chain B, Oxidized, Bovine, 3,496 Da 3.50; Aprotinin, Bovine Lung, 6,500 Da; α -Lactalbumin, Bovine Milk, 14,200 Da; Myoglobin, Horse Heart, 17,000 Da; Triose Phosphate Isomerase, Rabbit Muscle 26,600 Da)

In particular, NCE-1271 and NCE-1284 suppressed the formation of higher order oligomers at 250 μ M; at the lower concentration only minor effects were discernible.

After thus confirming that the LED irradiator did in fact produce the desired results, this concept was taken a step further. In order to irradiate multiple samples at a time, a new model

was designed and built (again by Brian Millier) that is capable of irradiating samples in a 96-well plate. It consists of an irradiator module featuring a 2 × 8 array of LEDs, a touch screen controller, and a plate holder with guide holes to allow precise positioning of the irradiator on top of the 96-well plate (see Figure V-25). The arrangement of the LEDs as a 2 × 8 array was chosen as a compromise between the time required to irradiate a full 96-well plate and the cost of the instrument.

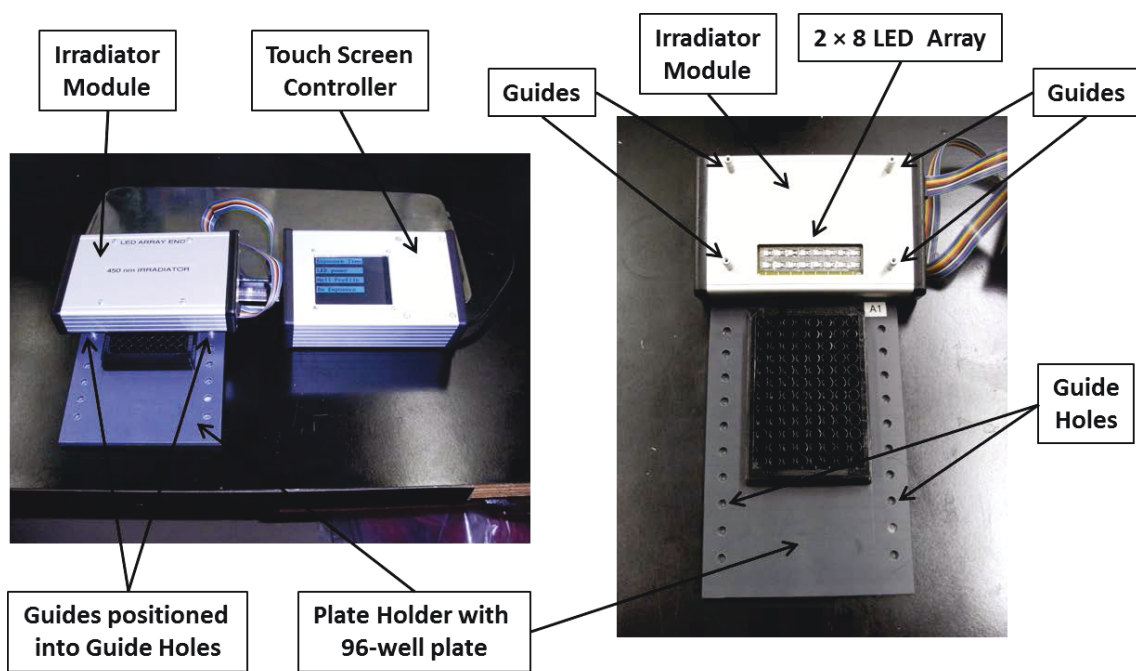


Figure V-25 The PICUP Multiplex LED Irradiator.

The PICUP Multiplex LED Irradiator consists of an irradiator module featuring a 2 × 8 array of LEDs, a touch screen controller, and a plate holder with guide holes to allow precise positioning of the irradiator on top of the 96-well plate. Left side shows setup ready for an irradiation; right side shows the underside of the irradiator module where the 2 × 8 LED array is located and the plate holder with guide holes. For details see text.

The LEDs used in the irradiator module (Kingbright, Blue (InGaN) Part #AA3535QB25Z1S, $\lambda_{\text{max}} = 445 \text{ nm}$) were smaller than the one previously used due to size restrictions; they had to be small enough to allow arrangement in a 2 × 8 matrix at exactly the same distances as the wells in a 96-well plate. The LEDs were matched before installation to ensure equal light intensity is

provided to each well; they provide a maximum of 2.5 lumens at 450 nm. With the plate holder fixing the 96-well plate, the guide holes and guides allow precise positioning of the irradiator module on top of the 96-well plate to irradiate two columns at a time; the distance of the LEDs from the top of the 96-well plate is about 2 mm.

The software for the controller allows setting of irradiation time from 0 – 99 s with a resolution of 0.025 s, and adjusting of LED power in 64 steps (0 – 63). Furthermore, a well profile can be defined, which allows modulation of the amount of radiation applied to each well. The amount of radiation is controlled via the exposure time, which is multiplied by the modulation factor (range: 0.000 – 1.000) to deliver the desired amount of radiation to each well. The modulation factor can be set for individual columns or rows, or an operator-specified range of wells.

To perform an irradiation, the operator enters the desired settings for exposure time, LED power, and well profile (modulation factor) and starts the exposure routine. After the irradiation of the first set of columns is completed, the operator is prompted to move the irradiator module to the next position and start the next irradiation. This process is repeated until the entire plate (or selected range) has been irradiated.

Considering that exposure times are typically only a few seconds long, one full 96-well plate can easily be irradiated in less than a minute. With these capabilities in hand, other processes in the PICUP assay become the rate-limiting step, most notably sample analysis. Most researchers use SDS-PAGE to analyse samples obtained through PICUP (78, 81, 83, 84), although other methods have been tried (85). However, SDS-PAGE is quite time-consuming, in particular for quantitative analyses, since visualisation of protein bands requires additional steps for staining or Western blots.

Here, the intent was to make use of the capability of the HPLC autosampler to take samples directly from a 96-well plate for injection onto the column since this would considerably reduce the hands-on time for the assay. However, due to time constraints, unfortunately this project did not advance past a few initial experiments and could not be completed.

A number of future experiments shall be suggested. Starting with FAM-A β (unlabeled A β proved undetectable by UV-Vis at the concentrations tried in the initial experiments (20 – 35 μ M)) and fluorescence detection, irradiation conditions should be optimised for the detection of oligomers. In a next step, unlabelled A β may be used in conjunction with pre-column derivatisation (e.g., with *o*-phthalaldehyde (OPA), an established derivatisation reagent; protocols are available to do this automatically with the autosampler) in order to reduce the cost of the assay. Subsequently, PICUP could be used to analyse samples obtained from the GM1 Assay as mentioned earlier. And finally, it may be attempted to develop a protocol that allows analysis of these samples by mass spectrometry.

3.6. Summary

The GM1 Assay was developed as an alternative to the well-established ThT aggregation assay, to assess the inhibitory effect of drug candidate molecules on the aggregation of A β . It avoids a number of issues associated with the ThT assay, namely the effect that the ThT dye itself has on the aggregation and on the binding of the tested compound, as well as possible quenching of the ThT fluorescence signal. Furthermore, it uses considerably lower amounts of A β , albeit of a more expensive (fluorescently labelled) form.

Competitive binding experiments with a number of A β antiaggregants showed comparable trends for IC₅₀ values obtained by the GM1 Assay and ThT assay, although at a higher level for

the former. While Cu^{2+} generally decreased the amount of GM1-bound $\text{A}\beta$ in presence of $\text{A}\beta$ antiaggregants, Zn^{2+} had a smaller opposite or no effect.

Two LED-based irradiators for the PICUP assay were designed and built; one for single samples, the other one for 96-well plates. Unfortunately, time constraints did not allow rigorous testing.

4. Conclusions

A β has been shown to interact with many different classes of molecules and ions; here, two aspects were investigated. First, the non-specific binding of A β to commonly used sample and reaction vessels was quantified in a range of conditions with the goal to identify measures to minimise sample loss in the handling of this expensive peptide. Losses of over 50% were observed for some vessels (glass), while one product consistently stood out with only minimal protein binding, the Eppendorf Protein LoBind microcentrifuge tubes. Second, the GM1 Assay was developed as an alternative to the ThT assay to determine the efficacy of A β antiaggregants. Experiments in this section actually covered a number of different interactions of A β ; the interaction with GM1, which leads to seed formation for its aggregation (i.e., its interaction with itself), interaction with metal ions (Cu²⁺, Zn²⁺), and interaction with small molecule antiaggregants. Finally, two LED irradiators were designed and built (one for single samples, the other for 96-well plates), to facilitate study of A β aggregation by photo-induced cross-linking of unmodified proteins (PICUP).

5. References

1. Verdier, Y.; Penke, B. Binding sites of amyloid β -peptide in cell plasma membrane and implications for Alzheimer's disease. *Curr. Protein Pept. Sci.* **2004**, *5*, 19-31.
2. Verdier, Y.; Zarandi, M.; Penke, B. Amyloid β -peptide interactions with neuronal and glial cell plasma membrane: binding sites and implications for Alzheimer's disease. *J. Pept. Sci.* **2004**, *10*, 229-248.
3. Kim, K. S.; Miller, D. L.; Sapienza, V. J.; Chen, C. - J.; Bai, C.; Grundke-Iqbal, I.; Currie, J. R.; Wisniewski, H. M. Production and characterization of monoclonal antibodies reactive to synthetic cerebrovascular amyloid peptide. *Neurosci. Res. Comm.* **1988**, *2*, 121-130.
4. Kim, K. S.; Wen, G. Y.; Bancher, C.; Chen, C. J. M.; Sapienza, V. J.; Hong, H.; Wisniewski, H. M. Detection and quantification of amyloid β -peptide with 2 monoclonal antibodies. *Neurosci. Res. Comm.* **1990**, *7*, 113-122.
5. Strittmatter, W. J.; Saunders, A. M.; Schmechel, D.; Pericak-Vance, M.; Enghild, J.; Salvesen, G. S.; Roses, A. D. Apolipoprotein E: high-avidity binding to β -amyloid and increased frequency of type 4 allele in late-onset familial Alzheimer disease. *Proc. Natl. Acad. Sci. U. S. A.* **1993**, *90*, 1977-1981.
6. Biancalana, M.; Koide, S. Molecular mechanism of Thioflavin-T binding to amyloid fibrils. *Biochim. Biophys. Acta* **2010**, *1804*, 1405-1412.
7. Strittmatter, W. J.; Huang, D. Y.; Bhasin, R.; Roses, A. D.; Goldgaber, D. Avid binding of β A amyloid peptide to its own precursor. *Exp. Neurol.* **1993**, *122*, 327-334.
8. Schwarzman, A. L.; Tsiper, M.; Gregori, L.; Goldgaber, D.; Frakowiak, J.; Mazur-Kolecka, B.; Taraskina, A.; Pchelina, S.; Vitek, M. P. Selection of peptides binding to the amyloid b-protein reveals potential inhibitors of amyloid formation. *Amyloid* **2005**, *12*, 199-209.
9. Grillo-Bosch, D.; Carulla, N.; Cruz, M.; Sanchez, L.; Pujol-Pina, R.; Madurga, S.; Rabanal, F.; Giralt, E. Retro-enantio N-methylated peptides as β -amyloid aggregation inhibitors. *ChemMedChem* **2009**, *4*, 1488-1494.
10. Zhang, L.; Yagnik, G.; Peng, Y.; Wang, J.; Xu, H. H.; Hao, Y.; Liu, Y. N.; Zhou, F. Kinetic studies of inhibition of the amyloid beta (1-42) aggregation using a ferrocene-tagged β -sheet breaker peptide. *Anal. Biochem.* **2013**, *434*, 292-299.
11. Hou, L.; Zagorski, M. G. NMR reveals anomalous copper(II) binding to the amyloid A β peptide of Alzheimer's disease. *J. Am. Chem. Soc.* **2006**, *128*, 9260-9261.

12. Atwood, C. S.; Scarpa, R. C.; Huang, X.; Moir, R. D.; Jones, W. D.; Fairlie, D. P.; Tanzi, R. E.; Bush, A. I. Characterization of copper interactions with alzheimer amyloid β peptides: identification of an attomolar-affinity copper binding site on amyloid β 1-42. *J. Neurochem.* **2000**, *75*, 1219-1233.
13. Syme, C. D.; Viles, J. H. Solution ^1H NMR investigation of Zn^{2+} and Cd^{2+} binding to amyloid- β peptide ($\text{A}\beta$) of Alzheimer's disease. *Biochim. Biophys. Acta* **2006**, *1764*, 246-256.
14. Danielsson, J.; Pierattelli, R.; Banci, L.; Graslund, A. High-resolution NMR studies of the zinc-binding site of the Alzheimer's amyloid β -peptide. *FEBS J.* **2007**, *274*, 46-59.
15. Yang, D. S.; McLaurin, J.; Qin, K.; Westaway, D.; Fraser, P. E. Examining the zinc binding site of the amyloid- β peptide. *Eur. J. Biochem.* **2000**, *267*, 6692-6698.
16. Bin, Y.; Chen, S.; Xiang, J. pH-dependent kinetics of copper ions binding to amyloid- β peptide. *J. Inorg. Biochem.* **2013**, *119*, 21-27.
17. Ghalebani, L.; Wahlstrom, A.; Danielsson, J.; Warmlander, S. K.; Graslund, A. pH-dependence of the specific binding of $\text{Cu}(\text{II})$ and $\text{Zn}(\text{II})$ ions to the amyloid- β peptide. *Biochem. Biophys. Res. Commun.* **2012**, *421*, 554-560.
18. Faller, P. Copper and zinc binding to amyloid- β : coordination, dynamics, aggregation, reactivity and metal-ion transfer. *Chembiochem* **2009**, *10*, 2837-2845.
19. Garzon-Rodriguez, W.; Yatsimirsky, A. K.; Glabe, C. G. Binding of $\text{Zn}(\text{II})$, $\text{Cu}(\text{II})$, and $\text{Fe}(\text{II})$ ions to alzheimer's $\text{A}\beta$ peptide studied by fluorescence. *Bioorg. Med. Chem. Lett.* **1999**, *9*, 2243-2248.
20. Brunden, K. R.; Richter-Cook, N. J.; Chaturvedi, N.; Frederickson, R. C. pH-dependent binding of synthetic β -amyloid peptides to glycosaminoglycans. *J. Neurochem.* **1993**, *61*, 2147-2154.
21. McLaurin, J. A.; Franklin, T.; Zhang, X.; Deng, J.; Fraser, P. E. Interactions of Alzheimer amyloid- β peptides with glycosaminoglycans effects on fibril nucleation and growth. *Eur. J. Biochem.* **1999**, *266*, 1101-1110.
22. Leveugle, B.; Scanameo, A.; Ding, W.; Fillit, H. Binding of heparan sulfate glycosaminoglycan to β -amyloid peptide: inhibition by potentially therapeutic polysulfated compounds. *Neuroreport* **1994**, *5*, 1389-1392.
23. Watson, D. J.; Lander, A. D.; Selkoe, D. J. Heparin-binding properties of the amyloidogenic peptides $\text{A}\beta$ and amylin. Dependence on aggregation state and inhibition by Congo red. *J. Biol. Chem.* **1997**, *272*, 31617-31624.

24. Sadler, I. I.; Hawtin, S. R.; Taylor, V.; Shearman, M. S.; Pollack, S. J. Glycosaminoglycans and sulphated polyanions attenuate the neurotoxic effects of β -amyloid. *Biochem. Soc. Trans.* **1995**, *23*, 106S.
25. Curtain, C. C.; Ali, F. E.; Smith, D. G.; Bush, A. I.; Masters, C. L.; Barnham, K. J. Metal ions, pH, and cholesterol regulate the interactions of Alzheimer's disease amyloid- β peptide with membrane lipid. *J. Biol. Chem.* **2003**, *278*, 2977-2982.
26. Devanathan, S.; Salamon, Z.; Lindblom, G.; Grobner, G.; Tollin, G. Effects of sphingomyelin, cholesterol and zinc ions on the binding, insertion and aggregation of the amyloid A β (1-40) peptide in solid-supported lipid bilayers. *FEBS J.* **2006**, *273*, 1389-1402.
27. Avdulov, N. A.; Chochina, S. V.; Igbavboa, U.; Warden, C. S.; Vassiliev, A. V.; Wood, W. G. Lipid binding to amyloid β -peptide aggregates: preferential binding of cholesterol as compared with phosphatidylcholine and fatty acids. *J. Neurochem.* **1997**, *69*, 1746-1752.
28. Hoshino, T.; Mahmood, M. I.; Mori, K.; Matsuzaki, K. Binding and Aggregation Mechanism of Amyloid β -Peptides onto the GM1 Ganglioside-Containing Lipid Membrane. *J Phys Chem B* **2013**, *117*, 8085-8094.
29. Ikeda, K.; Matsuzaki, K. Driving force of binding of amyloid β -protein to lipid bilayers. *Biochem. Biophys. Res. Commun.* **2008**, *370*, 525-529.
30. Shao, H.; Jao, S.; Ma, K.; Zagorski, M. G. Solution structures of micelle-bound amyloid β -(1-40) and β -(1-42) peptides of Alzheimer's disease. *J. Mol. Biol.* **1999**, *285*, 755-773.
31. Kisilevsky, R.; Lemieux, L. J.; Fraser, P. E.; Kong, X.; Hultin, P. G.; Szarek, W. A. Arresting amyloidosis in vivo using small-molecule anionic sulphonates or sulphates: implications for Alzheimer's disease. *Nat. Med.* **1995**, *1*, 143-148.
32. Carter, D. B.; Chou, K. C. A model for structure-dependent binding of Congo red to Alzheimer β -amyloid fibrils. *Neurobiol. Aging* **1998**, *19*, 37-40.
33. Kuner, P.; Bohrmann, B.; Tjernberg, L. O.; Naslund, J.; Huber, G.; Celenk, S.; Gruninger-Leitch, F.; Richards, J. G.; Jakob-Roetne, R.; Kemp, J. A.; Nordstedt, C. Controlling polymerization of β -amyloid and prion-derived peptides with synthetic small molecule ligands. *J. Biol. Chem.* **2000**, *275*, 1673-1678.
34. Talafous, J.; Marcinowski, K. J.; Klopman, G.; Zagorski, M. G. Solution structure of residues 1-28 of the amyloid β -peptide. *Biochemistry* **1994**, *33*, 7788-7796.
35. Salomon, A. R.; Marcinowski, K. J.; Friedland, R. P.; Zagorski, M. G. Nicotine inhibits amyloid formation by the β -peptide. *Biochemistry* **1996**, *35*, 13568-13578.

36. Seed, B. Silanizing glassware. *Curr. Protoc. Mol. Biol.* **2001**, Appendix 3, Appendix 3B.
37. Macdonell, M. T.; Hansen, J. N.; Ortiz-Conde, B. A. In *9 Isolation, Purification and Enzymatic Sequencing of RNA*; Colwell, R. R., Grigorova, R., Eds.; Methods in Microbiology; Academic Press: **1988**; Vol. 19, pp. 357-404.
38. Gibbs, J. Effective Blocking Procedures. *ELISA Technical Bulletin - No 3* **2001**, 1-6.
39. Pica-Mendez, A. M.; Tanen, M.; Dallob, A.; Tanaka, W.; Laterza, O. F. Nonspecific binding of A β 42 to polypropylene tubes and the effect of Tween-20. *Clin. Chim. Acta* **2010**, *411*, 1833.
40. Goebel-Stengel, M. The importance of using the optimal plasticware and glassware in studies involving peptides. *Anal. Biochem.* **2011**, *414*, 38-46.
41. Weiss, N.; Wentz, W.; Mueller, P. Eppendorf LoBind: Evaluation of protein recovery in Eppendorf Protein LoBind Tubes and Plates. *Eppendorf Application Note* **2010**, *180*, 1-5.
42. Nag, S.; Sarkar, B.; Bandyopadhyay, A.; Sahoo, B.; Sreenivasan, V. K.; Kombrabail, M.; Muralidharan, C.; Maiti, S. Nature of the amyloid- β monomer and the monomer-oligomer equilibrium. *J. Biol. Chem.* **2011**, *286*, 13827-13833.
43. Axelsson, I. Characterization of proteins and other macromolecules by agarose gel chromatography. *Journal of Chromatography A* **1978**, *152*, 21-32.
44. Wright, A. K.; Thompson, M. R. Hydrodynamic structure of bovine serum albumin determined by transient electric birefringence. *Biophys. J.* **1975**, *15*, 137-141.
45. Ge, S.; Kojio, K.; Takahara, A.; Kajiyama, T. Bovine serum albumin adsorption onto immobilized organotrichlorosilane surface: influence of the phase separation on protein adsorption patterns. *J. Biomater. Sci. Polym. Ed.* **1998**, *9*, 131-150.
46. Vassar, P. S.; Culling, C. F. A. Fluorescent stains, with special reference to amyloid and connective tissues. *Arch. Pathol.* **1959**, *68*, 487-498.
47. Kelenyi, G. On the histochemistry of azo group-free thiazole dyes. *J. Histochem. Cytochem.* **1967**, *15*, 172-180.
48. Kelenyi, G. Thioflavin S fluorescent and Congo red anisotropic stainings in the histologic demonstration of amyloid. *Acta Neuropathol.* **1967**, *7*, 336-348.
49. LeVine, H., 3rd Quantification of β -sheet amyloid fibril structures with thioflavin T. *Methods Enzymol.* **1999**, *309*, 274-284.

50. Wolfe, L. S.; Calabrese, M. F.; Nath, A.; Blaho, D. V.; Miranker, A. D.; Xiong, Y. Protein-induced photophysical changes to the amyloid indicator dye thioflavin T. *Proc. Natl. Acad. Sci. U. S. A.* **2010**, *107*, 16863-16868.
51. Klunk, W. E.; Jacob, R. F.; Mason, R. P. Quantifying amyloid β -peptide (A β) aggregation using the Congo red-A β (CR-A β) spectrophotometric assay. *Anal. Biochem.* **1999**, *266*, 66-76.
52. Pratim Bose, P.; Chatterjee, U.; Xie, L.; Johansson, J.; Gothelid, E.; Arvidsson, P. I. Effects of Congo Red on A β ₁₋₄₀ Fibril Formation Process and Morphology. *ACS Chem. Neurosci.* **2010**, *1*, 315-324.
53. Lorenzo, A.; Yankner, B. A. β -amyloid neurotoxicity requires fibril formation and is inhibited by congo red. *Proc. Natl. Acad. Sci. U. S. A.* **1994**, *91*, 12243-12247.
54. Podlisny, M. B.; Walsh, D. M.; Amarante, P.; Ostaszewski, B. L.; Stimson, E. R.; Maggio, J. E.; Teplow, D. B.; Selkoe, D. J. Oligomerization of endogenous and synthetic amyloid β -protein at nanomolar levels in cell culture and stabilization of monomer by Congo red. *Biochemistry* **1998**, *37*, 3602-3611.
55. Alavez, S.; Vantipalli, M. C.; Zucker, D. J.; Klang, I. M.; Lithgow, G. J. Amyloid-binding compounds maintain protein homeostasis during ageing and extend lifespan. *Nature* **2011**, *472*, 226-229.
56. Porat, Y.; Abramowitz, A.; Gazit, E. Inhibition of amyloid fibril formation by polyphenols: structural similarity and aromatic interactions as a common inhibition mechanism. *Chem. Biol. Drug Des.* **2006**, *67*, 27-37.
57. Inbar, P.; Bautista, M. R.; Takayama, S. A.; Yang, J. Assay to screen for molecules that associate with Alzheimer's related β -amyloid fibrils. *Anal. Chem.* **2008**, *80*, 3502-3506.
58. Rodriguez-Rodriguez, C.; Sanchez de Groot, N.; Rimola, A.; Alvarez-Larena, A.; Lloveras, V.; Vidal-Gancedo, J.; Ventura, S.; Vendrell, J.; Sodupe, M.; Gonzalez-Duarte, P. Design, selection, and characterization of thioflavin-based intercalation compounds with metal chelating properties for application in Alzheimer's disease. *J. Am. Chem. Soc.* **2009**, *131*, 1436-1451.
59. Inbar, P.; Li, C. Q.; Takayama, S. A.; Bautista, M. R.; Yang, J. Oligo(ethylene glycol) derivatives of thioflavin T as inhibitors of protein-amyloid interactions. *Chembiochem* **2006**, *7*, 1563-1566.
60. Hudson, S. A.; Ecroyd, H.; Kee, T. W.; Carver, J. A. The thioflavin T fluorescence assay for amyloid fibril detection can be biased by the presence of exogenous compounds. *FEBS J.* **2009**, *276*, 5960-5972.

61. Christie, W. W. Gangliosides - Structure, Occurrence, Biology, and Analysis. <http://lipidlibrary.aocs.org/Lipids/gang/index.htm> (accessed 02/10, 2014).
62. Ariga, T.; Yu, R. K. GM1 inhibits amyloid β -protein-induced cytokine release. *Neurochem. Res.* **1999**, *24*, 219-226.
63. Williamson, M. P.; Suzuki, Y.; Bourne, N. T.; Asakura, T. Binding of amyloid β -peptide to ganglioside micelles is dependent on histidine-13. *Biochem. J.* **2006**, *397*, 483-490.
64. Kakio, A.; Nishimoto, S. I.; Yanagisawa, K.; Kozutsumi, Y.; Matsuzaki, K. Cholesterol-dependent formation of GM1 ganglioside-bound amyloid β -protein, an endogenous seed for Alzheimer amyloid. *J. Biol. Chem.* **2001**, *276*, 24985-24990.
65. Ikeda, K.; Yamaguchi, T.; Fukunaga, S.; Hoshino, M.; Matsuzaki, K. Mechanism of amyloid β -protein aggregation mediated by GM1 ganglioside clusters. *Biochemistry* **2011**, *50*, 6433-6440.
66. Yanagisawa, M.; Ariga, T.; Yu, R. K. Cytotoxic effects of G(M1) ganglioside and amyloid β -peptide on mouse embryonic neural stem cells. *ASN Neuro* **2010**, *2*, e00029.
67. Dawson, R. M. Characterization of the binding of cholera toxin to ganglioside GM1 immobilized onto microtitre plates. *J. Appl. Toxicol.* **2005**, *25*, 30-38.
68. Schagger, H.; von Jagow, G. Tricine-sodium dodecyl sulfate-polyacrylamide gel electrophoresis for the separation of proteins in the range from 1 to 100 kDa. *Anal. Biochem.* **1987**, *166*, 368-379.
69. Schagger, H. Tricine-SDS-PAGE. *Nat. Protoc.* **2006**, *1*, 16-22.
70. Ogawa, M.; Tsukuda, M.; Yamaguchi, T.; Ikeda, K.; Okada, T.; Yano, Y.; Hoshino, M.; Matsuzaki, K. Ganglioside-mediated aggregation of amyloid β -proteins (A β): comparison between A β -(1-42) and A β -(1-40). *J. Neurochem.* **2011**, *116*, 851-857.
71. Feng, Y.; Wang, X.; Yang, S.; Wang, Y.; Zhang, X.; Du, X.; Sun, X.; Zhao, M.; Huang, L.; Liu, R. Resveratrol inhibits β -amyloid oligomeric cytotoxicity but does not prevent oligomer formation. *Neurotoxicology* **2009**, *30*, 986-995.
72. Ladiwala, A. R.; Lin, J. C.; Bale, S. S.; Marcelino-Cruz, A. M.; Bhattacharya, M.; Dordick, J. S.; Tessier, P. M. Resveratrol selectively remodels soluble oligomers and fibrils of amyloid A β into off-pathway conformers. *J. Biol. Chem.* **2010**, *285*, 24228-24237.
73. Yang, F.; Lim, G. P.; Begum, A. N.; Ubeda, O. J.; Simmons, M. R.; Ambegaokar, S. S.; Chen, P. P.; Kaye, R.; Glabe, C. G.; Frautsch, S. A.; Cole, G. M. Curcumin inhibits formation of

- amyloid β oligomers and fibrils, binds plaques, and reduces amyloid in vivo. *J. Biol. Chem.* **2005**, *280*, 5892-5901.
74. Ono, K.; Hasegawa, K.; Naiki, H.; Yamada, M. Curcumin has potent anti-amyloidogenic effects for Alzheimer's β -amyloid fibrils in vitro. *J. Neurosci. Res.* **2004**, *75*, 742-750.
75. Hulme, E. C.; Trevethick, M. A. Ligand binding assays at equilibrium: validation and interpretation. *Br. J. Pharmacol.* **2010**, *161*, 1219-1237.
76. Choo-Smith, L. P.; Garzon-Rodriguez, W.; Glabe, C. G.; Surewicz, W. K. Acceleration of amyloid fibril formation by specific binding of A β -(1-40) peptide to ganglioside-containing membrane vesicles. *J. Biol. Chem.* **1997**, *272*, 22987-22990.
77. Ariga, T.; Kobayashi, K.; Hasegawa, A.; Kiso, M.; Ishida, H.; Miyatake, T. Characterization of high-affinity binding between gangliosides and amyloid β -protein. *Arch. Biochem. Biophys.* **2001**, *388*, 225-230.
78. Fancy, D. A.; Kodadek, T. Chemistry for the analysis of protein-protein interactions: rapid and efficient cross-linking triggered by long wavelength light. *Proc. Natl. Acad. Sci. U. S. A.* **1999**, *96*, 6020-6024.
79. Mattson, G.; Conklin, E.; Desai, S.; Nielander, G.; Savage, M. D.; Morgensen, S. A practical approach to crosslinking. *Mol. Biol. Rep.* **1993**, *17*, 167-183.
80. Tang, X.; Bruce, J. E. Chemical cross-linking for protein-protein interaction studies. *Methods Mol. Biol.* **2009**, *492*, 283-293.
81. Bitan, G.; Lomakin, A.; Teplow, D. B. Amyloid β -protein oligomerization: prenucleation interactions revealed by photo-induced cross-linking of unmodified proteins. *J. Biol. Chem.* **2001**, *276*, 35176-35184.
82. Bitan, G.; Teplow, D. B. Rapid photochemical cross-linking--a new tool for studies of metastable, amyloidogenic protein assemblies. *Acc. Chem. Res.* **2004**, *37*, 357-364.
83. LeVine, H., 3rd. Alzheimer's β -peptide oligomer formation at physiologic concentrations. *Anal. Biochem.* **2004**, *335*, 81-90.
84. Crouch, P. J.; Blake, R.; Duce, J. A.; Ciccotosto, G. D.; Li, Q. X.; Barnham, K. J.; Curtain, C. C.; Cherny, R. A.; Cappai, R.; Dyrks, T.; Masters, C. L.; Trounce, I. A. Copper-dependent inhibition of human cytochrome c oxidase by a dimeric conformer of amyloid- β ₁₋₄₂. *J. Neurosci.* **2005**, *25*, 672-679.

85. Bitan, G. In *Structural Study of Metastable Amyloidogenic Protein Oligomers by Photo-Induced Cross-Linking of Unmodified Proteins*; Indu Kheterpal and Ronald Wetzel, Ed.; Methods in Enzymology; Academic Press: **2006**; *413*, pp. 217-236.
86. Kalyanasundaram, K. Photophysics, photochemistry and solar energy conversion with tris(bipyridyl)ruthenium(II) and its analogues. *Coord. Chem. Rev.* **1982**, *46*, 159-244.
87. Wallin, S.; Davidsson, J.; Modin, J.; Hammarstroem, L. Femtosecond Transient Absorption Anisotropy Study on $[\text{Ru}(\text{bpy})_3]^{2+}$ and $[\text{Ru}(\text{bpy})(\text{py})_4]^{2+}$. Ultrafast Interlig and Randomization of the MLCT State. *J. Phys. Chem. A* **2005**, *109*, 4697-4704.
88. Wikipedia Luminous efficacy. http://en.wikipedia.org/wiki/Luminous_efficacy#Overall_luminous_efficacy (accessed 01/15, 2014).

CHAPTER VI.

Conclusions and Future Directions

1. Conclusions

Alzheimer's disease is a chronic, progressive condition. Attempts to understand its underlying mechanisms have only been able to detail smaller components of the process without tying all aspects together; AD cannot be explained by a simple linear model such as the β -amyloid cascade.

This work integrates new experimental evidence with data from numerous research groups across multiple branches of science to challenge our previous thinking of AD. Traditionally, AD was considered a type of protein folding disorder. Here, the concept of AD as autoimmune disease — one of the innate immune system (1) for which autoimmunity has not been previously described — pioneers a new direction in AD research. The chapters of this thesis provide experimental data in support of this new hypothesis. Chapter II addressed some of the shortcomings of current AD hypotheses and provided solutions for unanswered questions about AD. Based on its structural similarity to established antimicrobial peptides (AMPs), as well as experiments demonstrating its increased production induced by (simulated) infection and its antibacterial and antiviral activity, it is proposed that the physiologic role of A β is as an AMP. In comparing several properties of different cell membranes, similarities between neuronal and bacterial cell membranes were identified as possible drivers for the attack of A β on neurons. After reproducing toxicity of A β against neuroblastoma and rat primary neuronal cells,

mitochondrial toxicity of A β was identified as another possible mechanism — besides its membrane destructing activity — for its neurotoxicity seen in AD. It is suggested that this mitochondrial toxicity is due to the similarity of bacteria with mitochondria, which may be explained by the evolutionary origin of mitochondria described in the endosymbiont theory as symbiotic bacteria that were engulfed by early eukaryotic cells. In reversing the concept of A β being an AMP, similarity of other AMPs to A β was shown by establishing neurotoxic activity of LL-37 and cecropin A against neuroblastoma and rat primary neuronal cells. It was shown that necrotic cell death caused by A β , but not apoptotic cell death, may spread to adjacent neurons. In conjunction with literature reports that A β prevents neurogenesis it was posited that A β thus may be responsible for the chronic and progressive character of AD. These findings were interpreted such that the processes involved in AD are not linear, as implied in the β -amyloid cascade, but are rather characterised by a positive feedback loop, which was termed the '*Vicious Cycle of Alzheimer's Disease*'. Integrating published data and research with results obtained through this work, a diagram was developed which shows the connections and feedback loops involved in the *Vicious Cycle of Alzheimer's Disease*.

Bacterial cell components can be potent stimulators of the immune system; gangliosides, and in particular GM1, are able to bind A β to form the toxic species that initiates and enters the *Vicious Cycle of AD*. In Chapter III, a question borne from A β 's activity as an AMP and its central role in the *Vicious Cycle of AD* was investigated: do antibiotics, such as penicillin, that cause release of bacterial endotoxins due to their mechanism of action, trigger the *Vicious Cycle of AD* and thus lead to the development of AD? Preliminary evidence supporting this notion was presented.

The synthesis by microwave-assisted solid-phase peptide synthesis of a number of peptides related to AD is described in Chapter IV. Problems occurring during the synthesis and

suggested solutions were discussed. The peptides that were successfully isolated and purified were used in experiments related to this thesis and the work of other members of this research group.

A β has been shown to interact with many different classes of molecules and ions; in Chapter V, two aspects were investigated. First, the non-specific binding of A β to commonly used sample and reaction vessels and resultant peptide loss was quantified in a range of conditions with the goal to identify measures to minimise sample loss in the handling of this expensive peptide. Losses of over 50% were observed for some vessels (glass), while one product consistently stood out with only minimal protein binding, the Eppendorf Protein LoBind microcentrifuge tubes. And second, the GM1 Assay was developed as an alternative to the ThT and Congo Red assays to determine the efficacy of A β antiaggregants. Experiments in this section actually covered a number of different interactions of A β ; the interaction with GM1, which leads to seed formation for its aggregation (i.e. its interaction with itself), interaction with metal ions (Cu²⁺, Zn²⁺), and interaction with small molecule antiaggregants. Finally, two LED irradiators were designed and built (one for single samples, the other for 96-well plates), to facilitate study of A β aggregation by photo-induced cross-linking of unmodified proteins (PICUP), a technique that has been employed successfully in the analysis of A β aggregation.

2. Future Directions

As often encountered in research, obtaining answers to one question leads to more questions not previously considered. Currently underway is research investigating the immunomodulatory role of A β and its connections to the Vicious Cycle of AD. qPCR experiments aimed at understanding the signalling pathways between different brain cells (neurons, microglia, astrocytes) involved in AD are being performed. One task with a high impact on many future experiments would be to improve current protocols for the preparation of A β and for 'quality control' of starting solutions in assays using A β . This might include finding a new standard for the A β quantitation in the BCA assay, as BSA has been shown to have a different response than A β in this assay (possibly due to the large difference in size and different relative abundance of amino acid residues). Scrambled A β may be a good candidate, since it has exactly the same amino acid residues as the native A β , and it has been shown not to aggregate. Other experiments that should be performed include obtaining a dose-response curve for A β production by cells upon incubation with LPS and LTA; repeating antibacterial assays with an improved formulation of A β ; obtaining a dose-response curve for the addition of cholesterol to the bacterial growth medium; determining the insertion of cholesterol into the bacterial membrane; determining the mechanism of action of A β against viruses and extending the spectrum of viruses tested; confirming that a viral infection can stimulate expression of A β ; and finally, using an AD-transgenic mouse model to find out whether a viral infection leads to earlier or increased symptoms of AD.

In regards to penicillin as a risk factor for AD, a number of experiments should be repeated to obtain better statistics. Additionally, some suggested experiments would include incubations

with antibiotics of other classes; determining cell wall integrity after killing bacteria, e.g. by Trypan Blue or Live/Dead® stain; quantifying how much LPS or LTA is actually released by each killing method using mass spectrometry or ELISA; testing dilution series of LPS/LTA and bacterial fragments for concentration dependence of the induced A β production; and determining the influence of added A β ₁₂₋₁₇ (VHHQKL, since BBXB is a possible binding motif for LPS and LTA) on the induced A β production.

An animal trial is in the planning stage pending the outcome of further in vitro test results. Performed by Kurt Stover, a Ph.D. student working under the supervision of Dr. Richard Brown at Dalhousie's Department of Psychology, it is intended to infect AD transgenic mice with bacteria, treat them with different antibiotics, and determine behaviour and brain pathology changes (in particular plaque load) over a time period of about six months in order to evaluate the influence that different classes of antibiotics may have on the progression of AD.

A number of peptides synthesised as part of this project should be resynthesized with improved protocols based on the results obtained here, e.g. A β ₁₋₄₀, A β ₁₋₄₂, A β ₁₂₋₁₇, and VHHQKLAAAA. Other peptides of interest might include scrambled A β _{1-40/42}, KLVFFAAAAA and GAIIGLAAAA, FAM-A β _{1-40/42}, and BHQ-10-A β _{1-40/42}. BHQ-10 (Biosearch Technologies, Novato, CA, USA) is a quencher for FAM fluorescence in Förster Resonance Energy Transfer (FRET), a technique used to investigate the distance between certain residues in a peptide. Here it is suggested to use mixed solutions of FAM-A β and BHQ-10-A β to investigate the aggregation of A β , and maybe utilise it to develop a new A β aggregation assay.

Suggested improvements for the peptide synthesis would be the use of a different resin, in particular the HMPB-ChemMatrix® resin, which has shown superior results in the synthesis of difficult peptides (2, 3). Another advantage, specifically in regards to the VHHQKLAAAA project,

would be that it allows cleavage of the peptide from the resin without prior deprotection of the side chains, thus avoiding an extra step to re-protect side chains and N-terminus for the attachment to the solid matrix. One way to avoid or remove peptide contaminants, such as deletion peptides seen in the synthesis of BBXB A β , may be the use of capping agents in the synthesis of this peptide. An intriguing method was published by Montanari and Kumar (4), which prevents formation of deletion peptides by capping in the coupling step unreacted N-termini of the growing peptide chain and allows removal of essentially all unwanted shorter fragments by the use of specially designed fluororous capping agents (4).

Another recommendation would be the introduction of routine amino acid analysis as a means of quality control for the synthesised and purified peptides.

The analysis of peptide/protein loss due to adsorption should be extended to include other low-binding tubes and plates, as well.

In regards to the GM1 Assay, a number of future experiments shall be suggested. Starting with FAM-A β (unlabeled A β proved undetectable by UV-Vis at the concentrations tried in the initial experiments (20 – 35 μ M)) and fluorescence detection, irradiation conditions should be optimised for the detection of oligomers. In a next step, unlabelled A β may be used in conjunction with pre-column derivatisation (e.g. with *o*-phthalaldehyde (OPA), an established derivatisation reagent; protocols are available to do this automatically with the autosampler) in order to reduce the cost of the assay. Subsequently, PICUP could be used to analyse samples obtained from the GM1 Assay as mentioned earlier. And finally, it may be attempted to develop a protocol that allows analysis of these samples by mass spectrometry.

3. References

1. Meier-Stephenson, V. C. Quantum Medicine: Novel Applications of Computational Chemistry to the Treatment of Neurological Diseases, Dalhousie University, Halifax, Nova Scotia, **2005**.
2. Garcia-Martin, F.; Quintanar-Audelo, M.; Garcia-Ramos, Y.; Cruz, L. J.; Gravel, C.; Furic, R.; Cote, S.; Tulla-Puche, J.; Albericio, F. ChemMatrix, a poly(ethylene glycol)-based support for the solid-phase synthesis of complex peptides. *J. Comb. Chem.* **2006**, *8*, 213-220.
3. Garcia-Martin, F.; White, P.; Steinauer, R.; Cote, S.; Tulla-Puche, J.; Albericio, F. The synergy of ChemMatrix resin and pseudoproline building blocks renders RANTES, a complex aggregated chemokine. *Biopolymers* **2006**, *84*, 566-575.
4. Montanari, V.; Kumar, K. Just add water: a new fluororous capping reagent for facile purification of peptides synthesized on the solid phase. *J. Am. Chem. Soc.* **2004**, *126*, 9528-9529.

APPENDIX A.

PREDICTION OF A β AS AMP

The sequence for A β ₁₋₄₀ was entered into the APD Prediction Tool (accessed: May 15, 2008) (http://aps.unmc.edu/AP/prediction/prediction_main.php), which returned the results shown in Figure A-1. Since the publication of work by Soscia et al. (1) in 2010 demonstrating the antimicrobial activity of A β against a number of bacterial strains, both A β ₁₋₄₀ and A β ₁₋₄₂ have been entered into the database with the ID numbers AP01675 and AP01676, respectively.

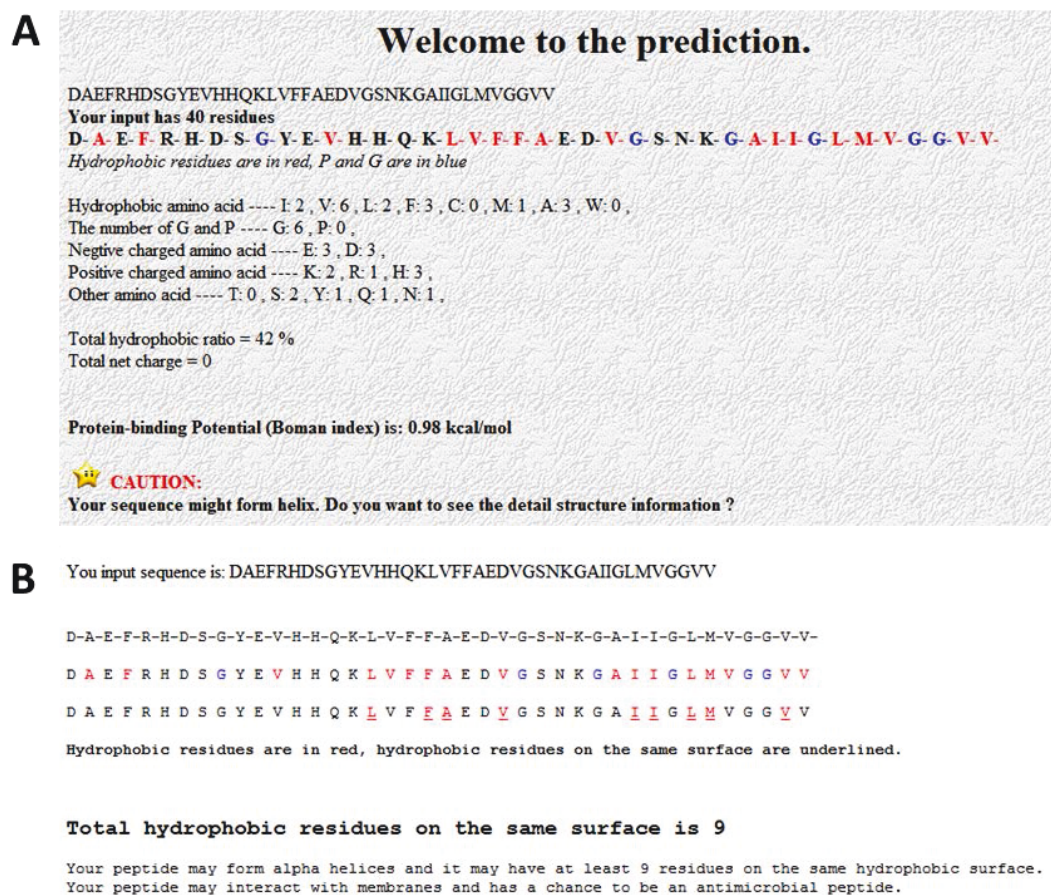


Figure A-1 Results for A β ₁₋₄₀ from APD Prediction Tool (2).

Screenshots of the results for A β ₁₋₄₀ from the APD Prediction Tool (1714) (accessed: May 15, 2008; http://aps.unmc.edu/AP/prediction/prediction_main.php) showing general information about the peptide in (A), and detailed structural information in (B) including the prediction that A β ₁₋₄₀ "has a chance to be an antimicrobial peptide".

References

1. Soccia, S. J.; Kirby, J. E.; Washicosky, K. J.; Tucker, S. M.; Ingelsson, M.; Hyman, B.; Burton, M. A.; Goldstein, L. E.; Duong, S.; Tanzi, R. E.; Moir, R. D. The Alzheimer's Disease-Associated Amyloid β -Protein Is an Antimicrobial Peptide. *PLoS One* **2010**, *5*, e9505.
2. Wang, Z.; Wang, G. APD: the Antimicrobial Peptide Database. *Nucleic Acids Res.* **2004**, *32*, D590-2.

APPENDIX B.

RADIAL DIFFUSION ASSAY

In order to facilitate a more thorough evaluation of the radial diffusion assay (RDA), here three tables are given looking at the same data in different ways. In Table B-1, the differences for all possible permutation of the samples were calculated for incubation without cholesterol, along with the corresponding statistical parameters; Table B-2 shows the respective results for incubation with cholesterol. In Table B-3, the influence of cholesterol and pH are determined. The colour coding scheme is as follows, red fill in the 't Stat' columns highlights negative values for the difference; green fill in the 'P(t<=T)' columns marks statistical significance below the 0.05 level, blue fill below the 0.01 level; '*' in the 'Significance' column stand for statistical significance below the 0.05 level, '**' below the 0.01 level, while a green fill is used for positive differences, and an orange fill for negative differences.

Table B-1 Results for incubation without cholesterol.

w/o Chol.	Δ		pH 7.3			pH 7.0			pH 6.5		
	pH 7.3	pH 7.0	pH 7.3	t Stat	P(T<=t) 1-tail	P(T<=t) 2-tail	Significance 2-tail	t Stat	P(T<=t) 1-tail	P(T<=t) 2-tail	Significance 2-tail
Cu ²⁺ - Blank	2.83	1.83	1.00	17.0000	3.51E-05	7.02E-05	**	11.0000	1.94E-04	3.88E-04	**
Zn ²⁺ - Blank	1.83	1.67	1.00	4.1576	0.00709	0.01417	*	10.0000	0.00028	0.00056	**
Pen-Strep - Blank	12.33	13.00	13.50	74.0000	9.99E-08	2.00E-07	**	45.0333	7.27E-07	1.45E-06	**
Aβ 90µM - Blank	0.00	0.00	0.00	#DIV/0!	#DIV/0!	#DIV/0!		#DIV/0!	#DIV/0!	#DIV/0!	
Aβ 50µM - Blank	1.50	1.50	0.67	3.0000	0.01997	0.03994	*	5.1962	0.00327	0.00653	**
Aβ 90µM / Cu ²⁺ - Blank	0.33	0.33	0.17	1.0000	0.1870	0.3739		1.0000	0.1870	0.3739	
Aβ 50µM / Zn ²⁺ - Blank	0.00	0.00	0.00	#DIV/0!	#DIV/0!	#DIV/0!		#DIV/0!	#DIV/0!	#DIV/0!	
Cu ²⁺ - Zn ²⁺	1.00	0.17	0.00	2.1213	0.05060	0.10119		0.7071	0.25926	0.51852	
Cu ²⁺ - Pen-Strep	-9.50	-11.17	-12.50	-40.3051	1.13E-06	2.26E-06	**	-33.5000	2.37E-06	4.74E-06	**
Cu ²⁺ - Aβ 90µM	2.83	1.83	1.00	17.0000	3.51E-05	7.02E-05	**	11.0000	1.94E-04	3.88E-04	**
Cu ²⁺ - Aβ 50µM	1.33	0.33	0.33	2.5298	0.03234	0.06468	**	1.0000	0.18695	0.37390	
Cu ²⁺ - Aβ 90µM / Cu ²⁺	2.50	1.50	0.83	6.7082	0.0013	0.0026	**	4.0249	0.0079	0.0158	*
Cu ²⁺ - Aβ 50µM / Zn ²⁺	2.83	1.83	1.00	17.0000	3.51E-05	7.02E-05	**	11.0000	1.94E-04	3.88E-04	**
Zn ²⁺ - Pen-Strep	-10.50	-11.33	-12.50	-22.2739	1.20E-05	2.41E-05	**	-34.0000	2.23E-06	4.46E-06	**
Zn ²⁺ - Aβ 90µM	1.83	1.67	1.00	4.1576	0.00709	0.01417	*	10.0000	0.00028	0.00056	**
Zn ²⁺ - Aβ 50µM	0.33	0.17	0.33	0.5000	0.32166	0.64333		0.5000	0.32166	0.64333	
Zn ²⁺ - Aβ 90µM / Cu ²⁺	1.50	1.33	0.83	2.7136	0.0267	0.0533		3.5777	0.0116	0.0232	*
Zn ²⁺ - Aβ 50µM / Zn ²⁺	1.83	1.67	1.00	4.1576	0.0071	0.0142	*	10.0000	0.0003	0.0006	**
Pen-Strep - Aβ 90µM	12.33	13.00	13.50	74.0000	9.99E-08	2.00E-07	**	45.0333	7.27E-07	1.45E-06	**
Pen-Strep - Aβ 50µM	10.83	11.50	12.83	20.5548	1.65E-05	3.31E-05	**	28.1691	4.72E-06	9.45E-06	**
Pen-Strep - Aβ 90µM / Cu ²⁺	12.00	12.67	13.33	32.1994	2.77E-06	5.55E-06	**	28.7253	4.37E-06	8.74E-06	**
Pen-Strep - Aβ 50µM / Zn ²⁺	12.33	13.00	13.50	74.0000	9.99E-08	2.00E-07	**	45.0333	7.27E-07	1.45E-06	**
Aβ 90µM - Aβ 50µM	-1.50	-1.50	-0.67	-3.0000	0.01997	0.03994	*	-5.1962	0.00327	0.00653	**
Aβ 90µM - Aβ 90µM / Cu ²⁺	-0.33	-0.33	-0.17	-1.0000	0.1870	0.3739		-1.0000	0.1870	0.3739	
Aβ 90µM - Aβ 50µM / Zn ²⁺	0.00	0.00	0.00	#DIV/0!	#DIV/0!	#DIV/0!		#DIV/0!	#DIV/0!	#DIV/0!	
Aβ 50µM - Aβ 90µM / Cu ²⁺	1.17	1.17	0.50	1.9415	0.0621	0.1242		2.6458	0.0286	0.0572	
Aβ 50µM - Aβ 50µM / Zn ²⁺	1.50	1.50	0.67	3.0000	0.0200	0.0399	*	5.1962	0.0033	0.0065	**
Aβ 90µM / Cu ²⁺ - Aβ 50µM / Zn ²⁺	0.33	0.33	0.17	1.0000	0.1870	0.3739		1.0000	0.1870	0.3739	

Table B-2 Results for incubation with cholesterol.

w/ Chol.	Δ		pH 7.3			pH 7.0			pH 6.5			Significance 2-tail
	pH 7.3	pH 7.0	t Stat	P(T<=t) 1-tail	P(T<=t) 2-tail	t Stat	P(T<=t) 1-tail	P(T<=t) 2-tail	t Stat	P(T<=t) 1-tail	P(T<=t) 2-tail	
Cu ²⁺ - Blank	1.17	2.00	2.6458	0.00666	5.72E-02	#DIV/0!	#DIV/0!	#DIV/0!	5.1962	3.27E-03	6.53E-03	**
Zn ²⁺ - Blank	2.67	0.67	8.0000	0.000132	0.00132	1.5119	0.10255	0.20511	#DIV/0!	#DIV/0!	#DIV/0!	
Pen-Strep - Blank	13.00	11.33	#DIV/0!	#DIV/0!	#DIV/0!	34.0000	2.23E-06	4.46E-06	35.5000	1.88E-06	3.76E-06	**
AP 90µM - Blank	0.00	0.00	#DIV/0!	#DIV/0!	#DIV/0!	#DIV/0!	#DIV/0!	#DIV/0!	#DIV/0!	#DIV/0!	#DIV/0!	
AP 50µM - Blank	1.17	0.00	7.0000	0.00110	0.00219	#DIV/0!	#DIV/0!	#DIV/0!	2.0000	0.05806	0.11612	
AP 90µM / Cu ²⁺ - Blank	0.00	0.00	#DIV/0!	#DIV/0!	#DIV/0!	#DIV/0!	#DIV/0!	#DIV/0!	5.0000	0.0037	0.0075	
AP 50µM / Zn ²⁺ - Blank	0.00	0.00	#DIV/0!	#DIV/0!	#DIV/0!	#DIV/0!	#DIV/0!	#DIV/0!	#DIV/0!	#DIV/0!	#DIV/0!	
Cu ²⁺ - Zn ²⁺	-1.50	1.33	-2.7136	0.02667	0.05334	3.0237	0.01951	0.03902	-1.7321	0.07915	0.15830	
Cu ²⁺ - Pen-Strep	-11.83	-9.33	-26.8355	5.73E-06	1.15E-05	-28.0000	4.84E-06	9.68E-06	-23.4338	9.83E-06	1.97E-05	**
Cu ²⁺ - AP 90µM	1.17	2.00	2.6458	2.86E-02	5.72E-02	#DIV/0!	#DIV/0!	#DIV/0!	1.8898	3.27E-03	6.53E-03	**
Cu ²⁺ - AP 50µM	0.00	2.00	0.0000	0.50000	1.00000	#DIV/0!	#DIV/0!	#DIV/0!	1.8898	0.06589	0.13178	
Cu ²⁺ - AP 90µM / Cu ²⁺	1.17	2.00	2.6458	0.0286	0.0572	#DIV/0!	#DIV/0!	#DIV/0!	2.0000	0.0581	0.1161	
Cu ²⁺ - AP 50µM / Zn ²⁺	1.17	2.00	2.6458	2.86E-02	5.72E-02	#DIV/0!	#DIV/0!	#DIV/0!	5.1962	3.27E-03	6.53E-03	**
Zn ²⁺ - Pen-Strep	-10.33	-10.67	-31.0000	3.23E-06	6.45E-06	-19.2967	2.13E-05	4.25E-05	-29.5000	3.93E-06	7.86E-06	**
Zn ²⁺ - AP 90µM	2.67	0.67	8.0000	0.00066	0.00132	1.5119	0.10255	0.20511	#DIV/0!	#DIV/0!	#DIV/0!	
Zn ²⁺ - AP 50µM	1.50	0.67	4.0249	0.00790	0.01580	1.5119	0.10255	0.20511	4.0000	0.00807	0.01613	*
Zn ²⁺ - AP 90µM / Cu ²⁺	2.67	0.67	8.0000	0.0007	0.0013	1.5119	0.1026	0.2051	7.0000	0.0011	0.0022	**
Zn ²⁺ - AP 50µM / Zn ²⁺	2.67	0.67	8.0000	0.0007	0.0013	1.5119	0.1026	0.2051	#DIV/0!	#DIV/0!	#DIV/0!	
Pen-Strep - AP 90µM	13.00	11.33	#DIV/0!	#DIV/0!	#DIV/0!	34.0000	2.23E-06	4.46E-06	35.5000	1.88E-06	3.76E-06	**
Pen-Strep - AP 50µM	11.83	11.33	71.0000	1.18E-07	2.36E-07	34.0000	2.23E-06	4.46E-06	23.6881	9.42E-06	1.88E-05	**
Pen-Strep - AP 90µM / Cu ²⁺	13.00	11.33	#DIV/0!	#DIV/0!	#DIV/0!	34.0000	2.23E-06	4.46E-06	29.5161	3.92E-06	7.85E-06	**
Pen-Strep - AP 50µM / Zn ²⁺	13.00	11.33	#DIV/0!	#DIV/0!	#DIV/0!	34.0000	2.23E-06	4.46E-06	35.5000	1.88E-06	3.76E-06	**
AP 90µM - AP 50µM	-1.17	0.00	-7.0000	0.00110	0.00219	#DIV/0!	#DIV/0!	#DIV/0!	-2.0000	0.05806	0.11612	
AP 90µM - AP 90µM / Cu ²⁺	0.00	0.00	#DIV/0!	#DIV/0!	#DIV/0!	#DIV/0!	#DIV/0!	#DIV/0!	-5.0000	0.0037	0.0075	**
AP 90µM - AP 50µM / Zn ²⁺	0.00	0.00	#DIV/0!	#DIV/0!	#DIV/0!	#DIV/0!	#DIV/0!	#DIV/0!	#DIV/0!	#DIV/0!	#DIV/0!	
AP 50µM - AP 90µM / Cu ²⁺	1.17	0.00	7.0000	0.0011	0.0022	#DIV/0!	#DIV/0!	#DIV/0!	-0.4472	0.3389	0.6779	
AP 50µM - AP 50µM / Zn ²⁺	1.17	0.00	7.0000	0.0011	0.0022	#DIV/0!	#DIV/0!	#DIV/0!	2.0000	0.0581	0.1161	
AP 90µM / Cu ²⁺ - AP 50µM / Zn ²⁺	0.00	0.00	#DIV/0!	#DIV/0!	#DIV/0!	#DIV/0!	#DIV/0!	#DIV/0!	5.0000	0.0037	0.0075	**

Table B-3 Results for influence of cholesterol and pH.

w/o - w/ Chol.	Δ		pH 7.3			pH 7.0			pH 6.5					
	pH 7.3 - pH 7.0	pH 7.0 - pH 6.5	t Stat	P(T<=t) 1-tail	P(T<=t) 2-tail	Significance 2-tail	t Stat	P(T<=t) 1-tail	P(T<=t) 2-tail	Significance 2-tail	t Stat	P(T<=t) 1-tail	P(T<=t) 2-tail	Significance 2-tail
Blank	0.0	0.0	#DIV/0!	#DIV/0!	#DIV/0!		#DIV/0!	#DIV/0!	#DIV/0!		#DIV/0!	#DIV/0!	#DIV/0!	
Cu ²⁺	1.7	-0.2	3.5355	0.01206	0.02411	*	-1.0000	0.18695	0.7390		-1.2247	0.14393	0.28786	
Zn ²⁺	-0.8	1.0	-1.5076	0.10308	0.20615		2.1213	0.05060	0.10119		#DIV/0!	#DIV/0!	#DIV/0!	
Pen-Strep	-0.7	1.7	-4.0000	0.00907	0.01613	*	3.7796	0.00972	0.01944	*	3.7796	0.00972	0.01944	*
Aβ 90µM	0.0	0.0	#DIV/0!	#DIV/0!	#DIV/0!		#DIV/0!	#DIV/0!	#DIV/0!		#DIV/0!	#DIV/0!	#DIV/0!	
Aβ 50µM	0.0	0.0	0.6325	0.28072	0.56144		5.1962	0.00327	0.00653	**	0.0000	0.50000	1.00000	
Aβ 90µM / Cu ²⁺	0.3	1.5	1.0000	0.18695	0.37390		1.0000	0.18695	0.37390		-2.8284	0.02371	0.04742	*
Aβ 50µM / Zn ²⁺	0.3	0.3	#DIV/0!	#DIV/0!	#DIV/0!		#DIV/0!	#DIV/0!	#DIV/0!		#DIV/0!	#DIV/0!	#DIV/0!	
w/o Cholesterol	Δ		pH 7.3 - pH 7.0			pH 7.3 - pH 6.5			pH 7.0 - pH 6.5					
	pH 7.3 - pH 7.0	pH 7.0 - pH 6.5	t Stat	P(T<=t) 1-tail	P(T<=t) 2-tail	Significance 2-tail	t Stat	P(T<=t) 1-tail	P(T<=t) 2-tail	Significance 2-tail	t Stat	P(T<=t) 1-tail	P(T<=t) 2-tail	Significance 2-tail
Blank	0.0	0.0	#DIV/0!	#DIV/0!	#DIV/0!		#DIV/0!	#DIV/0!	#DIV/0!		#DIV/0!	#DIV/0!	#DIV/0!	
Cu ²⁺	1.0	1.8	4.2426	0.00662	0.01324	*	5.5000	0.00266	0.00533	**	2.5000	0.03338	0.06677	
Zn ²⁺	0.2	0.8	0.3536	0.37076	0.74152		1.8898	0.06589	0.13178		4.0000	0.00807	0.01613	*
Pen-Strep	-0.7	-1.2	-2.0000	0.05806	0.11612		-3.5000	0.01245	0.02490	*	-1.2247	0.14393	0.28786	
Aβ 90µM	0.0	0.0	#DIV/0!	#DIV/0!	#DIV/0!		#DIV/0!	#DIV/0!	#DIV/0!		#DIV/0!	#DIV/0!	#DIV/0!	
Aβ 50µM	0.0	0.8	0.0000	0.50000	1.00000		1.2500	0.13972	0.27944		1.5811	0.09450	0.18900	
Aβ 90µM / Cu ²⁺	0.0	0.0	0.0000	0.50000	1.00000		0.4472	0.33893	0.67787		0.4472	0.33893	0.67787	
Aβ 50µM / Zn ²⁺	0.0	0.2	#DIV/0!	#DIV/0!	#DIV/0!		#DIV/0!	#DIV/0!	#DIV/0!		#DIV/0!	#DIV/0!	#DIV/0!	
w/ Cholesterol	Δ		pH 7.3 - pH 7.0			pH 7.3 - pH 6.5			pH 7.0 - pH 6.5					
	pH 7.3 - pH 7.0	pH 7.0 - pH 6.5	t Stat	P(T<=t) 1-tail	P(T<=t) 2-tail	Significance 2-tail	t Stat	P(T<=t) 1-tail	P(T<=t) 2-tail	Significance 2-tail	t Stat	P(T<=t) 1-tail	P(T<=t) 2-tail	Significance 2-tail
Blank	0.0	0.0	#DIV/0!	#DIV/0!	#DIV/0!		#DIV/0!	#DIV/0!	#DIV/0!		#DIV/0!	#DIV/0!	#DIV/0!	
Cu ²⁺	-0.8	-0.3	-1.8898	0.06589	0.13178		-0.6325	0.28072	0.56144		1.7321	0.07915	0.15830	
Zn ²⁺	2.0	0.7	3.6181	0.01120	0.02239	*	2.0000	0.05806	0.11612		-3.0237	0.01951	0.03902	*
Pen-Strep	1.7	1.2	5.0000	0.00375	0.00749	**	3.5000	0.01245	0.02490	*	-1.0607	0.17482	0.34864	
Aβ 90µM	0.0	0.0	#DIV/0!	#DIV/0!	#DIV/0!		#DIV/0!	#DIV/0!	#DIV/0!		#DIV/0!	#DIV/0!	#DIV/0!	
Aβ 50µM	1.2	0.5	7.0000	0.00110	0.00219	**	1.3416	0.12541	0.25082		-2.0000	0.05806	0.11612	
Aβ 90µM / Cu ²⁺	0.0	-0.8	#DIV/0!	#DIV/0!	#DIV/0!		-5.0000	0.00375	0.00749	**	-5.0000	0.00375	0.00749	**
Aβ 50µM / Zn ²⁺	0.0	-0.8	#DIV/0!	#DIV/0!	#DIV/0!		#DIV/0!	#DIV/0!	#DIV/0!		#DIV/0!	#DIV/0!	#DIV/0!	

APPENDIX C.

THE GROWTH CURVE ASSAY

C.1. Parameter Selection

For the Growth Curve Assay (GCA), ten parameters had been identified that might help in characterising a bacterial growth curve and identifying factors that influence different aspects related to bacterial growth. To facilitate displaying the results in a clear manner, it was decided to select six of those parameters based on their average correlation and mechanistic considerations.

For each parameter, the correlation coefficient, r , for the correlation with all other parameters was determined for each bacterial strain according to Equation (C-1):

$$r = \frac{\sum xy}{\sqrt{\sum x^2 \sum y^2}} \quad (\text{C-1})$$

where

$$\sum xy = \sum_{i=1}^n (X_i - \bar{X})(Y_i - \bar{Y}) \quad (\text{C-2})$$

and,

$$\sum x^2 = \sum (X_i - \bar{X})^2 \quad (\text{C-3})$$

$$\sum y^2 = \sum (Y_i - \bar{Y})^2 \quad (\text{C-4})$$

with X and Y as the independent variables that are being subjected to correlation analysis (in this case, two of the different parameters), i as the sample number, and n as the total number of samples. Then, the average correlation coefficient, r_{avg} , was calculated for each parameter (Equation (C-5)):

$$r_{avg} = \frac{\sum_{j=1}^n |r_j|}{m} \quad (C-5)$$

with j being the parameter number, and m the total number of parameters. Results are shown in Table C-1 - Table C-5; Table C-6 shows for each parameter pair the averages of the absolute correlation coefficients of all five bacterial strains. Values are colour-coded by their absolute correlation coefficient $|r|$:

- $r = 0 - 0.2$: red (very low correlation)
- $r = >0.2 - 0.4$: orange (low correlation)
- $r = >0.4 - 0.6$: yellow (medium correlation)
- $r = >0.6 - 0.8$: light green (high correlation)
- $r = >0.8 - 1.0$: dark green (very high correlation)

Table C-1 Correlation coefficients (r), average correlation coefficients (r_{avg}) and their ranking for *E. coli*.

<i>E. coli</i>	Slope _{max}	t _{onset}	OD _{12h}	OD _{max}	t _{ODmax}	t _{slope_{max}}	ΔOD _{final}	t _{2x}	Δt _{max}	OD _{slope_{max}}	r _{avg}	Rank
Slope _{max}		-0.4426	0.8126	0.7762	-0.6813	-0.5483	0.2648	-0.8305	-0.5428	0.9043	0.6124	3
t _{onset}	-0.4426		-0.7752	-0.6245	0.7156	0.9528	-0.4711	0.3659	0.0485	-0.4762	0.5495	7
OD _{12h}	0.8126	-0.7752		0.9161	-0.8797	-0.8421	0.4282	-0.5414	-0.5023	0.8592	0.7122	1
OD _{max}	0.7762	-0.6245	0.9161		-0.7344	-0.6670	0.2303	-0.4821	-0.4414	0.8417	0.6090	6
t _{ODmax}	-0.6813	0.7156	-0.8797	-0.7344		0.7290	-0.4805	0.3839	0.7324	-0.7447	0.6671	2
t _{slope_{max}}	-0.5483	0.9528	-0.8421	-0.6670	0.7290		-0.5437	0.4930	0.1137	-0.5345	0.6112	4
ΔOD _{final}	0.2648	-0.4711	0.4282	0.2303	-0.4805	-0.5437		-0.2373	-0.2277	0.2200	0.3605	9
t _{2x}	-0.8305	0.3659	-0.5414	-0.4821	0.3839	0.4930	-0.2373		0.1922	-0.5559	0.4408	8
Δt _{max}	-0.5428	0.0485	-0.5023	-0.4414	0.7324	0.1137	-0.2277	0.1922		0.3608	0.3501	10
OD _{slope_{max}}	0.9043	-0.4762	0.8592	0.8417	-0.7447	-0.5345	0.2200	-0.5559	0.3608		0.6108	5

Table C-2 Correlation coefficients (r), average correlation coefficients (r_{avg}) and their ranking for *S. marcescens*.

<i>S. marcescens</i>	Slope _{max}	t _{onset}	OD _{12h}	OD _{max}	t _{ODmax}	tslope _{max}	ΔOD _{final}	t _{2x}	Δt _{max}	OD _{slope_{max}}	r _{avg}	Rank
Slope _{max}		-0.8296	0.8663	0.8707	-0.7959	-0.8513	0.7724	-0.8500	0.4162	0.7908	0.7816	5
t _{onset}	-0.8296		-0.9764	-0.9197	0.7297	0.9979	-0.7271	0.6992	-0.7309	-0.7530	0.8263	3
OD _{12h}	0.8663	-0.9764		0.9482	-0.7229	-0.9782	0.7058	-0.7147	0.7033	0.7688	0.8270	2
OD _{max}	0.8707	-0.9197	0.9482		-0.6283	-0.9247	0.6581	-0.7355	0.7149	0.7818	0.8000	4
t _{ODmax}	-0.7959	0.7297	-0.7229	-0.6283		0.7386	-0.8028	0.6159	-0.0667	-0.6838	0.6376	9
tslope _{max}	-0.8513	0.9979	-0.9782	-0.9247	0.7386		-0.7338	0.7414	-0.7190	-0.7362	0.8356	1
ΔOD _{final}	0.7724	-0.7271	0.7058	0.6581	-0.8028	-0.7338		-0.6436	0.2596	0.7052	0.6629	7
t _{2x}	-0.8500	0.6992	-0.7147	-0.7355	0.6159	0.7414	-0.6436		-0.4055	-0.4236	0.6757	6
Δt _{max}	0.4162	-0.7309	0.7033	0.7149	-0.0667	-0.7190	0.2596	-0.4055		0.1733	0.5020	10
OD _{slope_{max}}	0.7908	-0.7530	0.7688	0.7818	-0.6838	-0.7362	0.7052	-0.4236	0.1733		0.6463	8

Table C-3 Correlation coefficients (r), average correlation coefficients (r_{avg}) and their ranking for *K. pneumoniae*.

<i>K. pneumoniae</i>	Slope _{max}	t _{onset}	OD _{12h}	OD _{max}	t _{ODmax}	tslope _{max}	ΔOD _{final}	t _{2x}	Δt _{max}	OD _{slope_{max}}	r _{avg}	Rank
Slope _{max}		-0.8798	0.9563	0.9713	-0.8537	-0.8870	0.8634	-0.9180	0.1628	0.9690	0.8115	5
t _{onset}	-0.8798		-0.9723	-0.9464	0.7255	0.9992	-0.6902	0.8316	-0.4943	-0.8636	0.8174	4
OD _{12h}	0.9563	-0.9723		0.9915	-0.7831	-0.9743	0.7707	-0.8923	0.3825	0.9393	0.8404	1
OD _{max}	0.9713	-0.9464	0.9915		-0.7811	-0.9499	0.7752	-0.9028	0.3484	0.9480	0.8333	2
t _{ODmax}	-0.8537	0.7255	-0.7831	-0.7811		0.7351	-0.9538	0.7429	0.2396	-0.8127	0.7269	8
tslope _{max}	-0.8870	0.9992	-0.9743	-0.9499	0.7351		-0.6976	0.8490	-0.4811	-0.8619	0.8216	3
ΔOD _{final}	0.8634	-0.6902	0.7707	0.7752	-0.9538	-0.6976		-0.7195	-0.2311	0.8441	0.7127	9
t _{2x}	-0.9180	0.8316	-0.8923	-0.9028	0.7429	0.8490	-0.7195		-0.2347	-0.8173	0.7613	7
Δt _{max}	0.1628	-0.4943	0.3825	0.3484	0.2396	-0.4811	-0.2311	-0.2347		0.0368	0.3218	10
OD _{slope_{max}}	0.9690	-0.8636	0.9393	0.9480	-0.8127	-0.8619	0.8441	-0.8173	0.0368		0.7881	6

Table C-4 Correlation coefficients (r), average correlation coefficients (r_{avg}) and their ranking for MRSA.

MRSA	Slope _{max}	t _{onset}	OD _{12h}	OD _{max}	t _{ODmax}	tslope _{max}	ΔOD _{final}	t _{2x}	Δt _{max}	OD _{slope_{max}}	r _{avg}	Rank
Slope _{max}		0.4959	-0.0561	0.6867	-0.5233	0.5895	0.9293	0.4503	-0.7093	0.7650	0.5550	3
t _{onset}	0.4959		-0.4378	0.6457	-0.0291	0.9294	0.5288	0.0770	-0.6516	0.0247	0.4744	6
OD _{12h}	-0.0561	-0.4378		0.1874	-0.5194	-0.4036	-0.1502	0.1370	-0.1186	0.4721	0.2513	10
OD _{max}	0.6867	0.6457	0.1874		-0.3780	0.6301	0.7079	0.2060	-0.6933	0.5026	0.5169	5
t _{ODmax}	-0.5233	-0.0291	-0.5194	-0.3780		-0.1017	-0.5254	-0.4697	0.7772	-0.7106	0.4155	8
tslope _{max}	0.5895	0.9294	-0.4036	0.6301	-0.1017		0.5583	0.2721	-0.6622	0.2189	0.5183	4
ΔOD _{final}	0.9293	0.5288	-0.1502	0.7079	-0.5254	0.5583		0.4205	-0.7317	0.6304	0.5690	2
t _{2x}	0.4503	0.0770	0.1370	0.2060	-0.4697	0.2721	0.4205		-0.4049	0.6321	0.3047	9
Δt _{max}	-0.7093	-0.6516	-0.1186	-0.6933	0.7772	-0.6622	-0.7317	-0.4049		0.3079	0.5936	1
OD _{slope_{max}}	0.7650	0.0247	0.4721	0.5026	-0.7106	0.2189	0.6304	0.6321	0.3079		0.4738	7

Table C-5 Correlation coefficients (r), average correlation coefficients (r_{avg}) and their ranking for MSSA.

MSSA	Slope _{max}	t _{onset}	OD _{12h}	OD _{max}	t _{ODmax}	t _{slope_{max}}	ΔOD _{final}	t _{2x}	Δt _{max}	OD _{slope_{max}}	r _{avg}	Rank
Slope _{max}		0.1539	0.1003	0.7526	0.0018	0.2589	0.4121	0.3416	0.0414	0.6011	0.2578	10
t _{onset}	0.1539		-0.6261	0.2960	0.4110	0.6808	0.2912	0.1106	-0.1405	0.3034	0.3388	6
OD _{12h}	0.1003	-0.6261		-0.2301	-0.4109	-0.2650	-0.3527	0.3667	0.4204	0.3107	0.3465	5
OD _{max}	0.7526	0.2960	-0.2301		0.2126	0.4567	0.7364	0.4344	0.1064	0.4853	0.4031	2
t _{ODmax}	0.0018	0.4110	-0.4109	0.2126		0.5333	-0.0833	0.1801	0.4247	0.0829	0.2822	9
t _{slope_{max}}	0.2589	0.6808	-0.2650	0.4567	0.5333		0.3664	0.6851	0.5633	0.6515	0.4762	1
ΔOD _{final}	0.4121	0.2912	-0.3527	0.7364	-0.0833	0.3664		0.3114	-0.0403	0.1931	0.3242	7
t _{2x}	0.3416	0.1106	0.3667	0.4344	0.1801	0.6851	0.3114		0.7647	0.7780	0.3993	4
Δt _{max}	0.0414	-0.1405	0.4204	0.1064	0.4247	0.5633	-0.0403	0.7647		0.1913	0.3127	8
OD _{slope_{max}}	0.6011	0.3034	0.3107	0.4853	0.0829	0.6515	0.1931	0.7780	0.1913		0.3997	3

Table C-6 Averages of the absolute correlation coefficients, |r| of all five bacterial strains.

Average r	Slope _{max}	t _{onset}	OD _{12h}	OD _{max}	t _{ODmax}	t _{slope_{max}}	ΔOD _{final}	t _{2x}	Δt _{max}	OD _{slope_{max}}
Slope _{max}		0.5604	0.5583	0.8115	0.5712	0.6270	0.6484	0.6781	0.3745	0.8061
t _{onset}	0.5604		0.7575	0.6864	0.5222	0.9120	0.5417	0.4169	0.4131	0.4842
OD _{12h}	0.5583	0.7575		0.6546	0.6632	0.6926	0.4815	0.5304	0.4254	0.6700
OD _{max}	0.8115	0.6864	0.6546		0.5469	0.7257	0.6216	0.5522	0.4609	0.7119
t _{ODmax}	0.5712	0.5222	0.6632	0.5469		0.5675	0.5691	0.4785	0.4481	0.6070
t _{slope_{max}}	0.6270	0.9120	0.6926	0.7257	0.5675		0.5800	0.6081	0.5079	0.6006
ΔOD _{final}	0.6484	0.5417	0.4815	0.6216	0.5691	0.5800		0.4665	0.2981	0.5186
t _{2x}	0.6781	0.4169	0.5304	0.5522	0.4785	0.6081	0.4665		0.4004	0.6414
Δt _{max}	0.3745	0.4131	0.4254	0.4609	0.4481	0.5079	0.2981	0.4004		0.2140
OD _{slope_{max}}	0.8061	0.4842	0.6700	0.7119	0.6070	0.6006	0.5186	0.6414	0.2140	

Finally, \bar{r}_{avg} , the global average correlation coefficient over all bacterial strains was calculated for each parameter using Equation (C-6):

$$\bar{r}_{avg} = \frac{\sum_{k=1}^o |r_{avg,k}|}{o} \quad (C-6)$$

with k being the bacterial strain number, and o the total number of bacterial strains. The data is displayed in Table C-7, which is sorted in ascending order of the parameters' global average correlation coefficient, \bar{r}_{avg} ; ultimately selected parameters are marked light green.

Table C-7 Average and global average correlation coefficients (\bar{r}_{avg}) of all parameters

Parameter	r_{avg}					\bar{r}_{avg}	
	E. coli	S. marcescens	K. pneumoniae	MRSA	MSSA	Avg.	S.E.M.
Δt_{max}	0.3501	0.5020	0.3218	0.5936	0.3127	0.4160	0.0560
t_{2x}	0.4408	0.6757	0.7613	0.3047	0.3993	0.5164	0.0865
ΔOD_{final}	0.3605	0.6629	0.7127	0.5690	0.3242	0.5259	0.0786
t_{ODmax}	0.6671	0.6376	0.7269	0.4155	0.2822	0.5458	0.0844
$OD_{Slopemax}$	0.6108	0.6463	0.7881	0.4738	0.3997	0.5837	0.0680
OD_{12h}	0.7122	0.8270	0.8404	0.2513	0.3465	0.5955	0.1240
t_{onset}	0.5495	0.8263	0.8174	0.4744	0.3388	0.6013	0.0962
$Slope_{max}$	0.6124	0.7816	0.8115	0.5550	0.2578	0.6037	0.0992
OD_{max}	0.6090	0.8000	0.8333	0.5169	0.4031	0.6325	0.0821
$t_{Slopemax}$	0.6112	0.8356	0.8216	0.5183	0.4762	0.6526	0.0751

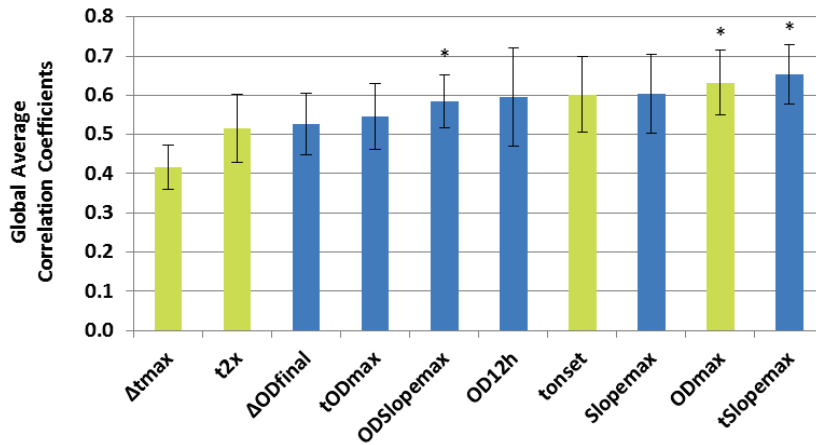


Figure C-1 Global Average Correlation Coefficients

Global Average Correlation Coefficients were calculated for each parameter using Equations (C-1) - (C-6); parameters were ranked from lowest to highest coefficient (see Table C-7). Parameters chosen for display (green bars) were selected based on this ranking and mechanistic considerations (see text for details). Error bars: \pm S.E.M. *: $P < 0.05$; ($n = 5$; one-tailed Student's t-test).

The Global Average Correlation Coefficients were calculated to determine which parameters show the lowest correlation. Selecting parameters with low correlation would supposedly allow the identification and differentiation of factors and assay conditions that affect bacterial growth through distinct mechanisms. As can be seen in Figure C-1, only the first parameter, Δt_{max} , is different from most of the other parameters; all the other ones have

overlapping error bars and are not significantly different from each other. It was therefore decided to additionally base the selection of parameters on mechanistic considerations.

t_{onset} was chosen over t_{Slopemax} and OD_{12h} (all three are highly or very highly correlated) as a parameter that is influenced by the initial number of bacteria, as well as bacterial processes that occur during the lag time. t_{ODmax} was not included, since it can be derived from t_{onset} and Δt_{max} ; furthermore, OD_{max} is included as parameter related to factors that prevent growth or accelerate bacterial death. Although ΔOD_{final} shows one of the lowest global average correlation coefficients, it was excluded since for this project factors that accelerate death after the stationary phase were not of high priority.

C.2. Results

Tables containing the results used to produce the graphs shown in the main part (see Chapter II, Section 2.8.4.3) are presented here (Table C-8 - Table C-12). For each bacterial strain, the table stretches over four pages to include all the data. The tables combine the results of two microplates each, one without cholesterol, and the second one with cholesterol. They first give the conditions (pH, presence of A β /Cu²⁺/Zn²⁺/cholesterol), and then the results for each of the ten parameters mentioned above; the value and standard error, followed by the difference of the samples without and with A β , with H₂O and with Cu²⁺ or Zn²⁺, respectively, and without and with cholesterol. The error for each of those differences was calculated according to the general equation for error propagation (Equation (C-8); given for the example of Slope_{max}):

$$\Delta\text{Slope}_{\text{max}} = \text{Slope}_{\text{max},1} - \text{Slope}_{\text{max},2} \quad (\text{C-7})$$

$$\pm\text{Error} (\Delta\text{Slope}_{\text{max}}) = \sqrt{\left(\text{S. E. M.} (\text{Slope}_{\text{max},1})\right)^2 + \left(\text{S. E. M.} (\text{Slope}_{\text{max},2})\right)^2} \quad (\text{C-8})$$

C.2.1. Incubation of *E. coli*

Table C-8 Incubation of *E. coli* with 10 μM AB₁₋₄₀ in presence of Cu²⁺, Zn²⁺ and cholesterol.

pH	AB	Cu	Zn	Chol.	Slope _{max}			Δ Slope _{max}			OD _{lagphase}			t _{onset}			Δ t _{onset}								
					(a.u./min *100)	S.E.M.	w/o-w/ AB	H ₂ O-Cu ²⁺ /Zn ²⁺	±Error	w/o-w/ Chol.	±Error	(a.u.)	S.E.M.	w/o-w/ AB	H ₂ O-Cu ²⁺ /Zn ²⁺	±Error	w/o-w/ Chol.	±Error	(min)	S.E.M.	w/o-w/ AB	H ₂ O-Cu ²⁺ /Zn ²⁺	±Error	w/o-w/ Chol.	±Error
7.3					0.421	0.0037					0.2482	0.0027				418	28								
7.3	x				0.368	0.0077	0.053	0.0085			0.2413	0.0025	0.069	0.0037		420	27	-2	38.8						
7.3	x	x			0.379	0.0132	0.042	0.0137			0.2606	0.0073	-0.0124	0.0078		383	4			35	28.4				
7.3	x	x	x		0.287	0.0013	0.092	0.0133	0.082	0.0078	0.2285	0.0063	0.0321	0.0097	0.0128	0.0068	379	8	5	9.2	41	28.0			
7.3	x	x	x	x	0.262	0.0050	0.159	0.0062	0.159	0.0062	0.1829	0.0019	0.0652	0.0033		408	2	11	28.1	11	28.1				
7.3	x	x	x	x	0.225	0.0053	0.036	0.0073	0.143	0.0093	0.1720	0.0018	0.0109	0.0026	0.0693	0.0031	453	37	-45	37.1	-33	45.8			
7.3	x	x	x	x	0.370	0.0014					0.2514	0.0028					330	1					88	28.1	
7.3	x	x	x	x	0.335	0.0088	0.035	0.0089			0.033	0.0117	0.2371	0.0009	0.0143	0.0029	333	3	-2	3.4			87	26.9	
7.3	x	x	x	x	0.347	0.0151	0.023	0.0152	0.033	0.0201	0.2650	0.0004			-0.0136	0.0028	323	1			7	1.6	60	4.6	
7.3	x	x	x	x	0.281	0.0053	0.065	0.0160	0.054	0.0103	0.1832	0.0076	0.0818	0.0076	0.0539	0.0077	317	3	7	3.0	16	4.2	62	8.6	
7.3	x	x	x	x	0.267	0.0078	0.102	0.0079	-0.006	0.0092	0.1871	0.0006	0.0643	0.0029	-0.0041	0.0020	358	2			-28	2.0	49	2.4	
7.3	x	x	x	x	0.226	0.0033	0.041	0.0085	0.109	0.0094	0.1631	0.0133	0.0240	0.0134	0.0740	0.0134	452	3	0	3.6	-25	4.5	95	37.2	
7.0					0.389	0.0085					0.2542	0.0058					402	28							
7.0	x				0.341	0.0132	0.049	0.0157			0.2406	0.0036	0.0136	0.0068			369	4	33	28.3					
7.0	x	x			0.363	0.0017	0.026	0.0086			0.2579	0.0075			-0.0037	0.0095	374	4			28	28.3			
7.0	x	x	x		0.291	0.0081	0.072	0.0082	0.050	0.0155	0.2065	0.0174	0.0514	0.0190	0.0340	0.0178	370	8	4	9.2	-1	9.3			
7.0	x	x	x	x	0.255	0.0030	0.135	0.0090	0.135	0.0090	0.1845	0.0021	0.0697	0.0062			503	13			-101	30.9			
7.0	x	x	x	x	0.218	0.0135	0.037	0.0138	0.123	0.0189	0.1653	0.0088	0.0192	0.0090	0.0752	0.0095	469	24	34	27.4	-100	24.4			
7.0	x	x	x	x	0.361	0.0083	0.029	0.0118	0.029	0.0118	0.2238	0.0073					326	1					76	28.0	
7.0	x	x	x	x	0.341	0.0113	0.020	0.0140	0.000	0.0173	0.2271	0.0129	-0.0034	0.0148			322	3	4	2.9			47	4.8	
7.0	x	x	x	x	0.350	0.0052	0.011	0.0098	0.014	0.0055	0.2524	0.0027			-0.0286	0.0077	320	2			7	2.6	54	4.4	
7.0	x	x	x	x	0.277	0.0091	0.064	0.0145	0.013	0.0122	0.2011	0.0162	0.0513	0.0164	0.0260	0.0207	309	2	10	3.4	13	3.6	61	8.8	
7.0	x	x	x	x	0.259	0.0072	0.102	0.0110	-0.005	0.0078	0.1829	0.0039	0.0409	0.0083	0.0016	0.0045	384	3			-58	3.0	119	13.4	
7.0	x	x	x	x	0.226	0.0035	0.033	0.0080	0.115	0.0118	0.1713	0.0032	0.0117	0.0050	0.0559	0.0132	381	5	3	5.8	-59	5.8	88	24.6	
6.5					0.390	0.0053					0.2494	0.0052					382	6							
6.5	x				0.311	0.0069	0.079	0.0087			0.2125	0.0118	0.0370	0.0129			371	6	11	8.6					
6.5	x	x			0.290	0.0033	0.100	0.0063	0.100	0.0063	0.2397	0.0020			0.0097	0.0056	388	2			-6	6.1			
6.5	x	x	x		0.230	0.0028	0.060	0.0044	0.081	0.0074	0.1895	0.0096	0.0503	0.0098	0.0230	0.0153	408	26	-20	26.2	-37	26.9			
6.5	x	x	x	x	0.209	0.0080	0.181	0.0096	0.181	0.0096	0.1679	0.0049	0.0815	0.0071			511	8			-129	9.6			
6.5	x	x	x	x	0.189	0.0023	0.021	0.0083	0.123	0.0073	0.1503	0.0027	0.0176	0.0056	0.0622	0.0121	532	16	-21	17.4	-161	16.9			
6.5	x	x	x	x	0.345	0.0084	0.045	0.0099	0.045	0.0099	0.2316	0.0133					323	2					59	6.1	
6.5	x	x	x	x	0.305	0.0209	0.039	0.0225	0.006	0.0220	0.2127	0.0160	0.0189	0.0208			321	5	2	5.1			50	7.9	
6.5	x	x	x	x	0.273	0.0047	0.072	0.0096	0.018	0.0057	0.2199	0.0114	0.0117	0.0175	0.0199	0.0115	339	0			-16	1.8	49	1.6	
6.5	x	x	x	x	0.249	0.0032	0.024	0.0057	0.0211	-0.019	0.0043	0.2133	0.0077	0.0066	0.0138	-0.0006	356	3	3	2.8	-16	5.5	72	26.3	
6.5	x	x	x	x	0.215	0.0021	0.030	0.0086	-0.005	0.0083	0.1625	0.0024	0.0691	0.0135	0.0691	0.0135	429	2			-107	2.4	82	7.8	
6.5	x	x	x	x	0.204	0.0039	0.011	0.0044	0.101	0.0213	0.1581	0.0070	0.0044	0.0074	0.0546	0.0174	431	3	-2	3.1	-110	5.4	101	15.9	

Table C-8 (cont'd) Incubation of *E. coli* with 10 μM AB_{1-40} in presence of Cu^{2+} , Zn^{2+} and cholesterol.

Conditions			t_{5x}			Δt_{5x}			OD_{max}			$\Delta \text{OD}_{\text{max}}$			Δt_{max}			$\Delta \Delta t_{\text{max}}$							
pH	AB	Cu Zn Chol.	(min)	s.E.M.	w/o-w/ w/AB	$\text{H}_2\text{O}-\text{w}/\text{Cu}^{2+}/\text{Zn}^{2+}$	w/o-w/ Chol.	(min)	s.E.M.	(a.u.)	w/o-w/ AB	$\text{H}_2\text{O}-\text{w}/\text{Cu}^{2+}/\text{Zn}^{2+}$	w/o-w/ Chol.	(min)	s.E.M.	w/o-w/ w/AB	$\text{H}_2\text{O}-\text{w}/\text{Cu}^{2+}/\text{Zn}^{2+}$	w/o-w/ Chol.	(min)	s.E.M.	w/o-w/ w/AB	$\text{H}_2\text{O}-\text{w}/\text{Cu}^{2+}/\text{Zn}^{2+}$	w/o-w/ Chol.		
7.3			27.85	0.22						0.7047±0.0064				423	29										
7.3	x		32.04	0.61	-4.19	0.65				0.7255±0.0091	-0.0208±0.0111			458	38	-35	47								
7.3	x	x	35.09	0.66		0.70				0.7240±0.0033		-0.0193±0.0072		462	18			-39	34						
7.3	x	x	36.25	0.44	-1.17	0.79				0.6725±0.0077	0.0514±0.0084	0.0530±0.0119		588	19	-126	26	-130	42						
7.3	x	x	36.98	0.40		0.46				0.5948±0.0072		0.1099±0.0096		532	20			-109	35						
7.3	x	x	37.94	0.45	-0.96	0.61				0.5598±0.0017	0.0350±0.0074	0.1657±0.0092		612	30	-80	36	-154	48						
7.3	x	x	32.11	0.04		0.22				0.7316±0.0074			-0.0269±0.0098	538	15								-115	33	
7.3	x	x	33.77	0.50	-1.66	0.50				0.7117±0.0021	0.0199±0.0077			520	10	17	18						-62	39	
7.3	x	x	37.34	1.20		1.37				0.7324±0.0012				503	43			35	45				-42	46	
7.3	x	x	34.35	0.74	2.99	1.41				0.6879±0.0085	0.0445±0.0086	0.0238±0.0088	-0.0154±0.0115	595	3	-92	43	-75	11				-7	19	
7.3	x	x	37.10	0.65		0.65				0.6048±0.0113		0.1268±0.0135	-0.0100±0.0133	502	11			36	19				31	23	
7.3	x	x	37.99	0.93	-0.89	1.14				0.5766±0.0027	0.0282±0.0116	0.1351±0.0034	-0.0168±0.0032	627	8	-125	14	-106	13				-15	30	
7.0			32.44	0.55						0.7351±0.0291				528	13										
7.0	x		33.36	1.12	-0.91	1.25				0.7286±0.0075	0.0065±0.0300			522	15	5	20								
7.0	x	x	34.63	0.26		0.61				0.6912±0.0163		0.0439±0.0334		424	11			103	17						
7.0	x	x	35.52	1.11	-0.89	1.14				0.6835±0.0139	0.0077±0.0215	0.0451±0.0158		570	19	-145	22	-47	24						
7.0	x	x	38.48	0.35		0.65				0.6101±0.0079		0.1250±0.0302		437	14			91	19						
7.0	x	x	38.65	0.77	-0.17	0.85				0.5758±0.0221	0.0344±0.0235	0.1528±0.0233		604	34	-167	36	-82	37						
7.0	x	x	27.77	0.37		0.66				0.6895±0.0040			0.0456±0.0294	495	18									32	22
7.0	x	x	32.00	0.73	-4.23	0.82				0.6993±0.0037	-0.0099±0.0055			506	14	-11	23						16	20	
7.0	x	x	33.80	0.21		0.33				0.7174±0.0038				432	6			63	19				-8	13	
7.0	x	x	35.50	0.95	0.30	0.97				0.7019±0.0047	0.0155±0.0061	-0.0026±0.0060	-0.0184±0.0147	566	8	-134	10	-59	16				4	21	
7.0	x	x	37.47	0.29		0.46				0.6166±0.0112		0.0729±0.0119	-0.0065±0.0137	454	8			41	20				-17	16	
7.0	x	x	38.49	0.33	-1.02	0.44				0.5895±0.0009	0.0271±0.0112	0.1098±0.0038	-0.0138±0.0221	572	9	-118	12	-66	17				32	35	
6.5			29.19	0.53		0.84				0.6650±0.0057				459	25										
6.5	x		32.76	0.09	-3.57	0.54				0.6724±0.0105	-0.0074±0.0119			512	18	-53	31								
6.5	x	x	41.18	0.64		0.83				0.6908±0.0100		-0.0258±0.0115		450	18			9	31						
6.5	x	x	41.18	1.52	0.00	1.65				0.6792±0.0053	0.0116±0.0113	-0.0068±0.0118		500	21	-50	27	12	27						
6.5	x	x	42.69	0.84		0.99				0.5967±0.0172		0.0683±0.0182		500	22			-41	33						
6.5	x	x	41.84	0.13	0.86	0.85				0.5608±0.0101	0.0359±0.0200	0.1116±0.0145		564	58	-64	62	-52	61						
6.5	x	x	33.25	0.37		0.65				0.6789±0.0012			-0.0138±0.0058	459	15								1	30	
6.5	x	x	34.47	0.51	-1.22	0.63				0.6930±0.0055	-0.0141±0.0056			509	10	-51	18						3	20	
6.5	x	x	41.18	1.00		1.19				0.7115±0.0026		-0.0326±0.0028	-0.0207±0.0103	464	11			-5	19				-14	21	
6.5	x	x	42.66	0.84	-1.48	1.30				0.7015±0.0052	0.0100±0.0058	-0.0085±0.0076	-0.0223±0.0074	510	10	-46	15	-1	14				-10	23	
6.5	x	x	42.34	0.90		1.23				0.6059±0.0067		0.0730±0.0068	-0.0092±0.0185	501	4			-42	16				0	22	
6.5	x	x	41.56	0.71	0.78	1.14				0.6043±0.0064	0.0015±0.0093	0.0886±0.0084	-0.0435±0.0119	577	19	-77	19	-68	21				-13	61	

Table C-8 (cont'd) Incubation of *E. coli* with 10 μM $\text{A}\beta_{1-40}$ in presence of Cu^{2+} , Zn^{2+} and cholesterol.

Conditions			OD ₇₂₀			ΔOD_{720}			$t_{\text{Espr,max}}$			$\Delta t_{\text{Espr,max}}$			
pH	AB	Cu Zn Chol.	(a.u.)	S.E.M.	W/o-w/ AB	H ₂ O-Cu ²⁺ /Zn ²⁺	W/o-w/ Chol.	(min)	S.E.M.	W/o-w/ AB	H ₂ O-Cu ²⁺ /Zn ²⁺	W/o-w/ Chol.	W/o-w/ AB	H ₂ O-Cu ²⁺ /Zn ²⁺	W/o-w/ Chol.
					±Error	±Error	±Error			±Error	±Error	±Error	±Error	±Error	±Error
7.3			0.6617	0.0066				452	1.7						
7.3	x		0.6562	0.0041	0.0055	0.0078		458	1.7	-6.7	2.4				
7.3		x	0.6688	0.0047		-0.0071	0.0081	453	3.3					-1.7	3.7
7.3	x	x	0.5758	0.0090	0.0931	0.0101	0.0805	455	10.4	-1.7	10.9	3.3	10.5		
7.3		x	0.5183	0.0113		0.1435	0.0131	478	1.7					-26.7	2.4
7.3	x	x	0.4413	0.0069	0.0770	0.0132	0.2150	493	4.4	-15.0	4.7			-35.0	4.7
7.3		x	0.6860	0.0086				398	1.7						53.3
7.3	x	x	0.6659	0.0065	0.0201	0.0108		403	3.3	-5.0	3.7			55.0	3.7
7.3		x	0.6914	0.0120				400	2.9					-1.7	3.3
7.3	x	x	0.6152	0.0086	0.0762	0.0148	0.0507	382	1.7	18.3	3.3	21.7	3.7	73.3	10.5
7.3		x	0.5614	0.0160		0.1246	0.0182	428	3.3					-30.0	3.7
7.3	x	x	0.4917	0.0060	0.0697	0.0171	0.1742	430	7.6	-1.7	8.3			-26.7	8.3
7.0			0.6356	0.0377				467	26.8						
7.0	x		0.6529	0.0068	-0.0173	0.0383		440	2.9	26.7	27.0				
7.0		x	0.6551	0.0135		-0.0195	0.0401	443	3.3					23.3	27.0
7.0	x	x	0.5874	0.0112	0.0677	0.0176	0.0655	430	5.8	13.3	6.7	10.0	6.5		
7.0		x	0.5141	0.0058		0.1215	0.0382	503	3.3					-36.7	27.0
7.0	x	x	0.4289	0.0249	0.0852	0.0256	0.2240	512	9.3	-8.3	9.9			-71.7	9.7
7.0		x	0.6561	0.0066				388	1.7						78.3
7.0	x	x	0.6581	0.0080	-0.0020	0.0103		388	3.3	0.0	3.7			51.7	4.4
7.0		x	0.6978	0.0034		-0.0417	0.0074	392	1.7					-3.3	2.4
7.0	x	x	0.6324	0.0085	0.0654	0.0092	0.0256	382	1.7	10.0	2.4	6.7	3.7	48.3	6.0
7.0		x	0.5668	0.0085		0.0893	0.0107	455	2.9					-66.7	3.3
7.0	x	x	0.5040	0.0035	0.0628	0.0092	0.1541	457	3.3	-1.7	4.4			-68.3	4.7
6.5			0.6229	0.0058				445	2.9						
6.5	x		0.5918	0.0043	0.0311	0.0073		435	5.0	10.0	5.8				
6.5		x	0.6268	0.0040		-0.0039	0.0071	470	0.0					-25.0	2.9
6.5	x	x	0.5660	0.0061	0.0608	0.0073	0.0259	463	6.0	6.7	6.0			-28.3	7.8
6.5		x	0.3822	0.0220		0.2407	0.0228	592	8.8					-146.7	9.3
6.5	x	x	0.3175	0.0061	0.0647	0.0228	0.2743	597	6.0	-5.0	10.7			-161.7	7.8
6.5		x	0.6508	0.0019				390	2.9						55.0
6.5	x	x	0.6451	0.0048	0.0057	0.0051		390	5.0	0.0	5.8			45.0	7.1
6.5		x	0.6646	0.0043		-0.0138	0.0047	420	2.9					-30.0	4.1
6.5	x	x	0.6334	0.0085	0.0312	0.0096	0.0117	432	6.0	-1.7	6.7			-31.7	7.8
6.5		x	0.4888	0.0098		0.1620	0.0100	505	2.9					-115.0	4.1
6.5	x	x	0.4550	0.0059	0.0338	0.0115	0.1901	508	4.4	-3.3	5.3			-118.3	6.7
															88.3
															7.5

Table C-8 (cont'd) Incubation of *E. coli* with 10 μM $\text{A}\beta_{1-40}$ in presence of Cu^{2+} , Zn^{2+} and cholesterol.

Conditions			t_{ADPmax}				Δt_{ADPmax}				ΔADPmax			
pH	AB	Cu:Zn:Chol.	(min)	s.E.M.	w/o-w/	H ₂ O-	w/o-w/	H ₂ O-	w/o-w/	H ₂ O-	s.E.M.	w/o-w/	H ₂ O-	w/o-w/
					AB	Cu ²⁺ /Zn ²⁺	AB	Cu ²⁺ /Zn ²⁺	AB	Cu ²⁺ /Zn ²⁺	(a.u.)	AB	Cu ²⁺ /Zn ²⁺	Chol.
					±Error	±Error	±Error	±Error	±Error	±Error		±Error	±Error	±Error
7.3			842	2							0.0565	0.0137		
7.3	x		878	14	-37	13.7					0.0477	0.0085	0.0087	0.0161
7.3	x	x	845	22			-3	21.9			0.0859	0.0152		-0.0294
7.3	x	x	967	24	-122	32.1	-88	27.2			0.0728	0.0127	0.0131	0.0199
7.3	x	x	940	22			-98	21.9			0.0933	0.0133		-0.0369
7.3	x	x	1065	18	-125	28.3	-187	22.6			0.0613	0.0116	0.0321	0.0177
7.3		x	868	16					-27	16.0	0.0643	0.0083		-0.0078
7.3	x	x	853	12	15	19.7			25	18.0	0.0688	0.0121	-0.0045	0.0147
7.3	x	x	827	42			42	45.0	18	47.4	0.0974	0.0158	-0.0331	0.0179
7.3	x	x	912	2	-85	42.1	-58	11.8	55	23.6	0.0893	0.0135	0.0081	0.0208
7.3	x	x	860	13			8	20.3	80	25.2	0.0972	0.0129	-0.0205	0.0181
7.3	x	x	985	10	-125	16.3	-132	15.6	80	20.8	0.0654	0.0106	0.0318	0.0167
7.0			930	15							0.0615	0.0056		
7.0	x		892	11	38	18.8					0.0682	0.0044	-0.0067	0.0071
7.0	x	x	798	12			132	19.4			0.1152	0.0057	-0.0537	0.0080
7.0	x	x	940	12	-142	16.7	-48	15.9			0.0891	0.0112	0.0261	0.0126
7.0	x	x	940	13			-10	19.8			0.0994	0.0074	-0.0379	0.0093
7.0	x	x	1073	13	-133	18.1	-182	17.0			0.0597	0.0113	0.0398	0.0135
7.0		x	822	18					108	23.3	0.0996	0.0035		-0.0381
7.0	x	x	828	13	-7	22.1			63	17.2	0.0959	0.0055	0.0037	0.0066
7.0	x	x	752	6			70	18.6	47	13.4	0.1224	0.0055	-0.0228	0.0079
7.0	x	x	875	10	-123	12.0	-47	16.9	65	15.5	0.1141	0.0104	0.0082	0.0117
7.0	x	x	838	7			-17	19.1	102	14.5	0.1075	0.0046	-0.0079	0.0058
7.0	x	x	953	11	-115	13.1	-125	17.2	120	17.0	0.0701	0.0074	0.0374	0.0087
6.5			842	29							0.0490	0.0057		-0.0105
6.5	x		883	22	-42	36.4					0.0520	0.0122	-0.0030	0.0135
6.5	x	x	838	17			3	33.4			0.0543	0.0050	-0.0053	0.0076
6.5	x	x	908	7	-70	18.2	-25	23.2			0.0473	0.0038	0.0070	0.0063
6.5	x	x	1012	27			-170	39.3			0.0534	0.0075	-0.0044	0.0094
6.5	x	x	1097	47	-85	54.1	-213	51.9			0.0273	0.0063	0.0261	0.0098
6.5		x	782	17					60	33.5	0.0739	0.0077		-0.0249
6.5	x	x	830	5	-48	17.6			53	22.6	0.0746	0.0075	-0.0007	0.0108
6.5	x	x	803	12			-22	20.5	35	20.3	0.0587	0.0043	0.0152	0.0089
6.5	x	x	847	12	-43	16.5	-17	12.7	62	13.7	0.0573	0.0050	0.0013	0.0066
6.5	x	x	930	5			-148	17.6	82	27.1	0.0547	0.0043	0.0175	0.0091
6.5	x	x	1008	19	-78	19.9	-178	19.9	88	50.8	0.0337	0.0029	0.0210	0.0052

C.2.2. Incubation of *S. marcescens*

Table C-9 Incubation of *S. marcescens* with 10 μM $\text{A}\beta_{1-40}$ in presence of Cu^{2+} , Zn^{2+} and cholesterol.

pH	Conditions AB: Cu: Zn: Chol.	Slope _{max}			Δ Slope _{max}			OD _{595max}			OD _{595max}			t _{onset}			Δ t _{onset}				
		(a.u./min *100)	w/o- w/AB	H ₂ O- Cu ²⁺ /Zn ²⁺	w/o-w/ Chol.	(a.u.)	S.E.M.	w/o- w/AB	H ₂ O- Cu ²⁺ /Zn ²⁺	w/o-w/ Chol.	(min)	S.E.M.	w/o- w/AB	H ₂ O- Cu ²⁺ /Zn ²⁺	w/o-w/ Chol.	(min)	S.E.M.	w/o- w/AB	H ₂ O- Cu ²⁺ /Zn ²⁺	w/o-w/ Chol.	
7.3		0.416	-0.0143			0.2605	-0.0201			0.0168	-0.0206			239	4						
7.3	x	0.347	-0.0082	0.070	0.0146	0.2477	-0.0211	0.0128	-0.0292					244	7	-6	7.9				
7.3	x	0.420	-0.0088			0.3455	-0.0118			-0.0850	-0.0233			238	1	1	4.0				
7.3	x	0.313	-0.0043	0.107	-0.0098	0.2422	-0.0029	0.1032	-0.0122	0.0055	-0.0213			237	0	1	1.4	7	7.0		
7.3	x	0.199	-0.0015			0.1892	-0.0075			0.0713	-0.0215			600	21			-361	21.3		
7.3	x	0.195	-0.0066	0.004	0.0068	0.1840	-0.0178	0.0052	-0.0194	0.0637	-0.0277			511	59	89	62.6	-267	59.4		
7.3	x	0.465	-0.0073			0.2437	-0.0043							281	1					-42	4.0
7.3 ^{a)}	x	0.355	-0.0127	0.110	0.0146	0.0131	-0.2643	-0.0118	-0.0206	0.0125				281	1	0	1.7			-37	7.0
7.3	x	0.434	-0.0080			0.031	-0.0108							272	6			9	6.2	-34	6.2
7.3 ^{b)}	x																				
7.3	x	0.208	-0.0049			0.0051	-0.2048	-0.0128						578	36			-298	36.5	21	42.0
7.3	x	0.204	-0.0019	0.005	-0.0052	0.0069	-0.1829	-0.0160	0.0219	-0.0205				502	28	77	45.7	-221	27.5	9	65.1
7.0		0.420	-0.0086			0.3107	-0.0291							244	4						
7.0	x	0.343	-0.0059	0.077	0.0105	0.2476	-0.0046	0.0631	-0.0295					243	2	2	4.3				
7.0	x	0.389	-0.0065			0.2538	-0.0031			0.0569	-0.0293			231	3			13	4.8		
7.0	x	0.344	-0.0196	0.045	-0.0207	0.2846	-0.0247	-0.0408	-0.0249	-0.0469	-0.0251			248	2	-17	3.4	-6	2.6		
7.0	x	0.198	-0.0050			0.2066	-0.0094			0.1041	-0.0306			667	16			-422	16.8		
7.0	x	0.210	-0.0117	-0.013	-0.0127	0.2060	-0.0155	0.0005	-0.0181	0.0416	-0.0162			664	2	3	16.5	-421	2.7		
7.0	x	0.458	-0.0067			0.0109	-0.3151	-0.0237						269	6			-0.0044	-0.0375	-25	7.4
7.0	x	0.324	-0.0214	0.134	0.0224	0.019	-0.2585	-0.0232	0.0566	-0.0331				271	4	-2	7.2			-29	4.0
7.0	x	0.386	-0.0115			0.072	-0.0133	0.003	0.0132	-0.3073	-0.0113			254	4			16	7.6	-22	5.2
7.0 ^{a)}	x	0.296	-0.0023	0.090	0.0117	0.048	-0.0198	-0.2783	-0.0730	0.0290	-0.0738			270	4	-16	5.9	2	5.4	-22	4.4
7.0	x	0.223	-0.0065			0.234	-0.0094	-0.026	0.0082	-0.2241	-0.0077			653	35			-384	35.9	14	38.9
7.0	x	0.227	-0.0015	-0.004	-0.0067	0.097	-0.0214	-0.017	-0.0118	-0.2143	-0.0172	0.0097	-0.0188	474	9	179	36.4	-203	9.6	190	9.1
6.5		0.385	-0.0216			0.2830	-0.0032							274	4						
6.5	x	0.314	-0.0093	0.071	0.0235	0.2775	-0.0246	0.0055	-0.0248					247	3	28	4.7				
6.5	x	0.337	-0.0042			0.3509	-0.0096			-0.0479	-0.0102			248	4			26	5.1		
6.5	x	0.311	-0.0115	0.026	0.0123	0.2918	-0.0426	0.0391	-0.0437	-0.0143	-0.0492			248	2	0	4.0	-1	3.4		
6.5	x	0.219	-0.0088			0.2633	-0.0566			0.0197	-0.0567			444	4			-169	5.1		
6.5	x	0.200	-0.0042	0.019	-0.0097	0.2001	-0.0066	0.0631	-0.0570	0.0774	-0.0254			490	6	-46	6.7	-243	6.3		
6.5	x	0.422	-0.0159			0.0268	-0.3048	-0.0103						286	4			-0.0218	-0.0108	-11	5.6
6.5	x	0.329	-0.0042	0.092	0.0164	0.0102	-0.2842	-0.0271	0.0207	-0.0290				287	3	-1	5.1			-40	4.0
6.5	x	0.332	-0.0170			0.0175	-0.2916	-0.0436						281	16			0.0133	-0.0448	4	16.2
6.5	x	0.318	-0.0050	0.014	0.0177	0.0126	-0.2359	-0.0358	0.0556	-0.0564	0.0483	-0.0449	0.0559	279	4	2	16.2	8	5.2	-31	4.8
6.5	x	0.233	-0.0025			0.189	-0.0161	-0.014	0.0092	-0.2229	-0.0084			486	10			0.0819	-0.0133	-200	11.3
6.5	x	0.231	-0.0045	0.002	-0.0051	0.098	-0.0061	-0.031	-0.0061	-0.2104	-0.0182	0.0125	-0.0201	511	7	-25	12.7	-0.0738	-0.0327	-224	7.7

a) data from two curves; one curve too noisy for data analysis

b) no data; all curves too noisy for data analysis

Table C-9 (cont'd) Incubation of *S. marcescens* with 10 μM AB_{1-40} in presence of Cu^{2+} , Zn^{2+} and cholesterol.

Conditions		t_{5x}			Δt_{5x}			OD _{max}			ΔOD_{max}			Δt_{max}			$\Delta \Delta t_{max}$						
pH	AB:Cu:Zn:Chol.	(min)	S.E.M.	w/o-w/ w/AB	H ₂ O- Cu ²⁺ /Zn ²⁺	±Error	w/o-w/ Chol.	(a.u)	S.E.M.	w/o-w/ w/AB	±Error	H ₂ O- Cu ²⁺ /Zn ²⁺	±Error	(min)	S.E.M.	w/o-w/ w/AB	±Error	H ₂ O- Cu ²⁺ /Zn ²⁺	±Error	w/o-w/ Chol.	±Error		
7.3		26.11	3.03					0.8170	0.0112					790	5								
7.3	x	34.96	2.59	-8.85	3.98			0.8555	0.0380	-0.0385	0.0397			804	40	-14	40						
7.3	x	37.88	0.55			-11.77	3.07	0.8169	0.0095		0.0002	0.0147		775	30			14	31				
7.3	x	35.85	0.06	2.03	0.55	-0.89	2.59	0.7711	0.0015	0.0458	0.0096	0.0844	0.0381	959	9	-184	32	-155	41				
7.3	x	51.01	1.13			-24.90	3.23	0.5564	0.0022		0.2807	0.0114		582	21			108	22				
7.3	x	51.32	1.76	-0.31	2.09	-16.36	3.13	0.5409	0.0201	-0.0045	0.0202	0.3146	0.0430	698	31	-16	38	107	51				
7.3	x	25.73	0.72			0.37	3.11	0.8649	0.0076					831	24					-41	24		
7.3 ^a	x	36.65	0.33	-10.92	0.80	-1.70	2.61	0.8690	0.0033	-0.0041	0.0083			922	8	-91	25			-118	41		
7.3	x	35.91	1.55			-10.18	1.71	0.8595	0.0120			0.0053	0.0142	865	31			-34	39	-89	43		
7.3 ^b	x																						
7.3	x	51.99	1.50			-26.26	1.67	0.5828	0.0144			0.2820	0.0163	713	29			118	37	-31	36		
7.3	x	51.58	1.92	0.41	2.44	-14.92	1.95	0.5771	0.0111	0.0057	0.0182	0.2918	0.0116	718	3	-5	29	204	9	-21	32		
7.0		33.42	4.20					0.8191	0.0115					675	40								
7.0	x	33.18	0.73	0.24	4.26			0.7953	0.0034	0.0239	0.0120			899	25	-224	47						
7.0	x	25.02	0.97			8.39	4.31	0.8259	0.0128			-0.0068	0.0172	857	21			-181	45				
7.0	x	45.02	3.16	-19.99	3.30	-11.84	3.24	0.8015	0.0086	0.0245	0.0154	-0.0062	0.0093	915	38	-58	43	-16	45				
7.0	x	55.55	2.46			-22.13	4.87	0.5544	0.0045			0.2648	0.0124	621	20			54	44				
7.0	x	54.20	2.54	1.35	3.54	-21.02	2.64	0.5463	0.0060	0.0081	0.0075	0.2490	0.0069	645	16	-23	26	254	29				
7.0	x	30.24	1.85			3.18	4.59	0.8788	0.0146					831	17					-155	43		
7.0	x	37.43	4.20	-7.19	4.59	-4.25	4.27	0.8828	0.0124	-0.0040	0.0192			932	19	-101	26			-33	31		
7.0	x	35.77	1.79			-5.54	2.57	0.8455	0.0225			0.0334	0.0268	858	32			-27	36	-1	38		
7.0 ^a	x	51.41	17.08	-15.63	17.17	-13.98	17.59	0.8187	0.0192	0.0268	0.0296	0.0642	0.0228	953	39	-95	50	-21	43	-38	54		
7.0	x	52.86	0.38			-22.62	1.89	0.6113	0.0154			0.2676	0.0212	635	19			195	26	-14	27		
7.0	x	51.82	1.47	1.03	1.52	-14.39	4.45	0.6453	0.0072	-0.0340	0.0170	0.2376	0.0143	753	7	-117	20	179	21	-108	18		
6.5		38.99	1.61					0.8093	0.0050					664	19								
6.5	x	44.14	4.88	-5.15	5.14			0.7906	0.0063	0.0187	0.0080			902	15	-238	24						
6.5	x	50.09	2.42			-11.10	2.91	0.8434	0.0061			-0.0342	0.0079	825	15			-161	24				
6.5	x	48.25	10.45	1.83	10.74	-4.12	11.54	0.8188	0.0007	0.0247	0.0062	-0.0282	0.0063	907	15	-82	21	-5	22				
6.5	x	72.92	15.56			-33.93	15.65	0.6325	0.0120			0.1768	0.0130	736	30			-73	35				
6.5	x	56.20	1.52	16.72	15.64	-12.07	5.11	0.5766	0.0107	0.0559	0.0161	0.2140	0.0124	795	43	-59	52	106	45				
6.5	x	33.55	3.12			5.43	3.51	0.8669	0.0105					809	36					-146	40		
6.5	x	43.59	5.68	-10.04	6.48	0.54	7.49	0.8580	0.0046	0.0089	0.0114			908	3	-99	36	-0.0674	0.0078	-7	15		
6.5	x	42.53	5.68			-8.98	6.48	0.8810	0.0101			-0.0141	0.0146	914	19			-104	41	-89	24		
6.5	x	35.10	5.38	7.43	7.82	8.49	7.82	0.8862	0.0009	-0.0051	0.0102	-0.0281	0.0047	944	25	-30	31	-36	25	-37	29		
6.5	x	53.36	1.46			-19.81	3.45	0.6837	0.0106			0.1832	0.0149	794	42			15	55	-58	51		
6.5	x	50.11	1.59	3.26	2.16	-6.51	5.90	0.6583	0.0061	0.0254	0.0122	0.1997	0.0077	784	49	10	65	124	49	11	65		

^a data from two curves; one curve too noisy for data analysis

^b no data; all curves too noisy for data analysis

Table C-9 (cont'd) Incubation of *S. marcescens* with 10 μM $\text{A}\beta_{1-40}$ in presence of Cu^{2+} , Zn^{2+} and cholesterol.

Conditions		OD _{12h}			ΔOD_{12h}			$t_{\text{Esop,max}}$			$\Delta t_{\text{Esop,max}}$						
pH	$\text{A}\beta$: Cu^{2+} : Zn^{2+} : Chol.	(a.u.)	S.E.M.	w/o- w/AB	\pm Error	$\text{H}_2\text{O}-$ $\text{Cu}^{2+}/\text{Zn}^{2+}$	\pm Error	w/o- w/Chol.	\pm Error	(min)	S.E.M.	w/o- w/AB	\pm Error	$\text{H}_2\text{O}-$ $\text{Cu}^{2+}/\text{Zn}^{2+}$	\pm Error	w/o- w/Chol.	\pm Error
7.3		0.7352	0.0136							302	4.4						
7.3	x	0.7377	0.0275	-0.0025	0.0307					315	0.0	-13.3	4.4				
7.3	x	0.7540	0.0145		-0.0188	0.0199				320	0.0			-18.3	4.4		
7.3	x	0.6556	0.0045	0.0984	0.0152	0.0279				315	0.0	5.0	0.0	0.0	0.0		
7.3	x	0.2334	0.0373		0.5019	0.0397				695	17.6			-993.3	18.1		
7.3	x	0.3410	0.0749	-0.1077	0.0837	0.0798				605	53.9	90.0	56.7	-290.0	53.9		
7.3	x	0.7596	0.0091				-0.0244	0.0163		333	1.7					-31.7	4.7
7.3 ^{a)}	x	0.7395	0.0038	0.0202	0.0099		-0.0018	0.0278		355	0.0	-21.7	1.7			-40.0	0.0
7.3	x	0.7685	0.0016				-0.0089	0.0092		352	8.3			-18.3	8.5	-31.7	8.3
7.3 ^{b)}	x																
7.3	x	0.2849	0.0720		0.4748	0.0726	-0.0515	0.0811		677	33.5					18.3	37.8
7.3	x	0.3830	0.0360	-0.0982	0.0805	0.3564	-0.0420	0.0831		592	25.2	85.0	41.9	-343.3	33.5	13.3	59.5
7.0		0.7533	0.0012							318	10.1						
7.0	x	0.6785	0.0077	0.0748	0.0078					315	0.0	3.3	10.1				
7.0	x	0.7416	0.0047		0.0117	0.0049				297	3.3			21.7	10.7		
7.0	x	0.6765	0.0063	0.0651	0.0079	0.0020	0.0099			332	3.3	-35.0	4.7	-16.7	3.3		
7.0	x	0.1146	0.0210		0.6388	0.0210				772	11.7			-453.3	15.5		
7.0	x	0.1230	0.0051	-0.0084	0.0216	0.5556	0.0092			762	7.3	10.0	13.7	-446.7	7.3		
7.0	x	0.7771	0.0091							338	10.1					-20.0	14.3
7.0	x	0.7400	0.0079	0.0371	0.0120		-0.0238	0.0091		352	6.0	-13.3	11.8			-96.7	6.0
7.0	x	0.7597	0.0126		0.0174	0.0155	-0.0181	0.0135		333	1.7			5.0	10.3	-36.7	3.7
7.0 ^{a)}	x	0.6715	0.0052	0.0883	0.0137	0.0686	0.0095	0.0051	0.0082	362	27.5	-29.2	27.6	-10.8	28.1	30.8	27.7
7.0	x	0.1703	0.0650		0.6068	0.0656	-0.0557	0.0683		753	34.7			-415.0	36.1	18.3	36.6
7.0	x	0.4639	0.0123	-0.2937	0.0661	0.2761	0.0146	-0.3409	0.0133	568	10.1	185.0	36.1	-216.7	11.8	193.3	12.5
6.5		0.7190	0.0084							348	4.4						
6.5	x	0.6577	0.0054	0.0614	0.0100					335	7.6	13.3	8.8				
6.5	x	0.7280	0.0045		-0.0090	0.0096				347	4.4			1.7	6.2		
6.5	x	0.6880	0.0026	0.0400	0.0052	-0.0304	0.0060			343	17.6	3.3	18.2	-8.3	19.2		
6.5	x	0.4806	0.0100		0.2385	0.0131				562	19.2			-213.3	19.7		
6.5	x	0.4073	0.0119	0.0732	0.0155	0.2503	0.0131			590	7.6	-28.3	20.7	-255.0	10.8		
6.5	x	0.7390	0.0069							358	1.7					-10.0	4.7
6.5	x	0.6902	0.0049	0.0488	0.0085		-0.0200	0.0109		373	8.3	-15.0	8.5			-38.3	11.3
6.5	x	0.7358	0.0222		0.0032	0.0233	-0.0078	0.0227		368	6.0			-10.0	6.2	-21.7	7.5
6.5	x	0.7233	0.0040	0.0125	0.0226	-0.0330	0.0063	-0.0533	0.0048	353	11.7	15.0	13.1	20.0	14.3	10.0	21.1
6.5	x	0.4796	0.0140		0.2594	0.0156	0.0010	0.0172		582	9.3			-223.3	9.4	-20.0	21.3
6.5	x	0.4428	0.0137	0.0568	0.0196	0.2475	0.0145	-0.0354	0.0181	602	4.4	-20.0	10.3	-228.3	9.4	-11.7	8.8

^{a)} data from two curves; one curve too noisy for data analysis

^{b)} no data; all curves too noisy for data analysis

Table C-9 (cont'd) Incubation of *S. marcescens* with 10 μM $\text{A}\beta_{1-40}$ in presence of Cu^{2+} , Zn^{2+} and cholesterol.

Conditions			$t_{\text{Log}_{\text{max}}}$				$\Delta t_{\text{Log}_{\text{max}}}$				$\Delta \text{AOD}_{\text{final}}$							
pH	A β	Cu Zn Chol	(min)	S.E.M.	w/o - w/A β	\pm Error	$\text{H}_2\text{O} - \text{Cu}^{2+}/\text{Zn}^{2+}$	\pm Error	w/o - w/Chol	\pm Error	(a.u.)	S.E.M.	w/o - w/A β	\pm Error	$\text{H}_2\text{O} - \text{Cu}^{2+}/\text{Zn}^{2+}$	\pm Error	w/o - w/Chol	\pm Error
7.3			1028	8							0.0590	0.0085						
7.3	x		1048	34	-20	35.2					0.0787	0.0101	-0.0198	0.0132				
7.3	x		1013	31			15	32.2			0.1065	0.0280			-0.0476	0.0293		
7.3	x	x	1197	9	-183	32.4	-148	35.3			0.0407	0.0055	0.0658	0.0285	0.0380	0.0115		
7.3	x	x	1282	15			-253	17.0			0.0190	0.0061			0.0400	0.0105		
7.3	x	x	1208	30	73	33.1	-160	45.2			0.0250	0.0071	-0.0060	0.0093	0.0537	0.0123		
7.3		x	1112	23					-83	24.8	0.0540	0.0054					0.0050	0.0101
7.3 ^{a)}	x	x	1202	8	-91	24.5			-154	35.0	0.0371	0.0075	0.0169	0.0092			0.0417	0.0126
7.3	x	x	1137	36			-25	43.2	-123	47.8	0.0551	0.0144			-0.0011	0.0154	0.0514	0.0315
7.3 ^{b)}	x	x																
7.3	x	x	1292	56			-180	60.9	-10	58.2	0.0170	0.0125			0.0370	0.0136	0.0020	0.0139
7.3	x	x	1220	25	72	61.6	-18	26.1	-12	38.8	0.0255	0.0097	-0.0085	0.0158	0.0116	0.0123	-0.0005	0.0120
7.0			920	37							0.0989	0.0137						
7.0	x		1142	26	-222	45.2					0.0637	0.0062	0.0352	0.0151				
7.0	x		1088	23			-168	43.6			0.1018	0.0049			-0.0029	0.0146		
7.0	x	x	1163	39	-75	45.8	-22	47.3			0.0744	0.0051	0.0275	0.0071	-0.0107	0.0080		
7.0		x	1288	8			-368	37.8			0.0200	0.0027			0.0788	0.0140		
7.0	x	x	1308	15	-20	17.0	-167	30.1			0.0194	0.0025	0.0006	0.0037	0.0443	0.0066		
7.0		x	1100	16					-180	40.2	0.0817	0.0085					0.0172	0.0162
7.0	x	x	1203	20	-103	26.0			-62	33.2	0.0504	0.0025	0.0313	0.0089			0.0133	0.0066
7.0	x	x	1112	36			-12	39.5	-23	43.0	0.0936	0.0126			-0.0119	0.0152	0.0082	0.0135
7.0 ^{a)}	x	x	1222	43	-111	55.8	-19	47.2	-59	58.0	0.0593	0.0000	0.0343	0.0126	-0.0089	0.0025	0.0150	0.0051
7.0		x	1288	23			-188	28.3	0	24.8	0.0212	0.0060			0.0605	0.0105	-0.0012	0.0066
7.0	x	x	1227	3	62	23.6	-23	20.7	82	15.2	0.0327	0.0051	-0.0115	0.0079	0.0177	0.0057	-0.0132	0.0057
6.5			938	16							0.0580	0.0050						
6.5	x		1148	13	-210	20.7					0.0330	0.0040	0.0250	0.0064				
6.5	x	x	1073	11			-135	19.3			0.0678	0.0095			-0.0098	0.0107		
6.5	x	x	1155	16	-82	19.4	-7	20.9			0.0494	0.0046	0.0184	0.0106	-0.0164	0.0061		
6.5		x	1180	30			-242	34.0			0.0281	0.0053			0.0299	0.0072		
6.5	x	x	1285	46	-105	55.3	-137	48.3			0.0064	0.0031	0.0217	0.0061	0.0266	0.0051		
6.5		x	1095	33					-157	36.2	0.0406	0.0022					0.0174	0.0054
6.5	x	x	1195	0	-100	32.5			-47	13.3	0.0240	0.0010	0.0167	0.0024			0.0091	0.0041
6.5	x	x	1195	29			-100	43.5	-122	30.9	0.0462	0.0144			-0.0055	0.0146	0.0216	0.0173
6.5	x	x	1223	21	-28	35.9	-28	21.3	-68	26.7	0.0375	0.0063	0.0087	0.0157	-0.0135	0.0064	0.0120	0.0078
6.5		x	1280	32			-185	45.7	-100	44.0	0.0207	0.0064			0.0199	0.0068	0.0074	0.0083
6.5	x	x	1295	52	-15	61.2	-100	52.0	-10	69.8	0.0061	0.0030	0.0146	0.0071	0.0178	0.0032	0.0002	0.0043

a) data from two curves; one curve too noisy for data analysis

b) no data; all curves too noisy for data analysis

C.2.3. Incubation of *K. pneumoniae*

Table C-10 Incubation of *K. pneumoniae* with 10 μM AB_{1-40} in presence of Cu^{2+} , Zn^{2+} and cholesterol.

Conditions			Slope _{max}			Δ Slope _{max}			OD _{logmax}			t _{onset}			Δ t _{onset}											
pH	AB	Cu Zn Chol.	(a.u./min; ±100)	w/o- w/AB	±Error	H ₂ O- Cu ²⁺ /Zn ²⁺	±Error	w/o-w/ Chol.	(a.u.)	±S.E.M.	w/o- w/AB	±Error	H ₂ O- Cu ²⁺ /Zn ²⁺	±Error	w/o-w/ Chol.	(min)	±S.E.M.	w/o- w/AB	±Error	H ₂ O- Cu ²⁺ /Zn ²⁺	±Error	w/o-w/ Chol.	±Error			
7.3			0.400	0.0127					0.3011	0.0052						313	3									
7.3	x		0.360	0.0135	0.041	0.0186			0.2863	0.0109	0.0147	0.0120				318	2	-5	3.2							
7.3	x	x	0.384	0.0105		0.016	0.0165		0.2778	0.0102		0.0233	0.0114			303	2			11	3.6					
7.3	x	x	0.335	0.0092	0.049	0.0139	0.025	0.0163	0.2701	0.0131	0.0077	0.0166	0.0163	0.0170		316	2	-13	3.4	2	2.9					
7.3	x	x	0.196	0.0018		0.204	0.0128		0.1545	0.0056		0.1465	0.0076			495	11			-181	11.6					
7.3	x	x	0.210	0.0038	-0.013	0.0042	0.150	0.0140	0.1882	0.0036	-0.0337	0.0067	0.0981	0.0114		458	10	36	15.0	-140	10.0					
7.3	x	x	0.433	0.0087					0.3111	0.0075						280	1			-0.0101	0.0091	33	2.8			
7.3	x	x	0.374	0.0057	0.059	0.0104			0.2915	0.0011	0.0197	0.0076				295	3	-16	2.9	-0.0051	0.0109	23	3.2			
7.3	x	x	0.398	0.0050		0.035	0.0100		0.2992	0.0016		0.0119	0.0077			287	1			-0.0215	0.0103	16	2.5			
7.3	x	x	0.334	0.0097	0.064	0.0109	0.040	0.0113	0.0134	0.2868	0.0016	0.0125	0.0023	0.0047	0.0020	294	5	-7	5.1	2	5.8	22	5.6			
7.3	x	x	0.222	0.0085		0.211	0.0121		0.1890	0.0090		0.1222	0.0117	0.0345	0.0106	445	15			-0.0345	0.0106	15.4	49	19.1		
7.3	x	x	0.213	0.0065	0.009	0.0106	0.161	0.0086	0.1686	0.0072	0.0203	0.0115	0.1228	0.0073		448	8	-2	17.2	-152	8.1	11	12.5			
7.0			0.417	0.0099					0.2937	0.0087						306	1									
7.0	x		0.384	0.0125	0.033	0.0159			0.2870	0.0046	0.0067	0.0098				319	2	-12	2.5							
7.0	x		0.432	0.0045		-0.015	0.0109		0.3177	0.0036		-0.0239	0.0094			308	1			-2	1.4					
7.0	x	x	0.371	0.0069	0.061	0.0083	0.014	0.0143	0.2872	0.0107	0.0305	0.0113	0.0001	0.0116		314	3	-6	3.0	5	3.6					
7.0	x	x	0.201	0.0041		0.216	0.0107		0.1575	0.0007		0.1362	0.0087			676	20			-370	19.7					
7.0	x	x	0.160	0.0100	0.041	0.0108	0.224	0.0160	0.1666	0.0075	-0.0090	0.0076	0.1205	0.0088		676	40	0	44.6	-358	40.1					
7.0	x	x	0.435	0.0111					0.3098	0.0029						274	1			-0.0161	0.0092	32	1.5			
7.0	x	x	0.366	0.0036	0.069	0.0117			0.2853	0.0016	0.0246	0.0033				296	5	-22	4.9	0.0018	0.0049	23	5.3			
7.0	x	x	0.425	0.0047		0.009	0.0121		0.3237	0.0014		-0.0139	0.0032			286	1			-0.0060	0.0039	12	1.3			
7.0	x	x	0.347	0.0059	0.079	0.0075	0.019	0.0069	0.2915	0.0029	0.0321	0.0033	-0.0063	0.0033		281	1	5	0.8	-0.0044	0.0111	8	3.8			
7.0	x	x	0.227	0.0066		0.208	0.0129		0.1905	0.0012		0.1193	0.0031	-0.0330	0.0014	476	13			-0.0330	0.0014	202	13.0	201	23.6	
7.0	x	x	0.218	0.0073	0.009	0.0098	0.148	0.0081	0.1892	0.0020	0.0013	0.0208	0.0961	0.0208		468	11	8	16.7	-0.0227	0.0221	11.6	208	41.4		
6.5			0.417	0.0031					0.3049	0.0077						309	1									
6.5	x		0.376	0.0099	0.041	0.0104			0.2832	0.0077	0.0217	0.0109				312	3	-3	3.4							
6.5	x	x	0.411	0.0024		0.006	0.0039		0.3307	0.0017		-0.0258	0.0079			331	1			-0.0039	0.0116	285	1			
6.5	x	x	0.391	0.0044	0.020	0.0050	-0.014	0.0108	0.3268	0.0033	0.0039	0.0037	-0.0436	0.0084		335	2	-3	2.0	-0.0209	0.0082	311	0			
6.5	x	x	0.166	0.0050		0.251	0.0059		0.1494	0.0083		0.1555	0.0114			785	53			0.0169	0.0037	313	3			
6.5	x	x	0.205	0.0051	-0.040	0.0071	0.171	0.0111	0.1966	0.0093	-0.0472	0.0125	0.0865	0.0121		697	11	87	53.8	-0.0476	0.0114	-386	12.0			
6.5	x	x	0.431	0.0085					0.3159	0.0021						277	1			-0.0110	0.0080	32	1.2			
6.5	x	x	0.364	0.0056	0.067	0.0102			0.2871	0.0087	0.0288	0.0089				285	1	-8	1.2	-0.0039	0.0116	27	3.4			
6.5	x	x	0.418	0.0041		0.012	0.0095		0.3367	0.0079		-0.0209	0.0082			311	0			-0.0060	0.0081	1.1	20	1.3		
6.5	x	x	0.377	0.0059	0.041	0.0072	-0.014	0.0082	0.3099	0.0017	0.0269	0.0081	-0.0228	0.0089		313	3	-2	3.4	-0.0228	0.0089	35	22	3.7		
6.5	x	x	0.241	0.0014		0.189	0.0087		0.2285	0.0037		0.0874	0.0043	-0.0791	0.0091	492	8			0.0874	0.0043	-215	7.9	293	53.1	
6.5	x	x	0.228	0.0038	0.013	0.0041	0.135	0.0068	0.2221	0.0016	0.0064	0.0040	0.0650	0.0088		490	1	2	7.8	-0.0254	0.0094	-205	1.1	208	11.5	

Table C-10 (cont'd) Incubation of *K. pneumoniae* with 10 μM AB_{1-40} in presence of Cu^{2+} , Zn^{2+} and cholesterol.

Conditions		t_{50}			Δt_{50}			OD_{600}			ΔOD_{600}			Δt_{max}			$\Delta \Delta t_{\text{max}}$										
pH	AB_{1-40}	Cu	Zn	Chol.	w/o-w/ w/ AB_{1-40}	S.E.M.	(min)	$\text{H}_2\text{O}-\text{Cu}^{2+}/\text{Zn}^{2+}$	\pm Error	w/o-w/ Chol.	(a.u.)	S.E.M.	(min)	w/o-w/ w/ AB_{1-40}	\pm Error	$\text{H}_2\text{O}-\text{Cu}^{2+}/\text{Zn}^{2+}$	\pm Error	w/o-w/ w/ AB_{1-40}	\pm Error	$\text{H}_2\text{O}-\text{Cu}^{2+}/\text{Zn}^{2+}$	\pm Error	w/o-w/ Chol.	\pm Error				
7.3					34.64	1.04					0.7065	0.0044						902	58								
7.3	x				38.21	2.09	-3.57	2.34			0.7043	0.0076	0.0022	0.0088				1028	10	-1.27	59						
7.3		x			37.64	0.30		-3.00	1.08		0.6762	0.0016		0.0303	0.0047			851	46			51	74				
7.3	x	x			39.93	1.59	-2.29	1.62	2.63		0.6366	0.0047	0.0396	0.0049	0.0677	0.0089		954	22	-1.03	51	74	24				
7.3			x		46.38	0.77		-11.74	1.30		0.4084	0.0061		0.2981	0.0075			915	28			-14	65				
7.3	x			x	49.64	1.78	-3.26	1.94	2.74		0.4613	0.0057	-0.0529	0.0084	0.2430	0.0095		967	14	-5.1	31	61	17				
7.3			x		34.05	0.13				0.59	1.05		0.7172	0.0053				860	16			-0.0107	0.0069	42	61		
7.3	x			x	37.70	0.75	-3.65	0.77		0.51	2.22		0.7007	0.0085	0.0165	0.0100		961	9	-1.01	18			67	13		
7.3		x		x	36.98	0.45				0.66	0.54		0.6573	0.0028		0.0600	0.0060	830	24			0.0189	0.0033	30	29	21	52
7.3	x	x		x	42.88	0.68	-5.90	0.82	1.02	-2.94	1.73		0.6208	0.0037	0.0364	0.0047	0.0799	0.0092	966	45	-1.36	51	-5	45	12	50	
7.3			x		46.29	0.01				0.09	0.77		0.4616	0.0152		0.2556	0.0161	772	4			-0.0532	0.0164	89	16	144	28
7.3	x			x	48.90	0.65	-2.61	0.65	1.00	0.74	1.89		0.4623	0.0054	-0.0006	0.0161	0.2385	0.0101	794	15	-2.3	16	167	18	173	21	
7.0					32.73	0.61					0.7080	0.0110						875	45								
7.0	x				35.19	0.31	-2.45	0.68			0.6932	0.0112	0.0149	0.0157				958	32	-8.3	55						
7.0		x			35.40	0.39				0.72			0.6890	0.0039		0.0190	0.0116	742	6					134	46		
7.0	x				38.88	1.82	-3.48	1.86	1.85		0.6596	0.0033	0.0294	0.0051	0.0336	0.0117		891	30	-1.49	31	67	44				
7.0			x		46.27	1.58				1.69			0.3528	0.0278		0.3553	0.0299	747	15					128	48		
7.0	x			x	60.08	3.25	-13.81	3.61	3.26		0.3485	0.0297	0.0043	0.0407	0.3447	0.0317		757	38	-1.0	41	201	50				
7.0			x		33.11	0.24				-0.38	0.65		0.7334	0.0100				809	9			-0.0254	0.0148	66	46		
7.0	x			x	37.85	0.09	-4.74	0.26		-2.66	0.32		0.6781	0.0048	0.0553	0.0111		968	32	-1.58	33			-10	45		
7.0		x			37.30	0.44				0.50	0.59		0.6897	0.0079		0.0437	0.0127	766	13					43	16	-24	14
7.0	x	x		x	42.74	0.36	-5.44	0.57	0.37	-3.86	1.86		0.6394	0.0073	0.0503	0.0107	0.0386	0.0087	932	15	-1.66	20	35	36	-42	34	
7.0			x		47.48	0.10				0.26	1.58		0.4457	0.0152		0.2877	0.0182	918	12					-108	16	-171	19
7.0	x			x	54.09	2.52	-6.61	2.52	2.52	5.99	4.11		0.4733	0.0052	-0.0276	0.0161	0.2048	0.0071	897	21	21	24	71	38	-140	44	
6.5					34.20	0.57					0.7107	0.0067						873	22								
6.5	x				35.45	0.19	-1.25	0.60			0.6818	0.0160	0.0289	0.0174				907	4			-34	23				
6.5		x			39.57	1.36				1.48			0.6832	0.0066		0.0275	0.0094	770	13					102	26		
6.5	x	x			42.13	0.99	-2.57	1.69	1.01		0.6765	0.0052	0.0067	0.0084	0.0053	0.0168		802	28	-3.2	31	104	28				
6.5			x		51.47	1.75				1.84			0.2818	0.0291		0.4289	0.0299	535	167					337	169		
6.5	x			x	54.08	1.85	-2.61	2.54	1.86		0.3684	0.0293	-0.0866	0.0413	0.3134	0.0334		737	11	-2.02	168	169	12				
6.5			x		34.49	0.28				-0.29	0.63		0.7349	0.0077				818	18			-0.0242	0.0102	55	29		
6.5	x			x	38.43	0.78	-3.95	0.83		-2.98	0.81		0.6760	0.0115	0.0589	0.0139		922	25	-1.04	31			-15	26		
6.5		x			39.96	0.52				0.59	1.46		0.6978	0.0055		0.0372	0.0095	749	17			-0.0146	0.0086	69	25	21	22
6.5	x	x		x	43.27	0.97	-3.31	1.10	1.25	-1.14	1.39		0.6657	0.0051	0.0321	0.0075	0.0104	0.0126	837	41	-8.8	45	85	48	-35	50	
6.5			x		49.10	0.87				0.92	1.95		0.4440	0.0063		0.2909	0.0100	-0.1622	0.0298	913	12			-95	22	-378	168
6.5	x			x	51.15	0.74	-2.05	1.14	1.08	2.93	1.99		0.4636	0.0058	-0.0196	0.0086	0.2124	0.0129	944	2	-3.1	12	-2.2	26	-206	12	

Table C-10 (cont'd) Incubation of *K. pneumoniae* with 10 μM $\text{A}\beta_{1-40}$ in presence of Cu^{2+} , Zn^{2+} and cholesterol.

Conditions		OD ₂₂₈		ΔOD_{228}			$t_{\text{Supp,max}}$		$\Delta t_{\text{Supp,max}}$					
pH	$\text{A}\beta$: Cu : Zn : Chol.	(a.u.)	S.E.M.	w/o- w/ $\text{A}\beta$	H_2O - $\text{Cu}^{2+}/\text{Zn}^{2+}$	\pm Error	w/o- w/Chol.	\pm Error	w/o- w/ $\text{A}\beta$	H_2O - $\text{Cu}^{2+}/\text{Zn}^{2+}$	\pm Error	w/o- w/Chol.	\pm Error	
7.3		0.6653	0.0010											
7.3	x	0.6583	0.0107	0.0070	0.0108				-10.0	3.7				
7.3	x	0.6560	0.0072		0.0092	0.0073					13.3	3.3		
7.3	x	0.6119	0.0035	0.0442	0.0080	0.0113			-21.7	4.4	1.7	4.7		
7.3	x	0.2725	0.0041		0.3928	0.0043					-185.0	13.1		
7.3	x	0.3061	0.0046	-0.0335	0.0062	0.0117			25.0	18.4	-150.0	13.4		
7.3	x	0.6903	0.0030			-0.0250	0.0032					36.7	2.4	
7.3	x	0.6704	0.0075	0.0199	0.0081		-0.0121	0.0131	-21.7	3.7		25.0	4.7	
7.3	x	0.6456	0.0040		0.0447	0.0050		0.0104			-10.0	2.4	3.3	
7.3	x	0.6058	0.0038	0.0399	0.0055	0.0084		0.0061	-18.3	3.3	-6.7	4.4	4.4	
7.3	x	0.3356	0.0144		0.3547	0.0147		-0.0631			-178.3	15.1	43.3	19.9
7.3	x	0.3294	0.0095	0.0063	0.0173	0.0121		-0.0233	3.3	17.6	-153.3	9.9	21.7	16.0
7.0		0.6732	0.0079											
7.0	x	0.6586	0.0071	0.0146	0.0106				-16.7	2.4				
7.0	x	0.6662	0.0054		0.0070	0.0096					-5.0	2.4		
7.0	x	0.6304	0.0024	0.0359	0.0059	0.0075			-10.0	4.7	1.7	4.7		
7.0	x	0.1010	0.0268		0.5723	0.0279					-378.3	19.0		
7.0	x	0.1055	0.0523	-0.0045	0.0588	0.0528			-26.7	53.2	-388.3	49.7		
7.0	x	0.7012	0.0110			-0.0279	0.0135					31.7	1.7	
7.0	x	0.6519	0.0030	0.0493	0.0114		0.0067	0.0077	-28.3	4.4		20.0	4.7	
7.0	x	0.6739	0.0046		0.0273	0.0119	-0.0077	0.0071			-16.7	1.7	20.0	2.4
7.0	x	0.6233	0.0015	0.0506	0.0048	0.0034	0.0070	0.0029	-3.3	1.7	8.3	4.4	26.7	4.4
7.0	x	0.3181	0.0091		0.3831	0.0142	-0.2171	0.0283			-215.0	15.3	195.0	24.3
7.0	x	0.3261	0.0071	-0.0080	0.0115	0.0077	-0.2207	0.0528	5.0	25.8	-181.7	21.3	226.7	53.9
6.5		0.6827	0.0024											
6.5	x	0.6522	0.0159	0.0305	0.0161				-5.0	3.7				
6.5	x	0.6620	0.0036		0.0207	0.0043					-30.0	2.4		
6.5	x	0.6424	0.0039	0.0196	0.0053	0.0164			-6.7	2.4	-31.7	3.7		
6.5	x	0.0304	0.0140		0.6524	0.0142					-493.3	48.1		
6.5	x	0.0826	0.0102	-0.0523	0.0174	0.0189			81.7	49.9	-406.7	14.0		
6.5	x	0.7014	0.0063			-0.0187	0.0068					31.7	1.7	
6.5	x	0.6499	0.0089	0.0515	0.0109		0.0023	0.0183	-13.3	1.7		23.3	3.7	
6.5	x	0.6739	0.0043		0.0281	0.0077	-0.0113	0.0056			-41.7	1.7	20.0	2.4
6.5	x	0.6322	0.0059	0.0411	0.0073	0.0107	0.0102	0.0071	-3.3	3.3	-31.7	3.3	28.3	3.3
6.5	x	0.3319	0.0042		0.3695	0.0076	-0.3016	0.0147			-236.7	9.3	288.3	48.9
6.5	x	0.3250	0.0039	0.0069	0.0057	0.0097	-0.2424	0.0109	0.0	9.4	-223.3	2.4	206.7	13.7

Table C-10 (cont'd) Incubation of *K. pneumoniae* with 10 μM AB_{1-40} in presence of Cu^{2+} , Zn^{2+} and cholesterol.

Conditions			$\Delta I_{\text{OD}_{600\text{nm}}}$				$\Delta \text{OD}_{600\text{nm}}$				$\Delta \text{AOD}_{600\text{nm}}$						
pH	AB	Cu : Zn : Chol.	(min)	S.E.M.	w/o- w/ AB	$\text{H}_2\text{O}-$ $\text{Cu}^{2+}/\text{Zn}^{2+}$	\pm Error	w/o- w/ Chol.	\pm Error	(a.u.)	S.E.M.	w/o- w/ AB	$\text{H}_2\text{O}-$ $\text{Cu}^{2+}/\text{Zn}^{2+}$	\pm Error	w/o- w/ Chol.	\pm Error	
7.3			1215	56						0.0164	0.0028						
7.3	x		1347	10	-132	56.7				0.0084	0.0009	0.0081	0.0029				
7.3	x		1153	43		62	70.6			0.0280	0.0056		-0.0116	0.0063			
7.3	x		1270	20	-117	47.7	77	22.4		0.0160	0.0021	0.0120	0.0060	-0.0076	0.0023		
7.3	x		1410	18		-195	58.5			0.0003	0.0001		0.0161	0.0028			
7.3	x		1425	5	-15	18.3	11.3			0.0009	0.0007	-0.0006	0.0007	0.0075	0.0011		
7.3	x	x	1140	15				75	57.7	0.0247	0.0014				-0.0082	0.0031	
7.3	x	x	1257	8	-117	17.2		90	13.1	0.0156	0.0008	0.0091	0.0016		-0.0072	0.0012	
7.3	x	x	1117	25				37	50.0	0.0309	0.0033		-0.0062	0.0036	-0.0029	0.0065	
7.3	x	x	1260	41	-143	47.9	-3	41.8	45.6	0.0162	0.0029	0.0147	0.0044	-0.0006	0.0030	-0.0002	0.0036
7.3	x	x	1217	12				193	21.1	0.0092	0.0006			0.0154	0.0015	-0.0089	0.0006
7.3	x	x	1242	9	-25	14.6	15	12.1	10.1	0.0061	0.0006	0.0031	0.0008	0.0094	0.0010	-0.0053	0.0009
7.0			1182	45						0.0250	0.0039						
7.0	x		1277	30	-95	54.0				0.0150	0.0026	0.0101	0.0047				
7.0	x		1050	6			132	45.5		0.0428	0.0016		-0.0178	0.0042			
7.0	x		1205	32	-155	32.7	72	43.7		0.0242	0.0030	0.0186	0.0034	-0.0092	0.0039		
7.0	x		1423	6			-242	45.5		0.0006	0.0003		0.0245	0.0039			
7.0	x		1433	2	-10	6.2	-157	29.7		0.0002	0.0002	0.0004	0.0004	0.0148	0.0026		
7.0	x	x	1083	8				98	45.9	0.0358	0.0011				-0.0108	0.0041	
7.0	x	x	1263	37	-180	37.7		13	47.2	0.0173	0.0040	0.0185	0.0042		-0.0024	0.0048	
7.0	x	x	1052	13			32	15.7	-2	0.0471	0.0012		-0.0113	0.0016	-0.0043	0.0020	
7.0	x	x	1213	15	-162	19.7	50	39.5	-8	0.0277	0.0015	0.0194	0.0019	-0.0104	0.0043	-0.0035	0.0033
7.0	x	x	1393	25			-310	26.6	30	0.0026	0.0008		0.0932	0.0014	-0.0020	0.0009	
7.0	x	x	1365	31	28	40.1	-102	48.2	68	0.0039	0.0015	-0.0013	0.0017	0.0134	0.0043	-0.0037	0.0015
6.5			1182	22						0.0318	0.0018						
6.5	x		1218	2	-37	21.7				0.0246	0.0006	0.0072	0.0019				
6.5	x		1102	14			80	25.6		0.0357	0.0011		-0.0038	0.0021			
6.5	x		1137	26	-35	29.5	82	26.2		0.0291	0.0023	0.0066	0.0025	-0.0044	0.0024		
6.5	x		1320	115			-138	117.0		0.0129	0.0129		0.0189	0.0131			
6.5	x		1435	0	-115	115.0	-217	1.7		0.0000	0.0000	0.0129	0.0129	0.0246	0.0006		
6.5	x	x	1095	18				87	27.9	0.0411	0.0014				-0.0093	0.0023	
6.5	x	x	1207	26	-112	31.3		12	25.9	0.0233	0.0016	0.0178	0.0021		0.0013	0.0017	
6.5	x	x	1060	17			35	24.7	42	0.0406	0.0026		0.0005	0.0029	-0.0050	0.0028	
6.5	x	x	1150	38	-90	41.6	57	45.9	-13	0.0363	0.0006	0.0043	0.0037	-0.0130	0.0017	-0.0072	0.0024
6.5	x	x	1405	15			-310	23.3	-85	0.0007	0.0007		0.0404	0.0015	0.0122	0.0130	
6.5	x	x	1433	2	-28	15.4	-227	25.9	2	0.0003	0.0003	0.0004	0.0007	0.0230	0.0016	-0.0003	0.0003

C.2.4. Incubation of methicillin-resistant *S. aureus* (MRSA)

Table C-11 Incubation of methicillin-resistant *S. aureus* (MRSA) with 10 μM AB_{1-40} in presence of Cu^{2+} , Zn^{2+} and cholesterol.

pH	Conditions			Slope _{max}			Δ Slope _{max}			OD _{500nm}			OD _{600nm}			Δ t _{onset}		
	AB	Cu	Zn	Chol	(a.u./min: \pm S.E.M. $\times 100$)	w/o- w/ AB	H ₂ O- Cu ²⁺ /Zn ²⁺ Error	w/o- w/ Chol	(a.u.)	S.E.M.	w/o- w/ AB	H ₂ O- Cu ²⁺ /Zn ²⁺ Error	w/o- w/ Chol	(min)	S.E.M.	w/o- w/ AB	H ₂ O- Cu ²⁺ /Zn ²⁺ Error	w/o- w/ Chol
7.3					0.342	0.0043			0.2834	0.0093				322	2			
7.3	x				0.309	0.0207	0.032	-0.0211	0.2640	0.0273	0.0194	0.0275		354	8	-32	7.8	
7.3 ^{a)}		x			0.357	0.0014	-0.015	-0.0045	0.3451	0.0028		-0.0617	0.0043	368	5			-46
7.3	x	x			0.350	0.0038	0.007	0.0041	0.2935	0.0247	0.0517	0.0248	-0.0295	366	2	2	5.2	-12
7.3 ^{d)}			x															
7.3 ^{d)}			x															
7.3 ^{a)}				x	0.357	0.0043	-0.015	0.0061	0.3182	0.0135				358	1			-36
7.3	x			x	0.448	0.1086	-0.092	0.1087	0.3062	0.0059	0.0120	0.0147	-0.0422	365	9	-7	8.9	-11
7.3	x	x		x	0.374	0.0043	-0.017	0.0061	0.2923	0.0252				412	12			-44
7.3 ^{d)}			x															
7.3 ^{d)}			x															
7.0 ^{a)}				x	0.336	0.0003			0.2705	0.0028				309	1			
7.0	x				0.349	0.0083	-0.012	0.0084	0.2743	0.0085	-0.0038	0.0089		311	1	-2	1.0	
7.0	x	x			0.358	0.0078	-0.022	0.0078	0.3327	0.0027		-0.0622	0.0039	363	4			-54
7.0 ^{b)}		x			0.350		-0.031		0.3596		-0.0069		-0.0653	365		-2		-54
7.0 ^{d)}			x															
7.0 ^{d)}			x															
7.0 ^{a)}				x	0.340	0.0023	-0.003	0.0023	0.2782	0.0010				352	1			-42
7.0	x				0.357	0.0104	-0.017	0.0106	0.3036	0.0040	-0.0254	0.0041	-0.0294	331	18	21	17.8	-19
7.0	x	x			0.387	0.0057	-0.048	0.0062	0.2681	0.0067				437	27			-74
7.0 ^{d)}		x			0.971	0.3186	-0.583	0.3187	0.4087	0.0267	-0.1406	0.0275	-0.0691	526	9	-89	28.4	-161
7.0 ^{d)}			x															
7.0 ^{d)}			x															
6.5					0.335	0.0007			0.2807	0.0010				308	2			
6.5	x				0.356	0.0008	-0.001	0.0010	0.2778	0.0040	0.0030	0.0041		311	1	-3	2.1	
6.5	x	x			0.333	0.0043	0.002	0.0044	0.2628	0.0188		0.0180	0.0188	361	4			-53
6.5	x	x			0.323	0.0070	0.010	0.0082	0.2618	0.0052	0.0010	0.0195	0.0160	392	4	-31	5.6	-82
6.5 ^{d)}			x															
6.5 ^{d)}			x															
6.5	x			x	0.331	0.0054	0.004	0.0055	0.2821	0.0077				350	1			-43
6.5	x	x			0.336	0.0036	-0.005	0.0065	0.2684	0.0077	0.0137	0.0108	0.0094	354	1	-3	1.7	-43
6.5	x	x			0.320	0.0099	0.011	0.0113	0.0108	0.2454	0.0148	0.0367	0.0167	475	33			-114
6.5	x	x		x	0.142	0.0483	0.178	0.0493	0.0488	0.0944	0.1610	0.0329	0.1840	477	21	-2	39.2	-123
6.5 ^{d)}			x															-85
6.5 ^{d)}			x															-20.9

a) data from two curves; one curve too noisy for data analysis

b) data from one curve; two curves too noisy for data analysis

c) no data; all curves show no growth, i.e. 1 mM Zn²⁺ completely suppresses growth of MRSA

d) no data; all curves too noisy for data analysis

Table C-11 (cont'd) Incubation of methicillin-resistant *S. aureus* (MRSA) with 10 μM AB_{1-40} in presence of Cu^{2+} , Zn^{2+} and cholesterol.

Conditions	$t_{5\%}$			$\Delta t_{5\%}$			OD_{max}			$\Delta \text{OD}_{\text{max}}$			Δt_{max}			$\Delta \Delta t_{\text{max}}$													
	pH	AB : Cu : Zn : Chol :	w/o - w/AB	S.E.M.	w/o - w/AB	\pm Error	H_2O - Cu^{2+} / Zn^{2+} :	H_2O - Cu^{2+} / Zn^{2+} :	\pm Error	(a.u.)	S.E.M.	w/o - w/AB	H_2O - Cu^{2+} / Zn^{2+} :	H_2O - Cu^{2+} / Zn^{2+} :	\pm Error	(min)	S.E.M.	w/o - w/AB	H_2O - Cu^{2+} / Zn^{2+} :	H_2O - Cu^{2+} / Zn^{2+} :	\pm Error	w/o - w/Chol	H_2O - Cu^{2+} / Zn^{2+} :	H_2O - Cu^{2+} / Zn^{2+} :	\pm Error				
7.3			42.56	1.35					0.9704	0.0016					888	2													
7.3	x		55.70	8.65	-13.14	8.75			0.9376	0.0105	0.0328	0.0106			899	27	-11	27											
7.3 ^{a)}	x		50.80	0.18		1.36	-8.25		1.0305	0.0008			-0.0601	0.0018	782	5			106	5									
7.3	x	x	47.48	2.44	3.32	2.44	8.22	8.99	1.0217	0.0096	0.0088	0.0097	-0.0841	0.0142	802	27	-21	27	97	38									
7.3 ^{d)}	x																												
7.3 ^{e)}	x																												
7.3 ^{a)}	x		45.38	0.70			-2.83	1.52	1.0328	0.0111					877	7													
7.3	x	x	41.29	4.78	4.09	4.83	14.41	9.88	1.0899	0.1112	-0.0570	0.1117			855	11	22	13											
7.3	x	x	42.82	1.93			2.56	2.06	1.0801	0.0050			-0.0473	0.0122	798	66			79	66									
7.3 ^{d)}	x																												
7.3 ^{e)}	x																												
7.3 ^{e)}	x																												
7.0 ^{a)}			41.74	0.38					0.9277	0.0095					854	23													
7.0	x		42.45	0.45	-0.72	0.59			0.9516	0.0024	-0.0239	0.0098			876	33	-22	40											
7.0	x		47.98	1.42			-6.24	1.47	0.9826	0.0081			-0.0549	0.0125	681	4			172	23									
7.0 ^{b)}	x	x	45.60	--	2.38	--	-3.15	--	1.0011	--	-0.0184	--	-0.0495	--	750	--	-68	--	126	--									
7.0 ^{d)}	x																												
7.0 ^{e)}	x																												
7.0 ^{a)}	x		41.72	0.69			0.02	0.79	0.9848	0.0044					887	70													
7.0	x	x	43.91	0.55	-2.20	0.88	-1.46	0.71	0.9911	0.0170	-0.0063	0.0176			852	35	35	79											
7.0	x	x	38.45	0.46			3.27	0.83	1.0910	0.0109			-0.1062	0.0117	686	68			200	98									
7.0 ^{d)}	x	x	49.06	16.65	-10.61	16.66	-5.14	16.66	1.1111	0.0150	-0.0201	0.0186			606	50	81	84	246	61	144								
7.0 ^{e)}	x																												
7.0 ^{e)}	x																												
6.5			40.70	0.18					0.9703	0.0010					899	15													
6.5	x		41.06	0.61	-0.36	0.63			0.9677	0.0082	0.0026	0.0083			881	32	18	36											
6.5	x		42.04	1.09			-1.34	1.10	0.9903	0.0098			-0.0200	0.0099	796	20			103	25									
6.5	x	x	40.10	0.22	1.95	1.11	0.97	0.65	0.9953	0.0019	-0.0049	0.0100	-0.0275	0.0085	859	59	-64	63	22	68									
6.5 ^{d)}	x																												
6.5 ^{e)}	x																												
6.5	x	x	42.22	0.57			-1.53	0.60	1.0213	0.0147					923	9													
6.5	x	x	39.77	0.73	2.45	0.93	1.29	0.95	0.9652	0.0079	0.0561	0.0168			936	32	-13	33											
6.5	x	x	41.72	0.80			0.50	0.99	1.0014	0.0166			0.0199	0.0222	800	46			123	47									
6.5	x	x	36.31	1.03	5.41	1.30	3.46	3.78	1.05	0.9850	0.0083	0.0165	0.0186		860	10	-60	48	77	34	0								
6.5 ^{d)}	x																												
6.5 ^{e)}	x																												

a) data from two curves; one curve too noisy for data analysis
 b) data from one curve; two curves too noisy for data analysis
 c) no data; all curves show no growth, i.e. 1 mM Zn^{2+} completely suppresses growth of MRSA
 d) no data; all curves too noisy for data analysis

Table C-11 (cont'd) Incubation of methicillin-resistant *S. aureus* (MRSA) with 10 μM AB_{1-40} in presence of Cu^{2+} , Zn^{2+} and cholesterol.

Conditions			OD _{2h}			ΔOD_{2h}			$t_{\text{Stop,max}}$			$\Delta t_{\text{Stop,max}}$						
pH	AB	Cu Zn Chol.	(a.u.)	S.E.M.	w/o- w/AB	\pm Error	H ₂ O- Cu ²⁺ /Zn ²⁺	\pm Error	w/o- w/Chol.	\pm Error	(min)	S.E.M.	w/o- w/AB	\pm Error	H ₂ O- Cu ²⁺ /Zn ²⁺	\pm Error	w/o- w/Chol.	\pm Error
7.3			0.7297	0.0123							405	2.9						
7.3	x		0.6930	0.0219	0.0367	0.0251					440	14.4	-35.0	14.7				
7.3 ^{a)}	x		0.8051	0.0075			-0.0754	0.0144			465	5.0			-60.0	5.8		
7.3	x	x	0.7536	0.0088	0.0515	0.0115	-0.0606	0.0236			450	10.4	15.0	11.5	-10.0	17.8		
7.3 ^{a)}	x																	
7.3 ^{a)}	x	x																
7.3 ^{a)}	x	x	0.7750	0.0053					-0.0454	0.0134	447	1.7					-41.7	3.3
7.3	x		0.7862	0.0770	-0.0111	0.0772			-0.0932	0.0800	437	7.5	9.2	7.7			2.5	16.3
7.3	x	x	0.7962	0.0180			-0.0212	0.0188	0.0088	0.0195	475	8.7			-28.3	8.8	-10.0	10.0
7.3 ^{a)}	x	x																
7.3 ^{a)}	x	x																
7.3 ^{a)}	x	x																
7.0 ^{a)}			0.7224	0.0094							390	0.0						
7.0	x		0.7505	0.0030	-0.0281	0.0098					390	0.0	0.0	0.0				
7.0	x	x	0.7962	0.0094			-0.0738	0.0133			457	6.7			-66.7	6.7		
7.0 ^{a)}	x	x	0.7791		0.0172		-0.0286				455		1.7		-65.0			
7.0 ^{a)}	x																	
7.0 ^{a)}	x	x																
7.0 ^{a)}	x	x	0.7245	0.0058					-0.0021	0.0111	433	1.7					-43.3	1.7
7.0	x		0.7307	0.0138	-0.0062	0.0150			0.0198	0.0141	437	2.5	-4.2	3.0			-47.5	2.5
7.0	x	x	0.8296	0.0091			-0.1051	0.0108	-0.0334	0.0131	453	1.7			-20.0	2.4	3.3	6.9
7.0 ^{a)}	x	x	0.6260	0.0333	0.2036	0.0346	0.1047	0.0361	0.1531		583	28.9	-130.0	29.0	-145.8	29.0	-128.3	
7.0 ^{a)}	x	x																
7.0 ^{a)}	x	x																
6.5			0.7333	0.0044							392	1.7						
6.5	x		0.7517	0.0080	-0.0184	0.0091					393	1.7	-1.7	2.4				
6.5	x	x	0.7665	0.0132			-0.0332	0.0139			440	7.6			-48.3	7.8		
6.5	x	x	0.7115	0.0068	0.0550	0.0148	0.0402	0.0105			473	4.4	-33.3	8.8	-80.0	4.7		
6.5 ^{a)}	x																	
6.5 ^{a)}	x	x																
6.5		x	0.7400	0.0090					-0.0066	0.0100	435	0.0					-43.4	1.7
6.5	x	x	0.7060	0.0060	0.0340	0.0108			0.0457	0.0100	433	1.7	1.7	1.7			-40.0	2.4
6.5	x	x	0.6842	0.0180			0.0557	0.0202	0.0823	0.0224	493	6.7			-58.3	6.7	-53.3	10.1
6.5	x	x	0.5421	0.0286	0.1421	0.0338	0.1639	0.0292	0.1694	0.0294	500	0.0	-6.7	6.7	-66.7	1.7	-26.7	4.4
6.5 ^{a)}	x	x																
6.5 ^{a)}	x	x																

a) data from two curves; one curve too noisy for data analysis
b) data from one curve; two curves too noisy for data analysis
c) no data; all curves show no growth, i.e. 1 mM Zn²⁺ completely suppresses growth of MRSA
d) no data; all curves too noisy for data analysis

Table C-11 (cont'd) Incubation of methicillin-resistant *S. aureus* (MRSA) with 10 μM AB_{1-40} in presence of Cu^{2+} , Zn^{2+} and cholesterol.

Conditions			$t_{\text{OD}_{\text{max}}}$				$\Delta t_{\text{OD}_{\text{max}}}$				$\Delta \text{OD}_{\text{Final}}$							
pH	AB	Cu Zn Chol.	(min)	S.E.M.	w/o - w/ AB	\pm Error	$\text{H}_2\text{O} -$ $\text{Cu}^{2+}/\text{Zn}^{2+}$	\pm Error	w/o - w/ Chol.	\pm Error	(a.u.)	S.E.M.	w/o - w/ AB	\pm Error	$\text{H}_2\text{O} -$ $\text{Cu}^{2+}/\text{Zn}^{2+}$	\pm Error	w/o - w/ Chol.	\pm Error
7.3			1210	0							0.0166	0.0024						
7.3	x		1253	32	-43	32.4					0.0098	0.0036	0.0068	0.0044				
7.3 ^{a)}	x		1150	0			60	0.0			0.0120	0.0005			0.0047	0.0025		
7.3	x	x	1168	25	-18	24.6	85	40.7			0.0125	0.0038	-0.0005	0.0038	-0.0027	0.0053		
7.3 ^{a)}	x		--	--	--	--	--	--			--	--			--	--		
7.3 ^{a)}	x	x	--	--	--	--	--	--			--	--			--	--		
7.3 ^{a)}	x	x	1235	8					-25	7.6	0.0152	0.0009					0.0014	0.0026
7.3	x	x	1220	20	15	21.4			33	38.1	0.0283	0.0145	-0.0130	0.0145			-0.0185	0.0149
7.3	x	x	1210	55			25	55.4	-60	54.9	0.0181	0.0045			-0.0029	0.0046	-0.0062	0.0045
7.3 ^{a)}	x	x	--	--	--	--	--	--	--	--	--	--			--	--	--	--
7.3 ^{a)}	x	x	--	--	--	--	--	--	--	--	--	--			--	--	--	--
7.3 ^{a)}	x	x	--	--	--	--	--	--	--	--	--	--			--	--	--	--
7.0 ^{a)}	x		1163	23							0.0251	0.0009						
7.0	x		1187	23	-24	32.4					0.0186	0.0000	0.0065	0.0009				
7.0	x	x	1045	0			118	23.3			0.0171	0.0010			0.0080	0.0013		
7.0 ^{a)}	x	x	1115	--	-70	--	73	--			0.0163	--	0.0008	--	0.0023	--	--	--
7.0 ^{a)}	x		--	--	--	--	--	--			--	--			--	--		
7.0 ^{a)}	x	x	--	--	--	--	--	--			--	--			--	--		
7.0 ^{a)}	x	x	1238	69					-75	73.1	0.0177	0.0018					0.0074	0.0020
7.0	x	x	1182	18	56	71.5			5	28.5	0.0187	0.0008	-0.0011	0.0020			-0.0001	0.0008
7.0	x	x	1123	41			115	80.5	-78	41.1	0.0253	0.0019			-0.0076	0.0027	-0.0082	0.0022
7.0 ^{a)}	x	x	1132	56	-8	69.8	51	59.1	-17	--	0.1030	0.0175	-0.0777	0.0176	-0.0842	0.0175	-0.0867	--
7.0 ^{a)}	x	x	--	--	--	--	--	--	--	--	--	--			--	--	--	--
7.0 ^{a)}	x	x	--	--	--	--	--	--	--	--	--	--			--	--	--	--
6.5			1207	16							0.0135	0.0026						
6.5	x		1192	33	15	37.0					0.0063	0.0008	0.0072	0.0028				
6.5	x	x	1157	16			50	22.5			0.0108	0.0005			0.0027	0.0027		
6.5	x	x	1252	60	-95	61.7	-60	68.4			0.0120	0.0016	-0.0013	0.0017	-0.0058	0.0018		
6.5 ^{a)}	x		--	--	--	--	--	--			--	--			--	--		
6.5 ^{a)}	x	x	--	--	--	--	--	--			--	--			--	--		
6.5		x	1273	8					-67	18.0	0.0160	0.0038					-0.0025	0.0046
6.5	x	x	1290	33	-17	34.3			-98	47.2	0.0056	0.0017	0.0104	0.0041			0.0007	0.0019
6.5	x	x	1275	20			-2	21.7	-118	25.5	0.0052	0.0009			0.0108	0.0039	0.0056	0.0010
6.5	x	x	1337	14	-62	24.6	-47	36.2	-85	61.3	0.0058	0.0023	-0.0007	0.0024	-0.0003	0.0029	0.0062	0.0028
6.5 ^{a)}	x	x	--	--	--	--	--	--	--	--	--	--			--	--	--	--
6.5 ^{a)}	x	x	--	--	--	--	--	--	--	--	--	--			--	--	--	--

a) data from two curves; one curve too noisy for data analysis
b) data from one curve; two curves too noisy for data analysis
c) no data; all curves show no growth, i.e. 1 mM Zn^{2+} completely suppresses growth of MRSA
d) no data; all curves too noisy for data analysis

C.2.5. Incubation of methicillin-susceptible *S. aureus* (MSSA)

Table C-12 Incubation of methicillin-susceptible *S. aureus* (MSSA) with 10 μM AB_{1-40} in presence of Cu^{2+} , Zn^{2+} and cholesterol.

pH	Conditions		Slope _{max}			Δ Slope _{max}			OD _{optmax}			OD _{optmax}			t _{opt}			Δ t _{opt}			
	AB	Cu:Zn:Chol.	(a.u./min *100)	S.E.M.	w/o- w/AB	H ₂ O- Cu ²⁺ :Zn ²⁺	w/o- w/Chol.	\pm Error	(a.u.)	S.E.M.	w/o- w/AB	H ₂ O- Cu ²⁺ :Zn ²⁺	w/o- w/Chol.	\pm Error	(min)	S.E.M.	w/o- w/AB	H ₂ O- Cu ²⁺ :Zn ²⁺	w/o- w/Chol.	\pm Error	
7.3			0.305	0.0119					0.2682	0.0202					561	30					
7.3 ^{a)}	x		0.279	0.0046	0.026	-0.0128			0.2730	0.0017	-0.0047	0.0203			528	2	33	29.6			
7.3	x		0.302	0.0042		0.003	-0.0127		0.2999	0.0014		0.0203			606	4			-45	29.9	
7.3	x	x	0.348	0.0292	-0.046	0.0295	-0.0296		0.3423	0.0425	-0.0423	0.0425	-0.0693	0.0425	604	4	2	6.0	-76	4.6	
7.3 ^{d)}	x																				
7.3 ^{d)}	x	x																			
7.3		x	0.345	0.0177		-0.040	0.0213		0.3205	0.0403					538	5					23
7.3 ^{e)}	x																				29.9
7.3 ^{e)}	x	x																			
7.3	x		0.332	0.0023		0.013	-0.0178	-0.030	0.0048	0.3217	0.0112				610	4			-73	6.5	6.2
7.3 ^{a)}	x	x	0.337	0.0113	-0.005	0.0116	-0.032	-0.0373	0.011	0.0313	-0.0054	0.0167	-0.1580	0.0282	579	40	31	40.0	-80	74.8	25
7.3 ^{d)}	x																				39.9
7.3 ^{d)}	x	x																			
7.0			0.294	0.0023					0.2796	0.0061					549	39					
7.0 ^{b)}	x		0.296		-0.002				0.2396		0.0400				510		39				
7.0	x		0.316	0.0038		-0.022	-0.0044		0.2810	0.0048		0.0078		694	20			-85	44.4		
7.0	x	x	0.293	0.0133	0.023	0.0139	0.003		0.2550	0.0031	0.0261	0.0057	-0.0154		692	4	2	20.6	-122		
7.0 ^{d)}	x																				
7.0 ^{d)}	x	x																			
7.0		x	0.312	0.0037		-0.018	0.0043		0.3018	0.0165					521	1			-0.0222	0.0176	28
7.0	x		0.336	0.0110	-0.024	0.0116	-0.040		0.2892	0.0123	0.0127	0.0206			532	42	-11	42.4	-0.0496		-22
7.0	x	x	0.355	0.0116		-0.043	-0.0122	-0.039	0.0122	0.3072	0.0091				602	8			-0.0054	0.0188	-81
7.0	x	x	0.331	0.0053	0.024	0.0128	0.005	-0.0122	-0.038	0.0144	0.2854	0.0234	0.0218	0.0251	676	39	-75	39.3	-0.0037	0.0265	-144
7.0 ^{d)}	x																				88.7
7.0 ^{d)}	x	x																			
7.0 ^{d)}	x	x																			
6.5			0.284	0.0028					0.2308	0.0039					613	15					
6.5	x		0.281	0.0055	0.003	0.0062			0.2344	0.0084	-0.0036	0.0092			554	33	59	36.4			
6.5	x		0.287	0.0022		-0.003	0.0036		0.2675	0.0110		0.0117			591	21			0.0368	0.0117	22
6.5	x	x	0.275	0.0119	0.012	0.0121	0.006	-0.0131	0.2312	0.0018	0.0363	0.0111	0.0032	0.0086	650	32	-39	38.4	-0.0032	0.0086	-76
6.5 ^{d)}	x																				46.5
6.5 ^{d)}	x	x																			
6.5		x	0.309	0.0025		-0.026	0.0037	0.0046	0.2482	0.0046					517	18			-0.0174	0.0060	95
6.5	x		0.301	0.0026	0.008	0.0036	-0.021	0.0061	0.2519	0.0066	-0.0037	0.0080			554	51	-37	54.3	-0.0175	0.0107	0
6.5	x	x	0.318	0.0027		-0.008	-0.0037	-0.031	0.0035	0.2902	0.0050				623	1			-0.0420	0.0068	-105
6.5	x	x	0.322	0.0351	-0.004	0.0352	-0.021	-0.0352	0.0371	0.2598	0.0060	0.0363	-0.0078	-0.0020	688	8	-65	7.9	-0.0027	0.0063	-133
6.5 ^{d)}	x																				52.0
6.5 ^{d)}	x	x																			
6.5 ^{d)}	x	x																			

a) data from two curves; one curve too noisy for data analysis

b) data from one curve; two curves too noisy for data analysis

c) no data; all curves show no growth, i.e. 1 mM Zn²⁺ completely suppresses growth of MSSA

d) no data; all curves too noisy for data analysis

Table C-12 (cont'd) Incubation of methicillin-susceptible *S. aureus* (MSSA) with 10 μM $\text{A}\beta_{1-40}$ in presence of Cu^{2+} , Zn^{2+} and cholesterol.

pH	AB	Cu:Zn:Chol.	t_{2x}			Δt_{2x}			OD _{max}			ΔOD_{max}			Δt_{max}			$\Delta\Delta t_{max}$					
			(min)	S.E.M.	w/o-w/ Chol.	H ₂ O- Cu ²⁺ /Zn ²⁺	w/o-w/ AB	S.E.M.	w/o-w/ AB	H ₂ O- Cu ²⁺ /Zn ²⁺	w/o-w/ AB	S.E.M.	w/o-w/ AB	H ₂ O- Cu ²⁺ /Zn ²⁺	w/o-w/ AB	S.E.M.	w/o-w/ AB	H ₂ O- Cu ²⁺ /Zn ²⁺	w/o-w/ Chol.	S.E.M.	w/o-w/ Chol.	H ₂ O- Cu ²⁺ /Zn ²⁺	
7.3			52.28	1.27				0.9692	0.0011						816	7							
7.3 ^a	x		53.90	0.99	-1.63	1.62		0.9635	0.0097	0.0057	0.0098				877	2	-61	7					
7.3	x	x	54.80	0.50		1.37	-2.52	1.0156	0.0041		-0.0464	0.0042			821	4					-5	8	
7.3	x	x	56.82	0.90	-2.02	1.03	-2.91	1.2053	0.0487	-0.1897	0.0489	-0.2418	0.0497		756	37	65	37			121	37	
7.3 ^b		x																					
7.3 ^b	x	x																					
7.3		x	54.40	5.23			-2.12	1.0271	0.0040						812	5							3
7.3 ^a	x	x																					9
7.3	x	x	56.35	1.52			-1.95	1.1555	0.0568						776	24					36	24	44
7.3 ^a	x	x	56.28	0.83	0.07	1.73	-3.29	1.1311	0.0361	0.0244	0.0673	-0.0413	0.0687	0.0742	839	47	-62	53			57	81	60
7.3 ^b		x																					
7.3 ^b	x	x																					
7.0			51.34	0.36				0.9339	0.0133						739	32							
7.0 ^a	x		51.21		0.13			0.9576		-0.0237					835		-95						
7.0	x	x	50.24	0.62		0.72	1.10	0.9869	0.0168			-0.0530	0.0215		783	20					-43	38	
7.0	x	x	51.97	1.80	-1.73	1.91	-0.76	1.0286	0.0049	-0.0417	0.0175	-0.0710			788	9	-5	22			47		
7.0 ^a		x																					
7.0 ^a	x	x																					
7.0		x	51.25	1.76			0.09	1.0208	0.0069						849	1							-109
7.0	x	x	54.29	1.56	-3.05	2.35	-3.09	1.0250	0.0110	-0.0043	0.0130				884	41	-35	41					-49
7.0	x	x	49.87	1.32		1.36	1.38	1.0784	0.0102			-0.0576	0.0123		823	8					25	8	-41
7.0	x	x	52.92	2.97	-3.05	3.25	1.37	1.1288	0.0419	-0.0504	0.0431	-0.1038	0.0433	-0.1002	747	37	76	38			137	56	41
7.0 ^a		x																					
7.0 ^a	x	x																					
6.5			47.39	0.71				0.9155	0.0150						759	3							
6.5	x		50.13	0.05	-2.74	0.71		0.9656	0.0123	-0.0501	0.0194				858	39	-99	39					
6.5	x	x	51.12	1.16		1.36	-3.73	0.9892	0.0026			-0.0737	0.0152		834	21					-75	21	
6.5	x	x	45.29	0.67	5.83	1.34	4.85	0.9755	0.0296	0.0140	0.0298	-0.0096	0.0321		798	31	36	37			60	50	
6.5 ^a		x																					
6.5 ^a	x	x																					
6.5		x	47.11	0.20			0.28	1.0176	0.0095						886	29					-0.1021	0.0177	-127
6.5	x	x	49.69	0.84	-2.59	0.86	0.44	1.0175	0.0104	0.0003	0.0141				867	50	19	58			-0.0517	0.0161	-10
6.5	x	x	51.41	0.34		0.39	-4.30	1.0678	0.0210			-0.0501	0.0230		804	3					82	29	63
6.5	x	x	43.83	1.71	7.58	1.75	5.86	1.0676	0.0221	0.0003	0.0305	-0.0503	0.0244		724	19	80	19			143	53	74
6.5 ^a		x																					
6.5 ^a	x	x																					

a) data from two curves; one curve too noisy for data analysis
 b) data from one curve; two curves too noisy for data analysis
 c) no data; all curves show no growth, i.e. 1 mM Zn²⁺ completely suppresses growth of MSSA
 d) no data; all curves too noisy for data analysis

Table C-12 (cont'd) Incubation of methicillin-susceptible *S. aureus* (MSSA) with 10 μM $\text{A}\beta_{1-40}$ in presence of Cu^{2+} , Zn^{2+} and cholesterol.

Conditions			OD _{12h}			ΔOD_{12h}			$t_{\text{Stop-max}}$			$\Delta t_{\text{Stop-max}}$			
pH	$\text{A}\beta$	Cu: Zn: Chol.	(a.u.)	S.E.M.	w/o - w/ $\text{A}\beta$	$\text{H}_2\text{O} - \text{Cu}^{2+}/\text{Zn}^{2+}$	\pm Error	w/o - w/ Chol.	(min)	S.E.M.	w/o - w/ $\text{A}\beta$	$\text{H}_2\text{O} - \text{Cu}^{2+}/\text{Zn}^{2+}$	\pm Error	w/o - w/ Chol.	\pm Error
7.3			0.4642	0.0057					615	7.6					
7.3 ^{a)}	x		0.4407	0.0040	0.0236	0.0069			625	0.0	-10.0	-90.0	7.6		
7.3		x	0.3401	0.0149		0.1242	0.0159		705	5.0				9.1	
7.3	x	x	0.3945	0.0474	-0.0545	0.0497	0.0476		702	4.4	3.3	-76.7	6.7	4.4	
7.3 ^{d)}		x													
7.3 ^{e)}	x	x													
7.3		x	0.5031	0.0050				-0.0389	630	13.2				-15.0	15.3
7.3 ^{d)}	x	x													
7.3 ^{e)}	x	x													
7.3	x	x	0.3618	0.0141		0.1414	0.0149	-0.0217	707	4.4		-76.7	13.9	-1.7	6.7
7.3 ^{d)}	x	x	0.3473	0.0026	0.0145	0.0143	-0.0279	0.0470	712	2.5	-5.8	-94.2	10.4	-10.8	5.1
7.3 ^{e)}		x													
7.3 ^{d)}	x	x													
7.0			0.5006	0.0068					603	1.7					
7.0 ^{b)}	x		0.4937		0.0069				590		13.3				
7.0		x	0.3407	0.0231		0.1599	0.0240		698	8.8		-95.0	9.0		
7.0	x	x	0.2566	0.0189	0.0841	0.0298	0.2372		718	6.7	-20.0	-128.3			
7.0 ^{d)}		x													
7.0 ^{e)}	x	x													
7.0		x	0.5100	0.0025				-0.0095	618	6.0				-15.0	6.2
7.0	x	x	0.4869	0.0070	0.0231	0.0075		0.0068	625	7.6	-6.7		9.7	-35.0	
7.0	x	x	0.4005	0.0319		0.1096	0.0320	-0.0598	688	9.3		-70.0	11.0	10.0	12.8
7.0	x	x	0.2702	0.0233	0.1303	0.0395	0.2168	0.0243	725	14.4	-36.7	-100.0	16.3	-6.7	15.9
7.0 ^{d)}		x													
7.0 ^{e)}	x	x													
6.5			0.4570	0.0030					598	1.7					
6.5	x		0.4544	0.0072	0.0026	0.0078			603	1.7	-5.0		2.4		
6.5		x	0.3033	0.0071		0.1537	0.0077		707	6.7		-108.3	6.9		
6.5	x	x	0.1792	0.0272	0.1242	0.0281	0.2752	0.0282	740	10.0	-33.3	-136.7	10.1		
6.5 ^{d)}		x													
6.5 ^{e)}	x	x													
6.5		x	0.4808	0.0060				-0.0237	617	1.7				-18.3	2.4
6.5	x	x	0.4667	0.0101	0.0141	0.0117		-0.0123	627	4.4	-10.0		4.7	-23.3	4.7
6.5		x	0.2989	0.0093		0.1819	0.0110	0.0044	717	1.7		-100.0	2.3	-10.0	6.9
6.5	x	x	0.1368	0.0039	0.1621	0.0100	0.3299	0.0108	762	1.7	-45.0	-135.0	4.7	-21.7	10.1
6.5 ^{d)}		x													
6.5 ^{e)}	x	x													

a) data from two curves; one curve too noisy for data analysis

b) data from one curve; two curves too noisy for data analysis

c) no data; all curves show no growth, i.e. 1 mM Zn^{2+} completely suppresses growth of MSSA

d) no data; all curves too noisy for data analysis

Table C-12 (cont'd) Incubation of methicillin-susceptible *S. aureus* (MSSA) with 10 μM $\text{A}\beta_{1-40}$ in presence of Cu^{2+} , Zn^{2+} and cholesterol.

Conditions			$t_{\text{OD}_{\text{max}}}$				$\Delta t_{\text{OD}_{\text{max}}}$				$\Delta \text{OD}_{\text{Final}}$			
pH	$\text{A}\beta$	Cu: Zn: Chol.	(min)	S.E.M.	w/o - w/AB	\pm Error	H ₂ O- Cu ²⁺ /Zn ²⁺	\pm Error	w/o - w/Chol.	\pm Error	H ₂ O- Cu ²⁺ /Zn ²⁺	\pm Error	w/o - w/Chol.	\pm Error
7.3			1377	25										
7.3 ^{a)}	x		1405	0	-28	24.5								
7.3	x		1427	2			-50	24.6						
7.3	x	x	1360	40	67	40.4	45	40.4						
7.3 ^{d)}	x		--	--	--	--	--	--						
7.3 ^{d)}	x	x	--	--	--	--	--	--						
7.3		x	1350	8					27	25.7				
7.3 ^{e)}	x		--	--	--	--	--	--						
7.3 ^{e)}	x	x	--	--	--	--	--	--						
7.3	x		1387	19			-37	20.7	40	19.3				
7.3 ^{e)}	x	x	1417	8	-31	20.6	-23	20.4	-58	41.1				
7.3 ^{d)}	x	x	--	--	--	--	--	--	--	--				
7.3 ^{d)}	x	x	--	--	--	--	--	--	--	--				
7.0			1288	10										
7.0 ^{b)}	x		1345	--	-57	--								
7.0	x		1417	8			-128	13.1						
7.0	x	x	1420	8	-3	11.3	-75	--						
7.0 ^{d)}	x		--	--	--	--	--	--						
7.0 ^{d)}	x	x	--	--	--	--	--	--						
7.0		x	1370	0					-82	10.1				
7.0	x		1417	6	-47	6.0			-72	--				
7.0	x	x	1425	0			-55	0.0	-8	8.3				
7.0	x	x	1423	2	2	1.7	-7	6.2	-3	7.8				
7.0 ^{d)}	x	x	--	--	--	--	--	--	--	--				
7.0 ^{d)}	x	x	--	--	--	--	--	--	--	--				
6.5			1372	13										
6.5	x		1412	12	-40	18.0								
6.5	x	x	1425	0			-53	13.3						
6.5	x	x	1428	3	-3	3.3	-17	12.5						
6.5 ^{d)}	x		--	--	--	--	--	--						
6.5 ^{d)}	x	x	--	--	--	--	--	--						
6.5		x	1403	17					-32	21.3				
6.5	x		1422	2	-18	16.8			-10	12.1				
6.5	x	x	1427	4			-23	17.2	-2	4.4				
6.5	x	x	1412	14	15	14.3	10	13.7	17	14.0				
6.5 ^{d)}	x	x	--	--	--	--	--	--	--	--				
6.5 ^{d)}	x	x	--	--	--	--	--	--	--	--				

a) data from two curves; one curve too noisy for data analysis

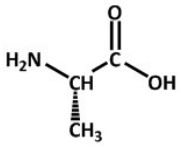
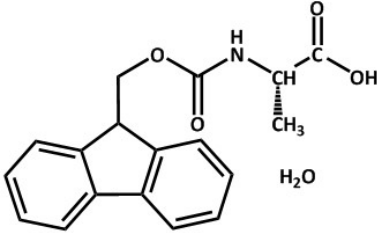
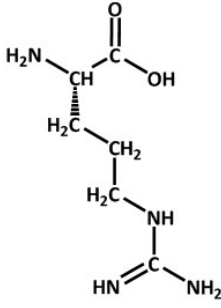
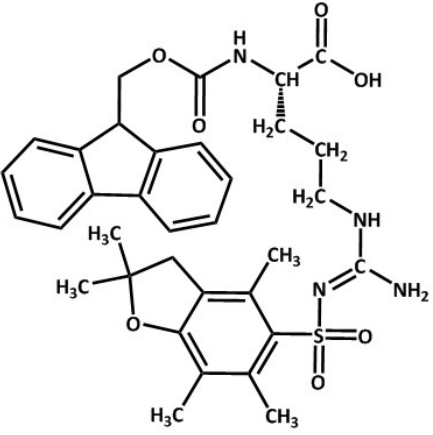
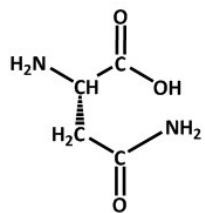
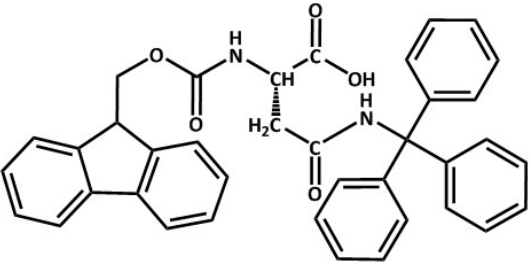
b) data from one curve; two curves too noisy for data analysis

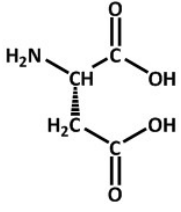
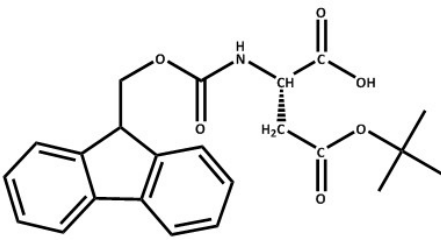
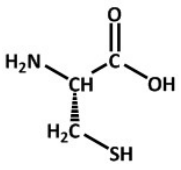
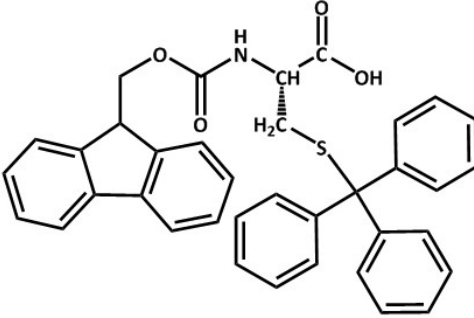
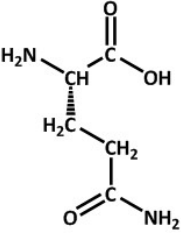
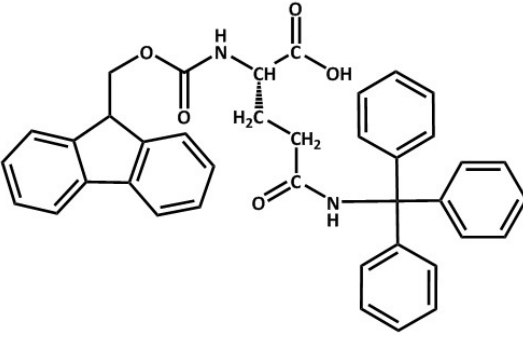
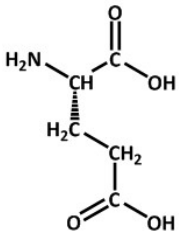
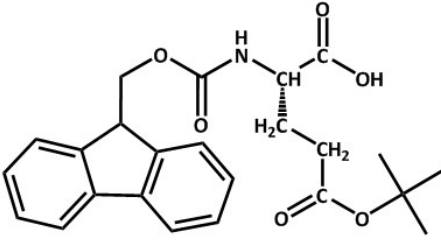
c) no data; all curves show no growth, i.e. 1 mM Zn²⁺ completely suppresses growth of MSSA

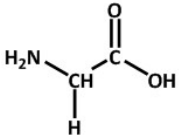
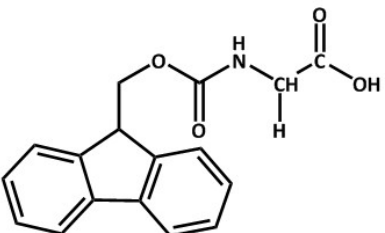
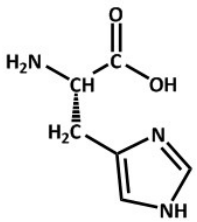
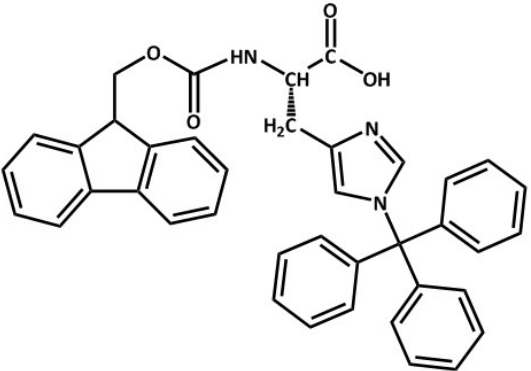
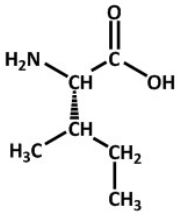
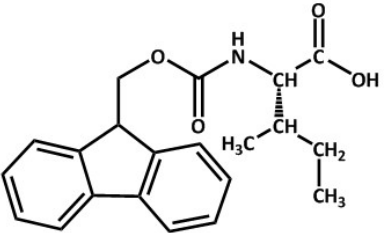
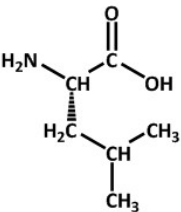
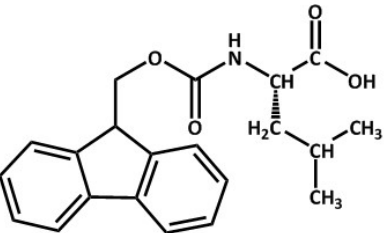
d) no data; all curves too noisy for data analysis

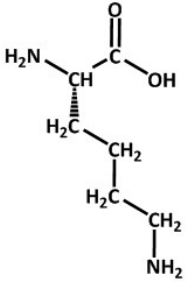
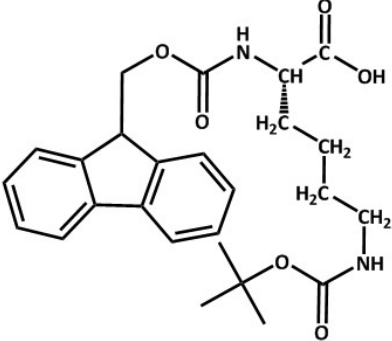
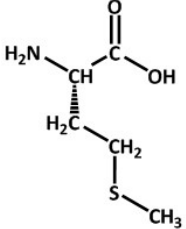
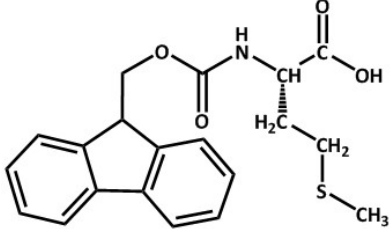
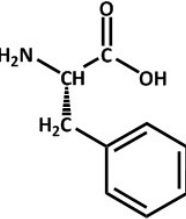
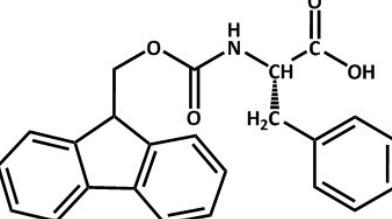
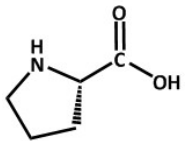
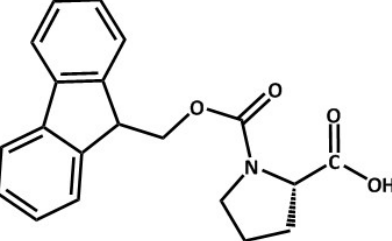
APPENDIX D. AMINO ACIDS

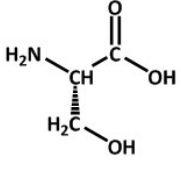
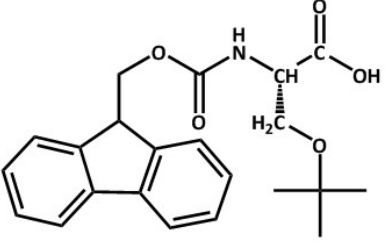
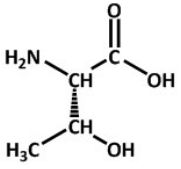
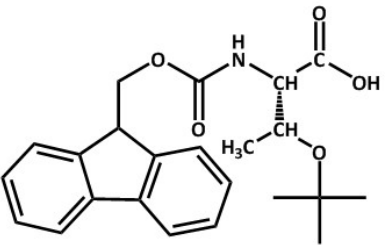
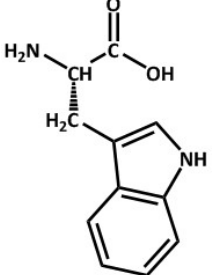
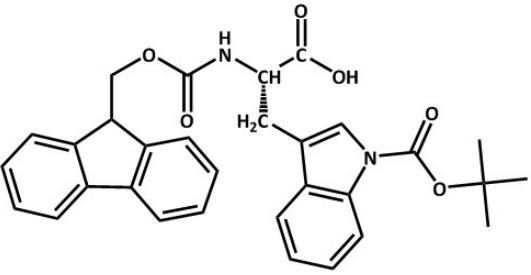
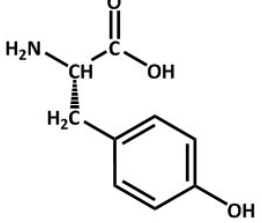
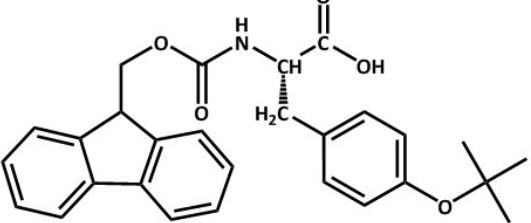
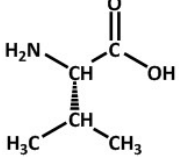
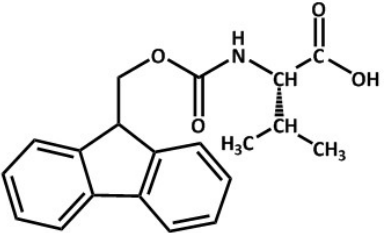
Table D-1 Symbols, structures and masses of amino acids and protected residues.

Residue 3- & 1-Letter Code Short Name of protected residues	Structure of amino acid	Structure of protected amino acid residue	Mass of amino acid/ (-H ₂ O)/ protected residue (g/mol)
L-Alanine Ala, A Fmoc-Ala-OH • H ₂ O			89.095/ 71.079/ 329.3
L-Arginine Arg, R Fmoc- Arg(Pbf)-OH			174.204/ 156.189/ 648.8
L-Asparagine Asn, N Fmoc- Asn(Trt)-OH			132.120/ 114.105/ 596.7

Residue 3- & 1-Letter Code	Structure of amino acid	Structure of protected amino acid residue	Mass of amino acid/ (-H ₂ O)/ protected residue (g/mol)
L-Aspartic Acid Asp, D Fmoc- Asp(OtBu)-OH			133.105/ 115.089/ 411.5
L-Cysteine Cys, C Fmoc-Cys(Trt)- OH			121.159/ 103.145/ 585.7
L-Glutamine Gln, Q Fmoc-Gln(Trt)- OH			146.147/ 128.132/ 610.7
L-Glutamic Acid Glu, E Fmoc- Glu(OtBu)-OH			147.132/ 129.116/ 425.5

Residue 3- & 1-Letter Code	Structure of amino acid	Structure of protected amino acid residue	Mass of amino acid/ (-H ₂ O)/ protected residue (g/mol)
Short Name of protected residues			
Glycine Gly, G Fmoc-Gly-OH			75.068/ 57.052/ 297.3
L-Histidine His, H Fmoc-His(Trt)- OH			155.158/ 137.142/ 619.7
L-Isoleucine Ile, I Fmoc-Ile-OH			131.176/ 113.161/ 353.4
L-Leucine Leu, L Fmoc-Leu-OH			131.176/ 113.161/ 353.4

Residue 3- & 1-Letter Code Short Name of protected residues	Structure of amino acid	Structure of protected amino acid residue	Mass of amino acid/ (-H ₂ O)/ protected residue (g/mol)
L-Lysine Lys, K Fmoc- Lys(Boc)-OH			146.191/ 128.175/ 468.5
L-Methionine Met, M Fmoc-Met-OH			149.213/ 131.198/ 371.5
L-Phenyl- alanine Phe, F Fmoc-Phe-OH			165.194/ 147.178/ 387.4
L-Proline Pro, P Fmoc-Pro-OH			115.133/ 97.118/ 337.4

Residue 3- & 1-Letter Code	Structure of amino acid	Structure of protected amino acid residue	Mass of amino acid/ (-H ₂ O)/ protected residue (g/mol)
Short Name of protected residues			
L-Serine Ser, S Fmoc- Ser(tBu)-OH			105.094/ 87.079/ 383.4
L-Threonine Thr, T Fmoc- Thr(tBu)-OH			119.121/ 101.106/ 397.5
L-Tryptophan Trp, W Fmoc- Trp(Boc)-OH			204.230/ 186.215/ 526.6
L-Tyrosine Tyr, Y Fmoc- Tyr(tBu)-OH			181.193/ 163.178/ 459.6
L-Valine Val, V Fmoc-Val-OH			117.149/ 99.134/ 339.4

APPENDIX E.

PEPTIDE SYNTHESIS CYCLES

Table E-1 Liberty 'Standard – Resin' cycle.

Step	Operation	Parameter	Volume	Drain	Cycles	Pause
1	Clean Reaction Vessel – Unfiltered		10	√	1	
2	Add DMF to Resin		7		1	
3	Add dichloromethane to Resin		7		1	
4	Transfer Resin to Reaction Vessel		10	√	1	
5	Add DMF to Resin		7		1	
6	Add dichloromethane to Resin		7		1	
7	Transfer Resin to Reaction Vessel		10	√	1	
8	Add DMF to Resin		7		1	
9	Add dichloromethane to Resin		7		1	
10	Transfer Resin to Reaction Vessel		10	√	1	
11	Add Reagent	Main Wash (DMF)	5		1	
12	Add Reagent	Secondary Wash (dichloromethane)	5		1	
13	Wait State		900		1	
14	Drain - Filtered			√	1	

Table E-2 Liberty '0.10 – Single' amino acid cycle.

Step	Operation	Parameter	Volume	Drain	Cycles	Pause
1	Clean Resin Dip Tube	Main Wash (DMF)		√	1	
2	Wash - Top	Main Wash (DMF)	7	√	1	
3	Add Deprotection	20% Piperidine w/ 0.1M HOBt	7		1	
4	Microwave Method	Initial Deprotection		√	1	
5	Clean Resin Dip Tube	Main Wash (DMF)		√	1	
6	Add Deprotection	20% Piperidine w/ 0.1M HOBt	7		1	
7	Microwave Method	Deprotection		√	1	
8	Wash - Top	Main Wash (DMF)	7	√	1	
9	Wash - Bottom	Main Wash (DMF)	7	√	1	
10	Wash - Top	Main Wash (DMF)	7	√	1	
11	Clean Resin Dip Tube	Main Wash (DMF)		√	1	
12	Wash - Top	Main Wash (DMF)	7	√	1	
13	Add Amino Acid		2.5		1	
14	Add Activator	HBTU	1		1	
15	Add Activator Base	DIEA	0.5		1	
16	Microwave Method	Coupling		√	1	

Table continued on next page.

Step	Operation	Parameter	Volume	Drain	Cycles	Pause
17	Wash - Top	Main Wash (DMF)	7	√	1	
18	Wash - Bottom	Main Wash (DMF)	7	√	1	
19	Wash - Top	Main Wash (DMF)	7	√	1	

Table E-3 Liberty '0.10' final deprotection cycle.

Step	Operation	Parameter	Volume	Drain	Cycles	Pause
1	Clean Resin Dip Tube	Main Wash (DMF)		√	1	
2	Wash - Top	Main Wash (DMF)	7	√	1	
3	Add Deprotection	20% Piperidine w/ 0.1M HOBt	7		1	
4	Microwave Method	Initial Deprotection		√	1	
5	Clean Resin Dip Tube	Main Wash (DMF)		√	1	
6	Add Deprotection	20% Piperidine w/ 0.1M HOBt	7		1	
7	Microwave Method	Deprotection		√	1	
8	Wash - Top	Main Wash (DMF)	7	√	1	
9	Wash - Bottom	Main Wash (DMF)	7	√	1	
10	Wash - Top	Main Wash (DMF)	7	√	1	

Table E-4 Liberty '0.10 – Cleavage' cycle

Step	Operation	Parameter	Volume	Drain	Cycles	Pause
1	Wash - Top	Secondary Wash (dichloromethane)	7	√	4	
2	Wash - Bottom	Secondary Wash (dichloromethane)	7	√	1	
3	Clean Resin Dip Tube	Secondary Wash (dichloromethane)		√	1	
4	Wash - Top	Secondary Wash (dichloromethane)	7	√	1	
5	Add Cleavage (TFA) – Sample Loop	TFA/TIS/H ₂ O	8		1	
6	Microwave Method	Cleaving 35min			1	
7	Transfer Product Cleaved				1	
8	Add Reagent	Secondary Wash (dichloromethane)	5		1	
9	Transfer Product Cleaved				1	
10	Add Reagent	Secondary Wash (dichloromethane)	5		1	
11	Transfer Product Cleaved				1	
12	Clean Reaction Vessel - Unfiltered		10		3	
13	Reaction Vessel Neutralization		10		3	
14	Wash - Top	Secondary Wash (dichloromethane)	7	√	2	

APPENDIX F. ANALYSIS AND PURIFICATION OF SYNTHESISED PEPTIDES

F.1. $A\beta_{1-40}$

F.1.1. Batch 1

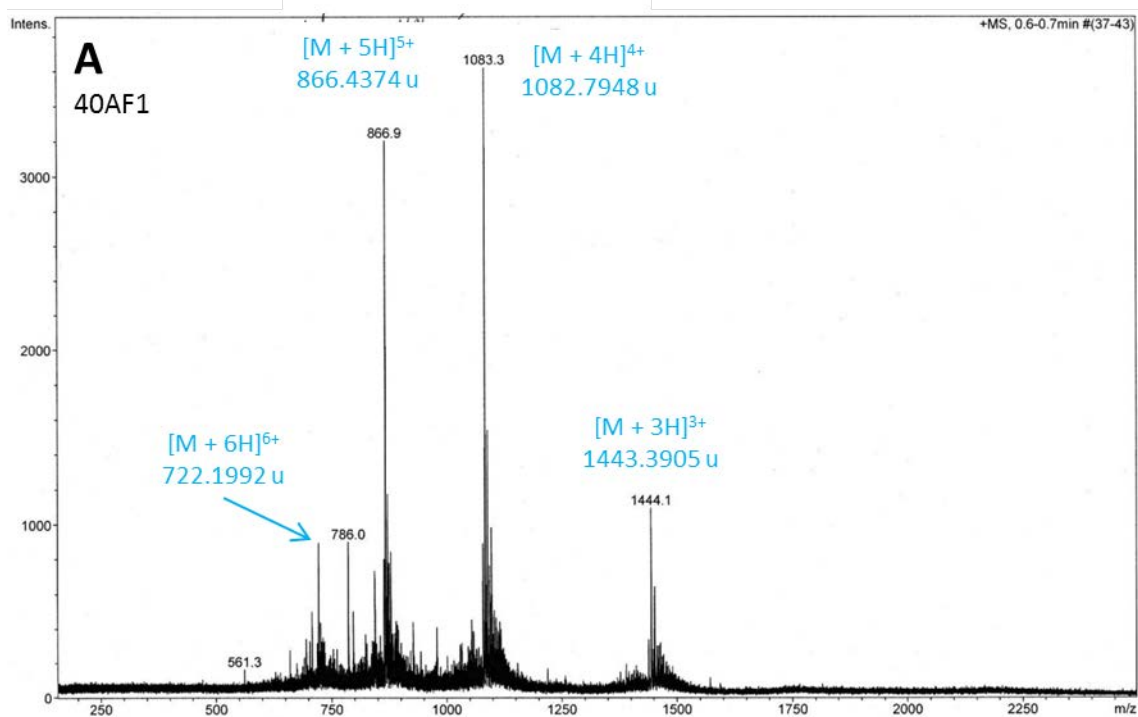


Figure F-1 Purification of $A\beta_{1-40}$ (Batch 1).
Mass spectrum of the first fraction of purified peptide.

F.1.2. Batch 2

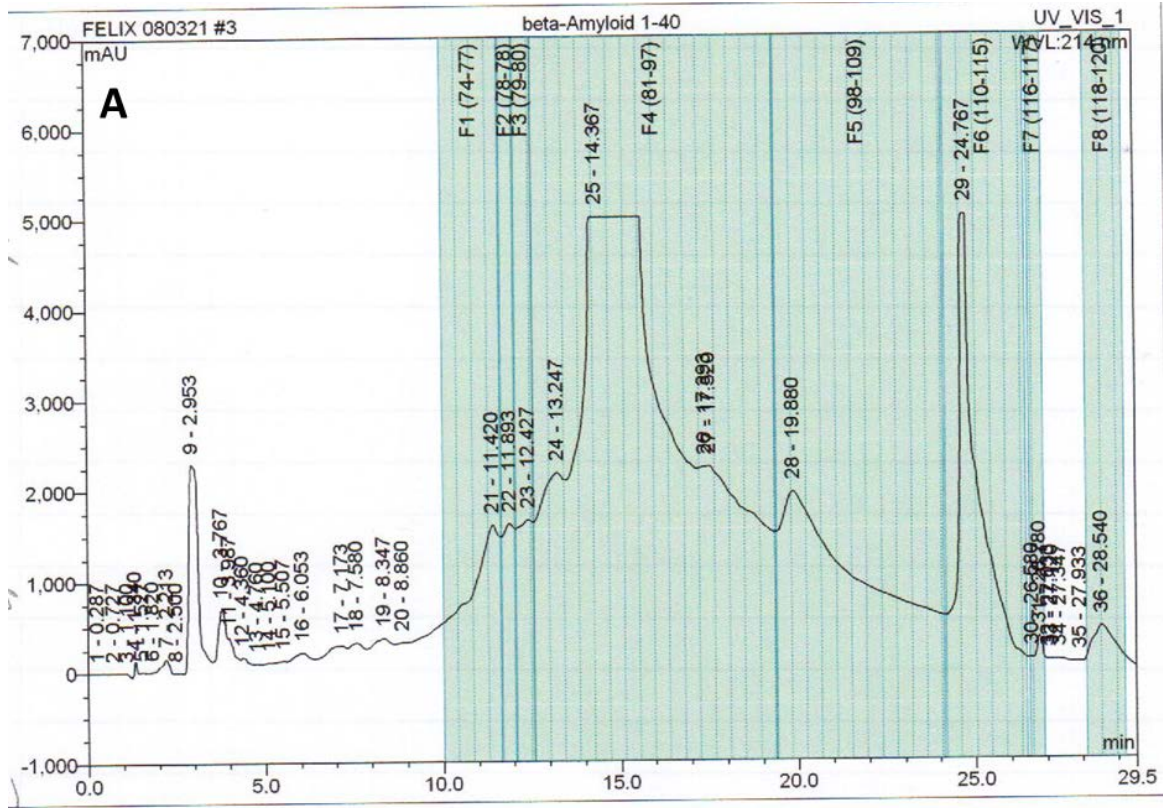


Figure F-2 Analysis and purification of A β ₁₋₄₀ (Batch 2).

Crude peptide was dissolved at 50.3 mg/mL in ultrapurified water and purified by semipreparative HPLC (A): flow rate: 21.240 mL/min, 500 μ L injection volume; gradient (A: ultrapurified water with 0.05% TFA, B: MeCN with 0.05% TFA): 5% B for 2 min, increase to 40% B over 20 min, ramp up to 100% B in 2 min, keep constant for 4 min, ramp down to 5% B in 2 min, equilibrate for 2 min. Green areas indicate collected fractions; vertical lines inside green areas indicate tube changes, with tube #s labelled in parentheses above peaks. Tubes #85 and #111 were analysed by MS (see B & C). Figure continued on next page.

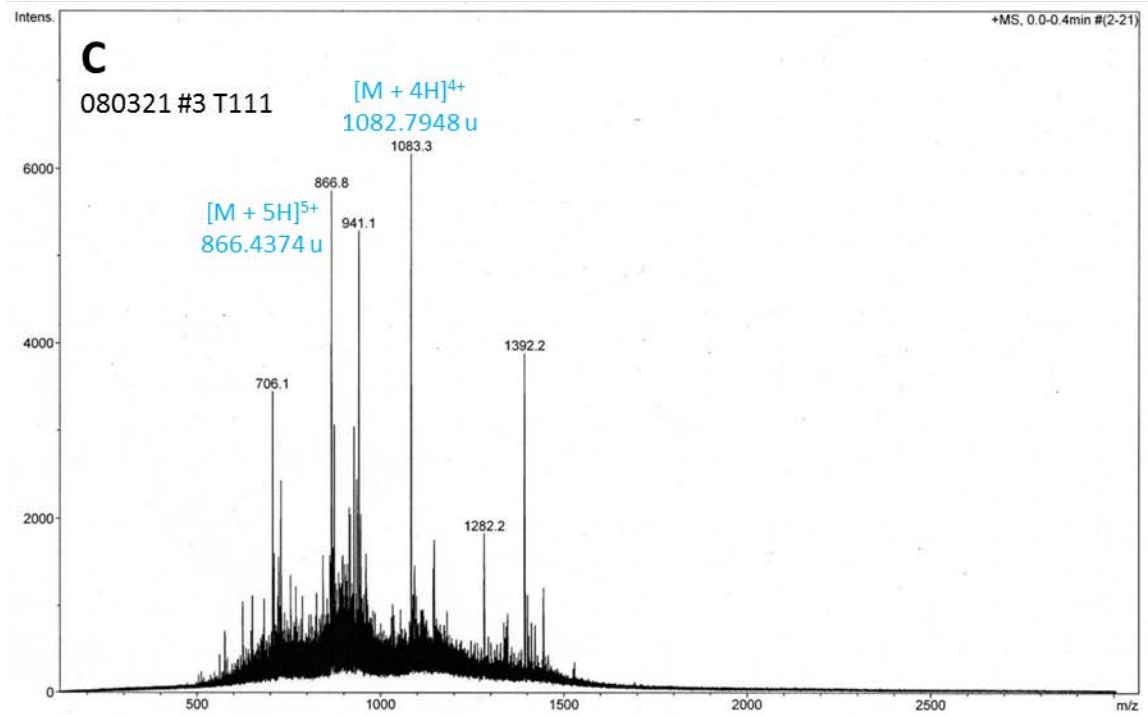
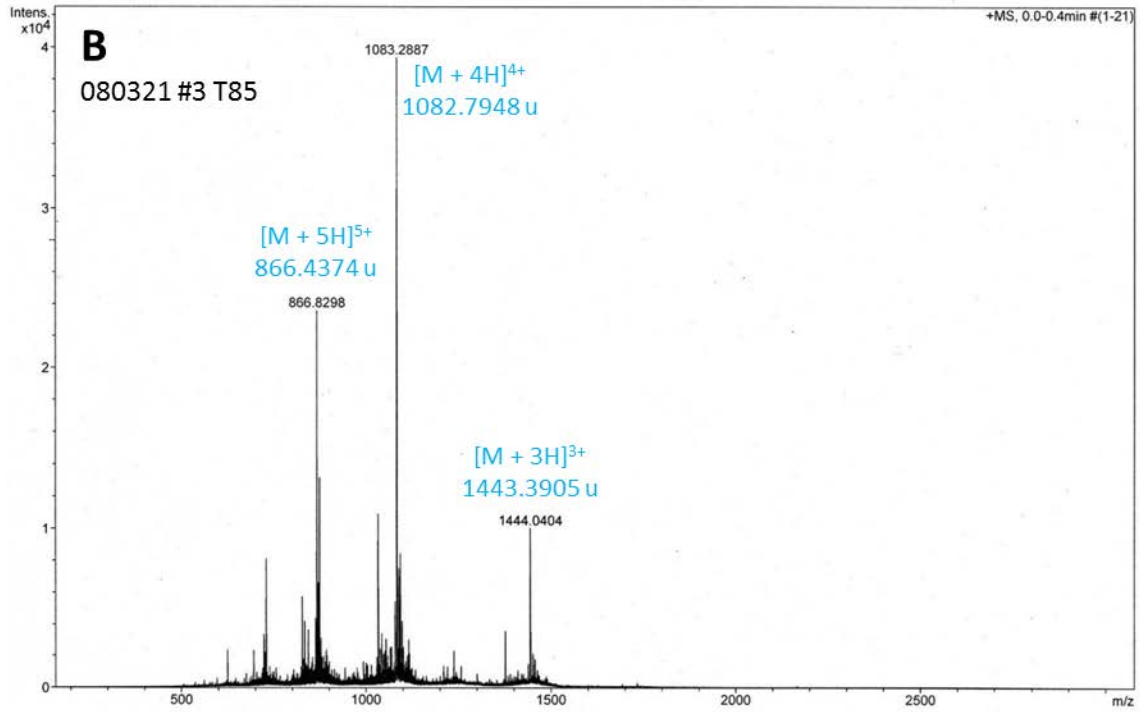


Figure F-2 Analysis and purification of A β ₁₋₄₀ (Batch 2); continued.

Mass Spectra of tubes #85 (B) and #111 (C); tube #85 shows mainly product in the spectrum, whereas tube #111 has a considerably larger background.

F.1.3. Batch 3

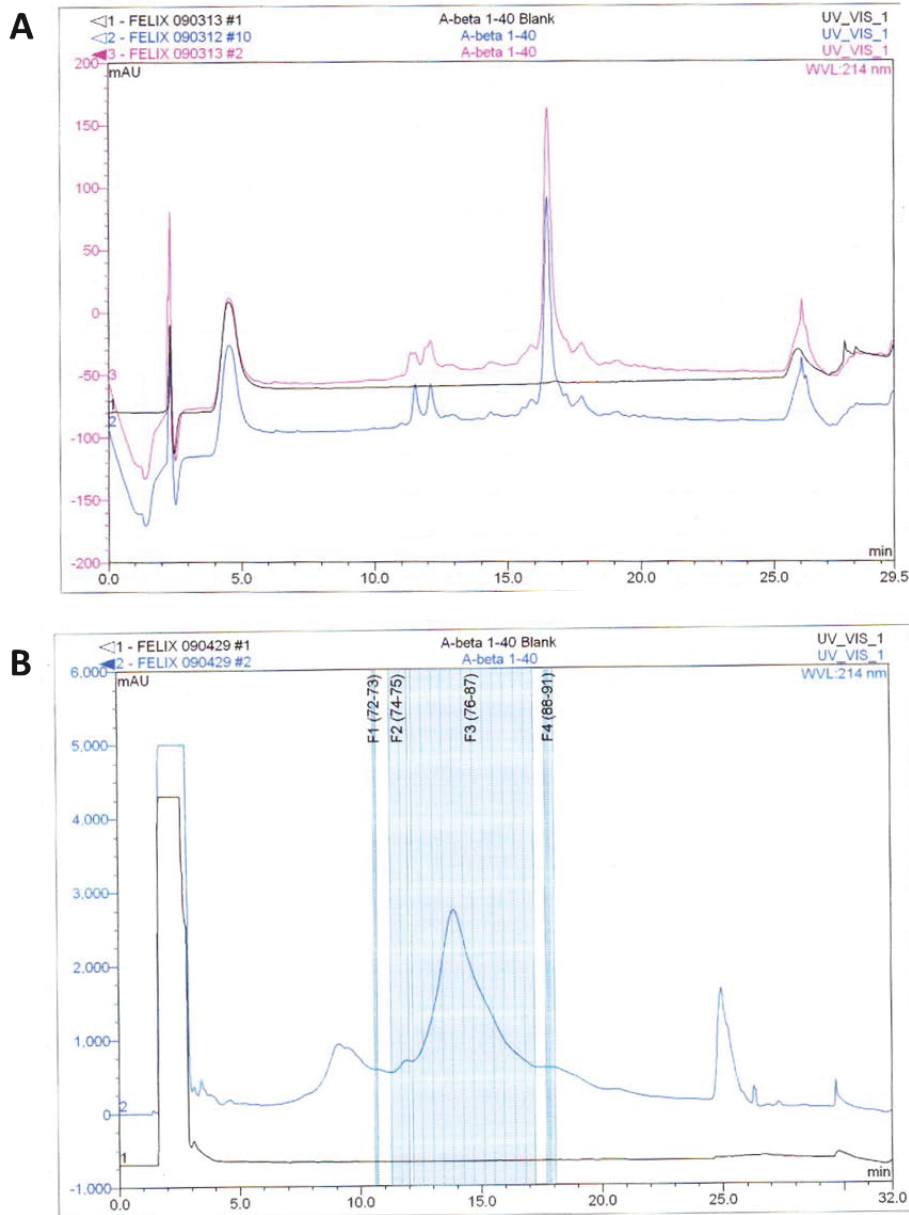


Figure F-3 Analysis and purification of Aβ₁₋₄₀ (Batch 3).

An unknown amount of crude peptide (tip of spatula of wet precipitate) was dissolved in 1:1 MeCN : ultrapurified water (with 0.025% TFA) and analysed by analytical HPLC (A): flow rate: 1 mL/min, 5 µL injection volume; gradient (A: ultrapurified water with 0.05% TFA, B: acetonitrile with 0.05% TFA): 5% B for 2 min, increase to 25% B over 20 min, ramp up to 95% B in 2 min, keep constant for 4 min, ramp down to 5% B in 2 min, equilibrate for 2 min. Black trace shows background (H₂O), blue trace the peptide. For purification, lyophilised crude peptide was dissolved at 50.875 mg/mL in DMSO and purified by semiprep HPLC (B): flow rate: 21.240 mL/min, 500 µL injection volume; the same mobile phases and gradient as for the analytical run were used. Green areas indicate collected fractions; vertical lines inside green areas indicate tube changes, with tube #s labelled in parentheses above peaks. Tubes #79 & #80 were submitted for MS analysis (C & D). Figure continued on next page.

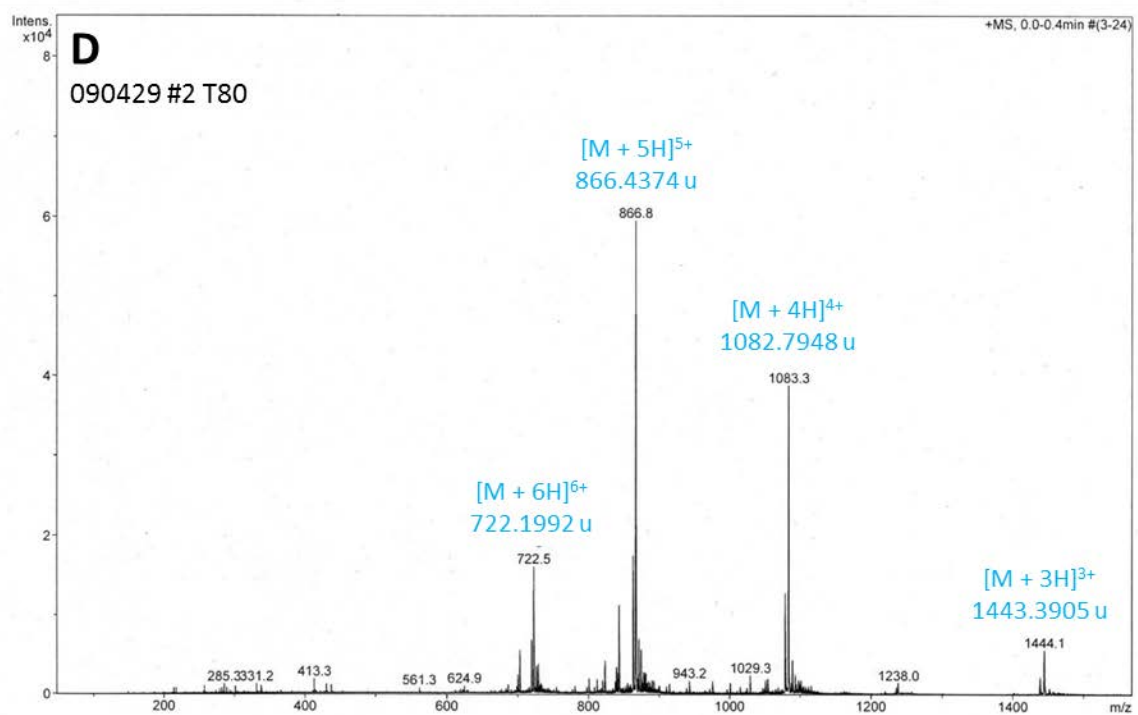
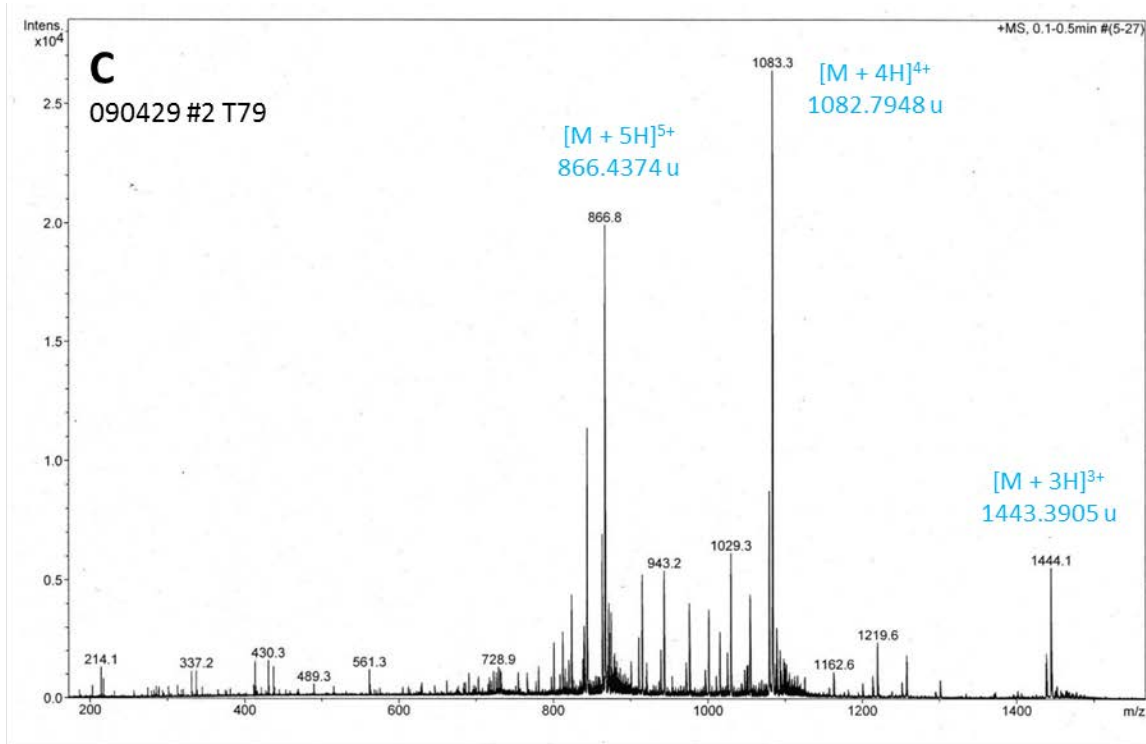


Figure F-3 Analysis and purification of A β ₁₋₄₀ (Batch 3); continued.

Mass Spectra of tubes #79 (C) and #80 (D); both tubes shows mainly product in the spectrum, however, tube #79 has more contaminants.

F.2. A β ₁₋₄₂

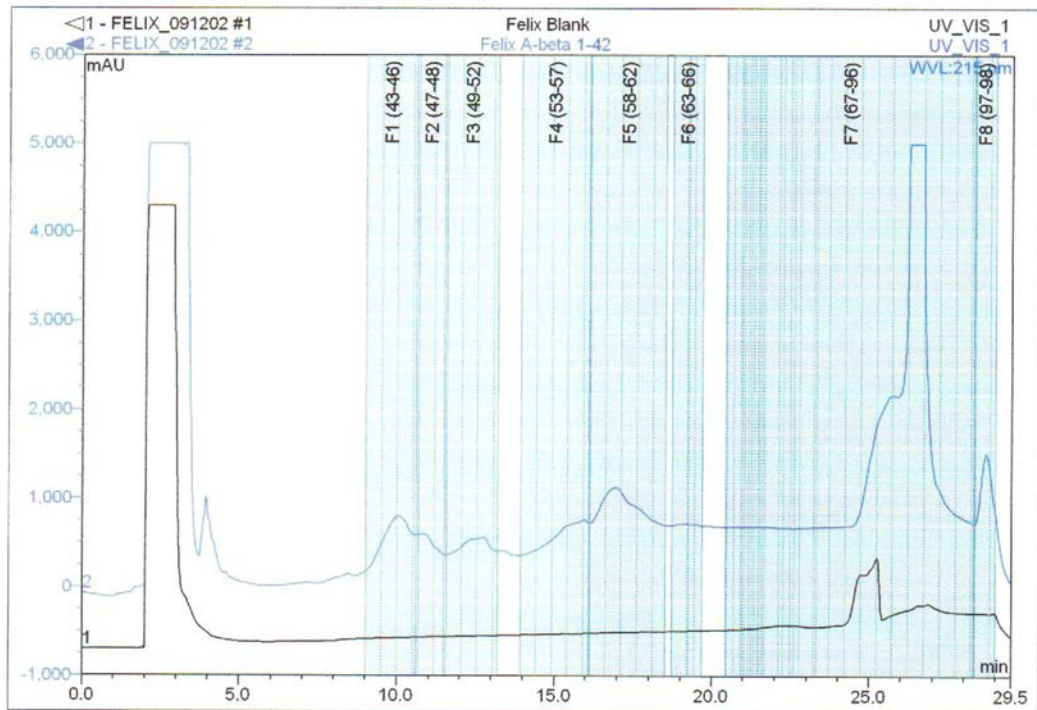


Figure F-4 Purification of A β ₁₋₄₂.

Crude peptide was dissolved at 50.0 mg/mL in ultrapurified water and purified by semipreparative HPLC (A): flow rate: 21.240 mL/min, 500 μ L injection volume; gradient (A: ultrapurified water with 0.05% TFA, B: MeCN with 0.05% TFA): 5% B for 2 min, increase to 40% B over 20 min, ramp up to 100% B in 2 min, keep constant for 4 min, ramp down to 5% B in 2 min, equilibrate for 2 min. Green areas indicate collected fractions; vertical lines inside green areas indicate tube changes, with tube #s labelled in parentheses above peaks.

F.3. A β ₁₋₄₀ K28A

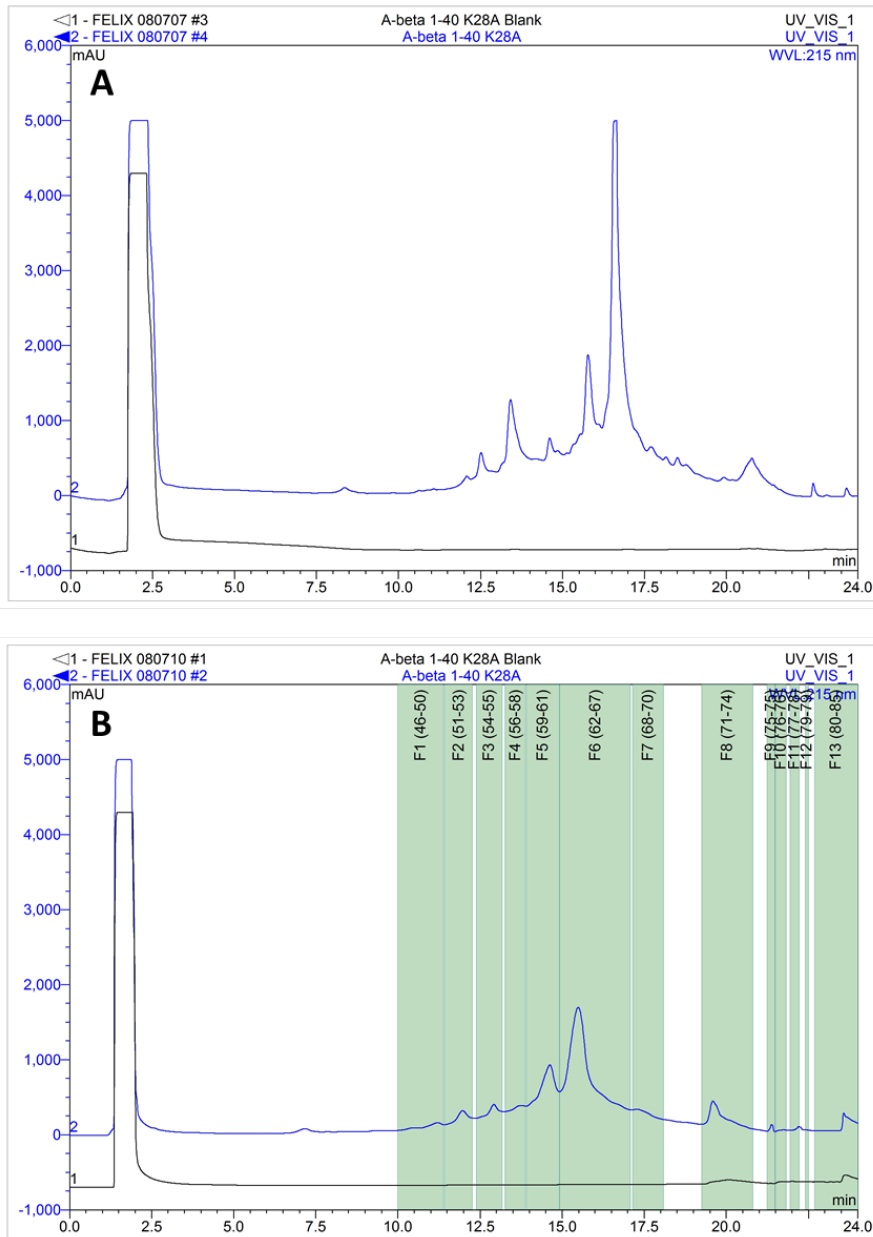


Figure F-5 Purification of A β ₁₋₄₀ K28A.

Crude peptide was dissolved at 30.7 mg/mL in DMSO and analysed by analytical HPLC (A): flow rate: 1 mL/min, 20 μ L injection volume; gradient (A: ultrapurified water with 0.05% TFA, B: acetonitrile with 0.05% TFA): 5% B for 2 min, increase to 25% B over 18 min, ramp up to 95% B in 2 min, keep constant for 4 min, ramp down to 5% B in 2 min, equilibrate for 2 min. Black trace shows background (H₂O), blue trace the peptide. For purification, lyophilised crude peptide was dissolved at 30.7 mg/mL in DMSO and purified by semiprep HPLC (B): flow rate: 21.240 mL/min, 500 μ L injection volume; the same mobile phases and gradient as for the analytical run were used. Green areas indicate collected fractions; vertical lines inside green areas indicate tube changes, with tube #s labelled in parentheses above peaks. Tubes #79 & #80 were submitted for MS analysis (C & D). Figure continued on next page.

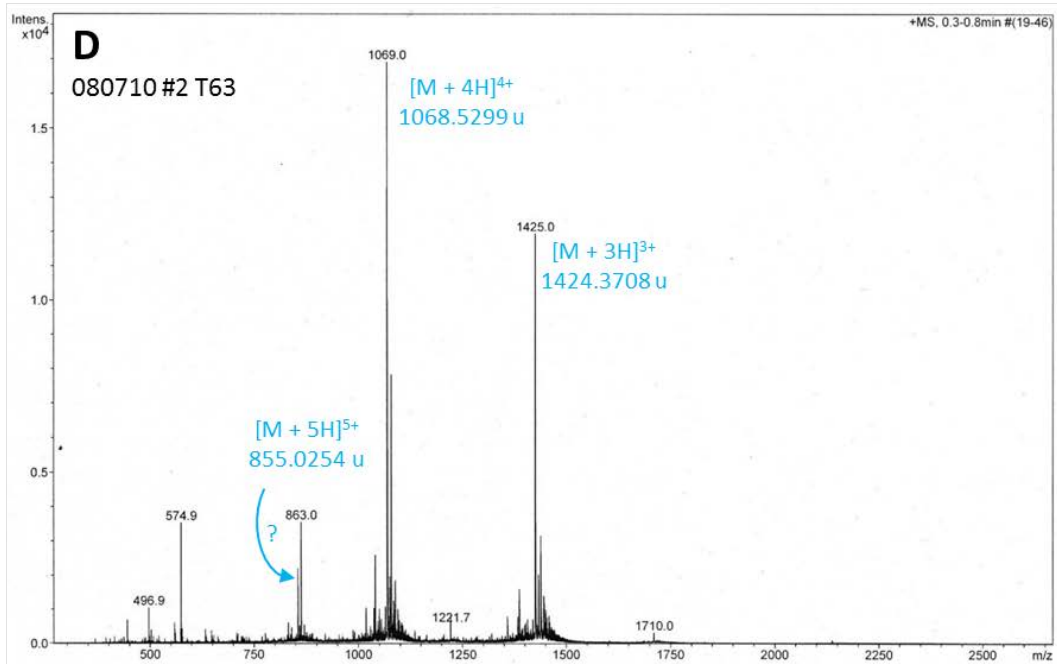
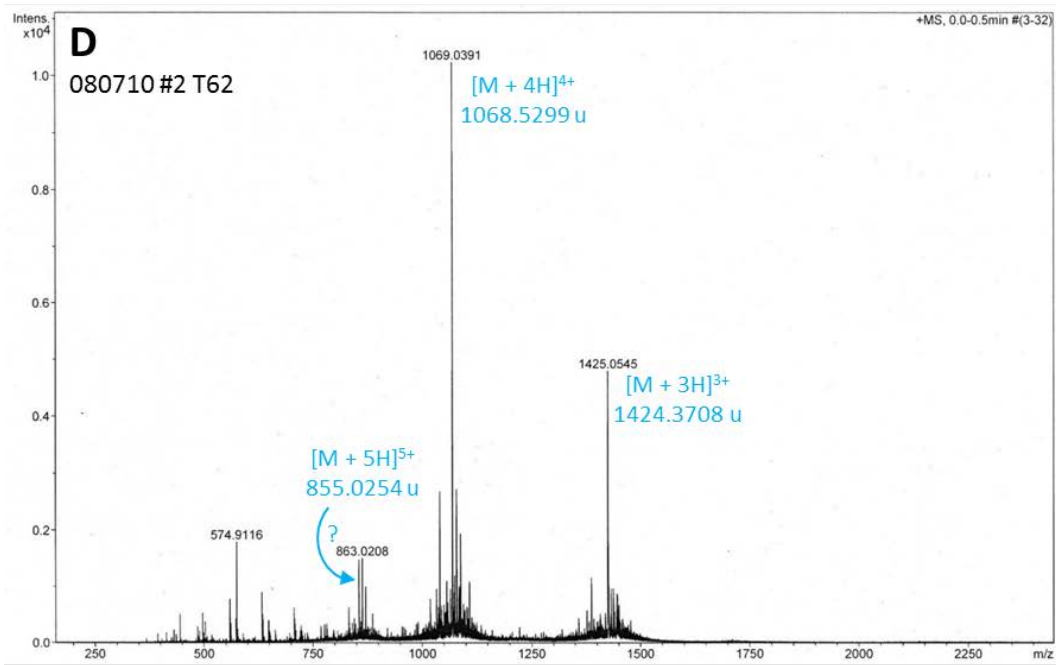


Figure F-5 Purification of A β 1-40 K28A; continued.

Mass Spectra of tubes #62 (C) and #63 (D); both tubes shows mainly product in the spectrum, however, tube #62 has more contaminants.

F.4. A β_{12-17}

F.4.1. Batch 1

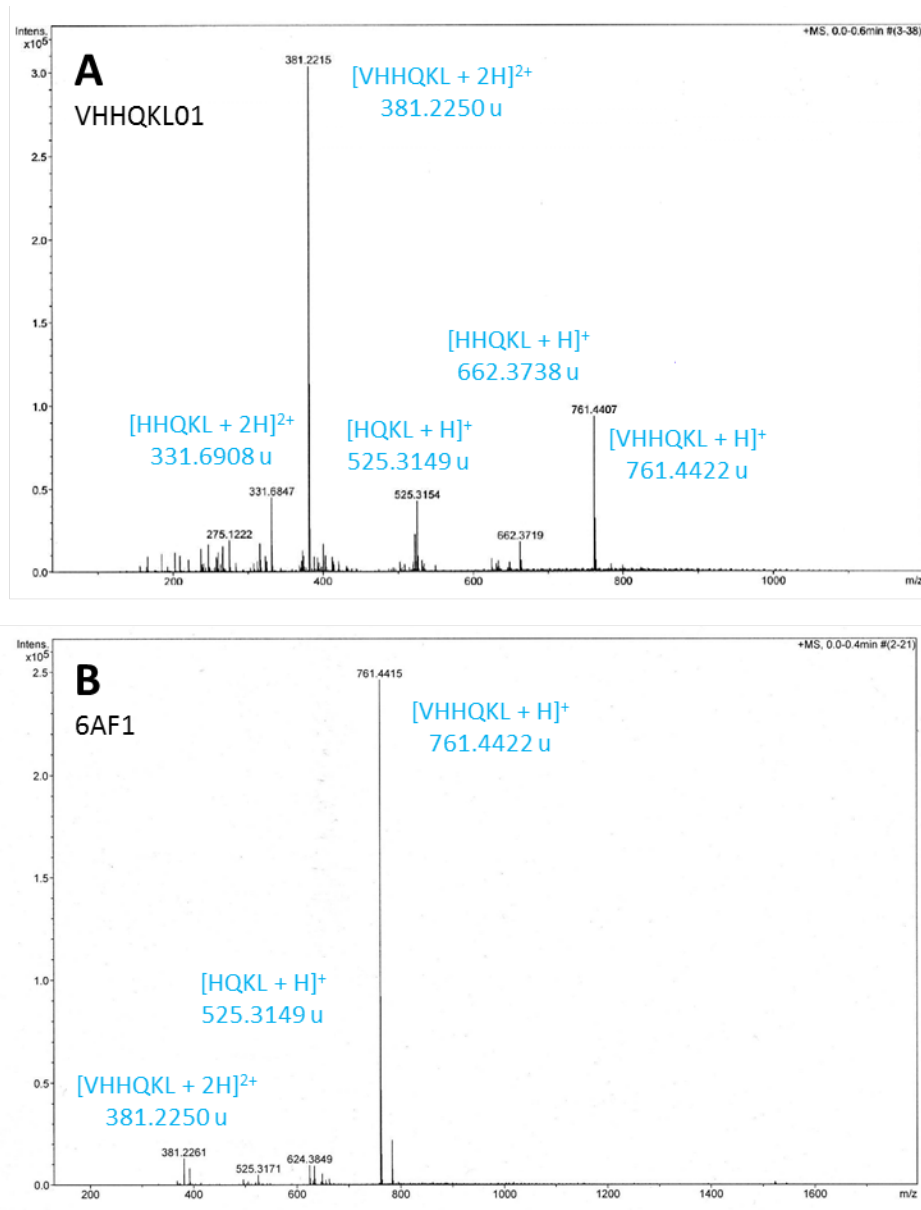


Figure F-6 Abeta₁₂₋₁₇ (Batch 1)

Mass spectrum of the crude (A), and the purified peptide (B) are shown; identified peaks are labelled in blue with ion formula and their respective theoretical monoisotopic mass. .

F.4.2. Batch 2

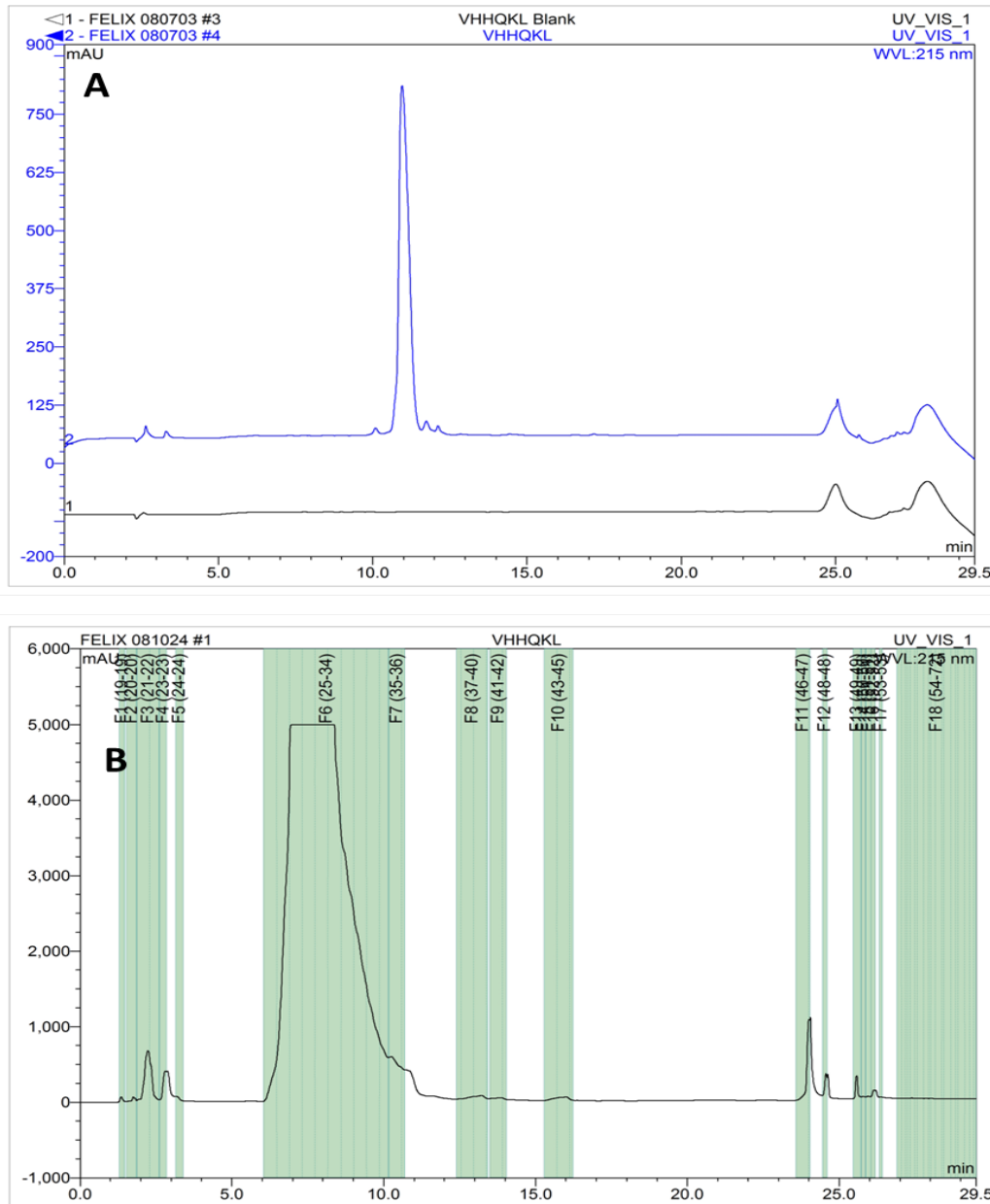


Figure F-7 Purification of A β ₁₂₋₁₇ (Batch 2).

Lyophilised crude peptide was dissolved at 5 mg/mL in ultrapurified water and analysed by analytical HPLC (A): flow rate: 1 mL/min, 5 μ L injection volume; gradient (A: ultrapurified water with 0.05% TFA, B: acetonitrile with 0.05% TFA): 5% B for 2 min, increase to 25% B over 20 min, ramp up to 95% B in 2 min, keep constant for 4 min, ramp down to 5% B in 2 min, equilibrate for 2 min. Black trace shows background (H₂O), blue trace the peptide. For purification, crude peptide was dissolved at 55.0 mg/mL in ultrapurified water and purified by semiprep HPLC (B): flow rate: 21.240 mL/min, 500 μ L injection volume; the same mobile phases and gradient as for the analytical run were used. Green areas indicate collected fractions; vertical lines inside green areas indicate tube changes, with tube #s labelled in parentheses above peaks. Tubes #27 - #30 were lyophilised and re-analysed by HPLC (C) as well as submitted for MS analysis (D). Figure continued on next page.

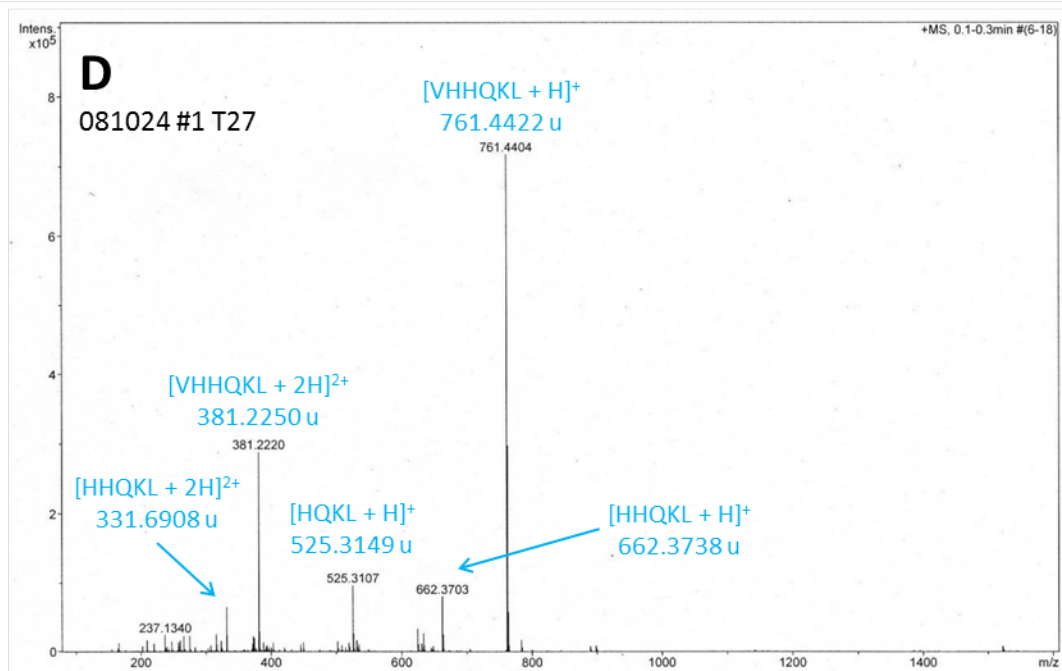
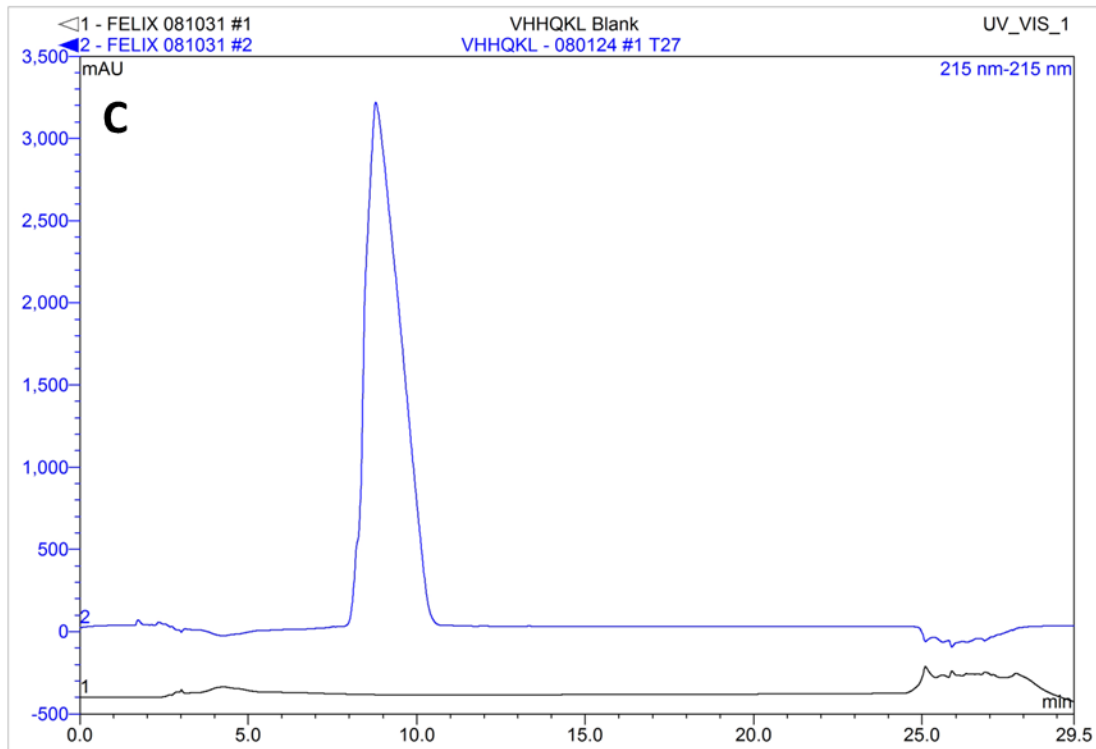


Figure F-7 Purification of A β ₁₂₋₁₇ (Batch 2); continued.

HPLC chromatogram for the re-analysis of tube #27 (C); conditions were the same as in A. The corresponding mass spectrum for tube #27 is shown in (D); identified peaks are labelled in blue with ion formula and their respective theoretical monoisotopic mass. Chromatograms and mass spectra for tubes #28 - #30 looked essentially identical to panels C and D, respectively.

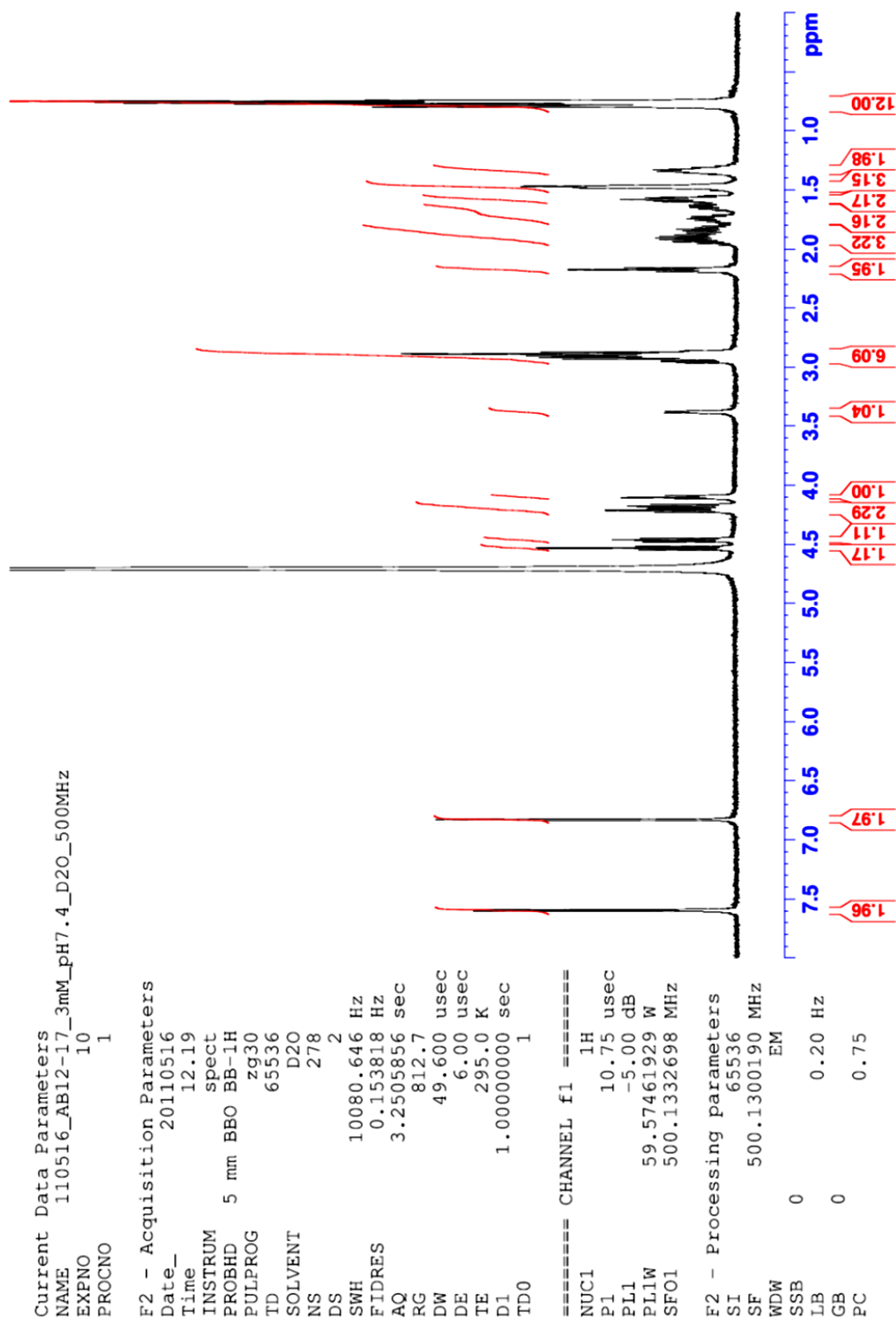


Figure F-8 $^1\text{H-NMR}$ to confirm identity of $\text{A}\beta_{12-17}$ (3 mM in D_2O , pH 7.4, 500 MHz).
 See Table F-1 below for peak assignment.

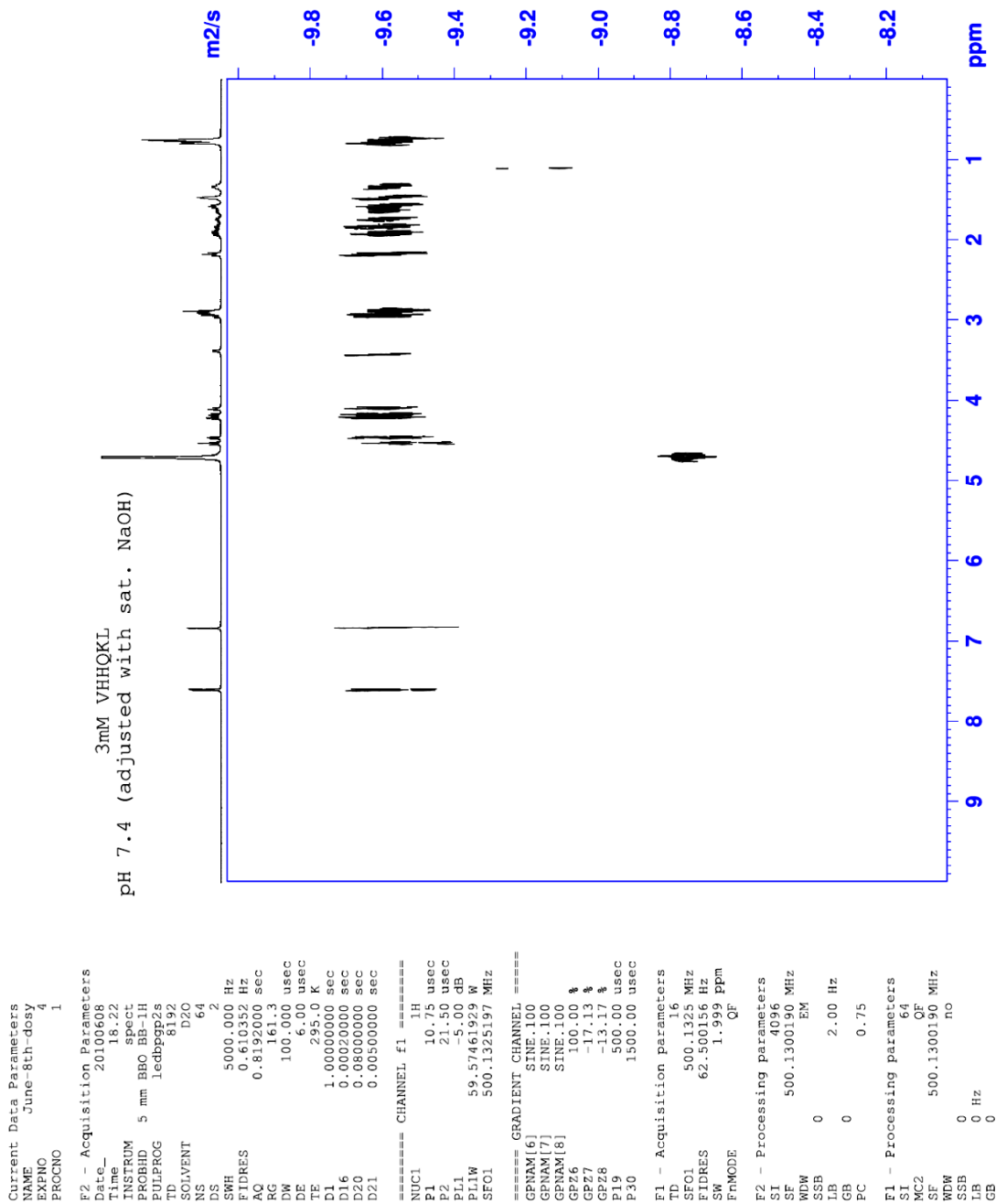


Figure F-9 DOSY-NMR to confirm identity of A β ₁₂₋₁₇ (3 mM in D₂O, pH 7.4, 500 MHz).
 See Table F-1 below for peak assignment.

Table F-1 1H-NMR of A β ₁₂₋₁₇ (3 mM in D₂O, pH 7.4, 500 MHz).

Amino Acid	Parameter	H α		H β	H γ	H δ	H ϵ	Total Integration
Valine	Shift (ppm)	3.38	-	1.80-1.97	0.73-0.80	-	-	
	Integration	1.03	-	*3.21 (1)	*12.00 (6)	-	-	8
	Splitting Pattern	d	-	m	m	-	-	
Histidine (2 \times)	Shift	#4.44-4.47	#4.53	2.86-2.97	-	6.83	7.59	
	Integration	#1.13	#1.17	*6.09 (4)	-	1.97	1.96	10\ddagger
	Splitting Pattern	#m	#t	m	-	d	dd	
Glutamine	Shift	4.15-4.23	-	1.80-1.97	2.18	-	-	
	Integration	*2.29 (1)	-	*3.21 (2)	1.95	-	-	5
	Splitting Pattern	m	-	m	t	-	-	
Lysine	Shift	4.15-4.23	-	1.63-1.79	1.29-1.37	1.58	2.86-2.97	
	Integration	*2.29 (1)	-	2.16	1.98	2.17	*6.09 (2)	9
	Splitting Pattern	m	-	m	m	qn	m	
Leucine	Shift	4.08-4.12	-	1.45-1.49	1.45-1.49	0.73-0.80	-	
	Integration	1.00	-	*3.15 (2)	*3.15 (1)	*12.00 (6)	-	10
	Splitting Pattern	m	-	m	m	m	-	

Total integration of peptide: 42

Notes:

Run in D₂O (a proton-exchangeable solvent) → signals from carboxylic acids, amines, aromatic amines and amides are not observed.

Shifts are given in ppm at the center points of well defined signals (m, d, dd, etc.), ranges are given for multiplets (ie. ppm-ppm)

Splitting pattern legend: m: multiplet, d: doublet, dd: doublet of doublets, t: triplet, qn: quintet
* overlaps with another signal (number inside bracket denotes the proton's contribution to total integration)

#H α are not equivalent for two histidines → two individual signals

\ddagger total integration for both histidines

F.5. VHHQKLA AAA

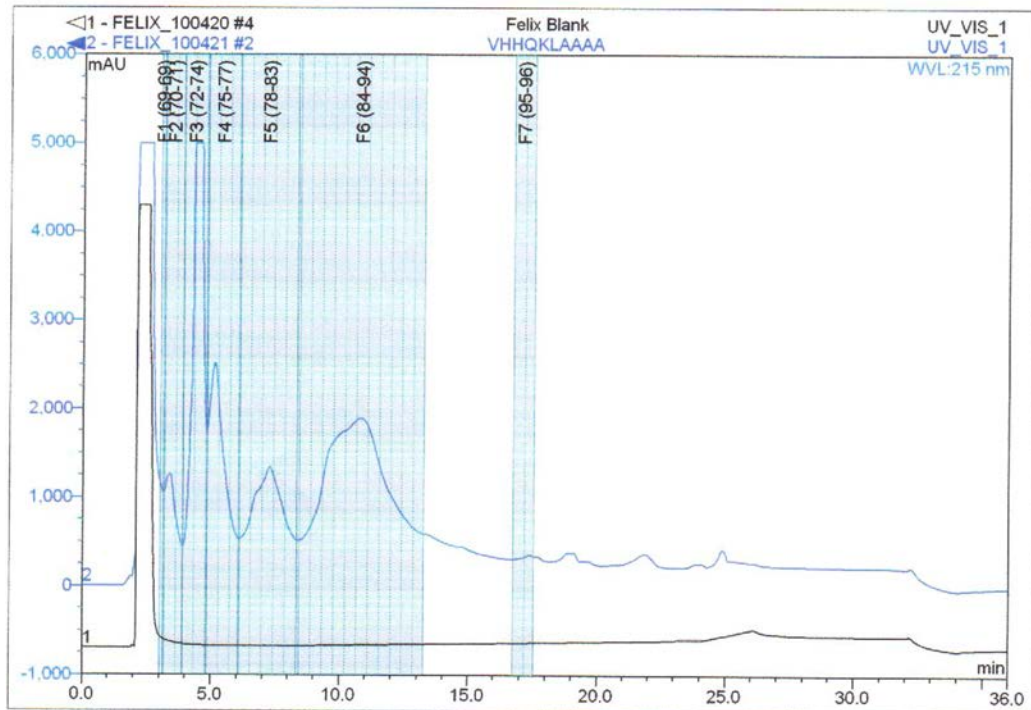


Figure F-10 Purification of VHHQKLA AAA.

Crude peptide was dissolved at 100.0 mg/mL in ultrapurified water and purified by semipreparative HPLC: flow rate: 21.240 mL/min, 165 μ L injection volume; gradient (A: ultrapurified water with 5% MeCN and 0.05% TFA, B: MeCN with 5 % ultrapurified water and 0.05% TFA): 0% B for 2 min, increase to 40% B over 22 min, ramp up to 100% B in 2 min, keep constant for 4 min, ramp down to 5% B in 2 min, equilibrate for 2 min. Green areas indicate collected fractions; vertical lines inside green areas indicate tube changes, with tube #s labelled in parentheses above peaks. Tubes #70, #72 - #76, #79 - #81, #86 - #90 were submitted to MS analysis, but no ions related to the desired product could be identified.

F.6. BBXB Peptides

F.6.1. BBXB A β (YEVHHQKLVF)

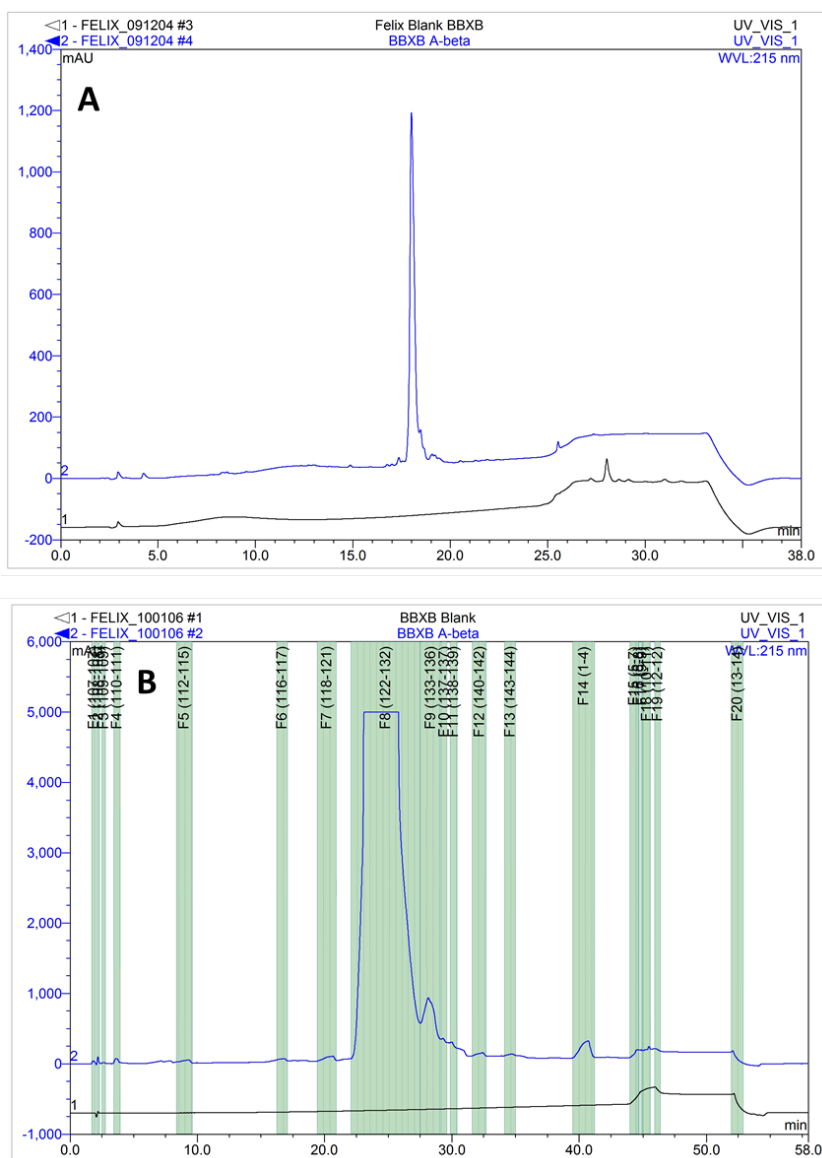


Figure F-11 Purification of BBXB A β .

Crude peptide was dissolved at 50.0 mg/mL in ultrapurified water and analysed by analytical HPLC (A): flow rate: 1 mL/min, 5 μ L injection volume; gradient (A: ultrapurified water with 5% MeCN and 0.05% TFA, B: MeCN with 5% ultrapurified water and 0.05% TFA): 0% B for 2 min, increase to 40% B over 22 min, ramp up to 100% B in 2 min, keep constant for 4 min, ramp down to 0% B in 2 min, equilibrate for 2 min. Black trace shows background (H₂O), blue trace the peptide. For isolation, the same solution was purified by semiprep HPLC (B): flow rate: 21.240 mL/min, 500 μ L injection volume; the same mobile phases as for the analytical run were used, the gradient was increased to 40 minutes. Green areas indicate collected fractions; vertical lines inside green areas indicate tube changes, with tube #s labelled in parentheses above peaks. Tubes #124 - #129 were submitted for MS analysis (C & D). Figure continued on next page.

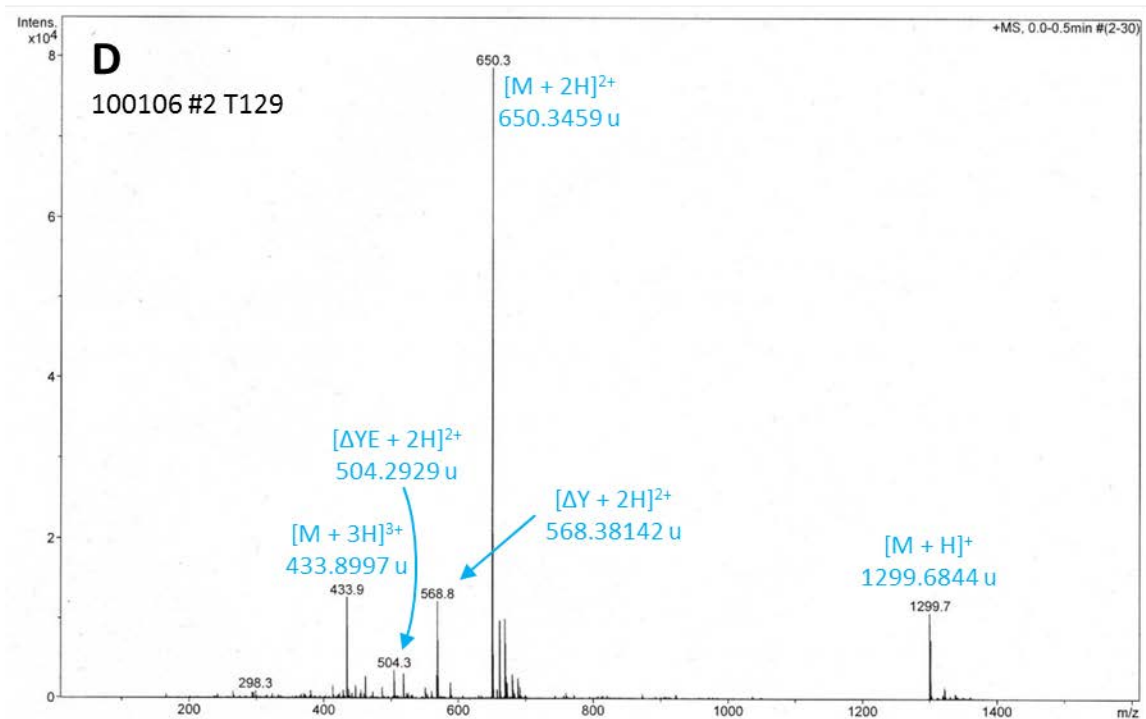
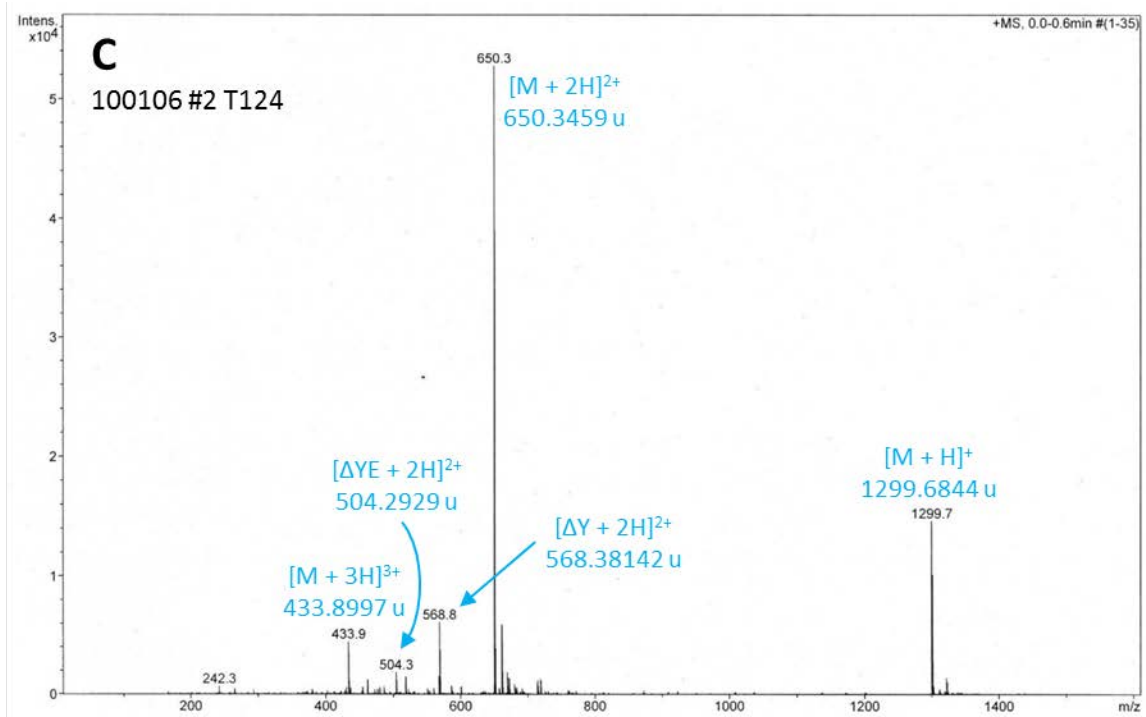


Figure F-11 Purification of BBXB Aβ; continued.

Mass Spectra of tubes #124 (C) and #129 (D); both tubes predominantly show ions related to the product; identified contaminants are deletion peptides missing the last residue (ΔY) and the two last residues (ΔYE), respectively.

F.6.2. BBXB Tau (SDDKKAKGAD)

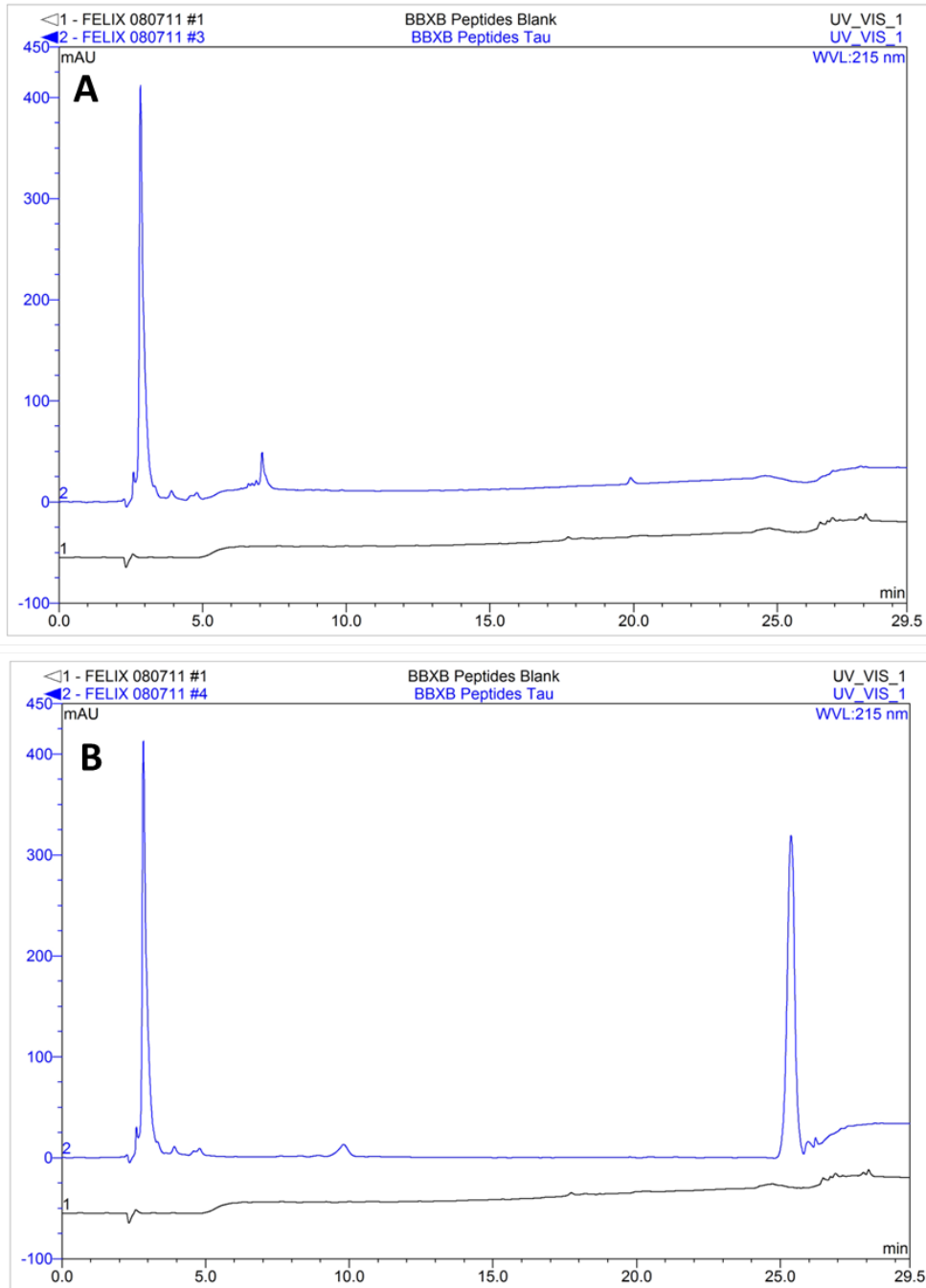


Figure F-12 Purification of BBXB Tau.

Crude peptide was dissolved at 50.0 mg/mL in ultrapurified water and analysed by analytical HPLC: flow rate: 1 mL/min, 5 μ L injection volume; gradient (A: ultrapurified water with 5% MeCN and 0.05% TFA, B: MeCN with 5% ultrapurified water and 0.05% TFA) for (A): 0% B for 2 min, increase to 40% B over 23 min, ramp up to 100% B in 2 min, keep constant for 4 min, ramp down to 0% B in 2 min, equilibrate for 2 min; (B) was run isocratically for 25 min at 5% B followed with a ramp to clean the column. Black trace shows background (H₂O), blue trace the peptide.

F.6.3. BBXB S100 β (GDKHKLKSEL)

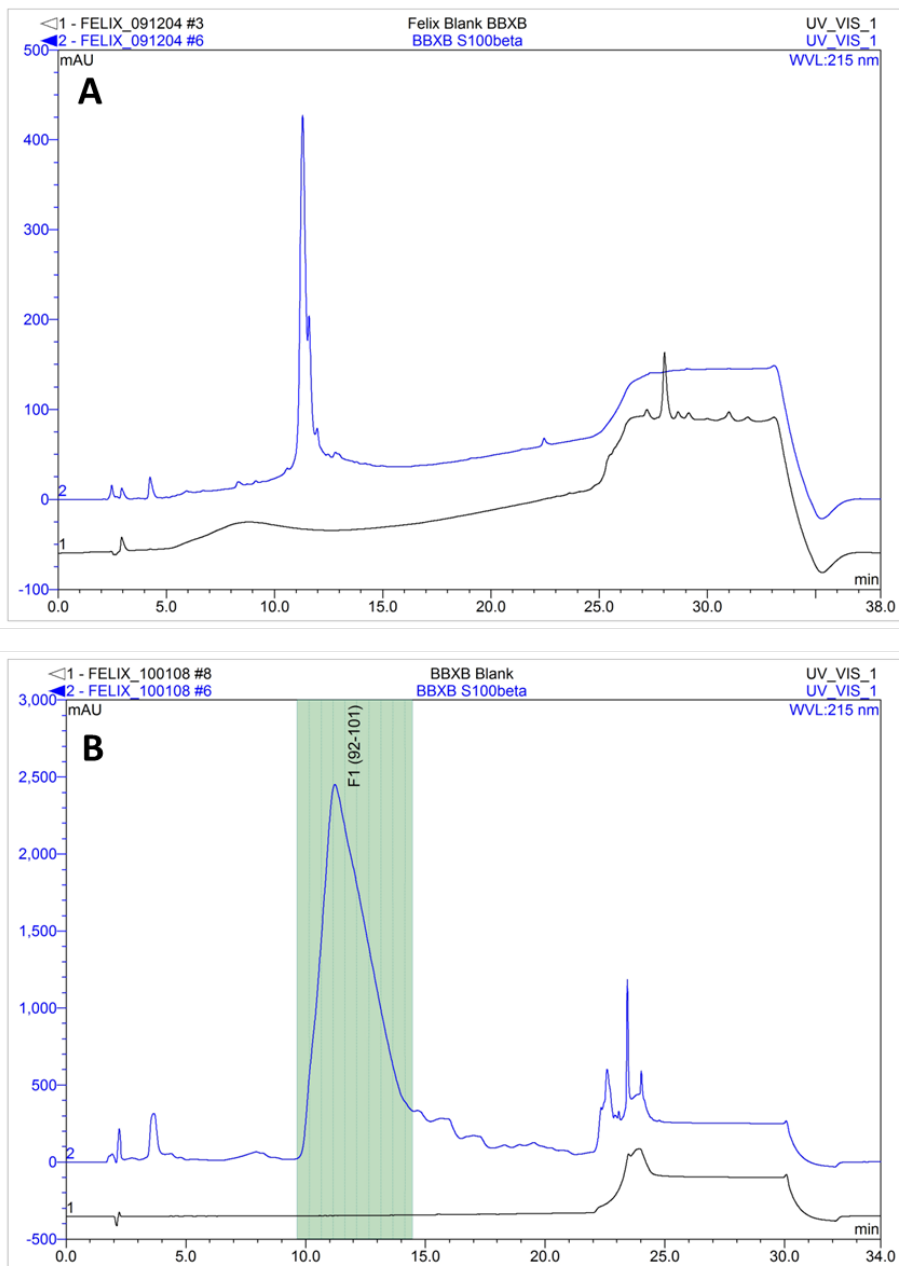


Figure F-13 Purification of BBXB S100 β .

Crude peptide was dissolved at 50.0 mg/mL in ultrapurified water and analysed by analytical HPLC (A): flow rate: 1 mL/min, 5 μ L injection volume; gradient (A: ultrapurified water with 5% MeCN and 0.05% TFA, B: MeCN with 5% ultrapurified water and 0.05% TFA): 0% B for 2 min, increase to 40% B over 22 min, ramp up to 100% B in 2 min, keep constant for 4 min, ramp down to 0% B in 2 min, equilibrate for 2 min. Black trace shows background (H₂O), blue trace the peptide. For isolation, the same solution was purified by semiprep HPLC (B): flow rate: 21.240 mL/min, 500 μ L injection volume; the same mobile phases as for the analytical run were used, the gradient was decreased to 20 minutes. Green areas indicate collected fractions; vertical lines inside green areas indicate tube changes, with tube #s labelled in parentheses above peaks. Tubes #94 - #96 were submitted for MS analysis (C & D). Figure continued on next page.

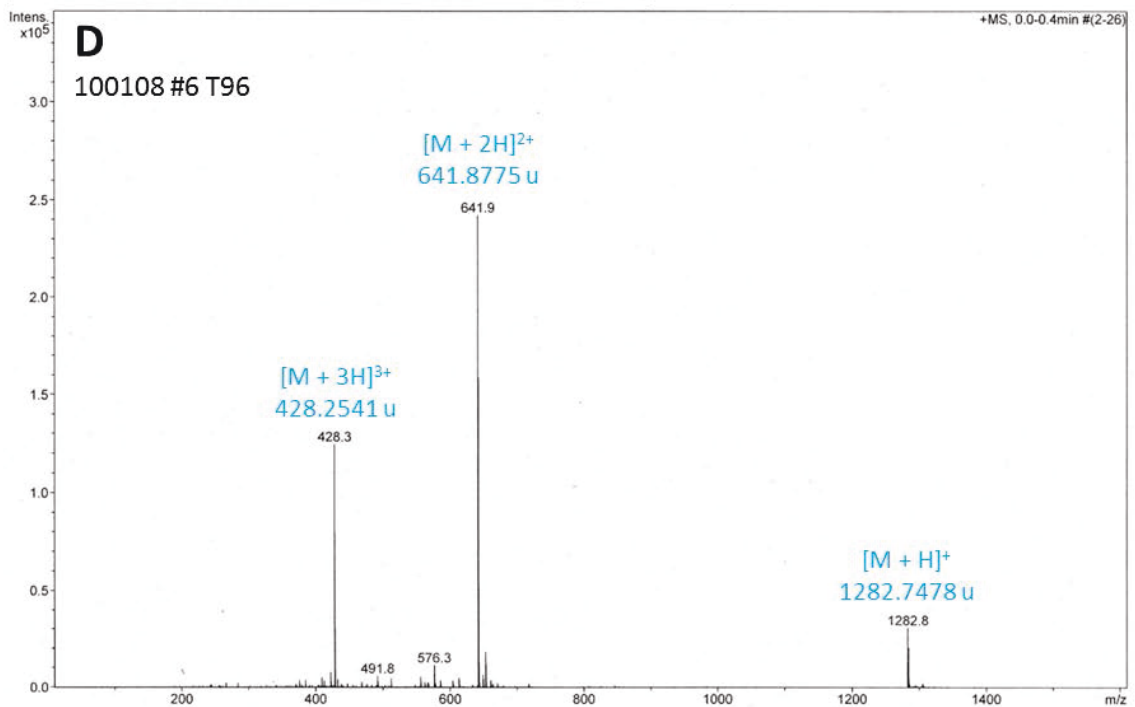
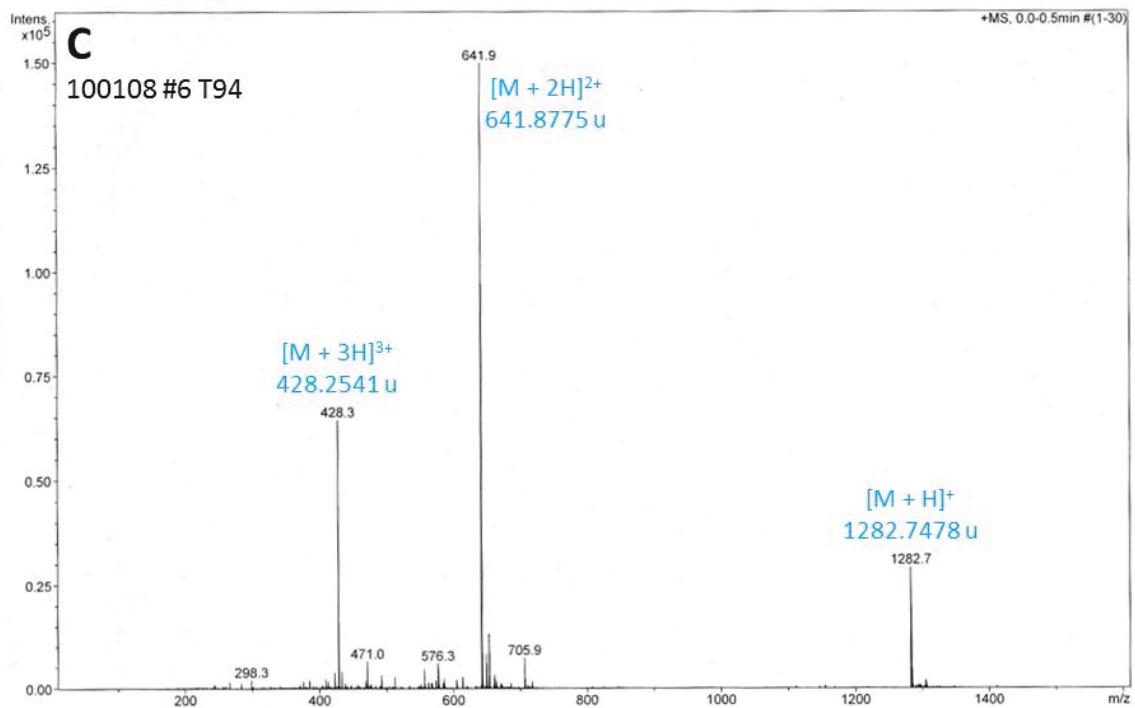


Figure F-13 Purification of BBXB S100 β ; continued.

Mass Spectra of tubes #94 (C) and #96 (D); both tubes show predominantly ions related to the product with only minor contaminant peaks; the spectrum for tube #95 looked essentially identical.

F.6.4. BBXB C1qA (KDPKKGHIYQ)

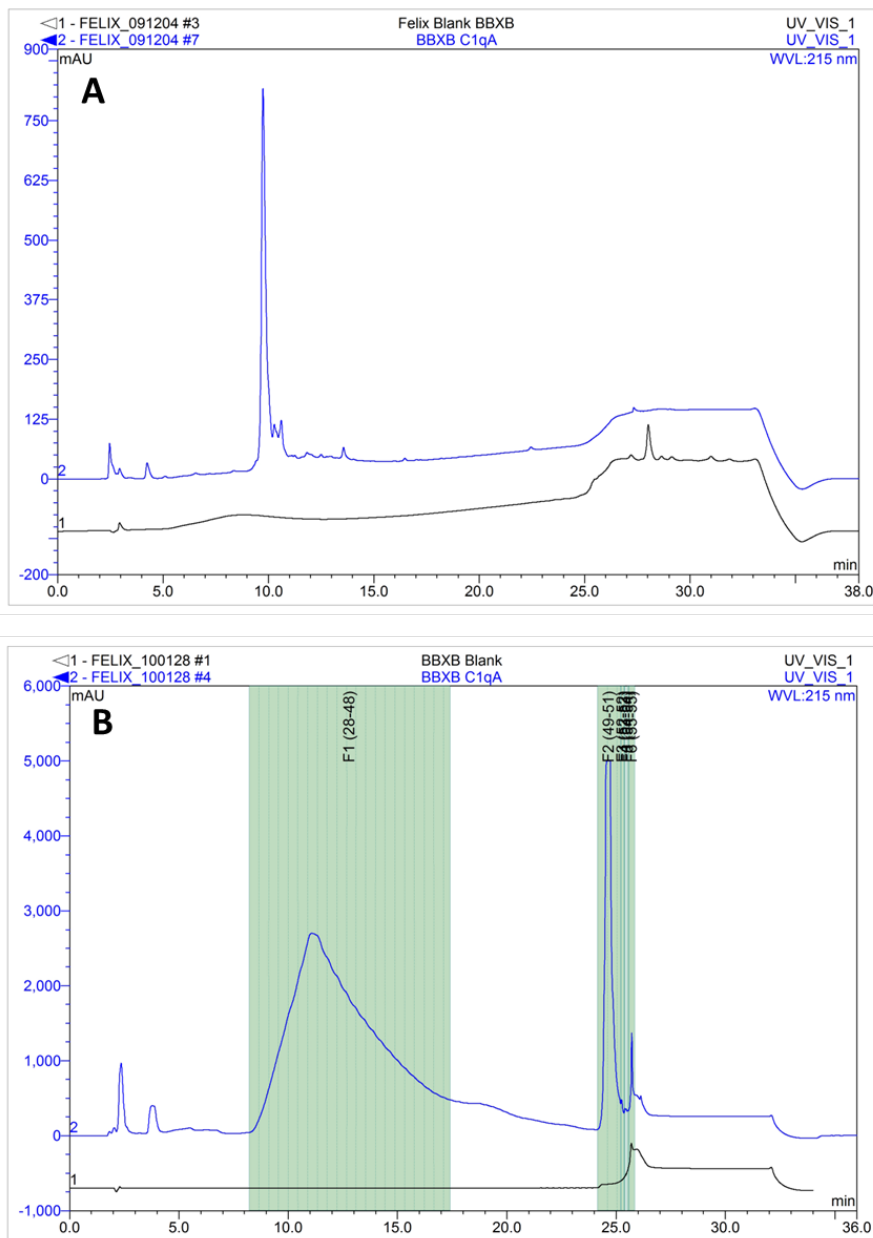


Figure F-14 Purification of BBXB C1qA.

Crude peptide was dissolved at 50.0 mg/mL in ultrapurified water and analysed by analytical HPLC (A): flow rate: 1 mL/min, 5 µL injection volume; gradient (A: ultrapurified water with 5% MeCN and 0.05% TFA, B: MeCN with 5% ultrapurified water and 0.05% TFA): 0% B for 2 min, increase to 40% B over 23 min, ramp up to 100% B in 2 min, keep constant for 4 min, ramp down to 0% B in 2 min, equilibrate for 2 min. Black trace shows background (H₂O), blue trace the peptide. For isolation, the same solution was purified by semiprep HPLC (B): flow rate: 21.240 mL/min, 500 µL injection volume; the same mobile phases as for the analytical run were used, the gradient was decreased to 20 minutes. Green areas indicate collected fractions; vertical lines inside green areas indicate tube changes, with tube #s labelled in parentheses above peaks. Tubes #33 - #35, and #50 were submitted for MS analysis (C & D). Figure continued on next page.

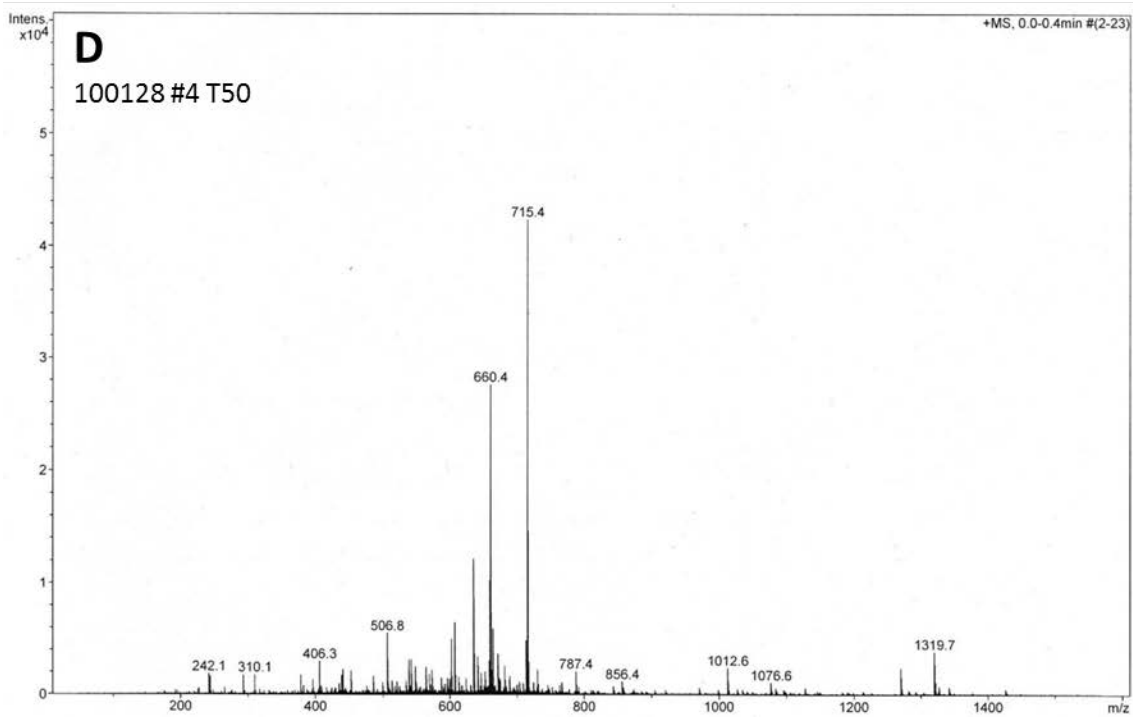
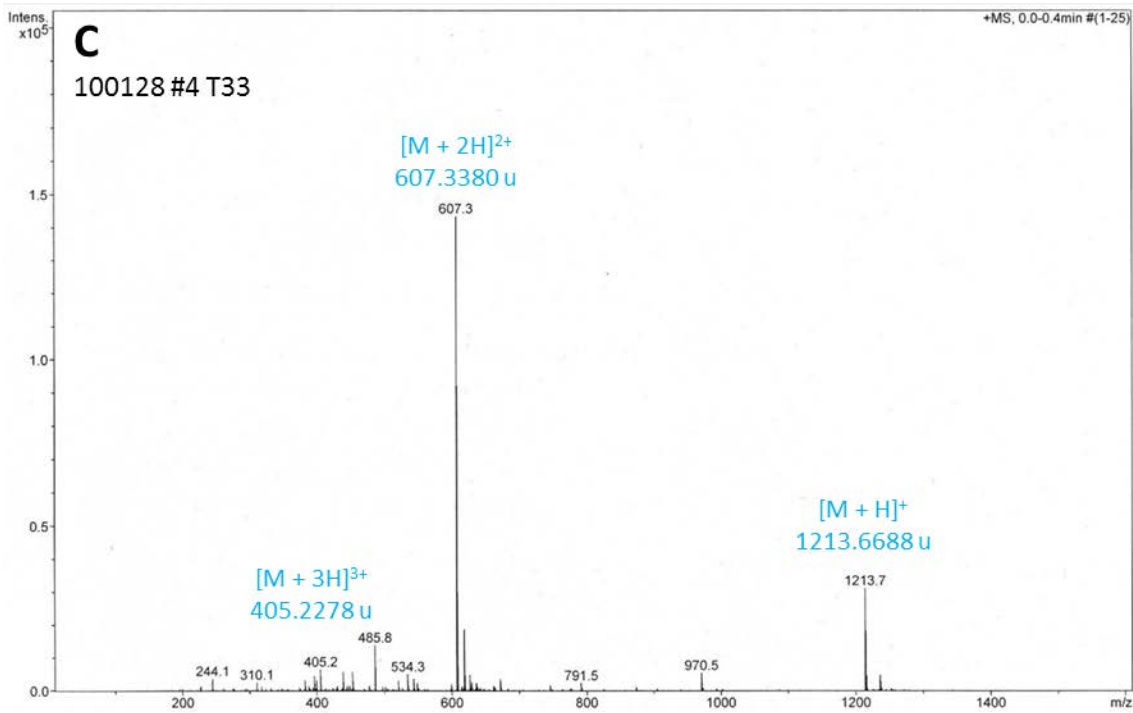


Figure F-14 Purification of BBXB C1qA; continued.

Mass Spectra of tubes #33 (C) and #50 (D); tube #33 shows predominantly ions related to the product with only minor contaminant peaks; the spectra for tubes #34 & #35 looked essentially identical. Tube #50 didn't show any ions related to the product.

F.6.5. BBXB IL4_a (FYSHHEKDTR)

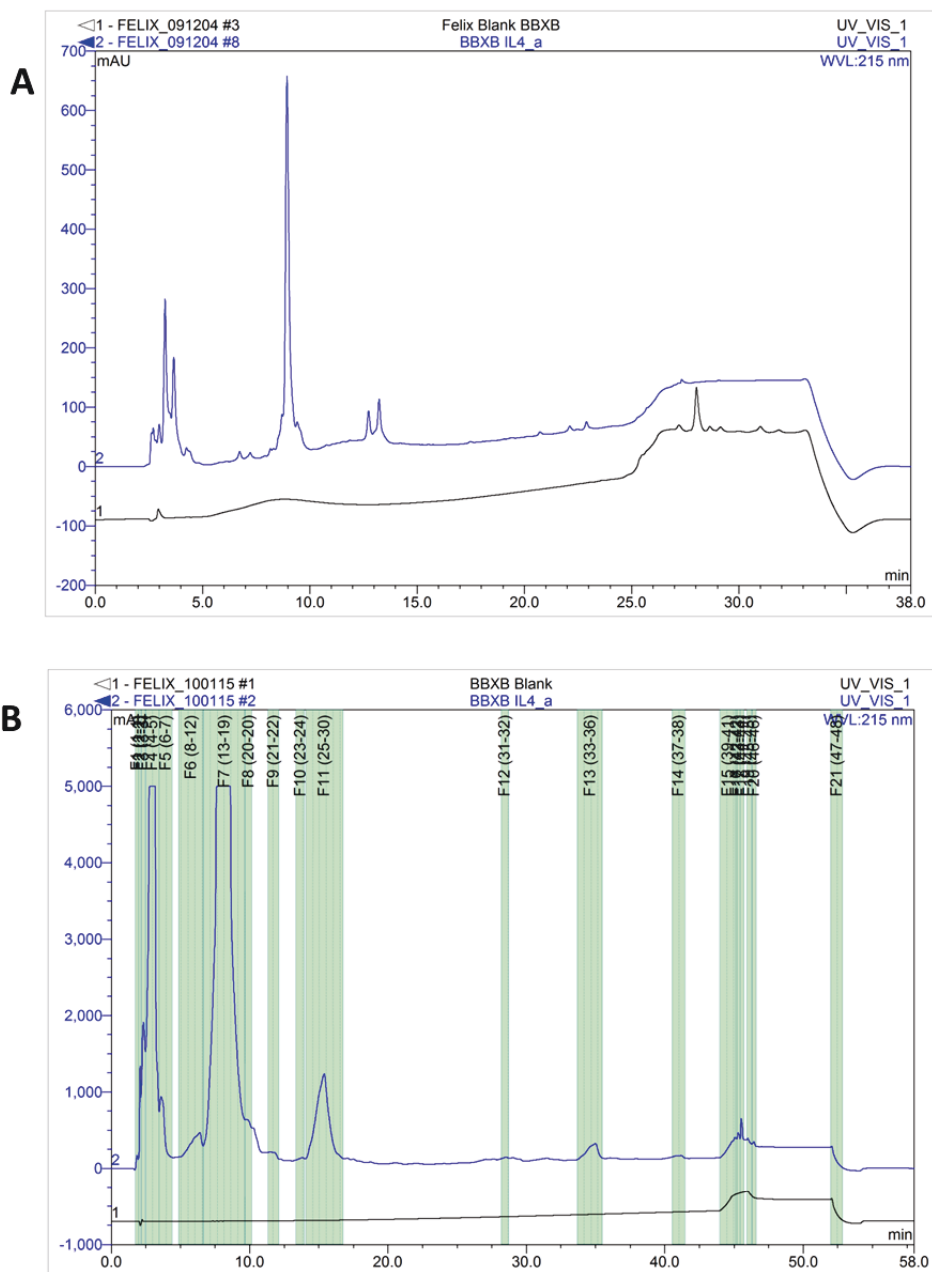


Figure F-15 Purification of BBXB IL4_a.

Crude peptide was dissolved at 50.0 mg/mL in ultrapurified water and analysed by analytical HPLC (A): flow rate: 1 mL/min, 5 μ L injection volume; gradient (A: ultrapurified water with 5% MeCN and 0.05% TFA, B: MeCN with 5% ultrapurified water and 0.05% TFA): 0% B for 2 min, increase to 40% B over 23 min, ramp up to 100% B in 2 min, keep constant for 4 min, ramp down to 0% B in 2 min, equilibrate for 2 min. Black trace shows background (H₂O), blue trace the peptide. For isolation, the same solution was purified by semiprep HPLC (B): flow rate: 21.240 mL/min, 500 μ L injection volume; the same mobile phases as for the analytical run were used, the gradient was increased to 42 minutes. Green areas indicate collected fractions; vertical lines inside green areas indicate tube changes, with tube #s labelled in parentheses above peaks.

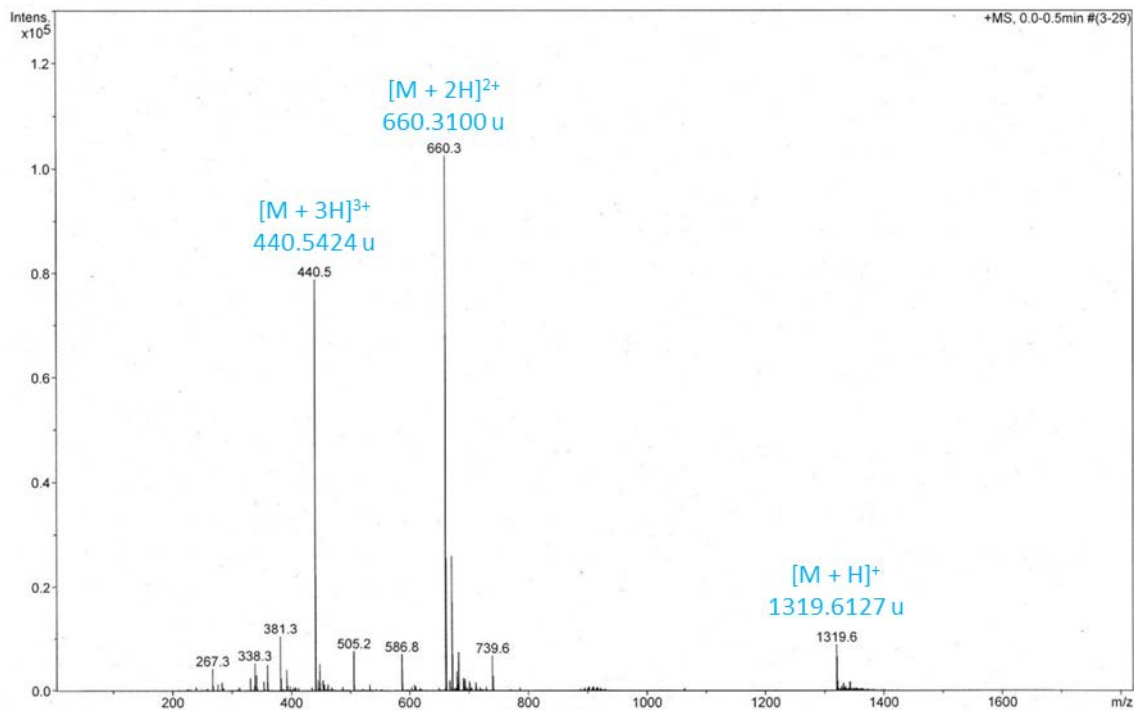


Figure F-15 Purification of BBXB IL4_a; continued.

The mass spectrum of BBXB IL4_a shows predominantly ions related to the product with only minor contaminant peaks.

F.6.6. BBXB IL4_b (Ac-QQFHRHKQLI)

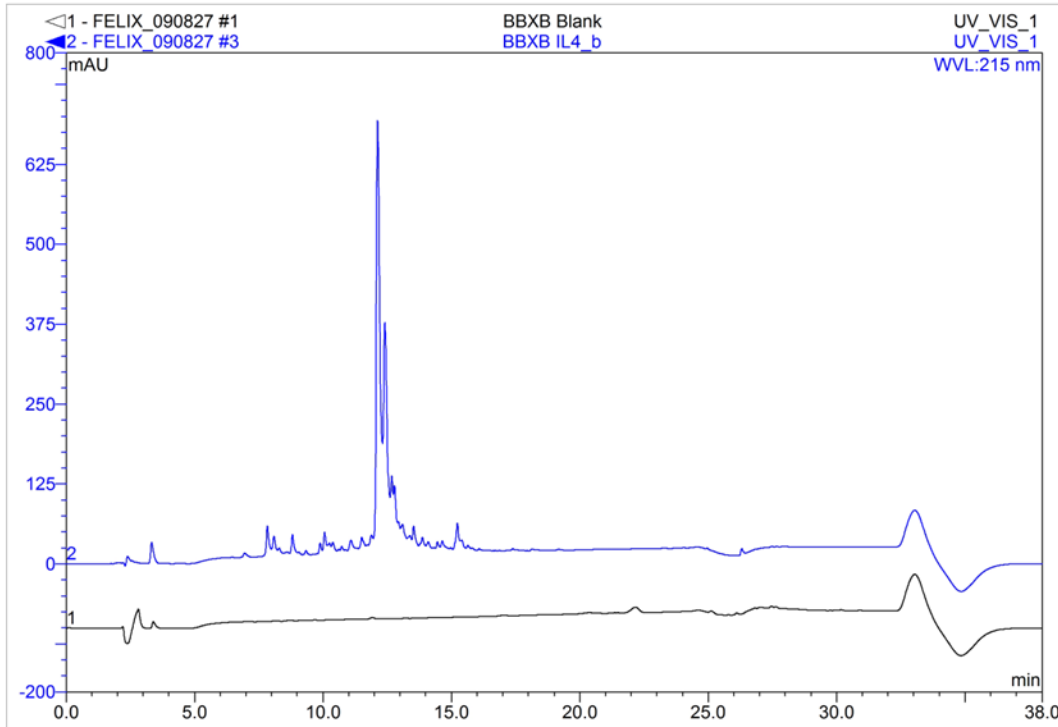


Figure F-16 Analysis of BBXB IL4_b.

Crude peptide was dissolved at 50.0 mg/mL in ultrapurified water and analysed by analytical HPLC: flow rate: 1 mL/min, 5 μ L injection volume; gradient (A: ultrapurified water with 5% MeCN and 0.05% TFA, B: MeCN with 5% ultrapurified water and 0.05% TFA): 0% B for 2 min, increase to 40% B over 23 min, ramp up to 100% B in 2 min, keep constant for 4 min, ramp down to 0% B in 2 min, equilibrate for 2 min.

F.6.7. BBXB IL6_a (FLQKKAKNLD)

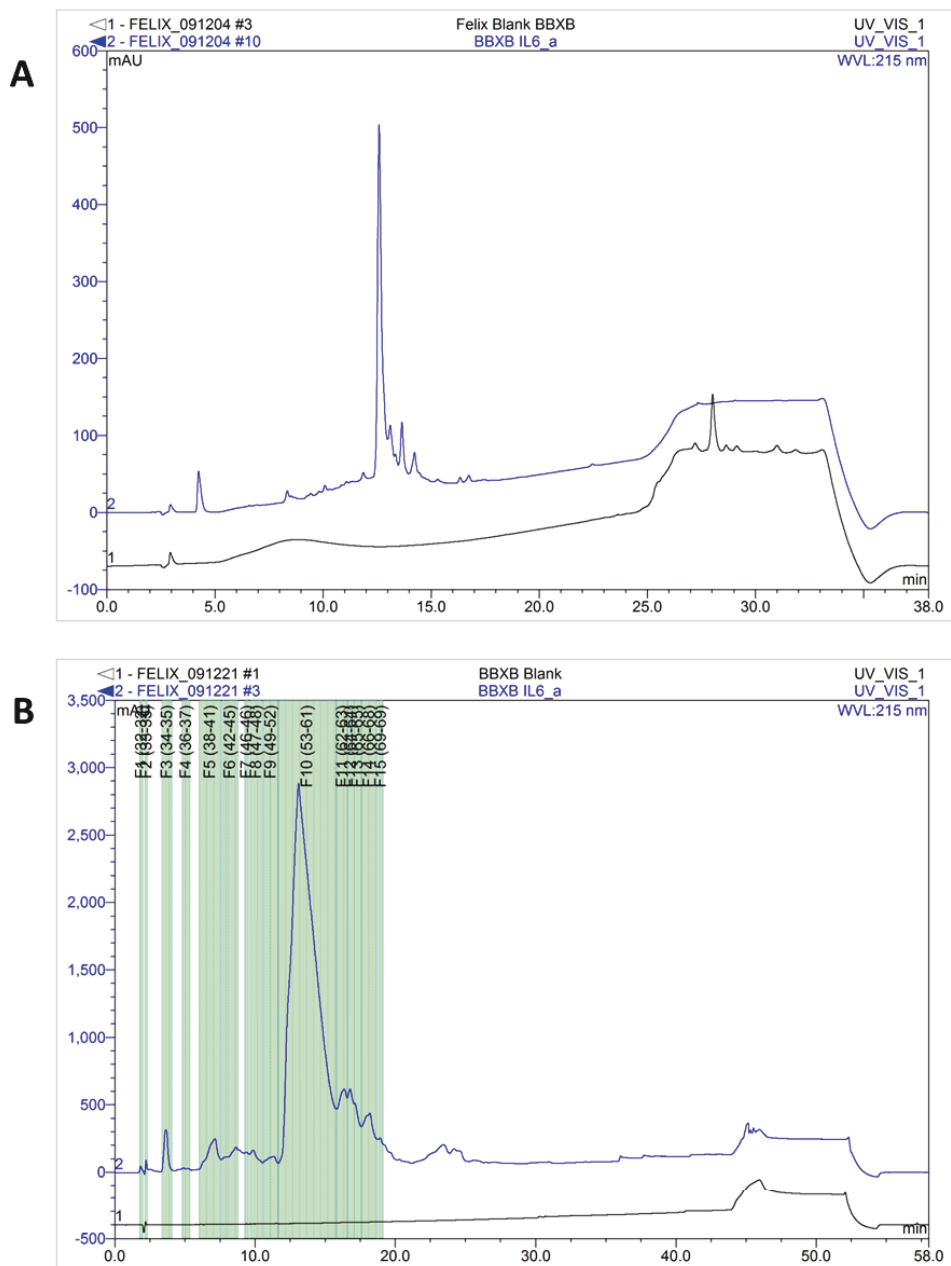


Figure F-17 Purification of BBXB IL6_a.

Crude peptide was dissolved at 50.0 mg/mL in ultrapurified water and analysed by analytical HPLC (A): flow rate: 1 mL/min, 5 μ L injection volume; gradient (A: ultrapurified water with 5% MeCN and 0.05% TFA, B: MeCN with 5% ultrapurified water and 0.05% TFA): 0% B for 2 min, increase to 40% B over 23 min, ramp up to 100% B in 2 min, keep constant for 4 min, ramp down to 0% B in 2 min, equilibrate for 2 min. Black trace shows background (H₂O), blue trace the peptide. For isolation, the same solution was purified by semiprep HPLC (B): flow rate: 21.240 mL/min, 500 μ L injection volume; the same mobile phases as for the analytical run were used, the gradient was increased to 40 minutes. Green areas indicate collected fractions; vertical lines inside green areas indicate tube changes, with tube #s labelled in parentheses above peaks.

F.6.8. BBXB IL6_b (NEGKKMRCEW)

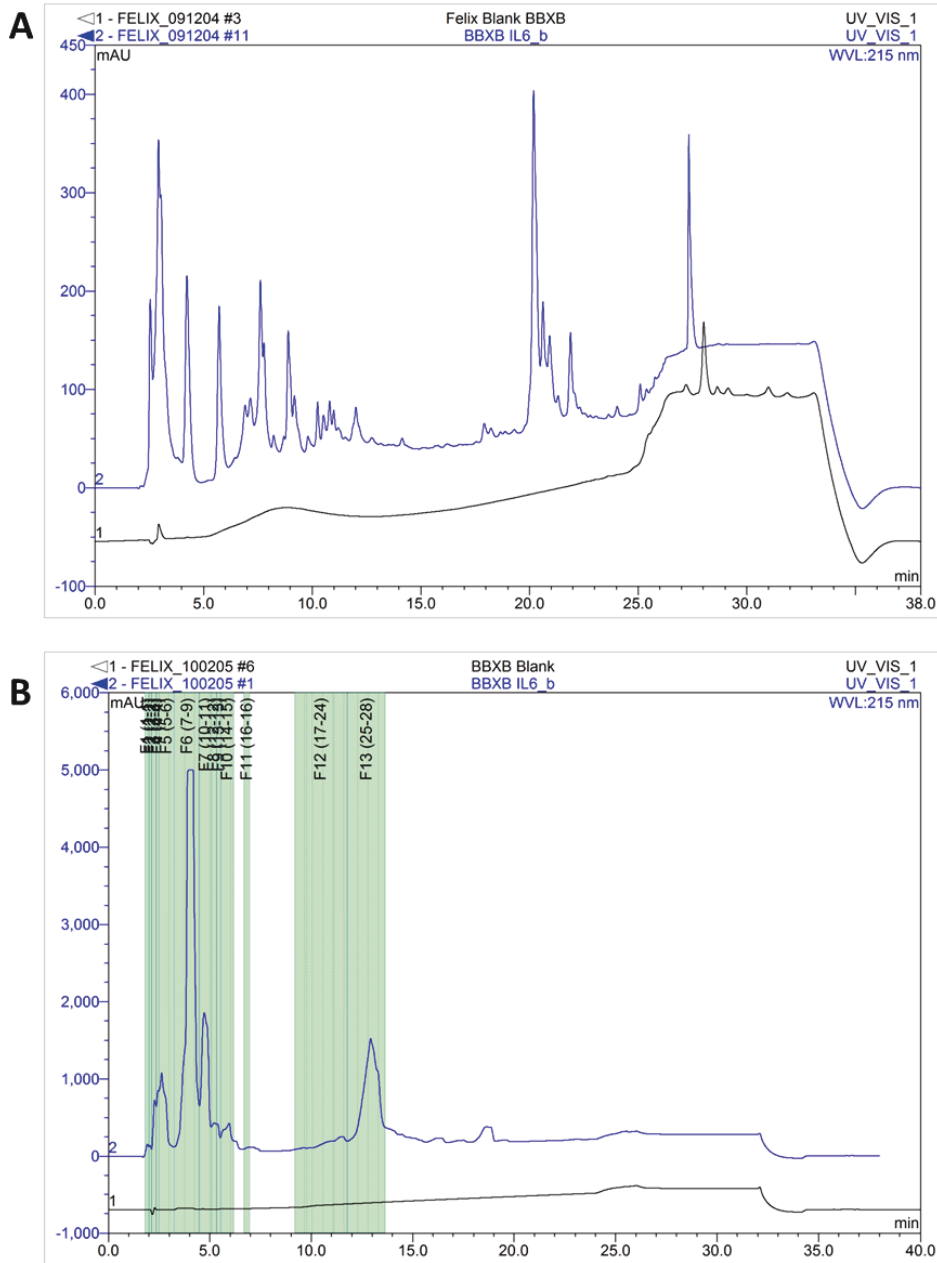


Figure F-18 Purification of BBXB IL6_b.

Crude peptide was dissolved at 25.0 mg/mL in ultrapurified water and analysed by analytical HPLC (A): flow rate: 1 mL/min, 5 µL injection volume; gradient (A: ultrapurified water with 5% MeCN and 0.05% TFA, B: MeCN with 5% ultrapurified water and 0.05% TFA): 0% B for 2 min, increase to 40% B over 23 min, ramp up to 100% B in 2 min, keep constant for 4 min, ramp down to 0% B in 2 min, equilibrate for 2 min. Black trace shows background (H₂O), blue trace the peptide. For isolation, the same solution was purified by semiprep HPLC (B): flow rate: 21.240 mL/min, 500 µL injection volume; the same mobile phases and gradient as for the analytical run were used. Green areas indicate collected fractions; vertical lines inside green areas indicate tube changes, with tube #s labelled in parentheses above peaks.

F.6.9. BBXB IL6_c (ADCKAKRDTP)

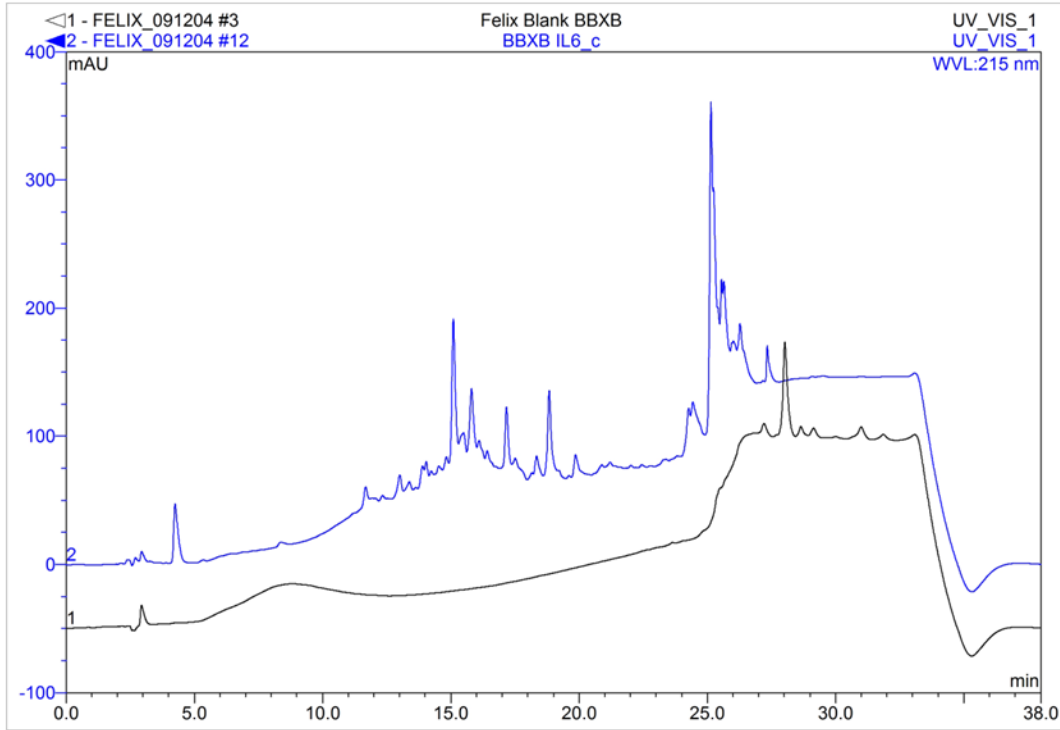


Figure F-19 Analysis of BBXB IL6_c.

Crude peptide was dissolved at 50.0 mg/mL in ultrapurified water and analysed by analytical HPLC: flow rate: 1 mL/min, 5 μ L injection volume; gradient (A: ultrapurified water with 5% MeCN and 0.05% TFA, B: MeCN with 5% ultrapurified water and 0.05% TFA): 0% B for 2 min, increase to 40% B over 23 min, ramp up to 100% B in 2 min, keep constant for 4 min, ramp down to 0% B in 2 min, equilibrate for 2 min.

APPENDIX G. PERMISSIONS

G.1. Permission for Figure I-1

ELSEVIER LICENSE TERMS AND CONDITIONS

Jan 20, 2014

This is a License Agreement between Felix S Meier-Stephenson ("You") and Elsevier ("Elsevier") provided by Copyright Clearance Center ("CCC"). The license consists of your order details, the terms and conditions provided by Elsevier, and the payment terms and conditions.

All payments must be made in full to CCC. For payment instructions, please see information listed at the bottom of this form.

Supplier	Elsevier Limited The Boulevard,Langford Lane Kidlington,Oxford,OX5 1GB,UK
Registered Company Number	1982084
Customer name	Felix S Meier-Stephenson
Customer address	4528 Vegas Rd. NW Calgary, AB T3A0N1
License number	3312860032619
License date	Jan 20, 2014
Licensed content publisher	Elsevier
Licensed content publication	Alzheimer's & Dementia
Licensed content title	Toward defining the preclinical stages of Alzheimer's disease: Recommendations from the National Institute on Aging-Alzheimer's Association workgroups on diagnostic guidelines for Alzheimer's disease
Licensed content author	Reisa A. Sperling,Paul S. Aisen,Laurel A. Beckett,David A. Bennett,Suzanne Craft,Anne M. Fagan,Takeshi Iwatsubo,Clifford R. Jack,Jeffrey Kaye,Thomas J. Montine,Denise C. Park,Eric M. Reiman,Christopher C. Rowe,Eric Siemers,Yaakov Stern, et al.
Licensed content date	May 2011
Licensed content volume number	7
Licensed content issue number	3
Number of pages	13
Start Page	280
End Page	292
Type of Use	reuse in a thesis/dissertation
Intended publisher of new work	other
Portion	figures/tables/illustrations

Number of figures/tables/illustrations	1
Format	both print and electronic
Are you the author of this Elsevier article?	No
Will you be translating?	No
Order reference number	#3800
Title of your thesis/dissertation	A New Theory of Alzheimer's Disease
Expected completion date	Feb 2014
Estimated size (number of pages)	300
Elsevier VAT number	GB 494 6272 12
Permissions price	0.00 USD
VAT/Local Sales Tax	0.00 USD / 0.00 GBP
Total	0.00 USD
Terms and Conditions	

INTRODUCTION

1. The publisher for this copyrighted material is Elsevier. By clicking 'accept' in connection with completing this licensing transaction, you agree that the following terms and conditions apply to this transaction (along with the Billing and Payment terms and conditions established by Copyright Clearance Center, Inc. ("CCC"), at the time that you opened your Rightslink account and that are available at any time at <http://myaccount.copyright.com>).

GENERAL TERMS

2. Elsevier hereby grants you permission to reproduce the aforementioned material subject to the terms and conditions indicated.

3. Acknowledgement: If any part of the material to be used (for example, figures) has appeared in our publication with credit or acknowledgement to another source, permission must also be sought from that source. If such permission is not obtained then that material may not be included in your publication/copies. Suitable acknowledgement to the source must be made, either as a footnote or in a reference list at the end of your publication, as follows:

“Reprinted from: Publication title, Vol /edition number, Author(s), Title of article / title of chapter, Pages No., Copyright (Year), with permission from Elsevier [OR APPLICABLE SOCIETY COPYRIGHT OWNER].” Also Lancet special credit - “Reprinted from: The Lancet, Vol. number, Author(s), Title of article, Pages No., Copyright (Year), with permission from Elsevier.”

4. Reproduction of this material is confined to the purpose and/or media for which permission is hereby given.

5. Altering/Modifying Material: Not Permitted. However figures and illustrations may be

altered/adapted minimally to serve your work. Any other abbreviations, additions, deletions and/or any other alterations shall be made only with prior written authorization of Elsevier Ltd. (Please contact Elsevier at permissions@elsevier.com)

6. If the permission fee for the requested use of our material is waived in this instance, please be advised that your future requests for Elsevier materials may attract a fee.

7. Reservation of Rights: Publisher reserves all rights not specifically granted in the combination of (i) the license details provided by you and accepted in the course of this licensing transaction, (ii) these terms and conditions and (iii) CCC's Billing and Payment terms and conditions.

8. License Contingent Upon Payment: While you may exercise the rights licensed immediately upon issuance of the license at the end of the licensing process for the transaction, provided that you have disclosed complete and accurate details of your proposed use, no license is finally effective unless and until full payment is received from you (either by publisher or by CCC) as provided in CCC's Billing and Payment terms and conditions. If full payment is not received on a timely basis, then any license preliminarily granted shall be deemed automatically revoked and shall be void as if never granted. Further, in the event that you breach any of these terms and conditions or any of CCC's Billing and Payment terms and conditions, the license is automatically revoked and shall be void as if never granted. Use of materials as described in a revoked license, as well as any use of the materials beyond the scope of an unrevoked license, may constitute copyright infringement and publisher reserves the right to take any and all action to protect its copyright in the materials.

9. Warranties: Publisher makes no representations or warranties with respect to the licensed material.

10. Indemnity: You hereby indemnify and agree to hold harmless publisher and CCC, and their respective officers, directors, employees and agents, from and against any and all claims arising out of your use of the licensed material other than as specifically authorized pursuant to this license.

11. No Transfer of License: This license is personal to you and may not be sublicensed, assigned, or transferred by you to any other person without publisher's written permission.

12. No Amendment Except in Writing: This license may not be amended except in a writing signed by both parties (or, in the case of publisher, by CCC on publisher's behalf).

13. Objection to Contrary Terms: Publisher hereby objects to any terms contained in any purchase order, acknowledgment, check endorsement or other writing prepared by you, which terms are inconsistent with these terms and conditions or CCC's Billing and Payment terms and conditions. These terms and conditions, together with CCC's Billing and Payment terms and conditions (which are incorporated herein), comprise the entire agreement between you and publisher (and CCC) concerning this licensing transaction. In the event of any conflict between your obligations established by these terms and conditions and those established by CCC's Billing and Payment terms and conditions, these terms and conditions shall control.

14. Revocation: Elsevier or Copyright Clearance Center may deny the permissions described in this License at their sole discretion, for any reason or no reason, with a full refund payable to you.

Notice of such denial will be made using the contact information provided by you. Failure to receive such notice will not alter or invalidate the denial. In no event will Elsevier or Copyright Clearance Center be responsible or liable for any costs, expenses or damage incurred by you as a result of a denial of your permission request, other than a refund of the amount(s) paid by you to Elsevier and/or Copyright Clearance Center for denied permissions.

LIMITED LICENSE

The following terms and conditions apply only to specific license types:

15. **Translation:** This permission is granted for non-exclusive world **English** rights only unless your license was granted for translation rights. If you licensed translation rights you may only translate this content into the languages you requested. A professional translator must perform all translations and reproduce the content word for word preserving the integrity of the article. If this license is to re-use 1 or 2 figures then permission is granted for non-exclusive world rights in all languages.

16. **Website:** The following terms and conditions apply to electronic reserve and author websites:
Electronic reserve: If licensed material is to be posted to website, the web site is to be password-protected and made available only to bona fide students registered on a relevant course if:

This license was made in connection with a course,

This permission is granted for 1 year only. You may obtain a license for future website posting. All content posted to the web site must maintain the copyright information line on the bottom of each image,

A hyper-text must be included to the Homepage of the journal from which you are licensing at <http://www.sciencedirect.com/science/journal/xxxxx> or the Elsevier homepage for books at <http://www.elsevier.com> , and

Central Storage: This license does not include permission for a scanned version of the material to be stored in a central repository such as that provided by Heron/XanEdu.

17. **Author website** for journals with the following additional clauses:

All content posted to the web site must maintain the copyright information line on the bottom of each image, and the permission granted is limited to the personal version of your paper. You are not allowed to download and post the published electronic version of your article (whether PDF or HTML, proof or final version), nor may you scan the printed edition to create an electronic version. A hyper-text must be included to the Homepage of the journal from which you are licensing at <http://www.sciencedirect.com/science/journal/xxxxx> . As part of our normal production process, you will receive an e-mail notice when your article appears on Elsevier's online service ScienceDirect (www.sciencedirect.com). That e-mail will include the article's Digital Object Identifier (DOI). This number provides the electronic link to the published article and should be included in the posting of your personal version. We ask that you wait until you receive this e-mail and have the DOI to do any posting.

Central Storage: This license does not include permission for a scanned version of the material to be stored in a central repository such as that provided by Heron/XanEdu.

18. **Author website** for books with the following additional clauses:

Authors are permitted to place a brief summary of their work online only.

A hyper-text must be included to the Elsevier homepage at <http://www.elsevier.com> . All content posted to the web site must maintain the copyright information line on the bottom of each image.

You are not allowed to download and post the published electronic version of your chapter, nor may you scan the printed edition to create an electronic version.

Central Storage: This license does not include permission for a scanned version of the material to be stored in a central repository such as that provided by Heron/XanEdu.

19. **Website** (regular and for author): A hyper-text must be included to the Homepage of the journal from which you are licensing at <http://www.sciencedirect.com/science/journal/xxxxx>. or for books to the Elsevier homepage at <http://www.elsevier.com>

20. **Thesis/Dissertation**: If your license is for use in a thesis/dissertation your thesis may be submitted to your institution in either print or electronic form. Should your thesis be published commercially, please reapply for permission. These requirements include permission for the Library and Archives of Canada to supply single copies, on demand, of the complete thesis and include permission for UMI to supply single copies, on demand, of the complete thesis. Should your thesis be published commercially, please reapply for permission.

21. **Other Conditions**:

v1.6

If you would like to pay for this license now, please remit this license along with your payment made payable to "COPYRIGHT CLEARANCE CENTER" otherwise you will be invoiced within 48 hours of the license date. Payment should be in the form of a check or money order referencing your account number and this invoice number RLNK501205613. Once you receive your invoice for this order, you may pay your invoice by credit card. Please follow instructions provided at that time.

**Make Payment To:
Copyright Clearance Center
Dept 001
P.O. Box 843006
Boston, MA 02284-3006**

For suggestions or comments regarding this order, contact RightsLink Customer Support: customercare@copyright.com or +1-877-622-5543 (toll free in the US) or +1-978-646-2777.

Gratis licenses (referencing \$0 in the Total field) are free. Please retain this printable license for your reference. No payment is required.

G.2. Permission for Figures I-2 & I-3

Re: permission to reproduce image

mhickey@alz.org on behalf of ALZ BrandHelp <brandhelp@alz.org>

Mon 22/07/2013 10:34 AM

To: Felix Meier-Stephenson <Felix.Meier@Dal.Ca>;

You have permission to reproduce Brain Tour images with the following credit:

© 2013 Alzheimer's Association. www.alz.org. All rights reserved. Illustrations by Stacy Jannis.

On Fri, Jul 19, 2013 at 11:01 AM, Felix Meier-Stephenson <felix.meier@dal.ca> wrote:

Good afternoon,

I would like to ask for permission to use the picture with the file name 'alzheimers_progression.jpeg' from your website (<http://www.alz.org/braintour/progression.asp>) in my Ph.D. thesis.

I would use it in a slightly modified form with the three brains next to each other and of course would cite it properly.

Thanks!

With kind regards,

Felix

Felix S. Meier-Stephenson
Graduate Student
Dalhousie University
Department of Chemistry
F.O. Box 15000
Halifax, Nova Scotia
E3H 4F2, Canada

Tel: [\(902\) 494-7183](tel:(902)494-7183)

Fax: [\(902\) 494-3110](tel:(902)494-3110)

email: felix.meier@dal.ca

G.3. Permission for Figure I-6

AW: Fermission to reproduce figure in dissertation

Rights and Permissions <permission@karger.com>

Tue 21/01/2014 1:25 AM

To: Felix Meier-Stephenson <Felix.Meier@Dal.Ca>;

Dear Dr. Meier-Stephenson,

Thank you for your email. As to your request, I am pleased to inform you that permission herewith is granted to use Figure 1B from the article

Finder, V.H. et al: Neurodegenerative Dis 2007;4:13–27 (DOI:10.1159/000100355)

to be reproduced in your PhD thesis, provided that full credit will be given to the original source and that S. Karger AG, Basel will be mentioned.

Please note that this is a non-exclusive permission, hence any further use or distribution, either in print or electronically, requires written permission again as this permission is valid for the above mentioned purpose only.

This permission applies only to copyrighted content that S. Karger AG owns, and not to copyrighted content from other sources. If any material in our work appears with credit to another source, you must also obtain permission from the original source cited in our work. All content reproduced from copyrighted material owned by S. Karger AG remains the sole and exclusive property of S. Karger AG. The right to grant permission to a third party is reserved solely by S. Karger AG.

Thank you for your understanding and cooperation.

Hopefully, I have been of assistance to you with the above.

Yours sincerely,

Silvia Meier
Rights Manager
t +41 61 306 14 75
permission@karger.com

S. Karger AG, Medical and Scientific Publishers, Allschwilerstrasse 10, 4009 Basel, Switzerland
t +41 61 306 11 11, f +41 61 306 12 34, www.karger.com



G.4. Permission for Figure I-7

THE AMERICAN ASSOCIATION FOR THE ADVANCEMENT OF SCIENCE LICENSE TERMS AND CONDITIONS

Jan 20, 2014

This is a License Agreement between Felix S Meier-Stephenson ("You") and The American Association for the Advancement of Science ("The American Association for the Advancement of Science") provided by Copyright Clearance Center ("CCC"). The license consists of your order details, the terms and conditions provided by The American Association for the Advancement of Science, and the payment terms and conditions.

All payments must be made in full to CCC. For payment instructions, please see information listed at the bottom of this form.

License Number	3313160182743
License date	Jan 20, 2014
Licensed content publisher	The American Association for the Advancement of Science
Licensed content publication	Science
Licensed content title	Alzheimer's disease: the amyloid cascade hypothesis
Licensed content author	JA Hardy, GA Higgins
Licensed content date	Apr 10, 1992
Volume number	256
Issue number	5054
Type of Use	Thesis / Dissertation
Requestor type	Scientist/individual at a research institution
Format	Print and electronic
Portion	Figure
Number of figures/tables	1
Order reference number	#2687
Title of your thesis / dissertation	A New Theory of Alzheimer's Disease
Expected completion date	Feb 2014
Estimated size(pages)	300
Total	0.00 USD

Terms and Conditions

American Association for the Advancement of Science TERMS AND CONDITIONS

Regarding your request, we are pleased to grant you non-exclusive, non-transferable permission, to republish the AAAS material identified above in your work identified above, subject to the terms and conditions herein. We must be contacted for permission for any uses other than those

specifically identified in your request above.

The following credit line must be printed along with the AAAS material: "From [Full Reference Citation]. Reprinted with permission from AAAS."

All required credit lines and notices must be visible any time a user accesses any part of the AAAS material and must appear on any printed copies and authorized user might make.

This permission does not apply to figures / photos / artwork or any other content or materials included in your work that are credited to non-AAAS sources. If the requested material is sourced to or references non-AAAS sources, you must obtain authorization from that source as well before using that material. You agree to hold harmless and indemnify AAAS against any claims arising from your use of any content in your work that is credited to non-AAAS sources.

If the AAAS material covered by this permission was published in Science during the years 1974 - 1994, you must also obtain permission from the author, who may grant or withhold permission, and who may or may not charge a fee if permission is granted. See original article for author's address. This condition does not apply to news articles.

The AAAS material may not be modified or altered except that figures and tables may be modified with permission from the author. Author permission for any such changes must be secured prior to your use.

Whenever possible, we ask that electronic uses of the AAAS material permitted herein include a hyperlink to the original work on AAAS's website (hyperlink may be embedded in the reference citation).

AAAS material reproduced in your work identified herein must not account for more than 30% of the total contents of that work.

AAAS must publish the full paper prior to use of any text.

AAAS material must not imply any endorsement by the American Association for the Advancement of Science.

This permission is not valid for the use of the AAAS and/or Science logos.

AAAS makes no representations or warranties as to the accuracy of any information contained in the AAAS material covered by this permission, including any warranties of

merchantability or fitness for a particular purpose.

If permission fees for this use are waived, please note that AAAS reserves the right to charge for reproduction of this material in the future.

Permission is not valid unless payment is received within sixty (60) days of the issuance of this permission. If payment is not received within this time period then all rights granted herein shall be revoked and this permission will be considered null and void.

In the event of breach of any of the terms and conditions herein or any of CCC's Billing and Payment terms and conditions, all rights granted herein shall be revoked and this permission will be considered null and void.

AAAS reserves the right to terminate this permission and all rights granted herein at its discretion, for any purpose, at any time. In the event that AAAS elects to terminate this permission, you will have no further right to publish, publicly perform, publicly display, distribute or otherwise use any matter in which the AAAS content had been included, and all fees paid hereunder shall be fully refunded to you. Notification of termination will be sent to the contact information as supplied by you during the request process and termination shall be immediate upon sending the notice. Neither AAAS nor CCC shall be liable for any costs, expenses, or damages you may incur as a result of the termination of this permission, beyond the refund noted above.

This Permission may not be amended except by written document signed by both parties.

The terms above are applicable to all permissions granted for the use of AAAS material. Below you will find additional conditions that apply to your particular type of use.

FOR A THESIS OR DISSERTATION

If you are using figure(s)/table(s), permission is granted for use in print and electronic versions of your dissertation or thesis. A full text article may be used in print versions only of a dissertation or thesis.

Permission covers the distribution of your dissertation or thesis on demand by ProQuest / UMI, provided the AAAS material covered by this permission remains in situ.

If you are an Original Author on the AAAS article being reproduced, please refer to your License to Publish for rules on reproducing your paper in a dissertation or thesis.

FOR JOURNALS:

Permission covers both print and electronic versions of your journal article, however the AAAS material may not be used in any manner other than within the context of your article.

FOR BOOKS/TEXTBOOKS:

If this license is to reuse figures/tables, then permission is granted for non-exclusive world rights in all languages in both print and electronic formats (electronic formats are defined below).

If this license is to reuse a text excerpt or a full text article, then permission is granted for non-exclusive world rights in English only. You have the option of securing either print or electronic rights or both, but electronic rights are not automatically granted and do garner additional fees. Permission for translations of text excerpts or full text articles into other languages must be obtained separately.

Licenses granted for use of AAAS material in electronic format books/textbooks are valid only in cases where the electronic version is equivalent to or substitutes for the print version of the book/textbook. The AAAS material reproduced as permitted herein must remain in situ and must not be exploited separately (for example, if permission covers the use of a full text article, the article

G.5. Permission for Figure I-8

SPRINGER LICENSE TERMS AND CONDITIONS

Jan 20, 2014

This is a License Agreement between Felix S Meier-Stephenson ("You") and Springer ("Springer") provided by Copyright Clearance Center ("CCC"). The license consists of your order details, the terms and conditions provided by Springer, and the payment terms and conditions.

All payments must be made in full to CCC. For payment instructions, please see information listed at the bottom of this form.

License Number	3312851135393
License date	Jan 20, 2014
Licensed content publisher	Springer
Licensed content publication	Springer eBook
Licensed content title	Alzheimer's Disease
Licensed content author	Dr Martin Beckerman
Licensed content date	Jan 1, 2009
Type of Use	Thesis/Dissertation
Portion	Figures
Author of this Springer article	No
Order reference number	
Title of your thesis / dissertation	A New Theory of Alzheimer's Disease
Expected completion date	Feb 2014
Estimated size(pages)	300
Total	0.00 USD

Terms and Conditions

Introduction

The publisher for this copyrighted material is Springer Science + Business Media. By clicking "accept" in connection with completing this licensing transaction, you agree that the following terms and conditions apply to this transaction (along with the Billing and Payment terms and conditions established by Copyright Clearance Center, Inc. ("CCC"), at the time that you opened your Rightslink account and that are available at any time at <http://myaccount.copyright.com>).

Limited License

With reference to your request to reprint in your thesis material on which Springer Science and Business Media control the copyright, permission is granted, free of charge, for the use indicated in

your enquiry.

Licenses are for one-time use only with a maximum distribution equal to the number that you identified in the licensing process.

This License includes use in an electronic form, provided its password protected or on the university's intranet or repository, including UMI (according to the definition at the Sherpa website: <http://www.sherpa.ac.uk/romeo/>). For any other electronic use, please contact Springer at (permissions.dordrecht@springer.com or permissions.heidelberg@springer.com).

The material can only be used for the purpose of defending your thesis, and with a maximum of 100 extra copies in paper.

Although Springer holds copyright to the material and is entitled to negotiate on rights, this license is only valid, subject to a courtesy information to the author (address is given with the article/chapter) and provided it concerns original material which does not carry references to other sources (if material in question appears with credit to another source, authorization from that source is required as well).

Permission free of charge on this occasion does not prejudice any rights we might have to charge for reproduction of our copyrighted material in the future.

Altering/Modifying Material: Not Permitted

You may not alter or modify the material in any manner. Abbreviations, additions, deletions and/or any other alterations shall be made only with prior written authorization of the author(s) and/or Springer Science + Business Media. (Please contact Springer at (permissions.dordrecht@springer.com or permissions.heidelberg@springer.com))

Reservation of Rights

Springer Science + Business Media reserves all rights not specifically granted in the combination of (i) the license details provided by you and accepted in the course of this licensing transaction, (ii) these terms and conditions and (iii) CCC's Billing and Payment terms and conditions.

Copyright Notice:Disclaimer

You must include the following copyright and permission notice in connection with any reproduction of the licensed material: "Springer and the original publisher /journal title, volume, year of publication, page, chapter/article title, name(s) of author(s), figure number(s), original copyright notice) is given to the publication in which the material was originally published, by adding: with kind permission from Springer Science and Business Media"

Warranties: None

Example 1: Springer Science + Business Media makes no representations or warranties with respect to the licensed material.

Example 2: Springer Science + Business Media makes no representations or warranties with respect to the licensed material and adopts on its own behalf the limitations and disclaimers established by CCC on its behalf in its Billing and Payment terms and conditions for this licensing

transaction.

Indemnity

You hereby indemnify and agree to hold harmless Springer Science + Business Media and CCC, and their respective officers, directors, employees and agents, from and against any and all claims arising out of your use of the licensed material other than as specifically authorized pursuant to this license.

No Transfer of License

This license is personal to you and may not be sublicensed, assigned, or transferred by you to any other person without Springer Science + Business Media's written permission.

No Amendment Except in Writing

This license may not be amended except in a writing signed by both parties (or, in the case of Springer Science + Business Media, by CCC on Springer Science + Business Media's behalf).

Objection to Contrary Terms

Springer Science + Business Media hereby objects to any terms contained in any purchase order, acknowledgment, check endorsement or other writing prepared by you, which terms are inconsistent with these terms and conditions or CCC's Billing and Payment terms and conditions. These terms and conditions, together with CCC's Billing and Payment terms and conditions (which are incorporated herein), comprise the entire agreement between you and Springer Science + Business Media (and CCC) concerning this licensing transaction. In the event of any conflict between your obligations established by these terms and conditions and those established by CCC's Billing and Payment terms and conditions, these terms and conditions shall control.

Jurisdiction

All disputes that may arise in connection with this present License, or the breach thereof, shall be settled exclusively by arbitration, to be held in The Netherlands, in accordance with Dutch law, and to be conducted under the Rules of the 'Netherlands Arbitrage Instituut' (Netherlands Institute of Arbitration). **OR:**

All disputes that may arise in connection with this present License, or the breach thereof, shall be settled exclusively by arbitration, to be held in the Federal Republic of Germany, in accordance with German law.

Other terms and conditions:

v1.3

If you would like to pay for this license now, please remit this license along with your payment made payable to "COPYRIGHT CLEARANCE CENTER" otherwise you will be invoiced within 48 hours of the license date. Payment should be in the form of a check or money order referencing your account number and this invoice number RLNK501205612. Once you receive your invoice for this order, you may pay your invoice by credit card. Please follow instructions provided at that time.

**Make Payment To:
Copyright Clearance Center
Dept 001
P.O. Box 843006**

G.6. Permission for Figure I-9

ELSEVIER LICENSE TERMS AND CONDITIONS

Jan 20, 2014

This is a License Agreement between Felix S Meier-Stephenson ("You") and Elsevier ("Elsevier") provided by Copyright Clearance Center ("CCC"). The license consists of your order details, the terms and conditions provided by Elsevier, and the payment terms and conditions.

All payments must be made in full to CCC. For payment instructions, please see information listed at the bottom of this form.

Supplier	Elsevier Limited The Boulevard,Langford Lane Kidlington,Oxford,OX5 1GB,UK
Registered Company Number	1982084
Customer name	Felix S Meier-Stephenson
Customer address	4528 Vegas Rd. NW Calgary, AB T3A0N1
License number	3312860473372
License date	Jan 20, 2014
Licensed content publisher	Elsevier
Licensed content publication	The Lancet Neurology
Licensed content title	Tracking pathophysiological processes in Alzheimer's disease: an updated hypothetical model of dynamic biomarkers
Licensed content author	Clifford R Jack,David S Knopman,William J Jagust,Ronald C Petersen,Michael W Weiner,Paul S Aisen,Leslie M Shaw,Prashanthi Vemuri,Heather J Wiste,Stephen D Weigand,Timothy G Lesnick,Vernon S Pankratz,Michael C Donohue,John Q Trojanowski
Licensed content date	February 2013
Licensed content volume number	12
Licensed content issue number	2
Number of pages	10
Start Page	207
End Page	216
Type of Use	reuse in a thesis/dissertation
Intended publisher of new work	other
Portion	figures/tables/illustrations

Number of figures/tables/illustrations	1
Format	both print and electronic
Are you the author of this Elsevier article?	No
Will you be translating?	No
Order reference number	#5268
Title of your thesis/dissertation	A New Theory of Alzheimer's Disease
Expected completion date	Feb 2014
Estimated size (number of pages)	300
Elsevier VAT number	GB 494 6272 12
Permissions price	0.00 USD
VAT/Local Sales Tax	0.00 USD / 0.00 GBP
Total	0.00 USD
Terms and Conditions	

INTRODUCTION

1. The publisher for this copyrighted material is Elsevier. By clicking "accept" in connection with completing this licensing transaction, you agree that the following terms and conditions apply to this transaction (along with the Billing and Payment terms and conditions established by Copyright Clearance Center, Inc. ("CCC"), at the time that you opened your Rightslink account and that are available at any time at <http://myaccount.copyright.com>).

GENERAL TERMS

2. Elsevier hereby grants you permission to reproduce the aforementioned material subject to the terms and conditions indicated.

3. Acknowledgement: If any part of the material to be used (for example, figures) has appeared in our publication with credit or acknowledgement to another source, permission must also be sought from that source. If such permission is not obtained then that material may not be included in your publication/copies. Suitable acknowledgement to the source must be made, either as a footnote or in a reference list at the end of your publication, as follows:

“Reprinted from Publication title, Vol /edition number, Author(s), Title of article / title of chapter, Pages No., Copyright (Year), with permission from Elsevier [OR APPLICABLE SOCIETY COPYRIGHT OWNER].” Also Lancet special credit - “Reprinted from The Lancet, Vol. number, Author(s), Title of article, Pages No., Copyright (Year), with permission from Elsevier.”

4. Reproduction of this material is confined to the purpose and/or media for which permission is hereby given.

5. Altering/Modifying Material: Not Permitted. However figures and illustrations may be altered/adapted minimally to serve your work. Any other abbreviations, additions, deletions and/or

any other alterations shall be made only with prior written authorization of Elsevier Ltd. (Please contact Elsevier at permissions@elsevier.com)

6. If the permission fee for the requested use of our material is waived in this instance, please be advised that your future requests for Elsevier materials may attract a fee.

7. Reservation of Rights: Publisher reserves all rights not specifically granted in the combination of (i) the license details provided by you and accepted in the course of this licensing transaction, (ii) these terms and conditions and (iii) CCC's Billing and Payment terms and conditions.

8. License Contingent Upon Payment: While you may exercise the rights licensed immediately upon issuance of the license at the end of the licensing process for the transaction, provided that you have disclosed complete and accurate details of your proposed use, no license is finally effective unless and until full payment is received from you (either by publisher or by CCC) as provided in CCC's Billing and Payment terms and conditions. If full payment is not received on a timely basis, then any license preliminarily granted shall be deemed automatically revoked and shall be void as if never granted. Further, in the event that you breach any of these terms and conditions or any of CCC's Billing and Payment terms and conditions, the license is automatically revoked and shall be void as if never granted. Use of materials as described in a revoked license, as well as any use of the materials beyond the scope of an unrevoked license, may constitute copyright infringement and publisher reserves the right to take any and all action to protect its copyright in the materials.

9. Warranties: Publisher makes no representations or warranties with respect to the licensed material.

10. Indemnity: You hereby indemnify and agree to hold harmless publisher and CCC, and their respective officers, directors, employees and agents, from and against any and all claims arising out of your use of the licensed material other than as specifically authorized pursuant to this license.

11. No Transfer of License: This license is personal to you and may not be sublicensed, assigned, or transferred by you to any other person without publisher's written permission.

12. No Amendment Except in Writing: This license may not be amended except in a writing signed by both parties (or, in the case of publisher, by CCC on publisher's behalf).

13. Objection to Contrary Terms: Publisher hereby objects to any terms contained in any purchase order, acknowledgment, check endorsement or other writing prepared by you, which terms are inconsistent with these terms and conditions or CCC's Billing and Payment terms and conditions. These terms and conditions, together with CCC's Billing and Payment terms and conditions (which are incorporated herein), comprise the entire agreement between you and publisher (and CCC) concerning this licensing transaction. In the event of any conflict between your obligations established by these terms and conditions and those established by CCC's Billing and Payment terms and conditions, these terms and conditions shall control.

14. Revocation: Elsevier or Copyright Clearance Center may deny the permissions described in this License at their sole discretion, for any reason or no reason, with a full refund payable to you. Notice of such denial will be made using the contact information provided by you. Failure to

receive such notice will not alter or invalidate the denial. In no event will Elsevier or Copyright Clearance Center be responsible or liable for any costs, expenses or damage incurred by you as a result of a denial of your permission request, other than a refund of the amount(s) paid by you to Elsevier and/or Copyright Clearance Center for denied permissions.

LIMITED LICENSE

The following terms and conditions apply only to specific license types:

15. **Translation:** This permission is granted for non-exclusive world **English** rights only unless your license was granted for translation rights. If you licensed translation rights you may only translate this content into the languages you requested. A professional translator must perform all translations and reproduce the content word for word preserving the integrity of the article. If this license is to re-use 1 or 2 figures then permission is granted for non-exclusive world rights in all languages.

16. **Website:** The following terms and conditions apply to electronic reserve and author websites:
Electronic reserve: If licensed material is to be posted to website, the web site is to be password-protected and made available only to bona fide students registered on a relevant course it:

This license was made in connection with a course,

This permission is granted for 1 year only. You may obtain a license for future website posting,

All content posted to the web site must maintain the copyright information line on the bottom of each image,

A hyper-text must be included to the Homepage of the journal from which you are licensing at <http://www.sciencedirect.com/science/journal/xxxxx> or the Elsevier homepage for books at <http://www.elsevier.com> , and

Central Storage: This license does not include permission for a scanned version of the material to be stored in a central repository such as that provided by Heron/XanEdu.

17. **Author website** for journals with the following additional clauses:

All content posted to the web site must maintain the copyright information line on the bottom of each image, and the permission granted is limited to the personal version of your paper. You are not allowed to download and post the published electronic version of your article (whether PDF or HTML, proof or final version), nor may you scan the printed edition to create an electronic version.

A hyper-text must be included to the Homepage of the journal from which you are licensing at <http://www.sciencedirect.com/science/journal/xxxxx> . As part of our normal production process, you will receive an e-mail notice when your article appears on Elsevier's online service ScienceDirect (www.sciencedirect.com). That e-mail will include the article's Digital Object Identifier (DOI). This number provides the electronic link to the published article and should be included in the posting of your personal version. We ask that you wait until you receive this e-mail and have the DOI to do any posting.

Central Storage: This license does not include permission for a scanned version of the material to be stored in a central repository such as that provided by Heron/XanEdu.

18. **Author website** for books with the following additional clauses:

Authors are permitted to place a brief summary of their work online only.

A hyper-text must be included to the Elsevier homepage at <http://www.elsevier.com> . All content posted to the web site must maintain the copyright information line on the bottom of each image. You are not allowed to download and post the published electronic version of your chapter, nor may you scan the printed edition to create an electronic version.

Central Storage: This license does not include permission for a scanned version of the material to be stored in a central repository such as that provided by Heron/XanEdu.

19. **Website** (regular and for author): A hyper-text must be included to the Homepage of the journal from which you are licensing at <http://www.sciencedirect.com/science/journal/xxxxx>. or for books to the Elsevier homepage at <http://www.elsevier.com>

20. **Thesis/Dissertation**: If your license is for use in a thesis/dissertation your thesis may be submitted to your institution in either print or electronic form. Should your thesis be published commercially, please reapply for permission. These requirements include permission for the Library and Archives of Canada to supply single copies, on demand, of the complete thesis and include permission for UMI to supply single copies, on demand, of the complete thesis. Should your thesis be published commercially, please reapply for permission.

21. **Other Conditions**:

v1.6

If you would like to pay for this license now, please remit this license along with your payment made payable to "COPYRIGHT CLEARANCE CENTER" otherwise you will be invoiced within 48 hours of the license date. Payment should be in the form of a check or money order referencing your account number and this invoice number RLNK501205614. Once you receive your invoice for this order, you may pay your invoice by credit card. Please follow instructions provided at that time.

**Make Payment To:
Copyright Clearance Center
Dept 001
P.O. Box 843006
Boston, MA 02284-3006**

For suggestions or comments regarding this order, contact RightsLink Customer Support: customercare@copyright.com or +1-877-622-5543 (toll free in the US) or +1-978-646-2777.

Gratis licenses (referencing \$0 in the Total field) are free. Please retain this printable license for your reference. No payment is required.

G.7. Permission for Figures II-7, II-8 & II-9

NATURE PUBLISHING GROUP LICENSE TERMS AND CONDITIONS

Jan 18, 2014

This is a License Agreement between Felix S Meier-Stephenson ("You") and Nature Publishing Group ("Nature Publishing Group") provided by Copyright Clearance Center ("CCC"). The license consists of your order details, the terms and conditions provided by Nature Publishing Group, and the payment terms and conditions.

All payments must be made in full to CCC. For payment instructions, please see information listed at the bottom of this form.

License Number	3311720577640
License date	Jan 18, 2014
Licensed content publisher	Nature Publishing Group
Licensed content publication	Nature Reviews Microbiology
Licensed content title	Antimicrobial peptides: pore formers or metabolic inhibitors in bacteria?
Licensed content author	Kim A. Brogden
Licensed content date	Mar 1, 2005
Volume number	3
Issue number	3
Type of Use	reuse in a dissertation / thesis
Requestor type	academic/educational
Format	print and electronic
Portion	figures/tables/illustrations
Number of figures/tables/illustrations	3
High-res required	no
Figures	Fig. 3 Fig. 4 Fig. 5
Author of this NPG article	no
Your reference number	
Title of your thesis / dissertation	A New Theory of Alzheimer's Disease
Expected completion date	Feb 2014
Estimated size (number of pages)	300
Total	0.00 USD
Terms and Conditions	

Terms and Conditions for Permissions

Nature Publishing Group hereby grants you a non-exclusive license to reproduce this material for this purpose, and for no other use, subject to the conditions below:

1. NPG warrants that it has, to the best of its knowledge, the rights to license reuse of this material. However, you should ensure that the material you are requesting is original to Nature Publishing Group and does not carry the copyright of another entity (as credited in the published version). If the credit line on any part of the material you have requested indicates that it was reprinted or adapted by NPG with permission from another source, then you should also seek permission from that source to reuse the material.
2. Permission granted free of charge for material in print is also usually granted for any electronic version of that work, provided that the material is incidental to the work as a whole and that the electronic version is essentially equivalent to, or substitutes for, the print version. Where print permission has been granted for a fee, separate permission must be obtained for any additional, electronic re-use (unless, as in the case of a full paper, this has already been accounted for during your initial request in the calculation of a print run). NB: In all cases, web-based use of full-text articles must be authorized separately through the 'Use on a Web Site' option when requesting permission.
3. Permission granted for a first edition does not apply to second and subsequent editions and for editions in other languages (except for signatories to the STM Permissions Guidelines, or where the first edition permission was granted for free).
4. Nature Publishing Group's permission must be acknowledged next to the figure, table or abstract in print. In electronic form, this acknowledgement must be visible at the same time as the figure/table/abstract, and must be hyperlinked to the journal's homepage.
5. The credit line should read:
Reprinted by permission from Macmillan Publishers Ltd: [JOURNAL NAME] (reference citation), copyright (year of publication)
For AOP papers, the credit line should read:
Reprinted by permission from Macmillan Publishers Ltd: [JOURNAL NAME], advance online publication, day month year (doi: 10.1038/sj.[JOURNAL ACRONYM].XXXXX)

Note: For republication from the *British Journal of Cancer*, the following credit lines apply.

Reprinted by permission from Macmillan Publishers Ltd on behalf of Cancer Research UK: [JOURNAL NAME] (reference citation), copyright (year of publication)
For AOP papers, the credit line should read:
Reprinted by permission from Macmillan Publishers Ltd on behalf of Cancer Research UK: [JOURNAL NAME], advance online publication, day month year (doi: 10.1038/sj.[JOURNAL ACRONYM].XXXXX)

6. Adaptations of single figures do not require NPG approval. However, the adaptation should be credited as follows:

Adapted by permission from Macmillan Publishers Ltd: [JOURNAL NAME] (reference citation), copyright (year of publication)

Note: For adaptation from the *British Journal of Cancer*, the following credit line applies.

Adapted by permission from Macmillan Publishers Ltd on behalf of Cancer Research UK: [JOURNAL NAME] (reference citation), copyright (year of publication)

7. Translations of 401 words up to a whole article require NPG approval. Please visit <http://www.macmillanmedicalcommunications.com> for more information. Translations of up to a 400 words do not require NPG approval. The translation should be credited as follows:

Translated by permission from Macmillan Publishers Ltd: [JOURNAL NAME] (reference citation), copyright (year of publication).

Note: For translation from the *British Journal of Cancer*, the following credit line applies.

Translated by permission from Macmillan Publishers Ltd on behalf of Cancer Research UK: [JOURNAL NAME] (reference citation), copyright (year of publication)

We are certain that all parties will benefit from this agreement and wish you the best in the use of this material. Thank you.

Special Terms:

v1.1

If you would like to pay for this license now, please remit this license along with your payment made payable to "COPYRIGHT CLEARANCE CENTER" otherwise you will be invoiced within 48 hours of the license date. Payment should be in the form of a check or money order referencing your account number and this invoice number RLNK501204966. Once you receive your invoice for this order, you may pay your invoice by credit card. Please follow instructions provided at that time.

**Make Payment To:
Copyright Clearance Center
Dept 001
P.O. Box 843006
Boston, MA 02284-3006**

For suggestions or comments regarding this order, contact RightsLink Customer Support: customercare@copyright.com or +1-877-622-5543 (toll free in the US) or +1-978-646-2777.

Gratis licenses (referencing \$0 in the Total field) are free. Please retain this printable license for your reference. No payment is required.

G.8. Permission for Figure IV-4

SPRINGER LICENSE TERMS AND CONDITIONS

Jan 20, 2014

This is a License Agreement between Felix S Meier-Stephenson ("You") and Springer ("Springer") provided by Copyright Clearance Center ("CCC"). The license consists of your order details, the terms and conditions provided by Springer, and the payment terms and conditions.

All payments must be made in full to CCC. For payment instructions, please see information listed at the bottom of this form.

License Number	3312860911945
License date	Jan 20, 2014
Licensed content publisher	Springer
Licensed content publication	Molecular Diversity
Licensed content title	Microwave synthesis solutions from personal chemistry
Licensed content author	Jon-Sverre Schanche
Licensed content date	Jan 1, 2003
Volume number	7
Issue number	2
Type of Use	Thesis/Dissertation
Portion	Figures
Author of this Springer article	No
Order reference number	#5982
Title of your thesis / dissertation	A New Theory of Alzheimer's Disease
Expected completion date	Feb 2014
Estimated size(pages)	300
Total	0.00 USD

Terms and Conditions

Introduction

The publisher for this copyrighted material is Springer Science + Business Media. By clicking "accept" in connection with completing this licensing transaction, you agree that the following terms and conditions apply to this transaction (along with the Billing and Payment terms and conditions established by Copyright Clearance Center, Inc. ("CCC"), at the time that you opened your Rightslink account and that are available at any time at <http://myaccount.copyright.com>).

Limited License

With reference to your request to reprint in your thesis material on which Springer Science and

Business Media control the copyright, permission is granted, free of charge, for the use indicated in your enquiry.

Licenses are for one-time use only with a maximum distribution equal to the number that you identified in the licensing process.

This License includes use in an electronic form, provided its password protected or on the university's intranet or repository, including UMI (according to the definition at the Sherpa website: <http://www.sherpa.ac.uk/romeo/>). For any other electronic use, please contact Springer at (permissions.dordrecht@springer.com or permissions.heidelberg@springer.com).

The material can only be used for the purpose of defending your thesis, and with a maximum of 100 extra copies in paper.

Although Springer holds copyright to the material and is entitled to negotiate on rights, this license is only valid, subject to a courtesy information to the author (address is given with the article/chapter) and provided it concerns original material which does not carry references to other sources (if material in question appears with credit to another source, authorization from that source is required as well).

Permission free of charge on this occasion does not prejudice any rights we might have to charge for reproduction of our copyrighted material in the future.

Altering/Modifying Material: Not Permitted

You may not alter or modify the material in any manner. Abbreviations, additions, deletions and/or any other alterations shall be made only with prior written authorization of the author(s) and/or Springer Science + Business Media. (Please contact Springer at (permissions.dordrecht@springer.com or permissions.heidelberg@springer.com))

Reservation of Rights

Springer Science + Business Media reserves all rights not specifically granted in the combination of (i) the license details provided by you and accepted in the course of this licensing transaction, (ii) these terms and conditions and (iii) CCC's Billing and Payment terms and conditions.

Copyright Notice:Disclaimer

You must include the following copyright and permission notice in connection with any reproduction of the licensed material: "Springer and the original publisher /journal title, volume, year of publication, page, chapter/article title, name(s) of author(s), figure number(s), original copyright notice) is given to the publication in which the material was originally published, by adding: with kind permission from Springer Science and Business Media"

Warranties: None

Example 1: Springer Science + Business Media makes no representations or warranties with respect to the licensed material.

Example 2: Springer Science + Business Media makes no representations or warranties with respect to the licensed material and adopts on its own behalf the limitations and disclaimers

established by CCC on its behalf in its Billing and Payment terms and conditions for this licensing transaction.

Indemnity

You hereby indemnify and agree to hold harmless Springer Science + Business Media and CCC, and their respective officers, directors, employees and agents, from and against any and all claims arising out of your use of the licensed material other than as specifically authorized pursuant to this license.

No Transfer of License

This license is personal to you and may not be sublicensed, assigned, or transferred by you to any other person without Springer Science + Business Media's written permission.

No Amendment Except in Writing

This license may not be amended except in a writing signed by both parties (or, in the case of Springer Science + Business Media, by CCC on Springer Science + Business Media's behalf).

Objection to Contrary Terms

Springer Science + Business Media hereby objects to any terms contained in any purchase order, acknowledgment, check endorsement or other writing prepared by you, which terms are inconsistent with these terms and conditions or CCC's Billing and Payment terms and conditions. These terms and conditions, together with CCC's Billing and Payment terms and conditions (which are incorporated herein), comprise the entire agreement between you and Springer Science + Business Media (and CCC) concerning this licensing transaction. In the event of any conflict between your obligations established by these terms and conditions and those established by CCC's Billing and Payment terms and conditions, these terms and conditions shall control.

Jurisdiction

All disputes that may arise in connection with this present License, or the breach thereof, shall be settled exclusively by arbitration, to be held in The Netherlands, in accordance with Dutch law, and to be conducted under the Rules of the 'Netherlands Arbitrage Instituut' (Netherlands Institute of Arbitration). **OR:**

All disputes that may arise in connection with this present License, or the breach thereof, shall be settled exclusively by arbitration, to be held in the Federal Republic of Germany, in accordance with German law.

Other terms and conditions:

v1.3

If you would like to pay for this license now, please remit this license along with your payment made payable to "COPYRIGHT CLEARANCE CENTER" otherwise you will be invoiced within 48 hours of the license date. Payment should be in the form of a check or money order referencing your account number and this invoice number RLNK501205615. Once you receive your invoice for this order, you may pay your invoice by credit card. Please follow instructions provided at that time.

Make Payment To:

**Copyright Clearance Center
Dept 001
P.O. Box 843006
Boston, MA 02284-3006**

**For suggestions or comments regarding this order, contact RightsLink Customer Support:
customercare@copyright.com or +1-877-622-5543 (toll free in the US) or +1-978-646-
2777.**

**Gratis licenses (referencing \$0 in the Total field) are free. Please retain this printable
license for your reference. No payment is required.**

G.9. Permission for Figure V-22A

ELSEVIER LICENSE TERMS AND CONDITIONS

Jan 29, 2014

This is a License Agreement between Felix S Meier-Stephenson ("You") and Elsevier ("Elsevier") provided by Copyright Clearance Center ("CCC"). The license consists of your order details, the terms and conditions provided by Elsevier, and the payment terms and conditions.

All payments must be made in full to CCC. For payment instructions, please see information listed at the bottom of this form.

Supplier	Elsevier Limited The Boulevard, Langford Lane Kidlington, Oxford, OX5 1GB, UK
Registered Company Number	1982084
Customer name	Felix S Meier-Stephenson
Customer address	4528 Vegas Rd. NW Calgary, AB T3A0N1
License number	3318310407112
License date	Jan 29, 2014
Licensed content publisher	Elsevier
Licensed content publication	Elsevier Books
Licensed content title	Methods in Enzymology, Volume 413
Licensed content author	Gal Bitan
Licensed content date	2006
Number of pages	20
Start Page	217
End Page	236
Type of Use	reuse in a thesis/dissertation
Intended publisher of new work	other
Portion	figures/tables/illustrations
Number of figures/tables/illustrations	1
Format	both print and electronic
Are you the author of this Elsevier chapter?	No
Will you be translating?	No
Order reference number	#2196
Title of your thesis/dissertation	A New Theory of Alzheimer's Disease
Expected completion date	Feb 2014
Estimated size (number of pages)	
Elsevier VAT number	GB 494 6272 12

Permissions price	0.00 USD
VAT/Local Sales Tax	0.00 USD / 0.00 GBP
Total	0.00 USD
Terms and Conditions	

INTRODUCTION

1. The publisher for this copyrighted material is Elsevier. By clicking "accept" in connection with completing this licensing transaction, you agree that the following terms and conditions apply to this transaction (along with the Billing and Payment terms and conditions established by Copyright Clearance Center, Inc. ("CCC"), at the time that you opened your Rightslink account and that are available at any time at <http://myaccount.copyright.com>).

GENERAL TERMS

2. Elsevier hereby grants you permission to reproduce the aforementioned material subject to the terms and conditions indicated.

3. Acknowledgement: If any part of the material to be used (for example, figures) has appeared in our publication with credit or acknowledgement to another source, permission must also be sought from that source. If such permission is not obtained then that material may not be included in your publication/copies. Suitable acknowledgement to the source must be made, either as a footnote or in a reference list at the end of your publication, as follows:

"Reprinted from Publication title, Vol /edition number, Author(s), Title of article / title of chapter, Pages No., Copyright (Year), with permission from Elsevier [OR APPLICABLE SOCIETY COPYRIGHT OWNER]." Also Lancet special credit -"Reprinted from The Lancet, Vol. number, Author(s), Title of article, Pages No., Copyright (Year), with permission from Elsevier."

4. Reproduction of this material is confined to the purpose and/or media for which permission is hereby given.

5. Altering/Modifying Material: Not Permitted. However figures and illustrations may be altered/adapted minimally to serve your work. Any other abbreviations, additions, deletions and/or any other alterations shall be made only with prior written authorization of Elsevier Ltd. (Please contact Elsevier at permissions@elsevier.com)

6. If the permission fee for the requested use of our material is waived in this instance, please be advised that your future requests for Elsevier materials may attract a fee.

7. Reservation of Rights: Publisher reserves all rights not specifically granted in the combination of (i) the license details provided by you and accepted in the course of this licensing transaction, (ii) these terms and conditions and (iii) CCC's Billing and Payment terms and conditions.

8. License Contingent Upon Payment: While you may exercise the rights licensed immediately upon issuance of the license at the end of the licensing process for the transaction, provided that you have disclosed complete and accurate details of your proposed use, no license is finally effective unless and until full payment is received from you (either by publisher or by CCC) as provided in CCC's Billing and Payment terms and conditions. If full payment is not received on a timely basis, then any license preliminarily granted shall be deemed automatically revoked and shall be void as if never granted. Further, in the event that you breach any of these terms and conditions or any of CCC's Billing and Payment terms and conditions, the license is automatically revoked and shall be void as if never granted. Use of materials as described in a revoked license, as well as any use of the materials beyond the scope of an unrevoked license, may constitute copyright infringement and publisher reserves the right to take any and all action to protect its copyright in the materials.

9. Warranties: Publisher makes no representations or warranties with respect to the licensed material.

10. Indemnity: You hereby indemnify and agree to hold harmless publisher and CCC, and their respective officers, directors, employees and agents, from and against any and all claims arising out of your use of the licensed material other than as specifically authorized pursuant to this license.

11. No Transfer of License: This license is personal to you and may not be sublicensed, assigned, or transferred by you to any other person without publisher's written permission.

12. No Amendment Except in Writing: This license may not be amended except in a writing signed by both parties (or, in the case of publisher, by CCC on publisher's behalf).

13. Objection to Contrary Terms: Publisher hereby objects to any terms contained in any purchase order, acknowledgment, check endorsement or other writing prepared by you, which terms are inconsistent with these terms and conditions or CCC's Billing and Payment terms and conditions. These terms and conditions, together with CCC's Billing and Payment terms and conditions (which are incorporated herein), comprise the entire agreement between you and publisher (and CCC) concerning this licensing transaction. In the event of any conflict between your obligations established by these terms and conditions and those established by CCC's Billing and Payment terms and conditions, these terms and conditions shall control.

14. Revocation: Elsevier or Copyright Clearance Center may deny the permissions described in this License at their sole discretion, for any reason or no reason, with a full refund payable to you. Notice of such denial will be made using the

contact information provided by you. Failure to receive such notice will not alter or invalidate the denial. In no event will Elsevier or Copyright Clearance Center be responsible or liable for any costs, expenses or damage incurred by you as a result of a denial of your permission request, other than a refund of the amount(s) paid by you to Elsevier and/or Copyright Clearance Center for denied permissions.

LIMITED LICENSE

The following terms and conditions apply only to specific license types:

15. Translation: This permission is granted for non-exclusive world **English** rights only unless your license was granted for translation rights. If you licensed translation rights you may only translate this content into the languages you requested. A professional translator must perform all translations and reproduce the content word for word preserving the integrity of the article. If this license is for use 1 or 2 figures then permission is granted for non-exclusive world rights in all languages.

16. Posting licensed content on any Website: The following terms and conditions apply as follows: Licensing material from an Elsevier journal: All content posted to the web site must maintain the copyright information line on the bottom of each image; A hyper-text must be included to the Homepage of the journal from which you are licensing at <http://www.sciencedirect.com/science/journal/xxxx> or the Elsevier homepage for books at <http://www.elsevier.com>;

Central Storage: This license does not include permission for a scanned version of the material to be stored in a central repository such as that provided by Heron/XanEdu.

Licensing material from an Elsevier book: A hyper-text link must be included to the Elsevier homepage at <http://www.elsevier.com>. All content posted to the web site must maintain the copyright information line on the bottom of each image.

Posting licensed content on Electronic reserve: In addition to the above the following clauses are applicable: The web site must be password-protected and made available only to bona fide students registered on a relevant course. This permission is granted for 1 year only. You may obtain a new license for future website posting.

For journal authors: the following clauses are applicable in addition to the above: Permission granted is limited to the author accepted manuscript version* of your paper.

***Accepted Author Manuscript (AAM) Definition:** An accepted author manuscript (AAM) is the author's version of the manuscript of an article that has been accepted for publication and which may include any author-incorporated changes suggested through the processes of submission processing, peer review, and editor-author communications. AAMs do not include other publisher value-added contributions such as copy-editing, formatting, technical enhancements and (if relevant) pagination.

You are not allowed to download and post the published journal article (whether PDF or HTML, proof or final version), nor may you scan the printed edition to create an electronic version. A hyper-text must be included to the Homepage of the journal from which you are licensing at <http://www.sciencedirect.com/science/journal/xxxx>. As part of our normal production process, you will receive an e-mail notice when your article appears on Elsevier's online service ScienceDirect (www.sciencedirect.com). That e-mail will include the article's Digital Object Identifier (DOI). This number provides the electronic link to the published article and should be included in the posting of your personal version. We ask that you wait until you receive this e-mail and have the DOI to do any posting.

Posting to a repository: Authors may post their AAM immediately to their employer's institutional repository for internal use only and may make their manuscript publicly available after the journal-specific embargo period has ended. Please also refer to Elsevier's Article Posting Policy for further information.

18. For book authors the following clauses are applicable in addition to the above: Authors are permitted to place a brief summary of their work online only. You are not allowed to download and post the published electronic version of your chapter, nor may you scan the printed edition to create an electronic version. Posting to a repository: Authors are permitted to post a summary of their chapter only in their institution's repository.

20. Thesis/Dissertation: If your license is for use in a thesis/dissertation your thesis may be submitted to your institution in either print or electronic form. Should your thesis be published commercially, please reapply for permission. These requirements include permission for the Library and Archives of Canada to supply single copies, on demand, of the complete thesis and include permission for UMI to supply single copies, on demand, of the complete thesis. Should your thesis be published commercially, please reapply for permission.

Elsevier Open Access Terms and Conditions

Elsevier publishes Open Access articles in both its Open Access journals and via its Open Access articles option in subscription journals.

Authors publishing in an Open Access journal or who choose to make their article Open Access in an Elsevier subscription journal select one of the following Creative Commons user licenses, which define how a reader may reuse their work: Creative Commons Attribution License (CC BY), Creative Commons Attribution – Non Commercial -

ShareAlike (CC BY NCSA) and Creative Commons Attribution – Non Commercial – No Derivatives (CC BYNC ND)

Terms & Conditions applicable to all Elsevier Open Access articles:

Any reuse of the article must not represent the author as endorsing the adaptation of the article nor should the article be modified in such a way as to damage the author's honour or reputation.

The author(s) must be appropriately credited.

If any part of the material to be used (for example, figures) has appeared in our publication with credit or acknowledgement to another source it is the responsibility of the user to ensure their reuse complies with the terms and conditions determined by the rights holder.

Additional Terms & Conditions applicable to each Creative Commons user license:

CC BY: You may distribute and copy the article, create extracts, abstracts, and other revised versions, adaptations or derivative works of or from an article (such as a translation), to include in a collective work (such as an anthology), to text or data mine the article, including for commercial purposes without permission from Elsevier

CC BY NC SA: For non-commercial purposes you may distribute and copy the article, create extracts, abstracts and other revised versions, adaptations or derivative works of or from an article (such as a translation), to include in a collective work (such as an anthology), to text and data mine the article and license new adaptations or creations under identical terms without permission from Elsevier

CC BY NC ND: For non-commercial purposes you may distribute and copy the article and include it in a collective work (such as an anthology), provided you do not alter or modify the article, without permission from Elsevier

Any commercial reuse of Open Access articles published with a CC BY NC SA or CC BY NC ND license requires permission from Elsevier and will be subject to a fee.

Commercial reuse includes:

- Promotional purposes (advertising or marketing)
 - Commercial exploitation (e.g. a product for sale or loan)
 - Systematic distribution (for a fee or free of charge)
- Please refer to Elsevier's Open Access Policy for further information.

21. Other Conditions:

v1.7

If you would like to pay for this license now, please remit this license along with your payment made payable to "COPYRIGHT CLEARANCE CENTER" otherwise you will be invoiced within 48 hours of the license date. Payment should be in the form of a check or money order referencing your account number and this invoice number RLNK501214162. Once you receive your invoice for this order, you may pay your invoice by credit card. Please follow instructions provided at that time.

Make Payment To:
Copyright Clearance Center
Dept 001
P.O. Box 843006
Boston, MA 02284-3006

For suggestions or comments regarding this order, contact RightsLink Customer Support:
customercare@copyright.com or +1-877-622-5543 (toll free in the US) or +1-978-646-2777.

Gratis licenses (referencing \$0 in the Total field) are free. Please retain this printable license for your reference. No payment is required.

G.10. Permission for Figure V-22B



RightsLink®

Home

Account Info

Help



ACS Publications
High quality. High impact.

Title: Femtosecond Transient Absorption Anisotropy Study on [Ru(bpy)₃]²⁺ and [Ru(bpy)₃(py)₂]²⁺. Ultrafast Interligand Randomization of the MLCT State

Logged in as:

Felix Meier

Account #:
3000740470

LOGOUT

Author: Staffan Wallin,[†] Jan Davidsson,[†] Judit Modin,[‡] and Leif Hammarström*,[†]

Publication: The Journal of Physical Chemistry A

Publisher: American Chemical Society

Date: Jun 1, 2005

Copyright © 2005, American Chemical Society

PERMISSION/LICENSE IS GRANTED FOR YOUR ORDER AT NO CHARGE

This type of permission/license, instead of the standard Terms & Conditions, is sent to you because no fee is being charged for your order. Please note the following:

- Permission is granted for your request in both print and electronic formats, and translations.
- If figures and/or tables were requested, they may be adapted or used in part.
- Please print this page for your records and send a copy of it to your publisher/graduate school.
- Appropriate credit for the requested material should be given as follows: "Reprinted (adapted) with permission from (COMPLETE REFERENCE CITATION). Copyright (YEAR) American Chemical Society." Insert appropriate information in place of the capitalized words.
- One-time permission is granted only for the use specified in your request. No additional uses are granted (such as derivative works or other editions). For any other uses, please submit a new request.

If credit is given to another source for the material you requested, permission must be obtained from that source.

BACK

CLOSE WINDOW

Copyright © 2014 Copyright Clearance Center, Inc. All Rights Reserved. [Privacy statement](#). Comments? We would like to hear from you. E-mail us at customercare@copyright.com

REFERENCES

Chapter I

1. Alzheimer, A. Über eine eigenartige Erkrankung der Hirnrinde. Vortrag in der Versammlung Südwestdeutscher Irrenärzte in Tübingen am 3. November 1906. *Allgemeine Zeitschrift für Psychiatrie und psychisch-gerichtliche Medizin* **1907**, *64*, 146-148.
2. Alzheimer, A.; Stelzmann, R. A.; Schnitzlein, H. N.; Murtagh, F. R. An English translation of Alzheimer's 1907 paper, "Über eine eigenartige Erkrankung der Hirnrinde". *Clin. Anat.* **1995**, *8*, 429-431.
3. Kraepelin, E. *Psychiatrie: ein Lehrbuch für Studierende und Ärzte. II. Band, Klinische Psychiatrie. I. Teil*; Johann Ambrosius Barth: Leipzig, 1910; , pp 1.
4. Kidd, M. Paired helical filaments in electron microscopy of Alzheimer's disease. *Nature* **1963**, *197*, 192-193.
5. Terry, R. D.; Gonatas, N. K.; Weiss, M. Ultrastructural Studies in Alzheimer's Presenile Dementia. *Am. J. Pathol.* **1964**, *44*, 269-297.
6. Glenner, G. G.; Wong, C. W. Alzheimer's disease: Initial report of the purification and characterization of a novel cerebrovascular amyloid protein. *Biochem. Biophys. Res. Commun.* **1984**, *120*, 885-890.
7. Heston, L. L.; Mastri, A. R. The genetics of Alzheimer's disease: associations with hematologic malignancy and Down's syndrome. *Arch. Gen. Psychiatry* **1977**, *34*, 976-981.
8. Schellenberg, G. D. Early Alzheimer's disease genetics. *J. Alzheimers Dis.* **2006**, *9*, 367-372.
9. Bertram, L.; Tanzi, R. E. The genetics of Alzheimer's disease. *Prog. Mol. Biol. Transl. Sci.* **2012**, *107*, 79-100.
10. Jack, C. R., Jr; Knopman, D. S.; Jagust, W. J.; Shaw, L. M.; Aisen, P. S.; Weiner, M. W.; Petersen, R. C.; Trojanowski, J. Q. Hypothetical model of dynamic biomarkers of the Alzheimer's pathological cascade. *Lancet Neurol.* **2010**, *9*, 119-128.

11. Ferri, C. P.; Sousa, R.; Albanese, E.; Ribeiro, W. S.; Honyashiki, M.; Acosta, D.; Blom, M.; Dudgeon, S.; Frantz, N.; Geiger, A.; Jansen, S.; Ketteringham, A.; Kinnaird, L.; Martensson, B.; Rees, G.; Schaper, F.; Splaine, M.; Tamitegama, T.; Westerlund, K.; Wortmann, M. *World Alzheimer Report 2009*. **2009**, *1*, 1-96.
12. Canadian study of health and aging: study methods and prevalence of dementia. *CMAJ* **1994**, *150*, 899-913.
13. Canadian Institute for Health Information. *The Burden of Neurologic Diseases, Disorders and Injuries in Canada*. **2007**.
14. Dudgeon, S. *Rising Tide - The Impact of Dementia on Canadian Society*. **2010**, 1-35.
15. Sperling, R. A.; Aisen, P. S.; Beckett, L. A.; Bennett, D. A.; Craft, S.; Fagan, A. M.; Iwatsubo, T.; Jack Jr., C. R.; Kaye, J.; Montine, T. J.; Park, D. C.; Reiman, E. M.; Rowe, C. C.; Siemers, E.; Stern, Y.; Yaffe, K.; Carrillo, M. C.; Thies, B.; Morrison-Bogorad, M.; Wagster, M. V.; Phelps, C. H. Toward defining the preclinical stages of Alzheimer's disease: Recommendations from the National Institute on Aging-Alzheimer's Association workgroups on diagnostic guidelines for Alzheimer's disease. *Alzheimer's and Dementia* **2011**, *7*, 280-292.
16. Braak, H.; Braak, E. Neuropathological staging of Alzheimer-related changes. *Acta Neuropathol.* **1991**, *82*, 239-259.
17. Braak, H.; Braak, E. Morphological criteria for the recognition of Alzheimer's disease and the distribution pattern of cortical changes related to this disorder. *Neurobiol. Aging* **1994**, *15*, 355-6; discussion 379-80.
18. Braak, H.; Braak, E.; Bohl, J. Staging of Alzheimer-related cortical destruction. *Eur. Neurol.* **1993**, *33*, 403-408.
19. Braak, H.; Braak, E. Staging of Alzheimer's disease-related neurofibrillary changes. *Neurobiol. Aging* **1995**, *16*, 271-8; discussion 278-84.
20. Braak, H.; Braak, E. Staging of Alzheimer-related cortical destruction. *Int. Psychogeriatr.* **1997**, *9 Suppl 1*, 257-61; discussion 269-72.
21. Braak, E.; Griffing, K.; Arai, K.; Bohl, J.; Bratzke, H.; Braak, H. Neuropathology of Alzheimer's disease: what is new since A. Alzheimer? *Eur. Arch. Psychiatry Clin. Neurosci.* **1999**, *249 Suppl 3*, 14-22.
22. Braak, H.; Braak, E. Evolution of neuronal changes in the course of Alzheimer's disease. *J. Neural Transm. Suppl.* **1998**, *53*, 127-140.

23. Braak, H.; Braak, E. Frequency of stages of Alzheimer-related lesions in different age categories. *Neurobiol. Aging* **1997**, *18*, 351-357.
24. Schoenheit, B.; Zarski, R.; Ohm, T. G. Spatial and temporal relationships between plaques and tangles in Alzheimer-pathology. *Neurobiol. Aging* **2004**, *25*, 697-711.
25. Duyckaerts, C.; Hauw, J. J. Diagnosis and staging of Alzheimer disease. *Neurobiol. Aging* **1997**, *18*, S33-42.
26. Dickson, D. W. Neuropathological diagnosis of Alzheimer's disease: a perspective from longitudinal clinicopathological studies. *Neurobiol. Aging* **1997**, *18*, S21-6.
27. Thal, D. R.; Braak, H. Post-mortem diagnosis of Alzheimer's disease. *Pathologie* **2005**, *26*, 201-213.
28. Mesulam, M. M. Neuroplasticity failure in Alzheimer's disease: bridging the gap between plaques and tangles. *Neuron* **1999**, *24*, 521-529.
29. Davies, P.; Maloney, A. J. Selective loss of central cholinergic neurons in Alzheimer's disease. *Lancet* **1976**, *2*, 1403.
30. Perry, E. K.; Gibson, P. H.; Blessed, G.; Perry, R. H.; Tomlinson, B. E. Neurotransmitter enzyme abnormalities in senile dementia. Choline acetyltransferase and glutamic acid decarboxylase activities in necropsy brain tissue. *J. Neurol. Sci.* **1977**, *34*, 247-265.
31. Bowen, D. M. Biochemistry of Dementias. *Proc. R. Soc. Med.* **1977**, *70*, 351-353.
32. Kril, J. J.; Patel, S.; Harding, A. J.; Halliday, G. M. Neuron loss from the hippocampus of Alzheimer's disease exceeds extracellular neurofibrillary tangle formation. *Acta Neuropathol.* **2002**, *103*, 370-376.
33. McKenzie, J. E.; Roberts, G. W.; Royston, M. C. Comparative investigation of neurofibrillary damage in the temporal lobe in Alzheimer's disease, Down's syndrome and dementia pugilistica. *Neurodegeneration* **1996**, *5*, 259-264.
34. Terry, R. D. Neuropathological changes in Alzheimer disease. *Prog. Brain Res.* **1994**, *101*, 383-390.
35. Dickson, T. C.; King, C. E.; McCormack, G. H.; Vickers, J. C. Neurochemical diversity of dystrophic neurites in the early and late stages of Alzheimer's disease. *Exp. Neurol.* **1999**, *156*, 100-110.
36. Hof, P.; Morrison, J. In *The cellular basis of cortical disconnection in Alzheimer disease and related dementing conditions*; Terry, R., Katzman, R. and Bick, K., Eds.; Alzheimer disease; Raven Press: New York, **1994**; pp. 197-229.

37. Masliah, E.; Mallory, M.; Deerinck, T.; DeTeresa, R.; Lamont, S.; Miller, A.; Terry, R. D.; Carragher, B.; Ellisman, M. Re-evaluation of the structural organization of neuritic plaques in Alzheimer's disease. *J. Neuropathol. Exp. Neurol.* **1993**, *52*, 619-632.
38. Praprotnik, D.; Smith, M. A.; Richey, P. L.; Vinters, H. V.; Perry, G. Filament heterogeneity within the dystrophic neurites of senile plaques suggests blockage of fast axonal transport in Alzheimer's disease. *Acta Neuropathol.* **1996**, *91*, 226-235.
39. Vickers, J. C.; Chin, D.; Edwards, A. M.; Sampson, V.; Harper, C.; Morrison, J. Dystrophic neurite formation associated with age-related β amyloid deposition in the neocortex: clues to the genesis of neurofibrillary pathology. *Exp. Neurol.* **1996**, *141*, 1-11.
40. Gray, E. G. Spongiform encephalopathy: a neurocytologist's viewpoint with a note on Alzheimer's disease. *Neuropathol. Appl. Neurobiol.* **1986**, *12*, 149-172.
41. Gray, E. G.; Paula-Barbosa, M.; Roher, A. Alzheimer's disease: paired helical filaments and cytomembranes. *Neuropathol. Appl. Neurobiol.* **1987**, *13*, 91-110.
42. Paula-Barbosa, M.; Tavares, M. A.; Cadete-Leite, A. A quantitative study of frontal cortex dendritic microtubules in patients with Alzheimer's disease. *Brain Res.* **1987**, *417*, 139-142.
43. Adlard, P. A.; Vickers, J. C. Morphologically distinct plaque types differentially affect dendritic structure and organisation in the early and late stages of Alzheimer's disease. *Acta Neuropathol.* **2002**, *103*, 377-383.
44. Knowles, R. B.; Gomez-Isla, T.; Hyman, B. T. A β associated neuropil changes: correlation with neuronal loss and dementia. *J. Neuropathol. Exp. Neurol.* **1998**, *57*, 1122-1130.
45. Knowles, R. B.; Wyart, C.; Buldyrev, S. V.; Cruz, L.; Urbanc, B.; Hasselmo, M. E.; Stanley, H. E.; Hyman, B. T. Plaque-induced neurite abnormalities: implications for disruption of neural networks in Alzheimer's disease. *Proc. Natl. Acad. Sci. U. S. A.* **1999**, *96*, 5274-5279.
46. Farfara, D.; Lifshitz, V.; Frenkel, D. Neuroprotective and Neurotoxic Properties of Glial Cells in the Pathogenesis of Alzheimer's Disease. *J. Cell. Mol. Med.* **2008**, *12*, 762-780.
47. Diamond, J. A Report on Alzheimer's Disease and Current Research. **2008**, *1*.
48. Ferri, C. P.; Prince, M.; Brayne, C.; Brodaty, H.; Fratiglioni, L.; Ganguli, M.; Hall, K.; Hasegawa, K.; Hendrie, H.; Huang, Y.; Jorm, A.; Mathers, C.; Menezes, P. R.; Rimmer, E.; Scazufca, M.; Alzheimer's Disease International. Global prevalence of dementia: a Delphi consensus study. *Lancet* **2005**, *366*, 2112-2117.
49. Mattson, M. P. Gene-diet interactions in brain aging and neurodegenerative disorders. *Ann. Intern. Med.* **2003**, *139*, 441-444.

50. Song, X.; Mitnitski, A.; Rockwood, K. Nontraditional risk factors combine to predict Alzheimer disease and dementia. *Neurology* **2011**, *77*, 227-234.
51. Scheuner, D.; Eckman, C.; Jensen, M.; Song, X.; Citron, M.; Suzuki, N.; Bird, T. D.; Hardy, J.; Hutton, M.; Kukull, W.; Larson, E.; Levy-Lahad, E.; Viitanen, M.; Peskind, E.; Poorkaj, P.; Schellenberg, G.; Tanzi, R.; Wasco, W.; Lannfelt, L.; Selkoe, D.; Younkin, S. Secreted amyloid β -protein similar to that in the senile plaques of Alzheimer's disease is increased in vivo by the presenilin 1 and 2 and APP mutations linked to familial Alzheimer's disease. *Nat. Med.* **1996**, *2*, 864-870.
52. De Jonghe, C.; Zehr, C.; Yager, D.; Prada, C. M.; Younkin, S.; Hendriks, L.; Van Broeckhoven, C.; Eckman, C. B. Flemish and Dutch mutations in amyloid β precursor protein have different effects on amyloid β secretion. *Neurobiol. Dis.* **1998**, *5*, 281-286.
53. Hendriks, L.; van Duijn, C. M.; Cras, P.; Cruts, M.; Van Hul, W.; van Harskamp, F.; Warren, A.; McInnis, M. G.; Antonarakis, S. E.; Martin, J. J. Presenile dementia and cerebral haemorrhage linked to a mutation at codon 692 of the β -amyloid precursor protein gene. *Nat. Genet.* **1992**, *1*, 218-221.
54. Nilsberth, C.; Westlind-Danielsson, A.; Eckman, C. B.; Condron, M. M.; Axelman, K.; Forsell, C.; Stenh, C.; Luthman, J.; Teplow, D. B.; Younkin, S. G.; Naslund, J.; Lannfelt, L. The 'Arctic' APP mutation (E693G) causes Alzheimer's disease by enhanced A β protofibril formation. *Nat. Neurosci.* **2001**, *4*, 887-893.
55. Suzuki, N.; Cheung, T. T.; Cai, X. D.; Odaka, A.; Otvos, L., Jr; Eckman, C.; Golde, T. E.; Younkin, S. G. An increased percentage of long amyloid β protein secreted by familial amyloid β protein precursor (β APP₇₁₇) mutants. *Science* **1994**, *264*, 1336-1340.
56. Cruts, M.; Theuns, J.; Van Broeckhoven, C. Locus-specific mutation databases for neurodegenerative brain diseases. *Hum. Mutat.* **2012**, *33*, 1340-1344.
57. Ankarcona, M. In *The Role of Presenilins in A β -Induced Cell Death in Alzheimer's Disease*; Barrow, C. J., Small, D. H., Eds.; A β peptide and Alzheimer's disease - Celebrating a century of research; Springer: London, **2007**; pp. 234-244.
58. Chan, Y.; Jan, Y. N. Presenilins, Processing of β -Amyloid Precursor Protein, and Notch Signaling. *Neuron* **1999**, *23*, 201-204.
59. Muller, U.; Winter, P.; Graeber, M. B. A presenilin 1 mutation in the first case of Alzheimer's disease. *Lancet Neurol.* **2013**, *12*, 129-130.
60. Verdile, G.; Gandy, S. E.; Martins, R. N. The role of presenilin and its interacting proteins in the biogenesis of Alzheimer's β amyloid. *Neurochem. Res.* **2007**, *32*, 609-623.

61. Sudoh, S.; Kawamura, Y.; Sato, S.; Wang, R.; Saido, T. C.; Oyama, F.; Sakaki, Y.; Komano, H.; Yanagisawa, K. Presenilin 1 mutations linked to familial Alzheimer's disease increase the intracellular levels of amyloid β -protein 1-42 and its N-terminally truncated variant(s) which are generated at distinct sites. *J. Neurochem.* **1998**, *71*, 1535-1543.
62. Li, Y. M.; Lai, M. T.; Xu, M.; Huang, Q.; DiMuzio-Mower, J.; Sardana, M. K.; Shi, X. P.; Yin, K. C.; Shafer, J. A.; Gardell, S. J. Presenilin 1 is linked with γ -secretase activity in the detergent solubilized state. *Proc. Natl. Acad. Sci. U. S. A.* **2000**, *97*, 6138-6143.
63. Sadowski, M. J.; Pankiewicz, J.; Scholtzova, H.; Mehta, P. D.; Prelli, F.; Quartermain, D.; Wisniewski, T. Blocking the apolipoprotein E/amyloid- β interaction as a potential therapeutic approach for Alzheimer's disease. *Proc. Natl. Acad. Sci. U. S. A.* **2006**, *103*, 18787-18792.
64. Ghebremedhin, E.; Schultz, C.; Braak, E.; Braak, H. High frequency of apolipoprotein E epsilon4 allele in young individuals with very mild Alzheimer's disease-related neurofibrillary changes. *Exp. Neurol.* **1998**, *153*, 152-155.
65. Adalbert, R.; Gilley, J.; Coleman, M. P. A β , tau and ApoE4 in Alzheimer's disease: the axonal connection. *Trends Mol. Med.* **2007**, *13*, 135-142.
66. Bell, R. D.; Sagare, A. P.; Friedman, A. E.; Bedi, G. S.; Holtzman, D. M.; Deane, R.; Zlokovic, B. V. Transport pathways for clearance of human Alzheimer's amyloid β -peptide and apolipoproteins E and J in the mouse central nervous system. *J. Cereb. Blood Flow Metab.* **2007**, *27*, 909-918.
67. Koffie, R. M.; Hashimoto, T.; Tai, H. C.; Kay, K. R.; Serrano-Pozo, A.; Joyner, D.; Hou, S.; Kopeikina, K. J.; Frosch, M. P.; Lee, V. M.; Holtzman, D. M.; Hyman, B. T.; Spires-Jones, T. L. Apolipoprotein E4 effects in Alzheimer's disease are mediated by synaptotoxic oligomeric amyloid- β . *Brain* **2012**, *135*, 2155-2168.
68. Corder, E. H.; Saunders, A. M.; Strittmatter, W. J.; Schmechel, D. E.; Gaskell, P. C.; Small, G. W.; Roses, A. D.; Haines, J. L.; Pericak-Vance, M. A. Gene dose of apolipoprotein E type 4 allele and the risk of Alzheimer's disease in late onset families. *Science* **1993**, *261*, 921-923.
69. Sing, C. F.; Davignon, J. Role of the apolipoprotein E polymorphism in determining normal plasma lipid and lipoprotein variation. *Am. J. Hum. Genet.* **1985**, *37*, 268-285.
70. Strittmatter, W. J.; Roses, A. D. Apolipoprotein E and Alzheimer disease. *Proc. Natl. Acad. Sci. U. S. A.* **1995**, *92*, 4725-4727.

71. Wu, C. W.; Liao, P. C.; Lin, C.; Kuo, C. J.; Chen, S. T.; Chen, H. I.; Kuo, Y. M. Brain region-dependent increases in β -amyloid and apolipoprotein E levels in hypercholesterolemic rabbits. *J. Neural Transm.* **2003**, *110*, 641-649.
72. Hayashi, H.; Igbavboa, U.; Hamanaka, H.; Kobayashi, M.; Fujita, S. C.; Wood, W. G.; Yanagisawa, K. Cholesterol is increased in the exofacial leaflet of synaptic plasma membranes of human apolipoprotein E4 knock-in mice. *Neuroreport* **2002**, *13*, 383-386.
73. Seshadri, S.; Drachman, D. A.; Lippa, C. F. Apolipoprotein E epsilon 4 allele and the lifetime risk of Alzheimer's disease. What physicians know, and what they should know. *Arch. Neurol.* **1995**, *52*, 1074-1079.
74. Yu, G.; Chen, F.; Levesque, G.; Nishimura, M.; Zhang, D.; Levesque, L.; Rogaeva, E.; Xu, D.; Liang, Y.; Duthie, M.; George-Hyslop, P. H. S.; Fraser, P. E. The Presenilin 1 Protein Is a Component of a High Molecular Weight Intracellular Complex That Contains β -Catenin. *Journal of Biological Chemistry* **1998**, *273*, 16470-16475.
75. Heston, L. L. Alzheimer's dementia and Down's syndrome: genetic evidence suggesting an association. *Ann. N. Y. Acad. Sci.* **1982**, *396*, 29-37.
76. Armstrong, R. A. Correlations between the morphology of diffuse and primitive β -amyloid ($A\beta$) deposits and the frequency of associated cells in Down's syndrome. *Neuropathol. Appl. Neurobiol.* **1996**, *22*, 527-530.
77. Glenner, G. G.; Wong, C. W. Alzheimer's disease and Down's syndrome: sharing of a unique cerebrovascular amyloid fibril protein. *Biochem. Biophys. Res. Commun.* **1984**, *122*, 1131-1135.
78. Masters, C. L.; Simms, G.; Weinman, N. A.; Multhaup, G.; McDonald, B. L.; Beyreuther, K. Amyloid plaque core protein in Alzheimer disease and Down syndrome. *Proc. Natl. Acad. Sci. U. S. A.* **1985**, *82*, 4245-4249.
79. Armstrong, R. A.; Myers, D. $\beta/A4$ deposits and their relationship to senile plaques in Alzheimer's disease. *Neuroreport* **1992**, *3*, 262-264.
80. Arnold, S. E.; Hyman, B. T.; Flory, J.; Damasio, A. R.; Van Hoesen, G. W. The topographical and neuroanatomical distribution of neurofibrillary tangles and neuritic plaques in the cerebral cortex of patients with Alzheimer's disease. *Cereb. Cortex* **1991**, *1*, 103-116.
81. Fiala, J. C. Mechanisms of amyloid plaque pathogenesis. *Acta Neuropathol.* **2007**, *114*, 551-571.
82. Klein, W. L.; Krafft, G. A.; Finch, C. E. Targeting small $A\beta$ oligomers: the solution to an Alzheimer's disease conundrum? *Trends Neurosci.* **2001**, *24*, 219-224.

83. Dahlgren, K. N.; Manelli, A. M.; Stine, W. B., Jr; Baker, L. K.; Krafft, G. A.; LaDu, M. J. Oligomeric and fibrillar species of amyloid- β peptides differentially affect neuronal viability. *J. Biol. Chem.* **2002**, *277*, 32046-32053.
84. Walsh, D. M.; Klyubin, I.; Fadeeva, J. V.; Rowan, M. J.; Selkoe, D. J. Amyloid- β oligomers: their production, toxicity and therapeutic inhibition. *Biochem. Soc. Trans.* **2002**, *30*, 552-557.
85. Walsh, D. M.; Klyubin, I.; Fadeeva, J. V.; Cullen, W. K.; Anwyl, R.; Wolfe, M. S.; Rowan, M. J.; Selkoe, D. J. Naturally secreted oligomers of amyloid β protein potently inhibit hippocampal long-term potentiation in vivo. *Nature* **2002**, *416*, 535-539.
86. Vekrellis, K.; Ye, Z.; Qiu, W. Q.; Walsh, D.; Hartley, D.; Chesneau, V.; Rosner, M. R.; Selkoe, D. J. Neurons regulate extracellular levels of amyloid β -protein via proteolysis by insulin-degrading enzyme. *J. Neurosci.* **2000**, *20*, 1657-1665.
87. Zhang, Y.; Hong, Y.; Bounhar, Y.; Blacker, M.; Roucou, X.; Tounekti, O.; Vereker, E.; Bowers, W. J.; Federoff, H. J.; Goodyer, C. G.; LeBlanc, A. P75 Neurotrophin Receptor Protects Primary Cultures of Human Neurons Against Extracellular Amyloid β Peptide Cytotoxicity. *J. Neurosci.* **2003**, *23*, 7385-7394.
88. DeMattos, R. B.; Cirrito, J. R.; Parsadanian, M.; May, P. C.; O'Dell, M. A.; Taylor, J. W.; Harmony, J. A.; Aronow, B. J.; Bales, K. R.; Paul, S. M.; Holtzman, D. M. ApoE and clusterin cooperatively suppress A β levels and deposition: evidence that ApoE regulates extracellular A β metabolism in vivo. *Neuron* **2004**, *41*, 193-202.
89. Grimm, H. S.; Beher, D.; Lichtenthaler, S. F.; Shearman, M. S.; Beyreuther, K.; Hartmann, T. γ -Secretase cleavage site specificity differs for intracellular and secretory amyloid β . *J. Biol. Chem.* **2003**, *278*, 13077-13085.
90. Hartmann, T.; Bieger, S. C.; Bruhl, B.; Tienari, P. J.; Ida, N.; Allsop, D.; Roberts, G. W.; Masters, C. L.; Dotti, C. G.; Unsicker, K.; Beyreuther, K. Distinct sites of intracellular production for Alzheimer's disease A $\beta_{40/42}$ amyloid peptides. *Nat. Med.* **1997**, *3*, 1016-1020.
91. Lee, H. K.; Kumar, P.; Fu, Q.; Rosen, K. M.; Querfurth, H. W. The insulin/Akt signaling pathway is targeted by intracellular β -amyloid. *Mol. Biol. Cell* **2009**, *20*, 1533-1544.
92. Walsh, D. M.; Tseng, B. P.; Rydel, R. E.; Podlisny, M. B.; Selkoe, D. J. The oligomerization of amyloid β -protein begins intracellularly in cells derived from human brain. *Biochemistry* **2000**, *39*, 10831-10839.
93. Friedrich, R. P.; Tepper, K.; Ronicke, R.; Soom, M.; Westermann, M.; Reymann, K.; Kaether, C.; Fandrich, M. Mechanism of amyloid plaque formation suggests an intracellular basis of A β pathogenicity. *Proc. Natl. Acad. Sci. U. S. A.* **2010**, *107*, 1942-1947.

94. Bayer, T. A.; Wirths, O. Intracellular accumulation of amyloid- β - a predictor for synaptic dysfunction and neuron loss in Alzheimer's disease. *Front. Aging Neurosci.* **2010**, *2*, 8.
95. LaFerla, F. M.; Green, K. N.; Oddo, S. Intracellular amyloid- β in Alzheimer's disease. *Nat. Rev. Neurosci.* **2007**, *8*, 499-509.
96. Li, M.; Chen, L.; Lee, D. H.; Yu, L. C.; Zhang, Y. The role of intracellular amyloid β in Alzheimer's disease. *Prog. Neurobiol.* **2007**, *83*, 131-139.
97. Wirths, O.; Multhaup, G.; Czech, C.; Blanchard, V.; Moussaoui, S.; Tremp, G.; Pradier, L.; Beyreuther, K.; Bayer, T. A. Intraneuronal A β accumulation precedes plaque formation in β -amyloid precursor protein and presenilin-1 double-transgenic mice. *Neurosci. Lett.* **2001**, *306*, 116-120.
98. Oddo, S.; Caccamo, A.; Shepherd, J. D.; Murphy, M. P.; Golde, T. E.; Kaye, R.; Metherate, R.; Mattson, M. P.; Akbari, Y.; LaFerla, F. M. Triple-transgenic model of Alzheimer's disease with plaques and tangles: intracellular A β and synaptic dysfunction. *Neuron* **2003**, *39*, 409-421.
99. Ohya, Y.; Yamada, T.; Nishioka, K.; Clarke, N. J.; Tomlinson, A. J.; Naylor, S.; Nakabeppu, Y.; Kira, J.; Younkin, S. G. Selective increase in cellular A β_{42} is related to apoptosis but not necrosis. *Neuroreport* **2000**, *11*, 167-171.
100. Small, S. A.; Gandy, S. Sorting through the cell biology of Alzheimer's disease: intracellular pathways to pathogenesis. *Neuron* **2006**, *52*, 15-31.
101. Ferretti, M. T.; Bruno, M. A.; Ducatzenzeiler, A.; Klein, W. L.; Cuello, A. C. Intracellular A β -oligomers and early inflammation in a model of Alzheimer's disease. *Neurobiol. Aging* **2012**, *33*, 1329-1342.
102. Turner, R. S.; Suzuki, N.; Chyung, A. S.; Younkin, S. G.; Lee, V. M. Amyloids β_{40} and β_{42} are generated intracellularly in cultured human neurons and their secretion increases with maturation. *J. Biol. Chem.* **1996**, *271*, 8966-8970.
103. Tabira, T.; Chui, D. H.; Kuroda, S. Significance of intracellular A β_{42} accumulation in Alzheimer's disease. *Front. Biosci.* **2002**, *7*, a44-9.
104. Yang, A. J.; Chandswangbhuvana, D.; Shu, T.; Henschen, A.; Glabe, C. G. Intracellular accumulation of insoluble, newly synthesized A β_{n-42} in amyloid precursor protein-transfected cells that have been treated with A β_{1-42} . *J. Biol. Chem.* **1999**, *274*, 20650-20656.
105. Zhang, Y.; McLaughlin, R. W.; Goodyer, C.; LeBlanc, A. Selective cytotoxicity of intracellular amyloid β peptide1-42 through p53 and Bax in cultured primary human neurons. *J. Cell Biol.* **2002**, *156*, 519-529.

106. Yang, T. T.; Hsu, C. T.; Kuo, Y. M. Cell-derived soluble oligomers of human amyloid- β peptides disturb cellular homeostasis and induce apoptosis in primary hippocampal neurons. *J. Neural Transm.* **2009**, *116*, 1561-1569.
107. Gouras, G. K.; Almeida, C. G.; Takahashi, R. H. Intraneuronal A β accumulation and origin of plaques in Alzheimer's disease. *Neurobiol. Aging* **2005**, *26*, 1235-1244.
108. Billings, L. M.; Oddo, S.; Green, K. N.; McGaugh, J. L.; LaFerla, F. M. Intraneuronal A β causes the onset of early Alzheimer's disease-related cognitive deficits in transgenic mice. *Neuron* **2005**, *45*, 675-688.
109. Fernandez-Vizarra, P.; Fernandez, A. P.; Castro-Blanco, S.; Serrano, J.; Bentura, M. L.; Martinez-Murillo, R.; Martinez, A.; Rodrigo, J. Intra- and extracellular A β and PHF in clinically evaluated cases of Alzheimer's disease. *Histol. Histopathol.* **2004**, *19*, 823-844.
110. Chui, D. H.; Tanahashi, H.; Ozawa, K.; Ikeda, S.; Checler, F.; Ueda, O.; Suzuki, H.; Araki, W.; Inoue, H.; Shirotani, K.; Takahashi, K.; Gallyas, F.; Tabira, T. Transgenic mice with Alzheimer presenilin 1 mutations show accelerated neurodegeneration without amyloid plaque formation. *Nat. Med.* **1999**, *5*, 560-564.
111. Bates, K. A.; Verdile, G.; Li, Q. X.; Ames, D.; Hudson, P.; Masters, C. L.; Martins, R. N. Clearance mechanisms of Alzheimer's amyloid- β peptide: implications for therapeutic design and diagnostic tests. *Mol. Psychiatry* **2009**, *14*, 469-486.
112. Tahara, K.; Kim, H. D.; Jin, J. J.; Maxwell, J. A.; Li, L.; Fukuchi, K. Role of toll-like receptor signalling in A β uptake and clearance. *Brain* **2006**, *129*, 3006-3019.
113. Fan, J.; Donkin, J.; Wellington, C. Greasing the wheels of A β clearance in Alzheimer's disease: the role of lipids and apolipoprotein E. *Biofactors* **2009**, *35*, 239-248.
114. Wang, Y. J.; Zhou, H. D.; Zhou, X. F. Clearance of amyloid- β in Alzheimer's disease: progress, problems and perspectives. *Drug Discov. Today* **2006**, *11*, 931-938.
115. Deane, R.; Wu, Z.; Zlokovic, B. V. RAGE (yin) versus LRP (yang) balance regulates alzheimer amyloid β -peptide clearance through transport across the blood-brain barrier. *Stroke* **2004**, *35*, 2628-2631.
116. Camacho, I. E.; Serneels, L.; Spittaels, K.; Merchiers, P.; Dominguez, D.; De Strooper, B. Peroxisome-proliferator-activated receptor γ induces a clearance mechanism for the amyloid- β peptide. *J. Neurosci.* **2004**, *24*, 10908-10917.
117. Hellström-Lindahl, E.; Ravid, R.; Nordberg, A. Age-dependent decline of neprilysin in Alzheimer's disease and normal brain: Inverse correlation with A β levels. *Neurobiol. Aging* **2008**, *29*, 210-221.

118. Apelt, J.; Ach, K.; Schliebs, R. Aging-related down-regulation of neprilysin, a putative β -amyloid-degrading enzyme, in transgenic Tg2576 Alzheimer-like mouse brain is accompanied by an astroglial upregulation in the vicinity of β -amyloid plaques. *Neurosci. Lett.* **2003**, *339*, 183-186.
119. Wang, D. S.; Lipton, R. B.; Katz, M. J.; Davies, P.; Buschke, H.; Kuslansky, G.; Verghese, J.; Younkin, S. G.; Eckman, C.; Dickson, D. W. Decreased neprilysin immunoreactivity in Alzheimer disease, but not in pathological aging. *J. Neuropathol. Exp. Neurol.* **2005**, *64*, 378-385.
120. Gao, W.; Eisenhauer, P. B.; Conn, K.; Lynch, J. A.; Wells, J. M.; Ullman, M. D.; McKee, A.; Thatté, H. S.; Fine, R. E. Insulin degrading enzyme is expressed in the human cerebrovascular endothelium and in cultured human cerebrovascular endothelial cells. *Neurosci. Lett.* **2004**, *371*, 6-11.
121. Kurochkin, I. V.; Goto, S. Alzheimer's β -amyloid peptide specifically interacts with and is degraded by insulin degrading enzyme. *FEBS Lett.* **1994**, *345*, 33-37.
122. Thal, D. R. The role of astrocytes in amyloid β -protein toxicity and clearance. *Exp. Neurol.* **2012**, *236*, 1-5.
123. Hickman, S. E.; Allison, E. K.; El Khoury, J. Microglial dysfunction and defective β -amyloid clearance pathways in aging Alzheimer's disease mice. *J. Neurosci.* **2008**, *28*, 8354-8360.
124. Iliff, J. J.; Wang, M.; Liao, Y.; Plogg, B. A.; Peng, W.; Gundersen, G. A.; Benveniste, H.; Vates, G. E.; Deane, R.; Goldman, S. A.; Nagelhus, E. A.; Nedergaard, M. A paravascular pathway facilitates CSF flow through the brain parenchyma and the clearance of interstitial solutes, including amyloid β . *Sci. Transl. Med.* **2012**, *4*, 147ra111.
125. Boche, D.; Nicoll, J. A. The role of the immune system in clearance of A β from the brain. *Brain Pathol.* **2008**, *18*, 267-278.
126. Michaelis, M. L.; Dobrowsky, R. T.; Li, G. Tau neurofibrillary pathology and microtubule stability. *J. Mol. Neurosci.* **2002**, *19*, 289-293.
127. Jellinger, K. A.; Bancher, C. Neuropathology of Alzheimer's disease: a critical update. *J. Neural Transm. Suppl.* **1998**, *54*, 77-95.
128. Lu, M.; Kosik, K. S. Competition for microtubule-binding with dual expression of tau missense and splice isoforms. *Mol. Biol. Cell* **2001**, *12*, 171-184.
129. Lovestone, S.; Reynolds, C. H. The phosphorylation of tau: a critical stage in neurodevelopment and neurodegenerative processes. *Neuroscience* **1997**, *78*, 309-324.

130. Forman, M. S.; Trojanowski, J. Q.; Lee, V. M. Neurodegenerative diseases: a decade of discoveries paves the way for therapeutic breakthroughs. *Nat. Med.* **2004**, *10*, 1055-1063.
131. Goedert, M.; Spillantini, M. G.; Cairns, N. J.; Crowther, R. A. Tau proteins of Alzheimer paired helical filaments: abnormal phosphorylation of all six brain isoforms. *Neuron* **1992**, *8*, 159-168.
132. Lee, G.; Leugers, C. J. Tau and tauopathies. *Prog. Mol. Biol. Transl. Sci.* **2012**, *107*, 263-293.
133. Avila, J. The tau code. *Front. Aging Neurosci.* **2009**, *1*, 1.
134. Avila, J. Tau phosphorylation and aggregation in Alzheimer's disease pathology. *FEBS Lett.* **2006**, *580*, 2922-2927.
135. Greenough, M. A.; Camakaris, J.; Bush, A. I. Metal dyshomeostasis and oxidative stress in Alzheimer's disease. *Neurochem. Int.* **2013**, *62*, 540-555.
136. Hureau, C.; Faller, P. A β -mediated ROS production by Cu ions: structural insights, mechanisms and relevance to Alzheimer's disease. *Biochimie* **2009**, *91*, 1212-1217.
137. Dikalov, S. I.; Vitek, M. P.; Mason, R. P. Cupric-amyloid β peptide complex stimulates oxidation of ascorbate and generation of hydroxyl radical. *Free Radic. Biol. Med.* **2004**, *36*, 340-347.
138. Adlard, P. A.; Bush, A. I. In *Metal Ions and Alzheimer's Disease*; Malva, J. O., Rego, A. C., Cunha, R. A. and Oliveira, C. R., Eds.; Interaction between neurons and glia in aging and disease; Springer Science+Business Media, LLC: New York, NY, 2007; pp. 333-362.
139. Atwood, C. S.; Huang, X.; Moir, R. D.; Tanzi, R. E.; Bush, A. I. Role of free radicals and metal ions in the pathogenesis of Alzheimer's disease. *Met. Ions Biol. Syst.* **1999**, *36*, 309-364.
140. Huang, X.; Cuajungco, M. P.; Atwood, C. S.; Hartshorn, M. A.; Tyndall, J. D.; Hanson, G. R.; Stokes, K. C.; Leopold, M.; Multhaup, G.; Goldstein, L. E.; Scarpa, R. C.; Saunders, A. J.; Lim, J.; Moir, R. D.; Glabe, C.; Bowden, E. F.; Masters, C. L.; Fairlie, D. P.; Tanzi, R. E.; Bush, A. I. Cu(II) potentiation of alzheimer A β neurotoxicity. Correlation with cell-free hydrogen peroxide production and metal reduction. *J. Biol. Chem.* **1999**, *274*, 37111-37116.
141. Huang, X.; Atwood, C. S.; Hartshorn, M. A.; Multhaup, G.; Goldstein, L. E.; Scarpa, R. C.; Cuajungco, M. P.; Gray, D. N.; Lim, J.; Moir, R. D.; Tanzi, R. E.; Bush, A. I. The A β peptide of Alzheimer's disease directly produces hydrogen peroxide through metal ion reduction. *Biochemistry* **1999**, *38*, 7609-7616.

142. Tabner, B. J.; Mayes, J.; Allsop, D. Hypothesis: soluble A β oligomers in association with redox-active metal ions are the optimal generators of reactive oxygen species in Alzheimer's disease. *Int. J. Alzheimers Dis.* **2010**, *2011*, 546380.
143. Cherny, R. A.; Atwood, C. S.; Xilinas, M. E.; Gray, D. N.; Jones, W. D.; McLean, C. A.; Barnham, K. J.; Volitakis, I.; Fraser, F. W.; Kim, Y.; Huang, X.; Goldstein, L. E.; Moir, R. D.; Lim, J. T.; Beyreuther, K.; Zheng, H.; Tanzi, R. E.; Masters, C. L.; Bush, A. I. Treatment with a Copper-Zinc Chelator Markedly and Rapidly Inhibits β -Amyloid Accumulation in Alzheimer's Disease Transgenic Mice. *Neuron* **2001**, *30*, 665-676.
144. Opazo, C.; Huang, X.; Cherny, R. A.; Moir, R. D.; Roher, A. E.; White, A. R.; Cappai, R.; Masters, C. L.; Tanzi, R. E.; Inestrosa, N. C.; Bush, A. I. Metalloenzyme-like activity of Alzheimer's disease β -amyloid. Cu-dependent catalytic conversion of dopamine, cholesterol, and biological reducing agents to neurotoxic H₂O₂. *J. Biol. Chem.* **2002**, *277*, 40302-40308.
145. Jomova, K.; Valko, M. Advances in metal-induced oxidative stress and human disease. *Toxicology* **2011**, *283*, 65-87.
146. Stohs, S. J.; Bagchi, D. Oxidative mechanisms in the toxicity of metal ions. *Free Radic. Biol. Med.* **1995**, *18*, 321-336.
147. Exley, C. The aluminium-amyloid cascade hypothesis and Alzheimer's disease. *Subcell. Biochem.* **2005**, *38*, 225-234.
148. Exley, C. A molecular mechanism of aluminium-induced Alzheimer's disease? *J. Inorg. Biochem.* **1999**, *76*, 133-140.
149. Bolognin, S.; Messori, L.; Drago, D.; Gabbiani, C.; Cendron, L.; Zatta, P. Aluminum, copper, iron and zinc differentially alter amyloid-A β ₁₋₄₂ aggregation and toxicity. *Int. J. Biochem. Cell Biol.* **2011**, *43*, 877-885.
150. Drago, D.; Cavaliere, A.; Mascetra, N.; Ciavardelli, D.; di Ilio, C.; Zatta, P.; Sensi, S. L. Aluminum modulates effects of β amyloid(1-42) on neuronal calcium homeostasis and mitochondria functioning and is altered in a triple transgenic mouse model of Alzheimer's disease. *Rejuvenation Res.* **2008**, *11*, 861-871.
151. Exley, C. Aluminium and iron, but neither copper nor zinc, are key to the precipitation of β -sheets of A β ₄₂ in senile plaque cores in Alzheimer's disease. *J. Alzheimers Dis.* **2006**, *10*, 173-177.
152. Trapp, G. A.; Miner, G. D.; Zimmerman, R. L.; Mastri, A. R.; Heston, L. L. Aluminum levels in brain in Alzheimer's disease. *Biol. Psychiatry* **1978**, *13*, 709-718.

153. Bolognin, S.; Zatta, P.; Lorenzetto, E.; Valenti, M. T.; Buffelli, M. β -Amyloid-aluminum complex alters cytoskeletal stability and increases ROS production in cortical neurons. *Neurochem. Int.* **2013**, *62*, 566-574.
154. Bahadi, R.; Farrelly, P. V.; Kenna, B. L.; Curtain, C. C.; Masters, C. L.; Cappai, R.; Barnham, K. J.; Kourie, J. I. Cu^{2+} -induced modification of the kinetics of $\text{A}\beta(1-42)$ channels. *Am. J. Physiol. Cell. Physiol.* **2003**, *285*, C873-C880.
155. Dai, X. L.; Sun, Y. X.; Jiang, Z. F. Cu(II) potentiation of Alzheimer $\text{A}\beta_{1-40}$ cytotoxicity and transition on its secondary structure. *Acta Biochim. Biophys. Sin. (Shanghai)* **2006**, *38*, 765-772.
156. Lin, C. J.; Huang, H. C.; Jiang, Z. F. Cu(II) interaction with amyloid- β peptide: a review of neuroactive mechanisms in AD brains. *Brain Res. Bull.* **2010**, *82*, 235-242.
157. Pedersen, J. T.; Ostergaard, J.; Rozlosnik, N.; Gammelgaard, B.; Heegaard, N. H. Cu(II) mediates kinetically distinct, non-amyloidogenic aggregation of amyloid- β peptides. *J. Biol. Chem.* **2011**, *286*, 26952-26963.
158. Smith, D. P.; Ciccotosto, G. D.; Tew, D. J.; Fodero-Tavoletti, M. T.; Johanssen, T.; Masters, C. L.; Barnham, K. J.; Cappai, R. Concentration Dependent Cu^{2+} Induced Aggregation and Dityrosine Formation of the Alzheimer's Disease Amyloid- β Peptide. *Biochemistry* **2007**.
159. Bush, A. I. Copper, zinc, and the metallobiology of Alzheimer disease. *Alzheimer Dis. Assoc. Disord.* **2003**, *17*, 147-150.
160. Jun, S.; Saxena, S. The aggregated state of amyloid- β peptide in vitro depends on Cu^{2+} ion concentration. *Angew. Chem. Int. Ed Engl.* **2007**, *46*, 3959-3961.
161. Karr, J. W.; Kaupp, L. J.; Szalai, V. A. Amyloid- β binds Cu^{2+} in a mononuclear metal ion binding site. *J. Am. Chem. Soc.* **2004**, *126*, 13534-13538.
162. Hureau, C.; Balland, V.; Coppel, Y.; Solari, P. L.; Fonda, E.; Faller, P. Importance of dynamical processes in the coordination chemistry and redox conversion of copper amyloid- β complexes. *J. Biol. Inorg. Chem.* **2009**, *14*, 995-1000.
163. Atwood, C. S.; Moir, R. D.; Huang, X.; Scarpa, R. C.; Bacarra, N. M.; Romano, D. M.; Hartshorn, M. A.; Tanzi, R. E.; Bush, A. I. Dramatic aggregation of Alzheimer $\text{A}\beta$ by Cu(II) is induced by conditions representing physiological acidosis. *J. Biol. Chem.* **1998**, *273*, 12817-12826.
164. Hayashi, T.; Shishido, N.; Nakayama, K.; Nunomura, A.; Smith, M. A.; Perry, G.; Nakamura, M. Lipid peroxidation and 4-hydroxy-2-nonenal formation by copper ion bound to amyloid- β peptide. *Free Radic. Biol. Med.* **2007**, *43*, 1552-1559.

165. Amit, T.; Avramovich-Tirosh, Y.; Youdim, M. B.; Mandel, S. Targeting multiple Alzheimer's disease etiologies with multimodal neuroprotective and neurorestorative iron chelators. *FASEB J.* **2008**, *22*, 1296-1305.
166. Collingwood, J. F.; Mikhaylova, A.; Davidson, M.; Batich, C.; Streit, W. J.; Terry, J.; Dobson, J. In situ characterization and mapping of iron compounds in Alzheimer's disease tissue. *J. Alzheimers Dis.* **2005**, *7*, 267-272.
167. Deibel, M. A.; Ehmann, W. D.; Markesbery, W. R. Copper, iron, and zinc imbalances in severely degenerated brain regions in Alzheimer's disease: possible relation to oxidative stress. *J. Neurol. Sci.* **1996**, *143*, 137-142.
168. House, E.; Collingwood, J.; Khan, A.; Korchazkina, O.; Berthon, G.; Exley, C. Aluminium, iron, zinc and copper influence the in vitro formation of amyloid fibrils of A β ₄₂ in a manner which may have consequences for metal chelation therapy in Alzheimer's disease. *J. Alzheimers Dis.* **2004**, *6*, 291-301.
169. Lovell, M. A.; Robertson, J. D.; Teesdale, W. J.; Campbell, J. L.; Markesbery, W. R. Copper, iron and zinc in Alzheimer's disease senile plaques. *J. Neurol. Sci.* **1998**, *158*, 47-52.
170. Khan, A.; Dobson, J. P.; Exley, C. Redox cycling of iron by A β ₄₂. *Free Radic. Biol. Med.* **2006**, *40*, 557-569.
171. Tougu, V.; Karafin, A.; Zovo, K.; Chung, R. S.; Howells, C.; West, A. K.; Palumaa, P. Zn(II)- and Cu(II)-induced Nonfibrillar Aggregates of Amyloid- β (1-42) Peptide are Transformed to Amyloid Fibrils, both Spontaneously and under the Influence of Metal Chelators. *J. Neurochem.* **2009**.
172. Miller, L. M.; Wang, Q.; Telivala, T. P.; Smith, R. J.; Lanzirrotti, A.; Miklossy, J. Synchrotron-based infrared and X-ray imaging shows focalized accumulation of Cu and Zn co-localized with β -amyloid deposits in Alzheimer's disease. *J. Struct. Biol.* **2006**, *155*, 30-37.
173. Ghalebani, L.; Wahlstrom, A.; Danielsson, J.; Warmlander, S. K.; Graslund, A. pH-dependence of the specific binding of Cu(II) and Zn(II) ions to the amyloid- β peptide. *Biochem. Biophys. Res. Commun.* **2012**, *421*, 554-560.
174. Bush, A. I.; Pettingell, W. H.; Multhaup, G.; d. Paradis, M.; Vonsattel, J. P.; Gusella, J. F.; Beyreuther, K.; Masters, C. L.; Tanzi, R. E. Rapid induction of Alzheimer A β amyloid formation by zinc. *Science* **1994**, *265*, 1464-1467.
175. Cuajungco, M. P.; Fagét, K. Y. Zinc takes the center stage: its paradoxical role in Alzheimer's disease. *Brain Res. Rev.* **2003**, *41*, 44-56.

176. Esler, W. P.; Stimson, E. R.; Jennings, J. M.; Ghilardi, J. R.; Mantyh, P. W.; Maggio, J. E. Zinc-induced aggregation of human and rat β -amyloid peptides in vitro. *J. Neurochem.* **1996**, *66*, 723-732.
177. Fitzgerald, D. J.; Maggio, J. E.; Esler, W. P.; Stimson, E. R.; Jennings, J. M.; Ghilardi, J. R.; Mantyh, P. W.; Bush, A. I.; Moir, R. D.; Rosenkranz, K. M.; Tanzi, R. E. Zinc and Alzheimer's disease. *Science* **1995**, *268*, 1920-1; author reply 1921-3.
178. Huang, X.; Atwood, C. S.; Moir, R. D.; Hartshorn, M. A.; Vonsattel, J. P.; Tanzi, R. E.; Bush, A. I. Zinc-induced Alzheimer's $A\beta_{1-40}$ aggregation is mediated by conformational factors. *J. Biol. Chem.* **1997**, *272*, 26464-26470.
179. Ichinohe, N.; Hayashi, M.; Wakabayashi, K.; Rockland, K. S. Distribution and progression of amyloid- β deposits in the amygdala of the aged macaque monkey, and parallels with zinc distribution. *Neuroscience* **2009**, *159*, 1374-1383.
180. Zhang, C. F.; Yang, P. Zinc-induced aggregation of $A\beta$ (10-21) potentiates its action on voltage-gated potassium channel. *Biochem. Biophys. Res. Commun.* **2006**, *345*, 43-49.
181. Faller, P. Copper and zinc binding to amyloid- β : coordination, dynamics, aggregation, reactivity and metal-ion transfer. *Chembiochem* **2009**, *10*, 2837-2845.
182. Yankner, B. A.; Duffy, L. K.; Kirschner, D. A. Neurotrophic and neurotoxic effects of amyloid β protein: reversal by tachykinin neuropeptides. *Science* **1990**, *250*, 279-282.
183. Jiang, D.; Li, X.; Liu, L.; Yagnik, G. B.; Zhou, F. Reaction rates and mechanism of the ascorbic acid oxidation by molecular oxygen facilitated by Cu(II)-containing amyloid- β complexes and aggregates. *J Phys Chem B* **2010**, *114*, 4896-4903.
184. Kang, J.; Park, E. J.; Jou, I.; Kim, J. H.; Joe, E. H. Reactive oxygen species mediate $A\beta$ (25-35)-induced activation of BV-2 microglia. *Neuroreport* **2001**, *12*, 1449-1452.
185. Multhaup, G.; Ruppert, T.; Schlicksupp, A.; Hesse, L.; Beher, D.; Masters, C. L.; Beyreuther, K. Reactive oxygen species and Alzheimer's disease. *Biochem. Pharmacol.* **1997**, *54*, 533-539.
186. Kadowaki, H.; Nishitoh, H.; Urano, F.; Sadamitsu, C.; Matsuzawa, A.; Takeda, K.; Masutani, H.; Yodoi, J.; Urano, Y.; Nagano, T.; Ichijo, H. Amyloid β induces neuronal cell death through ROS-mediated ASK1 activation. *Cell Death Differ.* **2005**, *12*, 19-24.
187. Spone, I.; Fifre, A.; Drouet, B.; Klein, C.; Koziel, V.; Pincon-Raymond, M.; Olivier, J. L.; Chambaz, J.; Pillot, T. Apoptotic neuronal cell death induced by the non-fibrillar amyloid- β peptide proceeds through an early reactive oxygen species-dependent cytoskeleton perturbation. *J. Biol. Chem.* **2003**, *278*, 3437-3445.

188. Butterfield, D. A.; Reed, T.; Newman, S. F.; Sultana, R. Roles of amyloid β -peptide-associated oxidative stress and brain protein modifications in the pathogenesis of Alzheimer's disease and mild cognitive impairment. *Free Radic. Biol. Med.* **2007**, *43*, 658-677.
189. Sultana, R.; Perluigi, M.; Butterfield, D. A. Oxidatively modified proteins in Alzheimer's disease (AD), mild cognitive impairment and animal models of AD: role of A β in pathogenesis. *Acta Neuropathol.* **2009**, *118*, 131-150.
190. Egana, J. T.; Zambrano, C.; Nunez, M. T.; Gonzalez-Billault, C.; Maccioni, R. B. Iron-induced oxidative stress modify tau phosphorylation patterns in hippocampal cell cultures. *Biometals* **2003**, *16*, 215-223.
191. Sjogren, M.; Mielke, M.; Gustafson, D.; Zandi, P.; Skoog, I. Cholesterol and Alzheimer's disease--is there a relation? *Mech. Ageing Dev.* **2006**, *127*, 138-147.
192. Eckert, G. P.; Kirsch, C.; Leutz, S.; Wood, W. G.; Muller, W. E. Cholesterol modulates amyloid β -peptide's membrane interactions. *Pharmacopsychiatry* **2003**, *36 Suppl 2*, S136-43.
193. Gong, J. S.; Sawamura, N.; Zou, K.; Sakai, J.; Yanagisawa, K.; Michikawa, M. Amyloid β -protein affects cholesterol metabolism in cultured neurons: implications for pivotal role of cholesterol in the amyloid cascade. *J. Neurosci. Res.* **2002**, *70*, 438-446.
194. Runz, H.; Rietdorf, J.; Tomic, I.; de Bernard, M.; Beyreuther, K.; Pepperkok, R.; Hartmann, T. Inhibition of intracellular cholesterol transport alters presenilin localization and amyloid precursor protein processing in neuronal cells. *J. Neurosci.* **2002**, *22*, 1679-1689.
195. Colell, A.; Fernandez, A.; Fernandez-Checa, J. C. Mitochondria, cholesterol and amyloid β peptide: a dangerous trio in Alzheimer disease. *J. Bioenerg. Biomembr.* **2009**.
196. Arispe, N.; Doh, M. Plasma membrane cholesterol controls the cytotoxicity of Alzheimer's disease A β P (1-40) and (1-42) peptides. *FASEB J.* **2002**, *16*, 1526-1536.
197. Yip, C. M.; Elton, E. A.; Darabie, A. A.; Morrison, M. R.; McLaurin, J. Cholesterol, a modulator of membrane-associated A β -fibrillogenesis and neurotoxicity. *J. Mol. Biol.* **2001**, *311*, 723-734.
198. McLaurin, J.; Darabie, A. A.; Morrison, M. R. Cholesterol, a modulator of membrane-associated A β -fibrillogenesis. *Pharmacopsychiatry* **2003**, *36 Suppl 2*, S130-5.
199. Vestergaard, M.; Hamada, T.; Takagi, M. Using model membranes for the study of amyloid β :lipid interactions and neurotoxicity. *Biotechnol. Bioeng.* **2008**, *99*, 753-763.

200. Michikawa, M.; Gong, J. S.; Fan, Q. W.; Sawamura, N.; Yanagisawa, K. A novel action of alzheimer's amyloid β -protein (A β): oligomeric A β promotes lipid release. *J. Neurosci.* **2001**, *21*, 7226-7235.
201. Fan, Q. W.; Yu, W.; Senda, T.; Yanagisawa, K.; Michikawa, M. Cholesterol-dependent modulation of tau phosphorylation in cultured neurons. *J. Neurochem.* **2001**, *76*, 391-400.
202. Fernandez, A.; Llacuna, L.; Fernandez-Checa, J. C.; Colell, A. Mitochondrial cholesterol loading exacerbates amyloid β peptide-induced inflammation and neurotoxicity. *J. Neurosci.* **2009**, *29*, 6394-6405.
203. Yanagisawa, K. Cholesterol and A β aggregation. *Pharmacopsychiatry* **2003**, *36 Suppl 2*, S127-9.
204. Lau, T. L.; Ambroggio, E. E.; Tew, D. J.; Cappai, R.; Masters, C. L.; Fidelio, G. D.; Barnham, K. J.; Separovic, F. Amyloid- β peptide disruption of lipid membranes and the effect of metal ions. *J. Mol. Biol.* **2006**, *356*, 759-770.
205. Curtain, C. C.; Ali, F. E.; Smith, D. G.; Bush, A. I.; Masters, C. L.; Barnham, K. J. Metal ions, pH, and cholesterol regulate the interactions of Alzheimer's disease amyloid- β peptide with membrane lipid. *J. Biol. Chem.* **2003**, *278*, 2977-2982.
206. Devanathan, S.; Salamon, Z.; Lindblom, G.; Grobner, G.; Tollin, G. Effects of sphingomyelin, cholesterol and zinc ions on the binding, insertion and aggregation of the amyloid A β (1-40) peptide in solid-supported lipid bilayers. *FEBS J.* **2006**, *273*, 1389-1402.
207. Lemkul, J. A.; Bevan, D. R. Lipid composition influences the release of Alzheimer's amyloid β -peptide from membranes. *Protein Sci.* **2011**, *20*, 1530-1545.
208. Widenbrant, M. J. O.; Rajadas, J.; Sutardja, C.; Fuller, G. G. Lipid-Induced β -Amyloid Peptide Assemblage Fragmentation. *Biophys. J.* **2006**, *91*, 4071-4080.
209. Eehalt, R.; Keller, P.; Haass, C.; Thiele, C.; Simons, K. Amyloidogenic processing of the Alzheimer β -amyloid precursor protein depends on lipid rafts. *J. Cell Biol.* **2003**, *160*, 113-123.
210. Friedman, R.; Pellarin, R.; Caflich, A. Amyloid aggregation on lipid bilayers and its impact on membrane permeability. *J. Mol. Biol.* **2009**, *387*, 407-415.
211. Yip, C. M.; Darabie, A. A.; McLaurin, J. A β ₄₂-peptide assembly on lipid bilayers. *J. Mol. Biol.* **2002**, *318*, 97-107.

212. Grösgen, S.; Grimm, M. O. W.; Frieß, P.; Hartmann, T. Role of amyloid β in lipid homeostasis. *Biochimica et Biophysica Acta (BBA) - Molecular and Cell Biology of Lipids* **2010**, *1801*, 966-974.
213. Cordy, J. M.; Hooper, N. M.; Turner, A. J. The involvement of lipid rafts in Alzheimer's disease. *Mol. Membr. Biol.* **2006**, *23*, 111-122.
214. Mielke, M. M.; Lyketsos, C. G. Lipids and the pathogenesis of Alzheimer's disease: is there a link? *Int. Rev. Psychiatry.* **2006**, *18*, 173-186.
215. Arlt, S.; Beisiegel, U.; Kontush, A. Lipid peroxidation in neurodegeneration: new insights into Alzheimer's disease. *Curr. Opin. Lipidol.* **2002**, *13*, 289-294.
216. Gonzalez, C.; Martin, T.; Cacho, J.; Brenas, M. T.; Arroyo, T.; Garcia-Berrocal, B.; Navajo, J. A.; Gonzalez-Buitrago, J. M. Serum zinc, copper, insulin and lipids in Alzheimer's disease epsilon 4 apolipoprotein E allele carriers. *Eur. J. Clin. Invest.* **1999**, *29*, 637-642.
217. Florent-Bechard, S.; Desbene, C.; Garcia, P.; Allouche, A.; Youssef, I.; Escanye, M. C.; Koziel, V.; Hanse, M.; Malaplate-Armand, C.; Stenger, C. The essential role of lipids in Alzheimer's disease. *Biochimie* **2009**, *91*, 804-809.
218. Martins, I. C.; Kuperstein, I.; Wilkinson, H.; Maes, E.; Vanbrabant, M.; Jonckheere, W.; Van Gelder, P.; Hartmann, D.; D'Hooge, R.; De Strooper, B.; Schymkowitz, J.; Rousseau, F. Lipids revert inert A β amyloid fibrils to neurotoxic protofibrils that affect learning in mice. *EMBO J.* **2008**, *27*, 224-233.
219. Vestergaard, M.; Hamada, T.; Morita, M.; Takagi, M. Cholesterol, lipids, amyloid β , and Alzheimer's. *Curr. Alzheimer Res.* **2010**, *7*, 262-270.
220. Camandola, S.; Poli, G.; Mattson, M. P. The lipid peroxidation product 4-hydroxy-2,3-nonenal inhibits constitutive and inducible activity of nuclear factor κ B in neurons. *Brain Res. Mol. Brain Res.* **2000**, *85*, 53-60.
221. Chaudhary, P.; Sharma, R.; Sharma, A.; Vatsyayan, R.; Yadav, S.; Singhal, S. S.; Rauniyar, N.; Prokai, L.; Awasthi, S.; Awasthi, Y. C. Mechanisms of 4-hydroxy-2-nonenal induced pro- and anti-apoptotic signaling. *Biochemistry* **2010**, *49*, 6263-6275.
222. Perluigi, M.; Coccia, R.; Butterfield, D. A. 4-Hydroxy-2-Nonenal, a Reactive Product of Lipid Peroxidation, and Neurodegenerative Diseases: A Toxic Combination Illuminated by Redox Proteomics Studies. *Antioxid. Redox Signal.* **2012**.
223. Butterfield, D. A.; Bader Lange, M. L.; Sultana, R. Involvements of the lipid peroxidation product, HNE, in the pathogenesis and progression of Alzheimer's disease. *Biochim. Biophys. Acta* **2010**, *1801*, 924-929.

224. Tang, S. C.; Lathia, J. D.; Selvaraj, P. K.; Jo, D. G.; Mughal, M. R.; Cheng, A.; Siler, D. A.; Markesbery, W. R.; Arumugam, T. V.; Mattson, M. P. Toll-like receptor-4 mediates neuronal apoptosis induced by amyloid β -peptide and the membrane lipid peroxidation product 4-hydroxynonenal. *Exp. Neurol.* **2008**, *213*, 114-121.
225. Butterfield, D. A.; Lauderback, C. M. Lipid peroxidation and protein oxidation in Alzheimer's disease brain: potential causes and consequences involving amyloid β -peptide-associated free radical oxidative stress. *Free Radic. Biol. Med.* **2002**, *32*, 1050-1060.
226. Castegna, A.; Lauderback, C. M.; Mohmmad-Abdul, H.; Butterfield, D. A. Modulation of phospholipid asymmetry in synaptosomal membranes by the lipid peroxidation products, 4-hydroxynonenal and acrolein: implications for Alzheimer's disease. *Brain Res.* **2004**, *1004*, 193-197.
227. Markesbery, W. R.; Lovell, M. A. Four-Hydroxynonenal, a Product of Lipid Peroxidation, is Increased in the Brain in Alzheimer's Disease. *Neurobiol. Aging* **1998**, *19*, 33-36.
228. Reed, T. T.; Pierce, W. M.; Markesbery, W. R.; Butterfield, D. A. Proteomic identification of HNE-bound proteins in early Alzheimer disease: Insights into the role of lipid peroxidation in the progression of AD. *Brain Res.* **2009**, *1274*, 66-76.
229. Pollard, H. B.; Rojas, E.; Arispe, N. A new hypothesis for the mechanism of amyloid toxicity, based on the calcium channel activity of amyloid β protein (A β P) in phospholipid bilayer membranes. *Ann. N. Y. Acad. Sci.* **1993**, *695*, 165-168.
230. Berridge, M. J. Calcium hypothesis of Alzheimer's disease. *Pflugers Arch.* **2010**, *459*, 441-449.
231. Berridge, M. J. Calcium signalling and Alzheimer's disease. *Neurochem. Res.* **2011**, *36*, 1149-1156.
232. Demuro, A.; Mina, E.; Kaye, R.; Milton, S. C.; Parker, I.; Glabe, C. G. Calcium dysregulation and membrane disruption as a ubiquitous neurotoxic mechanism of soluble amyloid oligomers. *J. Biol. Chem.* **2005**, *280*, 17294-17300.
233. Isaacs, A. M.; Senn, D. B.; Yuan, M.; Shine, J. P.; Yankner, B. A. Acceleration of amyloid β -peptide aggregation by physiological concentrations of calcium. *J. Biol. Chem.* **2006**, *281*, 27916-27923.
234. Kawahara, M.; Kuroda, Y. Molecular mechanism of neurodegeneration induced by Alzheimer's β -amyloid protein: channel formation and disruption of calcium homeostasis. *Brain Res. Bull.* **2000**, *53*, 389-397.

235. Suo, Z.; Fang, C.; Crawford, F.; Mullan, M. Superoxide free radical and intracellular calcium mediate A β ₁₋₄₂ induced endothelial toxicity. *Brain Res.* **1997**, *762*, 144-152.
236. Buxbaum, J. D.; Ruefli, A. A.; Parker, C. A.; Cypess, A. M.; Greengard, P. Calcium regulates processing of the Alzheimer amyloid protein precursor in a protein kinase C-independent manner. *Proc. Natl. Acad. Sci. U. S. A.* **1994**, *91*, 4489-4493.
237. Demuro, A.; Parker, I.; Stutzmann, G. E. Calcium signaling and amyloid toxicity in Alzheimer disease. *J. Biol. Chem.* **2010**, *285*, 12463-12468.
238. Ferreira, E.; Oliveira, C. R.; Pereira, C. M. The release of calcium from the endoplasmic reticulum induced by amyloid- β and prion peptides activates the mitochondrial apoptotic pathway. *Neurobiol. Dis.* **2008**, *30*, 331-342.
239. Supnet, C.; Bezprozvanny, I. The dysregulation of intracellular calcium in Alzheimer disease. *Cell Calcium* **2010**, *47*, 183-189.
240. Casley, C. S.; Canevari, L.; Land, J. M.; Clark, J. B.; Sharpe, M. A. β -amyloid inhibits integrated mitochondrial respiration and key enzyme activities. *J. Neurochem.* **2002**, *80*, 91-100.
241. Lustbader, J. W.; Cirilli, M.; Lin, C.; Xu, H. W.; Takuma, K.; Wang, N.; Caspersen, C.; Chen, X.; Pollak, S.; Chaney, M.; Trinchese, F.; Liu, S.; Gunn-Moore, F.; Lue, L. F.; Walker, D. G.; Kuppusamy, P.; Zewier, Z. L.; Arancio, O.; Stern, D.; Yan, S. S.; Wu, H. ABAD directly links A β to mitochondrial toxicity in Alzheimer's disease. *Science* **2004**, *304*, 448-452.
242. Manczak, M.; Anekonda, T. S.; Henson, E.; Park, B. S.; Quinn, J.; Reddy, P. H. Mitochondria are a direct site of A β accumulation in Alzheimer's disease neurons: implications for free radical generation and oxidative damage in disease progression. *Hum. Mol. Genet.* **2006**, *15*, 1437-1449.
243. Swerdlow, R. H.; Khan, S. M. A "mitochondrial cascade hypothesis" for sporadic Alzheimer's disease. *Med. Hypotheses* **2004**, *63*, 8-20.
244. Swerdlow, R. H.; Burns, J. M.; Khan, S. M. The Alzheimer's disease mitochondrial cascade hypothesis. *J. Alzheimers Dis.* **2010**, *20 Suppl 2*, S265-79.
245. Wang, X.; Perry, G.; Smith, M. A.; Zhu, X. Amyloid- β -derived diffusible ligands cause impaired axonal transport of mitochondria in neurons. *Neurodegener Dis.* **2010**, *7*, 56-59.
246. Eckert, A.; Schulz, K. L.; Rhein, V.; Gotz, J. Convergence of amyloid- β and tau pathologies on mitochondria in vivo. *Mol. Neurobiol.* **2010**, *41*, 107-114.

247. Eckert, A.; Schmitt, K.; Gotz, J. Mitochondrial dysfunction - the beginning of the end in Alzheimer's disease? Separate and synergistic modes of tau and amyloid- β toxicity. *Alzheimers Res. Ther.* **2011**, *3*, 15.
248. Keil, U.; Hauptmann, S.; Bonert, A.; Scherping, I.; Eckert, A.; Muller, W. E. Mitochondrial dysfunction induced by disease relevant A β PP and tau protein mutations. *J. Alzheimers Dis.* **2006**, *9*, 139-146.
249. Atamna, H.; Frey, W. H., 2nd Mechanisms of mitochondrial dysfunction and energy deficiency in Alzheimer's disease. *Mitochondrion* **2007**, *7*, 297-310.
250. Davis, J. N.; Hunnicutt Jr, E. J.; Chisholm, J. C. A mitochondrial bottleneck hypothesis of Alzheimer's disease. *Mol. Med. Today* **1995**, *1*, 240-247.
251. Gibson, G. E.; Starkov, A.; Blass, J. P.; Ratan, R. R.; Beal, M. F. Cause and consequence: Mitochondrial dysfunction initiates and propagates neuronal dysfunction, neuronal death and behavioral abnormalities in age-associated neurodegenerative diseases. *Biochimica et Biophysica Acta (BBA) - Molecular Basis of Disease* **2010**, *1802*, 122-134.
252. Dragicevic, N.; Mamcarz, M.; Zhu, Y.; Buzzeo, R.; Tan, J.; Arendash, G. W.; Bradshaw, P. C. Mitochondrial amyloid- β levels are associated with the extent of mitochondrial dysfunction in different brain regions and the degree of cognitive impairment in Alzheimer's transgenic mice. *J. Alzheimers Dis.* **2010**, *20 Suppl 2*, S535-50.
253. Hsu, M. J.; Sheu, J. R.; Lin, C. H.; Shen, M. Y.; Hsu, C. Y. Mitochondrial mechanisms in amyloid β peptide-induced cerebrovascular degeneration. *Biochim. Biophys. Acta* **2010**, *1800*, 290-296.
254. Riemer, J.; Kins, S. Axonal Transport and Mitochondrial Dysfunction in Alzheimer's Disease. *Neurodegener Dis.* **2012**.
255. Peters, I.; Igbavboa, U.; Schutt, T.; Haidari, S.; Hartig, U.; Rosello, X.; Bottner, S.; Copanaki, E.; Deller, T.; Kogel, D.; Wood, W. G.; Muller, W. E.; Eckert, G. P. The interaction of β -amyloid protein with cellular membranes stimulates its own production. *Biochim. Biophys. Acta* **2009**, *1788*, 964-972.
256. Lau, T.; Gehman, J. D.; Wade, J. D.; Perez, K.; Masters, C. L.; Barnham, K. J.; Separovic, F. Membrane interactions and the effect of metal ions of the amyloidogenic fragment A β (25–35) in comparison to A β (1–42). *Biochimica et Biophysica Acta (BBA) - Biomembranes* **2007**, *1768*, 2400-2408.
257. Askarova, S.; Yang, X.; Lee, J. C. Impacts of membrane biophysics in Alzheimer's disease: from amyloid precursor protein processing to A β Peptide-induced membrane changes. *Int. J. Alzheimers Dis.* **2011**, *2011*, 134971.

258. Price, K. A.; Crouch, P. J.; Donnelly, P. S.; Masters, C. L.; White, A. R.; Curtain, C. C. Membrane-targeted strategies for modulating APP and A β -mediated toxicity. *J. Cell. Mol. Med.* **2009**, *13*, 249-261.
259. Williams, T. L.; Serpell, L. C. Membrane and surface interactions of Alzheimer's A β peptide--insights into the mechanism of cytotoxicity. *FEBS J.* **2011**, *278*, 3905-3917.
260. Eikelenboom, P.; Veerhuis, R. The role of complement and activated microglia in the pathogenesis of Alzheimer's disease. *Neurobiol. Aging* **1996**, *17*, 673-680.
261. Siu, G.; Clifford, P.; Kosciuk, M.; Venkataraman, V.; Nagele, R. G. In *Glial Cells and A β Peptides in Alzheimer's Disease Pathogenesis*; Barrow, C. J., Small, D. H., Eds.; A β peptide and Alzheimer's disease - Celebrating a century of research; Springer: London, 2007; pp. 216-233.
262. Mrak, R. E.; Sheng, J. G.; Griffin, W. S. Glial cytokines in Alzheimer's disease: review and pathogenic implications. *Hum. Pathol.* **1995**, *26*, 816-823.
263. Walsh, D. T.; Bresciani, L.; Saunders, D.; Manca, M. F.; Jen, A.; Gentleman, S. M.; Jen, L. S. Amyloid β peptide causes chronic glial cell activation and neuro-degeneration after intravitreal injection. *Neuropathol. Appl. Neurobiol.* **2005**, *31*, 491-502.
264. Meda, L.; Baron, P.; Scarlato, G. Glial activation in Alzheimer's disease: the role of A β and its associated proteins. *Neurobiol. Aging* **2001**, *22*, 885-893.
265. Holcomb, L. A.; Gordon, M. N.; Benkovic, S. A.; Morgan, D. G. A β and perlecan in rat brain: glial activation, gradual clearance and limited neurotoxicity. *Mech. Ageing Dev.* **2000**, *112*, 135-152.
266. Haertig, W.; Bruckner, G.; Schmidt, C.; Brauer, K.; Bodewitz, G.; Turner, J. D.; Bigl, V. Co-localization of β -amyloid peptides, apolipoprotein E and glial markers in senile plaques in the prefrontal cortex of old rhesus monkeys. *Brain Res.* **1997**, *751*, 315-322.
267. Mohamed, A.; Posse de Chaves, E. A β internalization by neurons and glia. *Int. J. Alzheimers Dis.* **2011**, *2011*, 127984.
268. Nagele, R. G.; Wegiel, J.; Venkataraman, V.; Imaki, H.; Wang, K. C.; Wegiel, J. Contribution of glial cells to the development of amyloid plaques in Alzheimer's disease. *Neurobiol. Aging* **2004**, *25*, 663-674.
269. Serrano-Pozo, A.; Mielke, M. L.; Gomez-Isla, T.; Betensky, R. A.; Growdon, J. H.; Frosch, M. P.; Hyman, B. T. Reactive glia not only associates with plaques but also parallels tangles in Alzheimer's disease. *Am. J. Pathol.* **2011**, *179*, 1373-1384.

270. Wisniewski, H. M.; Wegiel, J. Spatial relationships between astrocytes and classical plaque components. *Neurobiol. Aging* **1991**, *12*, 593-600.
271. Thal, D. R.; Schultz, C.; Dehghani, F.; Yamaguchi, H.; Braak, H.; Braak, E. Amyloid β -protein (A β)-containing astrocytes are located preferentially near N-terminal-truncated A β deposits in the human entorhinal cortex. *Acta Neuropathol.* **2000**, *100*, 608-617.
272. Nagele, R. G.; D'Andrea, M. R.; Lee, H.; Venkataraman, V.; Wang, H. Y. Astrocytes accumulate A β ₄₂ and give rise to astrocytic amyloid plaques in Alzheimer disease brains. *Brain Res.* **2003**, *971*, 197-209.
273. Thal, D. R.; Hartig, W.; Schober, R. Diffuse plaques in the molecular layer show intracellular A β ₈₋₁₇-immunoreactive deposits in subpial astrocytes. *Clin. Neuropathol.* **1999**, *18*, 226-231.
274. Paresce, D. M.; Ghosh, R. N.; Maxfield, F. R. Microglial cells internalize aggregates of the Alzheimer's disease amyloid β -protein via a scavenger receptor. *Neuron* **1996**, *17*, 553-565.
275. Akiyama, H.; Mori, H.; Saido, T.; Kondo, H.; Ikeda, K.; McGeer, P. L. Occurrence of the diffuse amyloid β -protein (A β) deposits with numerous A β -containing glial cells in the cerebral cortex of patients with Alzheimer's disease. *Glia* **1999**, *25*, 324-331.
276. Ard, M. D.; Cole, G. M.; Wei, J.; Mehrle, A. P.; Fratkin, J. D. Scavenging of Alzheimer's amyloid β -protein by microglia in culture. *J. Neurosci. Res.* **1996**, *43*, 190-202.
277. Chung, H.; Brazil, M. I.; Soe, T. T.; Maxfield, F. R. Uptake, degradation, and release of fibrillar and soluble forms of Alzheimer's amyloid β -peptide by microglial cells. *J. Biol. Chem.* **1999**, *274*, 32301-32308.
278. DeWitt, D. A.; Perry, G.; Cohen, M.; Doller, C.; Silver, J. Astrocytes regulate microglial phagocytosis of senile plaque cores of Alzheimer's disease. *Exp. Neurol.* **1998**, *149*, 329-340.
279. Kurt, M. A.; Davies, D. C.; Kidd, M. β -Amyloid immunoreactivity in astrocytes in Alzheimer's disease brain biopsies: an electron microscope study. *Exp. Neurol.* **1999**, *158*, 221-228.
280. Wegiel, J.; Wang, K. C.; Tarnawski, M.; Lach, B. Microglia cells are the driving force in fibrillar plaque formation, whereas astrocytes are a leading factor in plaque degradation. *Acta Neuropathol.* **2000**, *100*, 356-364.
281. Balin, B. J.; Gerard, H. C.; Arking, E. J.; Appelt, D. M.; Branigan, P. J.; Abrams, J. T.; Whittum-Hudson, J. A.; Hudson, A. P. Identification and localization of *Chlamydia pneumoniae* in the Alzheimer's brain. *Med. Microbiol. Immunol.* **1998**, *187*, 23-42.
282. Kamer, A. R.; Craig, R. G.; Pirraglia, E.; Dasanayake, A. P.; Norman, R. G.; Boylan, R. J.; Nehorayoff, A.; Glodzik, L.; Brys, M.; de Leon, M. J. TNF- α and antibodies to periodontal

- bacteria discriminate between Alzheimer's disease patients and normal subjects. *J. Neuroimmunol.* **2009**, *216*, 92-97.
283. Urosevic, N.; Martins, R. N. Infection and Alzheimer's disease: the APOE epsilon4 connection and lipid metabolism. *J. Alzheimers Dis.* **2008**, *13*, 421-435.
284. Honjo, K.; van Reekum, R.; Verhoeff, N. P. Alzheimer's disease and infection: do infectious agents contribute to progression of Alzheimer's disease? *Alzheimers Dement.* **2009**, *5*, 348-360.
285. Nicolson, G. L. Chronic Bacterial and Viral Infections in Neurodegenerative and Neurobehavioral Diseases. *Lab Medicine* **2008**, *39*, 291-299.
286. Carter, C. Alzheimer's Disease: APP, γ Secretase, APOE, CLU, CR1, PICALM, ABCA7, BIN1, CD2AP, CD33, EPHA1, and MS4A2, and Their Relationships with Herpes Simplex, C. *Pneumoniae*, Other Suspect Pathogens, and the Immune System. *Int. J. Alzheimers Dis.* **2011**, *2011*, 501862.
287. Yucesan, C.; Sriram, S. *Chlamydia pneumoniae* infection of the central nervous system. *Curr. Opin. Neurol.* **2001**, *14*, 355-359.
288. Letenneur, L.; Peres, K.; Fleury, H.; Garrigue, I.; Barberger-Gateau, P.; Helmer, C.; Orgogozo, J. M.; Gauthier, S.; Dartigues, J. F. Seropositivity to herpes simplex virus antibodies and risk of Alzheimer's disease: a population-based cohort study. *PLoS One* **2008**, *3*, e3637.
289. Wozniak, M. A.; Mee, A. P.; Itzhaki, R. F. Herpes simplex virus type 1 DNA is located within Alzheimer's disease amyloid plaques. *J. Pathol.* **2009**, *217*, 131-138.
290. Kammerman, E. M.; Neumann, D. M.; Ball, M. J.; Lukiw, W.; Hill, J. M. Senile plaques in Alzheimer's diseased brains: possible association of β -amyloid with herpes simplex virus type 1 (HSV-1) L-particles. *Med. Hypotheses* **2006**, *66*, 294-299.
291. Katan, M.; Moon, Y. P.; Paik, M. C.; Sacco, R. L.; Wright, C. B.; Elkind, M. S. Infectious burden and cognitive function: the Northern Manhattan Study. *Neurology* **2013**, *80*, 1209-1215.
292. Itzhaki, R. F.; Lin, W. R.; Shang, D.; Wilcock, G. K.; Faragher, B.; Jamieson, G. A. Herpes simplex virus type 1 in brain and risk of Alzheimer's disease. *Lancet* **1997**, *349*, 241-244.
293. Carter, C. J. Alzheimer's disease plaques and tangles: cemeteries of a pyrrhic victory of the immune defence network against herpes simplex infection at the expense of complement and inflammation-mediated neuronal destruction. *Neurochem. Int.* **2011**, *58*, 301-320.
294. Carter, C. J. APP, APOE, complement receptor 1, clusterin and PICALM and their involvement in the herpes simplex life cycle. *Neurosci. Lett.* **2010**, *483*, 96-100.

295. Wang, Z.; Zhang, X.; Wang, H.; Qi, L.; Lou, Y. Neuroprotective effects of icaritin against β amyloid-induced neurotoxicity in primary cultured rat neuronal cells via estrogen-dependent pathway. *Neuroscience* **2007**, *145*, 911-922.
296. Henderson, V. W. Estrogen-containing hormone therapy and Alzheimer's disease risk: Understanding discrepant inferences from observational and experimental research. *Neuroscience* **2006**, *138*, 1031-1039.
297. Yue, X.; Lu, M.; Lancaster, T.; Cao, P.; Honda, S.; Staufenbiel, M.; Harada, N.; Zhong, Z.; Shen, Y.; Li, R. Brain estrogen deficiency accelerates A β plaque formation in an Alzheimer's disease animal model. *Proc. Natl. Acad. Sci. U. S. A.* **2005**, *102*, 19198-19203.
298. Nilsen, J.; Chen, S.; Irwin, R. W.; Iwamoto, S.; Brinton, R. D. Estrogen protects neuronal cells from amyloid β -induced apoptosis via regulation of mitochondrial proteins and function. *BMC Neurosci.* **2006**, *7*, 74.
299. Xu, H.; Wang, R.; Zhang, Y. W.; Zhang, X. Estrogen, β -amyloid metabolism/trafficking, and Alzheimer's disease. *Ann. N. Y. Acad. Sci.* **2006**, *1089*, 324-342.
300. Selkoe, D. J. Soluble oligomers of the amyloid β -protein impair synaptic plasticity and behavior. *Behav. Brain Res.* **2008**, *192*, 106-113.
301. Arendt, T. Synaptic degeneration in Alzheimer's disease. *Acta Neuropathol.* **2009**, *118*, 167-179.
302. Armstrong, R. A. The spatial pattern of discrete β -amyloid deposits in Alzheimer's disease reflects synaptic disconnection. *Dementia* **1996**, *7*, 86-90.
303. Cirrito, J. R.; Yamada, K. A.; Finn, M. B.; Sloviter, R. S.; Bales, K. R.; May, P. C.; Schoepp, D. D.; Paul, S. M.; Mennerick, S.; Holtzman, D. M. Synaptic activity regulates interstitial fluid amyloid- β levels in vivo. *Neuron* **2005**, *48*, 913-922.
304. Lacor, P. N.; Buniel, M. C.; Furlow, P. W.; Clemente, A. S.; Velasco, P. T.; Wood, M.; Viola, K. L.; Klein, W. L. A β oligomer-induced aberrations in synapse composition, shape, and density provide a molecular basis for loss of connectivity in Alzheimer's disease. *J. Neurosci.* **2007**, *27*, 796-807.
305. Blenow, K.; Bogdanovic, N.; Alafuzoff, I.; Ekman, R.; Davidsson, P. Synaptic pathology in Alzheimer's disease: relation to severity of dementia, but not to senile plaques, neurofibrillary tangles, or the ApoE4 allele. *J. Neural Transm.* **1996**, *103*, 603-618.
306. Callahan, L. M.; Coleman, P. D. Neurons bearing neurofibrillary tangles are responsible for selected synaptic deficits in Alzheimer's disease. *Neurobiol. Aging* **1995**, *16*, 311-314.

307. Cerpa, W.; Dinamarca, M. C.; Inestrosa, N. C. Structure-function implications in Alzheimer's disease: effect of A β oligomers at central synapses. *Curr. Alzheimer Res.* **2008**, *5*, 233-243.
308. Evans, N. A.; Facci, L.; Owen, D. E.; Soden, P. E.; Burbidge, S. A.; Prinjha, R. K.; Richardson, J. C.; Skaper, S. D. A β ₁₋₄₂ reduces synapse number and inhibits neurite outgrowth in primary cortical and hippocampal neurons: a quantitative analysis. *J. Neurosci. Methods* **2008**, *175*, 96-103.
309. De Felice, F. G.; Vieira, M. N.; Bomfim, T. R.; Decker, H.; Velasco, P. T.; Lambert, M. P.; Viola, K. L.; Zhao, W. Q.; Ferreira, S. T.; Klein, W. L. Protection of synapses against Alzheimer's-linked toxins: insulin signaling prevents the pathogenic binding of A β oligomers. *Proc. Natl. Acad. Sci. U. S. A.* **2009**, *106*, 1971-1976.
310. Viola, K. L.; Velasco, P. T.; Klein, W. L. Why Alzheimer's is a disease of memory: the attack on synapses by A β oligomers (ADDLs). *J. Nutr. Health Aging* **2008**, *12*, 51S-7S.
311. Mandelkow, E. M.; Stamer, K.; Vogel, R.; Thies, E.; Mandelkow, E. Clogging of axons by tau, inhibition of axonal traffic and starvation of synapses. *Neurobiol. Aging* **2003**, *24*, 1079-1085.
312. Borlikova, G. G.; Trejo, M.; Mably, A. J.; Mc Donald, J. M.; Sala Frigerio, C.; Regan, C. M.; Murphy, K. J.; Masliah, E.; Walsh, D. M. Alzheimer brain-derived amyloid β -protein impairs synaptic remodeling and memory consolidation. *Neurobiol. Aging* **2013**, *34*, 1315-1327.
313. Du, H.; Guo, L.; Yan, S. S. Synaptic mitochondrial pathology in Alzheimer's disease. *Antioxid. Redox Signal.* **2012**, *16*, 1467-1475.
314. Selkoe, D. J. Alzheimer's disease is a synaptic failure. *Science* **2002**, *298*, 789-791.
315. Masliah, E. Alzheimer's in real time. *Nature* **2008**, *451*, 638-639.
316. Coleman, P. D.; Yao, P. J. Synaptic slaughter in Alzheimer's disease. *Neurobiol. Aging* **2003**, *24*, 1023-1027.
317. Miklossy, J. Chronic inflammation and amyloidogenesis in Alzheimer's disease -- role of Spirochetes. *J. Alzheimers Dis.* **2008**, *13*, 381-391.
318. Rojo, L. E.; Fernández, J. A.; Maccioni, A. A.; Jimenez, J. M.; Maccioni, R. B. Neuroinflammation: Implications for the Pathogenesis and Molecular Diagnosis of Alzheimer's Disease. *Arch. Med. Res.* **2008**, *39*, 1-16.
319. Eikelenboom, P.; van Gool, W. A. Neuroinflammatory perspectives on the two faces of Alzheimer's disease. *J. Neural Transm.* **2004**, *111*, 281-294.

320. Eikelenboom, P.; Rozemuller, J. M.; van Muiswinkel, F. L. Inflammation and Alzheimer's disease: relationships between pathogenic mechanisms and clinical expression. *Exp. Neurol.* **1998**, *154*, 89-98.
321. Sheng, J. G.; Bora, S. H.; Xu, G.; Borchelt, D. R.; Price, D. L.; Koliatsos, V. E. Lipopolysaccharide-induced-neuroinflammation increases intracellular accumulation of amyloid precursor protein and amyloid β peptide in APPswe transgenic mice. *Neurobiol. Dis.* **2003**, *14*, 133-145.
322. Morishima, Y.; Gotoh, Y.; Zieg, J.; Barrett, T.; Takano, H.; Flavell, R.; Davis, R. J.; Shirasaki, Y.; Greenberg, M. E. β -amyloid induces neuronal apoptosis via a mechanism that involves the c-Jun N-terminal kinase pathway and the induction of Fas ligand. *J. Neurosci.* **2001**, *21*, 7551-7560.
323. Mattson, M. P.; Partin, J.; Begley, J. G. Amyloid β -peptide induces apoptosis-related events in synapses and dendrites. *Brain Res.* **1998**, *807*, 167-176.
324. Forloni, G.; Bugiani, O.; Tagliavini, F.; Salmona, M. Apoptosis-mediated neurotoxicity induced by β -amyloid and PrP fragments. *Mol. Chem. Neuropathol.* **1996**, *28*, 163-171.
325. LeBlanc, A.; Liu, H.; Goodyer, C.; Bergeron, C.; Hammond, J. Caspase-6 role in apoptosis of human neurons, amyloidogenesis, and Alzheimer's disease. *J. Biol. Chem.* **1999**, *274*, 23426-23436.
326. Guo, H.; Albrecht, S.; Bourdeau, M.; Petzke, T.; Bergeron, C.; LeBlanc, A. C. Active caspase-6 and caspase-6-cleaved tau in neuropil threads, neuritic plaques, and neurofibrillary tangles of Alzheimer's disease. *Am. J. Pathol.* **2004**, *165*, 523-531.
327. Galli, C.; Piccini, A.; Ciotti, M. T.; Castellani, L.; Calissano, P.; Zaccheo, D.; Tabaton, M. Increased amyloidogenic secretion in cerebellar granule cells undergoing apoptosis. *Proc. Natl. Acad. Sci. U. S. A.* **1998**, *95*, 1247-1252.
328. Gervais, F. G.; Xu, D.; Robertson, G. S.; Vaillancourt, J. P.; Zhu, Y.; Huang, J.; LeBlanc, A.; Smith, D.; Rigby, M.; Shearman, M. S.; Clarke, E. E.; Zheng, H.; Van Der Ploeg, L. H.; Ruffolo, S. C.; Thornberry, N. A.; Xanthoudakis, S.; Zamboni, R. J.; Roy, S.; Nicholson, D. W. Involvement of caspases in proteolytic cleavage of Alzheimer's amyloid- β precursor protein and amyloidogenic A β peptide formation. *Cell* **1999**, *97*, 395-406.
329. Esposito, L.; Gan, L.; Yu, G. Q.; Essrich, C.; Mucke, L. Intracellularly generated amyloid- β peptide counteracts the antiapoptotic function of its precursor protein and primes proapoptotic pathways for activation by other insults in neuroblastoma cells. *J. Neurochem.* **2004**, *91*, 1260-1274.

330. Zhang, Y.; Goodyer, C.; LeBlanc, A. Selective and protracted apoptosis in human primary neurons microinjected with active caspase-3, -6, -7, and -8. *J. Neurosci.* **2000**, *20*, 8384-8389.
331. Li, Y. P.; Bushnell, A. F.; Lee, C. M.; Perlmutter, L. S.; Wong, S. K. β -amyloid induces apoptosis in human-derived neurotypic SH-SY5Y cells. *Brain Res.* **1996**, *738*, 196-204.
332. LaFerla, F. M.; Tinkle, B. T.; Bieberich, C. J.; Haudenschild, C. C.; Jay, G. The Alzheimer's A β peptide induces neurodegeneration and apoptotic cell death in transgenic mice. *Nat. Genet.* **1995**, *9*, 21-30.
333. Kienlen-Campard, P.; Miolet, S.; Tasiaux, B.; Octave, J. N. Intracellular amyloid- β_{1-42} , but not extracellular soluble amyloid- β peptides, induces neuronal apoptosis. *J. Biol. Chem.* **2002**, *277*, 15666-15670.
334. Behl, C.; Davis, J. B.; Klier, F. G.; Schubert, D. Amyloid β peptide induces necrosis rather than apoptosis. *Brain Res.* **1994**, *645*, 253-264.
335. Kang, J.; Lemaire, H. G.; Unterbeck, A.; Salbaum, J. M.; Masters, C. L.; Grzeschik, K. H.; Multhaup, G.; Beyreuther, K.; Muller-Hill, B. The precursor of Alzheimer's disease amyloid A4 protein resembles a cell-surface receptor. *Nature* **1987**, *325*, 733-736.
336. Konig, G.; Salbaum, J. M.; Wiestler, O.; Lang, W.; Schmitt, H. P.; Masters, C. L.; Beyreuther, K. Alternative splicing of the β A4 amyloid gene of Alzheimer's disease in cortex of control and Alzheimer's disease patients. *Brain Res. Mol. Brain Res.* **1991**, *9*, 259-262.
337. Sandbrink, R.; Masters, C. L.; Beyreuther, K. APP gene family: unique age-associated changes in splicing of Alzheimer's β A4-amyloid protein precursor. *Neurobiol. Dis.* **1994**, *1*, 13-24.
338. Panegyres, P. K. The functions of the amyloid precursor protein gene. *Rev. Neurosci.* **2001**, *12*, 1-39.
339. Wertkin, A. M.; Turner, R. S.; Pleasure, S. J.; Golde, T. E.; Younkin, S. G.; Trojanowski, J. Q.; Lee, V. M. Human neurons derived from a teratocarcinoma cell line express solely the 695-amino acid amyloid precursor protein and produce intracellular β -amyloid or A4 peptides. *Proc. Natl. Acad. Sci. U. S. A.* **1993**, *90*, 9513-9517.
340. Sandbrink, R.; Masters, C. L.; Beyreuther, K. Similar alternative splicing of a non-homologous domain in β A4-amyloid protein precursor-like proteins. *J. Biol. Chem.* **1994**, *269*, 14227-14234.

341. Beyreuther, K.; Pollwein, P.; Multhaup, G.; Monning, U.; König, G.; Dyrks, T.; Schubert, W.; Masters, C. L. Regulation and expression of the Alzheimer's β /A4 amyloid protein precursor in health, disease, and Down's syndrome. *Ann. N. Y. Acad. Sci.* **1993**, *695*, 91-102.
342. Mattson, M. P.; Cheng, B.; Culwell, A. R.; Esch, F. S.; Lieberburg, I.; Rydel, R. E. Evidence for excitoprotective and intraneuronal calcium-regulating roles for secreted forms of the β -amyloid precursor protein. *Neuron* **1993**, *10*, 243-254.
343. Small, D. H.; Nurcombe, V.; Reed, G.; Clarris, H.; Moir, R.; Beyreuther, K.; Masters, C. L. A heparin-binding domain in the amyloid protein precursor of Alzheimer's disease is involved in the regulation of neurite outgrowth. *J. Neurosci.* **1994**, *14*, 2117-2127.
344. Schubert, D.; Jin, L. W.; Saitoh, T.; Cole, G. The regulation of amyloid β protein precursor secretion and its modulatory role in cell adhesion. *Neuron* **1989**, *3*, 689-694.
345. Van Nostrand, W. E.; Schmaier, A. H.; Farrow, J. S.; Cunningham, D. D. Protease nexin-II (amyloid β -protein precursor): a platelet α -granule protein. *Science* **1990**, *248*, 745-748.
346. Van Nostrand, W. E. Zinc (II) selectively enhances the inhibition of coagulation factor XIa by protease nexin-2/amyloid β -protein precursor. *Thromb. Res.* **1995**, *78*, 43-53.
347. Smith, R. P.; Higuchi, D. A.; Broze, G. J., Jr Platelet coagulation factor XIa-inhibitor, a form of Alzheimer amyloid precursor protein. *Science* **1990**, *248*, 1126-1128.
348. Henry, A.; Li, Q. X.; Galatis, D.; Hesse, L.; Multhaup, G.; Beyreuther, K.; Masters, C. L.; Cappai, R. Inhibition of platelet activation by the Alzheimer's disease amyloid precursor protein. *Br. J. Haematol.* **1998**, *103*, 402-415.
349. White, A. R.; Reyes, R.; Mercer, J. F.; Camakaris, J.; Zheng, H.; Bush, A. I.; Multhaup, G.; Beyreuther, K.; Masters, C. L.; Cappai, R. Copper levels are increased in the cerebral cortex and liver of APP and APLP2 knockout mice. *Brain Res.* **1999**, *842*, 439-444.
350. Bentahir, M.; Nyabi, O.; Verhamme, J.; Tolia, A.; Horre, K.; Wiltfang, J.; Esselmann, H.; De Strooper, B. Presenilin clinical mutations can affect γ -secretase activity by different mechanisms. *J. Neurochem.* **2006**, *96*, 732-742.
351. Greenfield, J. P.; Tsai, J.; Gouras, G. K.; Hai, B.; Thinakaran, G.; Checler, F.; Sisodia, S. S.; Greengard, P.; Xu, H. Endoplasmic reticulum and trans-Golgi network generate distinct populations of Alzheimer β -amyloid peptides. *Proc. Natl. Acad. Sci. U. S. A.* **1999**, *96*, 742-747.
352. Bouwman, F. H.; Schoonenboom, N. S.; Verwey, N. A.; van Elk, E. J.; Kok, A.; Blankenstein, M. A.; Scheltens, P.; van der Flier, W. M. CSF biomarker levels in early and late onset Alzheimer's disease. *Neurobiol. Aging* **2008**.

353. Bateman, R. J.; Munsell, L. Y.; Morris, J. C.; Swarm, R.; Yarasheski, K. E.; Holtzman, D. M. Human amyloid- β synthesis and clearance rates as measured in cerebrospinal fluid in vivo. *Nat. Med.* **2006**, *12*, 856-861.
354. Zou, K.; Gong, J. S.; Yanagisawa, K.; Michikawa, M. A novel function of monomeric amyloid β -protein serving as an antioxidant molecule against metal-induced oxidative damage. *J. Neurosci.* **2002**, *22*, 4833-4841.
355. Kontush, A. Alzheimer's amyloid- β as a preventive antioxidant for brain lipoproteins. *Cell. Mol. Neurobiol.* **2001**, *21*, 299-315.
356. Atwood, C. S.; Bowen, R. L.; Smith, M. A.; Perry, G. Cerebrovascular requirement for sealant, anti-coagulant and remodeling molecules that allow for the maintenance of vascular integrity and blood supply. *Brain Res. Brain Res. Rev.* **2003**, *43*, 164-178.
357. Meier-Stephenson, V. C. Quantum Medicine: Novel Applications of Computational Chemistry to the Treatment of Neurological Diseases, Dalhousie University, Halifax, Nova Scotia, 2005.
358. Soccia, S. J.; Kirby, J. E.; Washicosky, K. J.; Tucker, S. M.; Ingelsson, M.; Hyman, B.; Burton, M. A.; Goldstein, L. E.; Duong, S.; Tanzi, R. E.; Moir, R. D. The Alzheimer's disease-associated amyloid β -protein is an antimicrobial peptide. *PLoS One* **2010**, *5*, e9505.
359. Nordstedt, C.; Naslund, J.; Tjernberg, L. O.; Karlstrom, A. R.; Thyberg, J.; Terenius, L. The Alzheimer A β peptide develops protease resistance in association with its polymerization into fibrils. *J. Biol. Chem.* **1994**, *269*, 30773-30776.
360. Shapira, R.; Austin, G. E.; Mirra, S. S. Neuritic plaque amyloid in Alzheimer's disease is highly racemized. *J. Neurochem.* **1988**, *50*, 69-74.
361. Roher, A. E.; Lowenson, J. D.; Clarke, S.; Woods, A. S.; Cotter, R. J.; Gowing, E.; Ball, M. J. β -Amyloid-(1-42) is a major component of cerebrovascular amyloid deposits: implications for the pathology of Alzheimer disease. *Proc. Natl. Acad. Sci. U. S. A.* **1993**, *90*, 10836-10840.
362. Roher, A. E.; Palmer, K. C.; Yurewicz, E. C.; Ball, M. J.; Greenberg, B. D. Morphological and biochemical analyses of amyloid plaque core proteins purified from Alzheimer disease brain tissue. *J. Neurochem.* **1993**, *61*, 1916-1926.
363. Vitek, M. P.; Bhattacharya, K.; Glendening, J. M.; Stopa, E.; Vlassara, H.; Bucala, R.; Manogue, K.; Cerami, A. Advanced glycation end products contribute to amyloidosis in Alzheimer disease. *Proc. Natl. Acad. Sci. U. S. A.* **1994**, *91*, 4766-4770.

364. Smith, M. A.; Taneda, S.; Richey, P. L.; Miyata, S.; Yan, S. D.; Stern, D.; Sayre, L. M.; Monnier, V. M.; Perry, G. Advanced Maillard reaction end products are associated with Alzheimer disease pathology. *Proc. Natl. Acad. Sci. U. S. A.* **1994**, *91*, 5710-5714.
365. Smith, M. A.; Sayre, L. M.; Monnier, V. M.; Perry, G. Radical AGEing in Alzheimer's disease. *Trends Neurosci.* **1995**, *18*, 172-176.
366. Atwood, C. S.; Huang, X.; Khatri, A.; Scarpa, R. C.; Kim, Y. S.; Moir, R. D.; Tanzi, R. E.; Roher, A. E.; Bush, A. I. Copper catalyzed oxidation of Alzheimer A β . *Cell. Mol. Biol. (Noisy-le-grand)* **2000**, *46*, 777-783.
367. Atwood, C. S.; Perry, G.; Zeng, H.; Kato, Y.; Jones, W. D.; Ling, K. Q.; Huang, X.; Moir, R. D.; Wang, D.; Sayre, L. M.; Smith, M. A.; Chen, S. G.; Bush, A. I. Copper mediates dityrosine cross-linking of Alzheimer's amyloid- β . *Biochemistry* **2004**, *43*, 560-568.
368. Chen, K.; Maley, J.; Yu, P. H. Potential implications of endogenous aldehydes in β -amyloid misfolding, oligomerization and fibrillogenesis. *J. Neurochem.* **2006**, *99*, 1413-1424.
369. Reddy, V. P.; Obrenovich, M. E.; Atwood, C. S.; Perry, G.; Smith, M. A. Involvement of Maillard reactions in Alzheimer disease. *Neurotox Res.* **2002**, *4*, 191-209.
370. Atwood, C. S.; Obrenovich, M. E.; Liu, T.; Chan, H.; Perry, G.; Smith, M. A.; Martins, R. N. Amyloid- β : a chameleon walking in two worlds: a review of the trophic and toxic properties of amyloid- β . *Brain Res. Brain Res. Rev.* **2003**, *43*, 1-16.
371. Araki, W.; Kitaguchi, N.; Tokushima, Y.; Ishii, K.; Aratake, H.; Shimohama, S.; Nakamura, S.; Kimura, J. Trophic effect of β -amyloid precursor protein on cerebral cortical neurons in culture. *Biochem. Biophys. Res. Commun.* **1991**, *181*, 265-271.
372. Takenouchi, T.; Munekata, E. Trophic effects of substance P and β -amyloid peptide on dibutyryl cyclic AMP-differentiated human leukemic (HL-60) cells. *Life Sci.* **1995**, *56*, PL479-84.
373. Halverson, K.; Fraser, P. E.; Kirschner, D. A.; Lansbury, P. T., Jr Molecular determinants of amyloid deposition in Alzheimer's disease: conformational studies of synthetic β -protein fragments. *Biochemistry* **1990**, *29*, 2639-2644.
374. Fraser, P. E.; Nguyen, J. T.; Inouye, H.; Surewicz, W. K.; Selkoe, D. J.; Podlisny, M. B.; Kirschner, D. A. Fibril formation by primate, rodent, and Dutch-hemorrhagic analogues of Alzheimer amyloid β -protein. *Biochemistry* **1992**, *31*, 10716-10723.
375. Soto, C.; Castano, E. M.; Kumar, R. A.; Beavis, R. C.; Frangione, B. Fibrillogenesis of synthetic amyloid- β peptides is dependent on their initial secondary structure. *Neurosci. Lett.* **1995**, *200*, 105-108.

376. Ma, K.; Clancy, E. L.; Zhang, Y.; Ray, D. G.; Wollenberg, K.; Zagorski, M. G. Residue-Specific pKa Measurements of the β -Peptide and Mechanism of pH-Induced Amyloid Formation. *J. Am. Chem. Soc.* **1999**, *121*, 8698-8706.
377. Crescenzi, O.; Tomaselli, S.; Guerrini, R.; Salvadori, S.; D'Ursi, A. M.; Temussi, P. A.; Picone, D. Solution structure of the Alzheimer amyloid β -peptide (1-42) in an apolar microenvironment. Similarity with a virus fusion domain. *Eur. J. Biochem.* **2002**, *269*, 5642-5648.
378. Giulian, D.; Haverkamp, L. J.; Yu, J.; Karshin, W.; Tom, D.; Li, J.; Kazanskaia, A.; Kirkpatrick, J.; Roher, A. E. The HHQK domain of β -amyloid provides a structural basis for the immunopathology of Alzheimer's disease. *J. Biol. Chem.* **1998**, *273*, 29719-29726.
379. Zagorski, M. G.; Barrow, C. J. NMR studies of amyloid β -peptides: proton assignments, secondary structure, and mechanism of an α -helix \rightarrow β -sheet conversion for a homologous, 28-residue, N-terminal fragment. *Biochemistry* **1992**, *31*, 5621-5631.
380. Tjernberg, L. O.; Callaway, D. J.; Tjernberg, A.; Hahne, S.; Lilliehook, C.; Terenius, L.; Thyberg, J.; Nordstedt, C. A molecular model of Alzheimer amyloid β -peptide fibril formation. *J. Biol. Chem.* **1999**, *274*, 12619-12625.
381. Fraser, P. E.; Nguyen, J. T.; Surewicz, W. K.; Kirschner, D. A. pH-dependent structural transitions of Alzheimer amyloid peptides. *Biophys. J.* **1991**, *60*, 1190-1201.
382. Finder, V. H.; Glockshuber, R. Amyloid- β aggregation. *Neurodegener Dis.* **2007**, *4*, 13-27.
383. Zhai, J.; Lee, T. H.; Small, D. H.; Aguilar, M. I. Characterization of early stage intermediates in the nucleation phase of A β aggregation. *Biochemistry* **2012**, *51*, 1070-1078.
384. Shankar, G. M.; Leissring, M. A.; Adame, A.; Sun, X.; Spooner, E.; Masliah, E.; Selkoe, D. J.; Lemere, C. A.; Walsh, D. M. Biochemical and immunohistochemical analysis of an Alzheimer's disease mouse model reveals the presence of multiple cerebral A β assembly forms throughout life. *Neurobiol. Dis.* **2009**, *36*, 293-302.
385. Selkoe, D. J. Cell biology of protein misfolding: the examples of Alzheimer's and Parkinson's diseases. *Nat. Cell Biol.* **2004**, *6*, 1054-1061.
386. Zhang, S.; Iwata, K.; Lachenmann, M. J.; Peng, J. W.; Li, S.; Stimson, E. R.; Lu, Y.; Felix, A. M.; Maggio, J. E.; Lee, J. P. The Alzheimer's peptide A β adopts a collapsed coil structure in water. *J. Struct. Biol.* **2000**, *130*, 130-141.
387. Barrow, C. J.; Zagorski, M. G. Solution structures of β peptide and its constituent fragments: relation to amyloid deposition. *Science* **1991**, *253*, 179-182.

388. Lazo, N. D.; Grant, M. A.; Condrón, M. C.; Rigby, A. C.; Teplow, D. B. On the nucleation of amyloid β -protein monomer folding. *Protein Sci.* **2005**, *14*, 1581-1596.
389. Xu, Y.; Shen, J.; Luo, X.; Zhu, W.; Chen, K.; Ma, J.; Jiang, H. Conformational transition of amyloid β -peptide. *Proc. Natl. Acad. Sci. U. S. A.* **2005**, *102*, 5403-5407.
390. Garzon-Rodriguez, W.; Sepulveda-Becerra, M.; Milton, S.; Glabe, C. G. Soluble amyloid A β -(1-40) exists as a stable dimer at low concentrations. *J. Biol. Chem.* **1997**, *272*, 21037-21044.
391. Roher, A. E.; Chaney, M. O.; Kuo, Y. M.; Webster, S. D.; Stine, W. B.; Haverkamp, L. J.; Woods, A. S.; Cotter, R. J.; Tuohy, J. M.; Krafft, G. A.; Bonnell, B. S.; Emmerling, M. R. Morphology and toxicity of A β -(1-42) dimer derived from neuritic and vascular amyloid deposits of Alzheimer's disease. *J. Biol. Chem.* **1996**, *271*, 20631-20635.
392. Podlisny, M. B.; Ostaszewski, B. L.; Squazzo, S. L.; Koo, E. H.; Rydell, R. E.; Teplow, D. B.; Selkoe, D. J. Aggregation of secreted amyloid β -protein into sodium dodecyl sulfate-stable oligomers in cell culture. *J. Biol. Chem.* **1995**, *270*, 9564-9570.
393. Hilbich, C.; Kisters-Woike, B.; Reed, J.; Masters, C. L.; Beyreuther, K. Substitutions of hydrophobic amino acids reduce the amyloidogenicity of Alzheimer's disease β A4 peptides. *J. Mol. Biol.* **1992**, *228*, 460-473.
394. Nakabayashi, J.; Yoshimura, M.; Morishima-Kawashima, M.; Funato, H.; Miyakawa, T.; Yamazaki, T.; Ihara, Y. Amyloid β -protein (A β) accumulation in the putamen and mammillary body during aging and in Alzheimer disease. *J. Neuropathol. Exp. Neurol.* **1998**, *57*, 343-352.
395. Lesne, S.; Koh, M. T.; Kotilinek, L.; Kaye, R.; Glabe, C. G.; Yang, A.; Gallagher, M.; Ashe, K. H. A specific amyloid- β protein assembly in the brain impairs memory. *Nature* **2006**, *440*, 352-357.
396. Townsend, M.; Shankar, G. M.; Mehta, T.; Walsh, D. M.; Selkoe, D. J. Effects of secreted oligomers of amyloid β -protein on hippocampal synaptic plasticity: a potent role for trimers. *J. Physiol.* **2006**, *572*, 477-492.
397. Chen, Y. R.; Glabe, C. G. Distinct early folding and aggregation properties of Alzheimer amyloid- β peptides A β ₄₀ and A β ₄₂: stable trimer or tetramer formation by A β ₄₂. *J. Biol. Chem.* **2006**, *281*, 24414-24422.
398. Kuo, Y. M.; Emmerling, M. R.; Vigo-Pelfrey, C.; Kasunic, T. C.; Kirkpatrick, J. B.; Murdoch, G. H.; Ball, M. J.; Roher, A. E. Water-soluble A β (N-40, N-42) oligomers in normal and Alzheimer disease brains. *J. Biol. Chem.* **1996**, *271*, 4077-4081.

399. McLean, C. A.; Cherny, R. A.; Fraser, F. W.; Fuller, S. J.; Smith, M. J.; Beyreuther, K.; Bush, A. I.; Masters, C. L. Soluble pool of A β amyloid as a determinant of severity of neurodegeneration in Alzheimer's disease. *Ann. Neurol.* **1999**, *46*, 860-866.
400. Bitan, G.; Kirkitadze, M. D.; Lomakin, A.; Vollers, S. S.; Benedek, G. B.; Teplow, D. B. Amyloid β -protein (A β) assembly: A β ₄₀ and A β ₄₂ oligomerize through distinct pathways. *Proc. Natl. Acad. Sci. U. S. A.* **2003**, *100*, 330-335.
401. Cleary, J. P.; Walsh, D. M.; Hofmeister, J. J.; Shankar, G. M.; Kuskowski, M. A.; Selkoe, D. J.; Ashe, K. H. Natural oligomers of the amyloid- β protein specifically disrupt cognitive function. *Nat. Neurosci.* **2005**, *8*, 79-84.
402. Chromy, B. A.; Nowak, R. J.; Lambert, M. P.; Viola, K. L.; Chang, L.; Velasco, P. T.; Jones, B. W.; Fernandez, S. J.; Lacor, P. N.; Horowitz, P.; Finch, C. E.; Krafft, G. A.; Klein, W. L. Self-Assembly of A₁₋₄₂ into Globular Neurotoxins. *Biochemistry* **2003**, *42*, 12749-12760.
403. Losic, D.; Martin, L. L.; Mechler, A.; Aguilar, M. I.; Small, D. H. High resolution scanning tunnelling microscopy of the β -amyloid protein (A β ₁₋₄₀) of Alzheimer's disease suggests a novel mechanism of oligomer assembly. *J. Struct. Biol.* **2006**, *155*, 104-110.
404. Nimmrich, V.; Grimm, C.; Draguhn, A.; Barghorn, S.; Lehmann, A.; Schoemaker, H.; Hillen, H.; Gross, G.; Ebert, U.; Bruehl, C. Amyloid β oligomers (A β ₁₋₄₂ globulomer) suppress spontaneous synaptic activity by inhibition of P/Q-type calcium currents. *J. Neurosci.* **2008**, *28*, 788-797.
405. Arimon, M.; Diez-Perez, I.; Kogan, M. J.; Durany, N.; Giralt, E.; Sanz, F.; Fernandez-Busquets, X. Fine structure study of A β ₁₋₄₂ fibrillogenesis with atomic force microscopy. *FASEB J.* **2005**, *19*, 1344-1346.
406. Gellermann, G. P.; Byrnes, H.; Striebinger, A.; Ullrich, K.; Mueller, R.; Hillen, H.; Barghorn, S. A β -globulomers are formed independently of the fibril pathway. *Neurobiol. Dis.* **2008**, *30*, 212-220.
407. Lashuel, H. A.; Hartley, D.; Petre, B. M.; Walz, T.; Lansbury, P. T., Jr Neurodegenerative disease: amyloid pores from pathogenic mutations. *Nature* **2002**, *418*, 291.
408. Quist, A.; Doudevski, I.; Lin, H.; Azimova, R.; Ng, D.; Frangione, B.; Kagan, B.; Ghiso, J.; Lal, R. Amyloid ion channels: a common structural link for protein-misfolding disease. *Proc. Natl. Acad. Sci. U. S. A.* **2005**, *102*, 10427-10432.
409. Kagan, B. L.; Hirakura, Y.; Azimov, R.; Azimova, R.; Lin, M. C. The channel hypothesis of Alzheimer's disease: current status. *Peptides* **2002**, *23*, 1311-1315.

410. Klein, W. L.; Stine, W. B., Jr; Teplow, D. B. Small assemblies of unmodified amyloid β -protein are the proximate neurotoxin in Alzheimer's disease. *Neurobiol. Aging* **2004**, *25*, 569-580.
411. Lambert, M. P.; Barlow, A. K.; Chromy, B. A.; Edwards, C.; Freed, R.; Liosatos, M.; Morgan, T. E.; Rozovsky, I.; Trommer, B.; Viola, K. L.; Wals, P.; Zhang, C.; Finch, C. E.; Krafft, G. A.; Klein, W. L. Diffusible, nonfibrillar ligands derived from $A\beta_{1-42}$ are potent central nervous system neurotoxins. *Proc. Natl. Acad. Sci. U. S. A.* **1998**, *95*, 6448-6453.
412. Harper, J. D.; Wong, S. S.; Lieber, C. M.; Lansbury, P. T., Jr Assembly of $A\beta$ amyloid protofibrils: an in vitro model for a possible early event in Alzheimer's disease. *Biochemistry* **1999**, *38*, 8972-8980.
413. Gong, Y.; Chang, L.; Viola, K. L.; Lacor, P. N.; Lambert, M. P.; Finch, C. E.; Krafft, G. A.; Klein, W. L. Alzheimer's disease-affected brain: presence of oligomeric $A\beta$ ligands (ADDLs) suggests a molecular basis for reversible memory loss. *Proc. Natl. Acad. Sci. U. S. A.* **2003**, *100*, 10417-10422.
414. Georganopoulou, D. G.; Chang, L.; Nam, J. M.; Thaxton, C. S.; Mufson, E. J.; Klein, W. L.; Mirkin, C. A. Nanoparticle-based detection in cerebral spinal fluid of a soluble pathogenic biomarker for Alzheimer's disease. *Proc. Natl. Acad. Sci. U. S. A.* **2005**, *102*, 2273-2276.
415. Harper, J. D.; Lansbury, P. T., Jr Models of amyloid seeding in Alzheimer's disease and scrapie: mechanistic truths and physiological consequences of the time-dependent solubility of amyloid proteins. *Annu. Rev. Biochem.* **1997**, *66*, 385-407.
416. Harper, J. D.; Wong, S. S.; Lieber, C. M.; Lansbury, P. T. Observation of metastable $A\beta$ amyloid protofibrils by atomic force microscopy. *Chem. Biol.* **1997**, *4*, 119-125.
417. Kheterpal, I.; Lashuel, H. A.; Hartley, D. M.; Walz, T.; Lansbury, P. T., Jr; Wetzel, R. $A\beta$ protofibrils possess a stable core structure resistant to hydrogen exchange. *Biochemistry* **2003**, *42*, 14092-14098.
418. Walsh, D. M.; Lomakin, A.; Benedek, G. B.; Condron, M. M.; Teplow, D. B. Amyloid β -protein fibrillogenesis. Detection of a protofibrillar intermediate. *J. Biol. Chem.* **1997**, *272*, 22364-22372.
419. Williams, A. D.; Segal, M.; Chen, M.; Kheterpal, I.; Geva, M.; Berthelie, V.; Kaleta, D. T.; Cook, K. D.; Wetzel, R. Structural properties of $A\beta$ protofibrils stabilized by a small molecule. *Proc. Natl. Acad. Sci. U. S. A.* **2005**, *102*, 7115-7120.
420. O'Quinn, P. R.; Koo, S. I.; Noh, S. K.; Nelssen, J. L.; Goodband, R. D.; Tokach, M. D. Effects of modified tall oil on body composition and serum and tissue levels of cholesterol, phospholipids, and α -tocopherol in adult ovariectomized rats. *Nutrition Research* **2003/4**, *23*, 549-566.

421. Hartley, D. M.; Walsh, D. M.; Ye, C. P.; Diehl, T.; Vasquez, S.; Vassilev, P. M.; Teplow, D. B.; Selkoe, D. J. Protofibrillar intermediates of amyloid β -protein induce acute electrophysiological changes and progressive neurotoxicity in cortical neurons. *J. Neurosci.* **1999**, *19*, 8876-8884.
422. Ward, R. V.; Jennings, K. H.; Jepras, R.; Neville, W.; Owen, D. E.; Hawkins, J.; Christie, G.; Davis, J. B.; George, A.; Karran, E. H.; Howlett, D. R. Fractionation and characterization of oligomeric, protofibrillar and fibrillar forms of β -amyloid peptide. *Biochem. J.* **2000**, *348 Pt 1*, 137-144.
423. Ban, T.; Morigaki, K.; Yagi, H.; Kawasaki, T.; Kobayashi, A.; Yuba, S.; Naiki, H.; Goto, Y. Real-time and single fibril observation of the formation of amyloid β spherulitic structures. *J. Biol. Chem.* **2006**, *281*, 33677-33683.
424. Mann, D. M.; Yates, P. O.; Marcyniuk, B.; Ravindra, C. R. The topography of plaques and tangles in Down's syndrome patients of different ages. *Neuropathol. Appl. Neurobiol.* **1986**, *12*, 447-457.
425. Shibata, C.; Kashima, T.; Ohuchi, K. Nonthermal Influence of Microwave Power on Chemical Reactions. *Jpn. J. Appl. Phys.* **1996**, *35*, 316-319.
426. Ross, C. A.; Poirier, M. A. Opinion: What is the role of protein aggregation in neurodegeneration? *Nat. Rev. Mol. Cell Biol.* **2005**, *6*, 891-898.
427. LeVine, H., 3rd Quantification of β -sheet amyloid fibril structures with thioflavin T. *Methods Enzymol.* **1999**, *309*, 274-284.
428. Klunk, W. E.; Jacob, R. F.; Mason, R. P. Quantifying amyloid β -peptide (A β) aggregation using the Congo red-A β (CR-A β) spectrophotometric assay. *Anal. Biochem.* **1999**, *266*, 66-76.
429. Kirschner, D. A.; Inouye, H.; Duffy, L. K.; Sinclair, A.; Lind, M.; Selkoe, D. J. Synthetic peptide homologous to β protein from Alzheimer disease forms amyloid-like fibrils in vitro. *Proc. Natl. Acad. Sci. U. S. A.* **1987**, *84*, 6953-6957.
430. Stromer, T.; Serpell, L. C. Structure and morphology of the Alzheimer's amyloid fibril. *Microsc. Res. Tech.* **2005**, *67*, 210-217.
431. Luhrs, T.; Ritter, C.; Adrian, M.; Riek-Loher, D.; Bohrmann, B.; Dobeli, H.; Schubert, D.; Riek, R. 3D structure of Alzheimer's amyloid- β (1-42) fibrils. *Proc. Natl. Acad. Sci. U. S. A.* **2005**, *102*, 17342-17347.
432. Malinchik, S. B.; Inouye, H.; Szumowski, K. E.; Kirschner, D. A. Structural analysis of Alzheimer's β (1-40) amyloid: protofilament assembly of tubular fibrils. *Biophys. J.* **1998**, *74*, 537-545.

433. Lansbury, P. T., Jr Evolution of amyloid: what normal protein folding may tell us about fibrillogenesis and disease. *Proc. Natl. Acad. Sci. U. S. A.* **1999**, *96*, 3342-3344.
434. Terry, R. D.; Masliah, E.; Salmon, D. P.; Butters, N.; DeTeresa, R.; Hill, R.; Hansen, L. A.; Katzman, R. Physical basis of cognitive alterations in Alzheimer's disease: synapse loss is the major correlate of cognitive impairment. *Ann. Neurol.* **1991**, *30*, 572-580.
435. Muller-Hill, B.; Beyreuther, K. Molecular biology of Alzheimer's disease. *Annu. Rev. Biochem.* **1989**, *58*, 287-307.
436. Dickson, D. W.; Crystal, H. A.; Bevona, C.; Honer, W.; Vincent, I.; Davies, P. Correlations of synaptic and pathological markers with cognition of the elderly. *Neurobiol. Aging* **1995**, *16*, 285-98; discussion 298-304.
437. Wang, H. Y.; D'Andrea, M. R.; Nagele, R. G. Cerebellar diffuse amyloid plaques are derived from dendritic A β_{42} accumulations in Purkinje cells. *Neurobiol. Aging* **2002**, *23*, 213-223.
438. Armstrong, R. A.; Cairns, N. J.; Lantos, P. L. Spatial distribution of diffuse, primitive, and classic amyloid- β deposits and blood vessels in the upper laminae of the frontal cortex in Alzheimer disease. *Alzheimer Dis. Assoc. Disord.* **1998**, *12*, 378-383.
439. Necula, M.; Breydo, L.; Milton, S.; Kaye, R.; van der Veer, W. E.; Tone, P.; Glabe, C. G. Methylene blue inhibits amyloid A β oligomerization by promoting fibrillization. *Biochemistry* **2007**, *46*, 8850-8860.
440. Necula, M.; Kaye, R.; Milton, S.; Glabe, C. G. Small molecule inhibitors of aggregation indicate that amyloid β oligomerization and fibrillization pathways are independent and distinct. *J. Biol. Chem.* **2007**, *282*, 10311-10324.
441. Jarrett, J. T.; Lansbury, P. T., Jr Amyloid fibril formation requires a chemically discriminating nucleation event: studies of an amyloidogenic sequence from the bacterial protein OsmB. *Biochemistry* **1992**, *31*, 12345-12352.
442. Lomakin, A.; Chung, D. S.; Benedek, G. B.; Kirschner, D. A.; Teplow, D. B. On the nucleation and growth of amyloid β -protein fibrils: detection of nuclei and quantitation of rate constants. *Proc. Natl. Acad. Sci. U. S. A.* **1996**, *93*, 1125-1129.
443. Lomakin, A.; Teplow, D. B.; Kirschner, D. A.; Benedek, G. B. Kinetic theory of fibrillogenesis of amyloid β -protein. *Proc. Natl. Acad. Sci. U. S. A.* **1997**, *94*, 7942-7947.
444. Wogulis, M.; Wright, S.; Cunningham, D.; Chilcote, T.; Powell, K.; Rydel, R. E. Nucleation-dependent polymerization is an essential component of amyloid-mediated neuronal cell death. *J. Neurosci.* **2005**, *25*, 1071-1080.

445. Naiki, H.; Nagai, Y. Molecular Pathogenesis of Protein Misfolding Diseases: Pathological Molecular Environments versus Quality Control Systems against Misfolded Proteins. *J. Biochem.* **2009**.
446. Jarrett, J. T.; Costa, P. R.; Griffin, R. G.; Lansbury, P. T., Jr. Models of the β -Protein C-Terminus: Differences in Amyloid Structure May Lead to Segregation of "Long" and "Short" Fibrils. *J. Am. Chem. Soc.* **1994**, *116*, 9741-9742.
447. Naiki, H.; Nakakuki, K. First-order kinetic model of Alzheimer's β -amyloid fibril extension in vitro. *Lab. Invest.* **1996**, *74*, 374-383.
448. Morinaga, A.; Hasegawa, K.; Nomura, R.; Ookoshi, T.; Ozawa, D.; Goto, Y.; Yamada, M.; Naiki, H. Critical role of interfaces and agitation on the nucleation of A β amyloid fibrils at low concentrations of A β monomers. *Biochim. Biophys. Acta* **2010**, *1804*, 986-995.
449. Cannon, M. J.; Williams, A. D.; Wetzel, R.; Myszka, D. G. Kinetic analysis of β -amyloid fibril elongation. *Anal. Biochem.* **2004**, *328*, 67-75.
450. Esler, W. P.; Stimson, E. R.; Jennings, J. M.; Vinters, H. V.; Ghilardi, J. R.; Lee, J. P.; Mantyh, P. W.; Maggio, J. E. Alzheimer's disease amyloid propagation by a template-dependent dock-lock mechanism. *Biochemistry* **2000**, *39*, 6288-6295.
451. Hasegawa, K.; Ono, K.; Yamada, M.; Naiki, H. Kinetic modeling and determination of reaction constants of Alzheimer's β -amyloid fibril extension and dissociation using surface plasmon resonance. *Biochemistry* **2002**, *41*, 13489-13498.
452. Jarrett, J. T.; Berger, E. P.; Lansbury, P. T., Jr. The carboxy terminus of the β amyloid protein is critical for the seeding of amyloid formation: implications for the pathogenesis of Alzheimer's disease. *Biochemistry* **1993**, *32*, 4693-4697.
453. Hasegawa, K.; Yamaguchi, I.; Omata, S.; Gejyo, F.; Naiki, H. Interaction between A β (1-42) and A β (1-40) in Alzheimer's β -amyloid fibril formation in vitro. *Biochemistry* **1999**, *38*, 15514-15521.
454. Huang, T. H.; Yang, D. S.; Fraser, P. E.; Chakrabartty, A. Alternate aggregation pathways of the Alzheimer β -amyloid peptide. An in vitro model of preamyloid. *J. Biol. Chem.* **2000**, *275*, 36436-36440.
455. Yan, Y.; Wang, C. A β 40 Protects Non-toxic A β 42 Monomer from Aggregation. *Journal of Molecular Biology* **2007/6/15**, *369*, 909-916.
456. Wood, S. J.; Maleeff, B.; Hart, T.; Wetzel, R. Physical, morphological and functional differences between pH 5.8 and 7.4 aggregates of the Alzheimer's amyloid peptide A β . *J. Mol. Biol.* **1996**, *256*, 870-877.

457. Klug, G. M.; Losic, D.; Subasinghe, S. S.; Aguilar, M. I.; Martin, L. L.; Small, D. H. β -amyloid protein oligomers induced by metal ions and acid pH are distinct from those generated by slow spontaneous ageing at neutral pH. *Eur. J. Biochem.* **2003**, *270*, 4282-4293.
458. Yang, X. H.; Huang, H. C.; Chen, L.; Xu, W.; Jiang, Z. F. Coordinating to three histidine residues: Cu(II) promotes oligomeric and fibrillar amyloid- β peptide to precipitate in a non- β aggregation manner. *J. Alzheimers Dis.* **2009**, *18*, 799-810.
459. Yanagisawa, K.; Odaka, A.; Suzuki, N.; Ihara, Y. GM1 ganglioside-bound amyloid β -protein (A β): a possible form of preamyloid in Alzheimer's disease. *Nat. Med.* **1995**, *1*, 1062-1066.
460. Choo-Smith, L. P.; Surewicz, W. K. The interaction between Alzheimer amyloid β (1-40) peptide and ganglioside GM1-containing membranes. *FEBS Lett.* **1997**, *402*, 95-98.
461. Choo-Smith, L. P.; Garzon-Rodriguez, W.; Glabe, C. G.; Surewicz, W. K. Acceleration of amyloid fibril formation by specific binding of A β -(1-40) peptide to ganglioside-containing membrane vesicles. *J. Biol. Chem.* **1997**, *272*, 22987-22990.
462. Kakio, A.; Nishimoto, S. I.; Yanagisawa, K.; Kozutsumi, Y.; Matsuzaki, K. Cholesterol-dependent formation of GM1 ganglioside-bound amyloid β -protein, an endogenous seed for Alzheimer amyloid. *J. Biol. Chem.* **2001**, *276*, 24985-24990.
463. Yamamoto, N.; Matsubara, T.; Sato, T.; Yanagisawa, K. Age-dependent high-density clustering of GM1 ganglioside at presynaptic neuritic terminals promotes amyloid β -protein fibrillogenesis. *Biochim. Biophys. Acta* **2008**, *1778*, 2717-2726.
464. Ikeda, K.; Yamaguchi, T.; Fukunaga, S.; Hoshino, M.; Matsuzaki, K. Mechanism of amyloid β -protein aggregation mediated by GM1 ganglioside clusters. *Biochemistry* **2011**, *50*, 6433-6440.
465. Fukunaga, S.; Ueno, H.; Yamaguchi, T.; Yano, Y.; Hoshino, M.; Matsuzaki, K. GM1 cluster mediates formation of toxic A β fibrils by providing hydrophobic environments. *Biochemistry* **2012**, *51*, 8125-8131.
466. Yamamoto, N.; Fukata, Y.; Fukata, M.; Yanagisawa, K. GM1-ganglioside-induced A β assembly on synaptic membranes of cultured neurons. *Biochim. Biophys. Acta* **2007**, *1768*, 1128-1137.
467. Mochizuki, A.; Tamaoka, A.; Shimohata, A.; Komatsuzaki, Y.; Shoji, S. A β 42-positive non-pyramidal neurons around amyloid plaques in Alzheimer's disease. *Lancet* **2000**, *355*, 42-43.
468. Wilson, C. A.; Doms, R. W.; Lee, V. M. Intracellular APP processing and A β production in Alzheimer disease. *J. Neuropathol. Exp. Neurol.* **1999**, *58*, 787-794.

469. Iwatsubo, T.; Odaka, A.; Suzuki, N.; Mizusawa, H.; Nukina, N.; Ihara, Y. Visualization of A β 42(43) and A β 40 in senile plaques with end-specific A β monoclonals: evidence that an initially deposited species is A β 42(43). *Neuron* **1994**, *13*, 45-53.
470. Rogers, J.; Morrison, J. H. Quantitative morphology and regional and laminar distributions of senile plaques in Alzheimer's disease. *J. Neurosci.* **1985**, *5*, 2801-2808.
471. Pike, C. J.; Cummings, B. J.; Cotman, C. W. Early association of reactive astrocytes with senile plaques in Alzheimer's disease. *Exp. Neurol.* **1995**, *132*, 172-179.
472. Akiyama, H.; Barger, S.; Barnum, S.; Bradt, B.; Bauer, J.; Cole, G. M.; Cooper, N. R.; Eikelenboom, P.; Emmerling, M.; Fiebich, B. L.; Finch, C. E.; Frautschy, S.; Griffin, W. S.; Hampel, H.; Hull, M.; Landreth, G.; Lue, L.; Mrak, R.; Mackenzie, I. R.; McGeer, P. L.; O'Banion, M. K.; Pachter, J.; Pasinetti, G.; Plata-Salman, C.; Rogers, J. T.; Rydel, R.; Shen, Y.; Streit, W.; Strohmeyer, R.; Tooyoma, I.; Van Muiswinkel, F. L.; Veerhuis, R.; Walker, D.; Webster, S.; Wegrzyniak, B.; Wenk, G.; Wyss-Coray, T. Inflammation and Alzheimer's disease. *Neurobiol. Aging* **2000**, *21*, 383-421.
473. Tagliavini, F.; Giaccone, G.; Frangione, B.; Bugiani, O. Preamyloid deposits in the cerebral cortex of patients with Alzheimer's disease and nondemented individuals. *Neurosci. Lett.* **1988**, *93*, 191-196.
474. Yamaguchi, H.; Hirai, S.; Morimatsu, M.; Shoji, M.; Harigaya, Y. Diffuse type of senile plaques in the brains of Alzheimer-type dementia. *Acta Neuropathol.* **1988**, *77*, 113-119.
475. Spillantini, M. G.; Goedert, M.; Jakes, R.; Klug, A. Different configurational states of β -amyloid and their distributions relative to plaques and tangles in Alzheimer disease. *Proc. Natl. Acad. Sci. U. S. A.* **1990**, *87*, 3947-3951.
476. Armstrong, R. A. β -amyloid plaques: stages in life history or independent origin? *Dement. Geriatr. Cogn. Disord.* **1998**, *9*, 227-238.
477. Dickson, D. W. The pathogenesis of senile plaques. *J. Neuropathol. Exp. Neurol.* **1997**, *56*, 321-339.
478. Kuo, Y. M.; Kokjohn, T. A.; Beach, T. G.; Sue, L. I.; Brune, D.; Lopez, J. C.; Kalback, W. M.; Abramowski, D.; Sturchler-Pierrat, C.; Staufenbiel, M.; Roher, A. E. Comparative analysis of amyloid- β chemical structure and amyloid plaque morphology of transgenic mouse and Alzheimer's disease brains. *J. Biol. Chem.* **2001**, *276*, 12991-12998.
479. Veerhuis, R.; Van Breemen, M. J.; Hoozemans, J. M.; Morbin, M.; Ouladhadj, J.; Tagliavini, F.; Eikelenboom, P. Amyloid β plaque-associated proteins C1q and SAP enhance the A β ₁₋₄₂ peptide-induced cytokine secretion by adult human microglia in vitro. *Acta Neuropathol.* **2003**, *105*, 135-144.

480. Selkoe, D. J. Alzheimer's disease: genes, proteins, and therapy. *Physiol. Rev.* **2001**, *81*, 741-766.
481. Burns, M. P.; Noble, W. J.; Olm, V.; Gaynor, K.; Casey, E.; LaFrancois, J.; Wang, L.; Duff, K. Co-localization of cholesterol, apolipoprotein E and fibrillar A β in amyloid plaques. *Brain Res. Mol. Brain Res.* **2003**, *110*, 119-125.
482. Bronfman, F. C.; Garrido, J.; Alvarez, A.; Morgan, C.; Inestrosa, N. C. Laminin inhibits amyloid- β -peptide fibrillation. *Neurosci. Lett.* **1996**, *218*, 201-203.
483. Glenner, G. G.; Wong, C. W.; Quaranta, V.; Eanes, E. D. The amyloid deposits in Alzheimer's disease: their nature and pathogenesis. *Appl. Pathol.* **1984**, *2*, 357-369.
484. Haass, C.; Schlossmacher, M. G.; Hung, A. Y.; Vigo-Pelfrey, C.; Mellon, A.; Ostaszewski, B. L.; Lieberburg, I.; Koo, E. H.; Schenk, D.; Teplow, D. B. Amyloid β -peptide is produced by cultured cells during normal metabolism. *Nature* **1992**, *359*, 322-325.
485. Grundke-Iqbal, I.; Iqbal, K.; George, L.; Tung, Y. C.; Kim, K. S.; Wisniewski, H. M. Amyloid protein and neurofibrillary tangles coexist in the same neuron in Alzheimer disease. *Proc. Natl. Acad. Sci. U. S. A.* **1989**, *86*, 2853-2857.
486. Gouras, G. K.; Tsai, J.; Naslund, J.; Vincent, B.; Edgar, M.; Checler, F.; Greenfield, J. P.; Haroutunian, V.; Buxbaum, J. D.; Xu, H.; Greengard, P.; Relkin, N. R. Intraneuronal A β 42 accumulation in human brain. *Am. J. Pathol.* **2000**, *156*, 15-20.
487. D'Andrea, M. R.; Nagele, R. G.; Wang, H. Y.; Peterson, P. A.; Lee, D. H. Evidence that neurones accumulating amyloid can undergo lysis to form amyloid plaques in Alzheimer's disease. *Histopathology* **2001**, *38*, 120-134.
488. Nagele, R. G.; D'Andrea, M. R.; Anderson, W. J.; Wang, H. Y. Intracellular accumulation of β -amyloid₁₋₄₂ in neurons is facilitated by the α 7 nicotinic acetylcholine receptor in Alzheimer's disease. *Neuroscience* **2002**, *110*, 199-211.
489. Lee, S. J.; Liyanage, U.; Bickel, P. E.; Xia, W.; Lansbury, P. T., Jr; Kosik, K. S. A detergent-insoluble membrane compartment contains A β in vivo. *Nat. Med.* **1998**, *4*, 730-734.
490. Strandberg, Y.; Gray, C.; Vuocolo, T.; Donaldson, L.; Broadway, M.; Tellam, R. Lipopolysaccharide and lipoteichoic acid induce different innate immune responses in bovine mammary epithelial cells. *Cytokine* **2005**, *31*, 72-86.
491. Xu, H.; Sweeney, D.; Wang, R.; Thinakaran, G.; Lo, A. C.; Sisodia, S. S.; Greengard, P.; Gandy, S. Generation of Alzheimer β -amyloid protein in the trans-Golgi network in the apparent absence of vesicle formation. *Proc. Natl. Acad. Sci. U. S. A.* **1997**, *94*, 3748-3752.

492. Chui, D. H.; Dobo, E.; Makifuchi, T.; Akiyama, H.; Kawakatsu, S.; Petit, A.; Checler, F.; Araki, W.; Takahashi, K.; Tabira, T. Apoptotic neurons in Alzheimer's disease frequently show intracellular A β 42 labeling. *J. Alzheimers Dis.* **2001**, *3*, 231-239.
493. Busciglio, J.; Gabuzda, D. H.; Matsudaira, P.; Yankner, B. A. Generation of β -amyloid in the secretory pathway in neuronal and nonneuronal cells. *Proc. Natl. Acad. Sci. U. S. A.* **1993**, *90*, 2092-2096.
494. LeBlanc, A. C.; Xue, R.; Gambetti, P. Amyloid precursor protein metabolism in primary cell cultures of neurons, astrocytes, and microglia. *J. Neurochem.* **1996**, *66*, 2300-2310.
495. LeBlanc, A. C.; Papadopoulos, M.; Belair, C.; Chu, W.; Crosato, M.; Powell, J.; Goodyer, C. G. Processing of amyloid precursor protein in human primary neuron and astrocyte cultures. *J. Neurochem.* **1997**, *68*, 1183-1190.
496. Echeverria, V.; Ducatzenzeiler, A.; Alhonen, L.; Janne, J.; Grant, S. M.; Wandosell, F.; Muro, A.; Baralle, F.; Li, H.; Duff, K.; Szyf, M.; Cuelllo, A. C. Rat transgenic models with a phenotype of intracellular A β accumulation in hippocampus and cortex. *J. Alzheimers Dis.* **2004**, *6*, 209-219.
497. Oddo, S.; Caccamo, A.; Smith, I. F.; Green, K. N.; LaFerla, F. M. A dynamic relationship between intracellular and extracellular pools of A β . *Am. J. Pathol.* **2006**, *168*, 184-194.
498. Masliah, E.; Sisk, A.; Mallory, M.; Mucke, L.; Schenk, D.; Games, D. Comparison of neurodegenerative pathology in transgenic mice overexpressing V717F β -amyloid precursor protein and Alzheimer's disease. *J. Neurosci.* **1996**, *16*, 5795-5811.
499. Hsia, A. Y.; Masliah, E.; McConlogue, L.; Yu, G. Q.; Tatsuno, G.; Hu, K.; Kholodenko, D.; Malenka, R. C.; Nicoll, R. A.; Mucke, L. Plaque-independent disruption of neural circuits in Alzheimer's disease mouse models. *Proc. Natl. Acad. Sci. U. S. A.* **1999**, *96*, 3228-3233.
500. Bayer, T. A.; Breyhan, H.; Duan, K.; Rettig, J.; Wirths, O. Intraneuronal β -amyloid is a major risk factor--novel evidence from the APP/PS1KI mouse model. *Neurodegener Dis.* **2008**, *5*, 140-142.
501. Takahashi, R. H.; Milner, T. A.; Li, F.; Nam, E. E.; Edgar, M. A.; Yamaguchi, H.; Beal, M. F.; Xu, H.; Greengard, P.; Gouras, G. K. Intraneuronal Alzheimer A β 42 accumulates in multivesicular bodies and is associated with synaptic pathology. *Am. J. Pathol.* **2002**, *161*, 1869-1879.
502. Takahashi, R. H.; Almeida, C. G.; Kearney, P. F.; Yu, F.; Lin, M. T.; Milner, T. A.; Gouras, G. K. Oligomerization of Alzheimer's β -amyloid within processes and synapses of cultured neurons and brain. *J. Neurosci.* **2004**, *24*, 3592-3599.

503. LaFerla, F. M.; Troncoso, J. C.; Strickland, D. K.; Kawas, C. H.; Jay, G. Neuronal cell death in Alzheimer's disease correlates with apoE uptake and intracellular A β stabilization. *J. Clin. Invest.* **1997**, *100*, 310-320.
504. Cook, D. G.; Forman, M. S.; Sung, J. C.; Leight, S.; Kolson, D. L.; Iwatsubo, T.; Lee, V. M.; Doms, R. W. Alzheimer's A β (1-42) is generated in the endoplasmic reticulum/intermediate compartment of NT2N cells. *Nat. Med.* **1997**, *3*, 1021-1023.
505. Skovronsky, D. M.; Moore, D. B.; Milla, M. E.; Doms, R. W.; Lee, V. M. Protein kinase C-dependent α -secretase competes with β -secretase for cleavage of amyloid- β precursor protein in the trans-golgi network. *J. Biol. Chem.* **2000**, *275*, 2568-2575.
506. Perez, R. G.; Soriano, S.; Hayes, J. D.; Ostaszewski, B.; Xia, W.; Selkoe, D. J.; Chen, X.; Stokin, G. B.; Koo, E. H. Mutagenesis identifies new signals for β -amyloid precursor protein endocytosis, turnover, and the generation of secreted fragments, including A β 42. *J. Biol. Chem.* **1999**, *274*, 18851-18856.
507. Burdick, D.; Kosmoski, J.; Knauer, M. F.; Glabe, C. G. Preferential adsorption, internalization and resistance to degradation of the major isoform of the Alzheimer's amyloid peptide, A β 1-42, in differentiated PC12 cells. *Brain Res.* **1997**, *746*, 275-284.
508. Skovronsky, D. M.; Zhang, B.; Kung, M. P.; Kung, H. F.; Trojanowski, J. Q.; Lee, V. M. In vivo detection of amyloid plaques in a mouse model of Alzheimer's disease. *Proc. Natl. Acad. Sci. U. S. A.* **2000**, *97*, 7609-7614.
509. Knauer, M. F.; Soreghan, B.; Burdick, D.; Kosmoski, J.; Glabe, C. G. Intracellular accumulation and resistance to degradation of the Alzheimer amyloid A4/ β protein. *Proc. Natl. Acad. Sci. U. S. A.* **1992**, *89*, 7437-7441.
510. Bahr, B. A.; Hoffman, K. B.; Yang, A. J.; Hess, U. S.; Glabe, C. G.; Lynch, G. Amyloid β protein is internalized selectively by hippocampal field CA1 and causes neurons to accumulate amyloidogenic carboxyterminal fragments of the amyloid precursor protein. *J. Comp. Neurol.* **1998**, *397*, 139-147.
511. Glabe, C. Intracellular mechanisms of amyloid accumulation and pathogenesis in Alzheimer's disease. *J. Mol. Neurosci.* **2001**, *17*, 137-145.
512. Oddo, S.; Billings, L.; Kesslak, J. P.; Cribbs, D. H.; LaFerla, F. M. A β Immunotherapy Leads to Clearance of Early, but Not Late, Hyperphosphorylated Tau Aggregates via the Proteasome. *Neuron* **2004**, *43*, 321-332.
513. Reddy, P. H. Abnormal tau, mitochondrial dysfunction, impaired axonal transport of mitochondria, and synaptic deprivation in Alzheimer's disease. *Brain Res.* **2011**, *1415*, 136-148.

514. Manczak, M.; Reddy, P. H. Abnormal Interaction of Oligomeric Amyloid- β with Phosphorylated Tau: Implications to Synaptic Dysfunction and Neuronal Damage. *J. Alzheimers Dis.* **2013**, *36*, 285-295.
515. Takahashi, R. H.; Capetillo-Zarate, E.; Lin, M. T.; Milner, T. A.; Gouras, G. K. Co-occurrence of Alzheimer's disease ss-amyloid and tau pathologies at synapses. *Neurobiol. Aging* **2010**, *31*, 1145-1152.
516. Caspersen, C.; Wang, N.; Yao, J.; Sosunov, A.; Chen, X.; Lustbader, J. W.; Xu, H. W.; Stern, D.; McKhann, G.; Yan, S. D. Mitochondrial A β : a potential focal point for neuronal metabolic dysfunction in Alzheimer's disease. *FASEB J.* **2005**, *19*, 2040-2041.
517. Suh, Y. H.; Checler, F. Amyloid precursor protein, presenilins, and α -synuclein: molecular pathogenesis and pharmacological applications in Alzheimer's disease. *Pharmacol. Rev.* **2002**, *54*, 469-525.
518. Oda, T.; Wals, P.; Osterburg, H. H.; Johnson, S. A.; Pasinetti, G. M.; Morgan, T. E.; Rozovsky, I.; Stine, W. B.; Snyder, S. W.; Holzman, T. F. Clusterin (apoJ) alters the aggregation of amyloid β -peptide (A β ₁₋₄₂) and forms slowly sedimenting A β complexes that cause oxidative stress. *Exp. Neurol.* **1995**, *136*, 22-31.
519. Serpell, L. C. Alzheimer's amyloid fibrils: structure and assembly. *Biochim. Biophys. Acta* **2000**, *1502*, 16-30.
520. Stine, W. B., Jr; Dahlgren, K. N.; Krafft, G. A.; LaDu, M. J. In vitro characterization of conditions for amyloid- β peptide oligomerization and fibrillogenesis. *J. Biol. Chem.* **2003**, *278*, 11612-11622.
521. Okada, T.; Ikeda, K.; Wakabayashi, M.; Ogawa, M.; Matsuzaki, K. Formation of Toxic A β (1-40) Fibrils on GM1 Ganglioside-Containing Membranes Mimicking Lipid Rafts: Polymorphisms in A β (1-40) Fibrils. *J. Mol. Biol.* **2008**, *382*, 1066-1074.
522. Crowther, R. A.; Olesen, O. F.; Smith, M. J.; Jakes, R.; Goedert, M. Assembly of Alzheimer-like filaments from full-length tau protein. *FEBS Lett.* **1994**, *337*, 135-138.
523. Couchie, D.; Mavilia, C.; Georgieff, I. S.; Liem, R. K.; Shelanski, M. L.; Nunez, J. Primary structure of high molecular weight tau present in the peripheral nervous system. *Proc. Natl. Acad. Sci. U. S. A.* **1992**, *89*, 4378-4381.
524. Hasegawa, M.; Morishima-Kawashima, M.; Takio, K.; Suzuki, M.; Titani, K.; Ihara, Y. Protein sequence and mass spectrometric analyses of tau in the Alzheimer's disease brain. *J. Biol. Chem.* **1992**, *267*, 17047-17054.

525. Geula, C.; Wu, C. K.; Saroff, D.; Lorenzo, A.; Yuan, M.; Yankner, B. A. Aging renders the brain vulnerable to amyloid β -protein neurotoxicity. *Nat. Med.* **1998**, *4*, 827-831.
526. Breuzard, G.; Hubert, P.; Nouar, R.; De Bessa, T.; Devred, F.; Barbier, P.; Sturgis, J. N.; Peyrot, V. Molecular mechanisms of Tau binding to microtubules and its role in microtubule dynamics in live cells. *J. Cell. Sci.* **2013**, *126*, 2810-2819.
527. Siegel, G. J.; Chauhan, N.; Karczmar, A. G. In *Links Between Amyloid and Tau Biology in Alzheimer's Disease and Their Cholinergic Aspects*; Karczmar, A. G., Ed.; Exploring the Vertebrate Central Cholinergic Nervous System; Springer Science+Business Media, LLC: New York, NY, **2007**; pp. 597-656.
528. Karp, G. *Cell and molecular biology: concepts and experiments*; J. Wiley: New York, **2002**; , pp 785.
529. Billingsley, M. L.; Kincaid, R. L. Regulated phosphorylation and dephosphorylation of tau protein: effects on microtubule interaction, intracellular trafficking and neurodegeneration. *Biochem. J.* **1997**, *323 (Pt 3)*, 577-591.
530. Alonso, A. D.; Grundke-Iqbal, I.; Barra, H. S.; Iqbal, K. Abnormal phosphorylation of tau and the mechanism of Alzheimer neurofibrillary degeneration: sequestration of microtubule-associated proteins 1 and 2 and the disassembly of microtubules by the abnormal tau. *Proc. Natl. Acad. Sci. U. S. A.* **1997**, *94*, 298-303.
531. Alonso, A. D.; Di Clerico, J.; Li, B.; Corbo, C. P.; Alaniz, M. E.; Grundke-Iqbal, I.; Iqbal, K. Phosphorylation of tau at Thr212, Thr231, and Ser262 combined causes neurodegeneration. *J. Biol. Chem.* **2010**, *285*, 30851-30860.
532. Avila, J.; Santa-Maria, I.; Perez, M.; Hernandez, F.; Moreno, F. Tau phosphorylation, aggregation, and cell toxicity. *J. Biomed. Biotechnol.* **2006**, *2006*, 74539.
533. Avila, J.; Lim, F.; Moreno, F.; Belmonte, C.; Cuello, A. C. Tau function and dysfunction in neurons: its role in neurodegenerative disorders. *Mol. Neurobiol.* **2002**, *25*, 213-231.
534. Ballatore, C.; Lee, V. M.; Trojanowski, J. Q. Tau-mediated neurodegeneration in Alzheimer's disease and related disorders. *Nat. Rev. Neurosci.* **2007**, *8*, 663-672.
535. Hernandez, F.; Avila, J. Tau aggregates and tau pathology. *J. Alzheimers Dis.* **2008**, *14*, 449-452.
536. O'Brien, J.; Ames, D.; Burns, A., Eds.; In *Dementia*; Arnold: London, **2000**; pp. 940.
537. Perl, D. P. Neuropathology of Alzheimer's disease and related disorders. *Neurol. Clin.* **2000**, *18*, 847-864.

538. Hill, J. M.; Steiner, I.; Matthews, K. E.; Trahan, S. G.; Foster, T. P.; Ball, M. J. Statins lower the risk of developing Alzheimer's disease by limiting lipid raft endocytosis and decreasing the neuronal spread of Herpes simplex virus type 1. *Med. Hypotheses* **2005**, *64*, 53-58.
539. Halle, A.; Hornung, V.; Petzold, G. C.; Stewart, C. R.; Monks, B. G.; Reinheckel, T.; Fitzgerald, K. A.; Latz, E.; Moore, K. J.; Golenbock, D. T. The NALP3 inflammasome is involved in the innate immune response to amyloid- β . *Nat. Immunol.* **2008**, *9*, 857-865.
540. Udan, M. L.; Ajit, D.; Crouse, N. R.; Nichols, M. R. Toll-like receptors 2 and 4 mediate A β (1-42) activation of the innate immune response in a human monocytic cell line. *J. Neurochem.* **2008**, *104*, 524-533.
541. Gasque, P.; Dean, Y. D.; McGreal, E. P.; VanBeek, J.; Morgan, B. P. Complement components of the innate immune system in health and disease in the CNS. *Immunopharmacology* **2000**, *49*, 171-186.
542. McGeer, P. L.; McGeer, E. G. Inflammation, autotoxicity and Alzheimer disease. *Neurobiol. Aging* **2001**, *22*, 799-809.
543. Bsibsi, M.; Persoon-Deen, C.; Verwer, R. W.; Meeuwssen, S.; Ravid, R.; Van Noort, J. M. Toll-like receptor 3 on adult human astrocytes triggers production of neuroprotective mediators. *Glia* **2006**, *53*, 688-695.
544. Husemann, J.; Loike, J. D.; Anankov, R.; Febbraio, M.; Silverstein, S. C. Scavenger receptors in neurobiology and neuropathology: their role on microglia and other cells of the nervous system. *Glia* **2002**, *40*, 195-205.
545. Kielian, T.; Mayes, P.; Kielian, M. Characterization of microglial responses to *Staphylococcus aureus*: effects on cytokine, costimulatory molecule, and Toll-like receptor expression. *J. Neuroimmunol.* **2002**, *130*, 86-99.
546. Gaskin, F.; Finley, J.; Fang, Q.; Xu, S.; Fu, S. M. Human antibodies reactive with β -amyloid protein in Alzheimer's disease. *J. Exp. Med.* **1993**, *177*, 1181-1186.
547. Hyman, B. T.; Smith, C.; Buldyrev, I.; Whelan, C.; Brown, H.; Tang, M. X.; Mayeux, R. Autoantibodies to amyloid- β and Alzheimer's disease. *Ann. Neurol.* **2001**, *49*, 808-810.
548. Hershey, C. O.; Hershey, L. A.; Varnes, A.; Vibhakar, S. D.; Lavin, P.; Strain, W. H. Cerebrospinal fluid trace element content in dementia: clinical, radiologic, and pathologic correlations. *Neurology* **1983**, *33*, 1350-1353.
549. Ehmann, W. D.; Markesbery, W. R.; Alauddin, M.; Hossain, T. I.; Brubaker, E. H. Brain trace elements in Alzheimer's disease. *Neurotoxicology* **1986**, *7*, 195-206.

550. Thompson, C. M.; Markesbery, W. R.; Ehmann, W. D.; Mao, Y. X.; Vance, D. E. Regional brain trace-element studies in Alzheimer's disease. *Neurotoxicology* **1988**, *9*, 1-7.
551. Vance, D. E.; Ehmann, W. D.; Markesbery, W. R. A search for longitudinal variations in trace element levels in nails of Alzheimer's disease patients. *Biol. Trace Elem. Res.* **1990**, *26-27*, 461-470.
552. Basun, H.; Forssell, L. G.; Wetterberg, L.; Winblad, B. Metals and trace elements in plasma and cerebrospinal fluid in normal aging and Alzheimer's disease. *J. Neural Transm. Park. Dis. Dement. Sect.* **1991**, *3*, 231-258.
553. Samudralwar, D. L.; Diprete, C. C.; Ni, B. F.; Ehmann, W. D.; Markesbery, W. R. Elemental imbalances in the olfactory pathway in Alzheimer's disease. *J. Neurol. Sci.* **1995**, *130*, 139-145.
554. Cornett, C. R.; Markesbery, W. R.; Ehmann, W. D. Imbalances of trace elements related to oxidative damage in Alzheimer's disease brain. *Neurotoxicology* **1998**, *19*, 339-345.
555. Bush, A. I. Metals and neuroscience. *Curr. Opin. Chem. Biol.* **2000**, *4*, 184-191.
556. Hou, L.; Zagorski, M. G. NMR reveals anomalous copper(II) binding to the amyloid A β peptide of Alzheimer's disease. *J. Am. Chem. Soc.* **2006**, *128*, 9260-9261.
557. Atwood, C. S.; Scarpa, R. C.; Huang, X.; Moir, R. D.; Jones, W. D.; Fairlie, D. P.; Tanzi, R. E.; Bush, A. I. Characterization of copper interactions with Alzheimer amyloid β peptides: identification of an attomolar-affinity copper binding site on amyloid β 1-42. *J. Neurochem.* **2000**, *75*, 1219-1233.
558. Syme, C. D.; Viles, J. H. Solution ^1H NMR investigation of Zn^{2+} and Cd^{2+} binding to amyloid- β peptide (A β) of Alzheimer's disease. *Biochim. Biophys. Acta* **2006**, *1764*, 246-256.
559. Danielsson, J.; Pierattelli, R.; Banci, L.; Graslund, A. High-resolution NMR studies of the zinc-binding site of the Alzheimer's amyloid β -peptide. *FEBS J.* **2007**, *274*, 46-59.
560. Yang, D. S.; McLaurin, J.; Qin, K.; Westaway, D.; Fraser, P. E. Examining the zinc binding site of the amyloid- β peptide. *Eur. J. Biochem.* **2000**, *267*, 6692-6698.
561. Bin, Y.; Chen, S.; Xiang, J. pH-dependent kinetics of copper ions binding to amyloid- β peptide. *J. Inorg. Biochem.* **2013**, *119*, 21-27.
562. Strozyk, D.; Launer, L. J.; Adlard, P. A.; Cherny, R. A.; Tsatsanis, A.; Volitakis, I.; Blennow, K.; Petrovitch, H.; White, L. R.; Bush, A. I. Zinc and copper modulate Alzheimer A β levels in human cerebrospinal fluid. *Neurobiol. Aging* **2009**, *30*, 1069-1077.

563. Curtain, C. C.; Ali, F.; Volitakis, I.; Cherny, R. A.; Norton, R. S.; Beyreuther, K.; Barrow, C. J.; Masters, C. L.; Bush, A. I.; Barnham, K. J. Alzheimer's disease amyloid- β binds copper and zinc to generate an allosterically ordered membrane-penetrating structure containing superoxide dismutase-like subunits. *J. Biol. Chem.* **2001**, *276*, 20466-20473.
564. Bush, A. I. The metallobiology of Alzheimer's disease. *Trends Neurosci.* **2003**, *26*, 207-214.
565. Crapper, D. R.; Krishnan, S. S.; Dalton, A. J. Brain aluminum distribution in Alzheimer's disease and experimental neurofibrillary degeneration. *Science* **1973**, *180*, 511-513.
566. Crapper, D. R.; Krishnan, S. S.; Quittkat, S. Aluminium, neurofibrillary degeneration and Alzheimer's disease. *Brain* **1976**, *99*, 67-80.
567. Sparks, D. L.; Friedland, R.; Petanceska, S.; Schreurs, B. G.; Shi, J.; Perry, G.; Smith, M. A.; Sharma, A.; Derosa, S.; Ziolkowski, C.; Stankovic, G. Trace copper levels in the drinking water, but not zinc or aluminum influence CNS Alzheimer-like pathology. *J. Nutr. Health Aging* **2006**, *10*, 247-254.
568. Zatta, P. Aluminum and Alzheimer's disease: a Vexata Questio between uncertain data and a lot of imagination. *J. Alzheimers Dis.* **2006**, *10*, 33-37.
569. Drago, D.; Bettella, M.; Bolognin, S.; Cendron, L.; Scancar, J.; Milacic, R.; Ricchelli, F.; Casini, A.; Messori, L.; Tognon, G.; Zatta, P. Potential pathogenic role of β -amyloid₁₋₄₂-aluminum complex in Alzheimer's disease. *Int. J. Biochem. Cell Biol.* **2008**, *40*, 731-746.
570. Banks, W. A.; Niehoff, M. L.; Drago, D.; Zatta, P. Aluminum complexing enhances amyloid β protein penetration of blood-brain barrier. *Brain Res.* **2006**, *1116*, 215-221.
571. Bush, A. I.; Huang, X.; Fairlie, D. P. The possible origin of free radicals from amyloid β peptides in Alzheimer's disease. *Neurobiol. Aging* **1999**, *20*, 335-7; discussion 339-42.
572. Huang, X.; Moir, R. D.; Tanzi, R. E.; Bush, A. I.; Rogers, J. T. Redox-active metals, oxidative stress, and Alzheimer's disease pathology. *Ann. N. Y. Acad. Sci.* **2004**, *1012*, 153-163.
573. Verdier, Y.; Penke, B. Binding sites of amyloid β -peptide in cell plasma membrane and implications for Alzheimer's disease. *Curr. Protein Pept. Sci.* **2004**, *5*, 19-31.
574. Verdier, Y.; Zarandi, M.; Penke, B. Amyloid β -peptide interactions with neuronal and glial cell plasma membrane: binding sites and implications for Alzheimer's disease. *J. Pept. Sci.* **2004**, *10*, 229-248.
575. Shao, H.; Jao, S.; Ma, K.; Zagorski, M. G. Solution structures of micelle-bound amyloid β -(1-40) and β -(1-42) peptides of Alzheimer's disease. *J. Mol. Biol.* **1999**, *285*, 755-773.

576. Kisilevsky, R.; Lemieux, L. J.; Fraser, P. E.; Kong, X.; Hultin, P. G.; Szarek, W. A. Arresting amyloidosis in vivo using small-molecule anionic sulphonates or sulphates: implications for Alzheimer's disease. *Nat. Med.* **1995**, *1*, 143-148.
577. Carter, D. B.; Chou, K. C. A model for structure-dependent binding of Congo red to Alzheimer β -amyloid fibrils. *Neurobiol. Aging* **1998**, *19*, 37-40.
578. Kuner, P.; Bohrmann, B.; Tjernberg, L. O.; Naslund, J.; Huber, G.; Celenk, S.; Gruninger-Leitch, F.; Richards, J. G.; Jakob-Roetne, R.; Kemp, J. A.; Nordstedt, C. Controlling polymerization of β -amyloid and prion-derived peptides with synthetic small molecule ligands. *J. Biol. Chem.* **2000**, *275*, 1673-1678.
579. Talafous, J.; Marcinowski, K. J.; Klopman, G.; Zagorski, M. G. Solution structure of residues 1-28 of the amyloid β -peptide. *Biochemistry* **1994**, *33*, 7788-7796.
580. Salomon, A. R.; Marcinowski, K. J.; Friedland, R. P.; Zagorski, M. G. Nicotine inhibits amyloid formation by the β -peptide. *Biochemistry* **1996**, *35*, 13568-13578.
581. Fonnum, F.; Myhrer, T.; Paulsen, R. E.; Wangen, K.; Oksengard, A. R. Role of glutamate and glutamate receptors in memory function and Alzheimer's disease. *Ann. N. Y. Acad. Sci.* **1995**, *757*, 475-486.
582. Kar, S.; Slowikowski, S. P.; Westaway, D.; Mount, H. T. Interactions between β -amyloid and central cholinergic neurons: implications for Alzheimer's disease. *J. Psychiatry Neurosci.* **2004**, *29*, 427-441.
583. Hasselmo, M. E.; Stern, C. E. Mechanisms underlying working memory for novel information. *Trends Cogn. Sci.* **2006**, *10*, 487-493.
584. Li, S.; Hong, S.; Shepardson, N. E.; Walsh, D. M.; Shankar, G. M.; Selkoe, D. Soluble oligomers of amyloid β protein facilitate hippocampal long-term depression by disrupting neuronal glutamate uptake. *Neuron* **2009**, *62*, 788-801.
585. Courtney, C.; Farrell, D.; Gray, R.; Hills, R.; Lynch, L.; Sellwood, E.; Edwards, S.; Hardyman, W.; Raftery, J.; Crome, P.; Lendon, C.; Shaw, H.; Bentham, P.; AD2000 Collaborative Group Long-term donepezil treatment in 565 patients with Alzheimer's disease (AD2000): randomised double-blind trial. *Lancet* **2004**, *363*, 2105-2115.
586. Vardy, E. R.; Hussain, I.; Hooper, N. M. Emerging therapeutics for Alzheimer's disease. *Expert Rev. Neurother* **2006**, *6*, 695-704.
587. Hardy, J. A.; Higgins, G. A. Alzheimer's disease: the amyloid cascade hypothesis. *Science* **1992**, *256*, 184-185.

588. Golde, T. E.; Dickson, D.; Hutton, M. Filling the gaps in the A β cascade hypothesis of Alzheimer's disease. *Curr. Alzheimer Res.* **2006**, *3*, 421-430.
589. Beckerman, M. In *Alzheimer's Disease; Cellular Signaling in Health and Disease*; Springer US: **2009**; pp. 369-389.
590. De Felice, F. G.; Ferreira, S. T. β -amyloid production, aggregation, and clearance as targets for therapy in Alzheimer's disease. *Cell. Mol. Neurobiol.* **2002**, *22*, 545-563.
591. Skovronsky, D. M.; Lee, V. M.; Trojanowski, J. Q. Neurodegenerative diseases: new concepts of pathogenesis and their therapeutic implications. *Annu. Rev. Pathol.* **2006**, *1*, 151-170.
592. Lee, V. M.; Trojanowski, J. Q. The disordered neuronal cytoskeleton in Alzheimer's disease. *Curr. Opin. Neurobiol.* **1992**, *2*, 653-656.
593. Iqbal, K.; Liu, F.; Gong, C. X.; Alonso Adel, C.; Grundke-Iqbal, I. Mechanisms of tau-induced neurodegeneration. *Acta Neuropathol.* **2009**, *118*, 53-69.
594. Rodríguez-Martín, T.; Cuchillo-Ibáñez, I.; Noble, W.; Nyenya, F.; Anderton, B. H.; Hanger, D. P. Tau phosphorylation affects its axonal transport and degradation. *Neurobiol. Aging* **2013**, *34*, 2146-2157.
595. Kowall, N. W.; Kosik, K. S. Axonal disruption and aberrant localization of tau protein characterize the neuropil pathology of Alzheimer's disease. *Ann. Neurol.* **1987**, *22*, 639-643.
596. Patterson, K. R.; Ward, S. M.; Combs, B.; Voss, K.; Kanaan, N. M.; Morfini, G.; Brady, S. T.; Gamblin, T. C.; Binder, L. I. Heat shock protein 70 prevents both tau aggregation and the inhibitory effects of preexisting tau aggregates on fast axonal transport. *Biochemistry* **2011**, *50*, 10300-10310.
597. Mattson, M. P.; Cheng, B.; Davis, D.; Bryant, K.; Lieberburg, I.; Rydel, R. E. β -Amyloid peptides destabilize calcium homeostasis and render human cortical neurons vulnerable to excitotoxicity. *J. Neurosci.* **1992**, *12*, 376-389.
598. LaFerla, F. M. Calcium dyshomeostasis and intracellular signalling in Alzheimer's disease. *Nat. Rev. Neurosci.* **2002**, *3*, 862-872.
599. Paschen, W. Mechanisms of neuronal cell death: diverse roles of calcium in the various subcellular compartments. *Cell Calcium* **2003**, *34*, 305-310.
600. Bush, A. I.; Tanzi, R. E. Therapeutics for Alzheimer's disease based on the metal hypothesis. *Neurotherapeutics* **2008**, *5*, 421-432.
601. Exley, C. Aluminum and Alzheimer's disease. *J. Alzheimers Dis.* **2001**, *3*, 551-552.

602. Exley, C.; Birchall, J. D. Aluminium and Alzheimer's disease. *Age Ageing* **1993**, *22*, 391-392.
603. Exley, C. Aluminium, tau and Alzheimer's disease. *J. Alzheimers Dis.* **2007**, *12*, 313-5; author reply 317-8.
604. Jaeger, L. B.; Dohgu, S.; Hwang, M. C.; Farr, S. A.; Murphy, M. P.; Fleegal-DeMotta, M. A.; Lynch, J. L.; Robinson, S. M.; Niehoff, M. L.; Johnson, S. N.; Kumar, V. B.; Banks, W. A. Testing the neurovascular hypothesis of Alzheimer's disease: LRP-1 antisense reduces blood-brain barrier clearance, increases brain levels of amyloid- β protein, and impairs cognition. *J. Alzheimers Dis.* **2009**, *17*, 553-570.
605. Robinson, S. R.; Bishop, G. M. A β as a bioflocculant: implications for the amyloid hypothesis of Alzheimer's disease. *Neurobiol. Aging* **2002**, *23*, 1051-1072.
606. Swerdlow, R. H.; Khan, S. M. The Alzheimer's disease mitochondrial cascade hypothesis: an update. *Exp. Neurol.* **2009**, *218*, 308-315.
607. Arispe, N.; Rojas, E.; Pollard, H. B. Alzheimer disease amyloid β protein forms calcium channels in bilayer membranes: blockade by tromethamine and aluminum. *Proc. Natl. Acad. Sci. U. S. A.* **1993**, *90*, 567-571.
608. Pollard, H. B.; Arispe, N.; Rojas, E. Ion channel hypothesis for Alzheimer amyloid peptide neurotoxicity. *Cell. Mol. Neurobiol.* **1995**, *15*, 513-526.
609. Arispe, N.; Pollard, H. B.; Rojas, E. β -Amyloid Ca²⁺-channel hypothesis for neuronal death in Alzheimer disease. *Mol. Cell. Biochem.* **1994**, *140*, 119-125.
610. Shirwany, N. A.; Payette, D.; Xie, J.; Guo, Q. The amyloid β ion channel hypothesis of Alzheimer's disease. *Neuropsychiatr. Dis. Treat.* **2007**, *3*, 597-612.
611. Strandberg, T. E.; Aiello, A. E. Is the microbe-dementia hypothesis finally ready for a treatment trial? *Neurology* **2013**, *80*, 1182-1183.
612. Robinson, S. R.; Dobson, C.; Lyons, J. Challenges and directions for the pathogen hypothesis of Alzheimer's disease. *Neurobiol. Aging* **2004**, *25*, 629-637.
613. Lee, H. G.; Zhu, X.; Nunomura, A.; Perry, G.; Smith, M. A. Amyloid β : the alternate hypothesis. *Curr. Alzheimer Res.* **2006**, *3*, 75-80.
614. Lee, H. G.; Casadesus, G.; Zhu, X.; Takeda, A.; Perry, G.; Smith, M. A. Challenging the amyloid cascade hypothesis: senile plaques and amyloid- β as protective adaptations to Alzheimer disease. *Ann. N. Y. Acad. Sci.* **2004**, *1019*, 1-4.

615. Small, S. A.; Duff, K. Linking A β and Tau in Late-Onset Alzheimer's Disease: A Dual Pathway Hypothesis. *Neuron* **2008**, *60*, 534-542.
616. Ittner, L. M.; Gotz, J. Amyloid- β and tau--a toxic pas de deux in Alzheimer's disease. *Nat. Rev. Neurosci.* **2011**, *12*, 65-72.
617. Li, B.; Chohan, M. O.; Grundke-Iqbal, I.; Iqbal, K. Disruption of microtubule network by Alzheimer abnormally hyperphosphorylated tau. *Acta Neuropathol.* **2007**, *113*, 501-511.
618. Gustke, N.; Trinczek, B.; Biernat, J.; Mandelkow, E. M.; Mandelkow, E. Domains of tau protein and interactions with microtubules. *Biochemistry* **1994**, *33*, 9511-9522.
619. Gustke, N.; Steiner, B.; Mandelkow, E. M.; Biernat, J.; Meyer, H. E.; Goedert, M.; Mandelkow, E. The Alzheimer-like phosphorylation of tau protein reduces microtubule binding and involves Ser-Pro and Thr-Pro motifs. *FEBS Lett.* **1992**, *307*, 199-205.
620. Weingarten, M. D.; Lockwood, A. H.; Hwo, S. Y.; Kirschner, M. W. A protein factor essential for microtubule assembly. *Proc. Natl. Acad. Sci. U. S. A.* **1975**, *72*, 1858-1862.
621. Sloboda, R. D.; Rudolph, S. A.; Rosenbaum, J. L.; Greengard, P. Cyclic AMP-dependent endogenous phosphorylation of a microtubule-associated protein. *Proc. Natl. Acad. Sci. U. S. A.* **1975**, *72*, 177-181.
622. Iqbal, K.; Grundke-Iqbal, I.; Zaidi, T.; Merz, P. A.; Wen, G. Y.; Shaikh, S. S.; Wisniewski, H. M.; Alafuzoff, I.; Winblad, B. Defective brain microtubule assembly in Alzheimer's disease. *Lancet* **1986**, *2*, 421-426.
623. Lindwall, G.; Cole, R. D. Phosphorylation affects the ability of tau protein to promote microtubule assembly. *J. Biol. Chem.* **1984**, *259*, 5301-5305.
624. Goedert, M.; Hasegawa, M.; Jakes, R.; Lawler, S.; Cuenda, A.; Cohen, P. Phosphorylation of microtubule-associated protein tau by stress-activated protein kinases. *FEBS Lett.* **1997**, *409*, 57-62.
625. Chevalier-Larsen, E.; Holzbaur, E. L. F. Axonal transport and neurodegenerative disease. *Biochimica et Biophysica Acta (BBA) - Molecular Basis of Disease* **2006**, *1762*, 1094-1108.
626. Goldstein, L. S. B. In *Axonal Transport and Alzheimer's Disease*; Editor-in-Chief: Larry R. Squire, Ed.; Encyclopedia of Neuroscience; Academic Press: Oxford, 2009; pp. 1189-1194.
627. Alonso, A. C.; Zaidi, T.; Grundke-Iqbal, I.; Iqbal, K. Role of abnormally phosphorylated tau in the breakdown of microtubules in Alzheimer disease. *Proc. Natl. Acad. Sci. U. S. A.* **1994**, *91*, 5562-5566.

628. Alonso, A. C.; Grundke-Iqbal, I.; Iqbal, K. Alzheimer's disease hyperphosphorylated tau sequesters normal tau into tangles of filaments and disassembles microtubules. *Nat. Med.* **1996**, *2*, 783-787.
629. Grundke-Iqbal, I.; Iqbal, K.; Quinlan, M.; Tung, Y. C.; Zaidi, M. S.; Wisniewski, H. M. Microtubule-associated protein tau. A component of Alzheimer paired helical filaments. *J. Biol. Chem.* **1986**, *261*, 6084-6089.
630. Grundke-Iqbal, I.; Iqbal, K.; Tung, Y. C.; Quinlan, M.; Wisniewski, H. M.; Binder, L. I. Abnormal phosphorylation of the microtubule-associated protein tau (tau) in Alzheimer cytoskeletal pathology. *Proc. Natl. Acad. Sci. U. S. A.* **1986**, *83*, 4913-4917.
631. Goedert, M.; Spillantini, M. G.; Jakes, R.; Rutherford, D.; Crowther, R. A. Multiple isoforms of human microtubule-associated protein tau: sequences and localization in neurofibrillary tangles of Alzheimer's disease. *Neuron* **1989**, *3*, 519-526.
632. Brion, J. P.; Hanger, D. P.; Bruce, M. T.; Couck, A. M.; Flament-Durand, J.; Anderton, B. H. Tau in Alzheimer neurofibrillary tangles. N- and C-terminal regions are differentially associated with paired helical filaments and the location of a putative abnormal phosphorylation site. *Biochem. J.* **1991**, *273(Pt 1)*, 127-133.
633. Seino, Y.; Kawarabayashi, T.; Wakasaya, Y.; Watanabe, M.; Takamura, A.; Yamamoto-Watanabe, Y.; Kurata, T.; Abe, K.; Ikeda, M.; Westaway, D.; Murakami, T.; Hyslop, P. S.; Matsubara, E.; Shoji, M. Amyloid β accelerates phosphorylation of tau and neurofibrillary tangle formation in an amyloid precursor protein and tau double-transgenic mouse model. *J. Neurosci. Res.* **2010**, *88*, 3547-3554.
634. Alonso, A.; Zaidi, T.; Novak, M.; Grundke-Iqbal, I.; Iqbal, K. Hyperphosphorylation induces self-assembly of tau into tangles of paired helical filaments/straight filaments. *Proc. Natl. Acad. Sci. U. S. A.* **2001**, *98*, 6923-6928.
635. Delacourte, A.; Sergeant, N.; Champain, D.; Wattez, A.; Maurage, C. A.; Lebert, F.; Pasquier, F.; David, J. P. Nonoverlapping but synergetic tau and APP pathologies in sporadic Alzheimer's disease. *Neurology* **2002**, *59*, 398-407.
636. Ghetti, B.; Murrell, J.; Spillantini, M. G. Mutations in the Tau gene cause frontotemporal dementia. *Brain Res. Bull.* **1999**, *50*, 471-472.
637. Spillantini, M. G.; Bird, T. D.; Ghetti, B. Frontotemporal dementia and Parkinsonism linked to chromosome 17: a new group of tauopathies. *Brain Pathol.* **1998**, *8*, 387-402.
638. Goate, A. Segregation of a missense mutation in the amyloid β -protein precursor gene with familial Alzheimer's disease. *J. Alzheimers Dis.* **2006**, *9*, 341-347.

639. Sherrington, R.; Rogaev, E. I.; Liang, Y.; Rogaeva, E. A.; Levesque, G.; Ikeda, M.; Chi, H.; Lin, C.; Li, G.; Holman, K.; Tsuda, T.; Mar, L.; Foncin, J. F.; Bruni, A. C.; Montesi, M. P.; Sorbi, S.; Rainero, I.; Pinessi, L.; Nee, L.; Chumakov, I.; Pollen, D.; Brookes, A.; Sanseau, P.; Polinsky, R. J.; Wasco, W.; Da Silva, H. A.; Haines, J. L.; Perkicak-Vance, M. A.; Tanzi, R. E.; Roses, A. D.; Fraser, P. E.; Rommens, J. M.; St George-Hyslop, P. H. Cloning of a gene bearing missense mutations in early-onset familial Alzheimer's disease. *Nature* **1995**, *375*, 754-760.
640. Hutton, M.; Lendon, C. L.; Rizzu, P.; Baker, M.; Froelich, S.; Houlden, H.; Pickering-Brown, S.; Chakraverty, S.; Isaacs, A.; Grover, A.; Hackett, J.; Adamson, J.; Lincoln, S.; Dickson, D.; Davies, P.; Petersen, R. C.; Stevens, M.; de Graaff, E.; Wauters, E.; van Baren, J.; Hillebrand, M.; Joosse, M.; Kwon, J. M.; Nowotny, P.; Che, L. K.; Norton, J.; Morris, J. C.; Reed, L. A.; Trojanowski, J.; Basun, H.; Lannfelt, L.; Neystat, M.; Fahn, S.; Dark, F.; Tannenberg, T.; Dodd, P. R.; Hayward, N.; Kwok, J. B.; Schofield, P. R.; Andreadis, A.; Snowden, J.; Craufurd, D.; Neary, D.; Owen, F.; Oostra, B. A.; Hardy, J.; Goate, A.; van Swieten, J.; Mann, D.; Lynch, T.; Heutink, P. Association of missense and 5'-splice-site mutations in tau with the inherited dementia FTDP-17. *Nature* **1998**, *393*, 702-705.
641. Götz, J.; David, D. C.; Ittner, L. M. In *Impact of β -Amyloid on the Tau Pathology in Tau Transgenic Mouse and Tissue Culture Models*; Barrow, C. J., Small, D. H., Eds.; A β peptide and Alzheimer's disease - Celebrating a century of research; Springer: London, 2007; pp. 198-215.
642. Götz, J.; Chen, F.; van Dorpe, J.; Nitsch, R. M. Formation of neurofibrillary tangles in P301L tau transgenic mice induced by A β 42 fibrils. *Science* **2001**, *293*, 1491-1495.
643. Lewis, J.; Dickson, D. W.; Lin, W. L.; Chisholm, L.; Corral, A.; Jones, G.; Yen, S. H.; Sahara, N.; Skipper, L.; Yager, D.; Eckman, C.; Hardy, J.; Hutton, M.; McGowan, E. Enhanced neurofibrillary degeneration in transgenic mice expressing mutant tau and APP. *Science* **2001**, *293*, 1487-1491.
644. De Felice, F. G.; Wu, D.; Lambert, M. P.; Fernandez, S. J.; Velasco, P. T.; Lacor, P. N.; Bigio, E. H.; Jerecic, J.; Acton, P. J.; Shughrue, P. J.; Chen-Dodson, E.; Kinney, G. G.; Klein, W. L. Alzheimer's disease-type neuronal tau hyperphosphorylation induced by A β oligomers. *Neurobiology of Aging* **2008**, *29*, 1334-1347.
645. Jin, M.; Shepardson, N.; Yang, T.; Chen, G.; Walsh, D.; Selkoe, D. J. Soluble amyloid β -protein dimers isolated from Alzheimer cortex directly induce Tau hyperphosphorylation and neuritic degeneration. *Proc. Natl. Acad. Sci. U. S. A.* **2011**, *108*, 5819-5824.
646. Roberson, E. D.; Scarce-Levie, K.; Palop, J. J.; Yan, F.; Cheng, I. H.; Wu, T.; Gerstein, H.; Yu, G. Q.; Mucke, L. Reducing endogenous tau ameliorates amyloid β -induced deficits in an Alzheimer's disease mouse model. *Science* **2007**, *316*, 750-754.

647. Ittner, L. M.; Ke, Y. D.; Delerue, F.; Bi, M.; Gladbach, A.; van Eersel, J.; Wolfing, H.; Chieng, B. C.; Christie, M. J.; Napier, I. A.; Eckert, A.; Staufenbiel, M.; Hardeman, E.; Gotz, J. Dendritic function of tau mediates amyloid- β toxicity in Alzheimer's disease mouse models. *Cell* **2010**, *142*, 387-397.
648. Jack, C. R., Jr.; Knopman, D. S.; Jagust, W. J.; Petersen, R. C.; Weiner, M. W.; Aisen, P. S.; Shaw, L. M.; Vemuri, P.; Wiste, H. J.; Weigand, S. D.; Lesnick, T. G.; Pankratz, V. S.; Donohue, M. C.; Trojanowski, J. Q. Tracking pathophysiological processes in Alzheimer's disease: an updated hypothetical model of dynamic biomarkers. *Lancet Neurol.* **2013**, *12*, 207-216.

Chapter II

1. Tosi, M. F. Innate immune responses to infection. *J. Allergy Clin. Immunol.* **2005**, *116*, 241-9; quiz 250.
2. Pancer, Z.; Cooper, M. D. The evolution of adaptive immunity. *Annu. Rev. Immunol.* **2006**, *24*, 497-518.
3. Iwasaki, A.; Medzhitov, R. Regulation of adaptive immunity by the innate immune system. *Science* **2010**, *327*, 291-295.
4. Schenten, D.; Medzhitov, R. The control of adaptive immune responses by the innate immune system. *Adv. Immunol.* **2011**, *109*, 87-124.
5. National Library of Medicine Autoimmune Diseases. http://www.nlm.nih.gov/cgi/mesh/2011/MB_cgi?mode=&term=Autoimmune+Diseases (accessed 02/10, 2014).
6. Akira, S.; Uematsu, S.; Takeuchi, O. Pathogen Recognition and Innate Immunity. *Cell* **2006**, *124*, 783-801.
7. Hancock, R. E.; Scott, M. G. The role of antimicrobial peptides in animal defenses. *Proc. Natl. Acad. Sci. U. S. A.* **2000**, *97*, 8856-8861.
8. Yoshio, H.; Lagercrantz, H.; Gudmundsson, G. H.; Agerberth, B. First line of defense in early human life. *Semin. Perinatol.* **2004**, *28*, 304-311.
9. Turvey, S. E.; Broide, D. H. Innate immunity. *J. Allergy Clin. Immunol.* **2010**, *125*, S24-32.

10. Beutler, B. Innate immunity: an overview. *Mol. Immunol.* **2004**, *40*, 845-859.
11. Nonaka, M.; Yoshizaki, F. Evolution of the complement system. *Mol. Immunol.* **2004**, *40*, 897-902.
12. Trouw, L. A.; Daha, M. R. Role of complement in innate immunity and host defense. *Immunol. Lett.* **2011**, *138*, 35-37.
13. Braff, M. H.; Bardan, A.; Nizet, V.; Gallo, R. L. Cutaneous defense mechanisms by antimicrobial peptides. *J. Invest. Dermatol.* **2005**, *125*, 9-13.
14. Bulet, P.; Stocklin, R.; Menin, L. Anti-microbial peptides: from invertebrates to vertebrates. *Immunol. Rev.* **2004**, *198*, 169-184.
15. De Smet, K.; Contreras, R. Human antimicrobial peptides: defensins, cathelicidins and histatins. *Biotechnol. Lett.* **2005**, *27*, 1337-1347.
16. Jenssen, H.; Hamill, P.; Hancock, R. E. Peptide antimicrobial agents. *Clin. Microbiol. Rev.* **2006**, *19*, 491-511.
17. Durr, M.; Peschel, A. Chemokines meet defensins: the merging concepts of chemoattractants and antimicrobial peptides in host defense. *Infect. Immun.* **2002**, *70*, 6515-6517.
18. Kamysz, W.; Okroj, M.; Lukasiak, J. Novel properties of antimicrobial peptides. *Acta Biochim. Pol.* **2003**, *50*, 461-469.
19. Barlow, P. G.; Li, Y.; Wilkinson, T. S.; Bowdish, D. M.; Lau, Y. E.; Cosseau, C.; Haslett, C.; Simpson, A. J.; Hancock, R. E.; Davidson, D. J. The human cationic host defense peptide LL-37 mediates contrasting effects on apoptotic pathways in different primary cells of the innate immune system. *J. Leukoc. Biol.* **2006**, *80*, 509-520.
20. Bowdish, D. M.; Davidson, D. J.; Hancock, R. E. A re-evaluation of the role of host defence peptides in mammalian immunity. *Curr. Protein Pept. Sci.* **2005**, *6*, 35-51.
21. Beisswenger, C.; Bals, R. Functions of antimicrobial peptides in host defense and immunity. *Curr. Protein Pept. Sci.* **2005**, *6*, 255-264.
22. Oppenheim, J. J.; Biragyn, A.; Kwak, L. W.; Yang, D. Roles of antimicrobial peptides such as defensins in innate and adaptive immunity. *Ann. Rheum. Dis.* **2003**, *62 Suppl 2*, ii17-21.
23. Brown, K. L.; Hancock, R. E. Cationic host defense (antimicrobial) peptides. *Curr. Opin. Immunol.* **2006**, *18*, 24-30.

24. Iwasaki, A.; Medzhitov, R. Toll-like receptor control of the adaptive immune responses. *Nat. Immunol.* **2004**, *5*, 987-995.
25. Shanker, A. Adaptive control of innate immunity. *Immunol. Lett.* **2010**, *131*, 107-112.
26. Zhao, J.; Yang, X.; Auh, S. L.; Kim, K. D.; Tang, H.; Fu, Y. Do adaptive immune cells suppress or activate innate immunity? *Trends Immunol.* **2009**, *30*, 8-12.
27. Kabelitz, D.; Medzhitov, R. Innate immunity — cross-talk with adaptive immunity through pattern recognition receptors and cytokines. *Curr. Opin. Immunol.* **2007**, *19*, 1-3.
28. Abdelsadik, A.; Trad, A. Toll-like receptors on the fork roads between innate and adaptive immunity. *Hum. Immunol.* **2011**, *72*, 1188-1193.
29. McGonagle, D.; Savic, S.; McDermott, M. The NLR network and the immunological disease continuum of adaptive and innate immune-mediated inflammation against self. *Seminars in Immunopathology* **2007**, *29*, 303-313.
30. Goldstein, D. R. Toll-like receptors and other links between innate and acquired alloimmunity. *Curr. Opin. Immunol.* **2004**, *16*, 538-544.
31. Kawai, T.; Akira, S. The role of pattern-recognition receptors in innate immunity: update on Toll-like receptors. *Nat. Immunol.* **2010**, *11*, 373-384.
32. O'Neill, L. Specificity in the innate response: pathogen recognition by Toll-like receptor combinations. *Trends Immunol.* **2001**, *22*, 70.
33. Akira, S.; Takeda, K.; Kaisho, T. Toll-like receptors: critical proteins linking innate and acquired immunity. *Nat. Immunol.* **2001**, *2*, 675.
34. Janeway, C. A., Jr; Medzhitov, R. Innate immune recognition. *Annu. Rev. Immunol.* **2002**, *20*, 197-216.
35. Theofilopoulos, A. N.; Baccala, R.; Beutler, B.; Kono, D. H. Type I interferons (alpha/beta) in immunity and autoimmunity. *Annu. Rev. Immunol.* **2005**, *23*, 307-336.
36. Takeda, K.; Akira, S. Toll-like receptors in innate immunity. *Int. Immunol.* **2005**, *17*, 1-14.
37. Takeda, K.; Kaisho, T.; Akira, S. Toll-like receptors. *Annu. Rev. Immunol.* **2003**, *21*, 335-376.
38. Creagh, E. M.; O'Neill, L. A. J. TLRs, NLRs and RLRs: a trinity of pathogen sensors that cooperate in innate immunity. *Trends Immunol.* **2006**, *27*, 352-357.
39. Newton, K.; Dixit, V. M. Signaling in innate immunity and inflammation. *Cold Spring Harb Perspect. Biol.* **2012**, *4*, 10.1101/cshperspect.a006049.

40. Medzhitov, R.; Preston-Hurlburt, P.; Janeway, C. A., Jr A human homologue of the Drosophila Toll protein signals activation of adaptive immunity. *Nature* **1997**, *388*, 394-397.
41. Rock, F. L.; Hardiman, G.; Timans, J. C.; Kastelein, R. A.; Bazan, J. F. A family of human receptors structurally related to Drosophila Toll. *Proc. Natl. Acad. Sci. U. S. A.* **1998**, *95*, 588-593.
42. Kumar, H.; Kawai, T.; Akira, S. Toll-like receptors and innate immunity. *Biochem. Biophys. Res. Commun.* **2009**, *388*, 621-625.
43. Onoguchi, K.; Yoneyama, M.; Fujita, T. Retinoic acid-inducible gene-I-like receptors. *J. Interferon Cytokine Res.* **2011**, *31*, 27-31.
44. Yoneyama, M.; Fujita, T. Structural Mechanism of RNA Recognition by the RIG-I-like Receptors. *Immunity* **2008**, *29*, 178-181.
45. Li, X.; Lu, C.; Stewart, M.; Xu, H.; Strong, R. K.; Igumenova, T.; Li, P. Structural basis of double-stranded RNA recognition by the RIG-I like receptor MDA5. *Arch. Biochem. Biophys.* **2009**, *488*, 23-33.
46. Li, X.; Ranjith-Kumar, C. T.; Brooks, M. T.; Dharmiah, S.; Herr, A. B.; Kao, C.; Li, P. The RIG-I-like Receptor LGP2 Recognizes the Termini of Double-stranded RNA. *Journal of Biological Chemistry* **2009**, *284*, 13881-13891.
47. Takahashi, K.; Kumeta, H.; Tsuduki, N.; Narita, R.; Shigemoto, T.; Hirai, R.; Yoneyama, M.; Horiuchi, M.; Ogura, K.; Fujita, T.; Inagaki, F. Solution Structures of Cytosolic RNA Sensor MDA5 and LGP2 C-terminal Domains: Identification of the RNA Recognition Loop in RIG-I-like Receptors. *Journal of Biological Chemistry* **2009**, *284*, 17465-17474.
48. Ting, J. P. -.; Lovering, R. C.; Alnemri, E. S.; Bertin, J.; Boss, J. M.; Davis, B. K.; Flavell, R. A.; Girardin, S. E.; Godzik, A.; Harton, J. A.; Hoffman, H. M.; Hugot, J.; Inohara, N.; MacKenzie, A.; Maltais, L. J.; Nunez, G.; Ogura, Y.; Otten, L. A.; Philpott, D.; Reed, J. C.; Reith, W.; Schreiber, S.; Steimle, V.; Ward, P. A. The NLR Gene Family: A Standard Nomenclature. *Immunity* **2008**, *28*, 285-287.
49. Shaw, M. H.; Reimer, T.; Kim, Y.; Nuñez, G. NOD-like receptors (NLRs): bona fide intracellular microbial sensors. *Curr. Opin. Immunol.* **2008**, *20*, 377-382.
50. Franchi, L.; Warner, N.; Viani, K.; Nunez, G. Function of Nod-like receptors in microbial recognition and host defense. *Immunol. Rev.* **2009**, *227*, 106-128.
51. Greenberg, J. W.; Fischer, W.; Joiner, K. A. Influence of lipoteichoic acid structure on recognition by the macrophage scavenger receptor. *Infect. Immun.* **1996**, *64*, 3318-3325.

52. Fischer, W. Pneumococcal lipoteichoic and teichoic acid. *Microb. Drug Resist.* **1997**, *3*, 309-325.
53. Xia, G.; Kohler, T.; Peschel, A. The wall teichoic acid and lipoteichoic acid polymers of *Staphylococcus aureus*. *International Journal of Medical Microbiology* **2010**, *300*, 148-154.
54. Schmidt, R. R.; Pedersen, C. M.; Qiao, Y.; Zahringer, U. Chemical synthesis of bacterial lipoteichoic acids: an insight on its biological significance. *Org. Biomol. Chem.* **2011**, *9*, 2040-2052.
55. Erridge, C.; Bennett-Guerrero, E.; Poxton, I. R. Structure and function of lipopolysaccharides. *Microb. Infect.* **2002**, *4*, 837-851.
56. Raetz, C. R.; Whitfield, C. Lipopolysaccharide endotoxins. *Annu. Rev. Biochem.* **2002**, *71*, 635-700.
57. Caroff, M.; Karibian, D. Structure of bacterial lipopolysaccharides. *Carbohydr. Res.* **2003**, *338*, 2431-2447.
58. Ozinsky, A.; Underhill, D. M.; Fontenot, J. D.; Hajjar, A. M.; Smith, K. D.; Wilson, C. B.; Schroeder, L.; Aderem, A. The repertoire for pattern recognition of pathogens by the innate immune system is defined by cooperation between toll-like receptors. *Proc. Natl. Acad. Sci. U. S. A.* **2000**, *97*, 13766-13771.
59. Takeuchi, O.; Hoshino, K.; Kawai, T.; Sanjo, H.; Takada, H.; Ogawa, T.; Takeda, K.; Akira, S. Differential roles of TLR2 and TLR4 in recognition of gram-negative and gram-positive bacterial cell wall components. *Immunity* **1999**, *11*, 443-451.
60. Takeuchi, O.; Hoshino, K.; Akira, S. TLR2-deficient and MyD88-deficient mice are highly susceptible to *Staphylococcus aureus* infection. *J. Immunol.* **2000**, *165*, 5392-5396.
61. Yoshimura, A.; Lien, E.; Ingalls, R. R.; Tuomanen, E.; Dziarski, R.; Golenbock, D. Recognition of Gram-positive bacterial cell wall components by the innate immune system occurs via Toll-like receptor 2. *J. Immunol.* **1999**, *163*, 1-5.
62. Ulevitch, R. J.; Tobias, P. S. Recognition of Gram-negative bacteria and endotoxin by the innate immune system. *Curr. Opin. Immunol.* **1999**, *11*, 19-22.
63. Shimazu, R.; Akashi, S.; Ogata, H.; Nagai, Y.; Fukudome, K.; Miyake, K.; Kimoto, M. MD-2, a molecule that confers lipopolysaccharide responsiveness on Toll-like receptor 4. *J. Exp. Med.* **1999**, *189*, 1777-1782.
64. Alexopoulou, L.; Holt, A. C.; Medzhitov, R.; Flavell, R. A. Recognition of double-stranded RNA and activation of NF-kappaB by Toll-like receptor 3. *Nature* **2001**, *413*, 732-738.

65. Takeuchi, O.; Kawai, T.; Muhlradt, P. F.; Morr, M.; Radolf, J. D.; Zychlinsky, A.; Takeda, K.; Akira, S. Discrimination of bacterial lipoproteins by Toll-like receptor 6. *Int. Immunol.* **2001**, *13*, 933-940.
66. Yamamoto, M.; Sato, S.; Mori, K.; Hoshino, K.; Takeuchi, O.; Takeda, K.; Akira, S. Cutting edge: a novel Toll/IL-1 receptor domain-containing adapter that preferentially activates the IFN-beta promoter in the Toll-like receptor signaling. *J. Immunol.* **2002**, *169*, 6668-6672.
67. Takeuchi, O.; Sato, S.; Horiuchi, T.; Hoshino, K.; Takeda, K.; Dong, Z.; Modlin, R. L.; Akira, S. Cutting edge: role of Toll-like receptor 1 in mediating immune response to microbial lipoproteins. *J. Immunol.* **2002**, *169*, 10-14.
68. Tobias, P. S.; Soldau, K.; Ulevitch, R. J. Isolation of a lipopolysaccharide-binding acute phase reactant from rabbit serum. *J. Exp. Med.* **1986**, *164*, 777-793.
69. Schumann, R. R.; Leong, S. R.; Flaggs, G. W.; Gray, P. W.; Wright, S. D.; Mathison, J. C.; Tobias, P. S.; Ulevitch, R. J. Structure and function of lipopolysaccharide binding protein. *Science* **1990**, *249*, 1429-1431.
70. Wright, S. D.; Tobias, P. S.; Ulevitch, R. J.; Ramos, R. A. Lipopolysaccharide (LPS) binding protein opsonizes LPS-bearing particles for recognition by a novel receptor on macrophages. *J. Exp. Med.* **1989**, *170*, 1231-1241.
71. Wright, S. D.; Ramos, R. A.; Tobias, P. S.; Ulevitch, R. J.; Mathison, J. C. CD14, a receptor for complexes of lipopolysaccharide (LPS) and LPS binding protein. *Science* **1990**, *249*, 1431-1433.
72. Miyake, K. Innate recognition of lipopolysaccharide by CD14 and toll-like receptor 4-MD-2: unique roles for MD-2. *Int. Immunopharmacol.* **2003**, *3*, 119-128.
73. Jiang, Q.; Akashi, S.; Miyake, K.; Petty, H. R. Lipopolysaccharide induces physical proximity between CD14 and toll-like receptor 4 (TLR4) prior to nuclear translocation of NF-kappa B. *J. Immunol.* **2000**, *165*, 3541-3544.
74. Akashi, S.; Saitoh, S.; Wakabayashi, Y.; Kikuchi, T.; Takamura, N.; Nagai, Y.; Kusumoto, Y.; Fukase, K.; Kusumoto, S.; Adachi, Y.; Kosugi, A.; Miyake, K. Lipopolysaccharide interaction with cell surface Toll-like receptor 4-MD-2: higher affinity than that with MD-2 or CD14. *J. Exp. Med.* **2003**, *198*, 1035-1042.
75. Fitzgerald, K. A.; Rowe, D. C.; Golenbock, D. T. Endotoxin recognition and signal transduction by the TLR4/MD2-complex. *Microbes Infect.* **2004**, *6*, 1361-1367.
76. Kawai, T.; Akira, S. Innate immune recognition of viral infection. *Nat. Immunol.* **2006**, *7*, 131-137.

77. Saito, T.; Gale Jr, M. Principles of intracellular viral recognition. *Curr. Opin. Immunol.* **2007**, *19*, 17-23.
78. Hartmann, T.; Bieger, S. C.; Bruhl, B.; Tienari, P. J.; Ida, N.; Allsop, D.; Roberts, G. W.; Masters, C. L.; Dotti, C. G.; Unsicker, K.; Beyreuther, K. Distinct sites of intracellular production for Alzheimer's disease A beta40/42 amyloid peptides. *Nat. Med.* **1997**, *3*, 1016-1020.
79. Sorensen, O. E.; Thapa, D. R.; Roupe, K. M.; Valore, E. V.; Sjobring, U.; Roberts, A. A.; Schmidtchen, A.; Ganz, T. Injury-induced innate immune response in human skin mediated by transactivation of the epidermal growth factor receptor. *J. Clin. Invest.* **2006**, *116*, 1878-1885.
80. Tahara, K.; Kim, H. D.; Jin, J. J.; Maxwell, J. A.; Li, L.; Fukuchi, K. Role of toll-like receptor signalling in Abeta uptake and clearance. *Brain* **2006**, *129*, 3006-3019.
81. Stewart, C. R.; Stuart, L. M.; Wilkinson, K.; van Gils, J. M.; Deng, J.; Halle, A.; Rayner, K. J.; Boyer, L.; Zhong, R.; Frazier, W. A.; Lacy-Hulbert, A.; El Khoury, J.; Golenbock, D. T.; Moore, K. J. CD36 ligands promote sterile inflammation through assembly of a Toll-like receptor 4 and 6 heterodimer. *Nat. Immunol.* **2010**, *11*, 155-161.
82. El Khoury, J. B.; Moore, K. J.; Means, T. K.; Leung, J.; Terada, K.; Toft, M.; Freeman, M. W.; Luster, A. D. CD36 mediates the innate host response to beta-amyloid. *J. Exp. Med.* **2003**, *197*, 1657-1666.
83. Moore, K. J.; El Khoury, J.; Medeiros, L. A.; Terada, K.; Geula, C.; Luster, A. D.; Freeman, M. W. A CD36-initiated signaling cascade mediates inflammatory effects of beta-amyloid. *J. Biol. Chem.* **2002**, *277*, 47373-47379.
84. Andreu, D.; Rivas, L. Animal antimicrobial peptides: an overview. *Biopolymers* **1998**, *47*, 415-433.
85. Huttner, K. M.; Bevins, C. L. Antimicrobial peptides as mediators of epithelial host defense. *Pediatr. Res.* **1999**, *45*, 785-794.
86. Devine, D. A.; Hancock, R. E. Cationic peptides: distribution and mechanisms of resistance. *Curr. Pharm. Des.* **2002**, *8*, 703-714.
87. Bowdish, D. M.; Davidson, D. J.; Scott, M. G.; Hancock, R. E. Immunomodulatory activities of small host defense peptides. *Antimicrob. Agents Chemother.* **2005**, *49*, 1727-1732.
88. Steinstraesser, L.; Kraneburg, U.; Jacobsen, F.; Al-Benna, S. Host defense peptides and their antimicrobial-immunomodulatory duality. *Immunobiology* **2011**, *216*, 322-333.

89. Bowdish, D. M.; Davidson, D. J.; Hancock, R. E. Immunomodulatory properties of defensins and cathelicidins. *Curr. Top. Microbiol. Immunol.* **2006**, *306*, 27-66.
90. Kolls, J. K.; McCray, P. B., Jr; Chan, Y. R. Cytokine-mediated regulation of antimicrobial proteins. *Nat. Rev. Immunol.* **2008**, *8*, 829-835.
91. Hancock, R. E. Cationic peptides: effectors in innate immunity and novel antimicrobials. *Lancet Infect. Dis.* **2001**, *1*, 156-164.
92. Hancock, R. E.; Diamond, G. The role of cationic antimicrobial peptides in innate host defences. *Trends Microbiol.* **2000**, *8*, 402-410.
93. Legrand, D.; Mazurier, J. A critical review of the roles of host lactoferrin in immunity. *Biometals* **2010**, *23*, 365-376.
94. Bowdish, D. M.; Davidson, D. J.; Lau, Y. E.; Lee, K.; Scott, M. G.; Hancock, R. E. Impact of LL-37 on anti-infective immunity. *J. Leukoc. Biol.* **2005**, *77*, 451-459.
95. Braff, M. H.; Gallo, R. L. Antimicrobial peptides: an essential component of the skin defensive barrier. *Curr. Top. Microbiol. Immunol.* **2006**, *306*, 91-110.
96. Bals, R.; Wilson, J. M. Cathelicidins--a family of multifunctional antimicrobial peptides. *Cell Mol. Life Sci.* **2003**, *60*, 711-720.
97. Mor, A.; Nguyen, V. H.; Delfour, A.; Migliore-Samour, D.; Nicolas, P. Isolation, amino acid sequence, and synthesis of dermaseptin, a novel antimicrobial peptide of amphibian skin. *Biochemistry* **1991**, *30*, 8824-8830.
98. Shinnar, A. E.; Butler, K. L.; Park, H. J. Cathelicidin family of antimicrobial peptides: proteolytic processing and protease resistance. *Bioorg. Chem.* **2003**, *31*, 425-436.
99. Nizet, V.; Gallo, R. L. Cathelicidins and innate defense against invasive bacterial infection. *Scand. J. Infect. Dis.* **2003**, *35*, 670-676.
100. Niyonsaba, F.; Hirata, M.; Ogawa, H.; Nagaoka, I. Epithelial cell-derived antibacterial peptides human beta-defensins and cathelicidin: multifunctional activities on mast cells. *Curr. Drug Targets Inflamm. Allergy* **2003**, *2*, 224-231.
101. Nielsen, J. E.; Hansen, M. A.; Jorgensen, M.; Tanaka, M.; Almstrup, K.; Skakkebaek, N. E.; Leffers, H. Germ cell differentiation-dependent and stage-specific expression of LANCL1 in rodent testis. *Eur. J. Histochem.* **2003**, *47*, 215-222.
102. Hao, H. N.; Zhao, J.; Lotoczky, G.; Grever, W. E.; Lyman, W. D. Induction of human beta-defensin-2 expression in human astrocytes by lipopolysaccharide and cytokines. *J. Neurochem.* **2001**, *77*, 1027-1035.

103. Zhao, X.; Wu, H.; Lu, H.; Li, G.; Huang, Q. LAMP: A Database Linking Antimicrobial Peptides. *PLoS One* **2013**, *8*, e66557.
104. Verkleij, A. J.; Zwaal, R. F.; Roelofsen, B.; Comfurius, P.; Kastelijn, D.; van Deenen, L. L. The asymmetric distribution of phospholipids in the human red cell membrane. A combined study using phospholipases and freeze-etch electron microscopy. *Biochim. Biophys. Acta* **1973**, *323*, 178-193.
105. Brewer, D.; Lajoie, G. Evaluation of the metal binding properties of the histidine-rich antimicrobial peptides histatin 3 and 5 by electrospray ionization mass spectrometry. *Rapid Commun. Mass Spectrom.* **2000**, *14*, 1736-1745.
106. Edstrom, A. M.; Malm, J.; Frohm, B.; Martellini, J. A.; Giwercman, A.; Morgelin, M.; Cole, A. M.; Sorensen, O. E. The major bactericidal activity of human seminal plasma is zinc-dependent and derived from fragmentation of the semenogelins. *J. Immunol.* **2008**, *181*, 3413-3421.
107. Dashper, S. G.; O'Brien-Simpson, N. M.; Cross, K. J.; Paolini, R. A.; Hoffmann, B.; Catmull, D. V.; Malkoski, M.; Reynolds, E. C. Divalent metal cations increase the activity of the antimicrobial Peptide kappacin. *Antimicrob. Agents Chemother.* **2005**, *49*, 2322-2328.
108. Rydengard, V.; Andersson Nordahl, E.; Schmidtchen, A. Zinc potentiates the antibacterial effects of histidine-rich peptides against *Enterococcus faecalis*. *FEBS J.* **2006**, *273*, 2399-2406.
109. Wang, M.; Liu, L. H.; Wang, S.; Li, X.; Lu, X.; Gupta, D.; Dziarski, R. Human peptidoglycan recognition proteins require zinc to kill both gram-positive and gram-negative bacteria and are synergistic with antibacterial peptides. *J. Immunol.* **2007**, *178*, 3116-3125.
110. Brodersen, D. E.; Nyborg, J.; Kjeldgaard, M. Zinc-binding site of an S100 protein revealed. Two crystal structures of Ca²⁺-bound human psoriasin (S100A7) in the Zn²⁺-loaded and Zn²⁺-free states. *Biochemistry* **1999**, *38*, 1695-1704.
111. Hancock, R. E.; Lehrer, R. I. Cationic peptides: a new source of antibiotics. *Trends Biotechnol.* **1998**, *16*, 82-88.
112. Wang, G.; Li, X.; Wang, Z. APD2: the updated antimicrobial peptide database and its application in peptide design. *Nucleic Acids Res.* **2009**, *37*, D933-7.
113. Tossi, A.; Sandri, L. Molecular diversity in gene-encoded, cationic antimicrobial polypeptides. *Curr. Pharm. Des.* **2002**, *8*, 743-761.
114. Piotto, S. P.; Sessa, L.; Concilio, S.; Iannelli, P. YADAMP: yet another database of antimicrobial peptides. *Int. J. Antimicrob. Agents* **2012**, *39*, 346-351.

115. Wang, G. Structures of human host defense cathelicidin LL-37 and its smallest antimicrobial peptide KR-12 in lipid micelles. *J. Biol. Chem.* **2008**, *283*, 32637-32643.
116. Schibli, D. J.; Hunter, H. N.; Aseyev, V.; Starner, T. D.; Wiencek, J. M.; McCray, P. B.; Tack, B. F.; Vogel, H. J. The Solution Structures of the Human β -Defensins Lead to a Better Understanding of the Potent Bactericidal Activity of HBD3 against *Staphylococcus aureus*. *Journal of Biological Chemistry* **2002**, *277*, 8279-8289.
117. Rozek, A.; Friedrich, C. L.; Hancock, R. E. Structure of the bovine antimicrobial peptide indolicidin bound to dodecylphosphocholine and sodium dodecyl sulfate micelles. *Biochemistry* **2000**, *39*, 15765-15774.
118. Tossi, A.; Sandri, L.; Giangaspero, A. Amphipathic, alpha-helical antimicrobial peptides. *Biopolymers* **2000**, *55*, 4-30.
119. Schiffer, M.; Edmundson, A. B. Use of helical wheels to represent the structures of proteins and to identify segments with helical potential. *Biophys. J.* **1967**, *7*, 121-135.
120. Boman, H. G. Antibacterial peptides: basic facts and emerging concepts. *J. Intern. Med.* **2003**, *254*, 197-215.
121. Andersson, E.; Rydengard, V.; Sonesson, A.; Morgelin, M.; Bjorck, L.; Schmidtchen, A. Antimicrobial activities of heparin-binding peptides. *Eur. J. Biochem.* **2004**, *271*, 1219-1226.
122. Lu, X.; Wang, M.; Qi, J.; Wang, H.; Li, X.; Gupta, D.; Dziarski, R. Peptidoglycan recognition proteins are a new class of human bactericidal proteins. *J. Biol. Chem.* **2006**, *281*, 5895-5907.
123. Wang, Z.; Wang, G. APD: the Antimicrobial Peptide Database. *Nucleic Acids Res.* **2004**, *32*, D590-2.
124. Breukink, E.; Wiedemann, I.; van Kraaij, C.; Kuipers, O. P.; Sahl, H.; de Kruijff, B. Use of the cell wall precursor lipid II by a pore-forming peptide antibiotic. *Science* **1999**, *286*, 2361-2364.
125. Terwilliger, T. C.; Eisenberg, D. The structure of melittin. I. Structure determination and partial refinement. *J. Biol. Chem.* **1982**, *257*, 6010-6015.
126. Holak, T. A.; Engstrom, A.; Kraulis, P. J.; Lindeberg, G.; Bennich, H.; Jones, T. A.; Gronenborn, A. M.; Clore, G. M. The solution conformation of the antibacterial peptide cecropin A: a nuclear magnetic resonance and dynamical simulated annealing study. *Biochemistry* **1988**, *27*, 7620-7629.

127. Zasloff, M. Magainins, a class of antimicrobial peptides from *Xenopus* skin: isolation, characterization of two active forms, and partial cDNA sequence of a precursor. *Proc. Natl. Acad. Sci. U. S. A.* **1987**, *84*, 5449-5453.
128. Mandard, N.; Sy, D.; Maufrais, C.; Bonmatin, J. M.; Bulet, P.; Hetru, C.; Vovelle, F. Androctonin, a novel antimicrobial peptide from scorpion *Androctonus australis*: solution structure and molecular dynamics simulations in the presence of a lipid monolayer. *J. Biomol. Struct. Dyn.* **1999**, *17*, 367-380.
129. Shai, Y. Mechanism of the binding, insertion and destabilization of phospholipid bilayer membranes by alpha-helical antimicrobial and cell non-selective membrane-lytic peptides. *Biochim. Biophys. Acta* **1999**, *1462*, 55-70.
130. Wu, M.; Maier, E.; Benz, R.; Hancock, R. E. Mechanism of interaction of different classes of cationic antimicrobial peptides with planar bilayers and with the cytoplasmic membrane of *Escherichia coli*. *Biochemistry* **1999**, *38*, 7235-7242.
131. Matsuzaki, K.; Sugishita, K.; Ishibe, N.; Ueha, M.; Nakata, S.; Miyajima, K.; Epanand, R. M. Relationship of membrane curvature to the formation of pores by magainin 2. *Biochemistry* **1998**, *37*, 11856-11863.
132. Oren, Z.; Shai, Y. Mode of action of linear amphipathic alpha-helical antimicrobial peptides. *Biopolymers* **1998**, *47*, 451-463.
133. Bulet, P.; Hetru, C.; Dimarcq, J. L.; Hoffmann, D. Antimicrobial peptides in insects; structure and function. *Dev. Comp. Immunol.* **1999**, *23*, 329-344.
134. Wade, D.; Boman, A.; Wahlin, B.; Drain, C. M.; Andreu, D.; Boman, H. G.; Merrifield, R. B. All-D amino acid-containing channel-forming antibiotic peptides. *Proc. Natl. Acad. Sci. U. S. A.* **1990**, *87*, 4761-4765.
135. Merrifield, R. B.; Juvvadi, P.; Andreu, D.; Ubach, J.; Boman, A.; Boman, H. G. Retro and retroenantio analogs of cecropin-melittin hybrids. *Proc. Natl. Acad. Sci. U. S. A.* **1995**, *92*, 3449-3453.
136. Bessalle, R.; Kapitkovsky, A.; Gorea, A.; Shalit, I.; Fridkin, M. All-D-magainin: chirality, antimicrobial activity and proteolytic resistance. *FEBS Lett.* **1990**, *274*, 151-155.
137. Hetru, C.; Letellier, L.; Oren, Z.; Hoffmann, J. A.; Shai, Y. Androctonin, a hydrophilic disulphide-bridged non-haemolytic anti-microbial peptide: a plausible mode of action. *Biochem. J.* **2000**, *345 Pt 3*, 653-664.

138. Fleury, Y.; Dayem, M. A.; Montagne, J. J.; Chaboisseau, E.; Le Caer, J. P.; Nicolas, P.; Delfour, A. Covalent structure, synthesis, and structure-function studies of mesentericin Y 105(37), a defensive peptide from gram-positive bacteria *Leuconostoc mesenteroides*. *J. Biol. Chem.* **1996**, *271*, 14421-14429.
139. Cudic, M.; Otvos, L., Jr Intracellular targets of antibacterial peptides. *Curr. Drug Targets* **2002**, *3*, 101-106.
140. Feder, R.; Dagan, A.; Mor, A. Structure-activity relationship study of antimicrobial dermaseptin S4 showing the consequences of peptide oligomerization on selective cytotoxicity. *J. Biol. Chem.* **2000**, *275*, 4230-4238.
141. Lehrer, R. I.; Ganz, T. Antimicrobial peptides in mammalian and insect host defence. *Curr. Opin. Immunol.* **1999**, *11*, 23-27.
142. Hancock, R. E.; Rozek, A. Role of membranes in the activities of antimicrobial cationic peptides. *FEMS Microbiol. Lett.* **2002**, *206*, 143-149.
143. Matsuzaki, K. Why and how are peptide-lipid interactions utilized for self-defense? Magainins and tachyplesins as archetypes. *Biochimica et Biophysica Acta (BBA) - Biomembranes* **1999/12/15**, *1462*, 1-10.
144. Bechinger, B. The structure, dynamics and orientation of antimicrobial peptides in membranes by multidimensional solid-state NMR spectroscopy. *Biochim. Biophys. Acta* **1999**, *1462*, 157-183.
145. Shai, Y. From innate immunity to de-novo designed antimicrobial peptides. *Curr. Pharm. Des.* **2002**, *8*, 715-725.
146. Brogden, K. A. Antimicrobial peptides: pore formers or metabolic inhibitors in bacteria? *Nat. Rev. Microbiol.* **2005**, *3*, 238-250.
147. Huang, H. W.; Chen, F. Y.; Lee, M. T. Molecular mechanism of Peptide-induced pores in membranes. *Phys. Rev. Lett.* **2004**, *92*, 198304.
148. van 't Hof, W.; Veerman, E. C.; Helmerhorst, E. J.; Amerongen, A. V. Antimicrobial peptides: properties and applicability. *Biol. Chem.* **2001**, *382*, 597-619.
149. Hancock, R. E.; Chapple, D. S. Peptide antibiotics. *Antimicrob. Agents Chemother.* **1999**, *43*, 1317-1323.
150. Chitnis, S. N.; Prasad, K. S.; Bhargava, P. M. Isolation and characterization of autolysis-defective mutants of *Escherichia coli* that are resistant to the lytic activity of seminalplasmin. *J. Gen. Microbiol.* **1990**, *136*, 463-469.

151. Boman, H. G.; Agerberth, B.; Boman, A. Mechanisms of action on *Escherichia coli* of cecropin P1 and PR-39, two antibacterial peptides from pig intestine. *Infect. Immun.* **1993**, *61*, 2978-2984.
152. Subbalakshmi, C.; Sitaram, N. Mechanism of antimicrobial action of indolicidin. *FEMS Microbiol. Lett.* **1998**, *160*, 91-96.
153. Skerlavaj, B.; Romeo, D.; Gennaro, R. Rapid membrane permeabilization and inhibition of vital functions of gram-negative bacteria by bactenecins. *Infect. Immun.* **1990**, *58*, 3724-3730.
154. Xiong, Y. Q.; Yeaman, M. R.; Bayer, A. S. In vitro antibacterial activities of platelet microbicidal protein and neutrophil defensin against *Staphylococcus aureus* are influenced by antibiotics differing in mechanism of action. *Antimicrob. Agents Chemother.* **1999**, *43*, 1111-1117.
155. Lehrer, R. I.; Barton, A.; Daher, K. A.; Harwig, S. S.; Ganz, T.; Selsted, M. E. Interaction of human defensins with *Escherichia coli*. Mechanism of bactericidal activity. *J. Clin. Invest.* **1989**, *84*, 553-561.
156. Patrzykat, A.; Friedrich, C. L.; Zhang, L.; Mendoza, V.; Hancock, R. E. Sublethal concentrations of pleurocidin-derived antimicrobial peptides inhibit macromolecular synthesis in *Escherichia coli*. *Antimicrob. Agents Chemother.* **2002**, *46*, 605-614.
157. Brotz, H.; Bierbaum, G.; Leopold, K.; Reynolds, P. E.; Sahl, H. G. The lantibiotic mersacidin inhibits peptidoglycan synthesis by targeting lipid II. *Antimicrob. Agents Chemother.* **1998**, *42*, 154-160.
158. Otvos, L., Jr.; O, I.; Rogers, M. E.; Consolvo, P. J.; Condie, B. A.; Lovas, S.; Bulet, P.; Blaszczyk-Thurin, M. Interaction between heat shock proteins and antimicrobial peptides. *Biochemistry* **2000**, *39*, 14150-14159.
159. Park, C. B.; Kim, H. S.; Kim, S. C. Mechanism of action of the antimicrobial peptide buforin II: buforin II kills microorganisms by penetrating the cell membrane and inhibiting cellular functions. *Biochem. Biophys. Res. Commun.* **1998**, *244*, 253-257.
160. Park, C. B.; Yi, K. S.; Matsuzaki, K.; Kim, M. S.; Kim, S. C. Structure-activity analysis of buforin II, a histone H2A-derived antimicrobial peptide: the proline hinge is responsible for the cell-penetrating ability of buforin II. *Proc. Natl. Acad. Sci. U. S. A.* **2000**, *97*, 8245-8250.
161. Kobayashi, S.; Takeshima, K.; Park, C. B.; Kim, S. C.; Matsuzaki, K. Interactions of the novel antimicrobial peptide buforin 2 with lipid bilayers: proline as a translocation promoting factor. *Biochemistry* **2000**, *39*, 8648-8654.

162. Zhang, L.; Benz, R.; Hancock, R. E. Influence of proline residues on the antibacterial and synergistic activities of alpha-helical peptides. *Biochemistry* **1999**, *38*, 8102-8111.
163. Yonezawa, A.; Kuwahara, J.; Fujii, N.; Sugiura, Y. Binding of tachyplesin I to DNA revealed by footprinting analysis: significant contribution of secondary structure to DNA binding and implication for biological action. *Biochemistry* **1992**, *31*, 2998-3004.
164. Shi, J.; Ross, C. R.; Chengappa, M. M.; Sylte, M. J.; McVey, D. S.; Blecha, F. Antibacterial activity of a synthetic peptide (PR-26) derived from PR-39, a proline-arginine-rich neutrophil antimicrobial peptide. *Antimicrob. Agents Chemother.* **1996**, *40*, 115-121.
165. Brogden, K. A.; Ackermann, M.; Huttner, K. M. Detection of anionic antimicrobial peptides in ovine bronchoalveolar lavage fluid and respiratory epithelium. *Infect. Immun.* **1998**, *66*, 5948-5954.
166. Otvos, L., Jr Antibacterial peptides and proteins with multiple cellular targets. *J. Pept. Sci.* **2005**, *11*, 697-706.
167. Gusman, H.; Lendenmann, U.; Grogan, J.; Troxler, R. F.; Oppenheim, F. G. Is salivary histatin 5 a metallopeptide? *Biochim. Biophys. Acta* **2001**, *1545*, 86-95.
168. McEntire, J. C.; Montville, T. J.; Chikindas, M. L. Synergy between nisin and select lactates against *Listeria monocytogenes* is due to the metal cations. *J. Food Prot.* **2003**, *66*, 1631-1636.
169. Ramachandran, R.; Tweten, R. K.; Johnson, A. E. Membrane-dependent conformational changes initiate cholesterol-dependent cytolysin oligomerization and intersubunit beta-strand alignment. *Nat. Struct. Mol. Biol.* **2004**, *11*, 697-705.
170. Giddings, K. S.; Johnson, A. E.; Tweten, R. K. Redefining cholesterol's role in the mechanism of the cholesterol-dependent cytolysins. *Proc. Natl. Acad. Sci. U. S. A.* **2003**, *100*, 11315-11320.
171. Prenner, E. J.; Lewis, R. N.; Jelokhani-Niaraki, M.; Hodges, R. S.; McElhaney, R. N. Cholesterol attenuates the interaction of the antimicrobial peptide gramicidin S with phospholipid bilayer membranes. *Biochim. Biophys. Acta* **2001**, *1510*, 83-92.
172. Barman, H.; Walch, M.; Latinovic-Golic, S.; Dumrese, C.; Dolder, M.; Groscurth, P.; Ziegler, U. Cholesterol in negatively charged lipid bilayers modulates the effect of the antimicrobial protein granulysin. *J. Membr. Biol.* **2006**, *212*, 29-39.
173. Meier-Stephenson, V. C. Quantum Medicine: Novel Applications of Computational Chemistry to the Treatment of Neurological Diseases, Dalhousie University, Halifax, Nova Scotia, 2005.

174. Matsuzaki, K.; Murase, O.; Fujii, N.; Miyajima, K. An antimicrobial peptide, magainin 2, induced rapid flip-flop of phospholipids coupled with pore formation and peptide translocation. *Biochemistry* **1996**, *35*, 11361-11368.
175. Zhang, L.; Rozek, A.; Hancock, R. E. Interaction of cationic antimicrobial peptides with model membranes. *J. Biol. Chem.* **2001**, *276*, 35714-35722.
176. Matsuzaki, K.; Murase, O.; Fujii, N.; Miyajima, K. Translocation of a channel-forming antimicrobial peptide, magainin 2, across lipid bilayers by forming a pore. *Biochemistry* **1995**, *34*, 6521-6526.
177. Yan, S. D.; Fu, J.; Soto, C.; Chen, X.; Zhu, H.; Al-Mohanna, F.; Collison, K.; Zhu, A.; Stern, E.; Saido, T.; Tohyama, M.; Ogawa, S.; Roher, A.; Stern, D. An intracellular protein that binds amyloid-beta peptide and mediates neurotoxicity in Alzheimer's disease. *Nature* **1997**, *389*, 689-695.
178. Abramov, A. Y.; Canevari, L.; Duchen, M. R. Beta-amyloid peptides induce mitochondrial dysfunction and oxidative stress in astrocytes and death of neurons through activation of NADPH oxidase. *J. Neurosci.* **2004**, *24*, 565-575.
179. Huang, H. M.; Fowler, C.; Xu, H.; Zhang, H.; Gibson, G. E. Mitochondrial function in fibroblasts with aging in culture and/or Alzheimer's disease. *Neurobiol. Aging* **2005**, *26*, 839-848.
180. Canevari, L.; Abramov, A. Y.; Duchen, M. R. Toxicity of amyloid beta peptide: tales of calcium, mitochondria, and oxidative stress. *Neurochem. Res.* **2004**, *29*, 637-650.
181. Casley, C. S.; Canevari, L.; Land, J. M.; Clark, J. B.; Sharpe, M. A. Beta-amyloid inhibits integrated mitochondrial respiration and key enzyme activities. *J. Neurochem.* **2002**, *80*, 91-100.
182. Bonev, B.; Watts, A.; Bokvist, M.; Gröbner, G. Electrostatic peptide–lipid interactions of amyloid-beta peptide and pentalysine with membrane surfaces monitored by ³¹P MAS NMR. *Phys. Chem. Chem. Phys.* **2001**, *3*, 2904-2910.
183. Saberwal, G.; Nagaraj, R. Cell-lytic and antibacterial peptides that act by perturbing the barrier function of membranes: facets of their conformational features, structure-function correlations and membrane-perturbing abilities. *Biochim. Biophys. Acta* **1994**, *1197*, 109-131.
184. Levy, O. Antibiotic proteins of polymorphonuclear leukocytes. *Eur. J. Haematol.* **1996**, *56*, 263-277.

185. Tossi, A.; Scocchi, M.; Zanetti, M.; Storici, P.; Gennaro, R. PMAP-37, a novel antibacterial peptide from pig myeloid cells. cDNA cloning, chemical synthesis and activity. *Eur. J. Biochem.* **1995**, *228*, 941-946.
186. Wong, H.; Bowie, J. H.; Carver, J. A. The solution structure and activity of caerin 1.1, an antimicrobial peptide from the Australian green tree frog, *Litoria splendida*. *Eur. J. Biochem.* **1997**, *247*, 545-557.
187. Crescenzi, O.; Tomaselli, S.; Guerrini, R.; Salvadori, S.; D'Ursi, A. M.; Temussi, P. A.; Picone, D. Solution structure of the Alzheimer amyloid beta-peptide (1-42) in an apolar microenvironment. Similarity with a virus fusion domain. *Eur. J. Biochem.* **2002**, *269*, 5642-5648.
188. Sticht, H.; Bayer, P.; Willbold, D.; Dames, S.; Hilbich, C.; Beyreuther, K.; Frank, R. W.; Rosch, P. Structure of amyloid A4-(1-40)-peptide of Alzheimer's disease. *Eur. J. Biochem.* **1995**, *233*, 293-298.
189. Mattson, M. P.; Cheng, B.; Davis, D.; Bryant, K.; Lieberburg, I.; Rydel, R. E. beta-Amyloid peptides destabilize calcium homeostasis and render human cortical neurons vulnerable to excitotoxicity. *J. Neurosci.* **1992**, *12*, 376-389.
190. Arispe, N.; Pollard, H. B.; Rojas, E. beta-Amyloid Ca(2+)-channel hypothesis for neuronal death in Alzheimer disease. *Mol. Cell. Biochem.* **1994**, *140*, 119-125.
191. Lin, H.; Bhatia, R.; Lal, R. Amyloid beta protein forms ion channels: implications for Alzheimer's disease pathophysiology. *FASEB J.* **2001**, *15*, 2433-2444.
192. Dulbecco, R.; Vogt, M. Plaque formation and isolation of pure lines with poliomyelitis viruses. *J. Exp. Med.* **1954**, *99*, 167-182.
193. Fonnum, F.; Myhrer, T.; Paulsen, R. E.; Wangen, K.; Oksengard, A. R. Role of glutamate and glutamate receptors in memory function and Alzheimer's disease. *Ann. N. Y. Acad. Sci.* **1995**, *757*, 475-486.
194. Demuro, A.; Parker, I.; Stutzmann, G. E. Calcium signaling and amyloid toxicity in Alzheimer disease. *J. Biol. Chem.* **2010**, *285*, 12463-12468.
195. Smith, P. K.; Krohn, R. I.; Hermanson, G. T.; Mallia, A. K.; Gartner, F. H.; Provenzano, M. D.; Fujimoto, E. K.; Goeke, N. M.; Olson, B. J.; Klenk, D. C. Measurement of protein using bicinchoninic acid. *Anal. Biochem.* **1985**, *150*, 76-85.
196. Walker, J. M., Ed.; In *The Protein Protocols Handbook*; Humana Press: Totowa, NJ, USA, **2002**; pp. 1146.

197. Akins, R. E.; Tuan, R. S. Measurement of protein in 20 seconds using a microwave BCA assay. *BioTechniques* **1992**, *12*, 496-499.
198. LeVine, H., 3rd Alzheimer's beta-peptide oligomer formation at physiologic concentrations. *Anal. Biochem.* **2004**, *335*, 81-90.
199. Brewer, G. J.; Torricelli, J. R.; Evege, E. K.; Price, P. J. Optimized survival of hippocampal neurons in B27-supplemented Neurobasal, a new serum-free medium combination. *J. Neurosci. Res.* **1993**, *35*, 567-576.
200. Otvos, L., Jr; Szendrei, G. I.; Lee, V. M.; Mantsch, H. H. Human and rodent Alzheimer beta-amyloid peptides acquire distinct conformations in membrane-mimicking solvents. *Eur. J. Biochem.* **1993**, *211*, 249-257.
201. Jensen, M.; Hartmann, T.; Engvall, B.; Wang, R.; Uljon, S. N.; Sennvik, K.; Naslund, J.; Muehlhauser, F.; Nordstedt, C.; Beyreuther, K.; Lannfelt, L. Quantification of Alzheimer amyloid beta peptides ending at residues 40 and 42 by novel ELISA systems. *Mol. Med.* **2000**, *6*, 291-302.
202. Neumann, H.; Wekerle, H. Neuronal control of the immune response in the central nervous system: linking brain immunity to neurodegeneration. *J. Neuropathol. Exp. Neurol.* **1998**, *57*, 1-9.
203. Cho, H.; Proll, S. C.; Szretter, K. J.; Katze, M. G.; Gale, M., Jr; Diamond, M. S. Differential innate immune response programs in neuronal subtypes determine susceptibility to infection in the brain by positive-stranded RNA viruses. *Nat. Med.* **2013**, *19*, 458-464.
204. Hung, J.; Chansard, M.; Ousman, S. S.; Nguyen, M. D.; Colicos, M. A. Activation of microglia by neuronal activity: Results from a new in vitro paradigm based on neuronal-silicon interfacing technology. *Brain Behav. Immun.* **2010**, *24*, 31-40.
205. Butovsky, O.; Talpalar, A. E.; Ben-Yaakov, K.; Schwartz, M. Activation of microglia by aggregated β -amyloid or lipopolysaccharide impairs MHC-II expression and renders them cytotoxic whereas IFN- γ and IL-4 render them protective. *Molecular and Cellular Neuroscience* **2005**, *29*, 381-393.
206. Biber, K.; Neumann, H.; Inoue, K.; Boddeke, H. W. Neuronal 'On' and 'Off' signals control microglia. *Trends Neurosci.* **2007**, *30*, 596-602.
207. Yates, C. M.; Butterworth, J.; Tennant, M. C.; Gordon, A. Enzyme activities in relation to pH and lactate in postmortem brain in Alzheimer-type and other dementias. *J. Neurochem.* **1990**, *55*, 1624-1630.

208. Clausen, T.; Khaldi, A.; Zauner, A.; Reinert, M.; Doppenberg, E.; Menzel, M.; Soukup, J.; Alves, O. L.; Bullock, M. R. Cerebral acid-base homeostasis after severe traumatic brain injury. *J. Neurosurg.* **2005**, *103*, 597-607.
209. Timofeev, I.; Carpenter, K. L.; Nortje, J.; Al-Rawi, P. G.; O'Connell, M. T.; Czosnyka, M.; Smielewski, P.; Pickard, J. D.; Menon, D. K.; Kirkpatrick, P. J.; Gupta, A. K.; Hutchinson, P. J. Cerebral extracellular chemistry and outcome following traumatic brain injury: a microdialysis study of 223 patients. *Brain* **2011**, *134*, 484-494.
210. DeSalles, A. A.; Kontos, H. A.; Becker, D. P.; Yang, M. S.; Ward, J. D.; Moulton, R.; Gruemer, H. D.; Lutz, H.; Maset, A. L.; Jenkins, L. Prognostic significance of ventricular CSF lactic acidosis in severe head injury. *J. Neurosurg.* **1986**, *65*, 615-624.
211. Ratledge, C.; Wilkinson, S. G. *Microbial lipids*; Academic Press: London ; Toronto, 1988; .
212. Lehrer, R. I.; Rosenman, M.; Harwig, S. S.; Jackson, R.; Eisenhauer, P. Ultrasensitive assays for endogenous antimicrobial polypeptides. *J. Immunol. Methods* **1991**, *137*, 167-173.
213. du Toit, E. A.; Rautenbach, M. A sensitive standardised micro-gel well diffusion assay for the determination of antimicrobial activity. *Journal of Microbiological Methods* **2000/10**, *42*, 159-165.
214. Patel, J. P.; Tenover, F. C.; Turnidge, J. D.; Jorgenson, J. H. In *Susceptibility Test Methods - Dilution and Disk Diffusion Methods*; Versalovic, J., Carroll, K. C., Funke, G., Jorgensen, J. H., Landry, M. L. and Warnock, D. W., Eds.; Manual of Clinical Microbiology; ASM Press: Washington, DC, USA, 2011; Vol. 1, pp. 1122-1143.
215. Socia, S. J.; Kirby, J. E.; Washicosky, K. J.; Tucker, S. M.; Ingelsson, M.; Hyman, B.; Burton, M. A.; Goldstein, L. E.; Duong, S.; Tanzi, R. E.; Moir, R. D. The Alzheimer's disease-associated amyloid beta-protein is an antimicrobial peptide. *PLoS One* **2010**, *5*, e9505.
216. Anantharaman, A.; Rizvi, M. S.; Sahal, D. Synergy with rifampin and kanamycin enhances potency, kill kinetics, and selectivity of de novo-designed antimicrobial peptides. *Antimicrob. Agents Chemother.* **2010**, *54*, 1693-1699.
217. Wang, M. S.; Boddapati, S.; Sierks, M. R. Cyclodextrins promote protein aggregation posing risks for therapeutic applications. *Biochem. Biophys. Res. Commun.* **2009**, *386*, 526-531.
218. Hassall, D. G.; Graham, A. Changes in free cholesterol content, measured by filipin fluorescence and flow cytometry, correlate with changes in cholesterol biosynthesis in THP-1 macrophages. *Cytometry* **1995**, *21*, 352-362.
219. Dobson, C. B.; Itzhaki, R. F. Herpes simplex virus type 1 and Alzheimer's disease. *Neurobiol. Aging* **1999**, *20*, 457-465.

220. Gajdusek, D. C. Unconventional viruses and the origin and disappearance of kuru. *Science* **1977**, *197*, 943-960.
221. Heston, L. L.; Mastri, A. R. The genetics of Alzheimer's disease: associations with hematologic malignancy and Down's syndrome. *Arch. Gen. Psychiatry* **1977**, *34*, 976-981.
222. Schellenberg, G. D. Early Alzheimer's disease genetics. *J. Alzheimers Dis.* **2006**, *9*, 367-372.
223. Bertram, L.; Tanzi, R. E. The genetics of Alzheimer's disease. *Prog. Mol. Biol. Transl. Sci.* **2012**, *107*, 79-100.
224. Wadsworth, J. D.; Joiner, S.; Linehan, J. M.; Asante, E. A.; Brandner, S.; Collinge, J. Review. The origin of the prion agent of kuru: molecular and biological strain typing. *Philos. Trans. R. Soc. Lond. B. Biol. Sci.* **2008**, *363*, 3747-3753.
225. Wadsworth, J. D.; Joiner, S.; Linehan, J. M.; Desbruslais, M.; Fox, K.; Cooper, S.; Cronier, S.; Asante, E. A.; Mead, S.; Brandner, S.; Hill, A. F.; Collinge, J. Kuru prions and sporadic Creutzfeldt-Jakob disease prions have equivalent transmission properties in transgenic and wild-type mice. *Proc. Natl. Acad. Sci. U. S. A.* **2008**, *105*, 3885-3890.
226. Ball, M. J. "Limbic predilection in Alzheimer dementia: is reactivated herpesvirus involved?". *Can. J. Neurol. Sci.* **1982**, *9*, 303-306.
227. Katan, M.; Moon, Y. P.; Paik, M. C.; Sacco, R. L.; Wright, C. B.; Elkind, M. S. Infectious burden and cognitive function: the Northern Manhattan Study. *Neurology* **2013**, *80*, 1209-1215.
228. Howell, M. D.; Jones, J. F.; Kisich, K. O.; Streib, J. E.; Gallo, R. L.; Leung, D. Y. Selective killing of vaccinia virus by LL-37: implications for eczema vaccinatum. *J. Immunol.* **2004**, *172*, 1763-1767.
229. Gordon, Y. J.; Huang, L. C.; Romanowski, E. G.; Yates, K. A.; Proske, R. J.; McDermott, A. M. Human cathelicidin (LL-37), a multifunctional peptide, is expressed by ocular surface epithelia and has potent antibacterial and antiviral activity. *Curr. Eye Res.* **2005**, *30*, 385-394.
230. Daher, K. A.; Selsted, M. E.; Lehrer, R. I. Direct inactivation of viruses by human granulocyte defensins. *J. Virol.* **1986**, *60*, 1068-1074.
231. Lehrer, R. I.; Daher, K.; Ganz, T.; Selsted, M. E. Direct inactivation of viruses by MCP-1 and MCP-2, natural peptide antibiotics from rabbit leukocytes. *J. Virol.* **1985**, *54*, 467-472.
232. Tamamura, H.; Murakami, T.; Masuda, M.; Otaka, A.; Takada, W.; Ibuka, T.; Nakashima, H.; Waki, M.; Matsumoto, A.; Yamamoto, N. Structure-activity relationships of an anti-HIV peptide, T22. *Biochem. Biophys. Res. Commun.* **1994**, *205*, 1729-1735.

233. Murakami, T.; Niwa, M.; Tokunaga, F.; Miyata, T.; Iwanaga, S. Direct virus inactivation of tachyplesin I and its isopeptides from horseshoe crab hemocytes. *Chemotherapy* **1991**, *37*, 327-334.
234. Wachinger, M.; Saermark, T.; Erfle, V. Influence of amphipathic peptides on the HIV-1 production in persistently infected T lymphoma cells. *FEBS Lett.* **1992**, *309*, 235-241.
235. Wachinger, M.; Kleinschmidt, A.; Winder, D.; von Pechmann, N.; Ludvigsen, A.; Neumann, M.; Holle, R.; Salmons, B.; Erfle, V.; Brack-Werner, R. Antimicrobial peptides melittin and cecropin inhibit replication of human immunodeficiency virus 1 by suppressing viral gene expression. *J. Gen. Virol.* **1998**, *79 (Pt. 4)*, 731-740.
236. Furman, P. A.; Coen, D. M.; St Clair, M. H.; Schaffer, P. A. Acyclovir-resistant mutants of herpes simplex virus type 1 express altered DNA polymerase or reduced acyclovir phosphorylating activities. *J. Virol.* **1981**, *40*, 936-941.
237. Uribe, L. H.; Olarte, E. C.; Castillo, G. T. In vitro antiviral activity of *Chamaecrista nictitans* (Fabaceae) against herpes simplex virus: Biological characterization of mechanisms of action. *Rev. Biol. Trop.* **2004**, *52*, 807-816.
238. Cummings, J. L. Alzheimer's disease clinical trials: changing the paradigm. *Curr. Psychiatry Rep.* **2011**, *13*, 437-442.
239. Mullane, K.; Williams, M. Alzheimer's therapeutics: continued clinical failures question the validity of the amyloid hypothesis-but what lies beyond? *Biochem. Pharmacol.* **2013**, *85*, 289-305.
240. Schillinger, J. A.; Xu, F.; Sternberg, M. R.; Armstrong, G. L.; Lee, F. K.; Nahmias, A. J.; McQuillan, G. M.; Louis, M. E.; Markowitz, L. E. National seroprevalence and trends in herpes simplex virus type 1 in the United States, 1976-1994. *Sex. Transm. Dis.* **2004**, *31*, 753-760.
241. Sperling, R. A.; Aisen, P. S.; Beckett, L. A.; Bennett, D. A.; Craft, S.; Fagan, A. M.; Iwatsubo, T.; Jack Jr., C. R.; Kaye, J.; Montine, T. J.; Park, D. C.; Reiman, E. M.; Rowe, C. C.; Siemers, E.; Stern, Y.; Yaffe, K.; Carrillo, M. C.; Thies, B.; Morrison-Bogorad, M.; Wagster, M. V.; Phelps, C. H. Toward defining the preclinical stages of Alzheimer's disease: Recommendations from the National Institute on Aging-Alzheimer's Association workgroups on diagnostic guidelines for Alzheimer's disease. *Alzheimer's and Dementia* **2011**, *7*, 280-292.
242. Bouwman, F. H.; Schoonenboom, N. S.; Verwey, N. A.; van Elk, E. J.; Kok, A.; Blankenstein, M. A.; Scheltens, P.; van der Flier, W. M. CSF biomarker levels in early and late onset Alzheimer's disease. *Neurobiol. Aging* **2009**, *30*, 1895-1901.

243. Bateman, R. J.; Munsell, L. Y.; Morris, J. C.; Swarm, R.; Yarasheski, K. E.; Holtzman, D. M. Human amyloid-beta synthesis and clearance rates as measured in cerebrospinal fluid in vivo. *Nat. Med.* **2006**, *12*, 856-861.
244. Matsuzaki, K.; Sugishita, K.; Fujii, N.; Miyajima, K. Molecular basis for membrane selectivity of an antimicrobial peptide, magainin 2. *Biochemistry* **1995**, *34*, 3423-3429.
245. Dathe, M.; Wieprecht, T. Structural features of helical antimicrobial peptides: their potential to modulate activity on model membranes and biological cells. *Biochim. Biophys. Acta* **1999**, *1462*, 71-87.
246. Glukhov, E.; Stark, M.; Burrows, L. L.; Deber, C. M. Basis for selectivity of cationic antimicrobial peptides for bacterial versus mammalian membranes. *J. Biol. Chem.* **2005**, *280*, 33960-33967.
247. Duckworth, D. H.; Bevers, E. M.; Verkleij, A. J.; Op den Kamp, J. A.; van Deenen, L. L. Action of phospholipase A2 and phospholipase C on *Escherichia coli*. *Arch. Biochem. Biophys.* **1974**, *165*, 379-387.
248. Rothman, J. E.; Kennedy, E. P. Asymmetrical distribution of phospholipids in the membrane of *Bacillus megaterium*. *J. Mol. Biol.* **1977**, *110*, 603-618.
249. Neville, F.; Cahuzac, M.; Konovalov, O.; Ishitsuka, Y.; Lee, K. Y.; Kuzmenko, I.; Kale, G. M.; Gidalevitz, D. Lipid headgroup discrimination by antimicrobial peptide LL-37: insight into mechanism of action. *Biophys. J.* **2006**, *90*, 1275-1287.
250. Helmerhorst, E. J.; Reijnders, I. M.; van 't Hof, W.; Veerman, E. C.; Nieuw Amerongen, A. V. A critical comparison of the hemolytic and fungicidal activities of cationic antimicrobial peptides. *FEBS Lett.* **1999**, *449*, 105-110.
251. Hong, J.; Oren, Z.; Shai, Y. Structure and organization of hemolytic and nonhemolytic diastereomers of antimicrobial peptides in membranes. *Biochemistry* **1999**, *38*, 16963-16973.
252. Tytler, E. M.; Anantharamaiah, G. M.; Walker, D. E.; Mishra, V. K.; Palgunachari, M. N.; Segrest, J. P. Molecular basis for prokaryotic specificity of magainin-induced lysis. *Biochemistry* **1995**, *34*, 4393-4401.
253. Turner, J. D.; Rouser, G. Precise quantitative determination of human blood lipids by thin-layer and triethylaminoethylcellulose column chromatography. I. Erythrocyte lipids. *Anal. Biochem.* **1970**, *38*, 423-436.
254. Sal-Man, N.; Oren, Z.; Shai, Y. Preassembly of membrane-active peptides is an important factor in their selectivity toward target cells. *Biochemistry* **2002**, *41*, 11921-11930.

255. de Kroon, A. I.; de Gier, J.; de Kruijff, B. The effect of a membrane potential on the interaction of mastoparan X, a mitochondrial presequence, and several regulatory peptides with phospholipid vesicles. *Biochim. Biophys. Acta* **1991**, *1068*, 111-124.
256. Sansom, M. S. The biophysics of peptide models of ion channels. *Prog. Biophys. Mol. Biol.* **1991**, *55*, 139-235.
257. Vaz Gomes, A.; de Waal, A.; Berden, J. A.; Westerhoff, H. V. Electric potentiation, cooperativity, and synergism of magainin peptides in protein-free liposomes. *Biochemistry* **1993**, *32*, 5365-5372.
258. Rink, T. J.; Hladky, S. B. In Ellory, J. C., Young, J. D., Eds.; Red Cell Membranes - A Methodological Approach; Academic Press: London, 1982; pp. 321-334.
259. Laris, P. C.; Pershadsingh, H. A. Estimations of membrane potentials in *Streptococcus faecalis* by means of a fluorescent probe. *Biochem. Biophys. Res. Commun.* **1974**, *57*, 620-626.
260. Zilberstein, D.; Schuldiner, S.; Padan, E. Proton electrochemical gradient in *Escherichia coli* cells and its relation to active transport of lactose. *Biochemistry* **1979**, *18*, 669-673.
261. Cruciani, R. A.; Barker, J. L.; Zasloff, M.; Chen, H. C.; Colamonici, O. Antibiotic magainins exert cytolytic activity against transformed cell lines through channel formation. *Proc. Natl. Acad. Sci. U. S. A.* **1991**, *88*, 3792-3796.
262. Diaz-Achirica, P.; Ubach, J.; Guinea, A.; Andreu, D.; Rivas, L. The plasma membrane of *Leishmania donovani* promastigotes is the main target for CA(1-8)M(1-18), a synthetic cecropin A-melittin hybrid peptide. *Biochem. J.* **1998**, *330 (Pt. 1)*, 453-460.
263. Karp, G. *Cell and molecular biology: concepts and experiments*; J. Wiley: New York, 2002; , pp 785.
264. Yankner, B. A.; Dawes, L. R.; Fisher, S.; Villa-Komaroff, L.; Oster-Granite, M. L.; Neve, R. L. Neurotoxicity of a fragment of the amyloid precursor associated with Alzheimer's disease. *Science* **1989**, *245*, 417-420.
265. Pike, C. J.; Walencewicz, A. J.; Glabe, C. G.; Cotman, C. W. In vitro aging of beta-amyloid protein causes peptide aggregation and neurotoxicity. *Brain Res.* **1991**, *563*, 311-314.
266. Mosmann, T. Rapid colorimetric assay for cellular growth and survival: application to proliferation and cytotoxicity assays. *J. Immunol. Methods* **1983**, *65*, 55-63.

267. Berridge, M. V.; Tan, A. S. Characterization of the cellular reduction of 3-(4,5-dimethylthiazol-2-yl)-2,5-diphenyltetrazolium bromide (MTT): subcellular localization, substrate dependence, and involvement of mitochondrial electron transport in MTT reduction. *Arch. Biochem. Biophys.* **1993**, *303*, 474-482.
268. Helmerhorst, E. J.; Breeuwer, P.; van't Hof, W.; Walgreen-Weterings, E.; Oomen, L. C.; Veerman, E. C.; Amerongen, A. V.; Abee, T. The cellular target of histatin 5 on *Candida albicans* is the energized mitochondrion. *J. Biol. Chem.* **1999**, *274*, 7286-7291.
269. Eliassen, L. T.; Berge, G.; Leknessund, A.; Wikman, M.; Lindin, I.; Lokke, C.; Ponthan, F.; Johnsen, J. I.; Sveinbjornsson, B.; Kogner, P.; Flaegstad, T.; Rekdal, O. The antimicrobial peptide, lactoferricin B, is cytotoxic to neuroblastoma cells in vitro and inhibits xenograft growth in vivo. *Int. J. Cancer* **2006**, *119*, 493-500.
270. Mereschkowsky, K. Theorie der zwei Plasmaarten als Grundlage der Symbiogenese, einer neuen Lehre von der Entstehung der Organismen. *Biol. Centralbl.* **1910**, *30*, 353-367.
271. Wallin, I. E. The Mitochondria Problem. *The American Naturalist* **1923**, *57*, 255-261.
272. Wallin, I. E. *Symbiogenesis and the Origin of Species*; The Williams & Wilkins Company: Baltimore, MD, U.S.A., 1927; , pp 171.
273. Lustbader, J. W.; Cirilli, M.; Lin, C.; Xu, H. W.; Takuma, K.; Wang, N.; Caspersen, C.; Chen, X.; Pollak, S.; Chaney, M.; Trinchese, F.; Liu, S.; Gunn-Moore, F.; Lue, L. F.; Walker, D. G.; Kuppusamy, P.; Zewier, Z. L.; Arancio, O.; Stern, D.; Yan, S. S.; Wu, H. ABAD directly links Abeta to mitochondrial toxicity in Alzheimer's disease. *Science* **2004**, *304*, 448-452.
274. Manczak, M.; Anekonda, T. S.; Henson, E.; Park, B. S.; Quinn, J.; Reddy, P. H. Mitochondria are a direct site of A beta accumulation in Alzheimer's disease neurons: implications for free radical generation and oxidative damage in disease progression. *Hum. Mol. Genet.* **2006**, *15*, 1437-1449.
275. Swerdlow, R. H.; Khan, S. M. A "mitochondrial cascade hypothesis" for sporadic Alzheimer's disease. *Med. Hypotheses* **2004**, *63*, 8-20.
276. Swerdlow, R. H.; Burns, J. M.; Khan, S. M. The Alzheimer's disease mitochondrial cascade hypothesis. *J. Alzheimers Dis.* **2010**, *20 Suppl 2*, S265-79.
277. Wang, X.; Perry, G.; Smith, M. A.; Zhu, X. Amyloid-beta-derived diffusible ligands cause impaired axonal transport of mitochondria in neurons. *Neurodegener Dis.* **2010**, *7*, 56-59.
278. Eckert, A.; Schulz, K. L.; Rhein, V.; Gotz, J. Convergence of amyloid-beta and tau pathologies on mitochondria in vivo. *Mol. Neurobiol.* **2010**, *41*, 107-114.

279. Eckert, A.; Schmitt, K.; Gotz, J. Mitochondrial dysfunction - the beginning of the end in Alzheimer's disease? Separate and synergistic modes of tau and amyloid-beta toxicity. *Alzheimers Res. Ther.* **2011**, *3*, 15.
280. Keil, U.; Hauptmann, S.; Bonert, A.; Scherping, I.; Eckert, A.; Muller, W. E. Mitochondrial dysfunction induced by disease relevant AbetaPP and tau protein mutations. *J. Alzheimers Dis.* **2006**, *9*, 139-146.
281. Atamna, H.; Frey, W. H., 2nd Mechanisms of mitochondrial dysfunction and energy deficiency in Alzheimer's disease. *Mitochondrion* **2007**, *7*, 297-310.
282. Davis, J. N.; Hunnicutt Jr, E. J.; Chisholm, J. C. A mitochondrial bottleneck hypothesis of Alzheimer's disease. *Mol. Med. Today* **1995**, *1*, 240-247.
283. Gibson, G. E.; Starkov, A.; Blass, J. P.; Ratan, R. R.; Beal, M. F. Cause and consequence: Mitochondrial dysfunction initiates and propagates neuronal dysfunction, neuronal death and behavioral abnormalities in age-associated neurodegenerative diseases. *Biochimica et Biophysica Acta (BBA) - Molecular Basis of Disease* **2010**, *1802*, 122-134.
284. Dragicevic, N.; Mamcarz, M.; Zhu, Y.; Buzzeo, R.; Tan, J.; Arendash, G. W.; Bradshaw, P. C. Mitochondrial amyloid-beta levels are associated with the extent of mitochondrial dysfunction in different brain regions and the degree of cognitive impairment in Alzheimer's transgenic mice. *J. Alzheimers Dis.* **2010**, *20 Suppl 2*, S535-50.
285. Hsu, M. J.; Sheu, J. R.; Lin, C. H.; Shen, M. Y.; Hsu, C. Y. Mitochondrial mechanisms in amyloid beta peptide-induced cerebrovascular degeneration. *Biochim. Biophys. Acta* **2010**, *1800*, 290-296.
286. Riemer, J.; Kins, S. Axonal Transport and Mitochondrial Dysfunction in Alzheimer's Disease. *Neurodegener Dis.* **2012**.
287. Ceron, J. M.; Contreras-Moreno, J.; Puertollano, E.; de Cienfuegos, G. A.; Puertollano, M. A.; de Pablo, M. A. The antimicrobial peptide cecropin A induces caspase-independent cell death in human promyelocytic leukemia cells. *Peptides* **2010**, *31*, 1494-1503.
288. Hoskin, D. W.; Ramamoorthy, A. Studies on anticancer activities of antimicrobial peptides. *Biochim. Biophys. Acta* **2008**, *1778*, 357-375.
289. Schweizer, F. Cationic amphiphilic peptides with cancer-selective toxicity. *Eur. J. Pharmacol.* **2009**, *625*, 190-194.
290. Bhutia, S. K.; Maiti, T. K. Targeting tumors with peptides from natural sources. *Trends Biotechnol.* **2008**, *26*, 210-217.

291. Han, S. I.; Kim, Y. S.; Kim, T. H. Role of apoptotic and necrotic cell death under physiologic conditions. *BMB Rep.* **2008**, *41*, 1-10.
292. Wiechelman, K. J.; Braun, R. D.; Fitzpatrick, J. D. Investigation of the bicinchoninic acid protein assay: identification of the groups responsible for color formation. *Anal. Biochem.* **1988**, *175*, 231-237.
293. Ray, S. D.; Mehendale, H. M. In *Apoptosis*; Editor-in-Chief: Philip Wexler, Ed.; Encyclopedia of Toxicology (Second Edition); Elsevier: New York, 2005; pp. 153-167.
294. Behl, C.; Davis, J. B.; Klier, F. G.; Schubert, D. Amyloid beta peptide induces necrosis rather than apoptosis. *Brain Res.* **1994**, *645*, 253-264.
295. Loo, D. T.; Copani, A.; Pike, C. J.; Whittemore, E. R.; Walencewicz, A. J.; Cotman, C. W. Apoptosis is induced by beta-amyloid in cultured central nervous system neurons. *Proc. Natl. Acad. Sci. U. S. A.* **1993**, *90*, 7951-7955.
296. LaFerla, F. M.; Tinkle, B. T.; Bieberich, C. J.; Haudenschild, C. C.; Jay, G. The Alzheimer's A beta peptide induces neurodegeneration and apoptotic cell death in transgenic mice. *Nat. Genet.* **1995**, *9*, 21-30.
297. Kienlen-Campard, P.; Miolet, S.; Tasiaux, B.; Octave, J. N. Intracellular amyloid-beta 1-42, but not extracellular soluble amyloid-beta peptides, induces neuronal apoptosis. *J. Biol. Chem.* **2002**, *277*, 15666-15670.
298. Cha, M. Y.; Han, S. H.; Son, S. M.; Hong, H. S.; Choi, Y. J.; Byun, J.; Mook-Jung, I. Mitochondria-specific accumulation of amyloid beta induces mitochondrial dysfunction leading to apoptotic cell death. *PLoS One* **2012**, *7*, e34929.
299. Yanagisawa, K.; Odaka, A.; Suzuki, N.; Ihara, Y. GM1 ganglioside-bound amyloid beta-protein (A beta): a possible form of preamyloid in Alzheimer's disease. *Nat. Med.* **1995**, *1*, 1062-1066.
300. Yanagisawa, K. GM1 ganglioside and the seeding of amyloid in Alzheimer's disease: endogenous seed for Alzheimer amyloid. *Neuroscientist* **2005**, *11*, 250-260.
301. Pakkenberg, B.; Gundersen, H. J. Neocortical neuron number in humans: effect of sex and age. *J. Comp. Neurol.* **1997**, *384*, 312-320.
302. Pakkenberg, B.; Pelvig, D.; Marnier, L.; Bundgaard, M. J.; Gundersen, H. J.; Nyengaard, J. R.; Regeur, L. Aging and the human neocortex. *Exp. Gerontol.* **2003**, *38*, 95-99.
303. Chudler, E. H. Brain Facts and Figures. <http://faculty.washington.edu/chudler/facts.html> (accessed 02/08, 2014).

304. Farfara, D.; Lifshitz, V.; Frenkel, D. Neuroprotective and Neurotoxic Properties of Glial Cells in the Pathogenesis of Alzheimer's Disease. *J. Cell. Mol. Med.* **2008**, *12*, 762-780.
305. LaFerla, F. M.; Green, K. N.; Oddo, S. Intracellular amyloid-beta in Alzheimer's disease. *Nat. Rev. Neurosci.* **2007**, *8*, 499-509.
306. Vina, J.; Lloret, A.; Valles, S. L.; Borrás, C.; Badia, M. C.; Pallardo, F. V.; Sastre, J.; Alonso, M. D. Effect of gender on mitochondrial toxicity of Alzheimer's Abeta peptide. *Antioxid. Redox Signal.* **2007**, *9*, 1677-1690.
307. Tang, Y.; Nyengaard, J. R.; De Groot, D. M.; Gundersen, H. J. Total regional and global number of synapses in the human brain neocortex. *Synapse* **2001**, *41*, 258-273.
308. Alvarez-Buylla, A.; Lim, D. A. For the long run: maintaining germinal niches in the adult brain. *Neuron* **2004**, *41*, 683-686.
309. Alvarez-Buylla, A.; Seri, B.; Doetsch, F. Identification of neural stem cells in the adult vertebrate brain. *Brain Res. Bull.* **2002**, *57*, 751-758.
310. Zhao, C.; Deng, W.; Gage, F. H. Mechanisms and Functional Implications of Adult Neurogenesis. *Cell* **2008**, *132*, 645-660.
311. Demars, M.; Hu, Y. S.; Gadadhar, A.; Lazarov, O. Impaired neurogenesis is an early event in the etiology of familial Alzheimer's disease in transgenic mice. *J. Neurosci. Res.* **2010**, *88*, 2103-2117.
312. Trouche, S.; Bontempi, B.; Roulet, P.; Rampon, C. Recruitment of adult-generated neurons into functional hippocampal networks contributes to updating and strengthening of spatial memory. *Proc. Natl. Acad. Sci. U. S. A.* **2009**, *106*, 5919-5924.
313. Aimone, J. B.; Wiles, J.; Gage, F. H. Potential role for adult neurogenesis in the encoding of time in new memories. *Nat. Neurosci.* **2006**, *9*, 723-727.
314. Haughey, N. J.; Nath, A.; Chan, S. L.; Borchard, A. C.; Rao, M. S.; Mattson, M. P. Disruption of neurogenesis by amyloid beta-peptide, and perturbed neural progenitor cell homeostasis, in models of Alzheimer's disease. *J. Neurochem.* **2002**, *83*, 1509-1524.
315. Millet, P.; Lages, C. S.; Haik, S.; Nowak, E.; Allemand, I.; Granotier, C.; Boussin, F. D. Amyloid-beta peptide triggers Fas-independent apoptosis and differentiation of neural progenitor cells. *Neurobiol. Dis.* **2005**, *19*, 57-65.
316. McLaurin, J.; Chakrabartty, A. Membrane disruption by Alzheimer beta-amyloid peptides mediated through specific binding to either phospholipids or gangliosides. Implications for neurotoxicity. *J. Biol. Chem.* **1996**, *271*, 26482-26489.

317. Lopez-Toledano, M. A.; Shelanski, M. L. Neurogenic effect of beta-amyloid peptide in the development of neural stem cells. *J. Neurosci.* **2004**, *24*, 5439-5444.
318. Lazarov, O.; Marr, R. A. Neurogenesis and Alzheimer's disease: At the crossroads. *Exp. Neurol.* **2010**, *223*, 267-281.
319. Estus, S.; Tucker, H. M.; van Rooyen, C.; Wright, S.; Brigham, E. F.; Wogulis, M.; Rydel, R. E. Aggregated amyloid-beta protein induces cortical neuronal apoptosis and concomitant "apoptotic" pattern of gene induction. *J. Neurosci.* **1997**, *17*, 7736-7745.
320. Waldner, H. The role of innate immune responses in autoimmune disease development. *Autoimmun. Rev.* **2009**, *8*, 400-404.
321. Witebsky, E.; Rose, N. R.; Terplan, K.; Paine, J. R.; Egan, R. W. Chronic thyroiditis and autoimmunization. *J. Am. Med. Assoc.* **1957**, *164*, 1439-1447.
322. Rose, N. R.; Bona, C. Defining criteria for autoimmune diseases (Witebsky's postulates revisited). *Immunol. Today* **1993**, *14*, 426-430.
323. Zagorski, M. G.; Yang, J.; Shao, H.; Ma, K.; Zeng, H.; Hong, A. Methodological and chemical factors affecting amyloid beta peptide amyloidogenicity. *Methods Enzymol.* **1999**, *309*, 189-204.
324. Christian, A. E.; Haynes, M. P.; Phillips, M. C.; Rothblat, G. H. Use of cyclodextrins for manipulating cellular cholesterol content. *J. Lipid Res.* **1997**, *38*, 2264-2272.
325. Zidovetzki, R.; Levitan, I. Use of cyclodextrins to manipulate plasma membrane cholesterol content: Evidence, misconceptions and control strategies. *Biochim. Biophys. Acta - Biomembranes* **2007**, *1768*, 1311-1324.

Chapter III

1. Tomasz, A.; Waks, S. Mechanism of action of penicillin: triggering of the pneumococcal autolytic enzyme by inhibitors of cell wall synthesis. *Proc. Natl. Acad. Sci. U. S. A.* **1975**, *72*, 4162-4166.

2. Nau, R.; Eiffert, H. Modulation of release of proinflammatory bacterial compounds by antibacterials: potential impact on course of inflammation and outcome in sepsis and meningitis. *Clin. Microbiol. Rev.* **2002**, *15*, 95-110.
3. Goto, H.; Nakamura, S. Liberation of endotoxin from *Escherichia coli* by addition of antibiotics. *Jpn. J. Exp. Med.* **1980**, *50*, 35-43.
4. Crosby, H. A.; Bion, J. F.; Penn, C. W.; Elliott, T. S. Antibiotic-induced release of endotoxin from bacteria in vitro. *J. Med. Microbiol.* **1994**, *40*, 23-30.
5. Soto, A.; Evans, T. J.; Cohen, J. Proinflammatory cytokine production by human peripheral blood mononuclear cells stimulated with cell-free supernatants of Viridans streptococci. *Cytokine* **1996**, *8*, 300-304.
6. van Langevelde, P.; van Dissel, J. T.; Ravensbergen, E.; Appelmelk, B. J.; Schrijver, I. A.; Groeneveld, P. H. Antibiotic-induced release of lipoteichoic acid and peptidoglycan from *Staphylococcus aureus*: quantitative measurements and biological reactivities. *Antimicrob. Agents Chemother.* **1998**, *42*, 3073-3078.
7. Mattie, H.; Stuertz, K.; Nau, R.; van Dissel, J. T. Pharmacodynamics of antibiotics with respect to bacterial killing of and release of lipoteichoic acid by *Streptococcus pneumoniae*. *J. Antimicrob. Chemother.* **2005**, *56*, 154-159.
8. Heumann, D.; Barras, C.; Severin, A.; Glauser, M. P.; Tomasz, A. Gram-positive cell walls stimulate synthesis of tumor necrosis factor α and interleukin-6 by human monocytes. *Infect. Immun.* **1994**, *62*, 2715-2721.
9. Heumann, D.; Roger, T. Initial responses to endotoxins and Gram-negative bacteria. *Clinica Chimica Acta* **2002**, *323*, 59-72.
10. Heumann, D.; Glauser, M. P.; Calandra, T. Molecular basis of host-pathogen interaction in septic shock. *Curr. Opin. Microbiol.* **1998**, *1*, 49-55.
11. Elson, G.; Dunn-Siegrist, I.; Daubeuf, B.; Pugin, J. Contribution of Toll-like receptors to the innate immune response to Gram-negative and Gram-positive bacteria. *Blood* **2007**, *109*, 1574-1583.
12. Ginsburg, I. The role of bacteriolysis in the pathophysiology of inflammation, infection and post-infectious sequelae. *APMIS* **2002**, *110*, 753-770.
13. Kirikae, T.; Nakano, M.; Morrison, D. C. Antibiotic-induced endotoxin release from bacteria and its clinical significance. *Microbiol. Immunol.* **1997**, *41*, 285-294.

14. Bucklin, S. E.; Fujihara, Y.; Leeson, M. C.; Morrison, D. C. Differential antibiotic-induced release of endotoxin from gram-negative bacteria. *Eur. J. Clin. Microbiol. Infect. Dis.* **1994**, *13 Suppl 1*, S43-51.
15. Utsui, Y.; Ohya, S.; Takenouchi, Y.; Tajima, M.; Sugawara, S.; Deguchi, K.; Suginaka, H. Release of lipoteichoic acid from *Staphylococcus aureus* by treatment with cefmetazole and other β -lactam antibiotics. *J. Antibiot. (Tokyo)* **1983**, *36*, 1380-1386.
16. Yao, J. D. C.; Moellering, J., Robert C. In *Antibacterial Agents*; Versalovic, J., Carroll, K. C., Funke, G., Jorgensen, J. H., Landry, M. L. and Warnock, D. W., Eds.; Manual of Clinical Microbiology; ASM Press: Washington, DC, USA, 2011; Vol. 1, pp. 1043-1081.
17. Page, B.; Page, M.; Noel, C. A new fluorometric assay for cytotoxicity measurements in-vitro. *Int. J. Oncol.* **1993**, *3*, 473-476.
18. Ahmed, S. A.; Gogal, R. M., Jr; Walsh, J. E. A new rapid and simple non-radioactive assay to monitor and determine the proliferation of lymphocytes: an alternative to [3H]thymidine incorporation assay. *J. Immunol. Methods* **1994**, *170*, 211-224.
19. O'Brien, J.; Wilson, I.; Orton, T.; Pognan, F. Investigation of the Alamar Blue (resazurin) fluorescent dye for the assessment of mammalian cell cytotoxicity. *Eur. J. Biochem.* **2000**, *267*, 5421-5426.
20. International Bureau of Weights and Measures. The International System of Units (SI). **2006**, 88.

Chapter IV

1. Sewald, N.; Jakubke, H., Eds.; In *Peptides: Chemistry and Biology*; Wiley-VCH: Weinheim, Germany, **2002**.
2. Delgado, C.; Francis, G. E.; Fisher, D. The uses and properties of PEG-linked proteins. *Crit. Rev. Ther. Drug Carrier Syst.* **1992**, *9*, 249-304.
3. Pettit, D. K.; Bonnert, T. P.; Eisenman, J.; Srinivasan, S.; Paxton, R.; Beers, C.; Lynch, D.; Miller, B.; Yost, J.; Grabstein, K. H.; Gombotz, W. R. Structure-function studies of interleukin 15 using site-specific mutagenesis, polyethylene glycol conjugation, and homology modeling. *J. Biol. Chem.* **1997**, *272*, 2312-2318.

4. Barany, G.; Kneib-Cordonier, N.; Mullen, D. G. Solid-phase peptide synthesis: a silver anniversary report. *Int. J. Pept. Protein Res.* **1987**, *30*, 705-739.
5. Merrifield, R. B. Solid Phase Peptide Synthesis. I. The Synthesis of a Tetrapeptide. *J. Am. Chem. Soc.* **1963**, *85*, 2149-2154.
6. Fields, G. B., Ed.; In *Solid-phase Peptide Synthesis*; **1997**; Vol. 289, pp. 780.
7. Howl, J., Ed.; In *Peptide Synthesis and Application*; Humana Press: Totowa, NJ, USA, **2005**; Vol. 298, pp. 262.
8. Bodanzky, M. *Principles of Peptide Synthesis*; Springer-Verlag: Berlin; New York, **1993**; pp. 329.
9. Spencer, P. L. Patent: US2495429 A, **1950**.
10. Gedye, R.; Smith, F.; Westaway, K.; Ali, H.; Baldisera, L.; Laberge, L.; Rousell, J. The use of microwave ovens for rapid organic synthesis. *Tetrahedron Letters*, **1986**, *27*, 279-282.
11. Giguere, R. J.; Bray, T. L.; Duncan, S. M.; Majetich, G. Application of commercial microwave ovens to organic synthesis. *Tetrahedron Letters*, **1986**, *27*, 4945-4948.
12. Nuechter, M.; Ondruschka, B.; Bonrath, W.; Gumb, A. Microwave assisted synthesis - a critical technology overview. *Green Chem.* **2004**, *6*, 128-141.
13. Neas, E.; Collins, M. In Kingston, H. M., Jassie, L. B., Eds.; *Introduction to Microwave Sample Preparation: Theory and Practice*; American Chemical Society: Washington, DC, 1988; .
14. Stuerger, D.; Delmotte, M. In *Wave-Material Interactions, Microwave Technology and Equipment*; Loupy, A., Ed.; *Microwaves in Organic Synthesis*; Wiley-VCH: Weinheim, **2002**; Vol. 1, pp. 1-33.
15. Mingos, D. M. P.; Baghurst, D. A. Applications of Microwave Dielectric Heating Effects to Synthetic Problems in Chemistry. *Chem. Soc. Rev.* **1991**, *20*, 1-47.
16. Gabriel, C.; Gabriel, S.; Grant, E. H.; Halstead, B. S. J.; Mingos, D. M. P. Dielectric parameters relevant to microwave dielectric heating. *Chem. Soc. Rev.* **1998**, *27*, 213-224.
17. Hayes, B. L. *Microwave Synthesis: Chemistry at the Speed of Light*; CEM Publishing: Matthews, NC, **2002**; pp. 289.
18. Lide, D. R. *CRC Handbook of Chemistry and Physics: A Ready-Reference Book of Chemical and Physical Data.* **2003**.

19. Schanche, J. S. Microwave synthesis solutions from Personal Chemistry. *Mol. Divers.* **2003**, *7*, 293-300.
20. de la Hoz, A.; Diaz-Ortiz, A.; Moreno, A. Microwaves in organic synthesis. Thermal and non-thermal microwave effects. *Chem. Soc. Rev.* **2005**, *34*, 164-178.
21. Perreux, L.; Loupy, A. A tentative rationalization of microwave effects in organic synthesis according to the reaction medium, and mechanistic considerations. *Tetrahedron*, **2001**, *57*, 9199-9223.
22. Kuhnert, N. Microwave-Assisted Reactions in Organic Synthesis - Are There Any Nonthermal Microwave Effects? *Angew. Chem. Int. Ed. Engl.* **2002**, *41*, 1863-1866.
23. Strauss, C. R. Microwave-Assisted Reactions in Organic Synthesis - Are There Any Nonthermal Microwave Effects? Response to the Highlight by N. Kuhnert. *Angew. Chem. Int. Ed. Engl.* **2002**, *41*, 3589-3591.
24. Hajek, M. In *Microwave Catalysis in Organic Synthesis*; Loupy, A., Ed.; Microwaves in Organic Synthesis; Wiley-VCH: Weinheim, Germany, **2002**; pp. 345-378 (Chapter 10).
25. Kappe, C. O. Controlled microwave heating in modern organic synthesis. *Angew. Chem. Int. Ed. Engl.* **2004**, *43*, 6250-6284.
26. Kappe, O. C.; Stadler, A., Eds.; In *Microwaves in Organic and Medicinal Chemistry*; Mannhold, R., Kubinyi, H. and Folkers, G., Eds.; Methods and Principles in Medicinal Chemistry; Wiley-VCH Verlag GmbH Co. KGaA: Weinheim, **2005**; Vol. 25, pp. 410.
27. Baghurst, D. A.; Mingos, D. M. P. Superheating effects associated with microwave dielectric heating. *J. Chem. Soc., Chem. Commun.* **1992**, 674-677.
28. Saillard, R.; Poux, M.; Berlan, J.; Audhuy-Peaudecerf, M. Microwave heating of organic solvents: Thermal effects and field modelling. *Tetrahedron*, **1995**, *51*, 4033-4042.
29. Chemat, F.; Esveld, E. Microwave Super-Heated Boiling of Organic Liquids: Origin, Effect and Application. *Chem. Eng. Technol.* **2001**, *24*, 735-744.
30. Shibata, C.; Kashima, T.; Ohuchi, K. Nonthermal Influence of Microwave Power on Chemical Reactions. *Jpn. J. Appl. Phys.* **1996**, *35*, 316-319.
31. Jacob, J.; Chia, L. H. L.; Boey, F. Y. C. *J. Mater. Sci.* **1995**, *301*, 5322-5327.
32. Binner, J. G. P.; Hassine, N. A.; Cross, T. E. *J. Mater. Sci.* **1955**, *30*, 5289-5322.

33. Berlan, J.; Giboreau, P.; Lefeuvre, S.; Marchand, C. Synthèse organique sous champ microondes : premier exemple d'activation spécifique en phase homogène. *Tetrahedron Lett.* **1991**, *32*, 2363-2366.
34. Lewis, D. A.; Summers, J. D.; Ward, T. C.; McGrath, J. E. Accelerated imidization reactions using microwave radiation. *J. Polym. Sci. Part A* **1992**, *30*, 1647-1653.
35. de La Hoz, A.; Díaz-Ortiz, A.; Moreno, A. Selectivity in Organic Synthesis Under Microwave Irradiation. *Curr. Org. Chem.* **2004**, *8*, 903-918.
36. Yu, H. M.; Chen, S. T.; Wang, K. T. Enhanced coupling efficiency in solid-phase peptide synthesis by microwave irradiation. *J. Org. Chem.* **1992**, *57*, 4781-4784.
37. Erdélyia, M.; Gogoll, A. Rapid Microwave-Assisted Solid Phase Peptide Synthesis. *Synthesis* **2002**, *2002*, 1592-1596.
38. Katritzky, A. R.; Zhang, Y.; Singh, S. K.; Steelb, P. J. 1,3-Dipolar cycloadditions of organic azides to ester or benzotriazolylcarbonyl activated acetylenic amides. *ARKIVOC* **2003**, 47-64.
39. Chen, J. J.; Deshpande, S. V. Rapid synthesis of α -ketoamides using microwave irradiation–simultaneous cooling method. *Tetrahedron Lett.* **2003**, *44*, 8873-8876.
40. Humphrey, C. E.; Easson, M. A. M.; Tierney, J. P.; Turner, N. J. Solid-Supported Cyclohexane-1,3-dione (CHD): A "Capture and Release" Reagent for the Synthesis of Amides and Novel Scavenger Resin. *Org. Lett.* **2003**, *5*, 849-852.
41. Hachmann, J.; Lebl, M. Alternative to piperidine in Fmoc solid-phase synthesis. *J. Comb. Chem.* **2006**, *8*, 149.
42. Wade, J. D.; Bedford, J.; Sheppard, R. C.; Tregear, G. W. DBU as an N^α -Deprotecting Reagent for the Fluorenylmethoxycarbonyl Group in Continuous Flow Solid-Phase Peptide Synthesis. *Pept. Res.* **1991**, *4*, 194-199.
43. Tickler, A. K.; Barrow, C. J.; Wade, J. D. Improved Preparation of Amyloid- β Peptides Using DBU as N^α -Fmoc Deprotection Reagent. *J. Pept. Sci.* **2001**, *7*, 488-494.
44. GraceVydac HPLC Catalog. **2008**, p. 208.
45. Mutter, M.; Nefzi, A.; Sato, T.; Sun, X.; Wahl, F.; Wohr, T. Pseudo-prolines (psi Pro) for accessing "inaccessible" peptides. *Pept. Res.* **1995**, *8*, 145-153.
46. Haack, T.; Mutter, M. Serine derived oxazolidines as secondary structure disrupting, solubilizing building blocks in peptide synthesis. *Tetrahedron Lett.* **1992**, *33*, 1589-1592.

47. Novabiochem Synthesis design using pseudoproline dipeptides. *Novabiochem innovations* **2004**, 4.
48. Syme, C. D.; Viles, J. H. Solution ¹H NMR investigation of Zn²⁺ and Cd²⁺ binding to amyloid-β peptide (Aβ) of Alzheimer's disease. *Biochim. Biophys. Acta* **2006**, 1764, 246-256.
49. Danielsson, J.; Pierattelli, R.; Banci, L.; Graslund, A. High-resolution NMR studies of the zinc-binding site of the Alzheimer's amyloid β-peptide. *FEBS J.* **2007**, 274, 46-59.
50. Yang, D. S.; McLaurin, J.; Qin, K.; Westaway, D.; Fraser, P. E. Examining the zinc binding site of the amyloid-β peptide. *Eur. J. Biochem.* **2000**, 267, 6692-6698.
51. Ariga, T.; Yu, R. K. GM1 inhibits amyloid β-protein-induced cytokine release. *Neurochem. Res.* **1999**, 24, 219-226.
52. Williamson, M. P.; Suzuki, Y.; Bourne, N. T.; Asakura, T. Binding of amyloid β-peptide to ganglioside micelles is dependent on histidine-13. *Biochem. J.* **2006**, 397, 483-490.
53. Brunden, K. R.; Richter-Cook, N. J.; Chaturvedi, N.; Frederickson, R. C. pH-dependent binding of synthetic β-amyloid peptides to glycosaminoglycans. *J. Neurochem.* **1993**, 61, 2147-2154.
54. Garcia-Martin, F.; Quintanar-Audelo, M.; Garcia-Ramos, Y.; Cruz, L. J.; Gravel, C.; Furic, R.; Cote, S.; Tulla-Puche, J.; Albericio, F. ChemMatrix, a poly(ethylene glycol)-based support for the solid-phase synthesis of complex peptides. *J. Comb. Chem.* **2006**, 8, 213-220.
55. Garcia-Martin, F.; White, P.; Steinauer, R.; Cote, S.; Tulla-Puche, J.; Albericio, F. The synergy of ChemMatrix resin and pseudoproline building blocks renders RANTES, a complex aggregated chemokine. *Biopolymers* **2006**, 84, 566-575.
56. Stephenson, V. C.; Heyding, R. A.; Weaver, D. F. The "promiscuous drug concept" with applications to Alzheimer's disease. *FEBS Lett.* **2005**, 579, 1338-1342.
57. Montanari, V.; Kumar, K. Just add water: a new fluororous capping reagent for facile purification of peptides synthesized on the solid phase. *J. Am. Chem. Soc.* **2004**, 126, 9528-9529.
58. Sohma, Y.; Hayashi, Y.; Kimura, M.; Chiyomori, Y.; Taniguchi, A.; Sasaki, M.; Kimura, T.; Kiso, Y. The 'O-acyl isopeptide method' for the synthesis of difficult sequence-containing peptides: application to the synthesis of Alzheimer's disease-related amyloid β peptide (Aβ) 1-42. *J. Pept. Sci.* **2005**, 11, 441-451.

Chapter V

1. Verdier, Y.; Penke, B. Binding sites of amyloid β -peptide in cell plasma membrane and implications for Alzheimer's disease. *Curr. Protein Pept. Sci.* **2004**, *5*, 19-31.
2. Verdier, Y.; Zarandi, M.; Penke, B. Amyloid β -peptide interactions with neuronal and glial cell plasma membrane: binding sites and implications for Alzheimer's disease. *J. Pept. Sci.* **2004**, *10*, 229-248.
3. Kim, K. S.; Miller, D. L.; Sapienza, V. J.; Chen, C. -. J.; Bai, C.; Grundke-Iqbal, I.; Currie, J. R.; Wisniewski, H. M. Production and characterization of monoclonal antibodies reactive to synthetic cerebrovascular amyloid peptide. *Neurosci. Res. Comm.* **1988**, *2*, 121-130.
4. Kim, K. S.; Wen, G. Y.; Bancher, C.; Chen, C. J. M.; Sapienza, V. J.; Hong, H.; Wisniewski, H. M. Detection and quantification of amyloid β -peptide with 2 monoclonal antibodies. *Neurosci. Res. Comm.* **1990**, *7*, 113-122.
5. Strittmatter, W. J.; Saunders, A. M.; Schmechel, D.; Pericak-Vance, M.; Enghild, J.; Salvesen, G. S.; Roses, A. D. Apolipoprotein E: high-avidity binding to β -amyloid and increased frequency of type 4 allele in late-onset familial Alzheimer disease. *Proc. Natl. Acad. Sci. U. S. A.* **1993**, *90*, 1977-1981.
6. Biancalana, M.; Koide, S. Molecular mechanism of Thioflavin-T binding to amyloid fibrils. *Biochim. Biophys. Acta* **2010**, *1804*, 1405-1412.
7. Strittmatter, W. J.; Huang, D. Y.; Bhasin, R.; Roses, A. D.; Goldgaber, D. Avid binding of β A amyloid peptide to its own precursor. *Exp. Neurol.* **1993**, *122*, 327-334.
8. Schwarzman, A. L.; Tsiper, M.; Gregori, L.; Goldgaber, D.; Frakowiak, J.; Mazur-Kolecka, B.; Taraskina, A.; Pchelina, S.; Vitek, M. P. Selection of peptides binding to the amyloid b-protein reveals potential inhibitors of amyloid formation. *Amyloid* **2005**, *12*, 199-209.
9. Grillo-Bosch, D.; Carulla, N.; Cruz, M.; Sanchez, L.; Pujol-Pina, R.; Madurga, S.; Rabanal, F.; Giralt, E. Retro-enantio N-methylated peptides as β -amyloid aggregation inhibitors. *ChemMedChem* **2009**, *4*, 1488-1494.
10. Zhang, L.; Yagnik, G.; Peng, Y.; Wang, J.; Xu, H. H.; Hao, Y.; Liu, Y. N.; Zhou, F. Kinetic studies of inhibition of the amyloid beta (1-42) aggregation using a ferrocene-tagged β -sheet breaker peptide. *Anal. Biochem.* **2013**, *434*, 292-299.
11. Hou, L.; Zagorski, M. G. NMR reveals anomalous copper(II) binding to the amyloid A β peptide of Alzheimer's disease. *J. Am. Chem. Soc.* **2006**, *128*, 9260-9261.

12. Atwood, C. S.; Scarpa, R. C.; Huang, X.; Moir, R. D.; Jones, W. D.; Fairlie, D. P.; Tanzi, R. E.; Bush, A. I. Characterization of copper interactions with alzheimer amyloid β peptides: identification of an attomolar-affinity copper binding site on amyloid β 1-42. *J. Neurochem.* **2000**, *75*, 1219-1233.
13. Syme, C. D.; Viles, J. H. Solution ^1H NMR investigation of Zn^{2+} and Cd^{2+} binding to amyloid- β peptide ($\text{A}\beta$) of Alzheimer's disease. *Biochim. Biophys. Acta* **2006**, *1764*, 246-256.
14. Danielsson, J.; Pierattelli, R.; Banci, L.; Graslund, A. High-resolution NMR studies of the zinc-binding site of the Alzheimer's amyloid β -peptide. *FEBS J.* **2007**, *274*, 46-59.
15. Yang, D. S.; McLaurin, J.; Qin, K.; Westaway, D.; Fraser, P. E. Examining the zinc binding site of the amyloid- β peptide. *Eur. J. Biochem.* **2000**, *267*, 6692-6698.
16. Bin, Y.; Chen, S.; Xiang, J. pH-dependent kinetics of copper ions binding to amyloid- β peptide. *J. Inorg. Biochem.* **2013**, *119*, 21-27.
17. Ghalebani, L.; Wahlstrom, A.; Danielsson, J.; Warmlander, S. K.; Graslund, A. pH-dependence of the specific binding of $\text{Cu}(\text{II})$ and $\text{Zn}(\text{II})$ ions to the amyloid- β peptide. *Biochem. Biophys. Res. Commun.* **2012**, *421*, 554-560.
18. Faller, P. Copper and zinc binding to amyloid- β : coordination, dynamics, aggregation, reactivity and metal-ion transfer. *Chembiochem* **2009**, *10*, 2837-2845.
19. Garzon-Rodriguez, W.; Yatsimirsky, A. K.; Glabe, C. G. Binding of $\text{Zn}(\text{II})$, $\text{Cu}(\text{II})$, and $\text{Fe}(\text{II})$ ions to alzheimer's $\text{A}\beta$ peptide studied by fluorescence. *Bioorg. Med. Chem. Lett.* **1999**, *9*, 2243-2248.
20. Brunden, K. R.; Richter-Cook, N. J.; Chaturvedi, N.; Frederickson, R. C. pH-dependent binding of synthetic β -amyloid peptides to glycosaminoglycans. *J. Neurochem.* **1993**, *61*, 2147-2154.
21. McLaurin, J. A.; Franklin, T.; Zhang, X.; Deng, J.; Fraser, P. E. Interactions of Alzheimer amyloid- β peptides with glycosaminoglycans effects on fibril nucleation and growth. *Eur. J. Biochem.* **1999**, *266*, 1101-1110.
22. Leveugle, B.; Scanameo, A.; Ding, W.; Fillit, H. Binding of heparan sulfate glycosaminoglycan to β -amyloid peptide: inhibition by potentially therapeutic polysulfated compounds. *Neuroreport* **1994**, *5*, 1389-1392.
23. Watson, D. J.; Lander, A. D.; Selkoe, D. J. Heparin-binding properties of the amyloidogenic peptides $\text{A}\beta$ and amylin. Dependence on aggregation state and inhibition by Congo red. *J. Biol. Chem.* **1997**, *272*, 31617-31624.

24. Sadler, I. I.; Hawtin, S. R.; Taylor, V.; Shearman, M. S.; Pollack, S. J. Glycosaminoglycans and sulphated polyanions attenuate the neurotoxic effects of β -amyloid. *Biochem. Soc. Trans.* **1995**, *23*, 106S.
25. Curtain, C. C.; Ali, F. E.; Smith, D. G.; Bush, A. I.; Masters, C. L.; Barnham, K. J. Metal ions, pH, and cholesterol regulate the interactions of Alzheimer's disease amyloid- β peptide with membrane lipid. *J. Biol. Chem.* **2003**, *278*, 2977-2982.
26. Devanathan, S.; Salamon, Z.; Lindblom, G.; Grobner, G.; Tollin, G. Effects of sphingomyelin, cholesterol and zinc ions on the binding, insertion and aggregation of the amyloid A β (1-40) peptide in solid-supported lipid bilayers. *FEBS J.* **2006**, *273*, 1389-1402.
27. Avdulov, N. A.; Chochina, S. V.; Igbavboa, U.; Warden, C. S.; Vassiliev, A. V.; Wood, W. G. Lipid binding to amyloid β -peptide aggregates: preferential binding of cholesterol as compared with phosphatidylcholine and fatty acids. *J. Neurochem.* **1997**, *69*, 1746-1752.
28. Hoshino, T.; Mahmood, M. I.; Mori, K.; Matsuzaki, K. Binding and Aggregation Mechanism of Amyloid β -Peptides onto the GM1 Ganglioside-Containing Lipid Membrane. *J Phys Chem B* **2013**, *117*, 8085-8094.
29. Ikeda, K.; Matsuzaki, K. Driving force of binding of amyloid β -protein to lipid bilayers. *Biochem. Biophys. Res. Commun.* **2008**, *370*, 525-529.
30. Shao, H.; Jao, S.; Ma, K.; Zagorski, M. G. Solution structures of micelle-bound amyloid β -(1-40) and β -(1-42) peptides of Alzheimer's disease. *J. Mol. Biol.* **1999**, *285*, 755-773.
31. Kisilevsky, R.; Lemieux, L. J.; Fraser, P. E.; Kong, X.; Hultin, P. G.; Szarek, W. A. Arresting amyloidosis in vivo using small-molecule anionic sulphonates or sulphates: implications for Alzheimer's disease. *Nat. Med.* **1995**, *1*, 143-148.
32. Carter, D. B.; Chou, K. C. A model for structure-dependent binding of Congo red to Alzheimer β -amyloid fibrils. *Neurobiol. Aging* **1998**, *19*, 37-40.
33. Kuner, P.; Bohrmann, B.; Tjernberg, L. O.; Naslund, J.; Huber, G.; Celenk, S.; Gruninger-Leitch, F.; Richards, J. G.; Jakob-Roetne, R.; Kemp, J. A.; Nordstedt, C. Controlling polymerization of β -amyloid and prion-derived peptides with synthetic small molecule ligands. *J. Biol. Chem.* **2000**, *275*, 1673-1678.
34. Talafous, J.; Marcinowski, K. J.; Klopman, G.; Zagorski, M. G. Solution structure of residues 1-28 of the amyloid β -peptide. *Biochemistry* **1994**, *33*, 7788-7796.
35. Salomon, A. R.; Marcinowski, K. J.; Friedland, R. P.; Zagorski, M. G. Nicotine inhibits amyloid formation by the β -peptide. *Biochemistry* **1996**, *35*, 13568-13578.

36. Seed, B. Silanizing glassware. *Curr. Protoc. Mol. Biol.* **2001**, Appendix 3, Appendix 3B.
37. Macdonell, M. T.; Hansen, J. N.; Ortiz-Conde, B. A. In *9 Isolation, Purification and Enzymatic Sequencing of RNA*; Colwell, R. R., Grigorova, R., Eds.; Methods in Microbiology; Academic Press: **1988**; Vol. 19, pp. 357-404.
38. Gibbs, J. Effective Blocking Procedures. *ELISA Technical Bulletin - No 3* **2001**, 1-6.
39. Pica-Mendez, A. M.; Tanen, M.; Dallob, A.; Tanaka, W.; Laterza, O. F. Nonspecific binding of A β 42 to polypropylene tubes and the effect of Tween-20. *Clin. Chim. Acta* **2010**, *411*, 1833.
40. Goebel-Stengel, M. The importance of using the optimal plasticware and glassware in studies involving peptides. *Anal. Biochem.* **2011**, *414*, 38-46.
41. Weiss, N.; Wentz, W.; Mueller, P. Eppendorf LoBind: Evaluation of protein recovery in Eppendorf Protein LoBind Tubes and Plates. *Eppendorf Application Note* **2010**, *180*, 1-5.
42. Nag, S.; Sarkar, B.; Bandyopadhyay, A.; Sahoo, B.; Sreenivasan, V. K.; Kombrabail, M.; Muralidharan, C.; Maiti, S. Nature of the amyloid- β monomer and the monomer-oligomer equilibrium. *J. Biol. Chem.* **2011**, *286*, 13827-13833.
43. Axelsson, I. Characterization of proteins and other macromolecules by agarose gel chromatography. *Journal of Chromatography A* **1978**, *152*, 21-32.
44. Wright, A. K.; Thompson, M. R. Hydrodynamic structure of bovine serum albumin determined by transient electric birefringence. *Biophys. J.* **1975**, *15*, 137-141.
45. Ge, S.; Kojio, K.; Takahara, A.; Kajiyama, T. Bovine serum albumin adsorption onto immobilized organotrichlorosilane surface: influence of the phase separation on protein adsorption patterns. *J. Biomater. Sci. Polym. Ed.* **1998**, *9*, 131-150.
46. Vassar, P. S.; Culling, C. F. A. Fluorescent stains, with special reference to amyloid and connective tissues. *Arch. Pathol.* **1959**, *68*, 487-498.
47. Kelenyi, G. On the histochemistry of azo group-free thiazole dyes. *J. Histochem. Cytochem.* **1967**, *15*, 172-180.
48. Kelenyi, G. Thioflavin S fluorescent and Congo red anisotropic stainings in the histologic demonstration of amyloid. *Acta Neuropathol.* **1967**, *7*, 336-348.
49. LeVine, H., 3rd Quantification of β -sheet amyloid fibril structures with thioflavin T. *Methods Enzymol.* **1999**, *309*, 274-284.

50. Wolfe, L. S.; Calabrese, M. F.; Nath, A.; Blaho, D. V.; Miranker, A. D.; Xiong, Y. Protein-induced photophysical changes to the amyloid indicator dye thioflavin T. *Proc. Natl. Acad. Sci. U. S. A.* **2010**, *107*, 16863-16868.
51. Klunk, W. E.; Jacob, R. F.; Mason, R. P. Quantifying amyloid β -peptide (A β) aggregation using the Congo red-A β (CR-A β) spectrophotometric assay. *Anal. Biochem.* **1999**, *266*, 66-76.
52. Pratim Bose, P.; Chatterjee, U.; Xie, L.; Johansson, J.; Gothelid, E.; Arvidsson, P. I. Effects of Congo Red on A β ₁₋₄₀ Fibril Formation Process and Morphology. *ACS Chem. Neurosci.* **2010**, *1*, 315-324.
53. Lorenzo, A.; Yankner, B. A. β -amyloid neurotoxicity requires fibril formation and is inhibited by congo red. *Proc. Natl. Acad. Sci. U. S. A.* **1994**, *91*, 12243-12247.
54. Podlisny, M. B.; Walsh, D. M.; Amarante, P.; Ostaszewski, B. L.; Stimson, E. R.; Maggio, J. E.; Teplow, D. B.; Selkoe, D. J. Oligomerization of endogenous and synthetic amyloid β -protein at nanomolar levels in cell culture and stabilization of monomer by Congo red. *Biochemistry* **1998**, *37*, 3602-3611.
55. Alavez, S.; Vantipalli, M. C.; Zucker, D. J.; Klang, I. M.; Lithgow, G. J. Amyloid-binding compounds maintain protein homeostasis during ageing and extend lifespan. *Nature* **2011**, *472*, 226-229.
56. Porat, Y.; Abramowitz, A.; Gazit, E. Inhibition of amyloid fibril formation by polyphenols: structural similarity and aromatic interactions as a common inhibition mechanism. *Chem. Biol. Drug Des.* **2006**, *67*, 27-37.
57. Inbar, P.; Bautista, M. R.; Takayama, S. A.; Yang, J. Assay to screen for molecules that associate with Alzheimer's related β -amyloid fibrils. *Anal. Chem.* **2008**, *80*, 3502-3506.
58. Rodriguez-Rodriguez, C.; Sanchez de Groot, N.; Rimola, A.; Alvarez-Larena, A.; Lloveras, V.; Vidal-Gancedo, J.; Ventura, S.; Vendrell, J.; Sodupe, M.; Gonzalez-Duarte, P. Design, selection, and characterization of thioflavin-based intercalation compounds with metal chelating properties for application in Alzheimer's disease. *J. Am. Chem. Soc.* **2009**, *131*, 1436-1451.
59. Inbar, P.; Li, C. Q.; Takayama, S. A.; Bautista, M. R.; Yang, J. Oligo(ethylene glycol) derivatives of thioflavin T as inhibitors of protein-amyloid interactions. *Chembiochem* **2006**, *7*, 1563-1566.
60. Hudson, S. A.; Ecroyd, H.; Kee, T. W.; Carver, J. A. The thioflavin T fluorescence assay for amyloid fibril detection can be biased by the presence of exogenous compounds. *FEBS J.* **2009**, *276*, 5960-5972.

61. Christie, W. W. Gangliosides - Structure, Occurrence, Biology, and Analysis. <http://lipidlibrary.aocs.org/Lipids/gang/index.htm> (accessed 02/10, 2014).
62. Ariga, T.; Yu, R. K. GM1 inhibits amyloid β -protein-induced cytokine release. *Neurochem. Res.* **1999**, *24*, 219-226.
63. Williamson, M. P.; Suzuki, Y.; Bourne, N. T.; Asakura, T. Binding of amyloid β -peptide to ganglioside micelles is dependent on histidine-13. *Biochem. J.* **2006**, *397*, 483-490.
64. Kakio, A.; Nishimoto, S. I.; Yanagisawa, K.; Kozutsumi, Y.; Matsuzaki, K. Cholesterol-dependent formation of GM1 ganglioside-bound amyloid β -protein, an endogenous seed for Alzheimer amyloid. *J. Biol. Chem.* **2001**, *276*, 24985-24990.
65. Ikeda, K.; Yamaguchi, T.; Fukunaga, S.; Hoshino, M.; Matsuzaki, K. Mechanism of amyloid β -protein aggregation mediated by GM1 ganglioside clusters. *Biochemistry* **2011**, *50*, 6433-6440.
66. Yanagisawa, M.; Ariga, T.; Yu, R. K. Cytotoxic effects of G(M1) ganglioside and amyloid β -peptide on mouse embryonic neural stem cells. *ASN Neuro* **2010**, *2*, e00029.
67. Dawson, R. M. Characterization of the binding of cholera toxin to ganglioside GM1 immobilized onto microtitre plates. *J. Appl. Toxicol.* **2005**, *25*, 30-38.
68. Schagger, H.; von Jagow, G. Tricine-sodium dodecyl sulfate-polyacrylamide gel electrophoresis for the separation of proteins in the range from 1 to 100 kDa. *Anal. Biochem.* **1987**, *166*, 368-379.
69. Schagger, H. Tricine-SDS-PAGE. *Nat. Protoc.* **2006**, *1*, 16-22.
70. Ogawa, M.; Tsukuda, M.; Yamaguchi, T.; Ikeda, K.; Okada, T.; Yano, Y.; Hoshino, M.; Matsuzaki, K. Ganglioside-mediated aggregation of amyloid β -proteins ($A\beta$): comparison between $A\beta$ -(1-42) and $A\beta$ -(1-40). *J. Neurochem.* **2011**, *116*, 851-857.
71. Feng, Y.; Wang, X.; Yang, S.; Wang, Y.; Zhang, X.; Du, X.; Sun, X.; Zhao, M.; Huang, L.; Liu, R. Resveratrol inhibits β -amyloid oligomeric cytotoxicity but does not prevent oligomer formation. *Neurotoxicology* **2009**, *30*, 986-995.
72. Ladiwala, A. R.; Lin, J. C.; Bale, S. S.; Marcelino-Cruz, A. M.; Bhattacharya, M.; Dordick, J. S.; Tessier, P. M. Resveratrol selectively remodels soluble oligomers and fibrils of amyloid $A\beta$ into off-pathway conformers. *J. Biol. Chem.* **2010**, *285*, 24228-24237.

73. Yang, F.; Lim, G. P.; Begum, A. N.; Ubada, O. J.; Simmons, M. R.; Ambegaokar, S. S.; Chen, P. P.; Kaye, R.; Glabe, C. G.; Frautschy, S. A.; Cole, G. M. Curcumin inhibits formation of amyloid β oligomers and fibrils, binds plaques, and reduces amyloid in vivo. *J. Biol. Chem.* **2005**, *280*, 5892-5901.
74. Ono, K.; Hasegawa, K.; Naiki, H.; Yamada, M. Curcumin has potent anti-amyloidogenic effects for Alzheimer's β -amyloid fibrils in vitro. *J. Neurosci. Res.* **2004**, *75*, 742-750.
75. Hulme, E. C.; Trevethick, M. A. Ligand binding assays at equilibrium: validation and interpretation. *Br. J. Pharmacol.* **2010**, *161*, 1219-1237.
76. Choo-Smith, L. P.; Garzon-Rodriguez, W.; Glabe, C. G.; Surewicz, W. K. Acceleration of amyloid fibril formation by specific binding of A β -(1-40) peptide to ganglioside-containing membrane vesicles. *J. Biol. Chem.* **1997**, *272*, 22987-22990.
77. Ariga, T.; Kobayashi, K.; Hasegawa, A.; Kiso, M.; Ishida, H.; Miyatake, T. Characterization of high-affinity binding between gangliosides and amyloid β -protein. *Arch. Biochem. Biophys.* **2001**, *388*, 225-230.
78. Fancy, D. A.; Kodadek, T. Chemistry for the analysis of protein-protein interactions: rapid and efficient cross-linking triggered by long wavelength light. *Proc. Natl. Acad. Sci. U. S. A.* **1999**, *96*, 6020-6024.
79. Mattson, G.; Conklin, E.; Desai, S.; Nielander, G.; Savage, M. D.; Morgensen, S. A practical approach to crosslinking. *Mol. Biol. Rep.* **1993**, *17*, 167-183.
80. Tang, X.; Bruce, J. E. Chemical cross-linking for protein-protein interaction studies. *Methods Mol. Biol.* **2009**, *492*, 283-293.
81. Bitan, G.; Lomakin, A.; Teplow, D. B. Amyloid β -protein oligomerization: prenucleation interactions revealed by photo-induced cross-linking of unmodified proteins. *J. Biol. Chem.* **2001**, *276*, 35176-35184.
82. Bitan, G.; Teplow, D. B. Rapid photochemical cross-linking--a new tool for studies of metastable, amyloidogenic protein assemblies. *Acc. Chem. Res.* **2004**, *37*, 357-364.
83. LeVine, H., 3rd. Alzheimer's β -peptide oligomer formation at physiologic concentrations. *Anal. Biochem.* **2004**, *335*, 81-90.
84. Crouch, P. J.; Blake, R.; Duce, J. A.; Ciccotosto, G. D.; Li, Q. X.; Barnham, K. J.; Curtain, C. C.; Cherny, R. A.; Cappai, R.; Dyrks, T.; Masters, C. L.; Trounce, I. A. Copper-dependent inhibition of human cytochrome c oxidase by a dimeric conformer of amyloid- β ₁₋₄₂. *J. Neurosci.* **2005**, *25*, 672-679.

85. Bitan, G. In *Structural Study of Metastable Amyloidogenic Protein Oligomers by Photo-Induced Cross-Linking of Unmodified Proteins*; Indu Kheterpal and Ronald Wetzel, Ed.; Methods in Enzymology; Academic Press: **2006**; *413*, pp. 217-236.
86. Kalyanasundaram, K. Photophysics, photochemistry and solar energy conversion with tris(bipyridyl)ruthenium(II) and its analogues. *Coord. Chem. Rev.* **1982**, *46*, 159-244.
87. Wallin, S.; Davidsson, J.; Modin, J.; Hammarstroem, L. Femtosecond Transient Absorption Anisotropy Study on $[\text{Ru}(\text{bpy})_3]^{2+}$ and $[\text{Ru}(\text{bpy})(\text{py})_4]^{2+}$. Ultrafast Interligand and Randomization of the MLCT State. *J. Phys. Chem. A* **2005**, *109*, 4697-4704.
88. Wikipedia Luminous efficacy. http://en.wikipedia.org/wiki/Luminous_efficacy#Overall_luminous_efficacy (accessed 01/15, 2014).

Chapter VI

1. Meier-Stephenson, V. C. *Quantum Medicine: Novel Applications of Computational Chemistry to the Treatment of Neurological Diseases*, Dalhousie University, Halifax, Nova Scotia, **2005**.
2. Garcia-Martin, F.; Quintanar-Audelo, M.; Garcia-Ramos, Y.; Cruz, L. J.; Gravel, C.; Furic, R.; Cote, S.; Tulla-Puche, J.; Albericio, F. ChemMatrix, a poly(ethylene glycol)-based support for the solid-phase synthesis of complex peptides. *J. Comb. Chem.* **2006**, *8*, 213-220.
3. Garcia-Martin, F.; White, P.; Steinauer, R.; Cote, S.; Tulla-Puche, J.; Albericio, F. The synergy of ChemMatrix resin and pseudoproline building blocks renders RANTES, a complex aggregated chemokine. *Biopolymers* **2006**, *84*, 566-575.
4. Montanari, V.; Kumar, K. Just add water: a new fluororous capping reagent for facile purification of peptides synthesized on the solid phase. *J. Am. Chem. Soc.* **2004**, *126*, 9528-9529.

Appendix A

1. Soccia, S. J.; Kirby, J. E.; Washicosky, K. J.; Tucker, S. M.; Ingelsson, M.; Hyman, B.; Burton, M. A.; Goldstein, L. E.; Duong, S.; Tanzi, R. E.; Moir, R. D. The Alzheimer's Disease-Associated Amyloid β -Protein Is an Antimicrobial Peptide. *PLoS One* **2010**, *5*, e9505.
2. Wang, Z.; Wang, G. APD: the Antimicrobial Peptide Database. *Nucleic Acids Res.* **2004**, *32*, D590-2.